PANDEMIC INFLUENZA VACCINE APPROACHES: CURRENT STATUS AND FUTURE DIRECTIONS

EDITED BY: Rebecca Jane Cox, Michael Schotsaert and Corey Patrick Mallett
PUBLISHED IN: Frontiers in Immunology

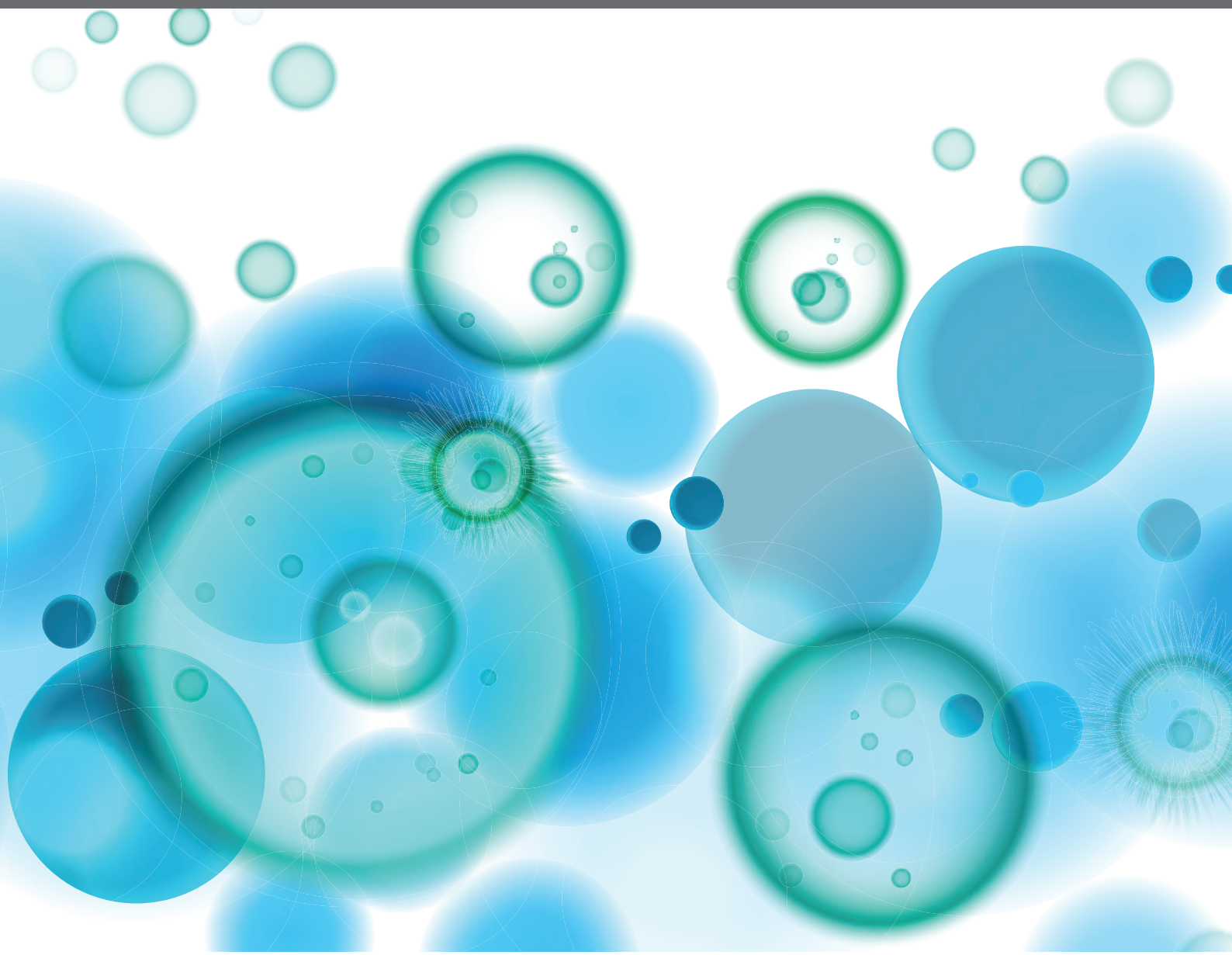

frontiers Research Topics

frontiers

ISSN 1664-8714
ISBN 978-2-83250-103-0
DOI 10.3389/978-2-83250-103-0

About Frontiers

Frontiers is more than just an open-access publisher of scholarly articles: it is a pioneering approach to the world of academia, radically improving the way scholarly research is managed. The grand vision of Frontiers is a world where all people have an equal opportunity to seek, share and generate knowledge. Frontiers provides immediate and permanent online open access to all its publications, but this alone is not enough to realize our grand goals.

Frontiers Journal Series

The Frontiers Journal Series is a multi-tier and interdisciplinary set of open-access, online journals, promising a paradigm shift from the current review, selection and dissemination processes in academic publishing. All Frontiers journals are driven by researchers for researchers; therefore, they constitute a service to the scholarly community. At the same time, the Frontiers Journal Series operates on a revolutionary invention, the tiered publishing system, initially addressing specific communities of scholars, and gradually climbing up to broader public understanding, thus serving the interests of the lay society, too.

Dedication to Quality

Each Frontiers article is a landmark of the highest quality, thanks to genuinely collaborative interactions between authors and review editors, who include some of the world's best academicians. Research must be certified by peers before entering a stream of knowledge that may eventually reach the public - and shape society; therefore, Frontiers only applies the most rigorous and unbiased reviews.
Frontiers revolutionizes research publishing by freely delivering the most outstanding research, evaluated with no bias from both the academic and social point of view. By applying the most advanced information technologies, Frontiers is catapulting scholarly publishing into a new generation.

What are Frontiers Research Topics?

Frontiers Research Topics are very popular trademarks of the Frontiers Journals Series: they are collections of at least ten articles, all centered on a particular subject. With their unique mix of varied contributions from Original Research to Review Articles, Frontiers Research Topics unify the most influential researchers, the latest key findings and historical advances in a hot research area! Find out more on how to host your own Frontiers Research Topic or contribute to one as an author by contacting the Frontiers Editorial Office: frontiersin.org/about/contact

PANDEMIC INFLUENZA VACCINE APPROACHES: CURRENT STATUS AND FUTURE DIRECTIONS

Topic Editors:
Rebecca Jane Cox, University of Bergen, Norway
Michael Schotsaert, Icahn School of Medicine at Mount Sinai, United States
Corey Patrick Mallett, GlaxoSmithKline, United States

Citation: Cox, R. J., Schotsaert, M., Mallett, C. P., eds. (2022). Pandemic Influenza Vaccine Approaches: Current Status and Future Directions.
Lausanne: Frontiers Media SA. doi: 10.3389/978-2-83250-103-0

Table of Contents

05 ***Editorial: Pandemic Influenza Vaccine Approaches: Current Status and Future Directions***
Michael Schotsaert, Rebecca Jane Cox and Corey P. Mallett

08 ***OVX836 Heptameric Nucleoprotein Vaccine Generates Lung Tissue-Resident Memory CD8+ T-Cells for Cross-Protection Against Influenza***
Judith Del Campo, Julien Bouley, Marion Chevandier, Carine Rousset, Marjorie Haller, Alice Indalecio, Delphine Guyon-Gellin, Alexandre Le Vert, Fergal Hill, Sophia Djebali, Yann Leverrier, Jacqueline Marvel, Béhazine Combadière and Florence Nicolas

21 ***Influenza Viruses: Innate Immunity and mRNA Vaccines***
SangJoon Lee and Jin-Hyeob Ryu

34 ***Mosaic Hemagglutinin-Based Whole Inactivated Virus Vaccines Induce Broad Protection Against Influenza B Virus Challenge in Mice***
Yonghong Liu, Shirin Strohmeier, Irene González-Domínguez, Jessica Tan, Viviana Simon, Florian Krammer, Adolfo García-Sastre, Peter Palese and Weina Sun

47 ***Pandemic Preparedness Against Influenza: DNA Vaccine for Rapid Relief***
Tor Kristian Andersen, Johanna Bodin, Fredrik Oftung, Bjarne Bogen, Siri Mjaaland and Gunnveig Grødeland

61 ***Bacteriophage T4 Vaccine Platform for Next-Generation Influenza Vaccine Development***
Mengling Li, Pengju Guo, Cen Chen, Helong Feng, Wanpo Zhang, Changqin Gu, Guoyuan Wen, Venigalla B. Rao and Pan Tao

73 ***Repeated Influenza Vaccination Boosts and Maintains H1N1pdm09 Neuraminidase Antibody Titers***
Lena Hansen, Fan Zhou, Håkon Amdam, Mai-Chi Trieu and Rebecca Jane Cox

84 ***Safety of Influenza A H1N1pdm09 Vaccines: An Overview of Systematic Reviews***
Lene Kristine Juvet, Anna Hayman Robertson, Ida Laake, Siri Mjaaland and Lill Trogstad

97 ***Influenza Neuraminidase Characteristics and Potential as a Vaccine Target***
Sarah Creytens, Mirte N. Pascha, Marlies Ballegeer, Xavier Saelens and Cornelis A. M. de Haan

116 ***Matrix M Adjuvanted H5N1 Vaccine Elicits Broadly Neutralizing Antibodies and Neuraminidase Inhibiting Antibodies in Humans That Correlate With In Vivo Protection***
Fan Zhou, Lena Hansen, Gabriel Pedersen, Gunnveig Grødeland and Rebecca Cox

129 ***Functional and Binding H1N1pdm09-Specific Antibody Responses in Occasionally and Repeatedly Vaccinated Healthcare Workers: A Five-Year Study (2009-2014)***
Håkon Amdam, Anders Madsen, Fan Zhou, Amit Bansal, Mai-Chi Trieu and Rebecca Jane Cox

140 ***Supplementation of H7N9 Virus-Like Particle Vaccine With Recombinant Epitope Antigen Confers Full Protection Against Antigenically Divergent H7N9 Virus in Chickens***
Dexin Kong, Taoran Chen, Xiaolong Hu, Shaorong Lin, Yinze Gao, Chunmei Ju, Ming Liao and Huiying Fan

frontiers | Frontiers in Immunology

TYPE Editorial
PUBLISHED 18 August 2022
DOI 10.3389/fimmu.2022.980956

OPEN ACCESS

EDITED AND REVIEWED BY
Denise L. Doolan,
James Cook University, Australia

*CORRESPONDENCE
Corey P. Mallett
corey.p.mallett@gsk.com

SPECIALTY SECTION
This article was submitted to Vaccines and Molecular Therapeutics, a section of the journal Frontiers in Immunology

RECEIVED 29 June 2022
ACCEPTED 25 July 2022
PUBLISHED 18 August 2022

CITATION
Schotsaert M, Cox RJ and Mallett CP (2022) Editorial: Pandemic influenza vaccine approaches: Current status and future directions.
Front. Immunol. 13:980956.
doi: 10.3389/fimmu.2022.980956

Editorial: Pandemic influenza vaccine approaches: Current status and future directions

Michael Schotsaert[1], Rebecca Jane Cox[2] and Corey P. Mallett[3]*

[1]Global Health and Emerging Pathogens Institute, Department of Microbiology, Icahn School of Medicine at Mount Sinai, New York, NY, United States, [2]Influenza Centre, Department of Clinical Science, University of Bergen, Bergen, Norway, [3]GSK, Rockville, MD, United States

KEYWORDS

pandemic, influenza vaccines, emergent influenza viruses, animal reservoir, human history

Editorial on the Research Topic
Pandemic influenza vaccine approaches: Current status and future directions

For over a hundred years, humanity was confronted with recurring pandemics caused by influenza viruses, over-burdening health care systems and disrupting societies worldwide. Since the beginning of the previous century, we have encountered four pandemics caused by H1N1, H2N2, and H3N2 viruses, with the last one in 2009 caused by an H1N1 swine-origin virus. With every pandemic a new influenza virus emerged that started circulating in a human population that was immunologically naive against the emerging virus. This condition allows us to study the response to a new vaccine that targets the emerging virus in the absence of pre-existing neutralizing antibodies that may affect vaccine effectiveness. In this Research Topic, Amdam et al., reported on the effect of vaccination history on the immune response to H1N1pdm09 vaccines in health care workers during the period 2009-2014, and Juvet et al., summarized data obtained in the years following the 2009 H1N1 pandemic on vaccine safety for the rolled-out pandemic influenza vaccines.

There is a constant fear that a new and potentially highly pathogenic influenza virus will make the cross-species jump from the animal reservoir to humans and start a new pandemic. Therefore, it came as a surprise for many of us when the second pandemic of this century was caused by SARS-CoV-2, a coronavirus. We are now over two years into the COVID-19 pandemic, and effective vaccines have saved many lives and allowed us to go from worldwide lockdowns towards less restricted travel. The fast response to this newly emerging coronavirus, also from an animal reservoir, was at least partly possible due to pandemic preparedness guided by our knowledge from previous preclinical and clinical research in the context of influenza virus-host interactions, influenza epidemiology, and influenza vaccine development. Interestingly, due to measures in place like social distancing, masking and creating awareness for respiratory virus

transmission during the COVID-19 pandemic, hospitalized cases due to influenza virus dropped drastically (1, 2). With easing of restrictions, more social interaction and international travel are again taking off, and thereby influenza cases are also on the rise. The absence of seasonal influenza in humans observed in the first year of the COVID-19 pandemic due to measures taken worldwide to mitigate the spread of SARS-CoV-2 made it difficult to predict the strains to be included in the vaccine, and antigenic mismatch for at least the H3 hemagglutinin (HA) vaccine component has been reported (3, 4). This highlights the need for further investment in pandemic influenza vaccine approaches, as outlined in the strategic plan for a Universal Influenza Vaccine from the National Institute of Allergy and Infectious Diseases (5). A recurring topic is the search for conserved antigens derived from influenza virus proteins and for strategies to make them immunogenic. Moreover, protection can be provided by immune mechanisms other than antibody-mediated virus neutralization, such as T cells or antibody-mediated cellular toxicity (ADCC). As such, different vaccine candidates based on different platforms are suggested. In this Research Topic, conventional (adjuvanted) inactivated influenza virus vaccines are discussed along with mRNA, DNA, virus like particles, T4 bacteriophage-based, and recombinant protein vaccines. Liu et. al., discussed a strategy based on targeting conserved epitopes in the influenza B HA using an engineered inactivated influenza B virus vaccine to induce antibody-mediated protection that correlates with ADCC. A strategy is also being tested in the clinic for an Influenza A universal vaccine that uses chimeric HA influenza vaccines (6, 7). Del Campo et al., described a recombinant protein-based approach to induce cross-reactive influenza nucleoprotein (NP)-specific CD8+ T cells. The nucleoprotein is a conserved influenza T cell antigen also in humans, and therefore targeting the NP may result in protection against influenza viruses from different subtypes. It was already suggested that infection induced NP-specific CD8+ T cells correlated with protection from influenza re-infection for several decades (8). Inducing them by vaccination, however, remained challenging. Interestingly, this methodology seems to be able to induce lung-resident memory CD8+ T cells by intramuscular vaccination, thereby promoting cellular mediated immunity in the tissue where infection starts, allowing for a faster response upon infection. Neuraminidase (NA) is the second major antigenic determinant on the surface of influenza viruses, and infected cells and antibodies against NA correlate with reduced shedding and shorter symptom duration in humans (9). In this Research Topic, Creytens et al., discussed the potential of NA as a vaccine antigen, and Hansen et al., reported that repeated vaccination with seasonal influenza vaccines can boost and maintain NA-specific humoral immunity health care workers in a five-year longitudinal study. The highly conserved ectodomain of the influenza matrix 2 protein (M2e) has been suggested as a good universal vaccine epitope, and antibodies targeting M2e correlated with protection in preclinical and clinical settings (10, 11). However, following natural infection, M2e-specific antibodies are not highly induced, and M2e is poorly immunogenic if not presented to the immune system with the help of a scaffold (12). Li et al., proposed to use the bacteriophage T4 vaccine platform combined with the M2e antigen as a scalable low-cost solution for producing a universal vaccine. Scalability and fast production are crucial for pandemic vaccines, and DNA- and RNA-based vaccine approaches are very attractive for this reason. Nucleic acid-based platforms hold the advantage that vaccine antigen is produced inside host cells and therefore can be efficiently presented to the immune system in the context of major histocompatibility complex proteins. This typically results in efficient T cell activation, as demonstrated by Andersen et al., Nucleic acid-based vaccines can also be recognized by innate immune receptors, thereby further adjuvanting vaccine responses against the antigen they encode, as discussed by Lee and Ryu. Pandemic vaccines often anticipate zoonotic spillover of (avian) influenza viruses from the animal reservoir. Therefore, H5N1 and H7N9-based pandemic vaccines have been tested in humans. Zhou et al., reported that an adjuvanted H5N1 vaccine can efficiently induce HA- and NA-specific antibodies in healthy volunteers that are protective in a preclinical animal model. Finally, preventing spillover of influenza viruses from the animal reservoir may reduce the risk of future pandemics. The one health approach is based on the concept of controlling viruses with zoonotic potential in animal reservoirs, for example poultry, not only to limit circulation of viruses with pandemic potential in the reservoir but also to prevent spread to humans. Kong et al., described in this Research Topic a virus-like particle supplemented with epitope antigens that can be effectively used to prevent H7N9 avian influenza virus from being shed by experimentally infected chickens.

In summary, *Pandemic Influenza Vaccine Approaches: Current Status and Future Directions* provided an interesting and timely update on the current research activities progressing in a highly relevant area of vaccine development that is part of an overall pandemic preparedness strategy, and the editors appreciated the many excellent contributions by several scientific teams.

Author contributions

All authors contributed to the preparation of the manuscript and reviewed the final content prior to journal submission.

Conflict of interest

CM is an employee of the GSK group of companies and reports owning shares in GSK.

The remaining authors declare that the research was conducted in the absence of any commercial or financial relationships that could be construed as a potential conflict of interest.

Publisher's note

References

1. Dhanasekaran V, Sullivan S, Edwards KM, Xie R, Khvorov A, Valkenburg SA, et al. Human seasonal influenza under COVID-19 and the potential consequences of influenza lineage elimination. *Nat Commun* (2022) 13:1721. doi: 10.1038/s41467-022-29402-5

2. Olsen SJ, Azziz-Baumgartner E, Budd AP, Brammer L, Sullivan S, Pineda RF, et al. Decreased influenza activity during the COVID-19 pandemic - united states, Australia, Chile, and south Africa, 2020. *Journal title MMWR Morb Mortal Wkly Rep* (2020) 37:1305–9. doi: 10.15585/mmwr.mm6937a6

3. Bolton MJ, Ort JT, McBride R, Swanson NJ, Wilson J, Awofolaju M, et al. Antigenic and virological properties of an H3N2 variant that will likely dominate the 2021-2022 northern hemisphere influenza season. (2021) 21267857. doi: 10.1101/2021.12.15.21267857

4. Bragstad K, et al. *Influenza virological and epidemiological season report prepared for the WHO consultation on the composition of influenza virus vaccines for the northern hemisphere 2022/2023*. Available at: https://www.fhi.no/globalassets/dokumenterfiler/rapporter/2022/niph_nic-norway-interim-2021-2022-influenza-season-report-for-who-vcm-february-2022.pdf.

5. Erbelding EJ, Post DJ, Stemmy EJ, Roberts PC, Augustine AD, Ferguson S, et al. A universal influenza vaccine: The strategic plan for the national institute of allergy and infectious diseases. *J Infect Dis* (2018) 218:347–54. doi: 10.1093/infdis/jiy103

6. Folschweiller N, Vanden Abeele C, Chu L, Van Damme P, García-Sastre A, Krammer F, et al. Reactogenicity, safety, and immunogenicity of chimeric haemagglutinin influenza split-virion vaccines, adjuvanted with AS01 or AS03 or non-adjuvanted: a phase 1-2 randomised controlled trial. *Lancet Infect Dis S1473-3099(22)00024-X* (2022) 7:1062–75. doi: 10.1016/S1473-3099(22)00024-X

7. Bernstein DI, Guptill J, Abdollah N, Nachbagauer R, Berlanda-Scorza F, Feser J, et al. Immunogenicity of chimeric haemagglutinin-based, universal influenza virus vaccine candidates: interim results of a randomised, placebo-controlled, phase 1 clinical trial. *Lancet Infect Dis* (2019) 1:80–91. doi: 10.1016/S1473-3099(19)30393-7

8. McMichael AJ, Gotch FM, Noble GR, Beare PA. Cytotoxic T-cell immunity to influenza. *N Engl J Med* (1983) 309:13–7. doi: 10.1056/NEJM198307073090103

9. Maier HE, Nachbagauer R, Kuan G, Ng S, Lopez R, Sanchez N, et al. Pre-existing anti-neuraminidase antibodies are associated with shortened duration of influenza a (H1N1)pdm virus shedding and illness in naturally infected adults. *Clin Infect Dis Off Publ Infect Dis Soc Am* (2019) 11:2290–7. doi: 10.1093/cid/ciz639

10. Neirynck S, Deroo T, Saelens X, Vanlandschoot P, Jou WM, Fiers W. A universal influenza a vaccine based on the extracellular domain of the M2 protein. *Nat Med* (1999) 5:1157–63. doi: 10.1038/13484

11. Ramos EL, Mitcham JL, Koller TD, Bonavia A, Usner DW, Balaratnam G, et al. Efficacy and safety of treatment with an anti-M2e monoclonal antibody in experimental human influenza. *J Infect Dis* (2015) 211:1038–44. doi: 10.1093/infdis/jiu539

12. Fiers W, De Filette M, El Bakkouri K, Schepens B, Roose K, Schotsaert M, et al. M2e-based universal influenza a vaccine. *Vaccine* (2009) 27:6280–3. doi: 10.1016/j.vaccine.2009.07.007

frontiers in Immunology

ORIGINAL RESEARCH
published: 10 June 2021
doi: 10.3389/fimmu.2021.678483

OVX836 Heptameric Nucleoprotein Vaccine Generates Lung Tissue-Resident Memory CD8+ T-Cells for Cross-Protection Against Influenza

Judith Del Campo[1], Julien Bouley[1], Marion Chevandier[1], Carine Rousset[1], Marjorie Haller[1], Alice Indalecio[1], Delphine Guyon-Gellin[1], Alexandre Le Vert[1], Fergal Hill[1], Sophia Djebali[2], Yann Leverrier[2], Jacqueline Marvel[2], Béhazine Combadière[3†] and Florence Nicolas[1†]*

[1] Research and Development Department, Osivax, Lyon, France, [2] Immunity and Cytotoxic Lymphocytes Team, Centre International de Recherche en Infectiologie, INSERM, U1111, Université Claude Bernard Lyon 1, CNRS, UMR5308, École Normale Supérieure de Lyon, Université de Lyon, Lyon, France, [3] Sorbonne Université, Inserm, Centre d'Immunologie et des Maladies Infectieuses (Cimi-Paris), Paris, France

OPEN ACCESS

Edited by:
Corey Patrick Mallett,
GlaxoSmithKline, United States

Reviewed by:
Kathrin Sutter,
University of Duisburg-Essen, Germany
David Pejoski,
Université de Genève, Switzerland

***Correspondence:**
Judith Del Campo
jdelcampo@osivax.com

†These authors share senior authorship

Specialty section:
This article was submitted to Vaccines and Molecular Therapeutics, a section of the journal Frontiers in Immunology

Received: 09 March 2021
Accepted: 18 May 2021
Published: 10 June 2021

Citation:
Del Campo J, Bouley J, Chevandier M, Rousset C, Haller M, Indalecio A, Guyon-Gellin D, Le Vert A, Hill F, Djebali S, Leverrier Y, Marvel J, Combadière B and Nicolas F (2021) OVX836 Heptameric Nucleoprotein Vaccine Generates Lung Tissue-Resident Memory CD8+ T-Cells for Cross-Protection Against Influenza. Front. Immunol. 12:678483. doi: 10.3389/fimmu.2021.678483

Tissue-resident memory (TRM) CD8+ T-cells play a crucial role in the protection against influenza infection but remain difficult to elicit using recombinant protein vaccines. OVX836 is a recombinant protein vaccine, obtained by the fusion of the DNA sequence of the influenza A nucleoprotein (NP) to the DNA sequence of the OVX313 heptamerization domain. We previously demonstrated that OVX836 provides broad-spectrum protection against influenza viruses. Here, we show that OVX836 intramuscular (IM) immunization induces higher numbers of NP-specific IFNγ-producing CD8+ T-cells in the lung, compared to mutant NP (NPm) and wild-type NP (NPwt), which form monomeric and trimeric structures, respectively. OVX836 induces cytotoxic CD8+ T-cells and high frequencies of lung TRM CD8+ T-cells, while inducing solid protection against lethal influenza virus challenges for at least 90 days. Adoptive transfer experiments demonstrated that protection against diverse influenza subtypes is mediated by NP-specific CD8+ T-cells isolated from the lung and spleen following OVX836 vaccination. OVX836 induces a high number of NP-specific lung CD8+ TRM-cells for long-term protection against influenza viruses.

Keywords: influenza vaccine, recombinant nucleoprotein, protection, cellular immunity, CD8+ T-cells

INTRODUCTION

Influenza A infection is a major cause of respiratory infections worldwide. Seasonal flu epidemics occur each year in autumn and winter, with a prevalence of 5 to 10%. They are caused by A/H1N1, A/H3N2, and B-type influenza viruses. Although most seasonal influenza infections are benign, they can cause hospitalization in severe cases, and even death in at-risk populations. Each year, up to 650,000 people

die from influenza around the world (https://www.who.int/influenza/surveillance_monitoring/en/). The "at-risk" populations include elderly people, children, immunosuppressed individuals, and people with chronic diseases.

Influenza viruses are extremely variable. This variability is mainly due to the nature of RNA and the segmentation of the virus' genome. Currently, the quadrivalent vaccines against seasonal influenza, which account for the majority of influenza vaccines worldwide, are inactivated, fragmented vaccines, administered in a single dose comprising 15 µg of hemagglutinin (HA) protein for four viral strains (1). These vaccines are composed of two type A (H1N1 and H3N2) viruses and two type B viruses, injected by the conventional IM route (1). The presence of antibodies directed against the HA glycoprotein on the virus surface which is subject to substantial immune selection pressure is considered the principal reference for protection against influenza viruses. However, vaccination strategies targeting influenza surface glycoproteins frequently have suboptimal effectiveness due to 1) virus mismatches (2, 3) and 2) low humoral responses in fragile populations (4). Nonetheless, CD8+ cytotoxic T-cells also play a role in the mechanisms that protect against influenza (5, 6). NP, in addition to the M1 and PB1 antigens, are significant sources of epitopes inducing cross-strain $CD8^+$ T-cell responses (6–8). McMichael et al. performed a clinical challenge study showing that, in individuals lacking specific antibodies, high levels of CD8+ T-cells correlate with reduced viral shedding following experimental infection (5). During the 1980s, Doherty's group also demonstrated the protective role of $CD8^+$ T-cells against influenza (8). These influenza-specific T-cells play a crucial role in the control of influenza; they are capable of producing cytokines and killing infected cells (7, 9). Various authors have proposed that these cytotoxic CD8+ T lymphocytes might provide protection against multiple subtypes (i.e. H1N1, H5N1, and H3N2) (10). The persistence of cellular immunity against influenza virus variants may play an important role in reducing the severity of infections during epidemics and pandemics (11). This cellular immune memory against influenza viruses is conferred during infections (12). These $CD8^+$ cell responses play a crucial role in viral infections, particularly in immunocompromised individuals (i.e. with an HIV infection or cancers) and the elderly (13, 14). Indeed T-cell responses may be a better correlate of protection in the elderly (5). In addition, their role as immune memory, able to persist and protect during influenza infections has moved forward substantially in the literature (15). Notably, the discovery of tissue localization of cellular immunity against infection has altered our understanding of adaptive immunity for protection. As a result, site-specific responses need to be taken into account in vaccine design (16, 17).

Lung tissue-resident memory (TRM) $CD4^+$ and $CD8^+$ T-cells generated following influenza infection have been shown to provoke viral clearance and survival after lethal challenge (18). Lung TRM T-cells are observed after viral infection and vaccination using live attenuated influenza viruses (LAIV) by the intranasal (IN) route (18). However, their induction remains insignificant when using recombinant protein or trivalent inactivated influenza vaccines. Compared with circulating T-cells, lung TRM cells protect animals against influenza infection (18). Mostly composed of $CD8^+$ T-cells that recognize conserved epitopes, their induction *via* vaccination might be a key aim for effective heterosubtypic protection (6, 19).

OVX836 (18) is a recombinant protein vaccine candidate obtained by genetically fusing the NP sequence of the Influenza A/WSN/1933(H1N1) virus to the OVX313 sequence (oligomerization domain). By spontaneous oligomerization during the production process, OVX836 forms a stable homo-heptameric recombinant protein, comprising seven copies of the NP antigen (19). OVX836 demonstrated a protective efficacy in mice challenges using various influenza A subtypes, thus minimizing the risks of lower protection linked to antigenic drift and even mismatches (19). However, the mechanism of protection needs to be elucidated.

In the present study, we analyzed the mechanism of protection conferred by OVX836 and compared the immune responses and protection produced by three distinct NP proteins, all based on the NP sequence from the Influenza A/WSN/1933 (H1N1) virus: monomeric E339A/R416A mutant NP (NPm), wild-type trimeric NP (NPwt), and heptameric NP (OVX836). Our findings demonstrate that the OVX836 vaccine, when compared to NPm and NPwt, generates higher proportions of lung TRM $CD8^+$ T-cells with cytotoxic activity, producing a higher level of protection against influenza viruses.

METHODS

Expression and Purification of Proteins

The amino acid sequence of NPm, NPwt, and OVX836 was based on influenza virus A/Wilson-Smith/1933. Synthetic genes, codon optimized for *Escherichia coli* expression, encoding NP-OVX313 (namely OVX836) and NPm (E339A/R416A) were purchased from ATUM Bio, USA. NP wild type (NPwt) was obtained by deletion of the OVX313 sequence from the OVX836 plasmid.

The recombinant NP proteins were produced using the *E. coli* BL21 (New England Biolabs) bacterial strain as previously described (19). After cell harvest by centrifugation, the pellets were resuspended in a phosphate buffer containing NaCl (supplemented with DNAse and RNAse for NPm), subsequently lysed by sonication on ice, and centrifuged. NPwt and OVX836 in supernatant were purified using a heparin affinity column followed by a diafiltration for OVX836 or gel filtration chromatography for NPwt. Supernatant containing soluble fraction of recombinant NPm was purified using a first ion exchange exclusion chromatography prior to the heparin and the gel filtration chromatography. Protein concentrations were determined by UV 280 nm measurement; their purity and identity were determined by SDS-PAGE, western blot and intact protein mass spectrometry.

Mass Spectrometry

Measurements of the average mass of intact proteins were performed on a UHR-QqTOF mass spectrometer (Impact II,

Bruker Daltonics) interfaced with a U3000 RSLC liquid chromatography system (CCSM, Lyon, France).

Dynamic Light Scattering Analysis

The measurements were performed on a Malvern Zetasizer Ultra apparatus thermostatted at 25°C. The scattering intensity data, from three measurement angles (MADLS, multi-angle dynamic light scattering), were processed using the instrument software, transformed into the intensity and volume distribution to obtain the hydrodynamic diameter (D_H) in each sample. The entire analysis was conducted in triplicate in 0.1 M Na/K_2 phosphate, 0.5 M Na_2SO_4. The protein concentrations were 0.8 mg/ml (NPm), 0.4 mg/ml (NPwt), and 0.2 mg/ml (OVX836).

Nano Differential Scanning Fluorimetry

nDSF (nano differential scanning fluorimetry) analysis (Tycho NT.6, Nanotemper) was performed to verify the structural integrity (or thermal stability) of NP constructs. The samples tested were the same as those used for the DLS experiments. After the capillaries were inserted into the Tycho NT.6, they were heated to 35–95°C at 20°C/min. The fluorescence was recorded during the thermal run, plotted as ratio and used to calculate the inflection temperature (Ti). These changes in fluorescence signal indicate transitions in the folding state of recombinant proteins. The Ti corresponds to the point at which half of the proteins in the solution have already unfolded.

Electron Microscopy

Samples (concentrations around 0.002–0.02 mg/ml) were applied between a carbon and a mica layer. The carbon was then floated on the top of a 1% (w/v) sodium silicotungstate, pH 7.0 solution. The carbon film was covered with a copper grid. Both were fished out using a small piece of journal paper and air dried before insertion into the electron microscope. Charge-coupled device (CCD) frames were taken with a FEI T12 microscope operating at 120 kV and a nominal magnification of 30,000 times. The dilutions for EM were performed with the 0.01 M Na phosphate pH 7.3, 0.5 M NaCl buffer (NPm and NPwt) or water (OVX836) right before preparing the grid.

Mice Immunizations and Influenza Virus Challenges

Six-week-old female C57BL/6 mice (Charles River Laboratories, Lyon, France) were used in all experiments. The animals were kept under specific pathogen-free conditions, with *ad libitum* access to food and water. All animal procedures were approved by the Institutional Animal Care ethics committee of the Plateau de Biologie Expérimental de la Souris (CECCAPP_ENS_2018_019, Lyon, France), and accreditations have been obtained from governmental agencies. The dose of 30 μg OVX836 used in this paper to characterize the mechanism of action of the vaccine was based on dose response studies in mice: this dose was selected as it provides high NP specific cellular responses and broad protection against influenza challenges. Mice were immunized twice, 21 days apart, with 30 μg of NPm and NPwt (0.536 μmol NP) and heptameric NP (OVX836, 0.476 μmol NP). Immunizations were performed by injection into the gastrocnemius muscle, with both injections being administered in the same hind limb. For immunogenicity studies, seven days after the second immunization, mice were sacrificed to collect serum, lungs, and splenocytes. All samples were processed individually immediately after collection.

For challenge studies, mice were infected 21 days after the last vaccination with the H1N1 influenza strain (A/California/07/2009) by intra-nasal administration of a $10^{4.7}$ Tissue Culture Infective Dose ($TCID_{50}$) in 20 μl (10 μl/nostril) after ketamine/xylazine anesthesia. Weight was recorded for 10 days after the challenge. Animals that lost more than 20% body weight were euthanized according to institutional guidelines by cervical dislocation.

Antibody Enzyme-Linked Immunosorbent Assay (ELISA)

Levels of immunoglobulin G (IgG) were measured in serum samples collected on D28 as previously described (19). Briefly, the 96-well ELISA plates were pre-coated with recombinant NPwt (OSIVAX) at 2.5 μg/ml overnight at 4°C. About 100 μl of serial 2-fold dilutions of serum (starting dilution 1/200) were added to each well and incubated for 2 h at 25°C. Bound antibodies were detected with goat anti-mouse IgG-HRP (Life Technology, USA) and finally, 100 μl of tetramethylbenzidine (TMB) (Interchim, France) substrate was added to each well. The antibody levels in the serum were expressed as a logarithm of endpoint dilution titer, defined as the reciprocal of the highest analytic dilution that gives a reading 3-fold over the mean O.D. 650 value of the negative-control mice serum at the 1/100 dilution.

IFNγ ELISpot Assays

Influenza NP-specific T-cells secreting IFNγ were enumerated using an IFNγ ELISpot assay (Mabtech, Sweden). Lymphocytes were isolated from the spleen and the lung from individual mice as previously described (19). ELISpot plates were coated with the capture mAb (#3321-2H) then incubated overnight at 4°C according to the instruction manual of Mabtech. Then 2×10^5 T-cells were cultured for 20 h at 37°C/5% CO_2 with 2 μg/ml of recombinant NPwt or with 2 μg/ml of the $NP_{366–374}$ (GenScript, Netherlands) immunodominant peptide epitope in C57BL/six mice. Concavalin A (Sigma-Aldrich, France) was used as a positive control and unstimulated splenocytes/lung cells were used as negative controls. Spots were counted with an ELISpot reader system (CTL-ImmunoSpot® S6 Ultra-V, Germany). The number of protein- or peptide-reactive cells was represented as spot-forming cells (SFCs) per 2×10^5 cells per well.

Flow Cytometry Staining

Spleens and lungs were harvested at D28, after intravascular (IV) staining with 200 μl of anti-CD45-BV421 antibody diluted 1/300 in PBS 1×, for the identification of vascular T-cells (clone 30-F11; BD Biosciences, USA). Lungs and spleens were dissociated as previously described (19). Red blood cells from lungs and spleens were lysed and cells were counted with the EVE system (Witec AG, Swiss). 2×10^6

cells of spleen and total lung cells were stained with 10 µl/sample of R-PE labelled Pro5 MHC H-2Db ASNENMETM ($_{366–374}$) Pentamer (Proimmune, U.K.) for 20 min at room temperature, before viability staining with Fixable Viable Dye efluor 506 (eBioscience, USA). For lung tissue-resident T-cell analysis, cells were stained with a mix of antibodies: CD103-APC (clone 2E7, Biolegend, USA), CD62L-BV786 (clone MEL-14; Biolegend, USA), CD8-Super Bright 645 (clone 53-6.7, eBioscience, USA), CD3-APC-Cyanine 7 (clone 17A2, BD Biosciences, USA), CD4-FITC (clone GK1.5, BD Biosciences), CD44- PerCP-Cy5.5 (clone IM7, eBioscience, USA), and CD69-PerCP-Cy7 (clone H1.2F3; BD Biosciences). Flow cytometry was performed with a Fortessa™ and data were analyzed with Flowjo™ software (BD Biosciences, USA).

DC Subset Isolation and *In Vitro* CD8+ T-Cell Stimulation

For isolation of dendritic cell (DC) subsets ($CD11c^+CD8^+$), a CD8+ Dendritic Cell Isolation Kit (Miltenyi, France) was used according to the manufacturer's instructions. Briefly, splenocytes were incubated with a cocktail of biotin-conjugated antibodies (CD90, CD45R, CD49b), followed by anti-biotin microbeads to deplete T, B, and NK cells. The $CD8\alpha^+$DC subset was isolated with $CD8^+$ selection. The CD8α+ DC subset was further purified using CD11c selection beads. The purity of the CD8α+ DC subset was 95%, as verified by flow cytometric analysis. The DC subsets were incubated with 2 µg/ml of either NPm, NPwt, or OVX836 at 37°C in the presence of 5% CO_2 for 18 h. Cells were washed and expression of CD40 and CD86 activation markers was measured on $CD8\alpha^+$ DCs by flow cytometry. DCs were stained with a combination of Abs to murine CD11c-FITC (clone HL3, eBioscience, USA), B220-PE (clone RA3-6B2, eBioscience, USA), CD11b-APC-Cy7 (clone M1/70, eBioscience, USA), SiglecH-eFluor 450 (clone eBio440c, eBioscience, USA), CD86-PE-Cy7 (clone B7-2, BD Biosciences, USA), and CD40-APC (clone 3.23, eBioscience, USA). Then, antigen-loaded DCs were incubated *in vitro* with purified $CD8^+$ T-cells from the spleen of mice immunized with 10 µg of $NP_{366–374}$ peptide in IFA (Ratio 5:1). Naive DC-loaded with $NP_{366–374}$ peptide and CpG 1826 (Invivogen, France), both at 2 µg/ml, were used as positive controls in the assay. After 2 h, brefeldin A (Sigma-Aldrich, France) was added at 5 µg/ml for 4 h of additional incubation. Lymphocytes were stained using CD8-Super Bright 645 (clone 53-6.7, eBioscience, USA) and CD3-APC-Cyanine 7 (clone 17A2, BD Biosciences, USA). For IFNγ intracellular cytokine staining, cells were fixed, permeabilized using CytoFix/CytoPerm (BD Biosciences, USA), and labeled with IFNγ–BV785 (clone XMG1.2, BD Biosciences, USA). Flow cytometry was performed with a Fortessa™ and data were analyzed with Flowjo™ software (BD Biosciences, USA).

Cytotoxic Assay

Splenocytes (5×10^7 cells/ml) from naive C57BL/6 mice were divided into two populations, labeled with two different concentrations of CFSE (Life Technology, USA). One population was pulsed with 4 µg/ml of $NP_{366–374}$ peptide (GenScript, Netherlands) for 1 h at 37°C and treated for 15 min at 37°C with 0.5 µM CFSE ($CFSE^{low}$). The other population remained un-pulsed and was treated with 5 µM CFSE ($CFSE^{high}$). The $CFSE^{low}$ (NP loaded) and $CFSE^{high}$ cells (control) were mixed at a 1:1 ratio, washed twice in PBS + 2% FBS and incubated for 16 h with CD8+ T-cells obtained from the spleen or lung of animals immunized with OVX836, and purified by positive selection using CD8a (Ly-2) (Miltenyi Biotec, USA). This assay allows for the measurement of the intrinsic capacity of CD8+ T-cells to kill target cells to determine the actual value of cell specific lysis: 1) Ratio = %[$CFSE^{high}$] peak/%[$CFSE^{low}$] peak, 2) Percent Specific Lysis = [1 − (Control ratio/Experimental ratio)] × 100, as described previously (20).

Adoptive Transfer Experiments and Influenza Virus Challenge

The experiment schema is represented in **Supplementary Figure 3**. Donor mice (n = 6–7 per group) were immunized twice (D0 and D21) intramuscularly (IM) with either 30 µg of OVX836 or Ovalbumin (OVA, 10 µg, Sigma-Aldrich, France) emulsified in IFA (Invivogen, France) or buffer. Mice of each group were sacrificed on D28 or D36. The lungs or spleens of the donor mice were processed individually to extract lung and spleen cells respectively as previously described (19). The cells were then pooled for cell sorting by positive selection with CD8α [MACS Isolation Kit CD8 (Ly-2)] or CD4 [MACS Isolation Kit CD4 (L3T4)] MicroBeads using MACS columns according to the manufacturer's protocol (Miltenyi Biotech, France). The purity of $CD8^+$ or $CD4^+$ T-cells was >95% as determined by flow cytometry. Some 5×10^5 lung-enriched CD8+ or $CD4^+$ T-cells were transferred by the intravenous route to each recipient mouse 24 h before challenge. In addition, NP immune serum of each immunized mouse was collected at D36, pooled and each recipient mouse received 300 µl of this serum pool by the intraperitoneal route 24 h prior to influenza challenge. Six OVX836-vaccinated mice were used as positive controls in each challenge study. Recipient mice (n = 6) and positive control mice (n = 6) were then infected by intranasal administration of $10^{4.7}$ $TCID_{50}$/20 µl (10 µl/nostril) of an H1N1 influenza strain (A/California/07/2009 or A/WSN/1933, Virpath, Lyon, France), after ketamine/xylazine anesthesia. Weight was recorded for 10 days after challenge. Animals that lost more than 20% body weight were euthanized according to institutional guidelines by cervical dislocation.

Statistical Analyses

Statistical analyses and graphic representations were performed with Prism 8.0 (GraphPad Software Inc.). Statistical significance was determined using the unpaired, one-way analysis of variance (ANOVA) with Tukey's multiple comparisons test or a non-parametric Kruskal–Wallis test followed by Dunn's multiple comparisons test. Differences were considered significant if the p value was <0.05: *, <0.05; **, <0.01; ***, <0.001; ****, <0.0001. Survival rates of mice were compared using Kaplan–Meier survival analysis, and statistical significance was assessed using the Log-Rank (Mantel–Cox) test. The radar charts were designed with R (http://www.r-project.org/).

RESULTS

NPm, NPwt, and OVX836 Proteins Display Different Physical Characteristics

We have previously proposed that heptameric influenza A NP proteins can be obtained by fusing OVX313 to the C-terminal sequence of NP, conferring a higher level of immunogenicity to the NP protein (19). Here, we produced in *Escherichia coli* and purified the three following recombinant proteins: the E339A/R416A mutant of strain A of NP (NPm), wild-type NP (NPwt), and NP-OVX313 (OVX836), prior to studying their immunogenicity. **Table 1** summarizes the structure and physicochemical characteristics of the three NP proteins. First, intact protein mass spectrometry confirmed the homogeneity and the expected mass of NPm and NPwt. Under conditions leading to complete reduction of the disulfide bonds, the primary structure of the OVX836 subunit was also ascertained by high-resolution mass spectrometry. Then, we assessed the degree of oligomerization of these three NP proteins by measuring their hydrodynamic diameter using dynamic light scattering. As shown in **Figure 1A** and in **Table 1**, we found that NPm remains monomeric in solution (D_H 6.5 nm), confirming previous findings (21, 22). NPwt protein forms oligomers with a D_H of 11.2 nm, whereas OVX836 displayed larger oligomers with a D_H of 41.0 nm and a rather multimodal size distribution. As shown in **Figure 1B** and in **Table 1**, the unfolding profiles of the three proteins were compared by nano differential scanning fluorimetry (nanoDSF). NPwt and OVX836 thermally unfolded at 75–76°C, a relatively high temperature, as compared to that of NPm (52–53°C). NPm is thus intrinsically more thermolabile than its wild-type counterparts. By negative stain electron microscopy (EM), we confirmed that NPm was monomeric

TABLE 1 | Structural characteristics of the NP proteins.

Construct	Mass (Da)$^{+}$	D_H (nm)*	EM**	Length (nm)**	Ti (°C)$^{++}$
NPm	56103.77	6.5 ± 0.3	Monomer	n/d	52.7
NPwt	56246.89	11.2 ± 0.3	Trimer	13 ± 2	75.1
			Heptamer to oligo-heptamer	18 ± 2 (heptamer)	
OVX836	62710.56	41.0 ± 1.4		43 ± 16 (di-heptamer)	76.0

The observed average masses of recombinant proteins by mass spectrometry agree with theoretical primary structures (+). Hydrodynamic diameters (D_H) obtained from scattering intensity DLS distributions (*). Main species and lengths seen in electron micrographs (**). Inflection temperatures (Ti) obtained from melting curves by nDSF measurements (++).

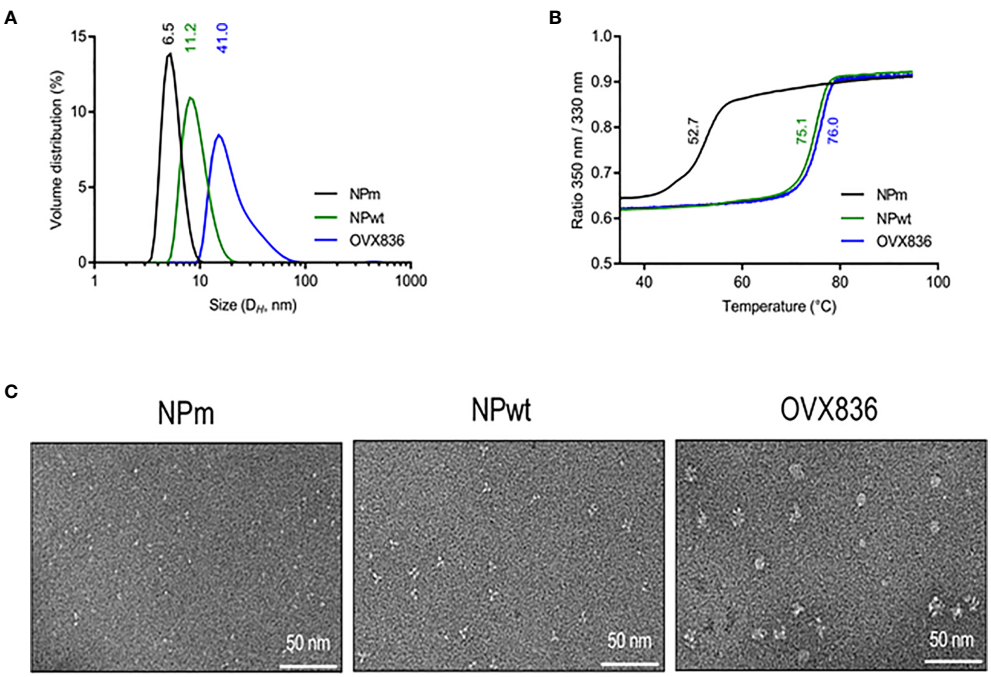

FIGURE 1 | Characterization of influenza A nucleoprotein (NP) constructs. **(A)** Size distribution as measured by dynamic light scattering (left panel). The x-axis shows a distribution of size classes (nm) and the y-axis shows the relative volume distribution. Hydrodynamic diameters are obtained from scattering intensity DLS distributions. **(B)** Thermal stability as measured by nano differential scanning fluorimetry (right panel). The inflection temperature (Ti) values are mentioned. **(C)** Electron microscopy images. NP protein vaccines show different oligomeric states.

(**Figure 1C**, left image) and showed that NPwt forms mainly trimers in solution (**Figure 1C**, middle image). When analyzing OVX836, EM images showed mainly heptameric NP structures, as well as higher-order structures formed through protein/protein interactions (**Figure 1C**, right image).

In conclusion, we characterized three NP proteins as defined by their physicochemical characteristics: monomeric NP (NPm), trimeric NP (NPwt), and heptameric NP (OVX836 vaccine candidate). Then, their immunogenicity and protective efficacy were compared in mice.

Compared to NPm and NPwt, OVX836 Vaccine Induces Higher Numbers of Persistent NP-Specific CD8+ T-Cells in Lung Tissue and Spleen, Providing Better Protection Against Influenza

In order to measure the immunogenicity and protective efficacy of NPm, NPwt, and OVX836, we immunized mice twice (D0, D21) by the IM route. Humoral and cellular immune responses were measured at D28 by ELISA, IFNγ ELISpot, and H-2Db $NP_{366–374}$ Pentamer staining (**Figure 2**). Whereas anti-NP IgG levels were significantly higher after NPwt and OVX836 compared to NPm immunization ($p < 0.0001$) (**Figure 2A**), $NP_{366–374}$-specific $CD8^+$ T-cell responses were significantly higher after OVX836 compared to NPwt ($p < 0.05$) and NPm ($p < 0.0001$) immunization, as measured by IFNγ ELISpot assays in both the spleen (**Figure 2B**) and lung (**Figure 2C**). The superior ability of OVX836 over NPwt and NPm to generate lung tissue-associated CD8 cellular responses was confirmed by H-2Db $NP_{366–374}$ Pentamer staining of $CD8^+$ T-cells (**Figures 2D, E**).

We also measured cellular and humoral effector memory responses at D90 (**Supplementary Figure S1** and **Figure 2E**). Whereas humoral responses were maintained at D90 for all NP proteins (**Supplementary Figure S1A**), only OVX836 induced persisting $NP_{366–374}$-specific IFNγ-producing CD8+ T-cells in the lung and spleen at this late time point (**Supplementary Figures S1B–E**). All immunogenicity results are compared and visualized in a radar chart (**Figure 2F**). Interestingly, at the memory phase, OVX836 induced persistent $NP_{366–374}$-specific IFNγ-producing $CD8^+$ T-cells, especially in the lung, whereas NPwt vaccination promoted persistent anti-NP antibodies (Abs), however, with reduced cellular responses over time. NPm is overall less immunogenic when compared to NPwt and OVX836.

Lethal challenge studies using the A/California/07/2009 virus were performed in mice vaccinated with OVX836, NPwt, and NPm both at D42 (**Figure 3A**) and D90 post-first vaccination (**Figure 3B**). A significantly higher protection rate was observed after OVX836 vaccination at the effector phase (D42) compared to NPwt ($p < 0.05$) and NPm ($p < 0.001$). At the memory phase (D90), the protection against lethal influenza challenge was lost following vaccination with NPwt and NPm, whereas it was maintained, although slightly decreased, after vaccination with OVX836 (**Figure 3B**). The level of protection was associated with a high number of NP-specific $CD8^+$ T-cells as observed in OVX836 compared to NPm and NPwt-immunized mice. In addition, the pronounced persistence of NP-specific CD8+ T-cells responses in the lung (**Figure 2F** and **Supplementary Figure S1**) suggests the important role of the lung CD8+ T-cells in animal protection.

In order to understand the mechanism of induction of CD8+ T-cell responses, we hypothesized that OVX836 might better stimulate these cells by inducing activation of DC. To test this hypothesis, we performed *in vitro* experiments assessing antigen presentation to CD8+ T-cells. First, we observed that purified $CD8\alpha^+CD11c^+$ DC expressed a higher level of CD40 (data not shown) and CD86 surface activation markers when incubated with OVX836 compared to NPm and NPwt (**Figure 4A**). Then, antigen-loaded $CD8\alpha^+CD11c^+$ DC were incubated with $NP_{366–374}$-specific $CD8^+$ T-cells isolated from mice immunized with $NP_{366–374}$ peptide plus Incomplete Freund Adjuvant (IFA). We observed a higher production of IFNγ by $NP_{366–374}$-specific $CD8^+$ T-cells when using DC incubated with $NP_{366–374}$ (positive control) and OVX836 compared to NPm and NPwt-loaded DC (**Figure 4B**). These results show that the OVX836 vaccine promotes DC activation favoring higher $CD8^+$ T-cell effector responses compared to NPm and NPwt.

OVX836 Generates a Higher Number of Lung TRM $CD8^+$ T-Cells With Cytotoxic Activity

Because the NP-specific CD8+ T-cells following vaccination was mainly persistent in the lung (**Figure 2A**), we investigated the presence of lung TRM $CD8^+$ T-cells that could rapidly control viral infection upon challenge (18), as well as their cytotoxic function. As shown in **Figure 5A**, when using *in vivo* CD45 staining to distinguish circulating and tissue-resident cells (23), we observed that OVX836 induced more resident CD8+ T-cells compared to NPwt and NPm. We also observed a significantly higher percentage of resident H-2Db $NP_{366–374}$ $Pentamer^+$ among $CD8^+$ T-cells following OVX836 immunization (**Figure 5B**). Likewise, the ratio of resident/circulating H-2Db $NP_{366–374}$ $Pentamer^+$ $CD8^+$ T-cells percentages was significantly higher after OVX836 vaccination compared to NPwt and NPm ($p < 0.01$ and 0.001, respectively) (**Figure 5C**). CD103 and CD69 integrins are markers of the TRM population in tissue (24). Representative flow cytometry analysis for the expression of CD103 and CD69 markers on $NP_{366–374}$ $Pentamer^+$ $CD8^+$ T-cells is shown in **Figure 5D**. We found a higher abundance of H-2Db $NP_{366–374}$ $Pentamer^+$ among $CD8^+$ $CD69^+CD103^+$ T-cells following vaccination with OVX836 compared to NPwt ($p < 0.05$) and NPm ($p < 0.0001$) vaccinated mice (**Figure 5E**). To our knowledge, this is the first demonstration that a NP protein vaccine favors the induction of TRM $CD8^+$ T-cells.

Of note, the effector memory (TEM) (*CD44*high*CD62L*neg) populations significantly expanded after OVX836 immunization compared to NPwt and NPm (**Supplementary Figure S2B**, gating strategy in **Figure S2A**). TEM cells are cytotoxic and present in the circulation. They can be easily recruited to sites of inflammation and could rapidly control viral infection upon challenge (25).

We then assessed the cytotoxic potency of the CD8+ T-cells (**Figure 6A**). CFSE-labeled splenocytes loaded with $NP_{366–374}$

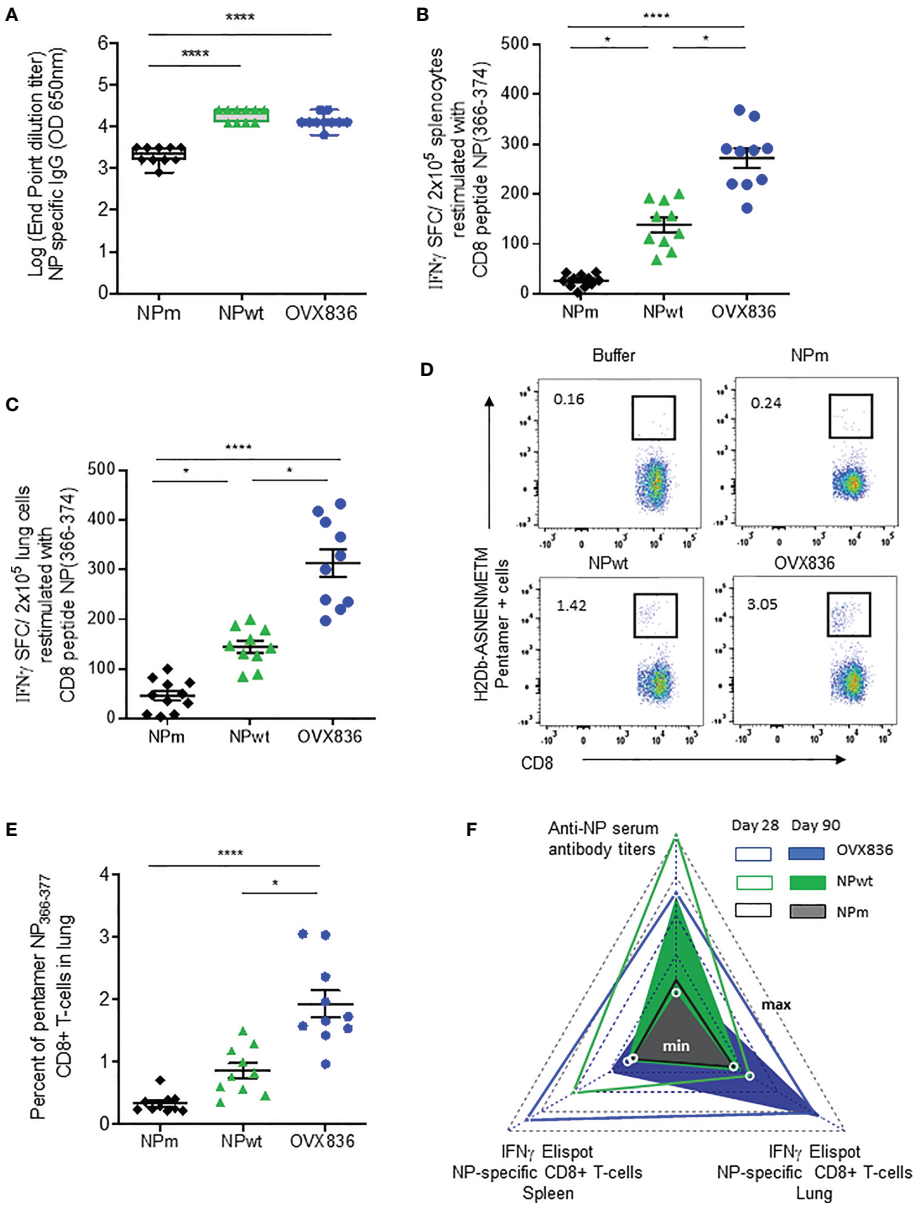

FIGURE 2 | OVX836 vaccine induces higher numbers of persistent NP-specific CD8+ T-cells in lung tissue and spleen compared to NPm and NPwt. C57BL/6 female mice (n = 10) were immunized twice (D0, D21) with 30 µg of NPm, NPwt, and OVX836 by the IM route. **(A)** NP-specific IgG were measured by ELISA in serum at D28. Levels of IgG are expressed as Log (endpoint dilution titer) and represented in box-and-whisker plots. **(B, C)** $NP_{366–374}$-specific IFNγ secreting T-cells (spot-forming cells (SFC)/2 × 10^5 cells) were measured by ELISpot in the spleen **(B)** and in the lung **(C)** at D28. **(D, E)** In the lung tissue, $NP_{366–374}$-specific CD8+ T-cells were detected by flow cytometry using pentamer staining (H2Db-$NP_{366–374}$). Representative flow cytometry plots show frequencies of $NP_{366–374}$-specific CD3+CD8+ T-cells in the lung **(D)**. Percentage of $NP_{366–374}$-specific CD3+CD8+ T-cells in the lungs of mice **(E)**. Individual data, mean (line), and SEM are represented, n = 10 mice per group in two independent experiments. Differences were assessed by one-way ANOVA followed by Tukey's multiple comparison test or with a Kruskal–Wallis test followed by Dunn's multiple comparison test. *p < 0.05; **** for p < 0.0001. **(F)** Radar chart presents the minimum (min) and maximum (max) values for each assay as indicated in log10 scale. Comparing the mean of antigen-specific immune responses at D28 (empty triangle) and D90 (plain triangle): NPm (black), NPwt (green), and OVX836 (blue).

(CFSE^{high}) or negative controls (CFSE^{low}) were used as target cells for effector CD8$^+$ T-cells isolated from the lung and spleen of OVX836-immunized mice (**Figure 6A**). We found that CD8$^+$ T-cells isolated from the lung and spleen of OVX836-immunized mice displayed significant cytotoxic function with about 35% (lung) and 25% (spleen) of killing activities (**Figure 6B**). Thus, the OVX836 vaccine induces NP-specific cytotoxic CD8$^+$ T-cells in the lung and spleen.

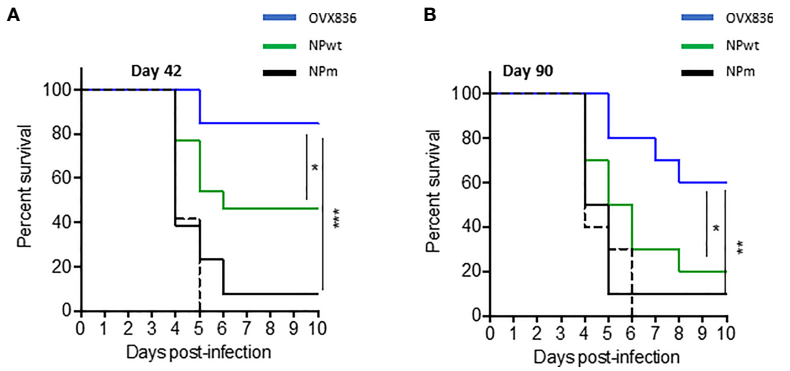

FIGURE 3 | Long-term protection against viral challenges following OVX836 vaccination compared to NPm and NPwt. C57BL/6 mice (n = 12) were immunized twice 3 weeks apart (D0, D21), with 30 µg of NPm, NPwt, OVX836, or buffer (control mice) by the IM route. **(A)** 42 days and **(B)** 90 days post-first vaccination, mice were infected by IN route with $10^{4.7}$ $TCID_{50}$/20 µl (10 µl/nostril) of influenza H1N1 A/California/7/2009. Graph shows the percentage of survival observed among each group of mice. Buffer (dashed black), NPm (plain black), NPwt (green), and OVX836 (blue). *p < 0.05, **p < 0.01 and ***p < 0.001 by Log-Rank (Mantel–Cox) test.

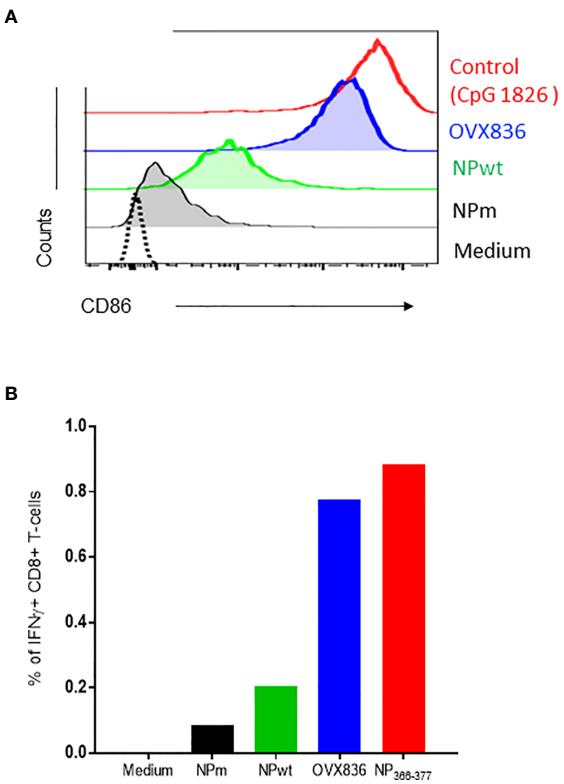

FIGURE 4 | OVX836 activates CD8α+ DC and promotes effector T-cell responses *in vitro*. **(A)** Mean CD86 expression on purified $CD8a^+$ DCs incubated for 18 h with 2 µg/ml NPm (36 nM NP), NPwt (36 nM NP), OVX836 (32 nM NP), or a positive control. **(B)** Graph shows the percentage of specific CD8+ T cells that were positive for IFNγ, measurement of IFNγ production by NP-specific $CD8^+$ T-cells incubated for 6 h with antigen-loaded DCs (as indicated) at a 5:1 (DC/CD8) ratio, then analyzed by flow cytometry. $CD8^+$ T-cells used in the assay were isolated from the spleen of mice immunized with 30 µg of $NP_{366–374}$ peptide in IFA. $NP_{366–374}$ was used as a positive control in the assay. Results are representative of two independent experiments.

OVX836 Heptameric NP Vaccine Generates Lung Tissue-Resident Memory CD8+ T-Cells for Cross-Protection Against Influenza

In order to determine the role of the different immune arms in the protection against lethal influenza challenge following OVX836 vaccination, we performed adoptive transfer of CD8+, CD4+ T-cells, or serum from vaccinated mice into recipient mice prior to influenza challenge. The experimental scheme is presented in **Supplementary Figure 3A**. Protection against the lethal A/California/07/2009 (H1N1) challenge was observed following adoptive transfer of sorted CD8+ T-cells from either lungs or spleens of OVX836-vaccinated mice, and not after transfer of either CD8+ T-cells from OVA-immunized mice or from unvaccinated mice (**Figure 7A**). Protection against the lethal A/WSN/1933 (H1N1) challenge was confirmed following adoptive transfer of sorted CD8+ T-cells from the spleens of OVX836-vaccinated mice (**Figure 7B**). In this lethal influenza challenge, the transfer of serum (**Figure 7B**) or sorted CD4+T cells from OVX836-immunized mice into recipient mice did not confer significant protection (**Supplementary Figure 3B**). In accordance with our previous findings, we observe cross-protection, since mice vaccinated with OVX836 or receiving CD8+ T-cells from OVX836 (containing NP of A/WSN/1933 (H1N1) were protected after both Influenza A/WSN/1933 (H1N1) virus (**Figure 7B**) and Influenza A/California/07/2009 (**Figure 7A**) challenges.

DISCUSSION

We have demonstrated that OVX836, a heptameric form of the influenza NP protein, has a high potency for the induction of both peripheral and lung-associated resident CD8+ T-cells as assessed by IFNγ production and cytotoxic function. The persistence of protective CD8+ T-cells is a striking feature of

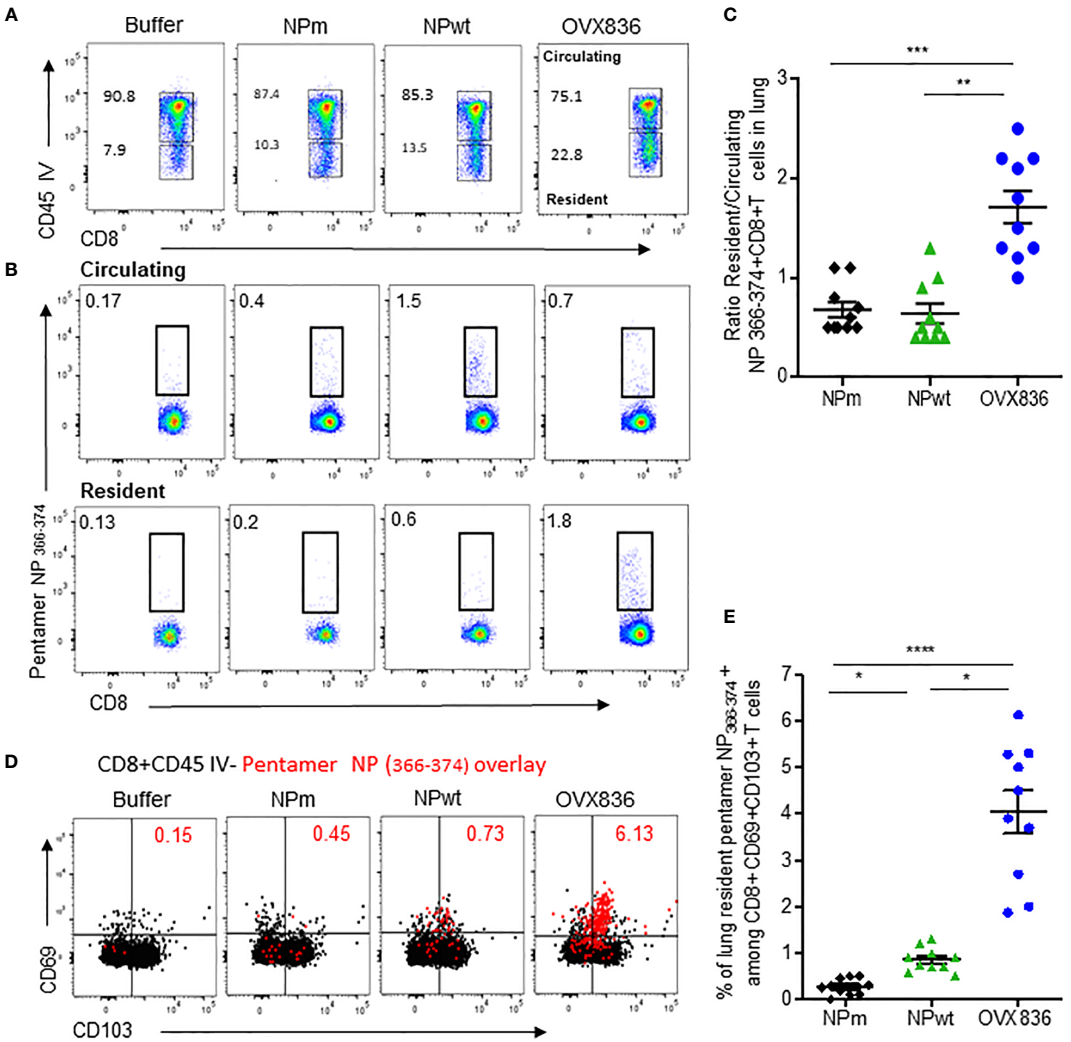

FIGURE 5 | OVX836 vaccine generates lung NP-specific CD8+ TRM cells. C57BL/6 mice (n = 9–10 in each group) were immunized twice 3 weeks apart, with 30 µg of NPm, NPwt, OVX836, or buffer (control) by the IM route. At D28, anti-CD45 Abs were administered by the IV route to label vascular cells. **(A)** Representative flow cytometry analysis of circulating (CD45+) and resident (CD45–) distribution in the lung after immunization. **(B)** Representative flow cytometry analysis of circulating and resident lung $NP_{366–374}$-specific CD8+ T-cells using H2-Db $NP_{366–374}$ pentamer staining. **(C)** Ratio resident/circulating of percent H-2Db $NP_{366–374}$ Pentamer + CD8+ T-cells of two independent experiments. **(D)** Representative overlay plots of flow cytometric analysis showing distribution of lung-resident H-2Db $NP_{366–374}$ $Pentamer^{+}CD8^{+}CD45^{-}$ T-cell (red dots) TRM generated following vaccination among the CD69+CD103+ (black) population. **(E)** Graph representing percent resident H-2Db-$NP_{366–374}$ Pentamer+ among CD8+CD69+CD103+ cells in the lung after vaccination of two pooled independent experiments. Individual data and mean ± SEM are represented. Differences were assessed by one-way ANOVA followed by Tukey's multiple comparison test. *p < 0.05, **p < 0.01, ***p < 0.001, ****p < 0.0001.

OVX836 compared to monomeric and trimeric NP. The identification of the mechanism of protection conferred by OVX836 provides a paradigm of the importance of NP $CD8^{+}$ T-cell-mediated vaccine for heterosubtypic protection (5, 19).

Some vaccination strategies attempt to promote induction of $CD8^{+}$ T-cell responses either by targeting the viral proteins that promote a cell-mediated response (M1, NP) or using vaccines in the form of particles (virosomes, virus-like particles, viral vectors, DNA, live attenuated influenza vaccine) to simultaneously promote humoral and cellular responses (10). In addition, the use of alternative routes of administration of vaccine formulations has provided evidence for the induction of systemic CD8+ T-cell responses (12, 26). Induction of lung-tissue CD8+ T-cell responses using protein-based vaccines remains challenging for vaccinologists. Inactivated influenza vaccines and LAIV are the two approved classes of influenza vaccine administered by the IM and IN routes, respectively (27). Both vaccines generate HA-specific antibodies while T-cell responses are significantly higher with LAIV (28). A single immunization with LAIV induces TRM, while vaccination with an inactivated influenza vaccine by a systemic or IN route is not sufficient to induce such T-cell responses in the lung (18). One of the main issues discussed for LAIV vaccination in adults, however, is the presence of

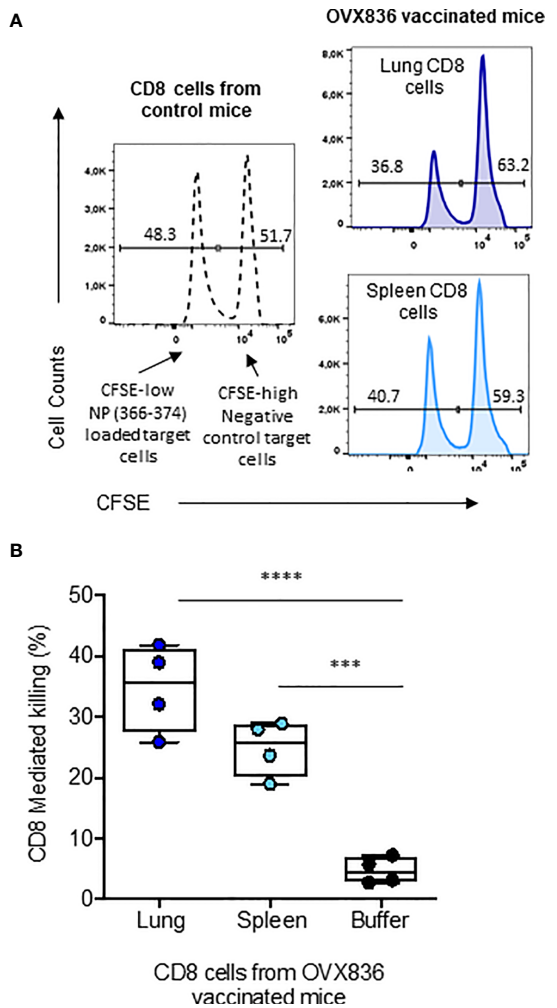

FIGURE 6 | NP-specific CD8+ T-cells from OVX836-immunized mice are cytotoxic effector cells. **(A)** Splenocytes from naive C57/B6 mice were labelled with CFSE: the $CFSE^{low}$ peak corresponds to $NP_{366–377}$-pulsed target cells, the $CFSE^{high}$ peak corresponds to unpulsed target cells. CFSE target cells were mixed at a 1:1 ratio and incubated for 16 h with sorted CD8+ T-cells isolated from the lungs and spleens of OVX836-vaccinated mice to measure antigen-specific CD8+ T-cell-mediated killing. **(B)** The data are representative of two separate experiments yielding similar results, represented in box-and-whisker plots (min and max, all points are shown) in the right panel. Differences were assessed by one-way ANOVA followed by Tukey's multiple comparison test. Significance was set at ***$p < 0.001$, ****$p < 0.0001$.

pre-existing Influenza-specific memory responses in the lung that may affect vaccine efficacy by the IN route. Our finding demonstrates that conventional IM administration of OVX836 can induce memory $CD8^+$ T-cells, both at the systemic level and in lung tissue, as well as protective efficacy against heterosubtypic influenza viruses.

The role of TRM in the lung has been evaluated for long-term protection in murine models, a question that cannot currently be addressed in humans (18, 29). Lessons learned from murine models of influenza infection have shown that the anti-viral activity of $CD8^+$ T-cells is strongly dependent on their ability to migrate and localize in the lung while the expansion is detected in the secondary lymphoid tissue (30). After OVX836 vaccination, we found that $CD8^+$ T-cells isolated from spleen and lung tissue display cytotoxic functions and IFNγ production. These cells can protect the animal against lethal influenza challenges, suggesting peripheral expansion of these cells into the secondary lymphoid tissue. Adoptive transfer experiments showed that lung-associated $CD8^+$ T-cells following OVX836 vaccination can protect the animals, whereas serum and $CD4^+$ T-cells from immunized mice were not similarly protective in the influenza challenge model. It has been shown that multiple mechanisms of effector $CD8^+$ T-cells can contribute to protection, including the release of anti-viral cytokines and perforin/granzyme, as well as the activation of the Fas/FasL pathway (31, 32). Despite the fact that adoptive transfer of $CD4^+$ T-cells isolated from OVX836-immunized mice did not confer full protection against influenza infection in our vaccination model, it has been proposed that $CD4^+$ T-cells guide the formation of TRM in the lung during influenza infection (33).

Antigen-specific CD8+ T-cells can be divided into central, effector, and resident memory cells based on the expression of CD62L, CCR7, CD69, and CD103. TRM expressing CD103+CD69+ are a highly specialized TRM population and are involved in viral clearance both in humans and in mice (34, 35). We demonstrated that OVX836 vaccination is more efficient than monomeric mutant NP (NPm) and trimeric wild-type NP (NPwt) at inducing $CD8^+$ TRM in the lung tissue. However, the mechanism for induction of TRM is currently unknown, as is the reason why these $CD8^+$ T-cells are localized in the lung. The site of antigen encounter as well as its transport and presentation to T-cells might play a role in programming T-cell migration to the tissue (26, 36). One could hypothesize that heptamerization would promote better uptake and processing for MHC-class I presentation on APC, leading to a higher number of antigen-specific $CD8^+$ T-cells. According to this hypothesis, we found that OVX836-loaded DC induced a higher effector $CD8^+$ T-cell activation compared to NPm and NPwt, suggesting involvement of DC cells in favoring CD8+ T-cell responses following OVX836 immunization. Of note, NPm, NPwt, and OVX836 exhibit different physicochemical characteristics. NPm is monomeric due to the mutation of two amino acids in the NP sequence (E339A/R416A), as the ionic bond between R416 and E339 involved in NP oligomerization is then disrupted (19, 21). This results in particle sizes smaller than 7 nm and greater sensitivity to thermal denaturation. NPwt is trimeric, with an average particle diameter smaller than 15 nm, and more stable to thermal denaturation. OVX836 forms heptamers due to the OVX313 moiety and higher-order structures related to the self-associative properties of NP, thus exhibiting the largest particle size (e.g. 20–40 nm) among the three NP proteins, without detrimental effects to its stability. In addition, ion exchange chromatography shows that OVX836 (apparent p*I* 9.8) is more cationic than NPwt (apparent p*I* 9.5), mainly due to the presence

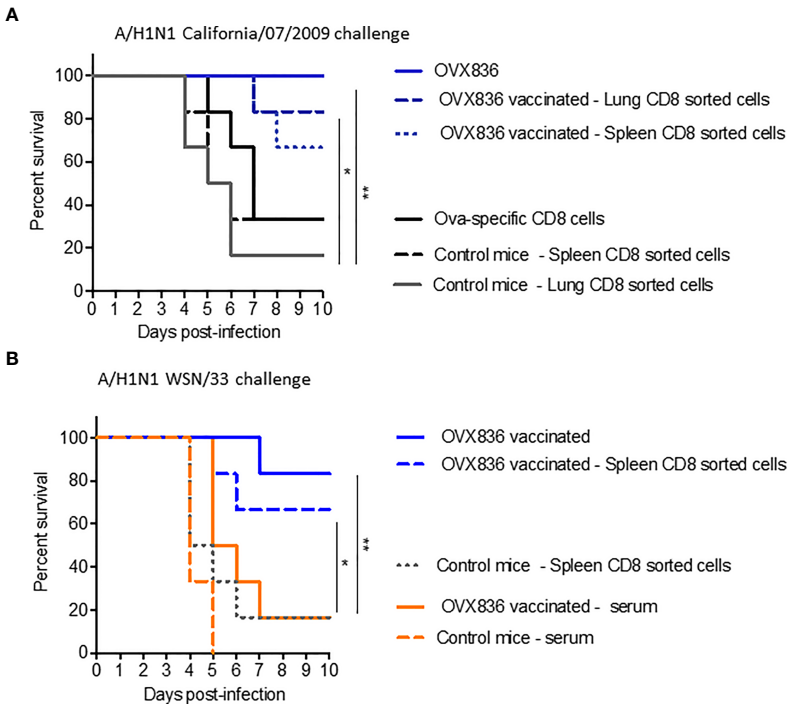

FIGURE 7 | NP-specific CD8+ T-cells protect mice from lethal influenza challenges. **(A, B)** Donor C57BL/6 mice (n = 6–7 in each group) received two IM immunizations (D0, D21) with OVX836 (30 µg), buffer (control mice), or OVA (10 µg) + IFA. Spleens and/or lungs were collected from the donor mice at D28 to obtain CD8+ T-cells for the transfer **(A)**. Lungs to obtain CD8+ T-cells and serum were collected from the donor mice at D36 for the transfer **(B)**. Naive C57BL/6 recipient mice (n = six in each group) received 5 × 10^5 lung-enriched CD8+ T-cells by the IV route or 300 µl of serum by the intraperitoneal (IP) route. Some 24 h after this adoptive transfer, all recipient mice were IN infected with $10^{4.7}$ $TCID_{50}$/20 µl of the influenza viral strain H1N1 A/California/07/2009 **(A)** or H1N1 A/WSN/33 **(B)**. OVX836-vaccinated mice were used as positive controls in each experiment. Mice were then observed daily for clinical signs and body weight changes for 10 days. Percent survival rates are presented. *p < 0.05, **p < 0.01 by Log-Rank (Mantel–Cox) test.

of arginine and lysine residues in OVX313. NPm is overall less cationic, with probably less cationic groups on its surface (apparent p*I* 8.6, data not shown). Thus, the properties of OVX836—higher particle size, high thermal stability, and more surface cationic groups—might contribute to DC maturation and activation during immunization. Further studies need to be performed on the mechanism of antigen-presentation by conventional DC for cross-presentation to T-cells.

The persistence and durability of memory responses is the cornerstone of successful vaccination. The presence of memory $CD8^+$ T-cells is potentially one of the contributing reasons that most healthy unvaccinated adults do not experience severe influenza disease on more than a few occasions. These T-cells might provide rapid and highly effective protective immunity during re-encounter of pathogens (15). In addition, $CD8^+$ T-cells can recognize more conserved epitopes of pathogens and provide protection against several viral proteins (37, 38). $CD8^+$ T-cell responses might diminish the morbidity and mortality typically caused by a newly emerging viral subtype (39, 40). In humans, resident effector cytotoxic T-cells are generated following multiple influenza infections. Epitopes of NP that are recognized by human cytotoxic T-cells have been identified (41). In addition, diverse TCR profiles of TRM cells and a high degree of clonal sharing with other CD8+ T-cell populations with polyfunctionality have been found in human lung tissue (42). This characteristic might be important for protection against the generation of viral-escape mutants. In pandemic situations or when influenza drifted strains circulate, available vaccines against conserved proteins of influenza virus would help to protect the population. Vaccines that promote cytotoxic T-cell responses in the lung could prevent seasonal or pandemic influenza, as a stand-alone and in combination with antibody approaches. Although cellular immunity is not sterilizing, it could contribute to significantly decreasing influenza illness, hospitalization, and death in humans (41). OVX836 is currently under clinical development: phase I was completed and Phase IIa was recently finalized (ClinicalTrials.gov Identifier: NCT03594890, NCT04192500).

DATA AVAILABILITY STATEMENT

The datasets presented in this study can be found in online repositories. The names of the repository/repositories and accession number(s) can be found in the article/**Supplementary Material**.

ETHICS STATEMENT

The animal study was reviewed and approved by CECCAPP_ENS_2018_019, Lyon, France.

AUTHOR CONTRIBUTIONS

Study conceptualization and supervision (JC, BC, FN, AV, DG, and FH). Methodology and experimental design (JC, BC, JB, SD, YL, JM, and FN). Conduction of experiments (JC, JB, MH, MC, CR, and AI). Collection and analysis of data (JC, BC, and JB. Manuscript writing (JC, BC, JB, and FN). All authors contributed to the article and approved the submitted version.

FUNDING

This project has received funding from Bpifrance (grant nos. DOS0058200/00, DOS0080075/00, & DOS0080076/00), from the European Union's Horizon 2020 research and innovation program under grant agreement no. 961112 and from the Region Auvergne-Rhône-Alpes. Bpifrance was not involved in the study design, collection, analysis, interpretation of data, the writing of this article or the decision to submit it for publication.

ACKNOWLEDGMENTS

We acknowledge the contribution of the AniRA-PBES core facility facilities (Plateau de Biologie Expérimentale de la Souris—Experimental Biology in Mice, Lyon), SFR BioSciences (UMS3444-CNRS/US8-INSERM, Ecole Normale Supérieure, University of Lyon), Thibault Andrieu and Sébastien Dussurgey (AniRA-Cytométrie), and the Instruct-ERIC Center (ISBG: UMS 3518 CNRS CEA-UGA-EMBL, Grenoble) within the Grenoble Partnership for Structural Biology (PSB). We thank Daphna Fenel and Dr. Guy Schoehn from the Electron Microscopy platform of the Integrated Structural Biology of Grenoble (ISBG, UMI3265) and Manuel Rosa-Calatrava and the team of Virpath Laboratories, Lyon.

SUPPLEMENTARY MATERIAL

The Supplementary Material for this article can be found online at: https://www.frontiersin.org/articles/10.3389/fimmu.2021.678483/full#supplementary-material

REFERENCES

1. Shasha D, Valinsky L, Hershkowitz Sikron F, Glatman-Freedman A, Mandelboim M, Toledano A, et al. Quadrivalent Versus Trivalent Influenza Vaccine: Clinical Outcomes in Two Influenza Seasons, Historical Cohort Study. *Clin Microbiol Infect* (2020) 26(1):101–6. doi: 10.1016/j.cmi.2019.05.003
2. Tricco AC, Chit A, Soobiah C, Hallett D, Meier G, Chen MH, et al. Comparing Influenza Vaccine Efficacy Against Mismatched and Matched Strains: A Systematic Review and Meta-Analysis. *BMC Med* (2013) 11 (153):1–19. doi: 10.1186/1741-7015-11-153
3. Xie H, Wan XF, Ye Z, Plant EP, Zhao Y, Xu Y, et al. H3n2 Mismatch of 2014–15 Northern Hemisphere Influenza Vaccines and Head-to-head Comparison Between Human and Ferret Antisera Derived Antigenic Maps. *Sci Rep* (2015) 15279:1–10. doi: 10.1038/srep15279
4. Meng Z, Zhang J, Shi J, Zhao W, Huang X, Cheng L, et al. Immunogenicity of Influenza Vaccine in Elderly People: A Systematic Review and Meta-Analysis of Randomized Controlled Trials, and Its Association With Real-World Effectiveness. *Hum Vaccines Immunother* (2020) 16(11):2680–9. doi: 10.1080/21645515.2020.1747375
5. McElhaney JE, Xie D, Hager WD, Barry MB, Wang Y, Kleppinger A, et al. T Cell Responses Are Better Correlates of Vaccine Protection in the Elderly. *J Immunol* (2006) 176(10):6333–9. doi: 10.4049/jimmunol.176.10.6333
6. Hayward AC, Wang L, Goonetilleke N, Fragaszy EB, Bermingham A, Copas A, et al. Natural T Cell–Mediated Protection Against Seasonal and Pandemic Influenza. Results of the Flu Watch Cohort Study. *Am J Respir Crit Care Med* (2015) 191(12):1422–31. doi: 10.1164/rccm.201411-1988OC
7. McMichael AJ, Gotch FM, Noble GR, Beare PA. Cytotoxic T-cell Immunity to Influenza. *N Engl J Med* (1983) 309(1):13–7. doi: 10.1056/NEJM198307073090103
8. Wang Z, Wan Y, Qiu C, Quiñones-Parra S, Zhu Z, Loh L, et al. Recovery From Severe H7N9 Disease is Associated With Diverse Response Mechanisms Dominated by CD8+ T Cells. *Nat Commun* (2015) 6833:1–12. doi: 10.1038/ncomms7833
9. McGraw C. Vaccines for Preventing Influenza in Healthy Adults (Review). *Prim Health Care* (2008) 18(8):31–1. doi: 10.7748/phc.18.8.31.s24
10. Doherty PC, Kelso A. Toward a Broadly Protective Influenza Vaccine. *J Clin Invest* (2018) 118(10):3273–5. doi: 10.1172/JCI37232
11. Brown LE, Kelso A. Prospects for an Influenza Vaccine That Induces Cross-Protective Cytotoxic T Lymphocytes. *Immunol Cell Biol* (2009) 87(4):300–8. doi: 10.1038/icb.2009.16
12. Bonduelle O, Carrat F, Luyt CE, Leport C, Mosnier A, Benhabiles N, et al. Characterization of Pandemic Influenza Immune Memory Signature After Vaccination or Infection. *J Clin Invest* (2014) 124(7):3129–36. doi: 10.1172/JCI74565
13. McElhaney JE, Kuchel GA, Zhou X, Swain SL, Haynes L. T-Cell Immunity to Influenza in Older Adults: A Pathophysiological Framework for Development of More Effective Vaccines. *Front Immunol* (2016) 7(14):1–11. doi: 10.3389/fimmu.2016.00041
14. Kumar A, McElhaney JE, Walrond L, Cyr TD, Merani S, Kollmann TR, et al. Cellular Immune Responses of Older Adults to Four Influenza Vaccines: Results of a Randomized, Controlled Comparison. *Hum Vaccines Immunother* (2017) 13(9):2048–57. doi: 10.1080/21645515.2017.1337615
15. Auladell M, Jia X, Hensen L, Chua B, Fox A, Nguyen THO, et al. Recalling the Future: Immunological Memory Toward Unpredictable Influenza Viruses. *Front Immunol* (2019) 10:1–18. doi: 10.3389/fimmu.2019.01400
16. Szabo PA, Miron M, Farber DL. Location, Location, Location: Tissue Resident Memory T Cells in Mice and Humans. *Sci Immunol* (2019) 4(34):1–10. doi: 10.1126/sciimmunol.aas9673
17. Uddbäck I, Kohlmeier JE, Thomsen AR, Christensen JP. Harnessing Cross-Reactive Cd8 $^{+}$ T $_{Rm}$ Cells for Long-Standing Protection Against Influenza A Virus. *Viral Immunol* (2020) 33(3):201–7. doi: 10.1089/vim.2019.0177
18. Zens KD, Chen JK, Farber DL. Vaccine-Generated Lung Tissue–Resident Memory T Cells Provide Heterosubtypic Protection to Influenza Infection. *JCI Insight* (2016) 1(10):1–13. doi: 10.1172/jci.insight.85832
19. Del Campo J, Pizzorno A, Djebali S, Bouley J, Haller M, Pérez-Vargas J, et al. OVX836 a Recombinant Nucleoprotein Vaccine Inducing Cellular Responses and Protective Efficacy Against Multiple Influenza A Subtypes. *NPJ Vaccines* (2019) 4(4):1–14. doi: 10.1038/s41541-019-0098-4
20. Durward M, Harms J, Splitter G. Antigen Specific *In Vivo* Killing Assay Using CFSE Labeled Target Cells. *J Vis Exp* (2010) (45):2250. doi: 10.3791/2250
21. Ye Q, Krug RM, Tao YJ. The Mechanism by Which Influenza A Virus Nucleoprotein Forms Oligomers and Binds RNA. *Nature* (2006) 444 (7122):1078–82. doi: 10.1038/nature05379

22. Shen Y-F, Chen Y-H, Chu S-Y, Lin M-I, Hsu H-T, Wu P-Y, et al. E339...R416 Salt Bridge of Nucleoprotein as a Feasible Target for Influenza Virus Inhibitors. *Proc Natl Acad Sci* (2011) 108(40):16515–20. doi: 10.1073/pnas.1113107108
23. Brinza L, Djebali S, Tomkowiak M, Mafille J, Loiseau C, Jouve PE, et al. Immune Signatures of Protective Spleen Memory CD8 T Cells. *Sci Rep* (2016) 6(1):1–12. doi: 10.1038/srep37651
24. Reilly EC, Lambert Emo K, Buckley PM, Reilly NS, Smith I, Chaves FA, et al. TRM Integrins CD103 and CD49a Differentially Support Adherence and Motility After Resolution of Influenza Virus Infection. *Proc Natl Acad Sci* (2020) 117(22):12306–14. doi: 10.1073/pnas.1915681117
25. Takamura S. Divergence of Tissue-Memory T Cells: Distribution and Function-Based Classification. *Cold Spring Harb Perspect Biol* (2020) 12(10): a037762. doi: 10.1101/cshperspect.a037762
26. Combadiere B, Liard C. Transcutaneous and Intradermal Vaccination. *Hum Vaccin* (2011) 7(8):811–27. doi: 10.4161/hv.7.8.16274
27. Belshe RB, Edwards KM, Vesikari T, Black SV, Walker RE, Hultquist M, et al. Live Attenuated Versus Inactivated Influenza Vaccine in Infants and Young Children. *N Engl J Med* (2007) 356(7):685–96. doi: 10.1056/NEJMoa065368
28. Basha S, Hazenfeld S, Brady RC, Subbramanian RA. Comparison of Antibody and T-cell Responses Elicited by Licensed Inactivated- and Live-Attenuated Influenza Vaccines Against H3N2 Hemagglutinin. *Hum Immunol* (2011) 72 (6):463–9. doi: 10.1016/j.humimm.2011.03.001
29. Snyder ME, Farber DL. Human Lung Tissue Resident Memory T Cells in Health and Disease. *Curr Opin Immunol* (2019) 59:101–8. doi: 10.1016/j.coi.2019.05.011
30. Cerwenka A, Morgan TM, Dutton RW. Naive, Effector, and Memory CD8 T Cells in Protection Against Pulmonary Influenza Virus Infection: Homing Properties Rather Than Initial Frequencies are Crucial. *J Immunol* (1999) 163 (10):5535–43.
31. Hamada H, Bassity E, Flies A, Strutt TM, Garcia-Hernandez Mde L, McKinstry KK, et al. Multiple Redundant Effector Mechanisms of CD8 $^{+}$ T Cells Protect Against Influenza Infection. *J Immunol* (2013) 190(1):296–306. doi: 10.4049/jimmunol.1200571
32. Topham DJ, Tripp RA, Doherty PC. Cd8+ T Cells Clear Influenza Virus by Perforin or Fas-dependent Processes. *J Immunol* (1997) 159(11):5197–200.
33. Laidlaw BJ, Zhang N, Marshall HD, Staron MM, Guan T, Hu Y, et al. Cd4+ T Cell Help Guides Formation of CD103+ Lung-Resident Memory Cd8+ T Cells During Influenza Viral Infection. *Immunity* (2014) 41(4):633–45. doi: 10.1016/j.immuni.2014.09.007
34. Purwar R, Campbell J, Murphy G, Richards WG, Clark RA, Kupper TS. Resident Memory T Cells (Trm) Are Abundant in Human Lung: Diversity, Function, and Antigen Specificity. *PloS One* (2011) 6(1):e16245. doi: 10.1371/journal.pone.0016245
35. Park CO, Kupper TS. The Emerging Role of Resident Memory T Cells in Protective Immunity and Inflammatory Disease. *Nat Med* (2015) 21(7):688–97. doi: 10.1038/nm.3883
36. Duffy D, Perrin H, Abadie V, Benhabiles N, Boissonnas A, Liard C, et al. Neutrophils Transport Antigen From the Dermis to the Bone Marrow, Initiating a Source of Memory Cd8+ T Cells. *Immunity* (2012) 37(5):917–29. doi: 10.1016/j.immuni.2012.07.015
37. Quinones-Parra S, Grant E, Loh L, Nguyen TH, Campbell KA, Tong SY, et al. Preexisting CD8+ T-Cell Immunity to the H7N9 Influenza A Virus Varies Across Ethnicities. *Proc Natl Acad Sci* (2014) 111(3):1049–54. doi: 10.1073/pnas.1322229111
38. Wang Z, Zhu L, Nguyen THO, Wan Y, Sant S, Quiñones-Parra SM, et al. Clonally Diverse CD38+HLA-DR+CD8+ T Cells Persist During Fatal H7N9 Disease. *Nat Commun* (2018) 9:824. doi: 10.1038/s41467-018-03243-7
39. Sridhar S, Begom S, Bermingham A, Hoschler K, Adamson W, Carman W, et al. Cellular Immune Correlates of Protection Against Symptomatic Pandemic Influenza. *Nat Med* (2013) 19(10):1305–12. doi: 10.1038/nm.3350
40. Tu W, Mao H, Zheng J, Liu Y, Chiu SS, Qin G, et al. Cytotoxic T Lymphocytes Established by Seasonal Human Influenza Cross-React Against 2009 Pandemic H1n1 Influenza Virus. *J Virol* (2010) 84(13):6527–35. doi: 10.1128/JVI.00519-10
41. Thomas PG, Keating R, Hulse-Post DJ, Doherty PC. Cell-Mediated Protection in Influenza Infection. *Emerg Infect Dis* (2006) 12(1):48–54. doi: 10.3201/eid1201.051237
42. Pizzolla A, Nguyen TH, Sant S, Jaffar J, Loudovaris T, Mannering SI, et al. Influenza-specific Lung-Resident Memory T Cells are Proliferative and Polyfunctional and Maintain Diverse TCR Profiles. *J Clin Invest* (2018) 128 (2):721–33. doi: 10.1172/JCI96957

Conflict of Interest: AV, DG, and FN are employed by and shareholders of Osivax. JC and FH are employed by Osivax and inventors of some of Osivax' patents. JC, JB, MC, CR, MH, and AI are employed by Osivax. BC is member of the advisory board of Osivax and receives honoraria.

The remaining authors declare that the research was conducted in the absence of any commercial or financial relationships that could be construed as a potential conflict of interest.

frontiers in Immunology

REVIEW
published: 31 August 2021
doi: 10.3389/fimmu.2021.710647

Influenza Viruses: Innate Immunity and mRNA Vaccines

SangJoon Lee[1] *and Jin-Hyeob Ryu*[2,3]*

[1] Department of Infection Biology, Faculty of Medicine, University of Tsukuba, Tsukuba, Japan, [2] BIORCHESTRA Co., Ltd, Daejeon, South Korea, [3] BIORCHESTRA Co., Ltd, Cambridge, MA, United States

The innate immune system represents the first line of defense against influenza viruses, which cause severe inflammation of the respiratory tract and are responsible for more than 650,000 deaths annually worldwide. mRNA vaccines are promising alternatives to traditional vaccine approaches due to their safe dosing, low-cost manufacturing, rapid development capability, and high efficacy. In this review, we provide our current understanding of the innate immune response that uses pattern recognition receptors to detect and respond to mRNA vaccination. We also provide an overview of mRNA vaccines, and discuss the future directions and challenges in advancing this promising therapeutic approach.

Keywords: mRNA, vaccine, influenza virus, innate immunity, inflammasome, cytokines, inflammation

OPEN ACCESS

Edited by:
Corey Patrick Mallett, GlaxoSmithKline, United States

Reviewed by:
Randy A. Albrecht, Icahn School of Medicine at Mount Sinai, United States
Takashi Imai, Gunma University, Japan

***Correspondence:**
Jin-Hyeob Ryu
branden.ryu@biorchestra.com

Specialty section:
This article was submitted to Vaccines and Molecular Therapeutics, a section of the journal Frontiers in Immunology

Received: *17 May 2021*
Accepted: *13 August 2021*
Published: *31 August 2021*

Citation:
Lee S and Ryu J-H (2021) Influenza Viruses: Innate Immunity and mRNA Vaccines. Front. Immunol. 12:710647. doi: 10.3389/fimmu.2021.710647

INTRODUCTION

The innate immune system serves as the first line of host immune response against pathogens but also virus-based vaccines containing either attenuated or inactivated viruses to prevent infectious diseases. After vaccination, the innate immune system identifies and removes vaccinated cells while coordinating the adaptive immune responses in the form of antigen-specific reactions, thereby sustaining long-term protection from the viral infection. To rapidly detect and defend against the various viruses, the immune cells have evolved to acquire multiple pattern-recognition receptors (PRRs) such as Toll-like receptors (TLRs), retinoic acid-inducible gene I (RIG-I)-like receptors (RLRs), and the nucleotide-binding oligomerization domain (NOD)-like receptor family proteins (NLRs) (1, 2). Through such receptors, the innate immune system is activated in a tightly regulated manner while retaining the adaptive immune response, but without excessive innate immune responses that can cause tissue damage and systemic inflammation, which are harmful to the host. In the present review, we discuss innate immune recognition, activation of inflammasome, and cytokine secretion in response to influenza virus infection and its mRNA vaccines. We also emphasize mRNA vaccines as promising tools for the prevention and control of influenza virus disease.

BRIEF HISTORY ON INFLUENZA VACCINES TO DATE

Influenza viruses cause some of the most virulent respiratory tract infections in humans. Seasonal influenza virus epidemics are estimated to lead to up to 290,000–650,000 deaths per year globally (3). Influenza viruses are enveloped, negative-sense, single-stranded RNA (ssRNA) viruses with a

segmented genome. For instance, the influenza A virus (IAV) contains eight RNA segments encoding the RNA polymerase subunits [polymerase acidic protein (PA), polymerase basic protein 1 (PB1), polymerase basic protein 2 (PB2)], viral glycoproteins [hemagglutinin (HA), which facilitates viral entry; and neuraminidase (NA), which facilitates viral release], viral nucleoprotein (NP), matrix protein (M1), membrane protein (M2), and nonstructural protein 1 (NS1) (**Figure 1A**). IAV infects the cell through endosomal uptake and release, and the viral ribonucleoproteins (vRNPs) enter the nucleus for mRNA transcription and replication *via* a positive-sense complementary ribonucleoprotein (cRNP) intermediate. Viral mRNA is then converted into viral proteins in cytoplasm, which are complex into new virions and released from the cell (**Figure 1B**).

There are four distinct types of seasonal influenza viruses: types A, B, C, and D. Types A and B influenza viruses are currently co-circulating in the human population and cause

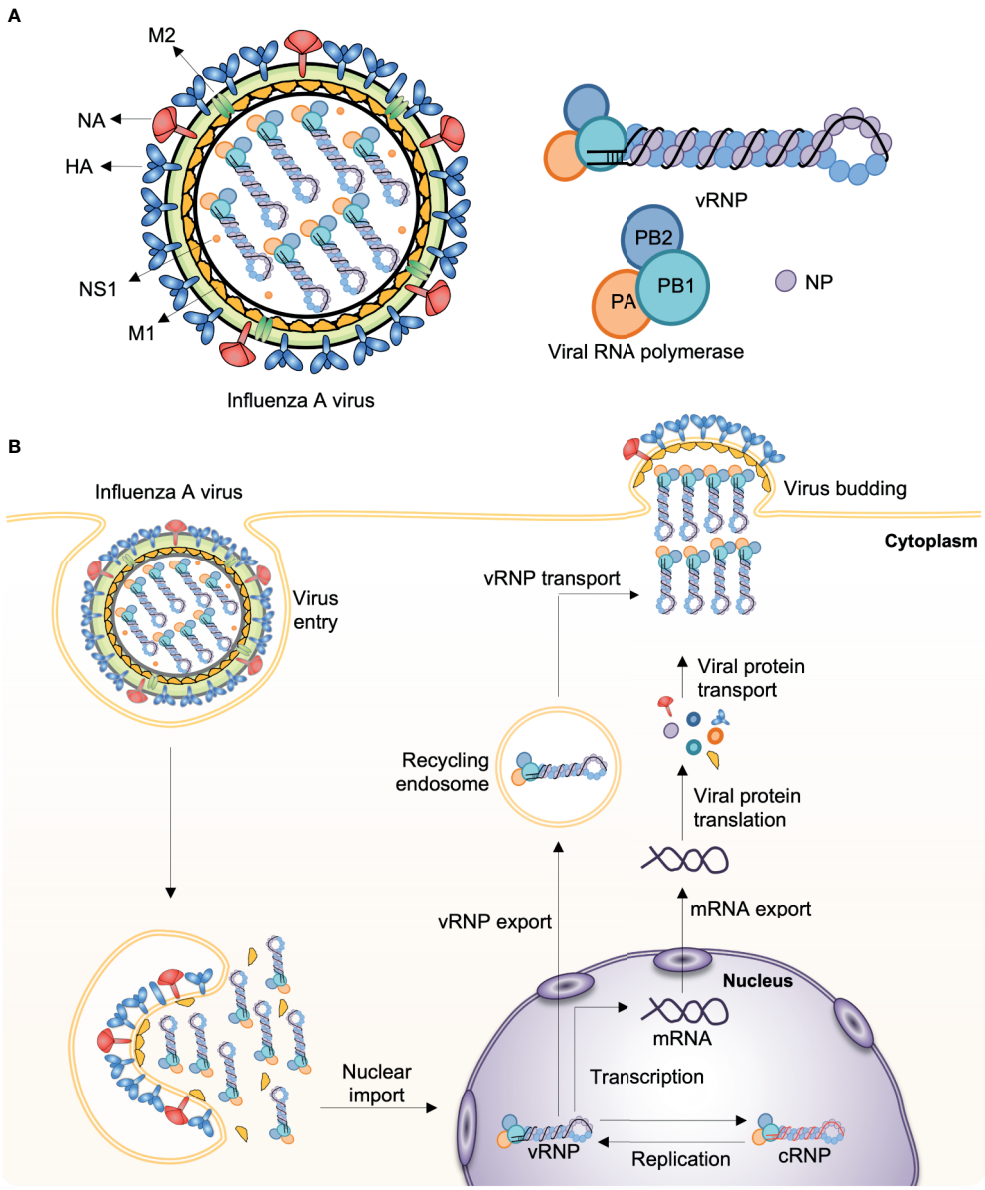

FIGURE 1 | Influenza A virus structure and replication. **(A)** The influenza A virus (IAV) genome comprises eight segmented, and single- and negative-stranded RNAs (vRNA). Each segment is encapsulated by a nucleoprotein (NP) and, mediated by the RNA polymerase, they form the viral ribonucleoprotein (vRNP) complex (PB1, PB2, PA, and NP), which is the essential unit for both transcription and replication. **(B)** Infecting vRNP is transported into the nucleus where viral transcription and replication occurs, followed by progeny vRNP production. After the progeny vRNP is exported to the cytoplasm, the virus is assembled. HA, haemagglutinin; M1, matrix protein; M2, membrane protein; NA, neuraminidase; NS1, nonstructural protein 1; PA, polymerase acidic protein; PB1, polymerase basic protein 1; PB2, polymerase basic protein 2.

seasonal epidemics: the H1N1 and the H3N2 subtypes of IAVs, and two divergent lineages (Yamagata lineage and Vitoria lineage) of the influenza B viruses (IBVs) (4). Through the coordination of World Health Organization Global Influenza Surveillance Network, seasonal influenza virus vaccines are designed annually and the formulations contain the two IAV strains and two IBV strains; however, the efficacy of seasonal influenza virus vaccines varies greatly each influenza season (5). Upon seasonal influenza vaccine injection, innate immune cells, including macrophages and dendritic cells (DCs) that are present in the muscle, cause an increase in the release of chemokines, which leads to the recruitment of more immune cells from the blood into the site of vaccination. The differentiated DCs act as antigen-presenting cells and migrate to the lymph nodes leading to the activation of T- and B-cells for the production of antibodies (6) (**Figure 2**). However, the vaccines induce narrow and strain-specific immunity that require constant updating (almost every year) due to the high frequency of point mutations, which ultimately represents a complex, expensive, and time-consuming process. In addition, various strains of influenza viruses, including avian and swine, have acquired the ability to grow efficiently in humans across species barriers from animal reservoirs and to disseminate between populations, posing a serious threat to humans. In addition to seasonal epidemics, influenza pandemics occur once every few decades and are caused by the swine-origin H1N1 IAVs, which

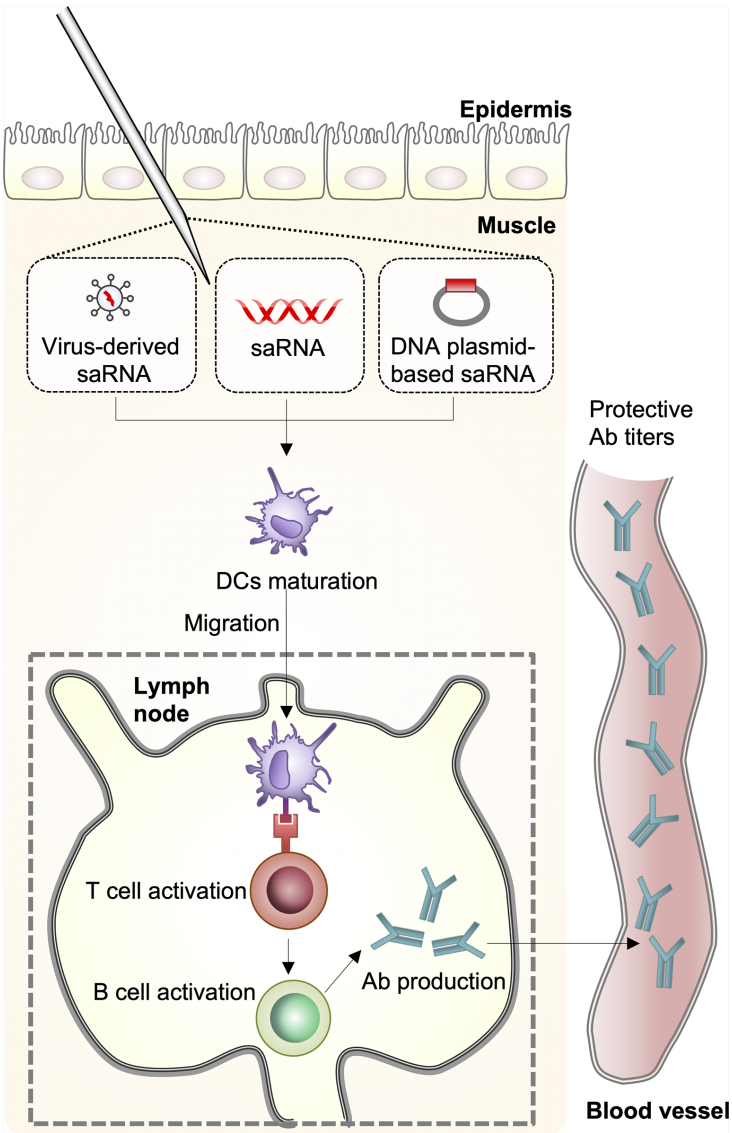

FIGURE 2 | Host immune response against mRNA vaccines. A self-amplifying RNA (saRNA) vaccine can be delivered in the form of virus-like RNA particles, *in vitro* transcribed RNA, and plasmid DNA. Dendritic cells (DCs) recognize saRNA in the muscle and the cells are differentiated. The differentiated DCs function as antigen-presenting cells and migrate to the lymph nodes leading to activation of T- and B-cells for antibody production.

have never circulated, and can spread rapidly across the human population. The H1N1 influenza virus pandemic in 1918 killed approximately 40 million people globally (7). Since then, pandemics have been caused by H2N2 in 1957, H3N2 in 1968, and again by H1N1pdm09 in 2009 (8). Considering seasonal influenza virus vaccines induce strain-specific immunity, which may not offer strong protection against infection by a pandemic-causing influenza virus, there is a need to develop novel influenza vaccines that induce broad immunity that is not focused on the corresponding vaccine strain (9).

Prior to the 1980s, inactivated and live-attenuated vaccines were established to protect humans against pathogenic microorganisms. Inactivated vaccines were manufactured by chemical or heat treatment, and live-attenuated vaccines were usually developed in animals or cell lines. The use of killed whole organism-based vaccines or live-attenuated vaccines had huge success in the reduction of viral infections including measles, mumps, rubella, and polio, and the eradication of smallpox infection (1). Despite the success, major concerns persist regarding conventional vaccination strategies. Infectious pathogens such as influenza virus are able to evade the adaptive immune response, and it is frequently difficult to develop live-attenuated or killed whole organism-based vaccines (10). In the case of the current influenza virus vaccine, the main challenge is its low effectiveness in the elderly (≥ 65 years old), who are more susceptible to influenza virus infection than children and adults (11). Such shortcomings of inactivated influenza virus vaccines are often attributed to mutations in surface antigens of the influenza virus. Other concerns regarding influenza virus live-attenuated vaccines include the potential to cause systemic inflammation and death, possibly due to back-mutations, acquisition of compensatory mutations, or recombination with circulating transmissible wild-type strains (12–14).

Generally, influenza virus infects the host *via* the nasal or oral cavities, where it makes the first contact with the respiratory epithelium, similar to live-attenuated influenza vaccines administered intranasally (15, 16). After infecting the respiratory epithelial cells, the virus or the intranasal influenza vaccine can induce both systemic and mucosal immune responses. The defense mechanisms of the innate immune cells, especially DCs, are a formidable barrier to the influenza virus. Particular immune systems exist at distinct mucosal surfaces to fighting invasion by influenza virus. The viral RNA that is present within infected cells is recognized as non-self by various pattern recognition receptors (PRRs), which leads to the release of proinflammatory cytokines, chemokines, and type I interferons (IFNs). Macrophages, pneumocytes, DCs, and plasmacytoid-DCs produce type I IFNs, which in turn stimulate the expression of IFN-stimulated genes (ISGs) in neighboring cells that induce antiviral states (17–19).

Unlike influenza virus infection or intranasal influenza vaccine, mRNA-based vaccines contain mRNAs that encode both the viral protein and immune-modulatory proteins as adjuvants, which enhance immunostimulatory properties. Upon mRNA entry into host cells, endosomal (e.g., TLR3, TLR7, and TLR8) and cytosolic innate immune sensors (e.g., RIG-I, PKR, NOD2, OAS, and MDA5) recognize mRNAs, including single-stranded RNA (ssRNA) and double-stranded RNA (dsRNA). Subsequently, the immune cells are activated and produce type I IFN and multiple inflammatory cytokines (20). However, single-stranded mRNAs in the vaccine are purified appropriately through *in vitro* transcription process to eliminate the interaction with innate immune sensors, which induce excessive secretion of type I IFN and its cellular dysfunction (20).

Furthermore, the adjuvant stimulates the innate immune response and drives antigen-specific T-cell responses without inducing systemic inflammation that could elicit severe side effects. In addition, injection site (e.g., subcutaneous, intramuscular, intradermal, and intravenous) and mRNA vaccine delivery formulations (e.g. lipid nanoparticle) influence the potency of the immune response (21). For instance, lipid nanoparticle carrier systems further protect mRNAs from nuclease, and can target delivery to lymphatics and promote protein translation in lymph nodes by intramuscular injection (20). In contrast to intranasal mRNA-mediated innate immune response, intramuscular mRNA will primarily be up taken by non-immune cells including local myocytes. Once in the lymph nodes, the lipid nanoparticle is eventually phagocytized by DCs, which consequently produce and present the antigen to T-cells to promote adaptive immune responses (22, 23). The capability of mRNA vaccines to induce the intracellular production of antigen proteins along with innate immune responses must prime both $CD8^+$ and $CD4^+$ T-cells to differentiate into effector and memory subsets for the protection from the infection (24).

The effective use of *in vitro* transcribed mRNA in mammals was first reported in 1990, with reporter gene mRNAs being injected into mice that induced the production of the target proteins (25). A subsequent study showed that administration of vasopressin-encoding mRNA in the hypothalamus could induce a physiological response in rats (26). However, such early promising results did not lead to significant investment for the development of mRNA vaccines because of anxieties associated with mRNA instability, severe innate immune responses, and ineffective *in vivo* delivery. Over the past decade, however, major technological innovations and investments in research have made mRNA a promising vaccination tool. The use of mRNA vaccines has several benefits over subunit, killed, and live-attenuated viruses. As mRNA is a non-infectious and non-integrating platform, there is no potential risk of infection or insertional mutagenesis. In addition, mRNA is degraded by normal cellular processes, and various modifications and delivery methods can modulate its half-life *in vivo* (27–29). Formulating mRNA into carrier molecules facilitates rapid uptake and expression in the cytoplasm, where it is stable and highly translatable (28, 30). Furthermore, mRNA vaccines have quick, inexpensive, and mountable manufacturing potential due to the high yield of *in vitro* transcription responses. Additionally, several elegant studies with non-human primate models of influenza mRNA vaccine have been carried out. After immunization of modified non-replicating mRNA encoding influenza H10 encapsulated in lipid nanoparticles in monkeys, protective levels of antibodies against hemagglutinin were dramatically increased, similar to observations following

seasonal influenza vaccination in humans (31). Using a novel imaging technology (positron emission tomography–computed tomography, PET–CT), an mRNA vaccine labeled with a probe is trafficked to assess bio-distribution in monkeys, providing insights of the mechanisms of the innate and adaptive immune responses following vaccine administration on site and at the draining lymph node, which translates into protective immunity (32).

INNATE IMMUNITY TO INFLUENZA VIRUSES

The IAV is recognized as foreign by PRRs including TLRs, RLRs, and NLRs, which leads to programmed cell death, secretion of type I IFNs, and proinflammatory cytokines, which induce excessive inflammation.

TLR- and RLR-Associated Influenza Virus Recognition

TLR- and RLR-mediated signals for influenza viruses induce to the release of type I IFNs and stimulate the expression of ISGs by infected and nearby cells to induce an antiviral state (33–36). Moreover, TLR and RLR signals also induce the release of proinflammatory cytokines, such as interleukin (IL)-6 and IL-8 (37, 38).

TLR3 senses dsRNA in endosomes. Although the cells infected by influenza virus do not produce dsRNA, *Tlr3*$^{-/-}$ mice have a longer lifespan compared with wild-type mice after deadly influenza virus infection (38), suggesting that TLR3 recognizes an unidentified RNA structure following viral infection. Furthermore, *Tlr3*$^{-/-}$ mice produce normal antibodies, and $CD4^+$ and $CD8^+$ T-cell responses after influenza virus infection (33), suggesting that TLR3 is dispensable for generating T-cell immunity. In plasmacytoid-DCs, TLR7 recognizes the ssRNA genomes of influenza virus (34, 35). TLR7 signaling *via* adaptor myeloid differentiation primary response 88 (MYD88) leads to the activation of transcription factors including nuclear factor-κB (NF-κB) and IFN-regulatory factor 7 (IRF7), which induce the production of type I IFNs and proinflammatory cytokines (39–41).

RIG-I is a cytosolic PRR that generally recognizes 5'ppp-double-stranded RNA (dsRNA). RIG-I also senses the 5'ppp-viral ssRNA that is produced following influenza viral replication (42–44). After detection of influenza viral RNA, the helicase domain of RIG-I interacts to ATP, which facilitates conformational changes of the caspase-recruitment domains (CARD) to interact with signaling adaptor mitochondrial antiviral signaling protein (MAVS) for type I IFN production (45, 46).

Inflammasome-Mediated Response to Influenza Virus

NLRs have an important role in antiviral immune response, inflammatory response, and cytokine induction. Proinflammatory signaling induces the recruitment of immune cell, such as macrophages and neutrophils, to eliminate pathogens and pathogen-derived molecules. IL-1β and IL-18 are key proinflammatory cytokines and are important for the protection against IAV infection (16, 47–49). Secretion of IL-1β and IL-18 requires the proteolytic maturation of pro-IL-1β and pro-IL-18, respectively, that is mediated by inflammasomes. Inflammasomes are multiprotein complexes consisting of caspase-1, ASC, and PRRs, such as NOD–like receptor family protein 3 (NLRP3) (16, 47–49). Upon viral ligand sensing, PRRs induce self-oligomerization and binds to the inflammasome adaptor protein ASC, which is composed of an N-terminal pyrin domain (PYD) and a C-terminal CARD. ASC oligomerizes *via* homotypic interactions of the PYD domain and then binds to caspase-1 *via* the CARD for the inflammasome formation, which ultimately induces inflammatory cell death.

In macrophages, influenza virus-induced NLRP3 inflammasome activation requires the Z-DNA binding protein 1 (ZBP1) to form the ZBP1–NLRP3 inflammasome (50, 51). When replicating, IAV generates Z-RNAs, which are transformed versions of an RNA double helix, that are sensed by ZBP1 and bind to the receptor interacting serine/threonine kinase 3 (RIPK3) and caspase-8 to activate the ZBP1–NLRP3 inflammasome (50–52). Recently, it has been shown that caspase-6 facilitates RHIM-dependent binding of RIPK3 with ZBP1, promoting ZBP1-mediated NLRP3 inflammasome activation (53). In respiratory epithelial cells, MxA functions as an inflammasome sensor that recognizes influenza viral protein NP and induces the release of IL-1β and IL-18 in an NLRP3-independent manner (15, 16).

NLRP3 and MxA inflammasome activation has been shown to be an important innate immune defense against influenza virus. After influenza virus strain A/Puerto Rico/8/34 (PR8) infection, NLRP3 was found to be important for the migration of leukocytes into the lungs and to protect the host from infection (47, 49). During influenza virus infection in human MxA transgenic mice, rapid activation of the MxA inflammasome in the respiratory epithelium showed to suppress viral spreading from the bronchioles to the distal alveolar regions (16). The results of such studies suggest that optimal inflammasome activation is beneficial for the host; however, abnormal activation can cause to harmful outcomes.

ADAPTIVE IMMUNITY TO INFLUENZA VIRUS

Innate and adaptive immune responses significantly protects the host from influenza viruses and are important for the production of strong antibody responses. After influenza virus infection, the innate immune system is critical for recognizing and removing vaccinated cells while also coordinating an adaptive immunity through an antigen-specific antibody reaction and providing long-term protection from the viral infection.

Upon recognition of viral antigens and interaction with cognate $CD4^+$ T-cells, naïve B-cells are activated (54). Some of the activated B-cells quickly differentiate into short-lived plasmablasts. Although other activated B-cells migrate to the

follicles of secondary lymphoid tissues and undergo a germinal center reaction, the plasmablasts produce the first wave of virus-specific antibodies in humans. If plasmablasts are derived from memory B-cells, the numbers of plasmablasts peak in the periphery at about 7 days post-infection (55). A small number of activated B-cells, however, will only differentiate into long-lived plasma cells, which migrate and resides in the bone marrow to produce antibodies, which provide the long-term serum antibody level and are associated with the defense against pathogen infection and disease. Another portion of the primarily activated B-cells differentiate into memory B-cells (56, 57), which do not release antibodies and remain in the periphery for immune surveillance, but they are long-lived and can be reactivated to become plasmablasts during infection for the production of new antibodies and further memory B-cells (55). Overall, the adaptive immunity-derived antibody response to influenza virus infection is relatively broad and long-lived; however, influenza viruses can deviate from the adaptive immune responses over time owing to their high mutation rates and antigenic flexibility. Further studies of how natural viral infection induces long-lived immune responses are required for the development of next-generation influenza virus vaccines.

CONVENTIONAL SEASONAL INFLUENZA VIRUS VACCINES

Seasonal influenza virus vaccines are produced using egg-, cell-, and protein-based technologies, and the entire processes typically take 6~8 months. Influenza vaccines against IAVs and IBVs were invented in the 1940s and such whole-virus inactivated vaccines were generated in embryonated chicken eggs that consisted of crudely purified whole virus inactivated with formalin and phenylmercuric nitrate (58, 59). In 2012, vaccine-containing cell-based virus emerged as an alternative method for producing inactivated and live-attenuated vaccines (60). The efficacy of trivalent inactivated and live-attenuated influenza vaccines is approximately 65% and 83% in adults and children, respectively (61). Live-attenuated influenza virus vaccines that are used are usually cold-adapted and temperature-sensitive, and efficiently replicate in the upper but not the lower respiratory tract (62–64). Collectively, such studies indicate that seasonal influenza virus vaccines present good protection against influenza virus infection.

However, there are also negative reports on such vaccines. A vaccine efficacy of 75% in adults declines suddenly in the elderly, who are more susceptible to influenza virus infection (65, 66). In addition, mismatches between vaccine and circulating strains sometimes occur and are generally associated to lower vaccine efficiency (67). Based on US virologic surveillance and US Influenza Vaccine Effectiveness (Flu VE) Network data, the estimated vaccine effectiveness (VE) against IAV or IBV decreased to 29% in all ages during the 2019–2020 influenza season (average VE in 2010–2018 was 44.1%) due to the spread of antigenically drifted IAV (H3N2), which has raised concerns about vaccine strain selection (68) (https://www.cdc.gov/flu/vaccines-work/past-seasons-estimates.html). Furthermore, the duration of protection is occasionally short (69, 70). To induce stronger, more sustained immune responses in the elderly, high-dose vaccines or advanced adjuvant vaccines including MF59 and AS03, have been tested. The doses in high-dose vaccines are 4-fold those in trivalent inactivated vaccines, which could induce higher amounts of antibodies than standard dose vaccines (71). MF59-adjuvanted seasonal vaccines have been licensed and marketed in more than 25 countries for the elderly population (72, 73). AS03-adjuvanted influenza virus vaccines are also under consideration for use in the elderly population (74).

CONVENTIONAL PANDEMIC INFLUENZA VIRUS VACCINES

IAVs are typically transmitted within one animal species but sometimes they can cross over and cause illness in another species. In the latter situation, more significant genetic changes are exhibited than in circulating human seasonal IAV. If the novel IAV is infectious and spreads easily in humans, it is considered an influenza virus pandemic. Because most of the human population has no or only limited natural immunity to novel influenza virus strains, pandemic IAV vaccine candidates have been developed using a range of production platforms. The inactivated split influenza virus vaccine platform with an adjuvant has advanced the furthest, and other platforms, including nucleic acid (DNA and mRNA), vector, recombinant protein (VLP; virus-like particle), and live virus are still under development (75). H5N1 avian influenza virus vaccine was the first U.S. FDA-approved vaccine for the human population because concerns were raised with regard to the potential of the highly pathogenic H5N1 virus to cause an influenza pandemic (76, 77).

One of the challenges in influenza pandemic management is the global vaccine production capacity within several months following the emergence of an outbreak. In the case of vaccines against H5N1 strains, the seed strains were generated using reverse genetics to remove the multi-basic cleavage site of the HA and to alter the backbone to that of a high-growth PR8 H1N1 strain, which exhibits relatively less pathogenicity (77). Such modifications facilitate the production of safer vaccine strains and at high quantities, because highly pathogenic IAVs frequently kill embryonated eggs, resulting in low production (77). A number of the H5N1 and H7N9 vaccines have been tested in humans and a high antigen dose or the use of an adjuvant is necessary to induce reliable hemagglutination inhibition titer (77, 78). A clinical trial of an H7N9 vaccine yielded an efficacy of approximately 60% despite the use of an adjuvant (79), indicating that adjuvants and multiple vaccinations are required for achieving sufficient vaccine efficiency.

MESSENGER RNA VACCINE STRATEGIES AGAINST INFLUENZA VIRUS

mRNA vaccines are extensively characterized by experimental approaches that improve mRNA stability and delivery, and

protein production. Such approaches involves the development of nanoparticle transport techniques that stabilize mRNA, enhance cellular uptake, and improve biological availability when mRNA enters the cell. A clear advantage of mRNA vaccines is that it does not need to enter the nucleus to promote antigen expression.

Self-Amplifying mRNA Vaccines Against Influenza Virus

A self-amplifying RNA (saRNA) vaccine can be carried in the form of plasmid DNA, virus-like RNA particles, and *in vitro* transcribed RNA (80) (**Figure 3**). DNA plasmid-based saRNA vaccines combine the advantages of a more stable DNA nucleic acid product with greater levels of antigen expression. saRNA vaccines have elicited strong immune responses in preclinical models (81). saRNA vaccines are derived from the genome backbone of an alphavirus, in which the genes encoding the viral RNA replication machinery are intact (82).

There are several reports on the use of saRNA vaccines against influenza virus. Immunization with 10 mg of saRNA vaccine encoding PR8 H1N1 IAV HA produced antibody responses and protection from lethal homologous viral challenge in mice (83). Another study showed development of saRNA vaccines where the A/California/07/2009 (H1N1) or A/Shanghai/2/2013 (H7N9) IAV HA-encoding saRNA was formulated in lipid nanoparticles, and small doses induced protective levels of hemagglutination inhibition titers after two intramuscular injections in mice (84). Consistent with this finding, another group showed that intramuscular administration of 0.1 or 0.2 mg of PR8 H1N1 IAV NP, M1, or combined NP+M1 self-amplifying RNA-lipid nanoparticle vaccines resulted in strong antigen-specific T-cell responses and protection from homologous viral infection (85). IAV HA and NP replicon RNA complexed with chitosan-containing lipid nanoparticles or polyethylenimine (PEI) has elicited T- and B-cell immune responses in mice after subcutaneous delivery (86, 87). A recent study revealed a delivery platform consisting of a chemically modified, ionizable dendrimer complexed into lipid nanoparticles. Using this platform, intramuscular delivery of RNA replicons encoding A/WSN/33 (H1N1) IAV HA successfully protected mice against lethal homologous virus challenge (88). A more recent study showed a direct comparison of the immune response and protective efficacy after self-replicating mRNA and non-replicating mRNA immunization in mice (80). Animals were intramuscularly immunized two times with increasing doses of PR8 H1N1 IAV

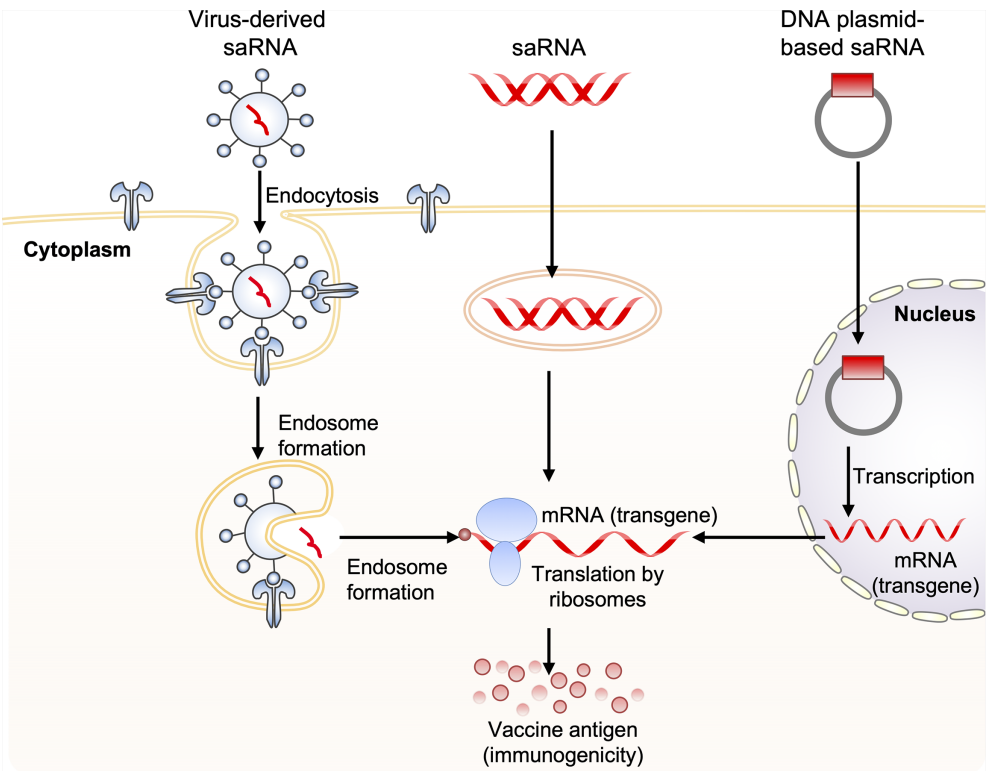

FIGURE 3 | Obtaining antigen expression by self-amplifying RNA vaccination. Three routes for the delivery of self-amplifying RNA (saRNA) are shown. These include: 1) virus-like RNA particles that deliver saRNA to the cytoplasm by receptor-mediated endocytosis, 2) direct delivery of *in vitro* transcribed replicon saRNA to cells either in saline or in synthetic formulations, and 3) plasmid DNA carrying replicase genes and the transgene into the nucleus, where it is transcribed, generating replicon saRNA, which is then transported to the cytoplasm. The three saRNA vaccination routes finally generate messenger RNA (mRNA), which is translated *via* ribosomes to produce vaccine antigen.

HA-encoding unformulated self-replicating mRNA or unmodified non-replicating mRNA and challenged eight weeks after the first vaccination. Both platforms induced protection against infection with the homologous influenza virus (80).

Non-Replicating Influenza Virus mRNA Vaccines

Non-replicating mRNA vaccines can be made with the incorporation of various modified nucleosides, and much effort has been invested in the development of directly injectable non-replicating mRNA vaccines. There are several studies of non-replicating mRNA vaccines against influenza virus. Administration of IAV NP-encoding mRNA complexed in liposomes induced cytotoxic T-cell responses in mice (89). Intradermally immunized mice, ferrets, and pigs with various IAV HA-, NP-, and NA-encoding RNActive vaccines produced protective immune responses after a single immunization (90). Intravenous immunizations in mice using PR8 H1N1 IAV HA-encoding unmodified mRNA-lipid complexes showed elevation of T-cell activation after administration of a single dose (91). Together, it will be important to determine if and how these findings translate to clinical trials and vaccination.

INNATE IMMUNITY TO mRNA Vaccines

The innate immune system acts as the first line of host immune response against mRNA vaccination. During an mRNA vaccination, the mRNA can be recognized by various PRRs, including TLRs, RLRs, and NLRs, for the production of IFNs and proinflammatory cytokines. Prototypically, IFNs and proinflammatory cytokines are largely beneficial to the host and trigger induction of IFN-inducible genes and the infiltration of immune cells to remove vaccinated cells. However, dysregulated IFNs and proinflammatory cytokines drive inhibition of efficacy of mRNA vaccines, detrimental systemic hyperinflammation, and tissue damage. Therefore, appropriate purification of *in vitro* transcribed mRNA is critical for maximizing immunogen production and avoiding undesired innate immune activation.

TLR3 senses dsRNA longer than 45 base pairs and those derived from ssRNA forming secondary structures or from viral replication intermediates. TLR7 can recognize both dsRNA and ssRNA, whereas TLR8 only senses ssRNA (92). The activation of TLR7 can stimulate antigen presentation, cytokine release, and induce B-cell responses (93). In particular, RIG-I senses ssRNA and dsRNA bearing a 5′-triphosphate and stimulates IFN production (44, 94).

mRNA vaccine-derived IFN production *via* RNA sensors is dependent on the quality of *in vitro* transcribed mRNA, the delivery vehicle, and the administration route. Recognition of *in vitro* transcribed mRNA contaminated with dsRNA cause rapid type I IFN induction, which upregulates the expression and activation of protein kinase R (PKR) and 2′-5′-oligoadenylate synthetase (OAS). This leads to the inhibition of translation and the degradation of cellular mRNA, ribosomal RNA, and *in vitro* transcribed mRNA (95–97) (**Figure 4**). Contaminating dsRNA can be efficiently removed from *in vitro* transcribed mRNA by chromatographic methods including reverse-phase fast protein liquid chromatography or high-performance liquid chromatography. Purification by these methods has been shown to increase antigen protein production from *in vitro* transcribed mRNA by up to about 1000-fold in human DCs (97). In addition to dsRNA contaminants, single-stranded mRNA molecules are recognized as a PAMP and detected by TLR7 and TLR8, resulting in type I IFN production and decreased antigen protein production from *in vitro* transcribed mRNA (98–100).

Given that reducing type I IFN signaling is critical for mRNA vaccine strategy, several studies revealed the development of modified mRNA that reduced type I IFN signaling. Incorporation of naturally occurring chemically modified nucleosides, including pseudouridine and 1-methylpseudouridine, prevented the activation of TLR7, TLR8, and other innate immune sensors, thereby reducing type I IFN signaling (27, 101–104). Another study also showed that nucleoside-modified mRNA translated better compared with that of unmodified mRNA *in vitro*, especially in primary DCs, and *in vivo* in mice (27, 103). Together, the balance between mRNA vaccines and the innate immune response is critical for potential vaccine approaches; this balance must be finely controlled to reduce excessive innate immune responses while retaining maximal immunogen production in DCs.

Note, that while the inflammasome-dependent release of IL-1b and IL-18 triggers further production in DCs for the induction of influenza virus-specific $CD8^+$ T-cell priming (49, 105), whether *in vitro* transcribed mRNA can be recognized by inflammasome sensors remains largely unknown. Future studies are needed to fully examine the factors required for the inflammasome-driven adaptive immune response.

mRNA-Based Influenza Virus Vaccine Development

mRNA vaccines have lately attracted substantial attention, involved massive academic and industrial investment, and biotechnology companies have succeeded in raising capital for the development of innovative RNA vaccines. The first directly injectable influenza RNA vaccine against H10N8 and H7N9 was developed by scientists at Moderna Therapeutics (USA), who demonstrated that it was possible to induce protective immunogenicity with acceptable tolerability profiles (106, 107). For the first human seasonal influenza virus RNA vaccine trial, CureVac AG company (Germany) developed a sequence-engineered mRNA-lipid nanoparticle strategy that enables an extraordinary level of *in vivo* protein translation without the use of modified nucleosides (29). Using this strategy, a recent study demonstrated that a single intramuscular immunization with 10 μg of A/Netherlands/602/2009 (H1N1) HA-encoding mRNA-lipid nanoparticles induce hemagglutination inhibition titers in the protective range (≥1:40) in non-human primates. Moreover,

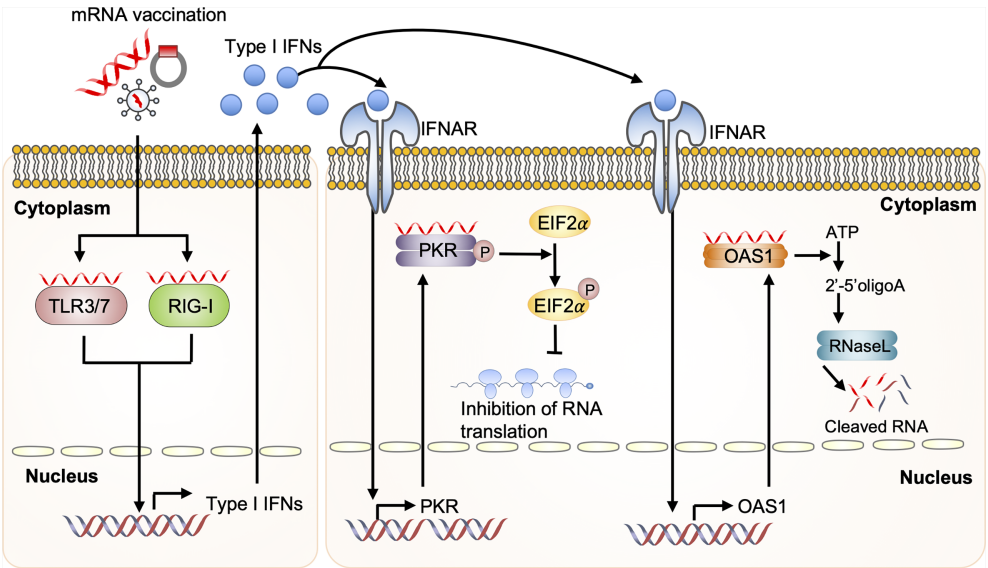

FIGURE 4 | Dysregulated innate immunity prevents mRNA vaccine efficacy Upon mRNA vaccination, incoming self-amplifying RNA (saRNA) is recognized by the Toll-like receptor (TLR) 3, TLR7, and retinoic acid-inducible gene I (RIG-I), which promotes their downstream signaling and consequent production of type I interferon (IFN). Recognition of *in vitro* transcribed mRNA contaminated with dsRNA causes rapid type I IFN production, which induces the expression and activation of protein kinase R (PKR) and 2′-5′-oligoadenylate synthetase (OAS). This will inhibit the translation and induce the degradation of cellular mRNA, ribosomal RNA, and *in vitro* transcribed mRNA. EIF2a, eukaryotic initiation factor 2a; IFNAR, interferon-alpha receptor.

inoculation of a second dose effectively boosted immune responses and resulted in hemagglutination inhibition titers ≥1:160 for over 1 year in all vaccinated animals (108). CureVac AG scientists provided evidence that two immunizations with mRNA-lipid nanoparticles encoding for HA from A/Hong Kong/4801/2014 (H3N2) induced stronger T- and B-cell immune responses than the licensed MF59-adjuvanted trivalent inactivated IAV vaccine.

LIMITATIONS OF mRNA Vaccine

mRNA vaccine-associated hypersensitivity reactions are not often observed. Similarly, severe acute-onset, presumably immunoglobulin-E (IgE)- or immunoglobulin-G (IgG)-mediated, and complement-mediated anaphylactic or severe delayed-onset T-cell-mediated systemic responses are considered very rare. Hypersensitivity to the active antigen of the vaccine can also be developed. Acute hypersensitivity responses following vaccination include self-limited local side effects and systemic responses can range from urticaria/angioedema to full-scale anaphylaxis with multisystem involvement (109).

Anaphylaxis is a rare life-threatening allergic reaction that usually occurs within minutes to hours after vaccination (109). Anaphylaxis induced by vaccines is generally rare. The coronavirus disease 2019 (COVID-19) pandemic highlighted the need for robust vaccine production *via* mRNA vaccines derived in lipid nanoparticles. Unexpectedly, there are fewer serious allergic reactions due to public vaccines and, as a result, there are considerable public concerns centered on atopic individuals. Previous research on the immune mechanism of vaccine-related anaphylaxis has focused on the presence of gelatin, latex, and egg proteins, and more recently on polysorbate 80, a widely used surfactant present in many vaccines (110). However, all of the above-mentioned excipients were not included in the Pfizer-BioNTech COVID-19 mRNA vaccine and no cases of anaphylaxis were observed in large-scale phase 2/3 clinical trials; thus, these events are unexpected (111, 112). Hence, occurrence of anaphylaxis upon initial exposure to the COVID-19 vaccine refers to pre-existing antibody-mediated immunity (allergy) or a pseudo-allergic reaction unrelated to previous exposure.

Anaphylaxis associated with known allergens is best understood through the classical paradigm of crosslinked IgE bound to fragment crystallizable region (Fc) ϵ receptors of mast cells and basophils, but nonclassical pathways including antibody-dependent activation of complement or IgG-associated mast cell/granulocyte/platelet/basophil-mediated mast cell/granulocyte/platelet/basophil activation *via* Fcγ receptors has been described in animal models and in human allergic responses to drugs (113–117). Unfortunately, information on the potential use of vaccines for testing to confirm the pathological etiology or predict reactivity risk remain scarce.

A rapid and thorough study-based evaluation of patients who have experienced anaphylactic vaccine reactions and prospective clinical trials in individuals at risk are requested to address these concerns during the public health crisis.

CONCLUSIONS AND FUTURE RESEARCH DIRECTIONS

We have highlighted the innate immune system response during IAV mRNA vaccination. Optimal innate immune sensing and inflammatory cytokine release are essential for T- and B-cell immune responses. However, excessive host innate immune responses possibly lead to cytokine storms and/or tissue damage (118, 119), inhibiting the efficacy of influenza virus mRNA vaccines. Therefore, mRNA-induced innate immunity must be controlled to reduce excessive inflammation while retaining antibody production.

Over the past decade, there has been a clear breakthrough in the field of influenza virus mRNA vaccines, demonstrating proof-of-concept in both preclinical and clinical settings (20). However, reducing the innate immune sensing of mRNA and maximizing translatability of the promising animal data to humans remains challenging. Further clinical trials examining the long-term safety and immunogenicity are required to evaluate the impact of RNA vaccines on the influenza virus vaccine field.

Currently, the COVID-19 pandemic continues to spread globally, urgently requiring effective vaccines to fight it. FDA-approved mRNA vaccines are greatly effective in working-age adults at preventing SARS-CoV-2 infection, with the vaccines attenuating the viral RNA load, risk of febrile symptoms, and duration of illness among those who have breakthrough infection despite vaccination (120). The future of mRNA vaccine field is potential, and the clinical data and resources provided by the associated companies and other academic institutions are likely to significantly build on and strengthen basic research into mRNA-based vaccines.

AUTHOR CONTRIBUTIONS

SL and J-HR conceived the outline of the manuscript. SL and J-HR. wrote the manuscript. SL and J-HR critically revised and approved the final version of the manuscript. All authors contributed to the article and approved the submitted version.

FUNDING

This research was supported in part by grants-in-aid from the Ministry of Education, Culture, Sports, Science, and Technology of Japan (19K16665 to SL).

ACKNOWLEDGMENTS

We apologize to our colleagues in the field whose work could not be cited due to space limitations. We thank all the members of the Biorchestra corporation for their comments and suggestions.

REFERENCES

1. Zhang C, Maruggi G, Shan H, Li J. Advances in mRNA Vaccines for Infectious Diseases. *Front Immunol* (2019) 10:594. doi: 10.3389/fimmu.2019.00594
2. Iwasaki A, Pillai PS. Innate Immunity to Influenza Virus Infection. *Nat Rev Immunol* (2014) 14(5):315–28. doi: 10.1038/nri3665
3. Iuliano AD, Roguski KM, Chang HH, Muscatello DJ, Palekar R, Tempia S, et al. Estimates of Global Seasonal Influenza-Associated Respiratory Mortality: A Modelling Study. *Lancet* (2018) 391(10127):1285–300. doi: 10.1016/S0140-6736(17)33293-2
4. Segaloff H, Melidou A, Adlhoch C, Pereyaslov D, Robesyn E, Penttinen P, et al. Co-Circulation of Influenza A(H1N1)pdm09 and Influenza A(H3N2) Viruses, World Health Organization (WHO) European Region, October 2018 to February 2019. *Euro Surveill* (2019) 24(9):1900125. doi: 10.2807/1560-7917.ES.2019.24.9.1900125
5. Gerdil C. The Annual Production Cycle for Influenza Vaccine. *Vaccine* (2003) 21(16):1776–9. doi: 10.1016/s0264-410x(03)00071-9
6. Seubert A, Monaci E, Pizza M, O'Hagan DT, Wack A. The Adjuvants Aluminum Hydroxide and MF59 Induce Monocyte and Granulocyte Chemoattractants and Enhance Monocyte Differentiation Toward Dendritic Cells. *J Immunol* (2008) 180(8):5402–12. doi: 10.4049/jimmunol.180.8.5402
7. Johnson NP, Mueller J. Updating the Accounts: Global Mortality of the 1918-1920 "Spanish" Influenza Pandemic. *Bull Hist Med* (2002) 76(1):105–15. doi: 10.1353/bhm.2002.0022
8. Palese P, Wang TT. Why do Influenza Virus Subtypes Die Out? A Hypothesis. *mBio* (2011) 2(5):e00150–11. doi: 10.1128/mBio.00150-11
9. Ross TM. Universal Influenza Vaccine Approaches Using Full-Length or Head-Only Hemagglutinin Proteins. *J Infect Dis* (2019) 219(Suppl_1):S57–61. doi: 10.1093/infdis/jiz004
10. Rodrigues CMC, Pinto MV, Sadarangani M, Plotkin SA. Whither Vaccines? *J Infect* (2017) 74 Suppl 1:S2–9. doi: 10.1016/S0163-4453(17)30184-6
11. Russell K, Chung JR, Monto AS, Martin ET, Belongia EA, McLean HQ, et al. Influenza Vaccine Effectiveness in Older Adults Compared With Younger Adults Over Five Seasons. *Vaccine* (2018) 36(10):1272–8. doi: 10.1016/j.vaccine.2018.01.045
12. Belshe RB, Edwards KM, Vesikari T, Black SV, Walker RE, Hultquist M, et al. Live-Attenuated Versus Inactivated Influenza Vaccine in Infants and Young Children. *N Engl J Med* (2007) 356(7):685–96. doi: 10.1056/NEJMoa065368
13. Li B, Fang L, Xu Z, Liu S, Gao J, Jiang Y, et al. Recombination in Vaccine and Circulating Strains of Porcine Reproductive and Respiratory Syndrome Viruses. *Emerg Infect Dis* (2009) 15(12):2032–5. doi: 10.3201/eid1512.090390
14. Zhou B, Meliopoulos VA, Wang W, Lin X, Stucker KM, Halpin RA, et al. Reversion of Cold-Adapted Live-Attenuated Influenza Vaccine Into a Pathogenic Virus. *J Virol* (2016) 90(19):8454–63. doi: 10.1128/JVI.00163-16
15. Lee S, Hirohama M, Noguchi M, Nagata K, Kawaguchi A. Influenza A Virus Infection Triggers Pyroptosis and Apoptosis of Respiratory Epithelial Cells Through the Type I Interferon Signaling Pathway in a Mutually Exclusive Manner. *J Virol* (2018) 92(14):e00396–18. doi: 10.1128/JVI.00396-18
16. Lee S, Ishitsuka A, Noguchi M, Hirohama M, Fujiyasu Y, Petric PP, et al. Influenza Restriction Factor Mxa Functions as Inflammasome Sensor in the Respiratory Epithelium. *Sci Immunol* (2019) 4(40):eaau4643. doi: 10.1126/sciimmunol.aau4643
17. Högner K, Wolff T, Pleschka S, Plog S, Gruber AD, Kalinke U, et al. Macrophage-Expressed IFN-β Contributes to Apoptotic Alveolar Epithelial Cell Injury in Severe Influenza Virus Pneumonia. *PloS Pathog* (2013) 9(2):e1003188. doi: 10.1371/journal.ppat.1003188
18. Kallfass C, Lienenklaus S, Weiss S, Staeheli P. Visualizing the Beta Interferon Response in Mice During Infection With Influenza A Viruses Expressing or Lacking Nonstructural Protein 1. *J Virol* (2013) 87(12):6925–30. doi: 10.1128/JVI.00283-13
19. Jewell NA, Vaghefi N, Mertz SE, Akter P, Peebles RSJr., Bakaletz LO, et al. Differential Type I Interferon Induction by Respiratory Syncytial Virus and Influenza a Virus In Vivo. *J Virol* (2007) 81(18):9790–800. doi: 10.1128/JVI.00530-07

20. Pardi N, Hogan MJ, Porter FW, Weissman D. mRNA Vaccines - a New Era in Vaccinology. *Nat Rev Drug Discov* (2018) 17(4):261–79. doi: 10.1038/nrd.2017.243
21. Heine A, Juranek S, Brossart P. Clinical and Immunological Effects of mRNA Vaccines in Malignant Diseases. *Mol Cancer* (2021) 20(1):52. doi: 10.1186/s12943-021-01339-1
22. Pardi N, Parkhouse K, Kirkpatrick E, McMahon M, Zost SJ, Mui BL, et al. Nucleoside-Modified Mrna Immunization Elicits Influenza Virus Hemagglutinin Stalk-Specific Antibodies. *Nat Commun* (2018) 9(1):3361. doi: 10.1038/s41467-018-05482-0
23. Sacks D, Baxter B, Campbell BCV, Carpenter JS, Cognard C, Dippel D, et al. Multisociety Consensus Quality Improvement Revised Consensus Statement for Endovascular Therapy of Acute Ischemic Stroke. *Int J Stroke* (2018) 13 (6):612–32. doi: 10.1177/1747493018778713
24. Teijaro JR, Farber DL. COVID-19 Vaccines: Modes of Immune Activation and Future Challenges. *Nat Rev Immunol* (2021) 21(4):195–7. doi: 10.1038/s41577-021-00526-x
25. Wolff JA, Malone RW, Williams P, Chong W, Acsadi G, Jani A, et al. Direct Gene Transfer Into Mouse Muscle In Vivo. *Science* (1990) 247(4949 Pt 1):1465–8. doi: 10.1126/science.1690918
26. Jirikowski GF, Sanna PP, Maciejewski-Lenoir D, Bloom FE. Reversal of Diabetes Insipidus in Brattleboro Rats: Intrahypothalamic Injection of Vasopressin mRNA. *Science* (1992) 255(5047):996–8. doi: 10.1126/science.1546298
27. Karikó K, Muramatsu H, Welsh FA, Ludwig J, Kato H, Akira S, et al. Incorporation of Pseudouridine Into mRNA Yields Superior Nonimmunogenic Vector With Increased Translational Capacity and Biological Stability. *Mol Ther* (2008) 16(11):1833–40. doi: 10.1038/mt.2008.200
28. Guan S, Rosenecker J. Nanotechnologies in Delivery of mRNA Therapeutics Using Nonviral Vector-Based Delivery Systems. *Gene Ther* (2017) 24 (3):133–43. doi: 10.1038/gt.2017.5
29. Thess A, Grund S, Mui BL, Hope MJ, Baumhof P, Fotin-Mleczek M, et al. Sequence-Engineered mRNA Without Chemical Nucleoside Modifications Enables an Effective Protein Therapy in Large Animals. *Mol Ther* (2015) 23 (9):1456–64. doi: 10.1038/mt.2015.103
30. Kauffman KJ, Webber MJ, Anderson DG. Materials for Non-Viral Intracellular Delivery of Messenger RNA Therapeutics. *J Control Release* (2016) 240:227–34. doi: 10.1016/j.jconrel.2015.12.032
31. Lindgren G, Ols S, Liang F, Thompson EA, Lin A, Hellgren F, et al. Induction of Robust B Cell Responses After Influenza Mrna Vaccination Is Accompanied by Circulating Hemagglutinin-Specific ICOS+ PD-1+ CXCR3+ T Follicular Helper Cells. *Front Immunol* (2017) 8:1539. doi: 10.3389/fimmu.2017.01539
32. Lindsay KE, Bhosle SM, Zurla C, Beyersdorf J, Rogers KA, Vanover D, et al. Visualization of Early Events in mRNA Vaccine Delivery in Non-Human Primates *via* PET-CT and Near-Infrared Imaging. *Nat BioMed Eng* (2019) 3 (5):371–80. doi: 10.1038/s41551-019-0378-3
33. Heer AK, Shamshiev A, Donda A, Uematsu S, Akira S, Kopf M, et al. TLR Signaling Fine-Tunes Anti-Influenza B Cell Responses Without Regulating Effector T Cell Responses. *J Immunol* (2007) 178(4):2182–91. doi: 10.4049/jimmunol.178.4.2182
34. Lund JM, Alexopoulou L, Sato A, Karow M, Adams NC, Gale NW, et al. Recognition Of Single-Stranded RNA Viruses by Toll-Like Receptor 7. *Proc Natl Acad Sci USA* (2004) 101(15):5598–603. doi: 10.1073/pnas.0400937101
35. Diebold SS, Kaisho T, Hemmi H, Akira S, Reis e Sousa C. Innate Antiviral Responses by Means of TLR7-Mediated Recognition of Single-Stranded RNA. *Science* (2004) 303(5663):1529–31. doi: 10.1126/science.1093616
36. Kato H, Sato S, Yoneyama M, Yamamoto M, Uematsu S, Matsui K, et al. Cell Type-Specific Involvement of RIG-I in Antiviral Response. *Immunity* (2005) 23(1):19–28. doi: 10.1016/j.immuni.2005.04.010
37. Wang JP, Bowen GN, Padden C, Cerny A, Finberg RW, Newburger PE, et al. Toll-Like Receptor-Mediated Activation of Neutrophils by Influenza A Virus. *Blood* (2008) 112(5):2028–34. doi: 10.1182/blood-2008-01-132860
38. Le Goffic R, Balloy V, Lagranderie M, Alexopoulou L, Escriou N, Flavell R, et al. Detrimental Contribution of the Toll-Like Receptor (TLR)3 to Influenza A Virus-Induced Acute Pneumonia. *PloS Pathog* (2006) 2(6): e53. doi: 10.1371/journal.ppat.0020053
39. Sasai M, Linehan MM, Iwasaki A. Bifurcation of Toll-Like Receptor 9 Signaling by Adaptor Protein 3. *Science* (2010) 329(5998):1530–4. doi: 10.1126/science.1187029
40. Honda K, Ohba Y, Yanai H, Negishi H, Mizutani T, Takaoka A, et al. Spatiotemporal Regulation of MyD88-IRF-7 Signalling for Robust Type-I Interferon Induction. *Nature* (2005) 434(7036):1035–40. doi: 10.1038/nature03547
41. Lande R, Gregorio J, Facchinetti V, Chatterjee B, Wang YH, Homey B, et al. Plasmacytoid Dendritic Cells Sense Self-DNA Coupled With Antimicrobial Peptide. *Nature* (2007) 449(7162):564–9. doi: 10.1038/nature06116
42. Pichlmair A, Schulz O, Tan CP, Näslund TI, Liljeström P, Weber F, et al. RIG-I-Mediated Antiviral Responses to Single-Stranded RNA Bearing 5'-Phosphates. *Science* (2006) 314(5801):997–1001. doi: 10.1126/science.1132998
43. Hornung V, Ellegast J, Kim S, Brzózka K, Jung A, Kato H, et al. 5'-Triphosphate RNA Is the Ligand for RIG-I. *Science* (2006) 314(5801):994–7. doi: 10.1126/science.1132505
44. Rehwinkel J, Tan CP, Goubau D, Schulz O, Pichlmair A, Bier K, et al. RIG-I Detects Viral Genomic RNA During Negative-Strand RNA Virus Infection. *Cell* (2010) 140(3):397–408. doi: 10.1016/j.cell.2010.01.020
45. Jiang F, Ramanathan A, Miller MT, Tang GQ, Gale MJr., Patel SS, et al. Structural Basis of RNA Recognition and Activation by Innate Immune Receptor RIG-I. *Nature* (2011) 479(7373):423–7. doi: 10.1038/nature10537
46. Kowalinski E, Lunardi T, McCarthy AA, Louber J, Brunel J, Grigorov B, et al. Structural Basis for the Activation of Innate Immune Pattern-Recognition Receptor RIG-I By Viral RNA. *Cell* (2011) 147(2):423–35. doi: 10.1016/j.cell.2011.09.039
47. Thomas PG, Dash P, Aldridge JRJr., Ellebedy AH, Reynolds C, Funk AJ, et al. The Intracellular Sensor NLRP3 Mediates Key Innate and Healing Responses to Influenza A Virus Via The Regulation of Caspase-1. *Immunity* (2009) 30(4):566–75. doi: 10.1016/j.immuni.2009.02.006
48. Allen IC, Scull MA, Moore CB, Holl EK, McElvania-TeKippe E, Taxman DJ, et al. The NLRP3 Inflammasome Mediates In Vivo Innate Immunity to Influenza A Virus Through Recognition of Viral RNA. *Immunity* (2009) 30 (4):556–65. doi: 10.1016/j.immuni.2009.02.005
49. Ichinohe T, Lee HK, Ogura Y, Flavell R, Iwasaki A. Inflammasome Recognition of Influenza Virus Is Essential for Adaptive Immune Responses. *J Exp Med* (2009) 206(1):79–87. doi: 10.1084/jem.20081667
50. Kuriakose T, Man SM, Malireddi RK, Karki R, Kesavardhana S, Place DE, et al. ZBP1/DAI Is An Innate Sensor of Influenza Virus Triggering the NLRP3 Inflammasome and Programmed Cell Death Pathways. *Sci Immunol* (2016) 1(2):aag2045. doi: 10.1126/sciimmunol.aag2045
51. Kesavardhana S, Kuriakose T, Guy CS, Samir P, Malireddi RKS, Mishra A, et al. ZBP1/DAI Ubiquitination and Sensing of Influenza Vrnps Activate Programmed Cell Death. *J Exp Med* (2017) 214(8):2217–29. doi: 10.1084/jem.20170550
52. Zhang T, Yin C, Boyd DF, Quarato G, Ingram JP, Shubina M, et al. Influenza Virus Z-RNAs Induce ZBP1-Mediated Necroptosis. *Cell* (2020) 180 (6):1115–29.e13. doi: 10.1016/j.cell.2020.02.050
53. Zheng M, Karki R, Vogel P, Kanneganti TD. Caspase-6 Is a Key Regulator of Innate Immunity, Inflammasome Activation, and Host Defense. *Cell* (2020) 181(3):674–87.e13. doi: 10.1016/j.cell.2020.03.040
54. Hufford MM, Kim TS, Sun J, Braciale TJ. The Effector T Cell Response to Influenza Infection. *Curr Top Microbiol Immunol* (2015) 386:423–55. doi: 10.1007/82_2014_397
55. Wrammert J, Smith K, Miller J, Langley WA, Kokko K, Larsen C, et al. Rapid Cloning of High-Affinity Human Monoclonal Antibodies Against Influenza Virus. *Nature* (2008) 453(7195):667–71. doi: 10.1038/nature06890
56. Ellebedy AH, Jackson KJ, Kissick HT, Nakaya HI, Davis CW, Roskin KM, et al. Defining Antigen-Specific Plasmablast and Memory B Cell Subsets in Human Blood After Viral Infection Or Vaccination. *Nat Immunol* (2016) 17 (10):1226–34. doi: 10.1038/ni.3533
57. Lau D, Lan LY, Andrews SF, Henry C, Rojas KT, Neu KE, et al. Low CD21 Expression Defines A Population of Recent Germinal Center Graduates Primed For Plasma Cell Differentiation. *Sci Immunol* (2017) 2(7):eaai8153. doi: 10.1126/sciimmunol.aai8153
58. Salk JE, Pearson HE, Brown PN, Francis T. Protective Effect of Vaccination Against Induced Influenza B. *J Clin Invest* (1945) 24(4):547–53. doi: 10.1172/JCI101634

59. Francis T, Salk JE, Pearson HE, Brown PN. Protective Effect of Vaccination Against Induced Influenza a. *J Clin Invest* (1945) 24(4):536–46. doi: 10.1172/JCI101633
60. Audsley JM, Tannock GA. Cell-Based Influenza Vaccines: Progress to Date. *Drugs* (2008) 68(11):1483–91. doi: 10.2165/00003495-200868110-00002
61. Tricco AC, Chit A, Soobiah C, Hallett D, Meier G, Chen MH, et al. Comparing Influenza Vaccine Efficacy Against Mismatched and Matched Strains: A Systematic Review and Meta-Analysis. *BMC Med* (2013) 11:153. doi: 10.1186/1741-7015-11-153
62. Jin H, Subbarao K. Live-Attenuated Influenza Vaccine. *Curr Top Microbiol Immunol* (2015) 386:181–204. doi: 10.1007/82_2014_410
63. Maassab HF. Adaptation and Growth Characteristics of Influenza Virus at 25 Degrees C. *Nature* (1967) 213(5076):612–4. doi: 10.1038/213612a0
64. Alexandrova GI, Budilovsky GN, Koval TA, Polezhaev FI, Garmashova LM, Ghendon Yu Z, et al. Study of Live Recombinant Cold-Adapted Influenza Bivalent Vaccine of Type A For Use in Children: An Epidemiological Control Trial. *Vaccine* (1986) 4(2):114–8. doi: 10.1016/0264-410x(86)90049-6
65. Beyer WE, McElhaney J, Smith DJ, Monto AS, Nguyen-Van-Tam JS, Osterhaus AD. Cochrane Re-Arranged: Support for Policies to Vaccinate Elderly People Against Influenza. *Vaccine* (2013) 31(50):6030–3. doi: 10.1016/j.vaccine.2013.09.063
66. Ohmit SE, Petrie JG, Malosh RE, Cowling BJ, Thompson MG, Shay DK, et al. Influenza Vaccine Effectiveness in the Community and the Household. *Clin Infect Dis* (2013) 56(10):1363–9. doi: 10.1093/cid/cit060
67. de Jong JC, Beyer WE, Palache AM, Rimmelzwaan GF, Osterhaus AD. Mismatch Between the 1997/1998 Influenza Vaccine and the Major Epidemic A(H3N2) Virus Strain as the Cause of an Inadequate Vaccine-Induced Antibody Response to This Strain in the Elderly. *J Med Virol* (2000) 61(1):94–9. doi: 10.1002/(SICI)1096-9071(200005)61:1<94::AID-JMV15>3.0.CO;2-C
68. Flannery B, Kondor RJG, Chung JR, Gaglani M, Reis M, Zimmerman RK, et al. Spread of Antigenically Drifted Influenza A(H3N2) Viruses and Vaccine Effectiveness in the United States During the 2018-2019 Season. *J Infect Dis* (2020) 221(1):8–15. doi: 10.1093/infdis/jiz543
69. Kissling E, Valenciano M, Larrauri A, Oroszi B, Cohen JM, Nunes B, et al. Low and Decreasing Vaccine Effectiveness Against Influenza A(H3) in 2011/12 Among Vaccination Target Groups In Europe: Results From The I-MOVE Multicentre Case-Control Study. *Euro Surveill* (2013) 18(5):20390. doi: 10.2807/ese.18.05.20390-en
70. Clark A, Potter CW, Jennings R, Nicholl JP, Langrick AF, Schild GC, et al. A Comparison of Live and Inactivated Influenza A (H1N1) Virus Vaccines. 2. Long-Term Immunity. *J Hyg (Lond)* (1983) 90(3):361–70. doi: 10.1017/s0022172400028990
71. DiazGranados CA, Dunning AJ, Kimmel M, Kirby D, Treanor J, Collins A, et al. Efficacy of High-Dose Versus Standard-Dose Influenza Vaccine in Older Adults. *N Engl J Med* (2014) 371(7):635–45. doi: 10.1056/NEJMoa1315727
72. O'Hagan DT, Ott GS, Nest GV, Rappuoli R, Giudice GD. The History of MF59(®) Adjuvant: A Phoenix That Arose From the Ashes. *Expert Rev Vaccines* (2013) 12(1):13–30. doi: 10.1586/erv.12.140
73. Del Giudice G, Rappuoli R. Inactivated and Adjuvanted Influenza Vaccines. *Curr Top Microbiol Immunol* (2015) 386:151–80. doi: 10.1007/82_2014_406
74. Ledgerwood JE. AS03-Adjuvanted Influenza Vaccine in Elderly People. *Lancet Infect Dis* (2013) 13(6):466–7. doi: 10.1016/S1473-3099(13)70038-0
75. Wei CJ, Crank MC, Shiver J, Graham BS, Mascola JR, Nabel GJ. Next-Generation Influenza Vaccines: Opportunities and Challenges. *Nat Rev Drug Discovery* (2020) 19(4):239–52. doi: 10.1038/s41573-019-0056-x
76. Kistner O, Howard MK, Spruth M, Wodal W, Brühl P, Gerencer M, et al. Cell Culture (Vero) Derived Whole Virus (H5N1) Vaccine Based on Wild-Type Virus Strain Induces Cross-Protective Immune Responses. *Vaccine* (2007) 25(32):6028–36. doi: 10.1016/j.vaccine.2007.05.013
77. Baz M, Luke CJ, Cheng X, Jin H, Subbarao K. H5N1 Vaccines in Humans. *Virus Res* (2013) 178(1):78–98. doi: 10.1016/j.virusres.2013.05.006
78. Belshe RB, Frey SE, Graham IL, Anderson EL, Jackson LA, Spearman P, et al. Immunogenicity of Avian Influenza A/Anhui/01/2005(H5N1) Vaccine With MF59 Adjuvant: A Randomized Clinical Trial. *Jama* (2014) 312(14):1420–8. doi: 10.1001/jama.2014.12609
79. Mulligan MJ, Bernstein DI, Winokur P, Rupp R, Anderson E, Rouphael N, et al. Serological Responses to an Avian Influenza A/H7N9 Vaccine Mixed at the Point-Of-Use With MF59 Adjuvant: A Randomized Clinical Trial. *Jama* (2014) 312(14):1409–19. doi: 10.1001/jama.2014.12854
80. Vogel AB, Lambert L, Kinnear E, Busse D, Erbar S, Reuter KC, et al. Self-Amplifying RNA Vaccines Give Equivalent Protection Against Influenza to mRNA Vaccines But at Much Lower Doses. *Mol Ther* (2018) 26(2):446–55. doi: 10.1016/j.ymthe.2017.11.017
81. Berglund P, Smerdou C, Fleeton MN, Tubulekas I, Liljeström P. Enhancing Immune Responses Using Suicidal DNA Vaccines. *Nat Biotechnol* (1998) 16(6):562–5. doi: 10.1038/nbt0698-562
82. Zhou X, Berglund P, Zhao H, Liljeström P, Jondal M. Generation of Cytotoxic and Humoral Immune Responses by Nonreplicative Recombinant Semliki Forest Virus. *Proc Natl Acad Sci USA* (1995) 92(7):3009–13. doi: 10.1073/pnas.92.7.3009
83. Fleeton MN, Chen M, Berglund P, Rhodes G, Parker SE, Murphy M, et al. Self-Replicative RNA Vaccines Elicit Protection Against Influenza A Virus, Respiratory Syncytial Virus, and a Tickborne Encephalitis Virus. *J Infect Dis* (2001) 183(9):1395–8. doi: 10.1086/319857
84. Hekele A, Bertholet S, Archer J, Gibson DG, Palladino G, Brito LA, et al. Rapidly Produced SAM(®) Vaccine Against H7N9 Influenza Is Immunogenic in Mice. *Emerg Microbes Infect* (2013) 2(8):e52. doi: 10.1038/emi.2013.54
85. Magini D, Giovani C, Mangiavacchi S, Maccari S, Cecchi R, Ulmer JB, et al. Self-Amplifying Mrna Vaccines Expressing Multiple Conserved Influenza Antigens Confer Protection Against Homologous and Heterosubtypic Viral Challenge. *PloS One* (2016) 11(8):e0161193. doi: 10.1371/journal.pone.0161193
86. McCullough KC, Bassi I, Milona P, Suter R, Thomann-Harwood L, Englezou P, et al. Self-Replicating Replicon-RNA Delivery to Dendritic Cells by Chitosan-Nanoparticles for Translation In Vitro And In Vivo. *Mol Ther Nucleic Acids* (2014) 3(7):e173. doi: 10.1038/mtna.2014.24
87. Démoulins T, Milona P, Englezou PC, Ebensen T, Schulze K, Suter R, et al. Polyethylenimine-Based Polyplex Delivery of Self-Replicating RNA Vaccines. *Nanomedicine* (2016) 12(3):711–22. doi: 10.1016/j.nano.2015.11.001
88. Chahal JS, Khan OF, Cooper CL, McPartlan JS, Tsosie JK, Tilley LD, et al. Dendrimer-RNA Nanoparticles Generate Protective Immunity Against Lethal Ebola, H1N1 Influenza, and Toxoplasma Gondii Challenges With a Single Dose. *Proc Natl Acad Sci USA* (2016) 113(35):E5250. doi: 10.1073/pnas.1612792113
89. Martinon F, Krishnan S, Lenzen G, Magné R, Gomard E, Guillet JG, et al. Induction of Virus-Specific Cytotoxic T Lymphocytes In Vivo by Liposome-Entrapped mRNA. *Eur J Immunol* (1993) 23(7):1719–22. doi: 10.1002/eji.1830230749
90. Kallen KJ, Heidenreich R, Schnee M, Petsch B, Schlake T, Thess A, et al. A Novel, Disruptive Vaccination Technology: Self-Adjuvanted Rnactive(®) Vaccines. *Hum Vaccin Immunother* (2013) 9(10):2263–76. doi: 10.4161/hv.25181
91. Kranz LM, Diken M, Haas H, Kreiter S, Loquai C, Reuter KC, et al. Systemic RNA Delivery to Dendritic Cells Exploits Antiviral Defence for Cancer Immunotherapy. *Nature* (2016) 534(7607):396–401. doi: 10.1038/nature18300
92. Ablasser A, Poeck H, Anz D, Berger M, Schlee M, Kim S, et al. Selection of Molecular Structure and Delivery of RNA Oligonucleotides to Activate TLR7 Versus TLR8 and to Induce High Amounts of IL-12p70 in Primary Human Monocytes. *J Immunol* (2009) 182(11):6824–33. doi: 10.4049/jimmunol.0803001
93. Hua Z, Hou B. TLR Signaling in B-Cell Development and Activation. *Cell Mol Immunol* (2013) 10(2):103–6. doi: 10.1038/cmi.2012.61
94. Goubau D, Schlee M, Deddouche S, Pruijssers AJ, Zillinger T, Goldeck M, et al. Antiviral Immunity Via RIG-I-Mediated Recognition of RNA Bearing 5'-Diphosphates. *Nature* (2014) 514(7522):372–5. doi: 10.1038/nature13590
95. Karikó K, Muramatsu H, Ludwig J, Weissman D. Generating the Optimal mRNA for Therapy: HPLC Purification Eliminates Immune Activation and Improves Translation of Nucleoside-Modified, Protein-Encoding mRNA. *Nucleic Acids Res* (2011) 39(21):e142. doi: 10.1093/nar/gkr695
96. de Haro C, Méndez R, Santoyo J. The eIF-2alpha Kinases and the Control of Protein Synthesis. *FASEB J* (1996) 10(12):1378–87. doi: 10.1096/fasebj.10.12.8903508

97. Liang SL, Quirk D, Zhou A. RNase L: Its Biological Roles and Regulation. *IUBMB Life* (2006) 58(9):508–14. doi: 10.1080/15216540600838232
98. Zhang Z, Ohto U, Shibata T, Krayukhina E, Taoka M, Yamauchi Y, et al. Structural Analysis Reveals That Toll-Like Receptor 7 Is a Dual Receptor for Guanosine and Single-Stranded RNA. *Immunity* (2016) 45(4):737–48. doi: 10.1016/j.immuni.2016.09.011
99. Tanji H, Ohto U, Shibata T, Taoka M, Yamauchi Y, Isobe T, et al. Toll-Like Receptor 8 Senses Degradation Products of Single-Stranded RNA. *Nat Struct Mol Biol* (2015) 22(2):109–15. doi: 10.1038/nsmb.2943
100. Isaacs A, Cox RA, Rotem Z. Foreign Nucleic Acids as the Stimulus to Make Interferon. *Lancet* (1963) 2(7299):113–6. doi: 10.1016/s0140-6736(63)92585-6
101. Schwartz S, Bernstein DA, Mumbach MR, Jovanovic M, Herbst RH, León-Ricardo BX, et al. Transcriptome-Wide Mapping Reveals Widespread Dynamic-Regulated Pseudouridylation of ncRNA and mRNA. *Cell* (2014) 159(1):148–62. doi: 10.1016/j.cell.2014.08.028
102. Carlile TM, Rojas-Duran MF, Zinshteyn B, Shin H, Bartoli KM, Gilbert WV. Pseudouridine Profiling Reveals Regulated Mrna Pseudouridylation in Yeast and Human Cells. *Nature* (2014) 515(7525):143–6. doi: 10.1038/nature13802
103. Andries O, Mc Cafferty S, De Smedt SC, Weiss R, Sanders NN, Kitada T. N(1)-Methylpseudouridine-Incorporated mRNA Outperforms Pseudouridine-Incorporated mRNA by Providing Enhanced Protein Expression and Reduced Immunogenicity in Mammalian Cell Lines and Mice. *J Control Release* (2015) 217:337–44. doi: 10.1016/j.jconrel.2015.08.051
104. Karikó K, Buckstein M, Ni H, Weissman D. Suppression of RNA Recognition by Toll-Like Receptors: The Impact of Nucleoside Modification and the Evolutionary Origin of RNA. *Immunity* (2005) 23 (2):165–75. doi: 10.1016/j.immuni.2005.06.008
105. Pang IK, Ichinohe T , Iwasaki A. IL-1r Signaling in Dendritic Cells Replaces Pattern-Recognition Receptors in Promoting $CD8^+$ T Cell Responses to Influenza A Virus. *Nat Immunol* (2013) 14(3):246–53. doi: 10.1038/ni.2514
106. Bahl K, Senn JJ, Yuzhakov O, Bulychev A, Brito LA, Hassett KJ, et al. Preclinical and Clinical Demonstration of Immunogenicity by mRNA Vaccines Against H10N8 and H7N9 Influenza Viruses. *Mol Ther* (2017) 25(6):1316–27. doi: 10.1016/j.ymthe.2017.03.035
107. Feldman RA, Fuhr R, Smolenov I, Mick Ribeiro A, Panther L, Watson M, et al. mRNA Vaccines Against H10N8 and H7N9 Influenza Viruses of Pandemic Potential Are Immunogenic and Well Tolerated in Healthy Adults in Phase 1 Randomized Clinical Trials. *Vaccine* (2019) 37(25):3326–34. doi: 10.1016/j.vaccine.2019.04.074
108. Lutz J, Lazzaro S, Habbeddine M, Schmidt KE, Baumhof P, Mui BL, et al. Unmodified mRNA in LNPs Constitutes a Competitive Technology for Prophylactic Vaccines. *NPJ Vaccines* (2017) 2:29. doi: 10.1038/s41541-017-0032-6
109. McNeil MM, DeStefano F. Vaccine-Associated Hypersensitivity. *J Allergy Clin Immunol* (2018) 141(2):463–72. doi: 10.1016/j.jaci.2017.12.971
110. Stone CAJr., Rukasin CRF, Beachkofsky TM, Phillips EJ. Immune-Mediated Adverse Reactions to Vaccines. *Br J Clin Pharmacol* (2019) 85(12):2694–706. doi: 10.1111/bcp.14112
111. Polack FP, Thomas SJ, Kitchin N, Absalon J, Gurtman A, Lockhart S, et al. Safety and Efficacy of the BNT162b2 mRNA Covid-19 Vaccine. *N Engl J Med* (2020) 383(27):2603–15. doi: 10.1056/NEJMoa2034577
112. Baden LR, El Sahly HM, Essink B, Kotloff K, Frey S, Novak R, et al. Efficacy and Safety of the mRNA-1273 SARS-CoV-2 Vaccine. *N Engl J Med* (2021) 384(5):403–16. doi: 10.1056/NEJMoa2035389
113. Finkelman FD, Khodoun MV, Strait R. Human IgE-Independent Systemic Anaphylaxis. *J Allergy Clin Immunol* (2016) 137(6):1674–80. doi: 10.1016/j.jaci.2016.02.015
114. Jimenez-Rodriguez TW, Garcia-Neuer M, Alenazy LA, Castells M. Anaphylaxis in the 21st Century: Phenotypes, Endotypes, and Biomarkers. *J Asthma Allergy* (2018) 11:121–42. doi: 10.2147/JAA.S159411
115. Jönsson F, de Chaisemartin L, Granger V, Gouel-Chéron A, Gillis CM, Zhu Q, et al. An IgG-Induced Neutrophil Activation Pathway Contributes to Human Drug-Induced Anaphylaxis. *Sci Transl Med* (2019) 11(500): eaat1479. doi: 10.1126/scitranslmed.aat1479
116. Balbino B, Herviou P, Godon O, Stackowicz J, Goff OR, Iannascoli B, et al. The Anti-IgE mAb Omalizumab Induces Adverse Reactions by Engaging Fcγ Receptors. *J Clin Invest* (2020) 130(3):1330–5. doi: 10.1172/JCI129697
117. Beutier H, Hechler B, Godon O, Wang Y, Gillis CM, de Chaisemartin L, et al. Platelets Expressing IgG Receptor Fcγriia/CD32A Determine the Severity of Experimental Anaphylaxis. *Sci Immunol* (2018) 3(22):eaan5997. doi: 10.1126/sciimmunol.aan5997
118. Karki R, Sharma BR, Tuladhar S, Williams EP, Zalduondo L, Samir P, et al. Synergism of TNF-α and IFN-γ Triggers Inflammatory Cell Death, Tissue Damage, and Mortality in SARS-CoV-2 Infection and Cytokine Shock Syndromes. *Cell* (2021) 184(1):149–68.e17. doi: 10.1016/j.cell.2020.11.025
119. Lee S, Channappanavar R, Kanneganti TD. Coronaviruses: Innate Immunity, Inflammasome Activation, Inflammatory Cell Death, and Cytokines. *Trends Immunol* (2020) 41(12):1083–99. doi: 10.1016/j.it.2020.10.005
120. Thompson MG, Burgess JL, Naleway AL, Tyner H, Yoon SK, Meece J, et al. Prevention and Attenuation of Covid-19 With the BNT162b2 and mRNA-1273 Vaccines. *N Engl J Med* (2021) 385:320–9. doi: 10.1056/NEJMoa2107058

Author Disclaimer: The content is solely the responsibility of the authors and does not necessarily represent the official views of the National Institutes of Health.

Conflict of Interest: Author J-HR was employed by company Biorchestra Co.

The remaining authors declare that the research was conducted in the absence of any commercial or financial relationships that could be construed as a potential conflict of interest.

Publisher's Note: All claims expressed in this article are solely those of the authors and do not necessarily represent those of their affiliated organizations, or those of the publisher, the editors and the reviewers. Any product that may be evaluated in this article, or claim that may be made by its manufacturer, is not guaranteed or endorsed by the publisher.

frontiers in Immunology

ORIGINAL RESEARCH
published: 16 September 2021
doi: 10.3389/fimmu.2021.746447

Mosaic Hemagglutinin-Based Whole Inactivated Virus Vaccines Induce Broad Protection Against Influenza B Virus Challenge in Mice

Yonghong Liu[1], Shirin Strohmeier[1], Irene González-Domínguez[1], Jessica Tan[1,2], Viviana Simon[1,2,3,4], Florian Krammer[1,4], Adolfo García-Sastre[1,2,3,4,5], Peter Palese[1,2] and Weina Sun[1]**

[1] Department of Microbiology, Icahn School of Medicine at Mount Sinai, New York, NY, United States, [2] Department of Medicine, Icahn School of Medicine at Mount Sinai, New York, NY, United States, [3] Global Health Emerging Pathogens Institute, Icahn School of Medicine at Mount Sinai, New York, NY, United States, [4] Department of Pathology, Molecular and Cell-Based Medicine, Icahn School of Medicine at Mount Sinai, New York, NY, United States, [5] The Tisch Cancer Institute, Icahn School of Medicine at Mount Sinai, New York, NY, United States

OPEN ACCESS

Edited by:
Rebecca Jane Cox,
University of Bergen, Norway

Reviewed by:
Oscar Taboga,
Instituto Nacional de Tecnología Agropecuaria, Argentina
Chunhong Dong,
Georgia State University, United States

***Correspondence:**
Peter Palese
peter.palese@mssm.edu
Weina Sun
weina.sun@mssm.edu

Specialty section:
This article was submitted to Vaccines and Molecular Therapeutics, a section of the journal Frontiers in Immunology

Received: 23 July 2021
Accepted: 31 August 2021
Published: 16 September 2021

Citation:
Liu Y, Strohmeier S, González-Domínguez I, Tan J, Simon V, Krammer F, García-Sastre A, Palese P and Sun W (2021) Mosaic Hemagglutinin-Based Whole Inactivated Virus Vaccines Induce Broad Protection Against Influenza B Virus Challenge in Mice. Front. Immunol. 12:746447. doi: 10.3389/fimmu.2021.746447

Influenza viruses undergo antigenic changes in the immuno-dominant hemagglutinin (HA) head domain, necessitating annual re-formulation of and re-vaccination with seasonal influenza virus vaccines for continuing protection. We previously synthesized mosaic HA (mHA) proteins of influenza B viruses which redirect the immune response towards the immuno-subdominant conserved epitopes of the HA *via* sequential immunization. As ~90% of current influenza virus vaccines are manufactured using the inactivated virus platform, we generated and sequentially vaccinated mice with inactivated influenza B viruses displaying either the homologous (same B HA backbones) or the heterologous (different B HA backbones) mosaic HAs. Both approaches induced long-lasting and cross-protective antibody responses showing strong antibody-dependent cellular cytotoxicity (ADCC) activity. We believe the B virus mHA vaccine candidates represent a major step towards a universal influenza B virus vaccine.

Keywords: influenza B virus, whole inactivated virus vaccine, immuno-subdominant epitopes, broad protection, universal influenza B vaccine

INTRODUCTION

Influenza B virus has been a significant public health burden on a global scale (1–3). Approximately 20 to 30% of all clinical influenza cases are caused by influenza B viruses. In some years, they are the most prominent circulating strains of influenza (4–7). Furthermore, influenza B viruses have been described to have significant and disproportionately higher mortality rates compared to influenza A strains in children and infants. For example, during the 2010-2011 epidemic in the United States, influenza B viruses caused 25% of all influenza cases while 38% of all pediatric deaths were attributed to influenza B infection (8). The impact of influenza B virus as a pediatric health problem has also been observed worldwide (7, 9, 10).

Currently, there are two antigenically distinct lineages of influenza B viruses co-circulating in the human population, the B/Yamagata/16/1988-like strains and the B/Victoria/02/1987-like strains, which diverged from a common ancestor in the 1980s (11). The influenza B virus HA contains four major antigenic sites in the globular head domain, the 120 loop, the 150 loop, the 160 loop and the 190 helix (12). These major antigenic sites are immuno-dominant, eliciting most of the HA-specific antibody responses in the host (13, 14). However, the immuno-dominant head domain has high plasticity and is subject to antigenic drift, which allows the virus to escape pre-existing immunity. Therefore, HA-based seasonal influenza virus vaccines need to be re-formulated and re-administered frequently based on surveillance of the circulating strains (15). Although the trivalent influenza virus vaccine (TIV) containing the influenza B virus components of one lineage offers cross-protection in some vaccine recipients (16, 17), a quadrivalent influenza virus vaccine (QIV) containing influenza B components of both lineages started to replace the TIV since 2013 in the United States and also in Europe, aiming for higher vaccine efficacy and broader protection (18–20). However, mismatches between the vaccine strains and circulating strains still substantially decrease vaccine efficacy (21, 22). To overcome such limitations, our group has developed two influenza B virus vaccine strategies, the chimeric HA (cHA) approach and the mosaic HA (mHA) approach (23–28). Both strategies were designed with the rationale of eliciting antibodies against the immuno-subdominant (SD) and more conserved epitopes of the HA protein. The mHA constructs had their immunodominant antigenic sites silenced and they were tested in the recombinant protein vaccine platform.

Because almost 90% of influenza virus vaccines are manufactured using the inactivated vaccine platform, the whole inactivated influenza B viruses (WIVs) displaying the mHAs were used for this study (29). Of note, in addition to the homologous B mHA viruses with the same B/Yamagata/16/1988 HA backbone, we rescued additional heterologous B mHA viruses in different HA backbones covering the two lineages (B/Phuket/3073/2013 and B/Brisbane/60/2008). In mice, we showed that sequential immunization with formaldehyde-inactivated WIVs expressing either the homologous or the heterologous B virus mHAs induced cross-reactive antibody responses against the SD epitopes that were long-lasting and highly cross-protective.

MATERIALS AND METHODS

Cell Culture

Human embryonic kidney 293T (HEK 293T) cells were maintained in Dulbecco's Modified Eagle Medium (DMEM; Gibco) supplemented with 10% (vol/vol) fetal bovine serum (FBS; Gibco) and 100 units/mL of penicillin, 100 μg/mL of streptomycin (P/S; Gibco). Madin-Darby canine kidney (MDCK) cells were maintained in Minimum Essential Medium (MEM; Gibco) supplemented with 10% (vol/vol) FBS, 100 units/mL of penicillin, 100 μg/mL of streptomycin (P/S; Gibco), 2 mM of L-glutamine (Gibco), 0.15% (w/vol) of sodium bicarbonate (Corning) and 20 mM of 4-(2-hydroxyethyl)-1-piperazineethanesulfonic acid (HEPES; Gibco). Cell lines were maintained at 37°C with 5% CO_2.

Recombinant HA Genes and Cloning

The mHA gene segments were based on the HA gene of the B/Yamagata/16/1988, B/Brisbane/60/2008 or B/Phuket/3073/2013 strains. The mosaic HA gene segments were designed by replacing the major antigenic sites of B HA with the corresponding sequences of H5, H8 or H13 viruses (H5, A/Vietnam/1203/2004 H5N1-PR8-IBCDC-RG/GLP; H8, A/mallard/Sweden/24/2002 H8N4; H13, A/black-headed gull/Sweden/1/1999 H13N6) as described before (28). The modified gene segments were obtained as synthetic double-stranded DNA fragments from Integrated DNA Technologies, using the gBlocks® Gene Fragments service, with 15 bp cloning sites specific for the pDZ vector at the 5' and 3' ends. The HA segments were subsequently cloned into the pDZ ambisense vector (30) through In-Fusion HD cloning (Takara Bio USA) according to the manufacturer's protocol. The pDZ B virus mHA plasmids were purified using NucleoBond Xtra Maxi Plus kit (Takara Bio USA) for rescue. Sequences of HA segments were confirmed by Sanger sequencing (Psomagen).

Rescue of Recombinant Influenza B Viruses

HEK 293T cells were seeded onto poly-D lysine-coated 6-well plates at a ratio of 1:4. The next day, each well of cells was transfected with 2.8 μg of pRS-B/Mal04 7-segment plasmid and 0.7 μg of modified pDZ plasmid encoding the HA segment as well as 0.5 μg of pCAGGS B/Mal04 HA helper plasmid using 20 μL of TransIT LT1 transfection reagent (Mirus Bio). The pRS-B/Mal04 7-segment plasmid drives ambisense expression of the seven gene segments (except HA) of the B/Malaysia/2506/2004 (B/Mal04) mouse-adapted (MA) virus strain and has been described previously (31). Transfected cells were incubated at 37°C for 16 to 20 hours and were then transferred to a 33°C incubator to achieve optimal rescue efficiency. Forty-eight hours post transfection, cells were scraped from the plates and collected along with cell supernatants and briefly homogenized through several syringe strokes. Subsequently, 200 μL of the cell and supernatant mixture were injected into the allantoic cavity of 8-day-old specific pathogen-free (SPF) embryonated chicken eggs (Charles River Laboratories). The eggs were incubated at 33°C. After a 3-day incubation, eggs were cooled to 4°C overnight, and allantoic fluid was harvested and clarified by low-speed centrifugation. A hemagglutination (HA) assay was used to examine the presence of rescued virus using 0.5% turkey red blood cells. HA-positive allantoic fluid samples were used to plaque-purify homogeneous virus clones on confluent MDCK cells. The plaque-purified viruses were further amplified in 10-day old embryonated chicken eggs. RNA was extracted from allantoic fluid containing the plaque-purified viruses using QIAamp Viral RNA Mini Kit (Qiagen). One-step RT-PCR was performed to amplify the HA segment DNA using SuperScript™ III One-Step RT-PCR System with Platinum™ Taq DNA

Polymerase (Invitrogen) and HA-specific primers. DNA was purified using NucleoSpin Gel and PCR Clean-up kit (Takara Bio USA) and then sequenced by Sanger sequencing (Genewiz).

Hemagglutination Inhibition (HI) Assay

Mouse sera were treated with receptor destroying enzyme (RDE; Denka Seiken) to eliminate non-specific inhibitors in the sera. Briefly, serum was mixed with RDE in a 1:3 ratio (vol/vol). RDE-treated samples were incubated at 37°C for 18-20 hours and the reaction was stopped by the addition of 2.5% sodium citrate solution in a 1:3 ratio (vol/vol). The samples were then heat-treated at 56°C for 30 minutes (32). Serum was finally diluted with sterile PBS to reach a final dilution of 1:10. To perform HI assays, virus stocks were diluted in PBS to a final HA titer of 8 HA units (4 wells of HA) per 50 µL sample. Two-fold dilutions (25 µL) of RDE-treated serum in PBS prepared in 96-well V-bottom microtiter plates (Thermo Fisher Scientific) were then combined with 25 µL of the diluted virus. The plates were incubated for 30 minutes at room temperature (RT) to allow HA-specific antibodies to bind to virus (32). Then 50 µL of a 0.5% suspension of turkey red blood cells (Lampire) were added to each well. HI titers were defined as the reciprocal of the highest dilution of serum that inhibited hemagglutination of red blood cells. Mouse antisera against the influenza B viruses used in the HI assays were generated from 6- to 8-week old female BALB/c mice with intranasal infection of either B/Phuket/3073/2013 virus (10^6 plaque forming units (PFU) per mouse) or reassortant B/Brisbane/60/2008 virus (10^4 PFU per mouse).

Preparation of Inactivated Viruses for Vaccination

Plaque-purified and sequence-confirmed B mHA viruses were expanded in 10-day-old SPF embryonated chicken eggs. Pooled allantoic fluids from eggs were treated with 0.03% (vol/vol) formaldehyde at 4°C under continuous shaking. After 72 hours, 25 mL of clarified allantoic fluid were added on top of 5 mL of a 30% sucrose (vol/vol) solution in 0.1 M sodium chloride (NaCl), 1 mM ethylenediaminetetraacetic acid (EDTA) and 10 mM Tris-HCl (pH 7.4) in round-bottom polypropylene copolymer (PPCO) centrifuge tubes (Thermo Fisher Scientific). After ultracentrifugation at 25,000 rpm in a Beckman L7-65 ultracentrifuge (Beckman Coulter) equipped with an SW28 rotor for 2 hours at 4°C, the supernatants were discarded and pellets were recovered in 1 mL of PBS. The total protein concentration of each stock was determined with the Pierce BCA Protein Assay Kit (Thermo Fisher Scientific) according to the manufacturer's protocol.

Immunization Studies

For animal immunizations, 6- to 8-week-old female BALB/c mice (Jackson Laboratories) were used for all experiments. Experiments were performed in accordance with protocols approved by the Icahn School of Medicine at Mount Sinai Institutional Animal Care and Use Committee (IACUC). Formaldehyde-inactivated viruses were administered intramuscularly at a dose of 1 µg HA per mouse diluted in a total volume of 100 µL sterile PBS with or without 50 µL of AddaVax adjuvant (Invivogen). PBS-vaccinated mice were included as negative controls. Vaccinations were given in 3- or 4-week intervals. Four weeks after the final immunization, mice were euthanized and blood was obtained by cardiac puncture. Sera were isolated by low-speed centrifugation and were stored at -80°C until use. Mice for longitudinal analysis of antibody dynamics were bled from the submandibular vein on study days 0, 28, 56, 84, 105, 147, 189, 231 and 292.

Passive Transfer and Challenge Studies

The challenge viruses B/New York/PV01181/2018 and B/New York/PV00094/2017 were isolated by the Personalized Virology Initiative at Icahn School of Medicine at Mount Sinai (ISMMS) and mouse-adapted. Six- to eight-week-old female BALB/c mice (Jackson Laboratories) received 100 or 150 µL of pooled sera *via* intraperitoneal (IP) injection. After 2 hours, mice were infected intranasally with 5 murine 50% lethal doses (5 mLD_{50}) of the mouse-adapted B/New York/PV01181/2018 virus, mouse-adapted B/New York/PV00094/2017 virus or B/Lee/1940 virus in a volume of 30 µL of sterile PBS after anesthesia with a ketamine/xylazine cocktail administered intraperitoneally. Animals were monitored for survival and weight loss for 14 days post-challenge and were scored dead and humanely euthanized if they lost more than 25% of their initial body weight.

Enzyme-Linked Immunosorbent Assay (ELISA)

Recombinant HA proteins were produced as described previously (33). Proteins were coated onto Immulon® 4 HBX 96-well microtiter plates (Thermo Fisher Scientific) at 2 µg/mL in 1x coating buffer (SeraCare Life Sciences Inc.) at 50 µL/well overnight at 4°C. All plates were washed 3 times with 225 µL PBS containing 0.1% (vol/vol) Tween-20 (PBST) and 220 µL blocking solution (3% goat serum, 0.5% non-fat dried milk powder, 96.5% PBST) was added to each well and incubated for 1 hour at RT. Individual serum samples or pooled sera were serially diluted 3-fold in blocking solution followed by a 2-hour incubation at RT. ELISA plates were washed 3 times with PBST and 50 µL of anti-mouse IgG-horseradish peroxidase (HRP) conjugated antibody (Cytiva) was added at a dilution of 1:3,000 in blocking solution. After 1 hour, plates were washed 3 times with PBST and developed using SigmaFast OPD (Sigma-Aldrich) for 10 minutes. Reactions were stopped by adding 50 µL 3M hydrochloric acid (HCl) and absorbance at 492 nm was determined on a Synergy 4 plate reader (BioTek) or similar. For each ELISA plate, the average plus 3 standard deviations of absorbance values of blank wells was used as a cutoff to determine endpoint titers using GraphPad Prism 7.0.

Antibody Dependent Cell-Mediated Cytotoxicity (ADCC) Reporter Assay

White flat-bottom 96-well plates (Corning) were seeded with 2×10^4 MDCK cells per well. After 24 hours at 37°C, the MDCK cells were washed once with PBS and then infected with influenza B viruses at a multiplicity of infection (MOI) of 5 for a single cycle of virus replication overnight. The next day, the culture medium

was removed and 25 µL of assay buffer (RPMI 1640 supplemented with 4% low-IgG FBS [Gibco]) was added to each well. Pooled mouse sera were diluted 1:2 (from a starting dilution of 1:30) in RPMI 1640 medium (Gibco) and added (25 µL per well) to the virus-infected MDCK cells in triplicates. The sera were then incubated with MDCK cells for 30 minutes at 37°C. Genetically modified Jurkat cells expressing the mouse FcγRIV with a luciferase reporter gene under transcriptional control of the nuclear factor-activated T (NFAT) cell promoter were then added to the plate at 7.5×10^4 cells in 25 µL/well (Promega) and incubated for 6 hours at 37°C. At the end of the incubation, a volume of 75 µL of Bio-Glo Luciferase assay reagent (Promega) was added to each well and luminescence was quantified using a Synergy 4 microplate reader (BioTek) using Gen5 2.09 software or similar. Fold induction was calculated as follows: $(RLU_{induced}-RLU_{background})/(RLU_{uninduced}-RLU_{background})$ and graphed using Prism 7.0.

Flow Cytometry Analysis

At 56 and 84 days post vaccination, the inguinal lymph nodes were harvested from euthanized mice. Lymph nodes were dispersed into single-cell suspensions by mechanical disruption through 40 µm cell strainer (Fisher Scientific) using syringe plungers into cold PBS. Red blood cells were lysed using ammonium-chloride-potassium (ACK) lysis buffer (0.15 M NH_4Cl, 10 mM $KHCO_3$ and 0.11 mM Na_2EDTA, pH 7.2-7.4). Cell debris was removed by passing samples through 40 µm cell strainers. Cells were pelleted by centrifugation (450 g, 5 minutes) and re-suspended in FACS buffer (PBS containing 0.1% bovine serum albumin [BSA] and 2 mM EDTA) containing Fc block anti-mouse CD16/CD32 (1:100, eBioscience) for 10 minutes at 4°C and then stained with primary surface antibodies (30 minutes, 4°C). The following antibodies were used for surface staining: Live/Dead™ Near-IR fluorescent reactive dye (Thermo Fisher Scientific), Brilliant Violet 605™ anti-mouse IgD (BioLegend), Pacific Blue™ anti-mouse CD3 (BioLegend), Alexa Fluor® 700 anti-mouse/human CD45R/B220 (BioLegend), PerCP/Cyanine 5.5 anti-MU/HU GL7 antigen (BioLegend) and PE/Cyanine 7 anti-mouse CD38 (BioLegend). Cells were washed in FACS buffer (500 g, 5 minutes) and then incubated in 2% methanol-free paraformaldehyde (PFA) fixation buffer for 20 minutes at 4°C. UltraComp eBeads™ Compensation Beads (Invitrogen) were used for compensation. Samples were washed and re-suspended in FACS buffer and transferred to cluster tubes (Corning) for acquisition. Data was acquired on an BD LSRFortessa cytometer (BD Biosciences) using FACSDiva v7.03 (BD Biosciences) with the appropriate fluorescent minus one (FMO) controls. The data were analyzed using FCS Express 7.0 software.

Statistics

Statistical analyses were performed using Prism 7.0 (GraphPad). Statistical differences in ELISA data were determined using Kruskal-Wallis one-way analysis of variance (ANOVA) corrected using Dunn's test for multiple comparisons and unpaired one-tailed t test when comparing two groups. The statistical analyses of FACS data were performed using one-way ANOVA corrected for multiple comparison using the Tukey test. Survival curves were compared using log-rank Mantel-Cox tests against the mock groups (PBS-treated or untreated). Levels of significance are indicated as follows: *P ≤ 0.05; **P ≤ 0.01; ***P ≤ 0.001; ****P ≤ 0.0001; ns, not significant.

RESULTS

Inactivated Homologous B mHA Viruses Induced Protective Antibody Responses to the Immuno-Subdominant (SD) Epitopes of the HA

The mHA approach aims to elicit antibodies not only against the conserved epitopes in the stalk domain but also against those conserved in the head domain outside of the variable antigenic sites. We have shown previously that the vaccine approach with B virus recombinant mHA proteins could induce strong cross-reactive antibody responses and broad protection against viral challenge in mice. Here we assessed whether the same principle holds true for the WIV platform. Three different B mHA viruses in which the major antigenic sites of the HA were replaced by corresponding sequences from H5, H8 or H13 have been constructed and characterized previously (28). The homologous B virus mHAs were based on the B/Yamagata/16/1988 (Yam) HA and designated as mosaic H5/B_{Yam} (mH5/B_{Yam}), mosaic H8/B_{Yam} (mH8/B_{Yam}), and mosaic H13/B_{Yam} (mH13/B_{Yam}) viruses. A virus with unchanged wild-type (WT) B/Yamagata/16/1988 HA served as the control. The B mHA viruses and the virus expressing the WT HA were propagated in embryonated chicken eggs, inactivated with formaldehyde and purified by ultracentrifugation through a sucrose cushion. To normalize HA content in the WIV preparations, we performed an ELISA using a monoclonal antibody (4G12) that broadly binds to an epitope within the stalk region of the influenza B virus HAs (34). The area under the curve (AUC) binding signal was used to calculate HA content relative to the recombinant Yam WT HA protein standard (data not shown). Two groups of 15 mice were vaccinated. Mice in the Yam mosaic group were primed with mH13/B_{Yam} WIV, boosted with mH5/B_{Yam} WIV and boosted again with mH8/B_{Yam} WIV. Mice in the Yam WT group received three doses of the WT WIV. The vaccines were administered with AddaVax, a squalene-based oil-in-water nano-emulsion with a formulation similar to that of MF59, which has been licensed in Europe for adjuvanted influenza virus vaccines (35). The vaccination was performed with a 3- to 4-week interval between doses. Then, mice were bled for serological analysis and passive transfer/viral challenge studies 3 to 4 weeks after the last boost (**Figure 1A**). First, we determined the antibody responses toward the stalk domain of HA by ELISAs using the chimeric H7/B_{Yam} (cH7/B_{Yam}) recombinant protein. The cH7/B_{Yam} has an H7 head domain on top of the stalk domain of the Yam HA. We observed that the Yam mosaic group developed significantly higher levels of stalk-reactive IgG than the Yam WT group (**Figure 1B**). Additionally, the antibody levels against the SD epitopes in both stalk and head domains were assessed by ELISAs using the mosaic H11/B_{Yam} (mH11/

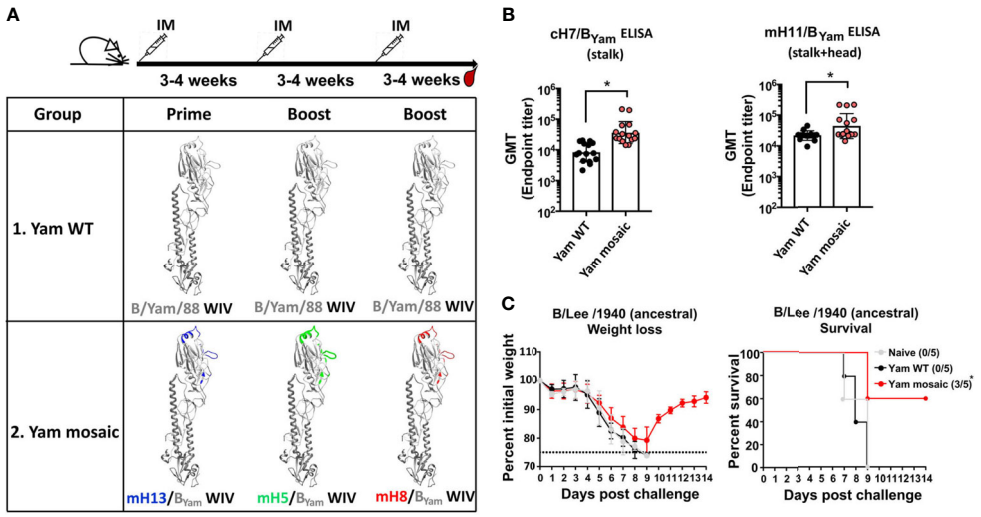

FIGURE 1 | The homologous B mHA viruses induced protective antibody responses to the SD epitopes of the HA. **(A)** Schematic representation of the vaccination groups and regimen [modeled based on the structure of the B/Brisbane/60/2008 HA, PDB accession no. 4FQM (36)]. Residues that were mutated in homologous monomeric B mHAs are shown in different colors which represent corresponding sequences from different influenza A HAs. BALB/c mice (n=15) in the Yam WT group received B/Yam/88 WT HA WIV three times. BALB/c mice (n=15) in the Yam mosaic group received the three B virus mHA WIVs in the order of mH13/B_{Yam} WIV - mH5/B_{Yam} WIV - mH8/B_{Yam} WIV. Each mouse received WIV containing 1 μg of HA. AddaVax was used as the adjuvant and the WIVs were given through intramuscular (IM) administration. Mice were bled 3-4 weeks after the second boost. **(B)** Binding of serum antibodies towards the SD epitopes. A cH7/B_{Yam} protein with a group 2 avian H7 head and the B/Yamagata/16/1988 HA stalk was used to measure stalk-specific antibodies. A mH11/B_{Yam} protein displaying the H11 sequences at the major antigenic sites within the B/Yamagata/16/1988 HA was used to measure antibody binding to SD conserved epitopes in the head and stalk domains. The geometric mean endpoint titer was calculated as the readout. The statistics were calculated using unpaired one-tailed t test (*P ≤ 0.05). **(C)** Cross-protection of serum antibodies against a distant influenza B strain in a passive transfer/viral challenge study. Six- to eight-week-old naïve female BALB/c mice (n=5) received 150 μL of pooled Yam WT, Yam mosaic or naïve sera intraperitoneally. Two hours after the transfer, mice were challenged with 5 mLD_{50} of the B/Lee/1940 strain intranasally. Weight loss and survival of mice were monitored for 2 weeks, with a humane endpoint of >25% loss of the initial weight. In the survival plots, the proportion of surviving animals in each group is shown in parentheses and statistical significance was determined by log-rank Mantel-Cox tests against the naïve group with *P ≤ 0.05.

B_{Yam}) protein displaying the H11 sequences at the major antigenic sites of the Yam HA. As expected, in comparison to the Yam WT group, the Yam mosaic group reached higher IgG titer against the mH11/B_{Yam} than the Yam WT group (**Figure 1B**). Next, we determined the ability of the antibodies induced by the Yam mHA vaccines to confer cross-protection against lethal challenge of the antigenically divergent ancestral B/Lee/1940 virus strain. Groups of 5 naïve mice received 150 μL per mouse of pooled sera intraperitoneally and were challenged 2 hours later with 5 mLD_{50} of B/Lee/1940 virus. Mice were observed daily for weight loss and mortality for 14 days post-challenge. All mice challenged with B/Lee/1940 virus showed substantial weight loss (**Figure 1C**). Of note, all mice in the naïve group and the Yam WT group succumbed to infection by day 9 post-challenge, whereas 60% of the animals in the Yam mosaic group survived. This showed that serum antibodies elicited by the homologous B virus mHA WIVs induced better cross-protection against challenge with an antigenically distinct virus than that provided by immunization with the WT WIV.

Rescue and Characterization of Heterologous B mHA Viruses

To improve the B virus mHA vaccine approach by introducing different HA backbones for the benefit of enriching cross-lineage antibodies, we rescued B mHA viruses either in the B/Phuket/3073/2013 (Phu, B/Yamagata/16/1988-like lineage) or the B/Brisbane/60/2008 (Bris, B/Victoria/2/1987-like lineage) HA backbones. We replaced the major antigenic sites with the corresponding sequences from H5 (Phu HA) or H13 (Bris HA) (**Figure 2A**). Those heterologous B mHA viruses were designated as mH5/B_{Phu} and mH13/B_{Bris} respectively. The amino acid sequence alignment of the B/Phuket/3073/2013 or B/Brisbane/60/2008 HA with mH5/B_{Phu} or mH13/B_{Bris} is shown in **Figure 2A**. Two viruses with WT B/Phuket/3073/2013 (Phu) or WT B/Brisbane/60/2008 (Bris) HA were also rescued as controls. The newly generated heterologous WT HA and B mHA viruses grew well in eggs, reaching a hemagglutination titer above 1:128 (**Figure 2B**) and an infectious titer of approximately 10^8 PFU/mL (**Figure 2C**). The major antigenic sites elicit most of the hemagglutination inhibition (HI) antibodies as they are relatively close to the receptor binding site (RBS) (13). To confirm the ablation of the original antigenic sites in the B virus mHAs, HI assays were performed using mouse sera raised against viruses with the WT HAs. As expected, mouse sera generated using the WT B/Brisbane/60/2008 HA virus inhibited hemagglutination strongly against the same virus. In contrast, no detectable HI reactivity was measured against the mH13/B_{Bris} (**Figure 2D**). Similarly, the mouse sera raised against

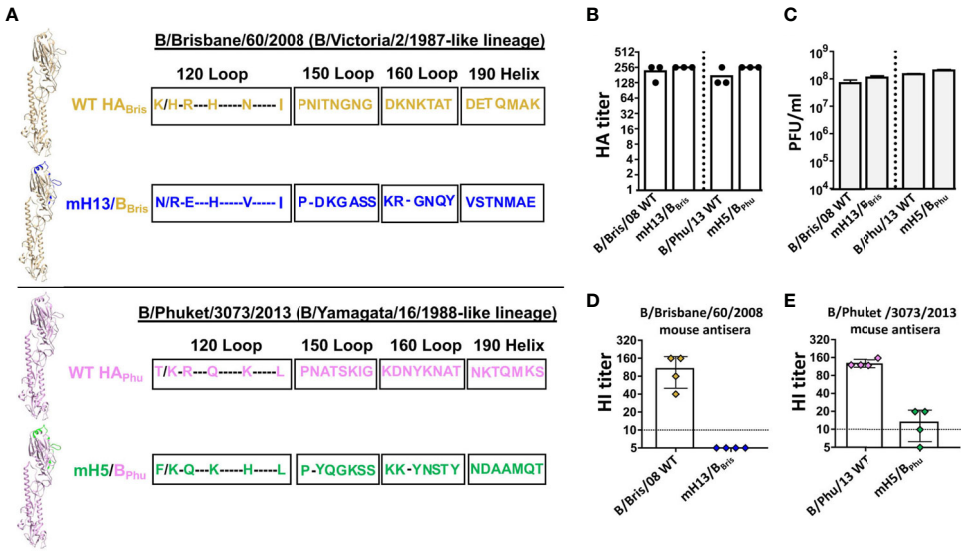

FIGURE 2 | Rescue and characterization of the heterologous B mHA viruses. **(A)** Schematic representation of the heterologous B mHAs design [modeled based on the structure of the B/Brisbane/60/2008 HA, PDB accession no. 4FQM (36)]. The left upper panel shows monomeric B/Brisbane/60/2008 WT HA and mHA. Residues that were mutated in monomeric mH13/B_{Bris} are shown in blue. The left lower panel shows monomeric B/Phuket/3073/2013 WT HA and mHA. Residues that were mutated in monomeric mH5/B_{Phu} are shown in green. Amino acid sequences of the major antigenic sites of the B virus mHA are aligned with the corresponding sequences of the WT HA. The sequence alignment was performed with the HAs of B/Brisbane/60/2008, mH13/B_{Bris}, B/Phuket/3073/2013 and mH5/B_{Phu} (H5: A/Vietnam/1203/04 H5N1-PR8-IBCDC-RG/GLP; H13: A/black-headed gull/Sweden/1/1999 H13N6). **(B)** HA titers and **(C)** plaque-forming units (PFU) of influenza B viruses grown from eggs. Allantoic fluid virus stocks were titrated by HA assay and plaque assay on MDCK cells in triplicate. Bars represent the mean ± SD. **(D)** HI assay using the indicated viruses and antisera of mice (n=4) raised against the reassortant B/Brisbane/60/2008. Symbols representing individual mice are color coded and the bars show the mean ± SD value of each group. **(E)** HI assay using the indicated viruses and antisera of mice (n=4) raised against the B/Phuket/3073/2013. Symbols representing individual mice are color coded and the bars show the mean ± SD value of each group.

B/Phuket/3073/2013 virus showed high HI titers against the same virus, while the HI titers against the mH5/B_{Phu} virus were nearly 10-fold lower (**Figure 2E**). These results confirmed that the original major antigenic sites had been successfully silenced in the two heterologous B mHA viruses.

Inactivated Heterologous B mHA Viruses Induced Protective Antibody Responses to the SD Epitopes of the HA

Humans are exposed to various strains of influenza B viruses *via* vaccinations and infections throughout life. Consequently, people of older age tend to have more stalk-specific antibodies than younger people (37). One way to demonstrate the value of the mosaic HA approach is to show that the heterologous B virus mHAs would elicit more antibodies to the SD epitopes than the heterologous WT HA. Therefore, we performed a similar immunization study as described in **Figure 1** using formaldehyde-inactivated WIVs (normalized to 1 μg HA per mouse) (**Figure 3A**). The WT group was primed with Bris WIV and subsequently boosted with the Phu WIV followed by the Yam WIV ("Mixed WT"). The B virus mHA group was primed with mH13/B_{Bris} WIV and boosted with mH5/B_{Phu} WIV then mH8/B_{Yam} WIV ("Mixed mosaic"). Three immunizations were given with a 4-week interval between doses. Each mouse was vaccinated with AddaVax as the adjuvant. Again, 4 weeks after the last immunization, mice were terminally bled to isolate sera. We performed ELISAs using cH7/B_{Yam} (stalk) or mH11/B_{Yam} (stalk and head) proteins to measure antibodies against the SD epitopes. In comparison to the Mixed WT group, the Mixed mosaic group demonstrated higher levels of antibodies targeting the SD epitopes of the B HA (**Figure 3B**). Then, we determined antibody-mediated cross-protection in mice by passive transfer and viral challenge study using the B/Lee/1940 strain. Groups of 5 naïve mice received 100 μL per mouse of pooled sera intraperitoneally and were lethally challenged 2 hours later with a dose of 5 mLD_{50}. All mice that received naïve mouse sera succumbed to infection by day 9. Importantly, 80% of animals in the Mixed mosaic group survived, while only 20% in the Mixed WT group survived (**Figure 3C**). These data indicated that the heterologous B virus mHA WIVs conferred better cross-protection than the heterologous WT HA WIVs, emphasizing that the B virus mHAs can induce cross-protective antibodies more efficiently than the heterologous WT HAs.

Head-to-Head Comparison of the Homologous B Virus mHA With the Heterologous B Virus mHA Vaccine Candidates

We have shown that both homologous and heterologous B virus mHA WIVs are efficient at inducing SD epitope-specific

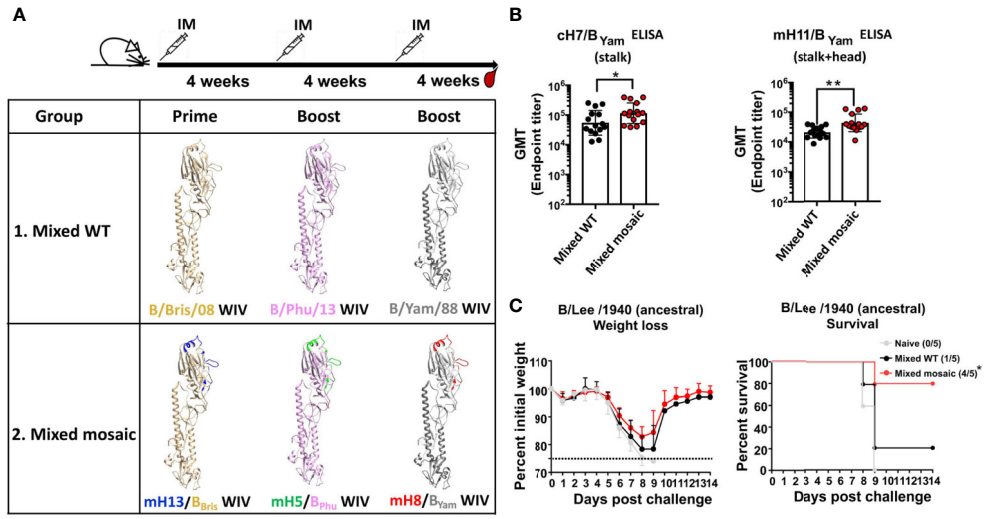

FIGURE 3 | The heterologous B virus mHA viruses induced protective antibodies responses to the subdominant epitopes of the HA. **(A)** Schematic of the vaccination groups and regimen [modeled based on the structure of the B/Brisbane/60/2008 HA, PDB accession no. 4FQM (36)]. Residues that were mutated in the heterologous monomeric B mHAs are indicated in different colors, representing corresponding sequences from different influenza A HAs. BALB/c mice (n=15) in the Mixed WT group received B/Bris/08 WT HA WIV followed by B/Phu/13 WT HA WIV and then B/Yam/88 WT HA WIV. Mice (n=15) in the Mixed mosaic group received the B virus mHA WIV sequentially as follows: mH13/B_{Bris} WIV - mH5/B_{Phu} WIV - mH8/B_{Yam} WIV. Each mouse received WIV containing 1 μg of HA. Each vaccination was given at 4-week intervals. AddaVax was used as the adjuvant and the WIVs were administered through intramuscular (IM) injection. Mice were bled 4 weeks after the second boost. **(B)** Binding of serum antibodies towards the SD epitopes. The cH7/B_{Yam} protein and the mH11/B Yam protein were used in ELISAs as described in **Figure 1**. The geometric mean endpoint titer (GMT) was calculated as the readout. The statistics were performed using the unpaired one-tailed t test (*P ≤ 0.05 and **P ≤ 0.01). **(C)** Cross-protection of serum antibodies against a distant influenza B strain in a passive transfer/viral challenge study. Naïve BALB/c mice (n=5) received 100 μL of pooled Mixed WT, Mixed mosaic or naïve sera intraperitoneally. Two hours after transfer, mice were challenged with 5 mLD_{50} of the B/Lee/1940 strain intranasally. Weight loss and survival of mice were monitored for 2 weeks, with a humane endpoint of >25% loss of the initial weight. In the survival plots, the proportion of surviving animals in each group is shown in parentheses and statistical significance was inferred by log-rank Mantel-Cox tests against the naïve group with *P ≤ 0.05.

antibodies. To determine if one approach is superior than the other in our mouse model, we performed a head-to-head comparison of sequential immunizations using homologous B mHA viruses (mH13/B_{Yam} - mH5/B_{Yam} - mH8/B_{Yam}, Yam mosaic) versus heterologous B mHA viruses (mH13/B_{Bris} -mH5/B_{Phu} - mH8/B_{Yam}, Mixed mosaic). The homologous WT HA virus (Yam WT) group, heterologous WT HA viruses (B/Bris - B/Phu - B/Yam, Mixed WT) group and PBS-treated group were included as controls (**Figure 4A**). The immunization was performed in the presence or absence of an adjuvant (AddaVax). Mice were bled periodically for serological assays. In fact, the animals were followed up to 292 days and bled on days 28, 56, 84, 105, 147, 189, 231 and 292 to assess the longevity of antibodies against the SD epitopes. Again, we determined the antibody responses of day 84 (D84) sera toward the SD epitopes by ELISA using cH7/B_{Yam} and mH11/B_{Yam} proteins (**Figure 4B**). Both mHAs vaccine strategies induced robust levels of SD epitope-reactive IgGs when the vaccines were adjuvanted. Additionally, we did not see differences in antibody titers between Yam mosaic and Mixed mosaic groups. Furthermore, as a universal vaccine candidate should provide durable protection, we performed a longitudinal analysis of antibody responses against the SD epitopes (**Figure 4C**). We found that: (i) the adjuvanted Yam mosaic and Mixed mosaic vaccines elicited the highest antibody titers among all the vaccines, (ii) antibody titers against SD epitopes of HA increased substantially after booster immunization and reached a plateau by day 105 and (iii) antibody titers against the SD epitopes remained at the plateau level up to day 292.

Next, we performed passive transfer/viral challenge studies using the day 292 (D292) sera to evaluate long-term protection. The challenge studies were performed using two recently circulating influenza B viruses representing the B/Victoria/2/1987-like lineage (B/New York/PV01181/2018) and the B/Yamagata/16/1988-like lineage (B/New York/PV00094/2017) that had been isolated from clinical samples and mouse-adapted. Sera were pooled within groups and then transferred into naïve mice. Each naïve mouse received 100 μL of pooled sera intraperitoneally. Two hours after serum transfer, mice were infected with a dose of 5 mLD_{50} of either virus. Challenge with the B/Victoria/2/1987-like strain B/New York/PV01181/2018 resulted in substantial weight loss in all groups (**Figure 5A**). All mice in the PBS control group succumbed to infection. Although more than 50% of the mice in all unadjuvanted groups succumbed to infection by day 9 post-challenge, the mosaic groups exhibited slightly better survival rates (Yam WT: 0%; Yam mosaic: 40%; Mixed WT: 20%; Mixed mosaic: 40%). In contrast, 80% of mice in the adjuvanted Yam mosaic

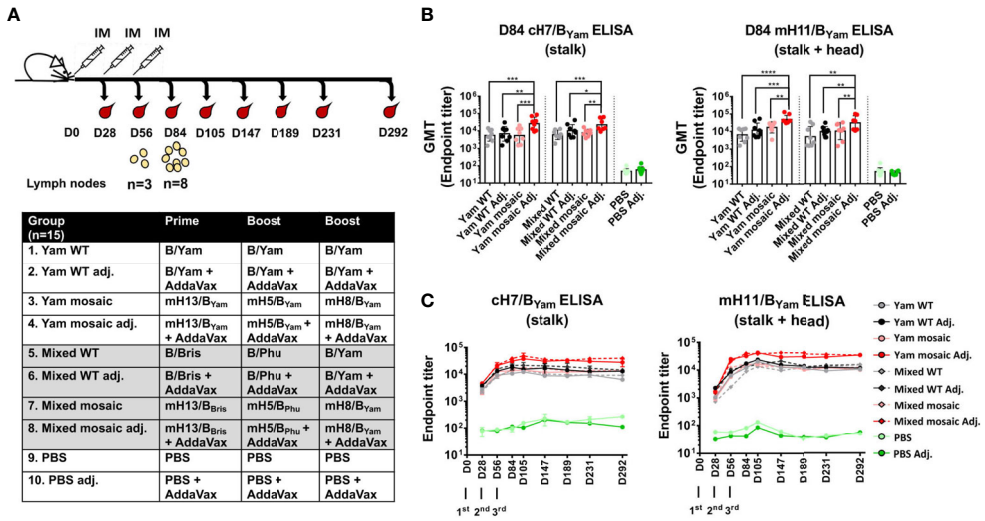

Group (n=15)	Prime	Boost	Boost
1. Yam WT	B/Yam	B/Yam	B/Yam
2. Yam WT adj.	B/Yam + AddaVax	B/Yam + AddaVax	B/Yam + AddaVax
3. Yam mosaic	mH13/B_{Yam}	mH5/B_{Yam}	mH8/B_{Yam}
4. Yam mosaic adj.	mH13/B_{Yam} + AddaVax	mH5/B_{Yam} + AddaVax	mH8/B_{Yam} + AddaVax
5. Mixed WT	B/Bris	B/Phu	B/Yam
6. Mixed WT adj.	B/Bris + AddaVax	B/Phu + AddaVax	B/Yam + AddaVax
7. Mixed mosaic	mH13/B_{Bris}	mH5/B_{Phu}	mH8/B_{Yam}
8. Mixed mosaic adj.	mH13/B_{Bris} + AddaVax	mH5/B_{Phu} + AddaVax	mH8/B_{Yam} + AddaVax
9. PBS	PBS	PBS	PBS
10. PBS adj.	PBS + AddaVax	PBS + AddaVax	PBS + AddaVax

FIGURE 4 | Immunogenicity of homologous versus heterologous B virus mHA constructs. **(A)** Vaccination groups and regimen. The groups (n=15) include homologous WT B/Yam (Yam WT), homologous B virus mHA (Yam mosaic), heterologous WT HA (Mixed WT), heterologous B virus mHA (Mixed mosaic) and PBS, each in the presence or absence of the adjuvant (AddaVax; Adj.). Mice were immunized with inactivated WIV at 4-week intervals *via* intramuscular injection. Two subsets of animals were euthanized on D56 and D84 to analyze germinal center reactions in the draining lymph nodes. Another subset of animals was terminally bled for serology. The remaining animals were kept until D292 and bled periodically to examine the longevity of antibody responses. **(B)** Serum IgG directed to the SD epitopes on D84. ELISAs were performed as described previously. The statistical analysis was performed using one-way ANOVA corrected for multiple comparison using Dunnett's test (*P ≤ 0.05; **P ≤ 0.01; ***P ≤ 0.001; ****P ≤ 0.0001). **(C)** Longevity of antibody responses. Pooled mouse sera from each group obtained on the indicated days were tested with a technical duplicate. Endpoint titers were plotted.

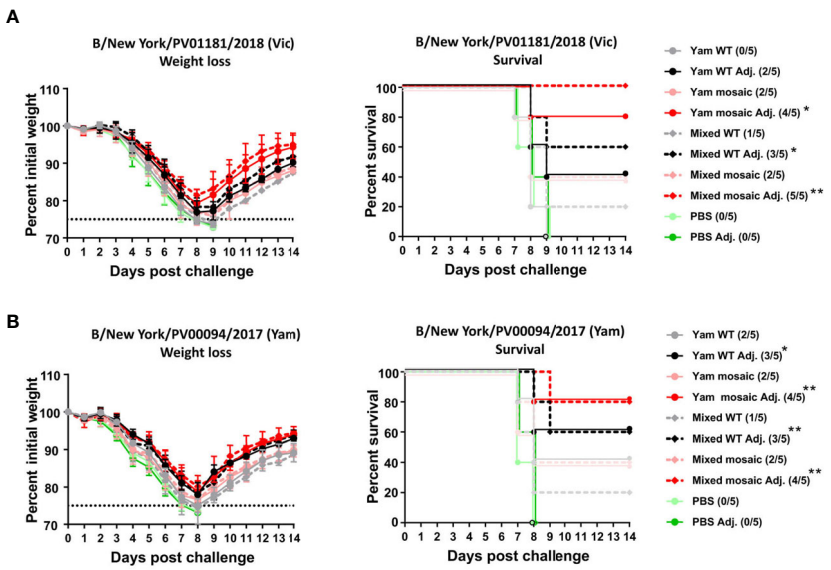

FIGURE 5 | Protection of D292 serum antibodies induced by homologous versus heterologous B virus mHAs vaccination. **(A)** Weight loss and survival of vaccination groups challenged with B/New York/PV01181/2018 virus. Mice (n = 5) received 100 µL of D292 pooled sera intraperitoneally and were challenged intranasally with 5 mLD_{50} of challenge virus. Weight loss and survival of mice were monitored for 2 weeks with a humane endpoint of >25% loss of the initial weight. In the survival plots, the proportion of surviving animals in each group is shown in parentheses and statistical significance was inferred by log-rank Mantel-Cox tests against the corresponding control group (PBS or PBS Adj.) with *P ≤ 0.05 and **P ≤ 0.01.**(B)** Weight loss and survival of vaccination groups challenged with B/New York/PV00094/2017 virus. Mice (n = 5) received 100 µL of D292 pooled sera intraperitoneally and were challenged intranasally with 5 mLD_{50} of challenge virus. Weight loss and survival of mice were monitored for 2 weeks with a humane endpoint of >25% loss of the initial weight. In the survival plots, the proportion of surviving animals in each group is shown in parentheses and statistical significance was inferred by log-rank Mantel-Cox tests against the corresponding control group (PBS or PBS Adj.) with *P ≤ 0.05 and **P ≤ 0.01.

group and 100% of mice in the adjuvanted Mixed mosaic group survived. The adjuvanted Yam WT group and Mixed WT group showed relatively lower survival rates (40% and 60%, respectively) than the adjuvanted mosaic groups (Yam mosaic: 80%; Mixed mosaic: 100%). No statistical difference in survival was detected in animals receiving Yam mosaic and Mixed mosaic vaccines. Lethal challenge with the B/Yamagata/16/1988-like virus B/New York/PV00094/2017 produced similar results (**Figure 5B**). All animals that were given PBS group sera succumbed to infection. For the unadjuvanted vaccination groups, more than 50% of mice in each group succumbed to infection by day 9 post-challenge. While 80% of mice that received sera from mice vaccinated with adjuvanted Yam mosaic or Mixed mosaic survived, 60% of mice that received adjuvanted Yam WT or Mixed WT sera survived. Similarly, no statistical difference in survival was detected in animals receiving the sera from Yam mosaic and Mixed mosaic vaccinations. In summary, both homologous and heterologous B virus mHA vaccine candidates elicited comparable antibody titers against the SD epitopes of HA and provided similar protection *in vivo*. Sequential immunization with mHA vaccines provided better cross-protection against divergent viruses than immunization with the WT HA viruses.

At last, we examined germinal center B cells in the draining lymph nodes as we were exploring the mechanism of action of the B virus mHA constructs. We took inguinal lymph nodes from a subset of animals at day 56 (D56, n=3) and day 84 (D84, n=8) and analyzed the relative abundance of germinal center B cells by flow cytometry (38–40). We observed that the sequential immunization with B virus mHA vaccines appeared to stimulate a stronger germinal center reaction, an effect which AddaVax strengthened significantly, even activating germinal center reactions when administered by itself in the PBS group (**Supplementary Figure 1**). We postulate that the sequential immunization of the B virus mHA constructs drives the memory B cells to re-enter a germinal center to undergo somatic hypermutations and affinity maturation as we expect the B cell receptors (BCRs) to the SD epitopes would have lower affinity to their epitopes than those that react to the immuno-dominant epitopes in the WT HA constructs. The MF59-like adjuvant AddaVax may increase antigen uptake or the adjuvant itself may promote a potent T follicular helper cell (Tfh) response and the persistence of germinal center B cells appeared to correlate with the levels of antibodies targeting the SD epitopes.

Both Homologous and Heterologous mHA Vaccines Induced Non-HI Active Antibodies With Antibody-Dependent Cellular Cytotoxicity (ADCC) Activity

Next, we sought to determine the activity of the antibodies induced by the vaccine candidates. HI activity is a known correlate of protection, with a titer of 1:40 considered to confer 50% protection against seasonal influenza in human adults (42). Consistently with our previous data (28), both B virus mHA vaccination sera showed no detectable HI titers against diverse influenza B viruses including B/Lee/1940, B/New York/PV01181/2018 and B/New York/PV00094/2017 (**Figure 6A**). Not surprisingly, we found the Mixed WT groups elicited detectable levels of HI titers against the B/New York/PV01181/

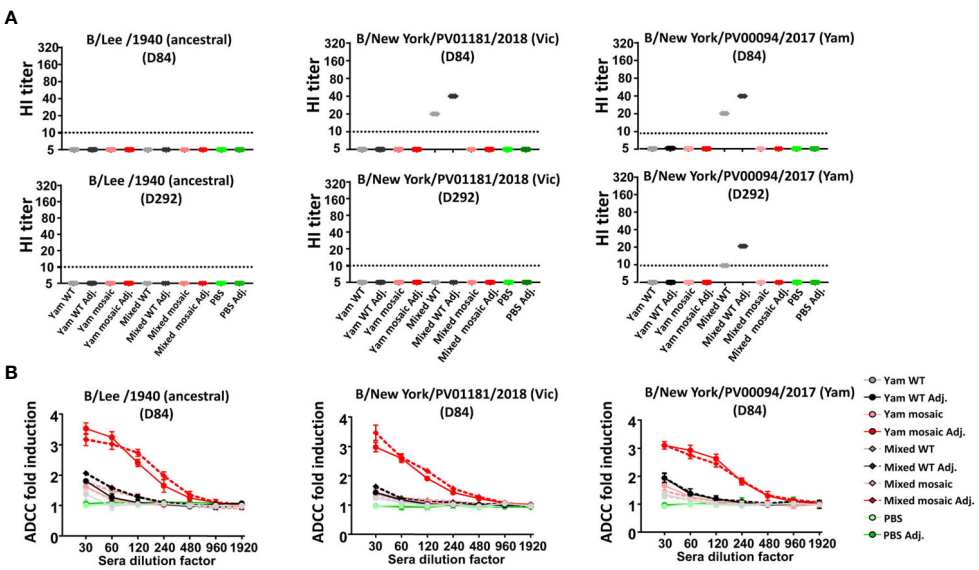

FIGURE 6 | Activity of serum antibodies induced by homologous versus heterologous B virus mHA constructs. **(A)** HI activity of D84 (upper panel) and D292 (lower panel) pooled sera against influenza B viruses including B/Lee/1940, B/New York/PV00094/2017 and B/New York/PV01181/2018. **(B)** ADCC activity of D84 pooled sera in a reporter assay. To perform ADCC reporter assay, MDCK cells were infected with each virus at an MOI of 5 with single-cycle replication. Fold induction of the reporter signal from the sera over those from the blanks were analyzed. Data points represent mean ± SD of pooled sera from 8 mice measured in technical triplicates.

2018 and B/New York/PV00094/2017 viruses. This result was expected because the B/Brisbane/2008 and B/Phuket/3073/2013 strains in the Mixed WT group are phylogenetically close to the B/New York/PV01181/2018 and B/New York/PV00094/2017 virus isolates, respectively. However, we observed that the HI-active antibodies against the B/New York/PV01181/2018 and B/New York/PV00094/2017 viruses on D292 declined significantly compared to those on D84, unlike the long-lasting antibodies targeting the SD epitopes (**Figure 4C**). These data suggested that the protection conferred by the B virus mHA vaccination approach was not through HI. Previously, we have described that Fc-mediated effector functions (such as ADCC) can be one of the mechanisms by which stalk-specific antibodies contribute to protection *in vivo* independently of HI activity (43–46). Therefore, we tested whether serum antibodies induced by B virus mHAs engaged in Fc-mediated effector functions using an ADCC reporter assay. We observed that D84 pooled sera of adjuvanted Yam mosaic or Mixed mosaic vaccinated mice showed strong induction of ADCC activity when incubated with MDCK cells infected with B/Lee/1940, B/New York/PV00094/2017 or B/New York/PV01181/2018 (**Figure 6B**). In contrast, the adjuvanted Yam WT or Mixed WT group elicited limited levels of antibodies with ADCC activity. Therefore, the B virus mHA vaccination approach likely conferred protection through non-HI-active antibodies that trigger Fc-mediated effector functions.

DISCUSSION

The development of universal influenza virus vaccines that can provide durable protection against multiple strains is one of the most critical global public health priorities. To date, the vast majority of these efforts have focused on influenza A viruses. Given the significant clinical burden and economic impact that influenza B viruses pose on the global population, more efforts should be made to design or refine influenza B virus vaccines. Importantly, in contrast to influenza A viruses, influenza B viruses lack animal reservoirs, except for rare spillovers into marine mammals (47). Another notable difference between influenza A and B viruses is that the evolutionary rate of influenza B viruses is much lower than that of influenza A viruses (48, 49). Both the host restriction and the low evolutionary rate allow for the possibility of eradicating influenza B viruses. Here, a broadly protective inactivated virus vaccine strategy using the B virus mosaic HAs is described, which builds on an earlier mosaic B virus HA protein study (28). The approach is based on the antigenic silencing of the major antigenic sites of the type B HA by replacing them with exotic sequences from HAs of avian influenza A viruses (H5, H8 and H13), yielding mosaic HAs. Compared to the recombinant B mHA proteins, the inactivated B mHA vaccines will provide additional protection mediated by other viral components such as the neuraminidase (NA) and internal proteins. Importantly, the inactivated virus vaccine platform is compatible with most of the influenza virus vaccine production capacity. As hypothesized, sequential vaccination with WIVs expressing the B virus mosaic HAs induced higher cross-reactive antibodies against the conserved epitopes than immunization with WIVs expressing the WT HAs. The mHA approach relies on the replacement of the hypervariable immunodominant epitopes. This can be achieved by either using exotic epitopes from other HA subtypes (as shown in this study) or by introducing irrelevant epitopes such as those consisting of glycines and/or alanines. The latter strategy would very much increase the number of possible mHAs.

Of note, the adjuvant AddaVax, an oil-in-water emulsion adjuvant, had a positive role in inducing antibodies against the conserved epitopes of HA. When adjuvanted with AddaVax, the B virus mHA vaccines induced significantly higher antibody titers than the unadjuvanted B virus mHA vaccines. This effect, to a lesser extent was also observed in WT HA vaccine groups. Interestingly, we also observed that sequential immunization with the B virus mHA vaccines adjuvanted with AddaVax generated higher levels of germinal center B cell reactions than non-adjuvanted B virus mHA vaccines. There seems to be a correlation between the antibody titers against the SD epitopes and the frequency of germinal center B cells. We speculate that this positive effect on germinal center reaction in B virus mHA immunization is due to a subset of recalled memory B cells with relatively low affinity re-entering germinal centers to undergo further somatic hypermutation and affinity maturation. AddaVax seems to facilitate a persistent activation of germinal centers, subsequently helping to boost the antibodies targeting SD epitopes. Furthermore, our results demonstrated that antibody titers against SD epitopes (e.g., stalk-specific antibodies) can be maintained at high levels over a long period of time in mice. We did not observe differences of SD epitope-specific antibodies induced by the homologous and heterologous B virus mHA vaccines. But the protection provided by the heterologous B virus mHAs in the B/Lee/1940 and B/Victoria/2/1987-like B/New York/PV01181/2018 challenge studies seemed to be better by a narrow margin than that provided by the homologous B virus mHAs (**Figures 1**, **3**, **5**). It is also worth noting that in the mouse study, we were comparing the B virus mHA vaccine with their corresponding WT HA constructs. In fact, the current seasonal influenza virus vaccine is a single immunization of a multi-valent vaccine instead of sequential vaccination with heterologous strains. Therefore, it is likely that one or two immunizations with the B virus mHA vaccines in the primed human population would enrich even more SD epitope-specific antibodies than one shot of TIV or QIV. Future clinical studies would be needed to recapitulate these findings and to evaluate the B virus mHA in combination with different adjuvants.

The B virus mHA approach using the inactivated virus vaccine platform induced broadly-reactive antibodies without detectable HI activities. We expect these antibodies are also non-neutralizing based on our previous study (28). Serum antibodies generated by a sequential vaccination with B virus mHA WIVs was highly active in an ADCC reporter assay that measures Fc-mediated effector functions. This was described as an important

mechanism of protection for HA stalk-reactive antibodies of influenza A viruses (43, 44). Here we showed that AddaVax enhanced ADCC activity of the antibodies resulting from vaccination with B virus mHAs. Although it was not measured in this study, a robust induction of IgG2a is expected in mice vaccinated with B mHA vaccines, as it was observed from our preclinical study involving the influenza A mHA vaccines (50). In contrast, sequential vaccination with WT HAs elicited limited levels of antibodies with ADCC reporter activity. Instead, the heterologous WT HA WIVs induced HI-active antibodies to the virus substrates due to the presence of similar immunodominant antigenic sites. However, the HI-active antibodies were not as long-lasting as the antibodies targeting the SD sites, explaining the lower protection of WT HA WIV sera as compared to mHA WIV sera collected at D292 in passive transfer/viral challenge studies. Consistent with what was observed in mice, a recent phase I clinical trial demonstrated that stalk-specific antibodies induced by sequential vaccination of group 1 cHA vaccines were long-lived (26).

Currently, the inactivated split-virion vaccine is most commonly used due to the relatively low production costs and high safety. Recombinant HA subunit vaccines are also available to effectively focus on HA-mediated protection. However, the production capacity of the subunit vaccine is limited (29). Despite the possible loss of immunogenicity, split-virion vaccines and subunit vaccines are used more frequently than the whole-virion vaccines in humans due to their reduced reactogenicity (51–53). Moreover, the recommended vaccine strains sometimes replicate poorly in eggs. Many passages of the vaccine strain in egg might be necessary to achieve high titers, yielding adaptive mutations. These changes, often within the major antigenic sites, can alter the antigenicity of the HAs, resulting in an antigenic mismatch of the vaccine and the circulating strain (54). Of note, the mHA vaccine approach provides durable and broad protection and is suitable for multiple vaccine platforms including inactivated, live attenuated and recombinant HA vaccines. Here, we only investigated the WIV as a platform. It would be of interest in the future to compare the B virus mHA WIV vaccine versus mHAs vaccine in other platforms. Finally, as we only show the activity of serum polyclonal antibodies in this study, further studies will focus on isolating and characterizing monoclonal antibodies targeting the SD epitopes after sequential immunization using mHA vaccines. The interaction of such monoclonal antibodies against the SD HA head epitopes will be studied by structural biology techniques including X-ray crystallography and cryo-EM.

DATA AVAILABILITY STATEMENT

The raw data supporting the conclusions of this article will be made available by the authors, without undue reservation.

ETHICS STATEMENT

The animal study was reviewed and approved by Icahn School of Medicine at Mount Sinai Institutional Animal Care and Use Committee (IACUC).

AUTHOR CONTRIBUTIONS

WS and PP initiated this study. WS, PP, FK, AG-S, and YL designed the experiments. YL, WS, and IG-D performed the experiments. YL and WS analyzed the data. SS, JT, and VS provided protein and virus reagents. YL, WS, and PP wrote the manuscript. All authors contributed to the article and approved the submitted version.

FUNDING

This work was partially funded by NIH (Centers of Excellence for influenza Research and Response, CEIRR,75N93021C00014, PP, FK, AG-S), (NIAID grant P01 AI097092-07, PP, AG-S), (NIAID grant R01 AI145870-03, PP) and by the Collaborative Influenza Vaccine Innovation centers (CIVICs) contract 75N93019C00051 (PP, FK, AG-S).

ACKNOWLEDGMENTS

We thank Dr. Guha Asthagiri Arunkumar for providing the monoclonal antibody 4G12. We thank Victoria Rosado and Dr. Alec Freyn for their assistance with the ADCC experiments, and Dr. Carly Bliss for the assistance with the flow cytometry. We also thank Dr. Jordi Ochando and Christopher Bare from the Flow Cytometry Core at ISMMS. Lastly, we thank the Mount Sinai Pathogen Surveillance Program (Drs. H. van Bakel and E.M. Sordillo) and the Clinical Microbiology Laboratories for providing access to clinical discard specimen.

SUPPLEMENTARY MATERIAL

The Supplementary Material for this article can be found online at: https://www.frontiersin.org/articles/10.3389/fimmu.2021.746447/full#supplementary-material

Supplementary Figure 1 | Frequency of germinal center B cells. Inguinal lymph nodes were collected on D56 **(A)** and D84 **(B)** and frequency of germinal center B cells ($CD3^-B220^+IgD^-GL7^+CD38^{low}$) was measured by FACS. The statistical analysis was performed using one-way ANOVA corrected for multiple comparison using the Tukey test (*P ≤ 0.05; **P ≤ 0.01; ***P ≤ 0.001; ****P ≤ 0.0001; ns, not significant).

REFERENCES

1. Paul Glezen W, Schmier JK, Kuehn CM, Ryan KJ, Oxford J. The Burden of Influenza B: A Structured Literature Review. *Am J Public Health* (2013) 103: e43–51. doi: 10.2105/AJPH.2012.301137
2. Koutsakos M, Nguyen TH, Barclay WS, Kedzierska K. Knowns and Unknowns of Influenza B Viruses. *Future Microbiol* (2016) 11:119–35. doi: 10.2217/fmb.15.120
3. Su S, Chaves SS, Perez A, Mello TD, Kirley PD, Yousey-Hindes KY, et al. Comparing Clinical Characteristics Between Hospitalized Adults With Laboratory-Confirmed Influenza A and B Virus Infection. *Clin Infect Dis* (2014) 59:252–5. doi: 10.1093/cid/ciu269
4. Molinari NAM, Ortega-Sanchez IR, Messonnier ML, Thompsonc WW, Wortley PM, Weintraub E, et al. The Annual Impact of Seasonal Influenza in the US: Measuring Disease Burden and Costs. *Vaccine* (2007) 25:5086–96. doi: 10.1016/j.vaccine.2007.03.046
5. Dijkstra F, Donker GA, Wilbrink B, Gageldonk-Lafeber ABV, van der Sande MAB. Long Time Trends in Influenza-Like Illness and Associated Determinants in The Netherlands. *Epidemiol Infect* (2009) 137:473–9. doi: 10.1017/S095026880800126X
6. Heikkinen T, Ikonen N, Ziegler T. Impact of Influenza B Lineage-Level Mismatch Between Trivalent Seasonal Influenza Vaccines and Circulating Viruses, 1999–2012. *Clin Infect Dis* (2014) 59:1519–24. doi: 10.1093/cid/ciu664
7. Kosasih H, Roselinda, Nurhayati, Klimov A, Xu X, Lindstrom S, et al. Surveillance of Influenza in Indonesia, 2003–2007. *Influenza Other Resp* (2012) 7:313–20. doi: 10.1111/j.1750-2659.2012.00403.x
8. McCullers JA, Hayden FG. Fatal Influenza B Infections: Time to Reexamine Influenza Research Priorities. *J Infect Dis* (2012) 205:870–2. doi: 10.1093/infdis/jir865
9. Chan PS, Chan MCW, Cheung JLK, Lee N, Leung TF, Yeung ACM, et al. Influenza B Lineage Circulation and Hospitalization Rates in a Subtropical City, Hong Kong, 2000–2010. *Clin Infect Dis* (2013) 56:677–84. doi: 10.1093/cid/cis885
10. Tran D, Vaudry W, Moore D, Bettinger JA, Halperin SA, Scheifele DW, et al. Hospitalization for Influenza A Versus B. *Pediatrics* (2016) 138:e20154643. doi: 10.1542/peds.2015-4643
11. Rota PA, Wallis TR, Harmon MW, Rota JS, Kendal AP, Nerome K. Cocirculation of Two Distinct Evolutionary Lineages of Influenza Type B Virus Since 1983. *Virology* (1990) 175:59–68. doi: 10.1016/0042-6822(90)90186-U
12. Wang Q, Cheng F, Lu M, Tian X, Ma J. Crystal Structure of Unliganded Influenza B Virus Hemagglutinin. *J Virol* (2008) 82:3011–20. doi: 10.1128/JVI.02477-07
13. Sun W, Kang DS, Zheng A, Liu STH, Broecker F, Simon V, et al. Antibody Responses Toward the Major Antigenic Sites of Influenza B Virus Hemagglutinin in Mice, Ferrets, and Humans. *J Virol* (2018) 93:e01673–01618. doi: 10.1128/JVI.01673-18
14. Zhirnov OP, Klenk HD. Influenza A Virus Proteins NS1 and Hemagglutinin Along With M2 Are Involved in Stimulation of Autophagy in Infected Cells. *J Virol* (2013) 87:13107–14. doi: 10.1128/JVI.02148-13
15. Krammer F, Palese P. Advances in the Development of Influenza Virus Vaccines. *Nat Rev Drug Discov* (2015) 14:167–82. doi: 10.1038/nrd4529
16. Skowronski DM, Janjua NZ, Sabaiduc S, Serres GD, Winter AL, Gubbay JB, et al. Influenza A/Subtype and B/Lineage Effectiveness Estimates for the 2011–2012 Trivalent Vaccine: Cross-Season and Cross-Lineage Protection With Unchanged Vaccine. *J Infect Dis* (2014) 210:126–37. doi: 10.1093/infdis/jiu048
17. Beyer WEP, Palache AM, Boulfich M, Osterhaus ADME. Rationale for Two Influenza B Lineages in Seasonal Vaccines: A Meta-Regression Study on Immunogenicity and Controlled Field Trials. *Vaccine* (2017) 35:4167–76. doi: 10.1016/j.vaccine.2017.06.038
18. Gaglani M, Vasudevan A, Raiyani C, Murthy K, Chen W, Reis M, et al. Effectiveness of Trivalent and Quadrivalent Inactivated Vaccines Against Influenza B in the United States, 2011–2012 to 2016–2017. *Clin Infect Dis* (2021) 72:1147–57. doi: 10.1093/cid/ciaa102
19. Crépey P, Redondo E, Díez-Domingo J, de LejarazuI RO, Martinón-Torres F, de Miguel AG, et al. From Trivalent to Quadrivalent Influenza Vaccines: Public Health and Economic Burden for Different Immunization Strategies in Spain. *PloS One* (2020) 15:e0233526. doi: 10.1371/journal.pone.0233526
20. Uhart M, Bricout H, Clay E, Largeron N. Public Health and Economic Impact of Seasonal Influenza Vaccination With Quadrivalent Influenza Vaccines Compared Totrivalent Influenza Vaccines in Europe. *Hum Vacc Immunother* (2016) 12:2259–68. doi: 10.1080/21645515.2016.1180490
21. Tricco AC, Chit A, Soobiah C, Hallett D, Meier G, Chen MH, et al. Comparing Influenza Vaccine Efficacy Against Mismatched and Matched Strains: A Systematic Review and Meta-Analysis. *BMC Med* (2013) 11:153. doi: 10.1186/1741-7015-11-153
22. Morimoto N, Takeishi K. Change in the Efficacy of Influenza Vaccination After Repeated Inoculation Under Antigenic Mismatch: A Systematic Review and Meta-Analysis. *Vaccine* (2018) 36:949–57. doi: 10.1016/j.vaccine.2018.01.023
23. Ermler ME, Kirkpatrick E, Sun W, Hai R, Amanat F, Chromikova V, et al. Chimeric Hemagglutinin Constructs Induce Broad Protection Against Influenza B Virus Challenge in the Mouse Model. *J Virol* (2017) 91:e00286–00217. doi: 10.1128/JVI.00286-17
24. Hai R, Krammer F, Tan GS, Pica N, Eggink D, Maamary J, et al. Influenza Viruses Expressing Chimeric Hemagglutinins: Globular Head and Stalk Domains Derived From Different Subtypes. *J Virol* (2012) 86:5774–81. doi: 10.1128/JVI.00137-12
25. Krammer F, Margine I, Hai R, Flood A, Hirsh A, Tsvetnitsky V, et al. H3 Stalk-Based Chimeric Hemagglutinin Influenza Virus Constructs Protect Mice From H7N9 Challenge. *J Virol* (2013) 88:2340–3. doi: 10.1128/JVI.03183-13
26. Nachbagauer R, Feser J, Naficy A, Bernstein DI, Guptill J, Walter EB, et al. A Chimeric Hemagglutinin-Based Universal Influenza Virus Vaccine Approach Induces Broad and Long-Lasting Immunity in A Randomized, Placebo-Controlled Phase I Trial. *Nat Med* (2021) 27:106–14. doi: 10.1038/s41591-020-1118-7
27. McMahon M, Arunkumar GA, Liu W, Stadlbauer D, Albrecht RA, Pavot V, et al. Vaccination With Viral Vectors Expressing Chimeric Hemagglutinin, NP and M1 Antigens Protects Ferrets Against Influenza Virus Challenge. *Front Immunol* (2019) 10:2005. doi: 10.3389/fimmu.2019.02005
28. Sun W, Kirkpatrick E, Ermler M, Nachbagauer R, Broecker F, Krammer F, et al. Development of Influenza B Universal Vaccine Candidates Using the "Mosaic" Hemagglutinin Approach. *J Viol* (2019) 93:e00333–00319. doi: 10.1128/JVI.00333-19
29. Sparrow E, Wood JG, Chadwick C, Newall AT, Torvaldsen S, Moen A, et al. Global Production Capacity of Seasonal and Pandemic Influenza Vaccines in 2019. *Vaccine* (2021) 39:512–20. doi: 10.1016/j.vaccine.2020.12.018
30. Martínez-Sobrido L, García-Sastre A. Generation of Recombinant Influenza Virus From Plasmid DNA. *J Vis Exp* (2010) 42:e2057. doi: 10.3791/2057
31. Fulton BO, Sun W, Heaton NS, Palese P. The Influenza B Virus Hemagglutinin Head Domain Is Less Tolerant to Transposon Mutagenesis Than That of the Influenza A Virus. *J Virol* (2018) 92:e00754–00718. doi: 10.1128/JVI.00754-18
32. Kaufmann L, Syedbasha M, Vogt D, Hollenstein Y, Hartmann J, Janina E, et al. An Optimized Hemagglutination Inhibition (HI) Assay to Quantify Influenzaspecific Antibody Titers. *J Vis Exp* (2017) 130:e55833. doi: 10.3791/55833
33. Krammer F, Margine I, Tan GS, Pica N, Krause JC, Palese P. A Carboxy-Terminal Trimerization Domain Stabilizes Conformational Epitopes on the Stalk Domain of Soluble Recombinant Hemagglutinin Substrates. *PloS One* (2012) 7:e43603. doi: 10.1371/journal.pone.0043603
34. Arunkumar GA, Ioannou A, Wohlbold TJ, Meade P, Aslam S, Amanat F, et al. Broadly Cross-Reactive, Nonneutralizing Antibodies Against Influenza B Virus Hemagglutinin Demonstrate Effector Function-Dependent Protection Against Lethal Viral Challenge in Mice. *J Virol* (2019) 93:e01696–e18. doi: 10.1128/JVI.01696-18
35. Calabroa S, Trittoa E, Pezzottia A, Tacconea M, Muzzia A, Bertholeta S, et al. The Adjuvant Effect of MF59 Is Due to the Oil-in-Water Emulsion Formulation, None of the Individual Components Induce a Comparable Adjuvant Effect. *Vaccine* (2013) 31:3363–9. doi: 10.1016/j.vaccine.2013.05.007
36. Dreyfus C, Laursen NS, Kwaks T, Zuijdgeest D, Khayat R, Ekiert DC, et al. Highly Conserved Protective Epitopes on Influenza B Viruses. *Science* (2012) 337:1343–8. doi: 10.1126/science.1222908
37. Nachbagauer R, Choi A, Izikson R, Cox MM, Palese P, Krammer F. Age Dependence and Isotype Specificity of Influenza Virus Hemagglutinin Stalk-

Reactive Antibodies in Humans. *mBio* (2017) 7:e01996–01915. doi: 10.1128/mBio.01996-15
38. Frank GM, Angeletti D, Ince WL, Gibbs JS, Khurana S, Wheatley AK, et al. A Simple Flow-Cytometric Method Measuring B Cell Surface Immunoglobulin Avidity Enables Characterization of Affinity Maturation to Influenza A Virus. *mBio* (2015) 6:e01156–01115. doi: 10.1128/mBio.01156-15
39. Angeletti D, Kosik I, Santos JJS, Yewdell WT, Boudreau CM, Mallajosyula VVA, et al. Outflanking Immunodominance to Target Subdominant Broadly Neutralizing Epitopes. *Proc Natl Acad Sci USA* (2019) 116:13474–9. doi: 10.1073/pnas.1816300116
40. Tan HX, Jegaskanda S, Juno JA, Esterbauer R, Wong J, Kelly HG, et al. Subdominance and Poor Intrinsic Immunogenicity Limit Humoral Immunity Targeting Influenza HA Stem. *J Clin Invest* (2019) 129:850–62. doi: 10.1172/JCI123366
41. Lofano G, Mancini F, Salvatore G, Cantisani R, Monaci E, Carrisi C, et al. Oil-In-Water Emulsion MF59 Increases Germinal Center B Cell Differentiation and Persistence in Response to Vaccination. *J Immunol* (2015) 195:1617–27. doi: 10.4049/jimmunol.1402604
42. Cox RJ. Correlates of Protection to Influenza Virus, Where Do We Go From Here? *Hum Vacc Immunother* (2013) 9:405–8. doi: 10.4161/hv.22908
43. Jacobsen H, Rajendran M, Choi A, Sjursen H, Brokstad KA, Cox RJ, et al. Influenza Virus Hemagglutinin Stalk-Specific Antibodies in Human Serum are a Surrogate Marker for In Vivo Protection in a Serum Transfer Mouse Challenge Model. *mBio* (2017) 8:e01463–01417. doi: 10.1128/mBio.01463-17
44. Leon PE, He W, Mullarkey CE, Bailey MJ, Miller MS, Krammer F, et al. Optimal Activation of Fc-Mediated Effector Functions by Influenza Virus Hemagglutinin Antibodies Requires Two Points of Contact. *Proc Natl Acad Sci USA* (2016) 113:E5944–51. doi: 10.1073/pnas.1613225113
45. Chai N, Swem LR, Park S, Nakamura G, Chiang N, Estevez A, et al. A Broadly Protective Therapeutic Antibody Against Influenza B Virus With Two Mechanisms of Action. *Nat Commun* (2016) 8:14234. doi: 10.1038/ncomms14234
46. DiLillo DJ, Tan GS, Palese P, Ravetch JV. Broadly Neutralizing Hemagglutinin Stalk–specific Antibodies Require Fcγr Interactions for Protection Against Influenza Virus In Vivo. *Nat Med* (2014) 20:3443. doi: 10.1038/nm.3443
47. Osterhaus ADME, Rimmelzwaan GF, Martina BEE, Bestebroer TM, Fouchier RAM. Influenza B Virus in Seals. *Science* (2000) 288:1051–3. doi: 10.1126/science.288.5468.1051
48. Nobusawa E, Sato K. Comparison of the Mutation Rates of Human Influenza A and B Viruses. *J Virol* (2006) 80:3675–8. doi: 10.1128/JVI.80.7.3675-3678.2006
49. Tan J, Arunkumar GA, Krammer F. Universal Influenza Virus Vaccines and Therapeutics: Where Do We Stand With Influenza B Virus? *Curr Opin Immunol* (2018) 53:45–50. doi: 10.1016/j.coi.2018.04.002
50. Broecker F, Liu STH, Suntronwong N, Sun W, Bailey MJ, Nachbagauer R, et al. A Mosaic Hemagglutinin-Based Influenza Virus Vaccine Candidate Protects Mice From Challenge With Divergent H3N2 Strains. *NPJ Vaccines* (2019) 4:31. doi: 10.1038/s41541-019-0126-4
51. Gross PA, Ennis FA. Influenza Vaccine: Split-Product Versus Whole-Virus Types — How Do They Differ? *N Engl J Med* (1977) 296:567–8. doi: 10.1056/NEJM197703102961012
52. Parkman PD, Hopps HE, Rastogi SC, Meyer.Jr HM. Summary of Clinical Trials of Influenza Virus Vaccines in Adults. *J Infect Dis* (1977) 136:S722–30. doi: 10.1093/infdis/136.Supplement_3.S722
53. Beyera WEP, Nautab JJP, Palachec AM, Giezemand KM, Osterhausa ADME. Immunogenicity and Safety of Inactivated Influenza Vaccines in Primed Populations: A Systematic Literature Review and Meta-Analysis. *Vaccine* (2011) 29:5785–92. doi: 10.1016/j.vaccine.2011.05.040
54. Zost SJ, Parkhouse K, Gumina ME, Kim K, Perez SD, Wilson PC, et al. Contemporary H3N2 Influenza Viruses Have a Glycosylation Site That Alters Binding of Antibodies Elicited by Egg-Adapted Vaccine Strains. *Proc Natl Acad Sci USA* (2017) 114:12578–83. doi: 10.1073/pnas.1712377114

Conflict of Interest: The Icahn School of Medicine at Mount Sinai has filed patent applications entitled "INFLUENZA VIRUS HEMAGGLUTININ PROTEINS AND USES THEREOF" which names PP, FK, AG-S as inventors.

The remaining authors declare that the research was conducted in the absence of any commercial or financial relationships that could be construed as a potential conflict of interest.

The handling Editor declared a past co-authorship with one of the authors FK.

Publisher's Note: All claims expressed in this article are solely those of the authors and do not necessarily represent those of their affiliated organizations, or those of the publisher, the editors and the reviewers. Any product that may be evaluated in this article, or claim that may be made by its manufacturer, is not guaranteed or endorsed by the publisher.

frontiers in Immunology

ORIGINAL RESEARCH
published: 08 October 2021
doi: 10.3389/fimmu.2021.747032

Pandemic Preparedness Against Influenza: DNA Vaccine for Rapid Relief

*Tor Kristian Andersen[1], Johanna Bodin[2], Fredrik Oftung[2], Bjarne Bogen[1,3], Siri Mjaaland[2] and Gunnveig Grødeland[1,3]**

[1] Department of Immunology and Transfusion Medicine, Institute of Clinical Medicine, University of Oslo, Oslo, Norway, [2] Division for Infection Control and Environmental Health, Norwegian Institute of Public Health, Oslo, Norway, [3] Department of Immunology and Transfusion Medicine, Clinic for Laboratory Medicine, Oslo University Hospital, Oslo, Norway

The 2009 "swine flu" pandemic outbreak demonstrated the limiting capacity for egg-based vaccines with respect to global vaccine supply within a timely fashion. New vaccine platforms that efficiently can quench pandemic influenza emergences are urgently needed. Since 2009, there has been a profound development of new vaccine platform technologies with respect to prophylactic use in the population, including DNA vaccines. These vaccines are particularly well suited for global pandemic responses as the DNA format is temperature stable and the production process is cheap and rapid. Here, we show that by targeting influenza antigens directly to antigen presenting cells (APC), DNA vaccine efficacy equals that of conventional technologies. A single dose of naked DNA encoding hemagglutinin (HA) from influenza/A/California/2009 (H1N1), linked to a targeting moiety directing the vaccine to major histocompatibility complex class II (MHCII) molecules, raised similar humoral immune responses as the adjuvanted split virion vaccine Pandemrix, widely administered in the 2009 pandemic. Both vaccine formats rapidly induced serum antibodies that could protect mice already 8 days after a single immunization, in contrast to the slower kinetics of a seasonal trivalent inactivated influenza vaccine (TIV). Importantly, the DNA vaccine also elicited cytotoxic T-cell responses that reduced morbidity after vaccination, in contrast to very limited T-cell responses seen after immunization with Pandemrix and TIV. These data demonstrate that DNA vaccines has the potential as a single dose platform vaccine, with rapid protective effects without the need for adjuvant, and confirms the relevance of naked DNA vaccines as candidates for pandemic preparedness.

Keywords: pandemic, vaccine, DNA vaccine, APC, APC-targeting, influenza, inactivated vaccine

OPEN ACCESS

Edited by:
Corey Patrick Mallett, GlaxoSmithKline, United States

Reviewed by:
Domenico Tortorella, Icahn School of Medicine at Mount Sinai, United States
Teodor Doru Brumeanu, Uniformed Services University of the Health Sciences, United States

***Correspondence:**
Gunnveig Grødeland
gunnveig.grodeland@medisin.uio.no

Specialty section:
This article was submitted to Vaccines and Molecular Therapeutics, a section of the journal Frontiers in Immunology

Received: *25 July 2021*
Accepted: *20 September 2021*
Published: *08 October 2021*

Citation:
Andersen TK, Bodin J, Oftung F, Bogen B, Mjaaland S and Grødeland G (2021) Pandemic Preparedness Against Influenza: DNA Vaccine for Rapid Relief. Front. Immunol. 12:747032. doi: 10.3389/fimmu.2021.747032

INTRODUCTION

Vaccines are highly efficient at prophylactic relief against infectious diseases, and vaccines against influenza, measles, and tuberculosis are examples of vaccines that annually save many lives (1, 2). The current SARS-CoV-2 pandemic has once again reminded us of the dependency on effective vaccines for control of a pandemic outbreak. In 2009, it became clear that the use of conventional

influenza vaccines based on egg-production had several shortcomings. In particular, the production time was prolonged, hampering efficient use even in a situation where the correlate of protection was well established, and approved vaccines against influenza were easily available (3, 4). For pandemic control, rapid availability of well-matched vaccines is key (5–7).

In 2009, the conventional vaccines against pandemic influenza was produced within 6 months, which represents a record fast production for this vaccine format (8). Thus, it should be no surprise that the frontrunner vaccines developed against SARS-CoV-2 in 2020 were based on more versatile technologies (9–11). In this study, we have compared the immunogenicity and efficacy of conventional influenza vaccines to that of a novel DNA vaccine format. DNA vaccines are rapid to produce, easy to store and deploy independent of a cold chain, and highly versatile with respect to updating the vaccine to match new antigenic variants (12). Furthermore, the development of minimally invasive DNA vaccine delivery systems, such as microneedle patches (13, 14) or needle-free jet delivery (15, 16), makes naked DNA vaccines highly applicable in a mass vaccination scenario.

While DNA vaccines against influenza has been in development since the 1990's with promising data in pre-clinical models, there are limited data from clinical trials due to low immunogenicity in larger animals (17). Some recent breakthrough has countered this, and most of the clinically approved DNA vaccines are based on delivery with viral vectors (11, 18, 19). While viral vector delivered DNA vaccines are attractive, the viral vector may in itself pose a risk for development of adverse events (20), and immune responses against the vector backbone may hamper repeated use, e.g. in prime boost vaccination schedules or updates for emerging viral variants.

Previously, we have developed a novel DNA vaccine format where the antigen was genetically linked to a targeting moiety specific for a selected receptor on antigen presenting cells (APC) (21–23). In brief, following delivery of naked DNA plasmids encoding the APC-targeted antigen under a single promotor, the cells at the injection site will secrete the corresponding proteins. The APC-specific targeting moiety will then direct the vaccine proteins specifically to the most relevant cells, and as such greatly enhance vaccine immunogenicity and efficacy (21–23). Of note, we have previously observed that steering of the APC-targeted vaccines to different APC receptors can polarize immune responses to either dominant antibody responses/Th2 or cellular responses/Th1 (24). As such, this vaccine platform could be tailored for enhanced induction of the most relevant correlate of protection for any disease (24–26). For influenza, the main correlate of protection against infection are neutralizing antibodies against the HA protein. We have previously found that targeting of HA to major histocompatibility complex class II (MHCII) molecules was superior at raising protective antibodies following vaccination, as compared to eight other APC specific targeting moieties (αCD11c, αCD40, Xcl-1, MIP-1α, FliC, GM-CSF, Flt-3L, αDEC205) (27). Hence, we have here used a plasmid encoding MHCII-targeted HA molecules for vaccination of mice (23, 28). Previously, such vaccination have demonstrated full protection against lethal influenza challenges in mice up to about a year after a single DNA vaccination (22, 24), as well as demonstrated promising efficacy in larger animals (23).

We have here compared the formation of immune responses in mice following vaccination with this MHCII-targeted DNA vaccine to that of conventional influenza vaccines. More specifically, we compared the MHCII-targeted DNA vaccine to Pandemrix, an adjuvanted inactivated split virion vaccine widely administered to counter the 2009 influenza pandemic, as well as the corresponding non-adjuvanted inactivated trivalent influenza vaccine (TIV) from the 2018/19 season.

We show that a single delivery of the MHCII-targeted DNA vaccine raised antibody responses similar to the adjuvanted Pandemrix, and both vaccines could offer long-lasting protection against a lethal influenza challenge. Interestingly, the MHCII-targeted DNA vaccine proved better than Pandemrix with respect to offering protection against a lethal influenza challenge one week after a single vaccination. This protection was likely attributed to the ability of the MHCII-targeted vaccine to also raise protective T cell responses.

MATERIALS AND METHODS

Mice and Cell Lines

Female BALB/c mice aged 6-8 weeks (Janvier, le Genest-Saint-Isle, France) were used in all experiments. All experiments involving research animals were pre-approved for ethics by the Norwegian Food Safety Authority. Cell work was performed with human embryonic kidney 293E cells purchased from the American Type Culture Collection (ATCC; Manassas, VA, USA).

Vaccines and Vaccination

Anesthetized mice [0.1mg/10g: cocktail of Zoletil Forte (250mg/ml; Virbac France), Rompun (20mg/ml; Bayer Animal Health GmbH), and fentanyl (50μg/ml; Actavis, Germany)] were vaccinated intra muscularly (i.m.) with 25μg DNA (αMHCII-HA) into each quadriceps femoris, immediately followed by electroporation over the injection site (Elgen; Inovio Biomedical Co., Blue Bell, PA). The αMHCII-HA plasmid encodes HA from influenza A/California/07/2009 (H1N1), aa 18-541, linked to the MHCII-specific scFv *via* a dimerization unit consisting of the C_H3 domain of human IgG3 (22). All DNA vaccines were purified by using an EndoFree Plasmid Mega kit (catalog no. 12381; Qiagen, Hilden, Germany) and dissolved in sterile injection fluid (0.9% NaCl). Alternatively, anaesthetized mice were vaccinated i.m. with 1/10 human dose of Pandemrix with AS03 adjuvant (GlaxoSmithKline, Belgium), or a non-adjuvanted trivalent inactivated seasonal influenza vaccine [strains: A/Michigan/45/2015 (H1N1)pdm09-like virus, A/Singapore/INFIMH-16-0019/2016(H3N2)-like virus B/Colorado/06/2017-like virus (B/Victoria/2/87 lineage)].

Viral Challenge

Mice were anaesthetized as described above, and a 5xLD_{50} dose of A/California/07/2009(H1N1) delivered in 10µl into each nostril. Mice were monitored daily for weight loss and euthanized at 80% of the original body weight. In figures, euthanized mice are scored as 80% for the remaining experimental time.

Flow Cytometry and Imaging

Draining LNs (iliac) were harvested and single cell suspensions prepared by GentleMACS dissociator (Miltenyi Biotech, Germany). Cells were stained with anti-CD3 (75-0032, Tonbo biosciences, San Diego, CA, USA), anti-GL7 (144603, Tonbo), anti-CD38 (102718, Tonbo), and anti-B220 (552771, BD Biosciences, Franklin Lakes, NJ, USA). HA reactivity was evaluated by binding to a His-tagged recombinant HA (Cal07) protein with an Y98F substitution (29) (rec.HA^{Y98F}), detected by anti-6xHis mAb (ab133714, Abcam, Cambridge, England). All samples were analyzed using an Attune NxT flow cytometer (Thermo Fisher Scientific, Waltham, MA, USA) and FlowJo software (ver.10).

Draining LNs were embedded in OCT mounting medium (00411243, Q Path, VWR, Radnor, PA, USA), immediately frozen on dry ice and stored at −80°C. Six-micrometer sections were collected on glass slides, air dried, fixed in room temperature acetone for 5 min, air dried, and blocked in 30% normal rat serum with FcRγ blocking reagent (10 µg/ml, HB-197). Sections were then incubated with 2µg/ml rec.HA^{Y98F}, followed by rabbit anti-HA(Cal07) pAb (11085-T54, Sino Biological, Inc) and anti-GL7-PE (144608, BioLegend, San Diego, CA, USA). Finally, colors were amplified using anti-FITC-Alexa Fluor 488 (A-11090, Thermo Fisher Scientific) and anti-R Phycoerythrin-Texas Red (ab34734, Abcam), and counterstained with DAPI. Sections were mounted with ProLong Diamond Antifade Mountant (P36970, Thermo Fisher Scientific). Images were acquired in a Nikon Eclipse Ti microscope using a Nikon S Plan Fluor 20x objective with a 0.60 numerical aperture and a Nikon Digital Sight Camera. All micrographs were analyzed and processed using ImageJ Version: 2.0.0-rc-69/1.52p, Build: 269a0ad53f.

Serum ELISA and Avidity Index ELISA

Blood was harvested by puncture of the saphenous vein, and sera collected by centrifugation. ELISA plates (Costar 5390, Corning, Corning, NY) were coated with 0.5µg/ml rec. HA from A/California/07/2009 (11085-V08H, Sino Biological, Inc., Wayne, PA, USA), blocked with 2% BSA/PBS, and incubated with serially diluted serum samples assayed for individual mice. Captured serum antibodies were detected with anti-mouse IgG1-bio (553500, BD Pharmingen, San Diego, CA, USA), or anti-mouse IgG2a- bio (553502, BD Pharmingen), and streptavidin-alkaline phosphatase (RPN1234, GE Healthcare, Buckinghamshire, UK), or alkaline phosphatase conjugated goat anti-mouse IgG (A2429, Saint-Louis, MO, USA). Plates were developed with phosphatase substrate (P4744, Sigma-Aldrich).

Resistance to UREA wash was used to calculate avidity index. Captured serum antibodies were incubated for 10min with 2M UREA or PBS before detecting remaining serum antibodies with alkaline phosphatase conjugated goat anti-mouse IgG (A9316, Sigma Aldrich). AUC was calculated for the dilution curves and baseline for AUC was calculated based on NaCl serum levels. Avidity index is defined as AUC for samples treated with UREA divided by AUC for the corresponding PBS treated sample.

ELISpot Assay

Bone marrow was harvested from femur and tibia. Single cell suspensions were prepared and seeded on MultiScreen HTS filter plates (MSIPS45, Merck Millipore Ltd., Tullagreen, Ireland) pre-coated overnight at 4°C with 0.5 µg/well of rec.HA (Cal07) (11085-V08H, Sino Biological), and incubated for 20h. Spots were detected with anti-mouse IgG (A1418, Sigma-Aldrich), developed with phosphatase substrate (P4744, Sigma-Aldrich) and analyzed in CTL- ImmunoSpot® analyzer (CTL, Shaker Heights, OH, USA).

In Vivo Cellular Cytotoxicity Assay

In vivo cellular cytotoxicity assay were adapted from Durward et al. (30). In brief, splenocytes were harvested and single cell suspensions prepared. Splenocytes were incubated with the MHC class I restricted influenza HA (Cal07) peptide IYSTVASSL, the NP peptide (RLIQNSLTIERMVLS), or a negative control peptide, at a density of 5x10^7 cells/mL for 1 h at 4°C followed by 30 min incubation at 37°C. Peptide-loaded cells were washed twice in PBS and subsequently stained with 5 µM CellTrace Violet (CTV) (C34557, Life Technologies) (HA peptide loaded cells), or 1 µM CellTrace Far Red (CTFR) (C34564, Life Technologies) (NP peptide loaded), or double stain (CTV and CTFR) (negative control) at a density of 5x10^7 cells/mL for 20 min at 37°C. Cells were mixed in equal ratios (1:1:1), and a total of 15x10^6 cells injected i.v. in a 100µl volume to vaccinated mice. Spleens were harvested 16h later, single cell suspensions prepared, and the presence of peptide loaded cells investigated by flow cytometry. The ratio of CTV to CTV/CTFR or CTFR to CTV/CTFR cells were calculated as % specific lysis = [1 – (average ratio in group with NaCl vaccinated mice/ experimental ratio)].

In Vitro T Cell Stimulation and Cytokine Staining

Spleens from mice were collected 9 and 21 days after vaccination and homogenized through a wire mesh to get a single cell suspension by Lympholyte M (Cedarlane, Burlington, US) gradient centrifugation, and thereafter kept frozen in Fetal Bovine Serum (FBS, Sigma/Merck) with 10% DMSO (Sigma/Merck) at -150°C. Splenocytes were thawed, washed in RPMI 1640 (Gibco, Thermo Fischer Scientific) with 10% FBS (Sigma/Merck) and rested for 24 hours prior to stimulation with 5.6 µg HA/ml (400HAU) of A/California/07/2009 (H1N1) for 4 hours at 37°C in the presence of 2.5 µg/ml brefeldin A (BFA, Sigma/Merck). Positive control was stimulated with 50 ng/ml phorbol myristate acetate (PMA, Sigma/Merck) and 1 µg/ml ionomycin (Sigma/Merck). Cells were stained for viability (Live/dead aqua,

Molecular Probes, Thermo Fischer Scientific) and extracellular markers in Brilliant staining buffer (BD Biosciences, San Antonia, CA, US) (each staining for 30 minutes at room temperature), then fixed and permeabilized (45 minutes at 4°C using Foxp3 fixation and permeabilization kit, eBioscience) prior to intracellular staining (1 hour 4°C). Percentage of positive CD3, CD4, CD8, CD44, CD62L, CD25, CD19, CD49b, Foxp3, CD107a, IFNγ, TNFα, IL-2 and IL-17A cells was analysed on a ZE5 flow cytometer (Bio-Rad, CA, US). Fractions of memory T cells; T effector memory (TEM) $CD44^+CD62L^-$, and T central memory (TCM) $CD44^+CD62L^+$, and naïve T cells $CD44^-CD62L^+$ as well as NK and NKT cells were also assessed using FlowJo_V10 (Tree Star, San Carlos, CA, US).

Splenocytes were harvested 21 days after vaccination, and single cell suspensions rested for 24 hours prior to stimulation with 5.6 μg HA/ml (400HAU) A/California/07/2009 (H1N1) for 4 hours at 37°C in the presence of 2.5 μg/ml brefeldin A (BFA, Sigma). Splenocytes were then stained for identification of IFNγ, IL-2, and TNFα positive CD4 and CD8 T-cells.

Statistical Analysis

The p-values represent exact values calculated by unpaired non-parametric two-tailed Mann-Whitney tests. Weight curves were analyzed with two-way ANOVA, and survival curves with the Gehan-Breslow-Wilcoxon test. Statistical analysis of flow cytometry was performed using one-way ANOVA with the Holm-Sidiak multiple-comparison test. All analysis was performed using GraphPad Prim 9 software.

RESULTS

Induction of Strong and Long Lasting Protective Antibodies up to 6 Months After a Single Vaccination

In order to compare the antibody kinetics of different vaccine strategies, we vaccinated mice once i.m. with either TIV, Pandemrix, or the MHCII-targeted DNA vaccine (αMHCII-HA). Both Pandemrix and αMHCII-HA are monovalent vaccines, designed to protect against A/California/07/2009 (H1N1), whereas TIV in addition to a pdm09 like strain contains an H3N2 strain and an influenza B strain. The plasmids encoding αMHCII-HA were formulated in a physiological saline solution (NaCl), while Pandemrix was formulated with the adjuvant solution AS03. Thus, both saline and AS03 were used as experimental negative controls.

Following a single vaccination with the different vaccines, serum samples were collected and monitored for HA specific antibodies over 180 days. Both αMHCII-HA and Pandemrix rapidly generated high titers of Cal07 HA specific IgG that were maintained over time. A peak was observed between 42 and 92 days post vaccination, and where the mice vaccinated with Pandemrix had significantly higher total IgG levels as compared to αMHCII-HA (**Figure 1A**). However, αMHCII-HA raised significantly higher antibody responses as compared to TIV, which only induced modest antibody responses in this system. After the peak, the responses seemed to reach a plateau from about day 106, and that were maintained for at least 180 days.

The antibody responses were highly strain specific, and only mild reactivity against the serologically different strain A/Puerto Rico/8/1934 (H1N1) (PR8) was detected after vaccination with Pandemrix or αMHCII-HA (**Figure 1B**). Interestingly, the difference between Pandemrix and αMHCII-HA seemed to be mostly due to a significantly higher amount of IgG1 antibodies following vaccination with Pandemrix (**Figure 1C**), while there were no significant differences in IgG2a levels (**Figure 1D**).

At day 180, mice were challenged with a lethal dose of influenza virus Cal07. Weight was monitored and used as an objective indicator of morbidity. As expected from the measured antibody responses, both αMHCII-HA and Pandemrix vaccination induced significantly improved protection as compared to TIV, characterized by near sterile protection and minimal weight loss after challenge (**Figure 1E**). In accordance with ethical requirements, mice that reached a 20% weight loss during the infection were euthanized. Importantly, none of the mice vaccinated with αMHCII-HA or Pandemrix reached this threshold (**Figure 1F**). Based on the low antibody levels associated with TIV, it may, however, be surprising that only 2/8 mice in this group lost 20% or more of their weight, as opposed to the negative control groups where 8/8 had to be euthanized. The mice receiving TIV lost weight until day 6 after infection, but from then on stabilized and regained weight (**Figure 1F**).

In sum, we observed that a single vaccination with either αMHCII-HA or Pandemrix could raise strong and long-lasting strain specific protective antibody responses against HA.

Rapid Induction of Antibodies and Protection Against a Lethal Challenge With Influenza Virus

Time is essential during a pandemic outbreak, with respect to both production time and the generation of protective immunity. Thus, we investigated how fast the different vaccines were able to induce protective immunity. BALB/c mice were vaccinated once with αMHCII-HA, Pandemrix, TIV, or controls, and sera examined for antibody responses at day 7 after vaccination. Importantly, a majority of the mice vaccinated with either αMHCII-HA or Pandemrix had detectable levels of HA specific IgG, but there were also some that had not yet seroconverted (**Figure 2A**). TIV immunized mice did not display any serum antibodies at day 7. Interestingly, αMHCII-HA was the only vaccine that could induced any antibody responses against the heterologous strain PR8, albeit only in 2 out of 16 mice in the group (**Figure 2B**). For homologous antibody responses against HA from Cal07, IgG1 and IgG2a levels were similar for Pandemrix and αMHCII-HA, but as was observed for total IgG, not all mice had seroconverted at this early time point (**Figures 2C, D**).

At day 8 after a single vaccination, mice were given a lethal dose of influenza Cal07 virus and weight was monitored. Interestingly, mice receiving αMHCII-HA lost significantly less

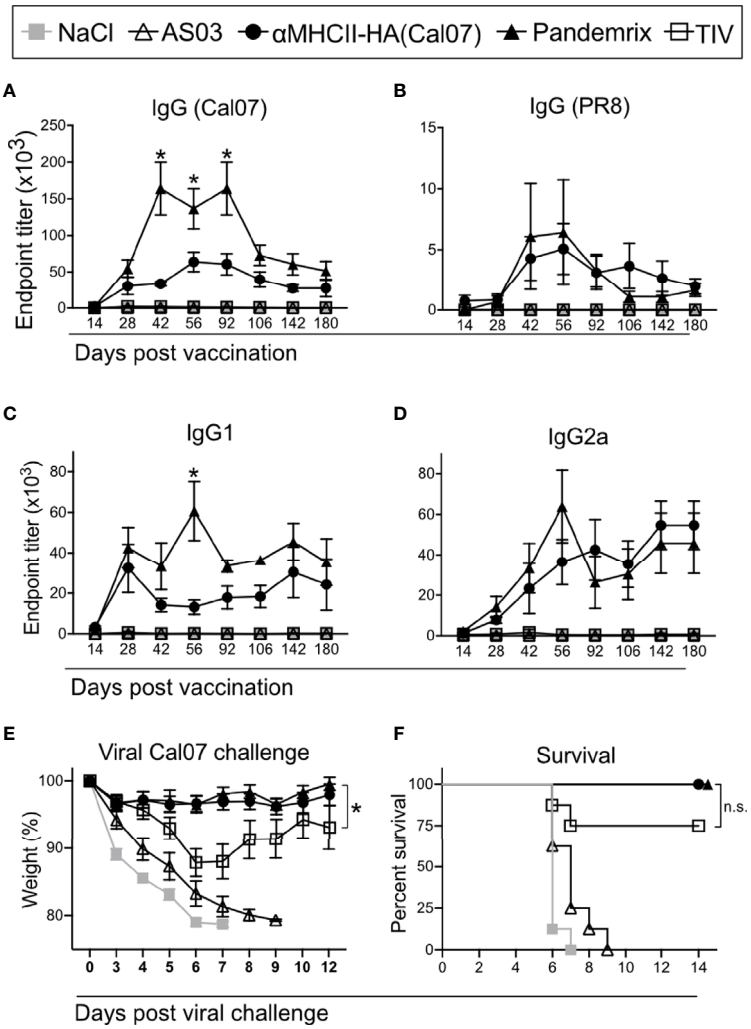

FIGURE 1 | Long term antibody responses and protection after a single vaccination. Mice (n=8/group) were vaccinated i.m. with the indicated vaccines. **(A–D)** Serum antibodies were monitored up to 6 months after vaccination in ELISA for **(A)** total IgG against HA from Cal07, **(B)** total IgG against HA from PR8, **(C)** IgG1 against HA from Cal07, and **(D)** IgG2a against HA from Cal07. *P < 0.05 for αMHCII-HA versus Pandemrix. **(E, F)** At 180 days after vaccination, mice were challenged with 5xLD_{50} dose of Cal07. **(E)** Weight was monitored. **(F)** Survival curve after challenge, defined by 20% weight loss. **(A–E)** Data shown are mean ± SEM, *P < 0.05 (two-way ANOVA) **(F)** *P < 0.05 (Gehan-Breslow-Wilcoxon test). n.s., not significant.

weight as compared to mice vaccinated with Pandemrix, but there was a smaller initial weight loss also in this group (**Figure 2E**). The trend also held when assessing survival as defined by a 20% weight loss, with αMHCII-HA displaying a 25% relative improved survival rate, albeit not statistically significant, when compared to Pandemrix (**Figure 2F**). Mice vaccinated with TIV were not protected 7 days after challenge. None of the vaccines induced protection against the heterologous PR8 virus at day 8 post vaccination (**Figures 2G, H**).

Taken together, we found that a single vaccination with either Pandemrix or αMHCII-HA could rapidly lead to seroconversion that translated into protection already one week after vaccination. In addition, vaccination with the MHCII-targeted DNA vaccine significantly improved morbidity as compared to Pandemrix.

Plasma Cells and High Avidity Antibodies After Vaccination

To characterize the antibody response induced after vaccination with the different vaccines in detail, we first investigated the presence of plasma cells in bone marrow following vaccination. Thus, bone marrow was harvested from mice that had been vaccinated once with αMHCII-HA or Pandemrix. Single cell suspensions were prepared, and the number of anti-HA (Cal07) secreting cells assayed by ELISpot. At day 9, we detected no anti-HA secreting cells in bone marrow, but by day 14 anti-HA secreting cells had formed for both these vaccines. Although low, at day 21 the levels had doubled, indicating a steady rise in anti-HA secreting cells in response to vaccination. The development was similar for both αMHCII-HA and Pandemrix, but there was

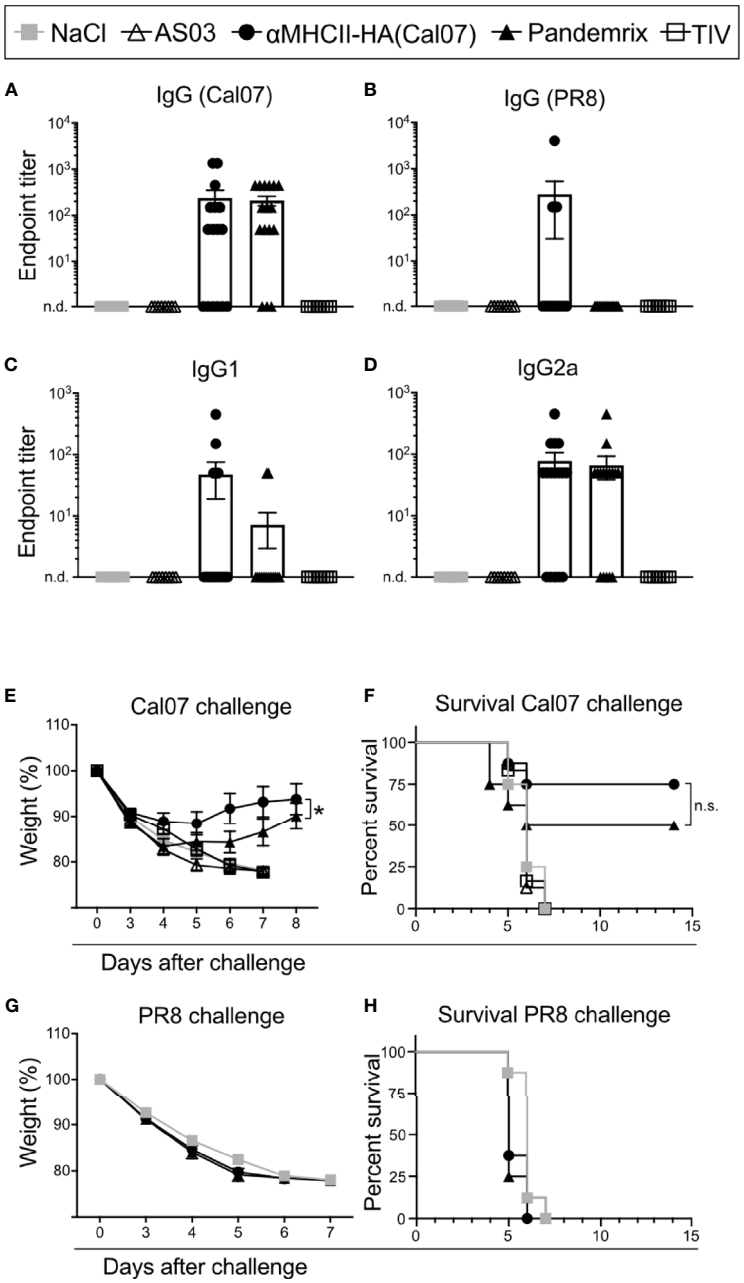

FIGURE 2 | Rapid induction of antibodies and protection after vaccination. Mice were vaccinated i.m. with the indicated vaccines. **(A–D)** Serum antibodies were monitored at day 7 after vaccination in ELISA for **(A)** total IgG against HA from Cal07, **(B)** total IgG against HA from PR8, **(C)** IgG1 against HA from Cal07, and **(D)** IgG2a against HA from Cal07. Pandemrix, αMHCII-HA, and NaCl: n=16/group. AS03 and TIV: n=8/group. **(E, F)** At day 8 after vaccination, mice (n=8/group) were challenged with a 5xLD_{50} dose of influenza Cal07. **(E)** Weight was monitored. **(F)** Survival curve, as defined by a 20% weight loss. **(G, H)** At day 8 after vaccination, mice (n=8/group) were challenged with a 5xLD_{50} dose of influenza PR8. **(G)** Weight was monitored. **(F)** Survival curve, as defined by a 20% weight loss. **(A, D, E, G)** Data shown are mean ± SEM, *P < 0.05 (two-way ANOVA); **(F, H)** *P < 0.05 (Gehan-Breslow-Wilcoxon test). n.s., not significant.

a tendency that Pandemrix had slightly higher numbers of plasma cells at day 14 and 21 (**Figure 3A**).

To evaluate long-term responses, we also examined plasma cells at day 180 in bone marrow following vaccination with TIV, αMHCII-HA, and Pandemrix. Interestingly, mice vaccinated with αMHCII-HA had significantly higher levels of plasma cells in the bone marrow as compared to mice receiving Pandemrix. Mice vaccinated with TIV did not show any plasma cells in response to vaccination after 180 days (**Figure 3B**).

Next, we wanted to investigate the avidity of the vaccine induced antibodies and set up an assay measuring the resistance to UREA wash as an indication of antibody binding avidity. In

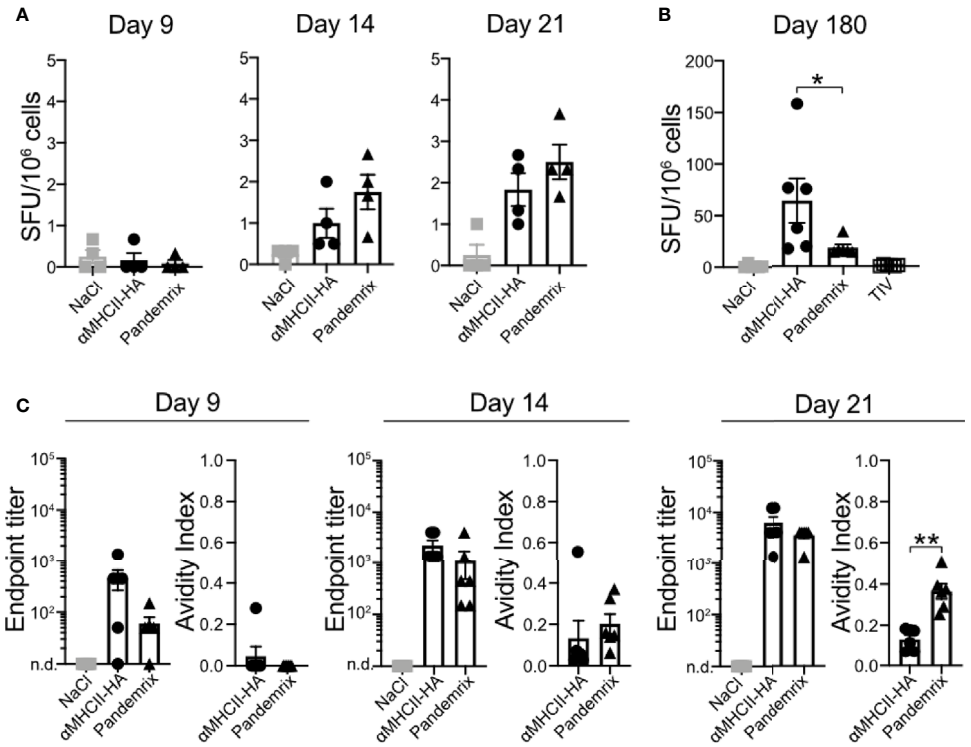

FIGURE 3 | Plasma cells in bone marrow and antibody avidity after vaccination. Mice (n=6/group) were vaccinated i.m. with the indicated vaccines. **(A, B)** Bone marrow (tibia) was harvested, and anti-HA secreting cells examined by ELISpot at **(A)** days 9, 14, and 21 after vaccination, or **(B)** day 180 post vaccination. **(C)** Antibody titers and avidity index of serum antibodies against HA as measured in ELISA from the indicated time points post vaccination. Data shown are mean ± SEM, *P < 0.05, **P < 0.01 (Mann-Whitney).

this assay, relative signals between washing with UREA or PBS in ELISA were compared, and an avidity index of 0 or 1 indicated no resistance or absolute resistance to UREA wash, respectively. Sera collected from mice at day 7, 14, and 21 post vaccination were assayed. In accordance with the above results from ELISA (**Figures 1**, **2**), we did not observe significant differences in antibody titers for Pandemrix and αMHCII-HA. However, mice vaccinated with Pandemrix demonstrated a steady increase in serum antibodies with higher avidity towards HA from Cal07 (**Figure 3C**), mimicking the tendency observed for plasma cells in bone marrow (**Figure 3A**). At day 21, mice vaccinated with Pandemrix had significantly more serum antibodies with increased avidity as compared to mice vaccinated with αMHCII-HA, even though serum antibody levels were similar between the two vaccines (**Figure 3C**).

In sum, we found that Pandemrix induced antibodies with higher avidity more rapidly than αMHCII-HA (day 21). However, with time (6 months) the level of plasma cells in response to αMHCII-HA vaccination was significantly higher than after vaccination with Pandemrix.

Germinal Center Induction After Vaccination and HA Reactive B Cells

The early presence of plasma cells in bone marrow could indicate a strong germinal center (GC) reaction to the vaccine antigen (**Figure 3A**). Thus, we wanted to investigate the formation of GCs, as well as the presence of HA reactive B cells with a GC phenotype.

Mice were vaccinated once and draining lymph nodes (LN) (iliac) harvested on days 9, 14, and 21. Cells from the prepared single cell suspensions were stained for GC B cells ($B220^+$ $CD38^{lo}$ $GL7^+$), identified by a recombinant HA probe (**Figure 4A**). A steady rise in HA reactivity among B cells was observed from day 9 through day 21 post vaccination (**Figure 4B**). Mice receiving αMHCII-HA had GC B cells with a significantly elevated HA reactivity. However, Pandemrix induced a stronger GC reaction, and although the percentage of GC HA reactivity was lower in these mice, the total number of HA reactive GC B cells was significantly higher than after vaccination with αMHCII-HA (**Figure 4C**).

The increased levels of GC B cells observed after vaccination with Pandemrix was likely augmented by the adjuvant AS03. Pandemrix is a split vaccine and also contains other antigens than HA. Thus, a new experiment was performed for day 21 post vaccination to also include an adjuvant control group and the non-adjuvanted split vaccine TIV. As expected, vaccination with αMHCII-HA again induced the highest percentages of HA reactive B cells with a GC phenotype in the LNs. The control groups vaccinated with NaCl or AS03 defined the background, and we observed that TIV induced low, but significant, levels of

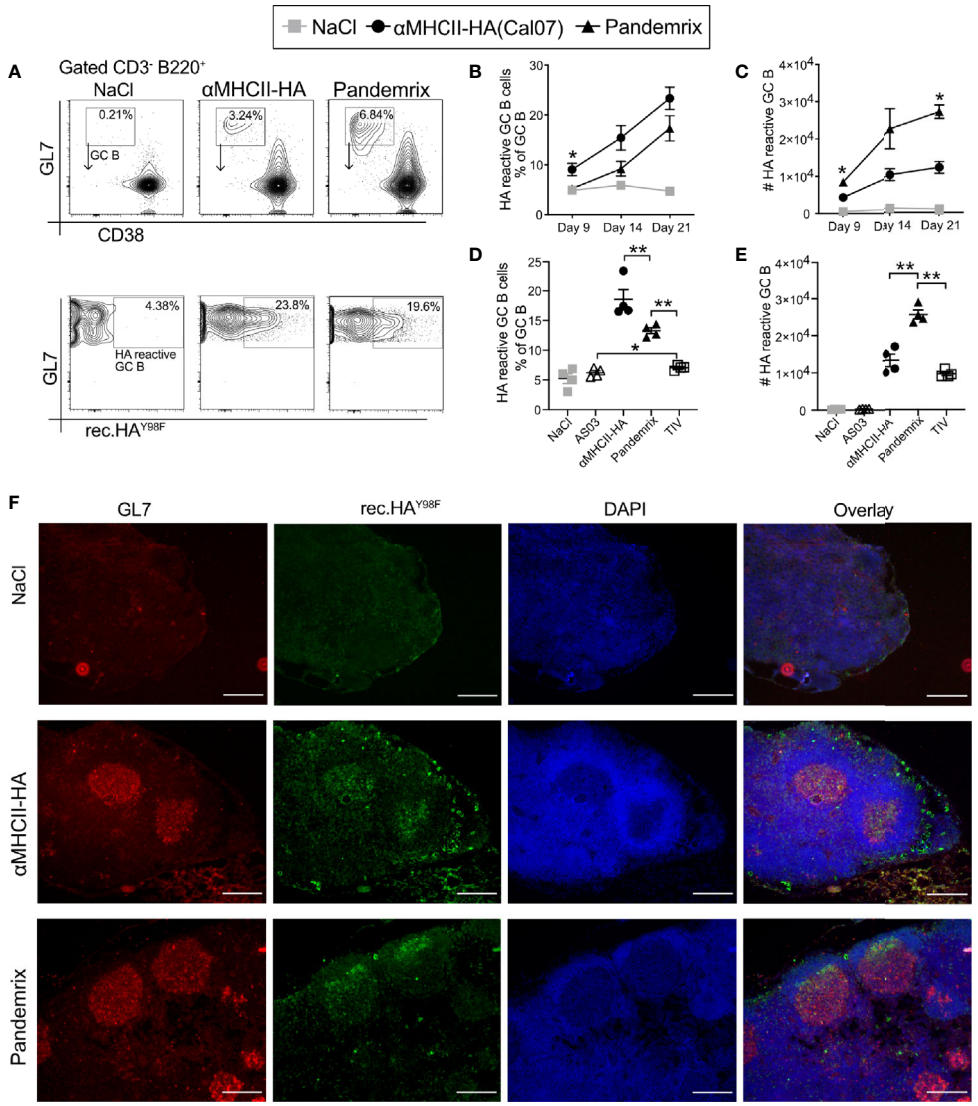

FIGURE 4 | Germinal center response and early formation of plasma cells after vaccination. Mice (n=4/group) were vaccinated i.m. with the indicated vaccines. **(A–E)** Draining lymph nodes (iliac) were harvested and examined for B cells ($CD3^-$ $B220^+$), GC markers ($GL7^+CD38^{lo}$), and binding to a recombinant HA probe by flow cytometry. **(A)** Gating strategy. Representative flow charts are shown. **(B)** Fraction of HA reactive B cells with a GC phenotype on the indicated time points. **(C)** Absolute numbers of HA reactive GC B cells from draining LNs at the indicated time points. **(D, E)** In a new experiment, the GC response was investigated at 21 days post vaccination. **(D)** Fraction of HA reactive B cells with a GC phenotype. **(E)** Absolute numbers of HA reactive GC B cells. **(F)** Cryosections of draining lymph nodes harvested 21 days after vaccinations, and stained with GL7 (red), rHA^{Y98F} (green), and DAPI (blue). Scale bar is 200μm. Data shown are mean ± SEM, *P < 0.05, **P < 0.01 (Mann-Whitney).

HA reactive GC B cells (**Figure 4D**). When looking at the total number of HA reactive GC B cells, however, we again observed that Pandemrix induced the highest absolute numbers (**Figure 4E**).

The formation of GC was also evaluated by microscopic imaging of LNs harvested at day 21 after vaccination. The cryopreserved LN sections were stained with the GC activation marker GL7, the recombinant HA probe, and DAPI (**Figure 4F**). Multiple GC structures with HA reactivity were observed for the mice receiving αMHCII-HA or Pandemrix, in accordance with the flow cytometry data.

Taken together, the data demonstrate that vaccination with αMHCII-HA induced a response where the reactivity of GC B cells was focused on HA. Pandemrix induce a stronger immune response in total, and as such had a higher total number of GC B cells and HA reactive GC B cells.

Strong Cytotoxic T-Cell Responses Induced by αMHCII-HA

The fairly similar B cell activation and antibody levels observed after vaccination with Pandemrix or αMHCII-HA led to the

question of whether differences in induction of cytotoxic T cells could explain the improved survival that was observed in mice at day 8 after vaccination with αMHCII-HA (**Figure 2**). Thus, single cell suspensions of splenocytes from naïve mice were loaded with MHC class I restricted peptides from HA, influenza nucleoprotein (NP), or an irrelevant peptide as negative control, and stained with cell trace dyes. Next, the peptide loaded splenocytes were injected i.p. into mice immunized 9 days or 8 weeks prior with TIV, Pandemrix, αMHCII-HA, or NaCl. Following a 16h incubation, spleens were harvested and the presence of transferred cells investigated by flow cytometry (**Figure 5A**). The ratios of HA or NP peptide loaded splenocytes to the irrelevant peptide negative control in NaCl treated mice was used as a reference to calculate the relative specific lysis of HA or NP peptide loaded cells in the vaccinated groups.

Importantly, mice vaccinated 9 days earlier with αMHCII-HA displayed a strong cytotoxic response towards the HA peptide that was about 10-fold higher than that observed in mice vaccinated with Pandemrix (**Figure 5B**). Vaccination with Pandemrix raised a similar cytotoxic response against both NP and HA, while αMHCII-HA, as expected, did not induce any cytotoxic activity towards the NP peptide (**Figure 5C**). Interestingly, TIV induced similar responses as Pandemrix

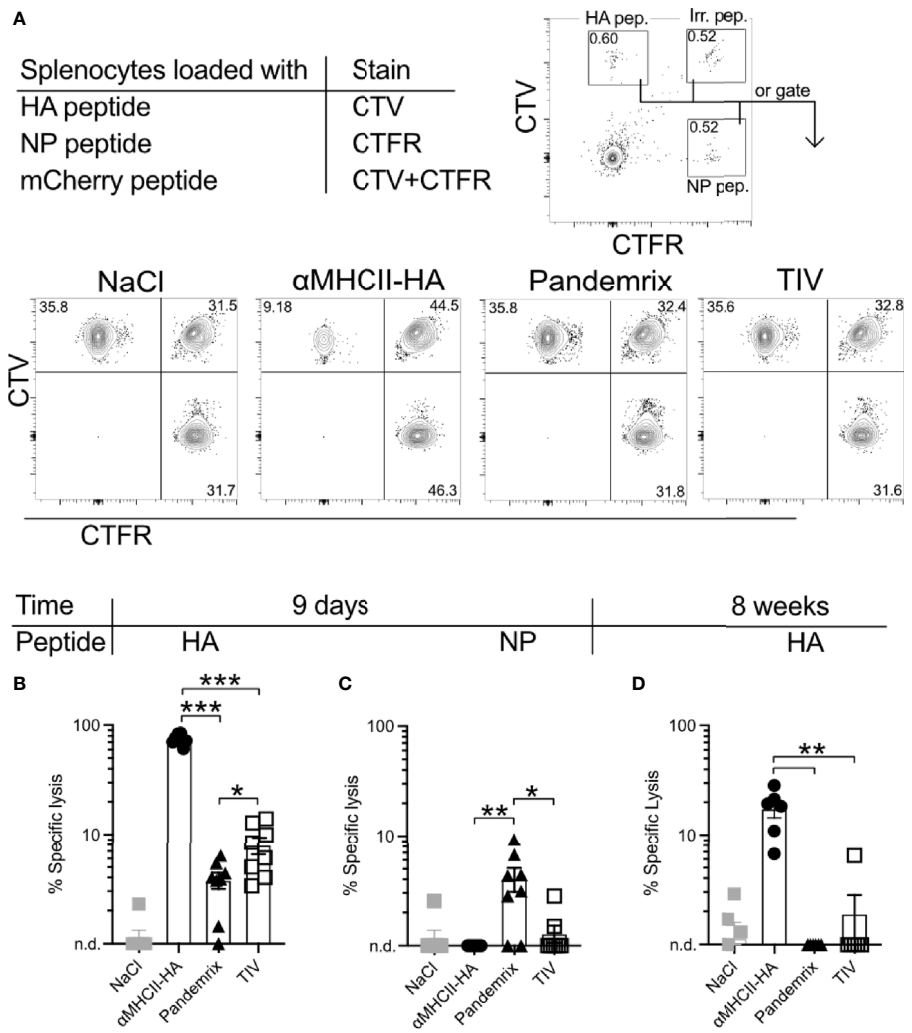

FIGURE 5 | Short and long-term antigen-specific cytotoxic responses after vaccination. Mice (n=6-8/group) were vaccinated once i.m. with the indicated vaccines. After 9 days or 8 weeks, splenocytes from naïve mice were loaded with MHC class I restricted peptides from HA (IYSTVASSL), NP (RLIQNSLTIERMVLS), or irrelevant peptide. Cells were stained with CellTrace Violet (CTV), CellTrace Far Red (CTFR), or double stained with CTV and CTFR, respectively. Cells were mixed in equal ratios and injected i.v. to vaccinated mice. 16h later, spleens were harvested and the presence of peptide loaded splenocytes were assessed by flow cytometry. **(A)** Gating strategy for identification of transferred cells. **(B)** HA-specific lysis of splenocytes 9 days after vaccination. **(C)** NP-specific lysis of splenocytes 9 days after vaccination. **(D)** HA-specific lysis of splenocytes 8 weeks after vaccination. Data shown are mean ± SEM, *P < 0.05, **P < 0.01, ***P < 0.001 (Mann-Whitney).

against both groups of peptides. In order to also examine the long-term cytotoxic potential, we set up a similar experiment 8 weeks post vaccination. The cytotoxic responses were markedly reduced in all the vaccine groups as compared to day 9, but the group vaccinated with αMHCII-HA maintained a significant and strong cytotoxic response (**Figure 5D**).

In sum, the data clearly demonstrated that αMHCII-HA induced a superior cytotoxic response both at early and later time points as compared to Pandemrix. The early induction of cytotoxic immunity could explain the improved protection observed after vaccination with αMHCII-HA and the viral challenge at 8 days post vaccination (**Figure 2**).

Cytokine Secretion Following Vaccination

T cells with an enhanced effector function have often been characterized by the dual secretion of two or more key cytokines (31), and the significant difference observed for cytotoxic responses between the vaccine groups (**Figure 5**) points towards different functional T cell profiles. Thus, we investigated the secretion of IFNγ, IL-2, and TNFα in T cells from splenocytes harvested 21 days after a single vaccination, and stimulated *ex vivo* with HA (Cal07). In accordance with the improved cytotoxic response following vaccination with αMHCII-HA (**Figure 5**), the highest numbers of IFNγ, IL-2, and TNFα secreting CD4 T-cells were observed for this group (**Figure 6A**). TIV induced somewhat higher numbers of cytokine secreting cells as compared to Pandemrix. The trend held also for double secreting CD4 T-cells. Triple secreting CD4 T-cells were not observed for any vaccine groups (**Figure 6A**). A similar trend was observed for the CD8 T-cells, but with somewhat higher levels (**Figure 6B**).

While the cytokine profiles indicated an increased level of effector T-cells, analysis of cells with effector memory (T_{EM}) and central memory (T_{CM}) phenotype was performed for CD4 and CD8 T-cells after *ex vivo* antigen stimulation. T_{EM} was identified as CD4/CD8$^+$ CD44$^+$ CD64L$^-$ cells and T_{CM} was identified as CD4/CD8$^+$ CD44$^+$ CD64L$^+$ cells. The T_{EM} subsets were slightly elevated in mice receiving αMHCII-HA for both CD4 and CD8 T-cells, whereas the other vaccine groups were similar to background (**Figures 6C, D**). T_{CM} were not clearly elevated above background levels (NaCl and AS03), although the percentage of CD8 T_{CM} seemed to be higher in mice receiving TIV compared to αMHCII-HA (**Figures 6E, F**).

Taken together, the data confirms an increased potential for activation of multifunctional T cells following vaccination with αMHCII-HA, as compared to Pandemrix and TIV. Further, immunization with αMHCII-HA increased the T_{EM} levels of both CD4 and CD8 T cells, indicating a strong protective effect. This is reflected in the highest survival rate after viral challenge compared across the vaccine platforms tested.

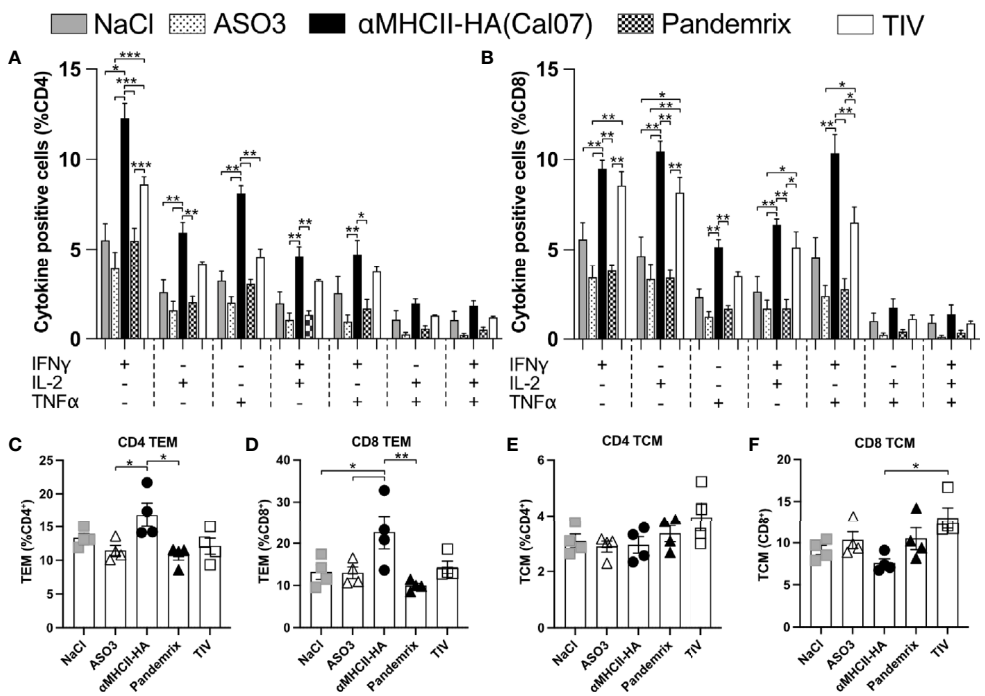

FIGURE 6 | Multifunctional T cell subsets after vaccination. Mice (n=4/group) were vaccinated once i.m. with the indicated vaccines. 21 days after vaccination, splenocytes were harvested, and following overnight resting stimulated for 4h with HA (Cal07) in the presence of a protein transport inhibitor. Single, double, or triple expression of cytokines IFNγ, IL-2, and TNFα were investigated for CD4 **(A)** and CD8 **(B)** T cell subsets. **(C, D)** Effector memory (T_{EM}) and central memory (T_{CM}) T cell subsets were defined as CD44$^+$ CD64L$^-$, and CD44$^+$ CD64L$^+$, respectively. **(C)** Presence of CD4 T_{EM}. **(D)** Presence of CD8 T_{EM}. **(E)** Presence of CD4 T_{CM}. **(F)** Presence of CD8 T_{CM}. Data shown are mean ± SEM, *P < 0.05, **P < 0.01, ***P < 0.001 (Anova og Tukey's multiple comparison).

DISCUSSION

The current SARS-CoV-2 pandemic has once again reminded us of our dependency on effective vaccines for control of a pandemic outbreak, and new vaccine platforms that efficiently can quench pandemic emergences are urgently needed. It is particularly important that the vaccines can be rapidly available for deployment in the population, and that protective immune responses are raised rapidly after vaccination.

In this study, we compared formation of immune responses in mice following vaccination with an MHCII-targeted DNA vaccine to that of conventional influenza vaccines. More specifically, we used an adjuvanted, inactivated split virion vaccine widely administered to counter the 2009 influenza pandemic (Pandemrix) and the corresponding conventional non-adjuvanted seasonal trivalent inactivated vaccine (TIV). A single delivery of the MHCII-targeted DNA vaccine raised HA-specific antibody responses with high avidity already after one week, similar to the responses induced by the adjuvanted Pandemrix, and both vaccines offered long-lasting protection against a lethal influenza challenge. Interestingly, the MHCII-targeted DNA vaccine proved even better than Pandemrix with respect to offering early protection against a lethal influenza challenge, probably due to the enhanced activation of cellular immunity after vaccination with αMHCII-HA.

DNA vaccines against influenza have been in development since the 1990's with promising data in pre-clinical models, but the reduced efficacy often observed in larger animals and humans has hampered progression to clinical application (17). New formulations such as lipid nanoparticles (32, 33), viral vector formulations (34, 35), and gene delivery methods (36) have increased vaccine efficacy, and a naked DNA vaccine from Inovio against SARS-CoV-2 just entered Phase 3 clinical testing (37).

The DNA vaccine format has several advantages for use in a pandemic setting, including advantageous price points and a cold chain independent distribution. A vaccine suited for pandemic preparedness against influenza should also be easily adaptable to match antigens of emerging strains and perform consistent across known influenza subtypes. Importantly, we have previously developed MHCII targeted DNA vaccines against several influenza subtypes, and observed a consistent and high immunogenicity in mice and larger animals (22, 23, 38, 39).

Besides the advantages of the DNA vaccine format, large-scale use of prophylactic DNA vaccines have also raised some safety concerns. Most pronounced is perhaps the potential for integration into host genomes (40, 41), antibiotic resistance (42), and DNA directed auto immunity (43). Fortunately, these phenomena have not been detected during clinical trials (37, 44–47). DNA vaccines have thus far demonstrated a good safety profile during clinical evaluations, but, as we have recently been reminded (48), rare adverse events are difficult to detect prior to use in a larger population.

The main correlate of protection against influenza is neutralizing antibodies that can block viral entry, and influenza vaccines typically aim for induction of these. Here, the rapid rise observed in antibody levels after vaccination with αMHCII-HA or Pandemrix was supported by increases in GC B-cells and plasma cells in bone marrow. These parameters were also reflected by the avidity index scores of serum antibodies for the two vaccines. Pandemrix induced a slightly stronger response than the DNA vaccine for practically all antibody or B-cell related measurements at early time points, although not statistically significant. Further, Pandemrix induced a very high number of GC B-cells, but the total HA reactivity was increased with αMHCII-HA. The adjuvant AS03 likely contributed to the high number of GC B cells found in draining lymph nodes after Pandemrix vaccination. AS03 is optimized for increased influx of immune cells to lymph nodes and B cell recruitment (49), and presumably contributed to a significant increase in the number of HA reactive GC B cells and the tendency of higher plasma cell numbers in the bone marrow at similar time points. Fluorescent micrographs demonstrated that the GCs with HA reactivity were slightly enhanced following vaccination with Pandemrix as compared to αMHCII-HA, in general accordance with GC B cell profile seen in the flow cytometry data (**Figure 4**).

Importantly, both Pandemrix and αMHCII-HA induced full protection against a lethal influenza challenge at 180 days post a single vaccination, with virtually no weight loss observed. Thus, the elevated IgG1 responses observed after vaccination with Pandemrix (**Figure 1**), as well as the increased avidity observed during the first weeks after vaccination (**Figure 3**), did not make a difference for the protective capacity long- or short-term as compared to MHCII-HA (**Figures 1**, **2**). At day 180 post a single vaccination, we also observed lower levels of anti-HA secreting plasma cells in bone marrow after Pandemrix vaccination as compared to αMHCII-HA. This also did not hamper protection, indicating that both vaccines were able to induce sufficient memory formation. TIV induced moderate long-term protection, in accordance with expectations for the single delivery of a non-adjuvanted vaccine administered to naïve mice.

In a pandemic setting, rapid formation of protective immunity is key. It is therefore important that both Pandemrix and αMHCII-HA were able to induce moderate protection against a lethal viral challenge already 8 days post a single vaccination. Interestingly, the DNA vaccine demonstrated a slight increase in survival as compared to Pandemrix, but significantly reduced morbidity. As expected, TIV did not induce any sign of immune resistance to challenge only 8 days after vaccination. At this time point, neither vaccine conferred sterilizing immunity against influenza. However, strong cytotoxic T-cell responses elicited by the MHCII targeted DNA vaccine are likely the underlying reason for the observed reduced morbidity in this vaccine group, as demonstrated by the significantly lower weight loss (**Figure 2**). This explanation was supported by observations of increased levels of CD4 and CD8 effector memory T cells after DNA vaccination. The clear differences in cytotoxicity observed *ex vivo* was also supported by the T cell cytokine profiles, with key cytokines such as IFN-γ, IL-2, and TNF-α elevated after DNA immunization both for the CD8 and CD4 T-cell compartment. The T cell responses raised at day 8 post vaccination were, however, not sufficient for

protection against a different strain of influenza H1N1 (**Figures 2G, H**). However, we have previously found that the cellular immune responses induced by αMHCII-HA can protect against antigenically variable strains at 4 weeks after a single DNA vaccination (22, 50).

The hemagglutination inhibition (HI) assay is currently at the core for regulatory assessments of influenza vaccine immunogenicity (51). It evaluates the ability of antibodies to prevent virus from binding to red blood cells. Concerns about considering the HI titer a lone predictor of vaccine efficacy have been raised (52), especially for strains with a pandemic potential (53). During the past 20 years, several influenza subtypes (e.g. H5, H7, H9, and H10) have been demonstrated to breach the zoonotic barrier (54). The influenza virus is prone to antigenic drift, potentially hampering the efficacy of vaccine induced strain specific and neutralizing antibodies. Vaccines against influenza pandemics should therefore ideally be able to raise a combination of protective antibodies and T cell responses, offering at least some protection also against strain variants that may emerge. The ability of the MHCII-targeted DNA vaccine to raise a broader type of immune response, including both strong antibody responses and T cells, is encouraging in this respect.

For pandemic preparedness, one should consider the contribution from cytotoxic T cells induced solely by vaccines or in combination with pre-existing immunity. T cells often react to conserved epitopes that are shared among many different strains or even subtypes of influenza, offering immune resistance in the absence of effective antibodies (55). An ideal vaccine for pandemic preparedness should therefor activate both arms of the immune system and induce neutralizing antibodies as well as cytotoxic T cell responses. T cell mediated immunity cannot confer sterilizing immunity, but the broader responses to more conserved epitopes in the virion may prevent progression to severe morbidity or mortality. Thus, it may be important to establish T cell based correlates of protection against disease for improved evaluation and approval of influenza vaccines.

In summary, DNA vaccines targeting HA to MHCII molecules demonstrated comparable antibody responses and efficacy to Pandemrix in a mouse model. A noteworthy difference between these two vaccines was the cytotoxic T-cell response after vaccination with αMHCII-HA, that likely improved symptomatic disease at an early time-point after a single vaccination. Due to the many advantages of the DNA vaccine format over egg-based split virus vaccines, these data confirms the relevance of DNA vaccines as an attractive approach for pandemic preparedness.

DATA AVAILABILITY STATEMENT

The original contributions presented in the study are included in the article/supplementary material. Further inquiries can be directed to the corresponding author.

ETHICS STATEMENT

The animal study was reviewed and approved by Norwegian Food Safety Authority.

AUTHOR CONTRIBUTIONS

GG, SM, TKA, and BB conceived and designed experiments. TKA, JB, SM, FO, and GG performed and analyzed experiments. TKA and GG wrote the paper. All authors edited and commented on the paper. All authors contributed to the article and approved the submitted version.

FUNDING

The work has been funded by the Research Council of Norway, as well as Helse Sør-Øst.

ACKNOWLEDGMENTS

We thank Kristina Randjelovic for technical help. Mice were housed at the Department of Comparative Medicine, Oslo University Hospital, and at the Animal Core Facility of the Norwegian Insitute of Public Health. We gratefully acknowledge the technical help from department staff at these two locations.

REFERENCES

1. Andersen P, Scriba TJ. Moving Tuberculosis Vaccines From Theory to Practice. *Nat Rev Immunol* (2019) 19:550–62. doi: 10.1038/s41577-019-0174-z
2. Orenstein WA, Ahmed R. Simply Put: Vaccination Saves Lives. *Proc Natl Acad Sci U S A* (2017) 114:4031–3. doi: 10.1073/pnas.1704507114
3. Blasio BF, Iversen BG, Tomba GS. Effect of Vaccines and Antivirals During the Major 2009 A(H1N1) Pandemic Wave in Norway–and the Influence of Vaccination Timing. *PLoS One* (2012) 7:e30018. doi: 10.1371/journal.pone.0030018
4. Paules CI, Fauci AS. Influenza Vaccines: Good, But We Can Do Better. *J Infect Dis* (2019) 219:S1–4. doi: 10.1093/infdis/jiy633
5. Conway JM, Tuite AR, Fisman DN, Hupert N, Meza R, Davoudi B, et al. Vaccination Against 2009 Pandemic H1N1 in a Population Dynamical Model of Vancouver, Canada: Timing Is Everything. *BMC Public Health* (2011) 11:932. doi: 10.1186/1471-2458-11-932
6. Matrajt L, Halloran ME, Longini IMJr. Optimal Vaccine Allocation for the Early Mitigation of Pandemic Influenza. *PLoS Comput Biol* (2013) 9: e1002964. doi: 10.1371/journal.pcbi.1002964
7. Mylius SD, Hagenaars TJ, Lugner AK, Wallinga J. Optimal Allocation of Pandemic Influenza Vaccine Depends on Age, Risk and Timing. *Vaccine* (2008) 26:3742–9. doi: 10.1016/j.vaccine.2008.04.043
8. Krammer F, Palese P. Advances in the Development of Influenza Virus Vaccines. *Nat Rev Drug Discov* (2015) 14:167–82. doi: 10.1038/nrd4529
9. Baden LR, El Sahly HM, Essink B, Kotloff K, Frey S, Novak R, et al. Efficacy and Safety of the mRNA-1273 SARS-CoV-2 Vaccine. *N Engl J Med* (2021) 384:403–16. doi: 10.1056/NEJMoa2035389

10. Polack FP, Thomas SJ, Kitchin N, Absalon J, Gurtman A, Lockhart S, et al. Safety and Efficacy of the BNT162b2 mRNA Covid-19 Vaccine. *N Engl J Med* (2020) 383:2603–15. doi: 10.1056/NEJMoa2034577
11. Voysey M, Clemens SAC, Madhi SA, Wecky LY, Folegatti PM, Aley PK, et al. Safety and Efficacy of the ChAdOx1 Ncov-19 Vaccine (AZD1222) Against SARS-CoV-2: An Interim Analysis of Four Randomised Controlled Trials in Brazil, South Africa, and the UK. *Lancet* (2021) 397:99–111. doi: 10.1016/S0140-6736(20)32661-1
12. Kutzler MA, Weiner DB. DNA Vaccines: Ready for Prime Time? *Nat Rev Genet* (2008) 9:776–88. doi: 10.1038/nrg2432
13. Fernando GJ, Zhang J, Ng H-I, Haigh OL, Yukiko SR, Kendall MAF. Influenza Nucleoprotein DNA Vaccination by a Skin Targeted, Dry Coated, Densely Packed Microprojection Array (Nanopatch) Induces Potent Antibody and CD8(+) T Cell Responses. *J Control Release* (2016) 237:35–41. doi: 10.1016/j.jconrel.2016.06.045
14. Song J-M, Kim Y-C, Compans RW, Prausnitz MR, Kang S-M. DNA Vaccination in the Skin Using Microneedles Improves Protection Against Influenza. *Mol Ther* (2012) 20:1472–80. doi: 10.1038/mt.2012.69
15. Diehl MC, Lee JC, Daniels SE, Tebas P, Khan AS, Giffear M, et al. Tolerability of Intramuscular and Intradermal Delivery by CELLECTRA((R)) Adaptive Constant Current Electroporation Device in Healthy Volunteers. *Hum Vaccin Immunother* (2013) 9:2246–52. doi: 10.4161/hv.24702
16. Graham BS, Enama ME, Nason MC, Gordon IJ, Peel SA, Ledgerwood JE, et al. DNA Vaccine Delivered by a Needle-Free Injection Device Improves Potency of Priming for Antibody and CD8+ T-Cell Responses After Rad5 Boost in a Randomized Clinical Trial. *PLoS One* (2013) 8:e59340. doi: 10.1371/journal.pone.0059340
17. Lee LYY, Izzard L, Hurt AC. A Review of DNA Vaccines Against Influenza. *Front Immunol* (2018) 9:1568. doi: 10.3389/fimmu.2018.01568
18. Pollard AJ, Launay O, Lelievre J-D, Lacabaratz C, Grande S, Goldstein N, et al. Safety and Immunogenicity of a Two-Dose Heterologous Ad26.ZEBOV and MVA-BN-Filo Ebola Vaccine Regimen in Adults in Europe (EBOVAC2): A Randomised, Observer-Blind, Participant-Blind, Placebo-Controlled, Phase 2 Trial. *Lancet Infect Dis* (2021) 21:493–506. doi: 10.1016/S1473-3099(20)30476-X
19. Wolf J, Jannat R, Dubey S, Troth S, Onorato MT, Coller B-A, et al. Development of Pandemic Vaccines: ERVEBO Case Study. *Vaccines (Basel)* (2021) 9. doi: 10.3390/vaccines9030190
20. Cines DB, Bussel JB. SARS-CoV-2 Vaccine-Induced Immune Thrombotic Thrombocytopenia. *N Engl J Med* (2021) 384:2254–6. doi: 10.1056/NEJMe2106315
21. Fredriksen AB, Sandlie I, Bogen B. DNA Vaccines Increase Immunogenicity of Idiotypic Tumor Antigen by Targeting Novel Fusion Proteins to Antigen-Presenting Cells. *Mol Ther* (2006) 13:776–85. doi: 10.1016/j.ymthe.2005.10.019
22. Grodeland G, Mjaaland S, Roux KH, Fredriksen AB, Bogen B. DNA Vaccine That Targets Hemagglutinin to MHC Class II Molecules Rapidly Induces Antibody-Mediated Protection Against Influenza. *J Immunol* (2013) 191:3221–31. doi: 10.4049/jimmunol.1300504
23. Grodeland G, Fredriksen AB, Løset GÅ, Vikse E, Fugger L, Bogen B. Antigen Targeting to Human HLA Class II Molecules Increases Efficacy of DNA Vaccination. *J Immunol* (2016) 197:3575–85. doi: 10.4049/jimmunol.1600893
24. Grodeland G, Mjaaland S, Tunheim G, Fredriksen AB, Bogen B. The Specificity of Targeted Vaccines for APC Surface Molecules Influences the Immune Response Phenotype. *PLoS One* (2013) 8:e80008. doi: 10.1371/journal.pone.0080008
25. Fossum E, Grødeland G, Terhorst D, Tveita AA, Vikse E, Mjaaland S, et al. Vaccine Molecules Targeting Xcr1 on Cross-Presenting DCs Induce Protective CD8+ T-Cell Responses Against Influenza Virus. *Eur J Immunol* (2015) 45:624–35. doi: 10.1002/eji.201445080
26. Grodeland G, Fossum E, Bogen B. Polarizing T and B Cell Responses by APC-Targeted Subunit Vaccines. *Front Immunol* (2015) 6:367. doi: 10.3389/fimmu.2015.00367
27. Braathen R, Spång HCL, Lindeberg MM, Fossum E, Grødeland G, Fredriksen AB, et al. The Magnitude and IgG Subclass of Antibodies Elicited by Targeted DNA Vaccines Are Influenced by Specificity for APC Surface Molecules. *Immunohorizons* (2018) 2:38–53. doi: 10.4049/immunohorizons.1700038
28. Grodeland G, Bogen B. Efficient Vaccine Against Pandemic Influenza: Combining DNA Vaccination and Targeted Delivery to MHC Class II Molecules. *Expert Rev Vaccines* (2015) 14:805–14. doi: 10.1586/14760584.2015.1029919
29. Frank GM, Angeletti D, Ince WL, Gibbs JS, Khurana S, Wheatley AK, et al. A Simple Flow-Cytometric Method Measuring B Cell Surface Immunoglobulin Avidity Enables Characterization of Affinity Maturation to Influenza A Virus. *MBio* (2015) 6:e01156. doi: 10.1128/mBio.01156-15
30. Durward M, Harms J, Splitter G. Antigen Specific Killing Assay Using CFSE Labeled Target Cells. *J Vis Exp* (2010) e2250. doi: 10.3791/2250
31. Seder RA, Darrah PA, Roederer M. T-Cell Quality in Memory and Protection: Implications for Vaccine Design. *Nat Rev Immunol* (2008) 8:247–58. doi: 10.1038/nri2274
32. Francis JE, Skakic I, Dekiwadia C, Shukla R, Taki AC, Walduck A, et al. Solid Lipid Nanoparticle Carrier Platform Containing Synthetic TLR4 Agonist Mediates Non-Viral DNA Vaccine Delivery. *Vaccines (Basel)* (2020) 8. doi: 10.3390/vaccines8030551
33. Mucker EM, Karmali PP, Vega J, Kwilas SA, Wu H, Joselyn M, et al. Lipid Nanoparticle Formulation Increases Efficiency of DNA-Vectored Vaccines/Immunoprophylaxis in Animals Including Transchromosomic Bovines. *Sci Rep* (2020) 10:8764. doi: 10.1038/s41598-020-65059-0
34. de Vries RD, Rimmelzwaan GF. Viral Vector-Based Influenza Vaccines. *Hum Vaccin Immunother* (2016) 12:2881–901. doi: 10.1080/21645515.2016.1210729
35. Rollier CS, Spencer AJ, Sogaard KC, Honeycutt J, Furze J, Bregu M, et al. Modification of Adenovirus Vaccine Vector-Induced Immune Responses by Expression of a Signalling Molecule. *Sci Rep* (2020) 10:5716. doi: 10.1038/s41598-020-61730-8
36. Suschak JJ, Williams JA, Schmaljohn CS. Advancements in DNA Vaccine Vectors, non-Mechanical Delivery Methods, and Molecular Adjuvants to Increase Immunogenicity. *Hum Vaccin Immunother* (2017) 13:2837–48. doi: 10.1080/21645515.2017.1330236
37. Tebas P, Yang S, Boyer JD, Reuschel EL, Patel A, Christensen-Quick A, et al. Safety and Immunogenicity of INO-4800 DNA Vaccine Against SARS-CoV-2: A Preliminary Report of an Open-Label, Phase 1 Clinical Trial. *EClinicalMedicine* (2021) 31:100689. doi: 10.1016/j.eclinm.2020.100689
38. Andersen TK, Zhou F, Cox R, Bogen B, Grodeland G. A DNA Vaccine That Targets Hemagglutinin to Antigen-Presenting Cells Protects Mice Against H7 Influenza. *J Virol* (2017) 91:e01340–17. doi: 10.1128/JVI.01340-17
39. Anderson AM, Baranowska-Hustad M, Braathen R, Grodeland G, Bogen B. Simultaneous Targeting of Multiple Hemagglutinins to APCs for Induction of Broad Immunity Against Influenza. *J Immunol* (2018) 200:2057–66. doi: 10.4049/jimmunol.1701088
40. Langer B, Renner M, Scherer J, Schule S, Cichutek K. Safety Assessment of Biolistic DNA Vaccination. *Methods Mol Biol* (2013) 940:371–88. doi: 10.1007/978-1-62703-110-3_27
41. Strain AJ. The Uptake and Fate of Exogenous Cellular DNA in Mammalian Cells. *Dev Biol (Basel)* (2006) 123:23–8.
42. Williams JA. Improving DNA Vaccine Performance Through Vector Design. *Curr Gene Ther* (2014) 14:170–89. doi: 10.2174/1566523214031408191225538
43. MacColl G, Bunn C, Goldspink G, Bouloux P, Gorecki DC. Intramuscular Plasmid DNA Injection can Accelerate Autoimmune Responses. *Gene Ther* (2001) 8:1354–6. doi: 10.1038/sj.gt.3301537
44. Carter C, Houser KV, Yamshchikov GV, Bellamy AR, May J, Enama ME, et al. Safety and Immunogenicity of Investigational Seasonal Influenza Hemagglutinin DNA Vaccine Followed by Trivalent Inactivated Vaccine Administered Intradermally or Intramuscularly in Healthy Adults: An Open-Label Randomized Phase 1 Clinical Trial. *PLoS One* (2019) 14:e0222178. doi: 10.1371/journal.pone.0222178
45. Danko JR, Kochel T, Teneza-Mora N, Luke TC, Raviprakash K, Sun P, et al. Safety and Immunogenicity of a Tetravalent Dengue DNA Vaccine Administered With a Cationic Lipid-Based Adjuvant in a Phase 1 Clinical Trial. *Am J Trop Med Hyg* (2018) 98:849–56. doi: 10.4269/ajtmh.17-0416
46. Elizaga ML, Li SS, Kochar NK, Wilson GJ, Allen MA, Tieu HVN, et al. Safety and Tolerability of HIV-1 Multiantigen pDNA Vaccine Given With IL-12 Plasmid DNA *via* Electroporation, Boosted With a Recombinant Vesicular Stomatitis Virus HIV Gag Vaccine in Healthy Volunteers in a Randomized, Controlled Clinical Trial. *PLoS One* (2018) 13:e0202753. doi: 10.1371/journal.pone.0202753
47. Richie TL, Charoenvit Y, Wang R, Epstein JE, Hedstrom RC, Kumar S, et al. Clinical Trial in Healthy Malaria-Naive Adults to Evaluate the Safety, Tolerability, Immunogenicity and Efficacy of MuStDO5, a Five-Gene, Sporozoite/Hepatic Stage Plasmodium Falciparum DNA Vaccine Combined With Escalating Dose Human GM-CSF DNA. *Hum Vaccin Immunother* (2012) 8:1564–84. doi: 10.4161/hv.22129
48. Schultz NH, Sørvoll IH, Michelsen AE, Munthe LA, Lund-Johansen F, Ahlen MT, et al. Thrombosis and Thrombocytopenia After ChAdOx1 Ncov-19 Vaccination. *N Engl J Med* (2021) 384:2124–30. doi: 10.1056/NEJMoa2104882

49. Galson JD, Truck J, Kelly DF, van der Most R. Investigating the Effect of AS03 Adjuvant on the Plasma Cell Repertoire Following Ph1n1 Influenza Vaccination. *Sci Rep* (2016) 6:37229. doi: 10.1038/srep37229
50. Lambert L, Kinnear E, McDonald JU, Grodeland G, Bogen B, Stubsrud E, et al. DNA Vaccines Encoding Antigen Targeted to MHC Class II Induce Influenza-Specific CD8(+) T Cell Responses, Enabling Faster Resolution of Influenza Disease. *Front Immunol* (2016) 7:321. doi: 10.3389/fimmu.2016.00321
51. Committee for Medicinal Products for Human Use. *Guideline on Influenza Vaccines: Non-Clinical and Clinical Module. EMA/CHMP/VWP/457259/2014*. European Medicines Agency (2016).
52. Cox RJ. Correlates of Protection to Influenza Virus, Where do We Go From Here? *Hum Vaccin Immunother* (2013) 9:405–8. doi: 10.4161/hv.22908
53. Krammer F, Cox RJ. The Emergence of H7N9 Viruses: A Chance to Redefine Correlates of Protection for Influenza Virus Vaccines. *Expert Rev Vaccines* (2013) 12:1369–72. doi: 10.1586/14760584.2013.850036
54. Bailey ES, Fieldhouse JK, Choi JY, Gray GC. A Mini Review of the Zoonotic Threat Potential of Influenza Viruses, Coronaviruses, Adenoviruses, and Enteroviruses. *Front Public Health* (2018) 6:104. doi: 10.3389/fpubh.2018.00104
55. Koutsakos M, Illing PT, Nguyen THO, Mifsud NA, Crawford JC, Rizzetto S, et al. Human CD8(+) T Cell Cross-Reactivity Across Influenza A, B and C Viruses. *Nat Immunol* (2019) 20:613–25. doi: 10.1038/s41590-019-0320-6

Conflict of Interest: GG and BB are inventors on a patent applications filed on an HLAII-specific targeting moiety according to institutional rules through the TTO offices of the University of Oslo and Oslo University Hospital. Further, BB is inventor of the core patent of Vaccibody AS, and hold shares in the company.

The remaining authors declare that the research was conducted in the absence of any commercial or financial relationships that could be construed as a potential conflict of interest.

Publisher's Note: All claims expressed in this article are solely those of the authors and do not necessarily represent those of their affiliated organizations, or those of the publisher, the editors and the reviewers. Any product that may be evaluated in this article, or claim that may be made by its manufacturer, is not guaranteed or endorsed by the publisher.

frontiers in Immunology

ORIGINAL RESEARCH
published: 12 October 2021
doi: 10.3389/fimmu.2021.745625

Bacteriophage T4 Vaccine Platform for Next-Generation Influenza Vaccine Development

Mengling Li[1,2,3,4], *Pengju Guo*[1,2,3,4], *Cen Chen*[1,2,3,4], *Helong Feng*[3,5], *Wanpo Zhang*[3], *Changqin Gu*[3], *Guoyuan Wen*[5*], *Venigalla B. Rao*[6*] *and Pan Tao*[1,2,3,4*]

[1] Key Laboratory of Development of Veterinary Diagnostic Products, Ministry of Agriculture, College of Veterinary Medicine, Huazhong Agricultural University, Wuhan, China, [2] The Cooperative Innovation Center for Sustainable Pig Production, Huazhong Agricultural University, Wuhan, China, [3] Division of Pathology, College of Veterinary Medicine, Huazhong Agricultural University, Wuhan, China, [4] Hongshan Lab, Wuhan, China, [5] Institute of Animal Husbandry and Veterinary Sciences, Hubei Academy of Agricultural Sciences, Wuhan, China, [6] Bacteriophage Medical Research Center, Department of Biology, The Catholic University of America, Washington, DC, United States

OPEN ACCESS

Edited by:
Corey Patrick Mallett, GlaxoSmithKline, United States

Reviewed by:
Chunhong Dong, Georgia State University, United States
Ze Chen, Hunan Normal University, China

***Correspondence:**
Pan Tao
taopan@mail.hzau.edu.cn
Venigalla B. Rao
rao@cua.edu
Guoyuan Wen
wgy_524@163.com

Specialty section:
This article was submitted to Vaccines and Molecular Therapeutics, a section of the journal Frontiers in Immunology

Received: *22 July 2021*
Accepted: *24 September 2021*
Published: *12 October 2021*

Citation:
Li M, Guo P, Chen C, Feng H, Zhang W, Gu C, Wen G, Rao VB and Tao P (2021) Bacteriophage T4 Vaccine Platform for Next-Generation Influenza Vaccine Development. Front. Immunol. 12:745625. doi: 10.3389/fimmu.2021.745625

Developing influenza vaccines that protect against a broad range of viruses is a global health priority. Several conserved viral proteins or domains have been identified as promising targets for such vaccine development. However, none of the targets is sufficiently immunogenic to elicit complete protection, and vaccine platforms that can enhance immunogenicity and deliver multiple antigens are desperately needed. Here, we report proof-of-concept studies for the development of next-generation influenza vaccines using the bacteriophage T4 virus-like particle (VLP) platform. Using the extracellular domain of influenza matrix protein 2 (M2e) as a readout, we demonstrate that up to ~1,281 M2e molecules can be assembled on a 120 x 86 nanometer phage capsid to generate M2e-T4 VLPs. These M2e-decorated nanoparticles, without any adjuvant, are highly immunogenic, stimulate robust humoral as well as cellular immune responses, and conferred complete protection against lethal influenza virus challenge. Potentially, additional conserved antigens could be incorporated into the M2e-T4 VLPs and mass-produced in *E. coli* in a short amount of time to deal with an emerging influenza pandemic.

Keywords: flu vaccine, virus-like particle, bacteriophage T4 platform, extracellular domain of matrix protein 2, phage display

INTRODUCTION

Influenza A (Flu) virus is a highly contagious infectious agent that can cause severe respiratory disease (1, 2). Although vaccines are available, they are strain-specific and mainly target the variable head domain of viral major envelope glycoprotein, hemagglutinin (HA) (3, 4). The stalk domain of HA exhibits a degree of conservation among influenza virus strains but cannot efficiently induce antibody responses in its native state due to the immunodominance of epitopes present in the head domain (5–8). The rapid evolution of influenza viruses through antigenic drift and shift in their surface glycoproteins, HA in particular, greatly limit the effectiveness of the current vaccines (9–12). Therefore, vaccines have to be reformulated annually using reference viruses recommended by

World Health Organization, based on the information provided by the Global Influenza Surveillance Network (13).

Vaccines that provide broader protection against diverse influenza virus strains are highly desired, and remain as one of the major challenges in Flu vaccine design. Many efforts have been focused on developing such vaccines, often referred to as "universal" Flu vaccines, using the conserved viral proteins or domains (12, 14). The internal virion proteins, nucleoprotein (NP) and matrix protein 1 (M1), were mainly used as immunogens to induce cellular immune responses, particularly CD8+ T cells with cross-protection against heterologous influenza viruses (15–17). Engineered headless HA stalk, in which the immunodominant head domain was removed, was mainly used to induce antibodies that recognize or neutralize diverse influenza virus strains (18, 19). Another widely used target for universal Flu vaccines is the extracellular domain of matrix protein 2 (M2e) that is highly conserved among divergent influenza virus strains (14, 20, 21). However, none of these vaccine targets are highly immunogenic and many strategies were employed to enhance their immunogenicity (22–25).

By taking advantage of *in vitro* assembly of antigen proteins on bacteriophage T4 capsid, we recently developed a virus-like nanoparticle (VLP) platform that can elicit robust immune responses against a variety of displayed antigens, without any adjuvants (26, 27). In this study, we aimed to develop an M2e-based influenza vaccine using this T4 VLP platform. The immunogenicity of M2e, a NH2-terminal 23-residue peptide of viral matrix protein 2 (M2), is otherwise quite low during natural infection due to its small size and low abundance on the virion surface (28). However, when displayed on a VLP, the M2e induced significant immune responses and provided variable protection against influenza virus infection (29, 30). Although many different platforms such as hepatitis B virus core particle (31), human papillomavirus particle (32), and tobacco mosaic virus (33) were used as VLP carriers for M2e, phage-based VLP platforms are more attractive for their cost-effectiveness and large-scale manufacturing potential that is critical during an influenza pandemic.

Several phage platforms have been tested for M2e Flu vaccine design. The M2e antigens displayed on T7 phage capsids, though immunogenic, failed to provide complete protection against lethal influenza virus challenge (34). This was probably due to the low copy number of M2e molecules on the phage capsid. Indeed, it was found that vaccines with higher M2e epitope densities resulted in higher protection efficacy (35, 36), and most of the licensed viral vaccines contain high density of antigens on the virion surface (37). Although phage fd can display up to 2,700 copies of peptide per capsid through its major coat protein pVIII, the display is sensitive to the size of the peptide (38). Therefore, only part of M2e (residues 2-16) could be displayed on phage fd, which still provided protection from death but the challenged mice showed severe body weight loss indicating its limited value as a vaccine (39).

We have previously reported that phage T4 can be used for efficient display of full-length proteins as large as 120 kDa at high density because of its unique capsid architecture (40). The 120 x 86 nm phage capsid is comprised of four major capsid proteins: two essential proteins, the capsid shell protein gp23* (930 copies) and the vertex protein gp24* (55 copies), and two non-essential proteins, the small outer capsid protein (Soc, 870 copies) and the highly antigenic outer capsid protein (Hoc, 155 copies) (**Figure 1A**) (26, 41). Deletion of Hoc and Soc (Hoc^-Soc^- T4) has no effect on the propagation of T4 under laboratory conditions, and recombinant antigens fused to Hoc or Soc specifically bind to Hoc^-Soc^- T4 capsids *in vitro* with high affinity (26, 27, 42, 43).

Here, we show that three variants of M2e peptide from human, swine, and avian influenza viruses tandemly fused to the COOH-terminus of Soc can be efficiently displayed on Hoc^-Soc^- T4 capsids at high density by *in vitro* assembly (**Figure 1**). The resultant M2e-decorated T4 nanoparticles are found to be highly immunogenic and induced complete protection against lethal influenza virus challenge, without any adjuvant. Importantly, the vaccinated mice showed no or minor symptoms after lethal influenza virus challenge, based on clinical observations including body weight and pathological analyses. These studies provide proof-of-concept for the development of next-generation influenza vaccines using the phage T4 VLP platform.

RESULTS

Construction of M2e-Decorated Bacteriophage T4 Nanoparticles

To stimulate increased breadth of immunogenicity and protection against Flu viruses, a 3M2e gene containing three types of M2e sequences from human, swine, and avian influenza viruses were synthesized (**Supplementary Table**) and fused to the COOH-terminus of Soc to generate Soc-3M2e. A flexible GGSSGGSS linker was introduced between each M2e segment as depicted in **Figure 1B**, to minimize any interference in the folding of the M2e domains. Hexa-histidine tags were also added to both termini of the Soc-3M2e protein. The fusion protein was expressed in *E. coli* and purified by Ni^{2+} affinity chromatography followed by size-exclusion chromatography. The major peak corresponding to a molecular weight of ~21.8 kDa (monomeric Soc-3M2e) was collected (**Figure 1B**, blue profile). The purity of the recombinant Soc-3M2e proteins was confirmed by sodium dodecyl sulfate–polyacrylamide gel electrophoresis (SDS-PAGE), which showed a single major band with a molecular mass of ~22 kDa, equivalent to the Soc-3M2e fusion protein (**Figure 1B**).

The 3M2e-decorated T4 nanoparticles (3M2e-T4 nanoparticles) were prepared by incubation of the purified Soc-3M2e protein with the CsCl-purified Hoc^-Soc^- T4 phages as previously described (44) (**Figure 1C**). To optimize the copy number of 3M2e, ~5×10^{10} T4 phages were incubated with different quantities of the Soc-3M2e protein (**Figure 1C**). The presence of bound Soc-3M2e was determined by SDS-PAGE analysis of 3M2e-T4 nanoparticles isolated by high-speed centrifugation. The data show that the Soc-3M2e protein bound efficiently to the Hoc^-Soc^- T4 phages, even at a 1:1 ratio

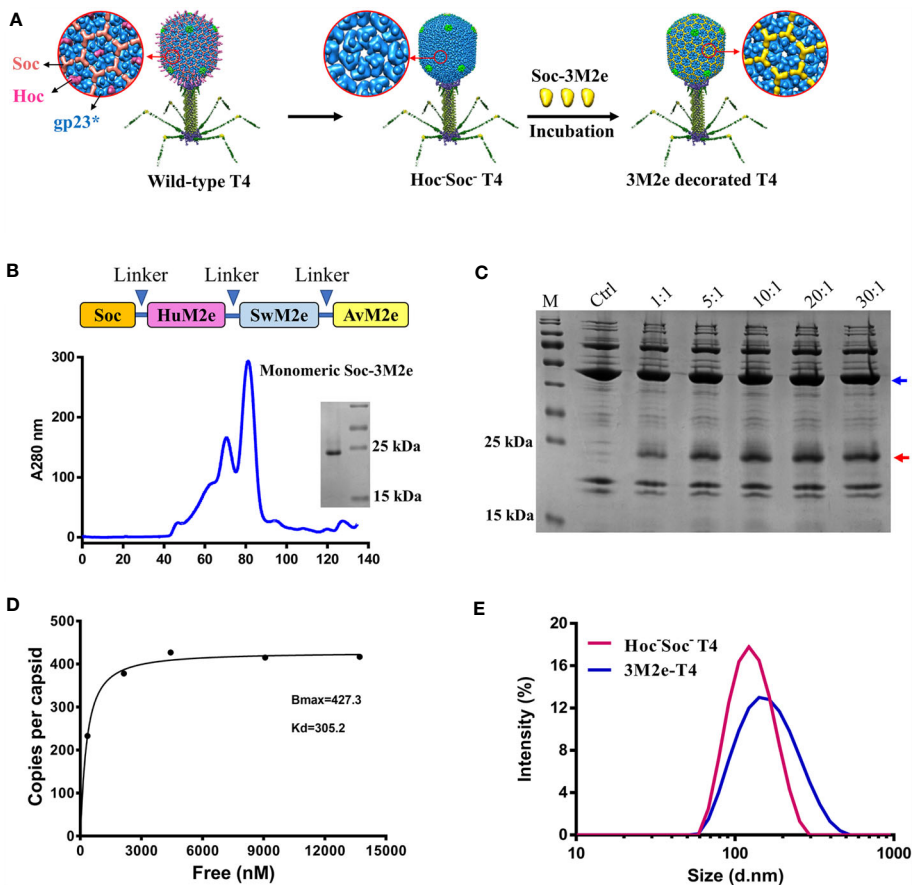

FIGURE 1 | Construction of 3M2e-T4 VLPs. **(A)** schematic diagram of 3M2e-T4 VLPs preparation. Structural models of wild-type T4 and Hoc$^-$Soc$^-$ T4 phages were shown. 3M2e decorated T4 nanoparticles were prepared by incubation of Soc-3M2e proteins with Hoc$^-$Soc$^-$ T4 phages as described in Materials and Methods. **(B)** Purification of Soc-3M2e. Soc-3M2e fusion was constructed by fusing 3M2e, which contains three tandem copies of M2e from human, swine, and avian influenza viruses, to the COOH-terminus of Soc. Arrows indicated the flexible linkers (GGSSGGSS) between each component. Soc-3M2e protein was purified by HisTrap affinity chromatography followed by size exclusion chromatography. Only the monomeric peak was collected, and the purity of Soc-3M2e protein was analyzed by SDS-PAGE. **(C)** Assembly of 3M2e-T4 VLPs *in vitro*. About 5×10^{10} Hoc$^-$Soc$^-$ T4 phages were incubated with at the indicated ratios of Soc-3M2e protein molecules to capsid binding sites (see Materials and Methods for the details). 3M2e-T4 VLPs were analyzed by SDS-PAGE. The same amount of Hoc$^-$Soc$^-$ T4 phages was used as a control. Blue and red arrows indicated gp23* and Soc-3M2e, respectively. **(D)** Saturation binding curve of Soc-3M2e. The bound and unbound (not shown) Soc-3M2e proteins were calculated using BSA a standard. The copy numbers of Soc-3M2e per capsid were determined using gp23* as internal control. The data were plotted as one-site saturation ligand binding curve. **(E)** The diameter distributions of Hoc$^-$Soc$^-$ T4 (red line) and 3M2e-T4 nanoparticles (blue line).

of Soc-3M2e molecules to Soc binding sites, and reached saturation at ratio of 10:1 (**Figure 1C**). The copy number of bound Soc-3M2e per capsid (B_{max}) calculated from the binding curve was 427, and the apparent binding constant (K_d) was 305 nM (**Figure 1D**). Since each Soc-3M2e protein contains three tandem copies of M2e peptide, there are ~1,281 M2e molecules assembled on each T4 nanoparticle, which is remarkably higher than any VLPs reported so far. The diameter distribution and zeta-potential of 3M2e-T4 nanoparticles was determined using Zetasizer Nano ZS. The average diameter of 3M2e-T4 nanoparticles is 150.9 nm, which is larger than the diameter of Hoc$^-$Soc$^-$ T4 phages (mean = 120.8 nm) (**Figure 1E**), indicating the binding of Soc-3M2e. We didn't observe significant difference in zeta-potentials between Hoc$^-$Soc$^-$ T4 (-26.7 ± 0.4 mV) and M2e-T4 nanoparticles (-24.3 ± 0.12 mV) (**Figure S1**).

3M2e-T4 Phage Nanoparticles Induced Robust M2e-Specific Antibodies

To determine the immunogenicity of 3M2e-T4 nanoparticles, mice were intramuscularly immunized with 3M2e-T4 nanoparticles displaying a total of 15μg 3M2e antigen on day 0, 14, and 28 (**Figure 2A**). Mice immunized with PBS, 15μg of Soc-3M2e soluble proteins, or a simple mixture of 15μg Soc-3M2e antigen and the same number of T4 phage nanoparticles (Soc-3M2e+T4) were used as controls. To minimize binding prior to immunization, the Soc-3M2e antigen was mixed with phage T4 at the time of immunization (most of the Soc-3M2e did not bind to capsid, see Materials and Methods for the details). Sera were collected according to the scheme shown in **Figure 2A**, and the titers of M2e-specific antibodies were determined by enzyme-linked immunosorbent assay (ELISA). All mice

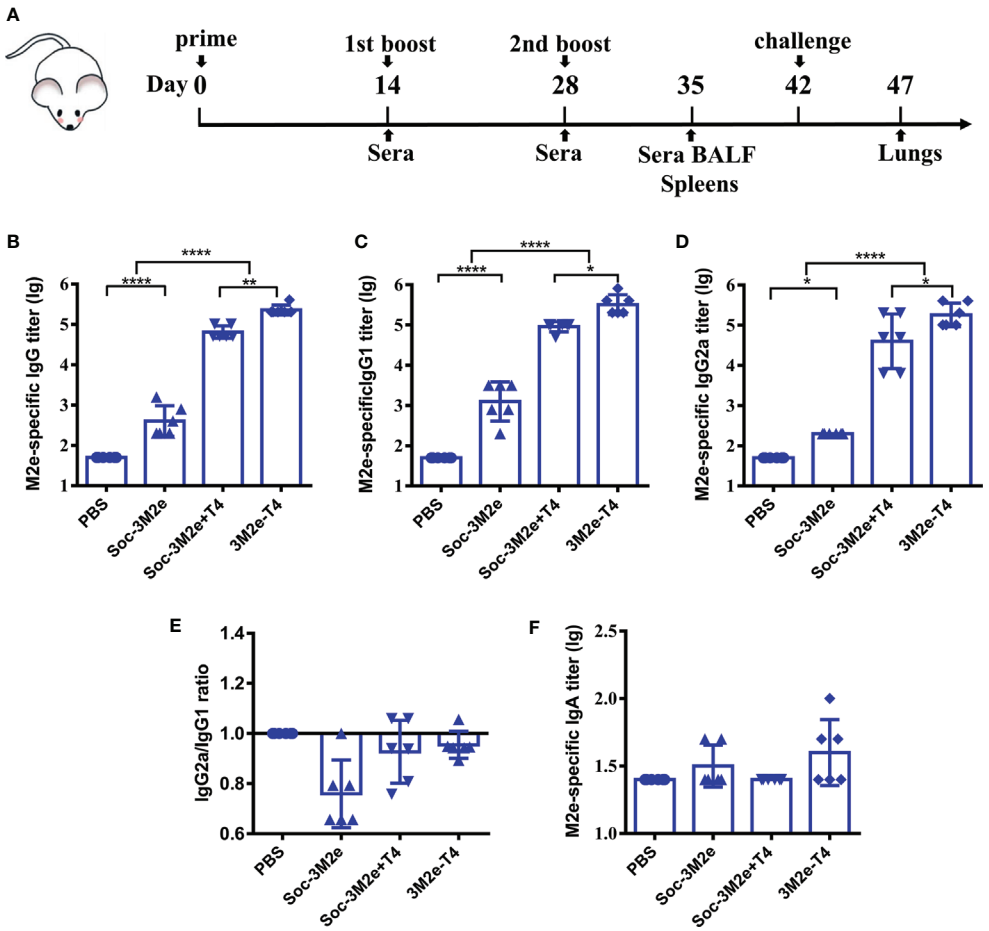

FIGURE 2 | M2e-specific humoral immune responses. **(A)** Scheme of mouse immunization. Sera were obtained before each immunization. The titers of M2e-specific IgG **(B)**, IgG1**(C)**, IgG2a **(D)**, and IgA **(F)** were determined by ELISA using peptides pool of M2e from human, swine, and avian influenza viruses. **(E)** Ratio of M2e-specific IgG2a to IgG1 were calculated. Date were shown as means ± S.D. *, **, and **** indicated $p < 0.05$, $p < 0.01$, and $p < 0.0001$ respectively (ANOVA).

immunized with PBS were negative for M2e-specific IgG even at a low sera dilution of 50. The Soc-3M2e soluble proteins induced very low levels of M2e-specific IgG antibodies. However, 3M2e-T4 nanoparticles), without any adjuvant, induced very high levels of 3M2e-specific IgG antibodies, with end point titers of ~4×10^5 (**Figure 2B**). Even a simple mixture of Soc-3M2e and T4 phage (Soc-3M2e+T4 mixture) generated high titers (~1×10^5) of M2e-specific antibodies when compared to the very low titers generated by the soluble Soc-3M2e antigen (**Figure 2B**, $p<0.0001$, ANOVA). These data point to the remarkable immune stimulatory effect of the T4 phage nanoparticles.

Since M2e-induced immune protection mainly depends on antibody-dependent cellular cytotoxicity (ADCC) and antibody-dependent cellular phagocytosis (ADCP), the efficiencies of which are different between IgG subtypes (45–47), we determined the titers of M2e-specific IgG1 (T_H2-biased) and IgG2a (T_H1-biased). The Soc-3M2e soluble antigen mainly induced IgG1 antibodies, whereas mice immunized with 3M2e-T4 nanoparticles or Soc-3M2e+T4 mixture produced similar levels of both IgG1 and IgG2a antibodies (**Figures 2C–E**). Elicitation of balanced T_H1 and T_H2 biased immune responses is a significant feature of the T4 vaccine delivery platform and generally important for protection against infectious disease. We have also determined the 3M2e-specific IgA antibodies in sera. Although 3M2e-T4 nanoparticles induced IgA antibodies in some of the mice, the data were not statistically significant ($p>0.05$, ANOVA. **Figure 2F**).

3M2e-T4 Nanoparticle-Induced Anti-M2e Antibodies Bind to Influenza Virions and Influenza Virus-Infected Cells

To determine whether 3M2e-T4 nanoparticles induced antibodies recognize M2e on influenza virions, A/Puerto Rico/8/34 (H1N1) virus was inactivated with β-propiolactone and used as the coating antigen in ELISA assays. The data revealed that these antibodies, regardless of the IgG subtype, specifically bound to the influenza virions (**Figures 3A–C**). Consistent with the end point titers (**Figure 2**), balanced levels of virion-binding titers were observed for both the IgG1 and IgG2a subtypes. As

expected, sera from PBS immunized mice showed negative results even at a low sera dilution of 10 (**Figures 3A–C**). Since M2e-induced immune protection mainly depends on ADCC and ADCP, we then examined whether M2e presented in plasma membranes of influenza virus-infected cells can be recognized by 3M2e-T4 induced antibodies. Madin-Darby canine kidney (MDCK) cells infected with A/Puerto Rico/8/34 (H1N1) influenza virus at a multiplicity of infection (MOI) of 1 were tested for the binding of M2e-specific antibodies by indirect immunofluorescence assay (**Figure 3D**). The data indicated that the sera from 3M2e-T4 VLPs immunized mice showed significant binding to influenza virus-infected cells, but not to mock-treated cells (**Figure 3D**). Together, these data demonstrated that the 3M2e-T4 nanoparticle can efficiently induce M2e-specific antibodies that recognize M2e presented both on influenza virions and on virus-infected cells, indicating their potential protection against influenza virus infection.

3M2e-T4 Nanoparticles Elicit Strong Cellular Immune Responses

To investigate whether the 3M2e-T4 nanoparticles elicited M2e-specific cellular immune responses, mice were sacrificed 7 days after the second boost, and spleens were collected to isolate peripheral blood mononuclear cells (PBMCs). The number of IFN-γ and IL-4 secreting cells were analyzed by ELISPOT using 10μg/ml M2e peptide as a stimulus. Neither the mice immunized with Soc-3M2e soluble antigen nor those immunized with the Soc-3M2e+T4 mixture generated IFN-γ and IL-4 secreting cells, while the mice immunized with 3M2e-T4 nanoparticles generated significant numbers of M2e-specific IFN-γ (**Figure 4A**) and IL-4 secreting cells (**Figure 4B**). These data demonstrate that assembly of 3M2e on T4 nanoparticles is essential to stimulate the cellular arm of the host immune system. This seems to be not that critical for the humoral arm because, as shown above, substantial induction of antibodies was evident with the Soc-3M2e+T4 mixture (**Figures 2B–D**).

3M2e-T4 Nanoparticles Elicited M2e-Specific Mucosal Antibodies

The mucosal surfaces of the respiratory tract are major ports of entry for influenza viruses, and previous studies indicated that both mucosal IgG and serum IgG are conducive for efficient protection (48). To determine if the 3M2e-T4 nanoparticles stimulated mucosal antibodies, bronchoalveolar lavage fluid

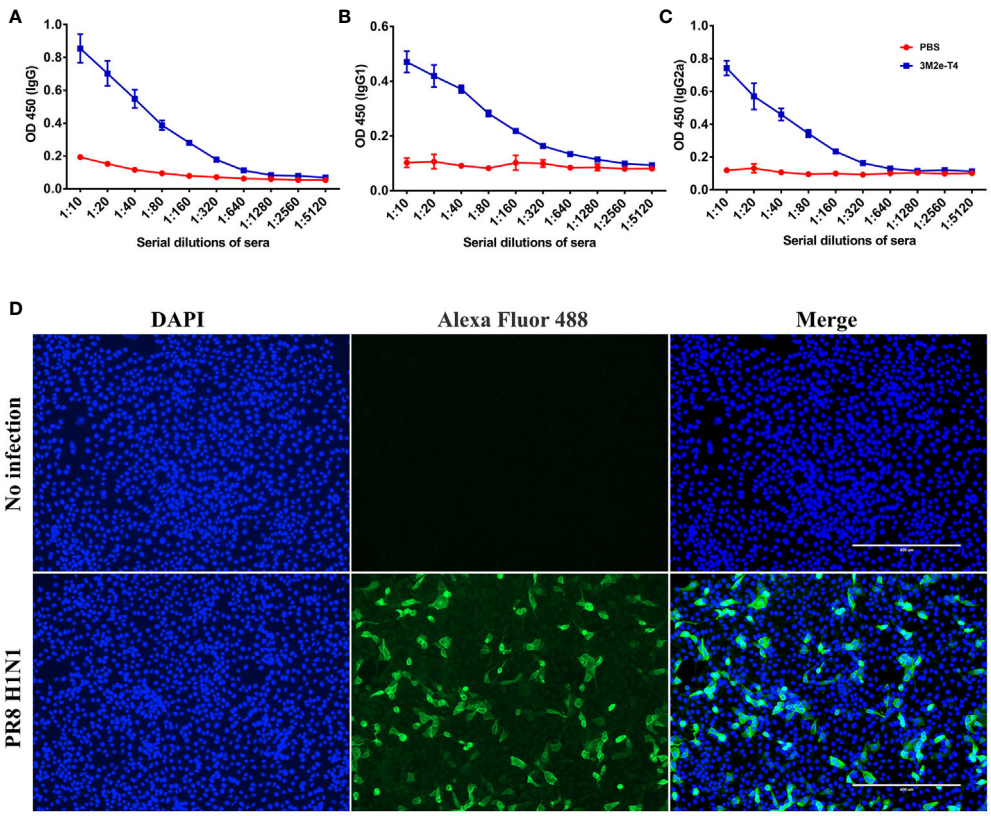

FIGURE 3 | Anti-M2e antibodies specifically bind to influenza virions and influenza virus-infected cells. The binding of M2e-specific IgG **(A)**, IgG1**(B)**, and IgG2a **(C)** to influenza virions were determined by ELISA using β-propiolactone-inactivated A/Puerto Rico/8/34 virus as the coating antigen. **(D)** The binding of M2e-specific IgG to influenza virus infected cells. MDCK cells were infected with A/Puerto Rico/8/34 virus at a MOI of 1, and the binding was determined by indirect immunofluorescence assay as described in Materials and Methods. Data were shown as means ± S.D.

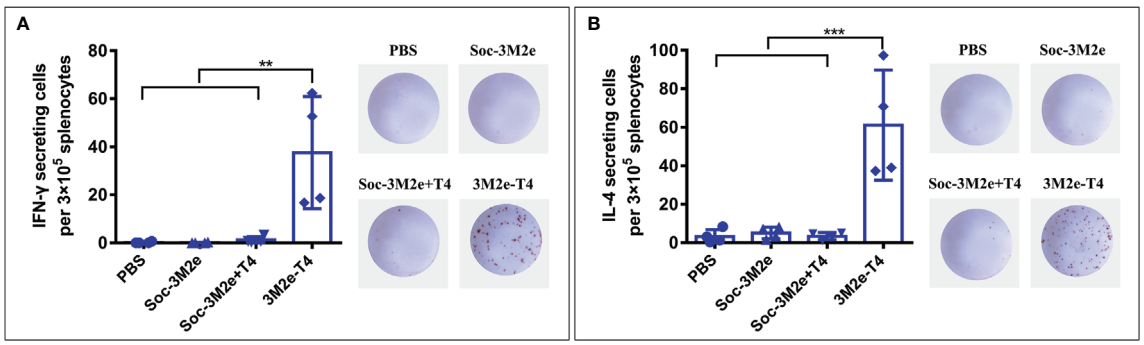

FIGURE 4 | M2e-specific cellular immune responses. Mice (n = 4) were immunized according to the scheme shown in **Figure 2A**, and splenocytes were isolated on day 35. The IFN-γ **(A)** and IL-4 **(B)** secreting lymphocytes were assayed by ELISPOT as described in Materials and Methods. The right images of each panel show the representative results of ELISPOT wells from each group. Data were represented as mean ± S.D. of four mice in each group. **p < 0.01; ***p < 0.001 (ANOVA).

(BALF) was collected 7 days post last immunization, and the presence of IgG and IgA antibodies were detected using ELISA. As shown in **Figure 5A**, soluble Soc-3M2e was able to induce low levels of M2e-specific IgG antibodies, whereas the 3M2e-T4 nanoparticles induced the highest levels. As in the case of serum IgG, the Soc-3M2e+T4 mixture could also induce mucosal IgG, much higher than the soluble antigen. As expected, the PBS control mice had no detectable levels of anti-M2e IgG antibodies (**Figure 5A**). Subtype analysis of the IgG antibodies showed that Soc-3M2e soluble antigens only elicited M2e-specific mucosal IgG1, whereas mice immunized with 3M2e-T4 nanoparticles or Soc-3M2e+T4 mixture induced balanced levels of both mucosal IgG1 and IgG2a antibodies (**Figures 5B, C**). However, all the groups failed to develop M2e-specific IgA antibodies in BALF (**Figure 5D**).

3M2e-T4 Nanoparticles Provided Complete Protection Against Influenza A Virus Challenge

To evaluate the protective efficacy of each formulation, immunized mice were challenged with $5LD_{50}$ of A/Puerto Rico/8/34 (H1N1) virus and monitored daily for body weight and survival for 14 days. As shown in **Figure 6A**, infection of influenza virus resulted in substantial weight loss of PBS control mice, or mice immunized with either the Soc-3M2e soluble antigen, or Soc-3M2e+T4 mixture, three days post infection. All the mice in the PBS control group died 10 days post challenge and five of the six mice immunized with the soluble Soc-3M2e died 9 days post challenge (**Figure 6B**), whereas 67% of the mice vaccinated with Soc-3M2e+T4 mixture recovered and survived (**Figure 6B**). In contrast, all the mice immunized with 3M2e-T4 nanoparticles not only survived the lethal challenges with the H1N1 virus infections (**Figure 6B**), but also, remarkably, showed no significant body weight loss (**Figure 6A**).

The protection efficacy was further evaluated by pathological analysis of the lungs of the immunized mice 5 days post-challenge. **Figure 6C** shows representative results of the lung lesions (column I) and pathological changes of alveoli (column II), bronchi (column III), and pulmonary vessels (column IV). Overall, mice immunized with Soc-3M2e+T4 mixture showed obvious, though less severe, lesions in the lungs when compared to the PBS control mice or mice immunized with soluble Soc-3M2e antigen, whereas no obvious lesions were found in 3M2e-T4 nanoparticle immunized mice (column I). The alveolar walls

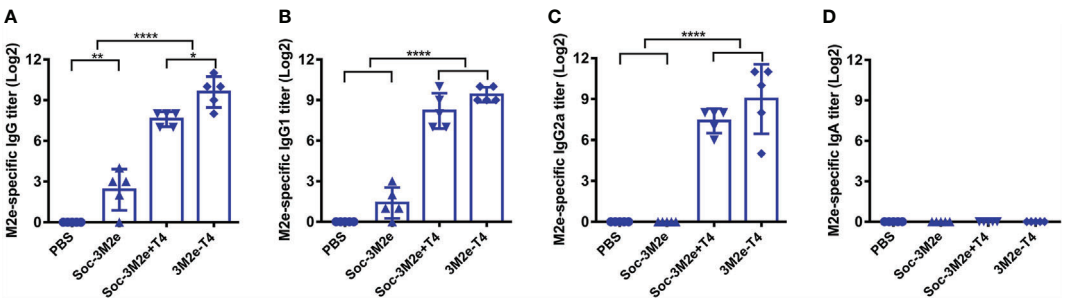

FIGURE 5 | M2e-specific antibodies in BALF. Bronchoalveolar lavage fluids were collected 7 days after last immunization (n = 5). M2e-specific total IgG **(A)**, IgG1 **(B)**, IgG2a **(C)**, and IgA **(D)** were determined by ELISA using a mixture of human, swine, avian influenza virus M2e peptides as the capture antigen (2 μg/ml). Date were presented as means ± S.D. *p < 0.05; **p < 0.01; ****p < 0.0001 (ANOVA).

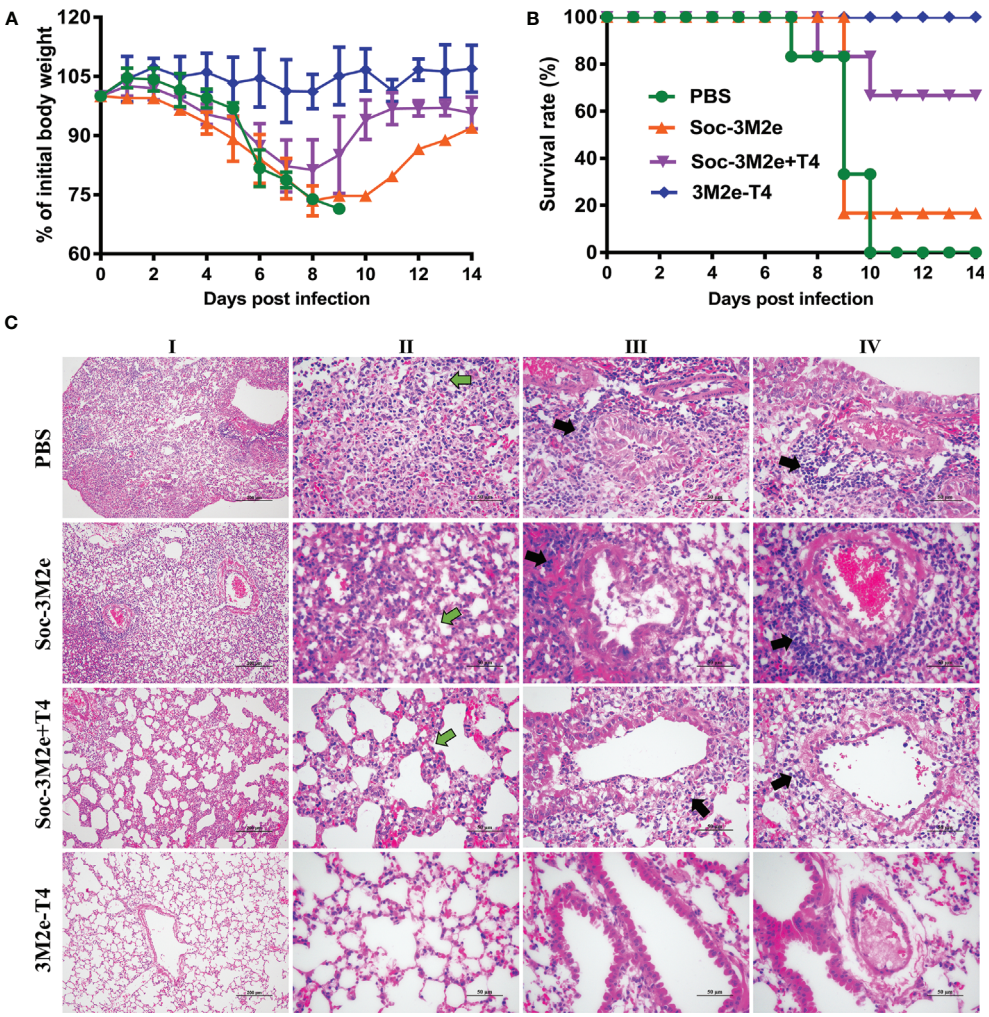

FIGURE 6 | 3M2e-T4 VLPs provided complete protection against influenza virus challenge. Mice (n = 6) were challenged with 5×LD_{50} of A/Puerto Rico/8/34 two weeks after last immunization. Weight loss **(A)** and survival rate **(B)** of mice were monitored daily for 14 days. **(C)** Pathological analysis of lungs from mice (n = 3) challenged with virus was carried out in a separate experiment, in which mice were immunized with the same immunization procedure described above. Five days post infection with 5×LD_{50} of A/Puerto Rico/8/34, mice were euthanized, and lung sections were prepared as described in Materials and Methods. The representative results from each group were shown (column I, scale bar, 200 μm; Columns II-IV, scale bar, 50 μm). Main pathological changes are thickening of alveolar septa of mice (column II, green arrows), inflammatory cells infiltrated around the bronchi (column III, black arrows), and pulmonary blood vessels (column IV, black arrows).

of PBS or soluble Soc-3M2e immunized mice were severely thickened (column II), and a large number of inflammatory cells infiltrated around the bronchi (column III) and pulmonary blood vessels (column IV). Mice immunized with Soc-3M2e+T4 mixture also exhibited similar but less severe pathological changes. However, in contrast, the mice vaccinated with 3M2e-T4 nanoparticles showed relatively normal alveolar wall thickness and negligible inflammatory infiltration (**Figure 6C**).

DISCUSSION

The influenza virus M2e antigen is considered to be an attractive target for the development of universal influenza vaccines (49–51). However, VLP carriers and/or adjuvants are absolutely needed for designing the M2e-based vaccines because of the poor immunogenicity of the M2e peptides. By taking advantage of the phage T4 nanoparticle platform, in this study, we developed a novel 3M2e-T4 VLP vaccine that, without any adjuvant, induced robust humoral and cellular immune responses and provided complete protection against influenza virus challenge.

The 3M2e-T4 nanoparticles were prepared by simply incubating the Soc-3M2e fusion protein with $Hoc^{-}Soc^{-}$ T4 phages, both of which can be produced in large-scale in *E. coli*. Therefore, our M2e-T4 nanoparticles provide an approach to manufacture influenza vaccines in a short amount of time, which is critical to deal with an emerging influenza pandemic. The

3M2e-T4 nanoparticles can be stored at 4°C for at least 6 days without significant degradation of the bound antigen (**Figure S2**), and it can also be lyophilized for long-term storage. Although phages T7 and fd have previously been used as carriers to present M2e, they conferred limited protection (34, 39). This is probably because these platforms cannot present full-length M2e peptides at high density, which is a key determinant for inducing strong and protective immune responses (52). Our data demonstrated that each T4 phage nanoparticle was decorated with ~427 copies of the 21.8 kDa Soc-3M2e, and each copy containing three tandem repeats of M2e peptide from human, swine, and avian influenza viruses. This means that ~1,281 copies of M2e molecules were presented on a 120 x 86 nm nanometer capsid particle, the highest density reported so far on any VLP. Such high density as well as the repetitive and symmetrical arrangement of M2e epitopes mimicking the surface structure of a viral pathogen, probably led to robust stimulation of the host immune system eliciting strong immune responses without the need for an adjuvant.

Apart from high epitope density, the high immunogenicity of 3M2e-T4 VLPs might also because the T4 phage was able to stimulate innate immune responses and may have natural adjuvant properties (26, 38). Indeed, a mixture of Soc-3M2e antigen and T4 phages (Soc-3M2e+T4) in which most of the antigen was not attached to capsid induced quite high levels of M2e-specific antibodies in sera (**Figures 2B**–**D**) and BALF (**Figure 5**). Importantly, however, the 3M2e-T4 nanoparticles elicited the strongest immune responses. This might be because display of 3M2e on T4 phage represents linkage of antigen to an adjuvant-loaded delivery system, which ensures simultaneous presentation of both to the same immune cell such as the antigen-presenting cells (APCs) that could significantly enhance the immune responses (53). T4 phages also induced vector-specific antibodies after immunization (**Figure S3A**), which could be a concern of T4 VLP platform. However, such antibodies did not interfere the immunogenicity of 3M2e displayed on T4 nanoparticles based on the observation that M2e-specific antibodies were boosted significantly after second and third immunizations (**Figure S3B**). This might because T4 phage is mainly used as a scaffold to efficiently deliver and present antigens to immune system, and it cannot replicate in mice as some other live viral vectors. The efficacy of such live viral vaccines depends on their replication *in vivo* to produce enough antigens, which might be inhibited by vector-specific immune responses. Our data indicated that the T4 vector immunogenicity is not a significant issue in the case of T4 VLP vaccines.

Unlike soluble Soc-3M2e protein that mainly elicited Th2-biased responses, the 3M2e-T4 VLPs induced balanced T_H1 and T_H2 immune responses (**Figures 2E**, **4**), which is vital for vaccine efficacy. T_H1-type cytokines such as IFN-γ tend to induce the proinflammatory responses, which could lead to tissue damage. T_H2-type cytokines such as IL-4 are mostly involved in mediating anti-inflammatory response, which will counteract the excessive microbicidal effect mediated by T_H1-based responses (54–56). Our results showed that mice immunized with 3M2e-T4 VLPs, but not soluble Soc-3M2e proteins, induced similar levels of M2e-specific IgG1 and IgG2a (**Figure 2E**). Similar results were also observed for the M2e-specific IFN-γ and IL-4 secreting cells (**Figure 4**) indicating that M2e-T4 VLPs facilitate both T_H1-type and T_H2-type immune responses. Additionally, M2e-specific antibodies generally are non-neutralizing and their protection is mainly dependent on antibody-dependent cellular cytotoxicity (ADCC) and antibody-dependent cellular phagocytosis (ADCP) (45–47, 57). Therefore, high levels of M2e-specific IgG2a antibodies, which are more potent than other IgG subclasses in directing ADCC, are desirable for M2e-based vaccines.

Previous studies have suggested that T-cell responses induced by M2e vaccines also contributed to the protection against influenza infections (49, 58). In our current study, we found that the 3M2e-T4 VLPs, but not the soluble Soc-3M2e or a mixture of T4 and Soc-3M2e, elicited high levels of M2e-specific IFN-γ and IL-4 secreting lymphocytes in the spleens of vaccinated mice. These might have contributed to the enhanced protections of 3M2e-T4 VLPs (**Figure 6**), and the expectation is that, since we have used three versions of M2e and that M2e as such is highly conserved among influenza viruses, these responses would afford cross-protection to diverse viruses belonging to different subtypes.

Although M2e-based universal influenza vaccines are promising, it is highly desirable to include other conserved antigens such as HA-stalk, NP, and M1 to cover a broad range of virus types. Other than displaying M2e on capsids, our T4 vaccine platform provides flexibility and capacity for next-generation multivalent vaccine design. For instance, we have demonstrated that the T4 platform can be used to simultaneously display and deliver different kinds of protein antigens or DNAs encoding antigen proteins, target antigens to dendritic cells, and co-deliver antigens and molecular adjuvants (27, 38, 40). Therefore, potent multivalent T4-Flu VLP vaccines can be designed and experiments are currently underway to develop such next-generation broadly effective Flu vaccines.

In conclusion, our studies demonstrated that the T4 phage nanoparticles displaying the Flu viral M2e peptides at high density, without the inclusion of an external adjuvant, stimulate strong humoral and cellular immune responses in mice against the virion-exposed M2e that is otherwise poorly immunogenic. These responses also afforded complete protection against lethal Flu virus challenge. These results, thus, provide a proof-of-concept for the development of potent next-generation influenza vaccines using the T4 VLP platform by incorporating additional conserved influenza antigens and other immunostimulatory molecules.

MATERIALS AND METHODS

Ethics Statement

All animal experiments were approved by the Research Ethics Committee (HZAUMO-2021-0023), Huazhong Agricultural University, Hubei, China and performed in the Laboratory Animal Center of Huazhong Agricultural University strictly in

accordance with the Guidelines for the Care and Use of Laboratory Animals, Huazhong Agricultural University.

Construction of Plasmids

The plasmid pET-RbSoc was constructed by inserting Soc gene of RB69 phage into pET28b expression vector using NheI and XhoI restriction sites. The 3M2e gene (**Table S1**) encoding three tandem copies of M2e from human, swine, and avian influenza viruses separated by two flexible linkers (GGSSGGSS) was synthesized and cloned into pUC19 vector using SalI and XhoI restriction sites. The 3M2e gene fragment was cut from pUC19 plasmid using SalI and XhoI and subcloned into pET-RbSoc plasmid at the XhoI site to generate the expression plasmid pRbSoc-3M2e, in which the 3M2e gene was fused to COOH-terminus of RB69 Soc.

Purification of Recombinant Soc-3M2e Protein

The pRbSoc-3M2e expression plasmid was transformed into *E. coli* BL21 (DE3) competent cells (Novagen), and a single colony was cultured overnight in LB medium supplemented with 50 μg/ml kanamycin. Ten ml of the overnight culture was inoculated into 1 L of fresh LB medium containing the antibiotic, and the expression of Soc-3M2e was induced with 1mM isopropyl-β-D-thiogalactoside (IPTG) at 30°C for 2 hours when the OD600 of culture reached 0.8. *E. coli* cells were collected by centrifugation at 4,300g for 15 min and resuspended with binding buffer (20 mM Tris-HCl pH 8.0, 100 mM NaCl, 10 mM imidazole, and 5 μg/ml DNase I). The cells were lysed by high-pressure cell disruptor at 4°C, and cell debris was removed by high-speed centrifugation (35,000g, 20 min, 4°C). The supernatant containing the recombinant Soc-3M2e proteins was passed through a 0.22 μm filter and loaded onto HisTrap column (Yeasen, Shanghai, China). After washing with 40 ml washing buffer (20 mM Tris-HCl pH 8.0, 100 mM NaCl, and 20 mM imidazole), the Soc-3M2e protein was eluted with elution buffer (20 mM Tris-HCl pH 8.0, 100 mM NaCl, and 400 mM imidazole). The peak fractions were collected and further purified by size-exclusion chromatography (Hi-load 16/60 Superdex 200 column, GE Healthcare Life Sciences) using gel filtration buffer (20 mM Tris-HCl pH 8.0, 100 mM NaCl). The purity of eluted Soc-3M2e protein was analyzed by SDS-PAGE, and protein concentration was determined with BSA as a standard. The endotoxin level present in purified Soc-3M2e protein was 0.05 EU/ml tested using Limulus Amebocyte Lysate (LAL) Endotoxin Quantitation Kit (Xiamen Bioendo Technology Co., Ltd, Xiamen China).

T4 Phage Purification

The propagation and purification of Hoc$^-$Soc$^-$ phage T4 were carried out as previously described (44, 59, 60). Briefly, an overnight culture of *E. coli* P301 was inoculated into LB/M9CA medium and incubated at 37°C until the cell density reaches 1.5-2.0×10^8 cells/ml. *E. coli* cells were then infected with Hoc$^-$Soc$^-$ phage T4 at a multiplicity of infection (MOI) of 0.2-0.4, and cultured at 37°C for another 2-3 h. The cultures were harvested by centrifugation at 30,000g for 30 min, and the pellet containing phages was suspended in Pi-Mg buffer (26 mM Na_2HPO_4, 22 mM KH_2PO_4, 79 mM NaCl, 1 mM $MgSO_4$) containing chloroform and DNase I. After 20 min incubation at 37°C, the suspension was centrifuged at 4,300g for 20 min to remove cell debris, and phages in the supernatant were collected by high-speed centrifugation (30,000g, 30 min). The phage pellet was resuspended in 1 ml Pi-Mg buffer and purified by CsCl step density gradient centrifugation. Finally, the phages were dialyzed against dialysis solution I (10 mM Tris pH 8.0, 200 mM NaCl, and 5 mM $MgCl_2$) for 5 h followed by dialysis solution II (10 mM Tris pH 8.0, 50 mM NaCl, and 5 mM $MgCl_2$) for overnight at 4°C. The endotoxin level present in purified Hoc$^-$Soc$^-$ phages was 1.53 EU/ml, which is well under the maximum recommended endotoxin levels, 20 EU/ml, in subunit vaccines (61).

Assembly of 3M2e Antigens on Hoc$^-$Soc$^-$ T4 Capsids *In Vitro*

In vitro assembly of proteins on Hoc$^-$Soc$^-$ T4 phages was performed as described previously (26, 44). To optimize the binding of Soc-3M2e, about 5 × 10^{10} phage particles were incubated at 4°C for 45 min with Soc-3M2e proteins at different ratios of antigen molecules to Soc binding sites (1:1 to 30:1, **Figure 1C**). The unbound Soc-3M2e proteins were removed by centrifugation at 21,130 g for 30 min, and the pellet of phage particles containing bound proteins were washed twice with PBS. The Soc-3M2e decorated phage particles were finally resuspended in PBS, transferred to a new tube, and analyzed by SDS-PAGE. The gp23* and Soc-3M2e proteins in each lane were quantified by Image-Pro Plus software using BSA as a standard. The copy number of bound Soc-3M2e proteins was determined using gp23* (49 kDa, 930 copies per capsid) as internal control. The saturation binding curve was generated using Prism GraphPad software as previously described (26, 27, 43). The y-axis showed the copy number at the different ratios, while x-axis represented the concentration of unbound Soc-3M2e. The apparent binding affinity (K_d) and the maximal number of bound molecules (B_{max}) were determined by nonlinear regression analysis with the methods of one site specific binding with a Hill slope. The diameter distribution and zeta-potential of the nanoparticles were determined using Zetasizer Nano ZS (Malvern Panalytical, UK).

Immunizations and Influenza A Virus Challenge

Six- to eight-week-old female BALB/c mice were purchased from Laboratory Animal Center of Huazhong Agricultural University, Hubei, China. The 3M2e-T4 nanoparticles were prepared as described above and injected intramuscularly into mice (15μg 3M2e per dose) at week 0, 2, and 4. Each batch of sample was analyzed by SDS-PAGE for consistency in the copy number of displayed antigens before injection (**Figure S4**). Mice immunized with the mixture of Soc-3M2e proteins (15μg 3M2e per dose) and T4 phages (9×10^{11} particles) were used as controls (Soc-3M2e+ T4). To minimize the binding of Soc-3M2e, the protein was mixed with T4 phages right before each immunization.

Other control groups included PBS, Soc-3M2e soluble proteins (15μg 3M2e per dose), and T4 phages (9×10^{11} particles). Two weeks post the third immunization, mice (n=6) were anaesthetized with ether and intranasally infected with 5 LD_{50} of influenza A/Puerto Rico/8/1934 virus. All mice were monitored daily for morbidity and mortality for 14 days. Animals with 30% or greater body weight loss were euthanized immediately and considered as death.

Quantification of Antibodies in Sera and BALF

The levels of antigen-specific antibodies in sera and bronchoalveolar lavage fluid (BALF) were quantified by enzyme-linked immunosorbent assay (ELISA). Blood samples (n=6) were collected on days 0, 14, 28, and 35. BALF samples (n=5) were collected 7 days after the third immunization. Briefly, the lungs from sacrificed mice were flushed three times with 1ml PBS, which was then centrifugated at 3,500 g for 10 min. The supernatant was harvested for analysis of M2e-specific antibody titers. The ELISA plates were coated overnight at 4°C with 200 ng/well of M2e peptide pool consisting of equal amounts of peptides from human, swine, and avian influenza viruses or β-propiolactone-inactivated influenza A virus (1×10^6 PFU/well) or Hoc^-Soc^- T4 phages (1×10^9 PFU/well). The plates were blocked with 3% BSA in PBS-T (PBS containing 0.05% Tween-20) for 1 hour at 37°C. Serially diluted sera and BALF (1% BSA in PBS-T) were then added to each well of plates, which were incubated at 37°C for 1 hour. After washing 5 times with PBS-T, the plates were incubated with secondary antibodies (horseradish peroxidase-conjugated goat anti-mouse IgG, IgG1, IgG2a, and IgA) at 37°C for 1 hour. Following five washes, 100 μl of TMB (3,3′,5,5′-tetramethylbenzidine) substrate was added to each well, and the reaction was stopped with 2 M H_2SO_4. The absorbance atOD450 was determined by a microplate reader.

Indirect Immunofluorescence Assay

About 2×10^5 MDCK cells in 500 μl of growth medium (DMEM supplemented with 10% fetal bovine serum) were seeded into an each well of 24-well plate and allowed to adhere overnight. The growth medium was removed, and cells were washed twice with PBS and mock infected or infected with A/Puerto Rico/8/1934 virus in serum-free DMEM at a MOI of 1 for 1 h. The cells were then washed three times with PBS and cultured in serum-free DMEM containing 1 μg/ml TPCK-trypsin for 20h. After washing with PBS, cells were fixed with 10% formalin for 10 min, permeabilized with 0.1% Triton X-100 for 20 min, and blocked with 5% BSA in PBS-T (PBS containing 0.05% Tween-20) for 1 hour at 37 °C. The cells were then incubated with the sera from immunized mice at a dilution of 1:100 for 1h. After 5 times wash with PBS-T, Alexa Fluor 488 goat anti-mouse IgG (Thermo Fisher Scientific) were used as secondary antibodies at a dilution of 1:1000. Following five washes, nuclei were counterstained with 1 μg/ml DAPI (BD Biosciences) for 5 min in the dark. Photography was performed on an inverted fluorescence microscope (Thermo Fisher Scientific).

Enzyme-Linked Immunosorbent Spot Assay

ELISPOT assay was performed to determine the number of M2e-specific IFN-γ and IL-4 secreting cells in spleen according to the manufacturer's protocol (DAKAWE, China). Briefly, 7 days post the last immunization, mice were sacrificed and the spleens were harvested to prepare single-cell suspensions. Around 3×10^5 splenocytes were seeded to each well of plates and stimulated with M2e peptides (equal amounts of M2e peptide from human, swine, and avian influenza viruses) at a final concentration of 10 μg/ml. After 32-34 hours of culture at 37°C, 5% CO_2, the splenocytes were removed by cell-cracking buffer of ice-cold deionized water. The plates were then incubated with biotinylated antibodies followed the addition of HRP-conjugated streptavidin. After washing 5 times, the reaction was developed with AEC (3-amino-9-ethylcarbazole) substrate and stopped with flowing water. Plates were dried at room temperature and spot-counted (DAKAWE, Wuhan, China).

Histopathologic Analyses

Mice (n=3) were immunized and challenged as described above. Five days after challenge with 5 LD_{50} of influenza A/PR/8/1934 virus, mice were sacrificed, and lungs were isolated. Lung tissues were fixed in 10% formalin, dehydrated through a graded series of ethanol, embedded in paraffin wax, and cut into 4 μm-thick sections. After deparaffinization, sections were stained with hematoxylin-eosin and observed under an optical microscope (Nikon, Japan).

Statistical Analysis

All the statistical analyses were performed using GraphPad Prism software. Comparisons among different groups were evaluated by one-way ANOVA. In all cases, $p< 0.05$ was considered as statistically significant difference.

DATA AVAILABILITY STATEMENT

The original contributions presented in the study are included in the article/**Supplementary Material**. Further inquiries can be directed to the corresponding authors.

ETHICS STATEMENT

The animal study was reviewed and approved by The Research Ethics Committee (HZAUMO-2021-0023), Huazhong Agricultural University, Hubei, China.

AUTHOR CONTRIBUTIONS

PT and ML designed the experiments. ML, PG, CC, and HF performed the experiments. ML, PG, WZ, and CG analyzed the data. ML, VR, and PT wrote the manuscript. PT directed

the project. All authors contributed to the article and approved the submitted version.

FUNDING

This work was supported by grants from National Natural Science Foundation of China [Grant No. 31870915 to PT], Fundamental Research Funds for the Central Universities [Program No. 2662019 PY002 to PT], and in part by National Institute of Allergy and Infectious Diseases, National Institutes of Health [AI081726 to VR].

SUPPLEMENTARY MATERIAL

The Supplementary Material for this article can be found online at: https://www.frontiersin.org/articles/10.3389/fimmu.2021.745625/full#supplementary-material

REFERENCES

1. Elbahesh H, Saletti G, Gerlach T, Rimmelzwaan GF. Broadly Protective Influenza Vaccines: Design and Production Platforms. *Curr Opin Virol* (2019) 34:1–9. doi: 10.1016/j.coviro.2018.11.005
2. Monto AS, Fukuda K. Lessons From Influenza Pandemics of the Last 100 Years. *Clin Infect Dis* (2020) 70:951–7. doi: 10.1093/cid/ciz803
3. Jang YH, Seong BL. The Quest for a Truly Universal Influenza Vaccine. *Front Cell Infect Microbiol* (2019) 9:344. doi: 10.3389/fcimb.2019.00344
4. Sautto GA, Kirchenbaum GA, Ross TM. Towards a Universal Influenza Vaccine: Different Approaches for One Goal. *Virol J* (2018) 15:17. doi: 10.1186/s12985-017-0918-y
5. Choi A, Bouzya B, Cortés Franco KD, Stadlbauer D, Rajabhathor A, Rouxel RN, et al. Chimeric Hemagglutinin-Based Influenza Virus Vaccines Induce Protective Stalk-Specific Humoral Immunity and Cellular Responses in Mice. *ImmunoHorizons* (2019) 3:133–48. doi: 10.4049/immunohorizons.1900022
6. Jang YH, Seong BL. Options and Obstacles for Designing a Universal Influenza Vaccine. *Viruses* (2014) 6:3159–80. doi: 10.3390/v6083159
7. Nachbagauer R, Kinzler D, Choi A, Hirsh A, Beaulieu E, Lecrenier N, et al. A Chimeric Haemagglutinin-Based Influenza Split Virion Vaccine Adjuvanted With AS03 Induces Protective Stalk-Reactive Antibodies in Mice. *NPJ Vaccines* (2016) 1:16015–. doi: 10.1038/npjvaccines.2016.15
8. Wong SS, Webby RJ. Traditional and New Influenza Vaccines. *Clin Microbiol Rev* (2013) 26:476–92. doi: 10.1128/CMR.00097-12
9. Jazayeri SD, Poh CL. Development of Universal Influenza Vaccines Targeting Conserved Viral Proteins. *Vaccines* (2019) 7:169. doi: 10.3390/vaccines7040169
10. Sah P, Alfaro-Murillo JA, Fitzpatrick MC, Neuzil KM, Meyers LA, Singer BH, et al. Future Epidemiological and Economic Impacts of Universal Influenza Vaccines. *Proc Natl Acad Sci USA* (2019) 116:20786–92. doi: 10.1073/pnas.1909613116
11. Webster RG, Govorkova EA. Continuing Challenges in Influenza. *Ann New Y Acad Sci* (2014) 1323:115–39. doi: 10.1111/nyas.12462
12. Wei CJ, Crank MC, Shiver J, Graham BS, Mascola JR, Nabel GJ. Next-Generation Influenza Vaccines: Opportunities and Challenges. *Nat Rev Drug Discov* (2020) 19:239–52. doi: 10.1038/s41573-019-0056-x
13. Pica N, Palese P. Toward a Universal Influenza Virus Vaccine: Prospects and Challenges. *Annu Rev Med* (2013) 64:189–202. doi: 10.1146/annurev-med-120611-145115
14. Nachbagauer R, Palese P. Is a Universal Influenza Virus Vaccine Possible? *Annu Rev Med* (2020) 71:315–27. doi: 10.1146/annurev-med-120617-041310
15. Herrera-Rodriguez J, Meijerhof T, Niesters HG, Stjernholm G, Hovden AO, Sorensen B, et al. A Novel Peptide-Based Vaccine Candidate With Protective Efficacy Against Influenza A in a Mouse Model. *Virology* (2018) 515:21–8. doi: 10.1016/j.virol.2017.11.018
16. Li ZT, Zarnitsyna VI, Lowen AC, Weissman D, Koelle K, Kohlmeier JE, et al. Why Are CD8 T Cell Epitopes of Human Influenza A Virus Conserved? *J Virol* (2019) 93:e01534-18. doi: 10.1128/JVI.01534-18
17. Pleguezuelos O, James E, Fernandez A, Lopes V, Rosas LA, Cervantes-Medina A, et al. Efficacy of FLU-V, a Broad-Spectrum Influenza Vaccine, in a Randomized Phase IIb Human Influenza Challenge Study. *NPJ Vaccines* (2020) 5:22. doi: 10.1038/s41541-020-0174-9
18. Krammer F. The Quest for a Universal Flu Vaccine: Headless HA 2.0. *Cell Host Microbe* (2015) 18:395–7. doi: 10.1016/j.chom.2015.10.003
19. Li CK, Rappuoli R, Xu XN. Correlates of Protection Against Influenza Infection in Humans–on the Path to a Universal Vaccine? *Curr Opin Immunol* (2013) 25:470–6. doi: 10.1016/j.coi.2013.07.005
20. Sei CJ, Rao M, Schuman RF, Daum LT, Matyas GR, Rikhi N, et al. Conserved Influenza Hemagglutinin, Neuraminidase and Matrix Peptides Adjuvanted With ALFQ Induce Broadly Neutralizing Antibodies. *Vaccines* (2021) 9:698. doi: 10.3390/vaccines9070698
21. Zharikova D, Mozdzanowska K, Feng J, Zhang M, Gerhard W. Influenza Type A Virus Escape Mutants Emerge *In Vivo* in the Presence of Antibodies to the Ectodomain of Matrix Protein 2. *J Virol* (2005) 79:6644–54. doi: 10.1128/JVI.79.11.6644-6654.2005
22. Deng L, Mohan T, Chang TZ, Gonzalez GX, Wang Y, Kwon YM, et al. Double-Layered Protein Nanoparticles Induce Broad Protection Against Divergent Influenza A Viruses. *Nat Commun* (2018) 9:359. doi: 10.1038/s41467-017-02725-4
23. Fiers W, De Filette M, El Bakkouri K, Schepens B, Roose K, Schotsaert M, et al. M2e-Based Universal Influenza A Vaccine. *Vaccine* (2009) 27:6280–3. doi: 10.1016/j.vaccine.2009.07.007
24. He F, Leyrer S, Kwang J. Strategies Towards Universal Pandemic Influenza Vaccines. *Expert Rev Vaccines* (2016) 15:215–25. doi: 10.1586/14760584.2016.1115352
25. Ibañez LI, Roose K, De Filette M, Schotsaert M, De Sloovere J, Roels S, et al. M2e-Displaying Virus-Like Particles With Associated RNA Promote T Helper 1 Type Adaptive Immunity Against Influenza A. *PLoS One* (2013) 8:e59081. doi: 10.1371/journal.pone.0059081
26. Tao P, Mahalingam M, Kirtley ML, van Lier CJ, Sha J, Yeager LA, et al. Mutated and Bacteriophage T4 Nanoparticle Arrayed F1-V Immunogens From Yersinia Pestis as Next Generation Plague Vaccines. *PLoS Pathog* (2013) 9:e1003495. doi: 10.1371/journal.ppat.1003495
27. Tao P, Mahalingam M, Zhu J, Moayeri M, Sha J, Lawrence WS, et al. A Bacteriophage T4 Nanoparticle-Based Dual Vaccine Against Anthrax and Plague. *mBio* (2018) 9:e01926-18. doi: 10.1128/mBio.01926-18
28. Schepens B, De Vlieger D, Saelens X. Vaccine Options for Influenza: Thinking Small. *Curr Opin Immunol* (2018) 53:22–9. doi: 10.1016/j.coi.2018.03.024
29. Kim KH, Kwon YM, Lee YT, Kim MC, Hwang HS, Ko EJ, et al. Virus-Like Particles Are a Superior Platform for Presenting M2e Epitopes to Prime Humoral and Cellular Immunity Against Influenza Virus. *Vaccines* (2018) 6:66. doi: 10.3390/vaccines6040066
30. Tao W, Hurst BL, Shakya AK, Uddin MJ, Ingrole RS, Hernandez-Sanabria M, et al. Consensus M2e Peptide Conjugated to Gold Nanoparticles Confers Protection Against H1N1, H3N2 and H5N1 Influenza A Viruses. *Antiviral Res* (2017) 141:62–72. doi: 10.1016/j.antiviral.2017.01.021
31. Neirynck S, Deroo T, Saelens X, Vanlandschoot P, Jou WM, Fiers W. A Universal Influenza A Vaccine Based on the Extracellular Domain of the M2 Protein. *Nat Med* (1999) 5:1157–63. doi: 10.1038/13484
32. Matić S, Rinaldi R, Masenga V, Noris E. Efficient Production of Chimeric Human Papillomavirus 16 L1 Protein Bearing the M2e Influenza Epitope in Nicotiana Benthamiana Plants. *BMC Biotechnol* (2011) 11:106. doi: 10.1186/1472-6750-11-106
33. Petukhova NV, Gasanova TV, Stepanova LA, Rusova OA, Potapchuk MV, Korotkov AV, et al. Immunogenicity and Protective Efficacy of Candidate Universal Influenza A Nanovaccines Produced in Plants by Tobacco Mosaic Virus-Based Vectors. *Curr Pharm Des* (2013) 19:5587–600. doi: 10.2174/13816128113199990337

34. Hashemi H, Pouyanfard S, Bandehpour M, Noroozbabaei Z, Kazemi B, Saelens X, et al. Immunization With M2e-Displaying T7 Bacteriophage Nanoparticles Protects Against Influenza A Virus Challenge. *PLoS One* (2012) 7:e45765. doi: 10.1371/journal.pone.0045765
35. Kim MC, Lee JS, Kwon YM, O E, Lee YJ, Choi JG, et al. Multiple Heterologous M2 Extracellular Domains Presented on Virus-Like Particles Confer Broader and Stronger M2 Immunity Than Live Influenza A Virus Infection. *Antiviral Res* (2013) 99:328–35. doi: 10.1016/j.antiviral.2013.06.010
36. Liu W, Peng Z, Liu Z, Lu Y, Ding J, Chen YH. High Epitope Density in a Single Recombinant Protein Molecule of the Extracellular Domain of Influenza A Virus M2 Protein Significantly Enhances Protective Immunity. *Vaccine* (2004) 23:366–71. doi: 10.1016/j.vaccine.2004.05.028
37. Cheng W. The Density Code for the Development of a Vaccine? *J Pharm Sci* (2016) 105:3223–32. doi: 10.1016/j.xphs.2016.07.020
38. Tao P, Zhu J, Mahalingam M, Batra H, Rao VB. Bacteriophage T4 Nanoparticles for Vaccine Delivery Against Infectious Diseases. *Adv Drug Deliv Rev* (2019) 145:57–72. doi: 10.1016/j.addr.2018.06.025
39. Deng L, Ibañez LI, Van den Bossche V, Roose K, Youssef SA, de Bruin A, et al. Protection Against Influenza A Virus Challenge With M2e-Displaying Filamentous Escherichia Coli Phages. *PLoS One* (2015) 10:e0126650. doi: 10.1371/journal.pone.0126650
40. Tao P, Mahalingam M, Marasa BS, Zhang Z, Chopra AK, Rao VB. *In Vitro* and *In Vivo* Delivery of Genes and Proteins Using the Bacteriophage T4 DNA Packaging Machine. *Proc Natl Acad Sci USA* (2013) 110:5846–51. doi: 10.1073/pnas.1300867110
41. Tao P, Wu X, Tang WC, Zhu J, Rao V. Engineering of Bacteriophage T4 Genome Using CRISPR-Cas9. *ACS Synth Biol* (2017) 6:1952–61. doi: 10.1021/acssynbio.7b00179
42. Sathaliyawala T, Rao M, Maclean DM, Birx DL, Alving CR, Rao VB. Assembly of Human Immunodeficiency Virus (HIV) Antigens on Bacteriophage T4: A Novel *in vitro* Approach to Construct Multicomponent HIV Vaccines. *J Virol* (2006) 80:7688–98. doi: 10.1128/JVI.00235-06
43. Shivachandra SB, Li Q, Peachman KK, Matyas GR, Leppla SH, Alving CR, et al. Multicomponent Anthrax Toxin Display and Delivery Using Bacteriophage T4. *Vaccine* (2007) 25:1225–35. doi: 10.1016/j.vaccine.2006.10.010
44. Tao P, Li Q, Shivachandra SB, Rao VB. Bacteriophage T4 as a Nanoparticle Platform to Display and Deliver Pathogen Antigens: Construction of an Effective Anthrax Vaccine. *Methods Mol Biol (Clifton NJ)* (2017) 1581:255–67. doi: 10.1007/978-1-4939-6869-5_15
45. Boudreau CM, Alter G. Extra-Neutralizing FcR-Mediated Antibody Functions for a Universal Influenza Vaccine. *Front Immunol* (2019) 10:440. doi: 10.3389/fimmu.2019.00440
46. Deloizy C, Fossum E, Barnier-Quer C, Urien C, Chrun T, Duval A, et al. The Anti-Influenza M2e Antibody Response Is Promoted by XCR1 Targeting in Pig Skin. *Sci Rep* (2017) 7:7639. doi: 10.1038/s41598-017-07372-9
47. Sedova ES, Scherbinin DN, Lysenko AA, Alekseeva SV, Artemova EA, Shmarov MM. Non-Neutralizing Antibodies Directed at Conservative Influenza Antigens. *Acta Naturae* (2019) 11:22–32. doi: 10.32607/20758251-2019-11-4-22-32
48. Qi M, Zhang XE, Sun X, Zhang X, Yao Y, Liu S, et al. Intranasal Nanovaccine Confers Homo- and Hetero-Subtypic Influenza Protection. *Small (Weinheim an der Bergstrasse Germany)* (2018) 14:e1703207. doi: 10.1002/smll.201703207
49. Eliasson DG, Omokanye A, Schön K, Wenzel UA, Bernasconi V, Bemark M, et al. M2e-Tetramer-Specific Memory CD4 T Cells Are Broadly Protective Against Influenza Infection. *Mucosal Immunol* (2018) 11:273–89. doi: 10.1038/mi.2017.14
50. Mezhenskaya D, Isakova-Sivak I, Rudenko L. M2e-Based Universal Influenza Vaccines: A Historical Overview and New Approaches to Development. *J BioMed Sci* (2019) 26:76. doi: 10.1186/s12929-019-0572-3
51. Saelens X. The Role of Matrix Protein 2 Ectodomain in the Development of Universal Influenza Vaccines. *J Infect Dis* (2019) 219:S68–s74. doi: 10.1093/infdis/jiz003
52. Sun X, Wang Y, Dong C, Hu J, Yang L. High Copy Numbers and N Terminal Insertion Position of Influenza A M2E Fused With Hepatitis B Core Antigen Enhanced Immunogenicity. *Biosci Trends* (2015) 9:221–7. doi: 10.5582/bst.2015.01060
53. Gomes AC, Flace A, Saudan P, Zabel F, Cabral-Miranda G, Turabi AE, et al. Adjusted Particle Size Eliminates the Need of Linkage of Antigen and Adjuvants for Appropriated T Cell Responses in Virus-Like Particle-Based Vaccines. *Front Immunol* (2017) 8:226. doi: 10.3389/fimmu.2017.00226
54. Azouz A, Razzaque MS, El-Hallak M, Taguchi T. Immunoinflammatory Responses and Fibrogenesis. *Med Electron Microsc* (2004) 37:141–8. doi: 10.1007/s00795-004-0255-2
55. Berger A. Th1 and Th2 Responses: What are They? *BMJ (Clin Res ed)* (2000) 321:424. doi: 10.1136/bmj.321.7258.424
56. Li X, Xing R, Xu C, Liu S, Qin Y, Li K, et al. Immunostimulatory Effect of Chitosan and Quaternary Chitosan: A Review of Potential Vaccine Adjuvants. *Carbohydr Polymers* (2021) 264:118050. doi: 10.1016/j.carbpol.2021.118050
57. Von Holle TA, Moody MA. Influenza and Antibody-Dependent Cellular Cytotoxicity. *Front Immunol* (2019) 10:1457. doi: 10.3389/fimmu.2019.01457
58. Kim MC, Lee YN, Ko EJ, Lee JS, Kwon YM, Hwang HS, et al. Supplementation of Influenza Split Vaccines With Conserved M2 Ectodomains Overcomes Strain Specificity and Provides Long-Term Cross Protection. *Mol Ther* (2014) 22:1364–74. doi: 10.1038/mt.2014.33
59. Tao P, Mahalingam M, Rao VB. Highly Effective Soluble and Bacteriophage T4 Nanoparticle Plague Vaccines Against Yersinia Pestis. *Methods Mol Biol (Clifton NJ)* (2016) 1403:499–518. doi: 10.1007/978-1-4939-3387-7_28
60. Zhu J, Ananthaswamy N, Jain S, Batra H, Tang WC, Lewry DA, et al. A Universal Bacteriophage T4 Nanoparticle Platform to Design Multiplex SARS-CoV-2 Vaccine Candidates by CRISPR Engineering. *Sci Adv* (2021) 7:eabh1547. doi: 10.1126/sciadv.abh1547
61. Brito LA, Singh M. Acceptable Levels of Endotoxin in Vaccine Formulations During Preclinical Research. *J Pharm Sci* (2011) 100:34–7. doi: 10.1002/jps.22267

Conflict of Interest: The authors declare that the research was conducted in the absence of any commercial or financial relationships that could be construed as a potential conflict of interest.

frontiers in Immunology

ORIGINAL RESEARCH
published: 14 October 2021
doi: 10.3389/fimmu.2021.748264

Repeated Influenza Vaccination Boosts and Maintains H1N1pdm09 Neuraminidase Antibody Titers

Lena Hansen[1]*, *Fan Zhou*[1], *Håkon Amdam*[1], *Mai-Chi Trieu*[1] and *Rebecca Jane Cox*[1,2]*

[1] Influenza Centre, Department of Clinical Science, University of Bergen, Bergen, Norway, [2] Department of Microbiology, Haukeland University Hospital, Bergen, Norway

Antibodies to influenza surface protein neuraminidase (NA) have been found to reduce disease severity and may be an independent correlate of protection. Despite this, current influenza vaccines have no regulatory requirements for the quality or quantity of the NA antigen and are not optimized for induction of NA-specific antibodies. Here we investigate the induction and durability of NA-specific antibody titers after pandemic AS03-adjuvanted monovalent H1N1 vaccination and subsequent annual vaccination in health care workers in a five-year longitudinal study. NA-specific antibodies were measured by endpoint ELISA and functional antibodies measured by enzyme-linked lectin assay (ELLA) and plaque reduction naturalisation assay. We found robust induction of NA inhibition (NAI) titers with a 53% seroconversion rate (>4-fold) after pandemic vaccination in 2009. Furthermore, the endpoint and NAI geometric mean titers persisted above pre-vaccination levels up to five years after vaccination in HCWs that only received the pandemic vaccine, which demonstrates considerable durability. Vaccination with non-adjuvanted trivalent influenza vaccines (TIV) in subsequent influenza seasons 2010/2011 – 2013/2014 further boosted NA-specific antibody responses. We found that each subsequent vaccination increased durable endpoint titers and contributed to maintaining the durability of functional antibody titers. Although the trivalent influenza vaccines boosted NA-specific antibodies, the magnitude of fold-increase at day 21 declined with repeated vaccination, particularly for functional antibody titers. High levels of pre-existing antibodies were associated with lower fold-induction in repeatedly vaccinated HCWs. In summary, our results show that durable NA-specific antibody responses can be induced by an adjuvanted influenza vaccine, which can be maintained and further boosted by TIVs. Although NA-specific antibody responses are boosted by annual influenza vaccines, high pre-existing titers may negatively affect the magnitude of fold-increase in repeatedly vaccinated individuals. Our results support continued development and standardization of the NA antigen to supplement current influenza vaccines and reduce the burden of morbidity and mortality.

Keywords: influenza, neuraminidase, neuraminidase inhibition, neuraminidase inhibition (NAI) titer, repeated vaccination, pre-existing immunity, pandemic vaccination

OPEN ACCESS

Edited by:
Cornelis Joseph Melief, Leiden University, Netherlands

Reviewed by:
Carolyn M. Nielsen, University of Oxford, United Kingdom
Osaretin Emmanuel Asowata, Population Council, United States

***Correspondence:**
Rebecca Jane Cox
Rebecca.Cox@uib.no
Lena Hansen
Lena.Hansen@uib.no

Specialty section:
This article was submitted to Vaccines and Molecular Therapeutics, a section of the journal Frontiers in Immunology

Received: *27 July 2021*
Accepted: *28 September 2021*
Published: *14 October 2021*

Citation:
Hansen L, Zhou F, Amdam H, Trieu M-C and Cox RJ (2021) Repeated Influenza Vaccination Boosts and Maintains H1N1pdm09 Neuraminidase Antibody Titers. Front. Immunol. 12:748264. doi: 10.3389/fimmu.2021.748264

INTRODUCTION

Influenza is an acute respiratory disease that is annually estimated to cause 3 – 5 million cases of severe illness and 290 000 – 650 000 deaths worldwide (1, 2). Influenza vaccines are currently the most effective method of prevention of influenza infection. Hemagglutinin (HA) is the major surface glycoprotein on the virus that mediates viral entry by binding to sialic acid receptors on the surface of host cells. Antibodies that target the HA globular head and block binding to sialic acids are considered the classical mediators of protection against influenza infection. These antibodies are measured by hemagglutination inhibition (HI) assay and the HI titer has been the gold standard for measuring vaccine immunogenicity for many years. Thus, current seasonal influenza vaccines are optimized for induction of HA-specific antibodies. Each vaccine dose is standardized by the HA content, however, there are no concentration requirements for the other vaccine components, such as neuraminidase. Neuraminidase (NA) is the second major surface glycoprotein. It is a sialidase that cleaves terminal sialic acids and facilitates the release and spread of newly formed viruses from host cells (3). HI antibodies tend to be strain-specific and have reduced cross-reactivity with new and drifted influenza strains due to the high mutation rate of the HA head region. Antigenic drift and shift may occur independently for HA and NA proteins and NA is a potential target for more broadly protective vaccines. Early studies established that NA is immunogenic and that NA-specific antibodies reduce disease in humans (4, 5). More recent studies have found that antibodies with NA inhibition (NAI) activity correlate with reduced viral shedding and clinical disease, and may be a possible correlate of protection (6, 7). Despite NA being an antigenic target for induction of protective antibody responses, the quantity and quality of NA is not regulated in current influenza vaccines. Consequently, the amount and stability of the NA antigen has been found to vary between influenza vaccines and key epitopes targeted by human monoclonal antibodies are poorly displayed (8, 9). Studies have reported variable seroconversion rates for NA-specific antibody responses after vaccination with inactivated influenza vaccines, ranging between 23 – 64% (7, 10, 11).

Annual vaccination is recommended due to antigenic drift of influenza viruses and waning of antibody titers. However, there is growing evidence showing that repeated influenza vaccination can lead to a diminished B cell response (12) and that high pre-existing antibody titers can reduce boosting of antibody titers after vaccination (13). The impact of repeated vaccination has mainly been studied in the context of HA-specific antibody responses (12, 13). Thus, there is limited data on whether repeated vaccination and pre-existing titers impact the induction of NA-specific antibody responses after vaccination.

This study aimed to investigate the induction and durability of NA-specific antibodies with AS03-adjuvanted pandemic H1N1pdm09 vaccination and determine the impact of subsequent annual vaccination with trivalent inactivated vaccines (TIV) in health care workers (HCWs). We found that AS03-adjuvanted monovalent H1N1pdm09 vaccination induced robust and durable NA-specific antibody responses. The antibody titers were further boosted after immunization with TIVs, however, we found that the magnitude of the functional NA antibody fold-increase declined with repeated vaccination.

MATERIALS AND METHODS

Study Design and Blood Sampling

Healthy HCWs (n=50) were vaccinated between October 2009 and March 2010 at Haukeland University Hospital, Norway with the AS03-adjuvanted pandemic H1N1pdm09 split virus vaccine (3.75 µg hemagglutinin A/California/7/2009 (H1N1) (Pandemrix, GlaxoSmithKline-GSK, Belgium). Written informed consent was obtained before inclusion in the study. Further informed consent was obtained for the 4-year extension between 2010/2011–2013/2014 where vaccination was with the trivalent seasonal inactivated influenza vaccine [TIV; either subunit (Influvac, Abbott Laboratories) or split-virion (Vaxigrip, Sanofi Pasteur)] containing 15 µg hemagglutinin per strain. Throughout the study, the A/H1N1 strain remained the same [A/California/07/2009 (H1N1)], however the A/H3N2 and B viruses changed between seasons. Demographic and clinical information including working department were collected. The study was approved by the regional ethics committee (REKVest-2012/1772) and the Norwegian Medicines Agency (Clinical trials.gov NCT01003288) (14).

Blood samples were collected pre-vaccination (D0), 21 days (D21), 3, 6, and 12 months (3M, 6M, 12M, respectively) after vaccination. Annual influenza vaccination is recommended, but not mandatory for HCWs in Norway. The HCWs were divided into two groups, repeated and single group, based on their vaccination status in influenza seasons 2010/2011 – 2013/2014. The single group did not receive any TIVs during the study. The repeated group was vaccinated with two or three TIVs in the four seasons following the 2009 pandemic. An overview of the number of vaccinations and the intervals that these were given for the repeated group can be found in **Supplemental Table 2**. The same sampling schedule was followed after all vaccinations. The 12M timepoint was collected from all HCW irrespective of vaccination and used as D0 for HCWs in the repeated group for each season. Blood samples collected before vaccination were considered as day 0 whenever HCWs had not been vaccinated during the previous season, which more accurately reflected the true baseline titers. HCWs in the single group (n=24) were only vaccinated in 2009 but provided yearly blood samples at the start of each influenza season, i.e. 24, 36, 48 and 60 months after H1N1pdm09 vaccination. The samples collected from the single group after the 2009 season were labelled as 12M for each subsequent season as seen in **Figure 2**. All serum samples were heat inactivated at 56°C for one hour before use in serological assays.

ELISA

Flat bottom 96-well plates (Invitrogen) were coated with recombinant N1 NA A/California/07/2009 (H1N1) (Cal09) produced in a baculovirus expression system as previously

described (15). N1 NA Cal09 (100 µl/well) diluted in PBS (1 µg/ml) was added and incubated overnight at 4°C. The plates were washed six times with PBS-T (PBS with 0.05% Tween 20) and blocked with 200 µl of blocking solution [PBS with 0.1% Tween-20 (Sigma), 1% BSA (Sigma), 5% milk (Marvel)] and incubated for 1 hour at 37°C. Sera were 4-fold serially diluted from 1:100 in blocking solution and 100 µl of diluted serum was added per well in duplicates and incubated at 37°C for 1 hour. Following incubation, the plates were washed six times with PBS-T and 100 µl horseradish peroxidase (HRP)-conjugated mouse anti-human IgG (BD Biosciences) diluted in blocking buffer (1:4000) was added per well and incubated at 37°C for 1 hour. The plates were washed six times with PBS-T and the secondary antibody signal was developed by adding 100 µl per well of 3,3′,5,5′-Tetramethylbenzidine (TMB) substrate (BD Biosciences). The reaction was stopped after 10 min by adding 100 µl of 1M HCl (Sigma). Absorbance was measured at 450 and 620 nm with a microplate reader (Bio-Tek). Background measured at 620 nm was subtracted from the absorbance measured at 450 nm. The endpoint titer was determined using a sigmoidal dose response curve in GraphPad Prism 9.

ELLA

Inhibition of NA enzyme activity was determined using enzyme-linked lectin assay (ELLA) using an influenza reassortant H7N1 virus (NIBSC, UK) with an irrelevant HA from A/Equine/Prague/56 (H7N7) and NA from A/California/07/09 (H1N1), matching the vaccine strain. ELLA was performed according to Couzens et al. (16). Briefly, 96-well plates were coated with 100 µl/well of fetuin (25 µg/ml) (Sigma) diluted in PBS and incubated at 4°C for a minimum of 18 hours. The plates were washed three times with PBS-T. Sera were 5-fold serially diluted from 1:50 in sample diluent (PBS with 0.9 mM $CaCl_2$ and 0.5 mM $MgCl_2$ (Life Technologies), 1% BSA (Sigma), 0.5% Tween-20) and 50 µl was added per well in duplicates. The virus was diluted in sample buffer at a concentration equivalent to 90% of the maximum signal and 50 µl was added per well. The plates were incubated at 37°C for 18 hours. After incubation, the plates were washed six times with PBS-T and 100 µl of HRP-conjugated peanut agglutinin (1 mg/ml) (Sigma) diluted in conjugate diluent (PBS with 0.9 mM $CaCl_2$ and 0.5 mM $MgCl_2$, 1% BSA) was added to per well and incubated in the dark at room temperature for 2 hours. The plates were washed three times with PBS-T. 100 µl of o-Phenylenediamine dihydrochloride (OPD) substrate (Sigma) in phosphate-citrate buffer (50 mM) (Sigma) was added to each well and incubated in the dark for 10 min. The reaction was stopped by adding 100 µl 1N sulfuric acid (Sigma). The absorbance was measured at 490 nm. 50% inhibitory concentration was calculated for each serum sample using a sigmoidal dose response curve in GraphPad Prism 9 and considered as the neuraminidase inhibition (NAI) titer.

Plaque Reduction Neutralization Assay

A 96-well microplate plaque reduction neutralization assay was used to measure the capacity of sera to inhibit viral replication *in vitro*. The reassortant H7N1 virus used in ELLA was used for this assay. The plaque reduction neutralization assay was performed according to Matrosovich et al. (17, 18). MDCK SIAT1 cells were seeded ($2x10^4$ per well) and incubated overnight at 37°C. The virus was diluted to a concentration that would generate 100 plaques per well. Sera were diluted 1:20 and 1:100 and mixed with the virus, and incubated at 37°C for one hour. This inoculum was added in quadruplets and incubated at 37°C for 40 min. A low-viscosity Avicel overlay (FMC BioPolymer) was added to each well and the plates were incubated with the inoculum-overlay mixture for 24 hours. The plaques were visualized by immunostaining of nucleoprotein and the plaques were counted using ELISpot counter (AID). The number of plaques in the control wells was used to determine 50% inhibition and the highest reciprocal dilution giving 50% reduction in plaque formation was defined as plaque reduction neutralizing titer ($PRNT_{50}$ titer). The NA inhibitor oseltamivir (Roche) was used as a positive control to confirm that the assay could detect reduction in plaque forming units (PFU) as a result of NA inhibition in a dose-dependent manner (**Supplementary Figure 1**). Human serum depleted for IgA, IgM, and IgG (Sigma) was used as negative control.

Statistical Analysis

Endpoint, NAI and $PRNT_{50}$ titers were log-transformed and analyzed by linear mixed effects model with adjustments for demographic factors and multiple comparisons by Sidak correction. Demographic factors used for adjustments included age, sex, influenza vaccination prior to 2009 and working department (**Table 1**). The linear-mixed effects model analyses were performed in IBM SPSS Statistics version 26 and was the statistical test used unless otherwise stated. Analyzes of statistical difference between the single and repeated group was done by non-parametric Kruskal-Wallis test in GraphPad Prism 9. Correlation coefficients were calculated by non-parametric

TABLE 1 | Demographics of the study participants.

Demographics	All HCWs	Single group	Repeated group
Number of participants	50	24	26
Male (%)	9 (18)	4 (17)	5 (19)
Female (%)	41 (82)	20 (83)	21 (81)
Median age (range)	39 (22 – 63)	38 (26 – 59)	43 (22 – 63)
Seasonal vaccination before 2009 (%)	32 (65.3)	11 (47.8)	21 (80.8)
Working department(non-clinical, clinical, infectious)	23, 21, 6	13, 9, 2	10, 12, 4

HCW healthcare workers (HCWs). The single group had only pandemic vaccination in 2009. The repeated group were vaccinated with pandemic vaccine in 2009 and trivalent influenza vaccine in two or three seasons after 2009.

Spearman correlation in GraphPad Prism 9. Statistical significance was defined as P<0.05 for all tests.

RESULTS

In this study we investigated NA-specific antibody responses after pandemic vaccination and subsequent annual influenza vaccination. Fifty HCWs were included in the study, which consisted of 9 men and 41 women. These numbers reflect the gender distribution in the Norwegian healthcare system. The median age at the start of the study was 38 years old (range 22 – 63). The majority of the HCWs (65%) had been vaccinated with TIVs before 2009 (**Table 1**).

Robust and Durable NA-Specific Antibody Responses After 2009 Pandemic Vaccination

One objective of this study was to investigate the induction of NA-specific antibody responses after AS03-adjuvanted monovalent pandemic vaccine (H1N1pdm09) in healthy adults. All HCWs in the study were vaccinated with the H1N1pdm09 vaccine in 2009 and blood samples were collected before and 21 days, 3, 6 and 12 months after vaccination. Endpoint titers were determined by ELISA against recombinant N1 NA Cal09 (**Figure 1A**). NA-specific endpoint titers were detected in all HCWs pre-vaccination with a geometric mean titer (GMT) of 322. The endpoint titers were significantly boosted to a GMT of 773, a geometric fold rise (GMFR) of 2.4, at 21 days post-vaccination (P<0.0001). The endpoint titers gradually waned during the following 12 months, although titers were significantly higher than pre-vaccination levels up to the 3-month time point (P=0.004).

The capacity of the antibody response to inhibit NA enzyme activity was measured by ELLA. A reassortant H7N1 virus, with an irrelevant H7 HA from A/Equine/Prague/02/56 and N1 NA from Cal09, was used to avoid interference from HA-specific antibodies. The H1N1pdm09 vaccine met the European Committee for Medicinal Products for Human Use (CHMP) criteria for immunogenicity set for HI titers (**Supplementary Table 1**). These criteria were used to assess induction of NAI titers. Pre-vaccination NAI titers were detected in all HCWs, albeit with a modest NAI GMT of 19. H1N1pdm09 vaccination significantly increased NAI GMT at 21 days post-vaccination to 84 (P<0.0001), a 4.4-fold increase from pre-vaccination levels (**Figure 1B**). The seroconversion rate for NAI titers was 53% (32/49). Similarly to endpoint titers, the NAI titers gradually waned but remained significantly higher than the pre-vaccination level up to 12 months after vaccination (P=0.014).

Approximately half of the HCWs (26/50) chose to receive two or three TIVs during the four-year follow-up study after the 2009 pandemic (repeated group). The remaining 24 HCWs chose not to be further vaccinated (single group) (**Figure 2A**). The repeated group had higher endpoint and NAI titers than the single group, especially during the influenza season (defined as November – April) (**Figures 2B, C**). Annual blood samples were collected prior to the start of each season from the single group, which allowed us to investigate the durability of antibody responses induced by the H1N1pdm09 vaccine. We found that three HCWs in the single group seroconverted during the study (HI titer >4-fold increase), probably due to infection. Samples collected after seroconversion were excluded to ensure that the durability was only measured from pandemic vaccination. Endpoint and NAI titers were maintained at low stable levels above baseline in the single group throughout the study (**Figures 2B, C**). The GMFR was 1.38- and 1.33-fold above pre-vaccination levels for endpoint and NAI titers, respectively, five years after H1N1pdm09 vaccination. This demonstrated that a single dose of AS03-adjuvanted H1N1pdm09 vaccine induced durable antibody responses that persisted for several years after vaccination, suggesting that long-lived plasma cells were generated.

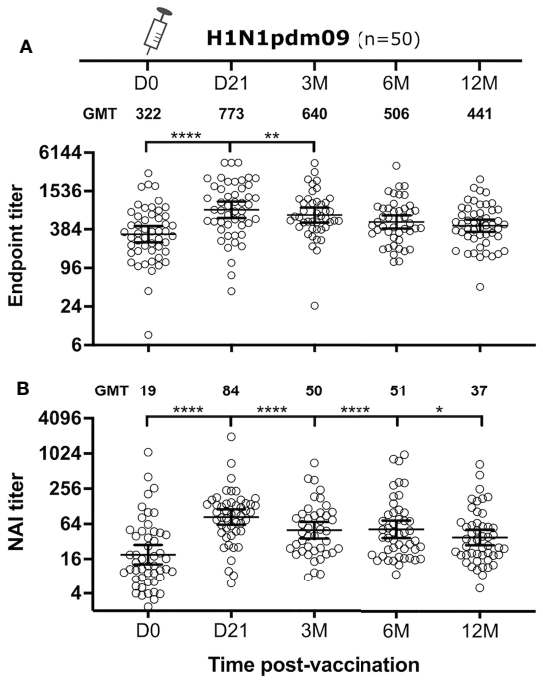

FIGURE 1 | NA-specific antibody responses after H1N1pdm09 vaccination. Health care workers (n = 50) were vaccinated with AS03-adjuvanted H1N1pdm09 vaccine. The NA-specific antibody response was measured before and 21 days, 3, 6 and 12 months after vaccination (D0, D21, 3M, 6M, 12M, respectively). Endpoint titers were measured by ELISA **(A)** and NA inhibition (NAI) titers were measured by ELLA **(B)**. Each subject is shown as one symbol with geometric mean and 95% confidence intervals. A linear mixed effects model was used for statistical analyses between pre- and post-vaccination titers with adjustments for demographic factors. *P ≤ 0.05, **P ≤ 0.01, ****P ≤ 0.0001.

Trivalent Influenza Vaccines Boost NA-Specific Antibody Responses

HCWs in the repeated group received two or three TIVs during the study, resulting in variation in vaccination intervals. The majority of the HCWs received three TIVs (81%), whereas the remaining HCWs received two TIVs (19%) (**Supplementary Table 2**). We observed that HCWs that had delayed their first TIV until the 2011/2012 season (6/26) had higher NAI titer than the HCWs

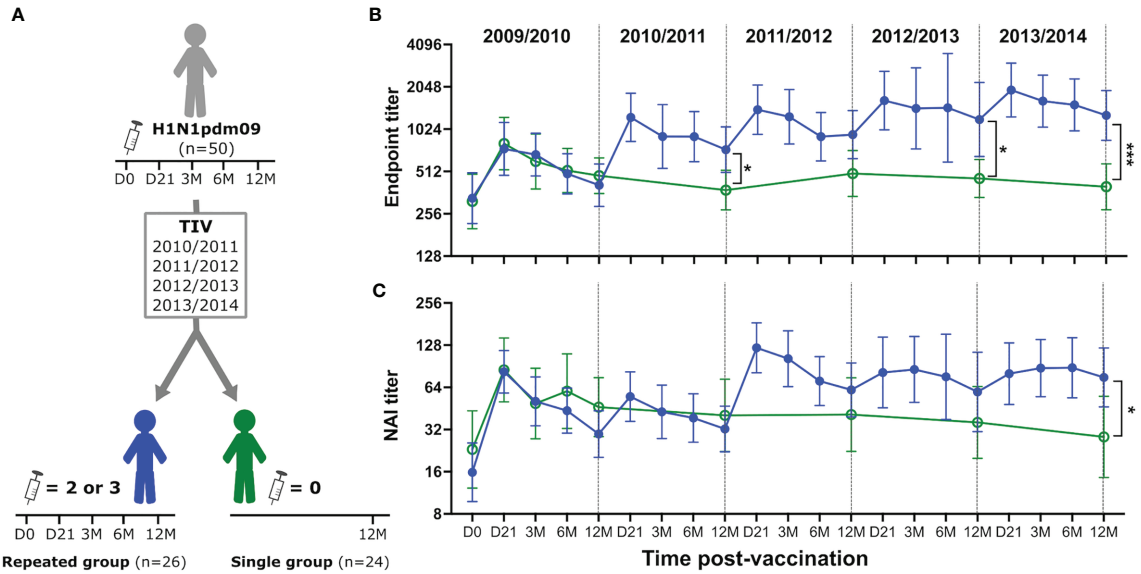

FIGURE 2 | H1N1pdm09 vaccination induced durable NA-specific antibody responses boosted by trivalent influenza vaccines. Study design **(A)**. Health care workers were divided into two groups based on their vaccination status after H1N1pdm09 vaccination in 2009. The repeated group (blue, filled circles) received two or three trivalent influenza vaccines (TIV) during seasons 2010/2011-2013/2014. Blood samples were collected 21 days (D21), and 3, 6, 12 months (3M, 6M, 12M, respectively) after vaccination. The single group (green, open circles) chose not to be further vaccinated but provided yearly blood samples prior to the start of each season (12M). NA-specific antibody responses were measured by ELISA **(B)** and ELLA **(C)** during each influenza season from 2009/2010 to 2013/2014. Data are shown as geometric mean with 95% confidence intervals. Analyzes of statistical difference between the single and repeated group was done by non-parametric Kruskal-Wallis test in GraphPad Prism 9. *P ≤ 0.05, ***P ≤ 0.001.

that received their second TIV that season. Therefore, HCWs in the repeated group were grouped based on number of vaccines, rather than season, in order to study the effect of each vaccine and the impact of repeated vaccination. The quantity of NA-specific antibodies were measured by ELISA and functional antibodies were measured by ELLA and a plaque reduction neutralisation assay in all HCWs in the repeated group. The three assays demonstrated that NA-specific antibody responses were boosted after TIV vaccination (**Figure 3**). These antibody titers gradually decreased but persisted above baseline levels throughout the influenza season. We found that endpoint titers were significantly boosted after the first (P=0.001) and second TIV (P=0.04) (**Figure 3A**), whereas the NAI titers were only significantly boosted on day 21 after the first TIV (P=0.018) (**Figure 3B**). Although the third TIV boosted endpoint and NAI titers, neither were significant. Plaque reduction neutralisation assay was used to further assess the functionality of the NA-specific antibody response *in vitro* using the same reassortant H7N1 virus with N1 NA Cal09. This assay measures inhibition of the viral replication cycle and NA-specific inhibition of plaque formation was confirmed using oseltamivir (**Supplementary Figure 1**). We found a significant increase in antibody titer that resulted in 50% reduction in plaque formation ($PRNT_{50}$ titer) 21 days after H1N1pdm09 (P<0.0001) (**Figure 3C**). Vaccination with TIVs boosted $PRNT_{50}$ titers, although not significant for any of the three TIVs. The $PRNT_{50}$ titers confirmed our findings in the ELLA and demonstrated that the vaccine-induced NA-specific antibodies were capable of inhibiting enzyme activity and viral replication *in vitro*. Collectively, our results show that seasonal TIV vaccination readily boosts NA-specific antibody responses following priming with AS03-adjuvanted H1N1pdm09 vaccination.

Repeated Vaccination Increases Durable Endpoint Titers and Maintains Durability of Functional Antibody Titers

Durable antibody titers were measured 12 months after vaccination. The H1N1 component remained the same in all vaccines used during this study, which allowed us to investigate the impact of repeated vaccination with the same antigen. We compared endpoint and NAI titres in the repeated and single group at the end of the 5-year study to assess the impact of TIVs on the durability of antibody titers. Only HCWs in the repeated group that had been vaccinated with TIV in the final season of the study were used for comparison using samples collected 12 months post-vaccination. 14/18 HCWs in the repeated group had received three TIVs and 4/18 had received two TIVs in that season (**Supplementary Table 2**). We found that the repeated group had 3.2-fold higher endpoint titers (P=0.0002) (**Figure 2A**) and 2.7-fold higher NAI titers (P=0.01) (**Figure 2B**) compared to the single group 5 years after H1N1pdm09 vaccination. This demonstrated that repeated vaccination with TIVs after AS03-adjuvanted H1N1pdm09 vaccination contributed to maintenance and further increase of the durable NA-specific antibody responses.

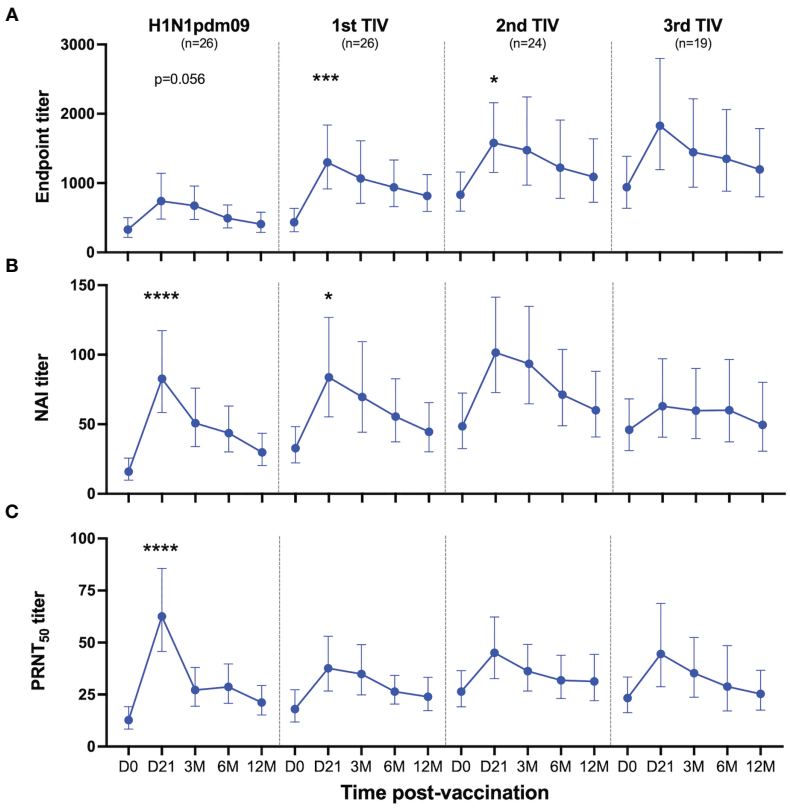

FIGURE 3 | Antibody responses to NA induced by H1N1pdm09 and TIV vaccination. Health care workers in the repeated group received two or three trivalent influenza vaccines (TIV) in the four subsequent seasons after the 2009 pandemic during the five-year study. Blood samples were collected pre-season (D0) and 21 days, 3, 6 and 12 months (D21, 3M, 6M, 12M, respectively) after each vaccination. Antibody responses were measured by ELISA **(A)**, ELLA **(B)** and plaque reduction neutralization assay **(C)** after vaccination with H1N1pdm09 and the first, second or third TIV. All vaccinated HCWs in the repeated group is included in this figure regardless of their vaccination intervals. Data are shown as geometric mean with 95% confidence intervals. A linear mixed effects model with adjustments for demographic factors was used to determine statistical difference between antibody titers measured on day 0 and day 21 for each vaccination. *P ≤ 0.05, ***P ≤ 0.001, ****P ≤ 0.0001.

Immunization with three TIVs gradually increased the magnitude of durable endpoint titers and collectively increased the GMT by 3-fold from titers measured 12 months after the H1N1pdm09 vaccination (**Figure 4B**). Durable antibody levels measured 12 months after the first (P=0.008), second (P=0.001) and third TIV (P<0.0001) were all significantly higher than the level measured after H1N1pdm09 vaccination (**Figure 4B**). This demonstrates that all TIVs contributed to further increase and maintenance of durable endpoint titers. The first TIV increased NAI titers 12 months after vaccination, which reached an antibody ceiling for the two subsequent TIVs (**Figure 4E**). No change was observed in $PRNT_{50}$ titers after vaccination with TIVs (**Figure 4H**). Overall, our results indicate that the TIVs increased durable endpoint titers and maintained the durability of functional antibody titers.

Repeated Vaccination Boosts Antibody Titers but With Reduced Fold-Increase

We analyzed the impact of repeated vaccination on endpoint titers, and functional NAI and $PRNT_{50}$ titers measured at 21 days and 12 months after vaccination in the repeated group. The TIVs boosted endpoint titers measured on day 21 and the endpoint GMT increased gradually with each TIV (**Figure 4A**). The endpoint GMT was measured at 740 after H1N1pdm09 vaccination and was significantly higher after the second TIV when GMT increased to 1579 (P=0.039). Among the HCWs receiving the second TIV, 7/26 had not been vaccinated the year before and one HCW had not been vaccinated for two years (**Supplementary Table 2**). The endpoint GMT further increased to 1827 after the third TIV, which was the highest level measured during the study, although this was not significantly different from the endpoint GMTs measured after H1N1pdm09 or the other TIVs. The number of HCWs that received a third TIV was 19/26, however, two HCWs did not provide day 21 samples. Of these 19 HCWs, only 4 had not been vaccinated the season prior to the third TIV (**Supplementary Table 2**). We observed a different trend for the functional NAI titers on day 21. Although NAI titers were boosted by the TIVs, there were minimal differences in GMT on day 21 after the first, second and third TIV (**Figure 4D**). In fact, NAI GMT measured on day 21 was lowest after the third TIV. $PRNT_{50}$ titers were also boosted after vaccination with TIVs and the highest GMT was observed 21 days after H1N1pdm09 vaccination, whereas TIVs induced lower but

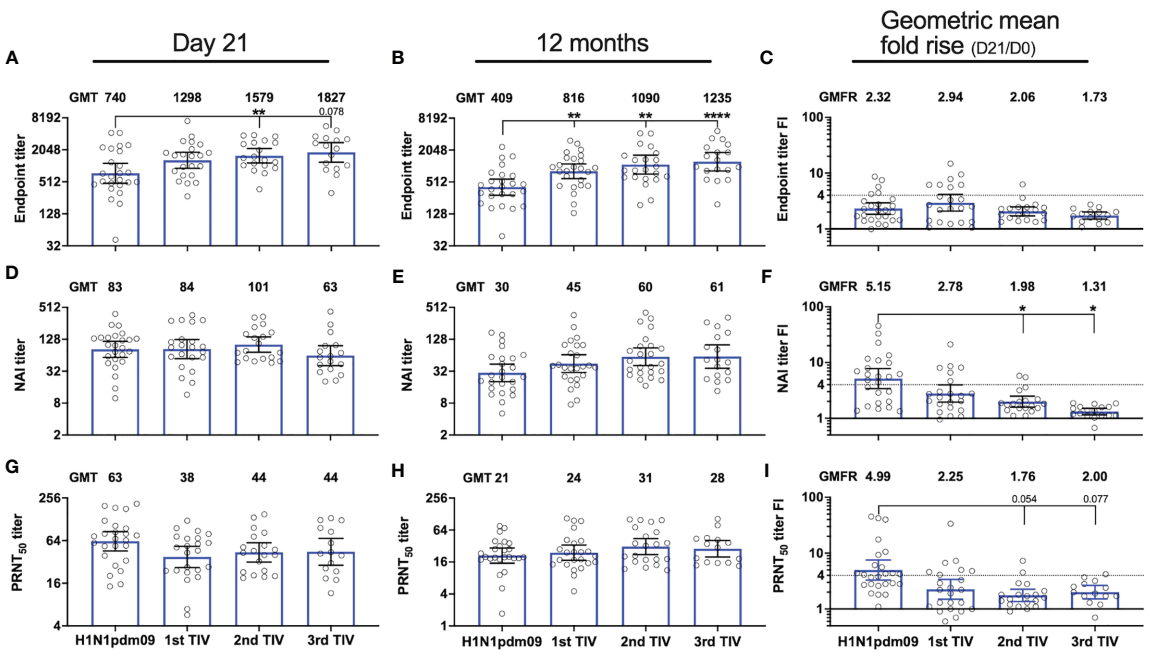

FIGURE 4 | Repeated influenza vaccination boosted durable NA-specific antibody titers but with diminished fold-induction. NA-specific antibody responses were measured 21 days and 12 months after vaccination with AS03-adjuvanted monovalent H1N1pdm09 vaccine and three trivalent influenza vaccines (TIVs) in the four subsequent years after the 2009 pandemic. Antibody titers were measured by ELISA **(A, B)**, ELLA **(D, E)** and plaque reduction neutralization assay **(G, H)** in the repeated group. Geometric mean titers (GMT) are indicated for each vaccine on top of all graphs **(A, B, D, E, G, H)**. Fold-increase (FI) for each subject on day 21 (day 21/day 0) was calculated for the individual vaccines and the geometric mean fold rise (GMFR) for the whole group is indicated on top of each graph **(C, F, I)**. The dotted line represents the threshold set for seroconversion (>4-fold increase). Results are grouped by H1N1pdm09 vaccination and number of trivalent influenza vaccines (TIV) received. The data are presented as geometric mean with 95% confidence intervals. A linear mixed effects model with adjustments for demographic factors was used to determine statistical difference between antibody titers measured after vaccination with H1N1pdm09 and TIVs. *P ≤ 0.05, **P ≤ 0.01, ****P ≤ 0.0001.

similar titers (**Figure 4G**). The level of $PRNT_{50}$ titers measured 21 days after vaccination was not significantly different among the TIVs.

Although TIV vaccination boosted NA-specific antibody responses, the magnitude of the fold- increase on day 21 was not augmented by the number of vaccinations reflecting an antibody ceiling (**Figures 4C, F, I**). The GMFR for functional NAI and $PRNT_{50}$ titers in the repeated group was highest after H1N1pdm09 vaccination and declined with each subsequent TIV (**Figures 4F, I**). The GMFR for NAI titers was significantly lower after the second (P=0.038) and third TIV (P=0.014) compared to H1N1pdm09 vaccination. A trend of decreasing GMFR for the $PRNT_{50}$ titers was observed after the second (P=0.054) and third TIVs (P=0.077) although not significant compared to H1N1pdm09 vaccination. The seroconversion rate for NAI titers also declined with each TIV, where none of the HCWs had >4-fold increase after the third TIV. Seroconversion rates for the first and second TIV were 27 and 11%, respectively. Reduction in GMFR for endpoint titers was also observed with repeated vaccination but the effect was less pronounced than for functional antibody titers (**Figure 4C**).

Pre-existing antibody titers to HA may have a negative effect on boosting of antibody titers after vaccination, however, it is unknown if this applies to NA-specific responses. Spearman correlation analysis was performed to investigate the relationship between baseline titers and fold-increase 21 days after vaccination (**Figure 5**). We found trends of inverse correlation, which was strongest for functional NAI (**Figures 5E–H**) and $PRNT_{50}$ titers (**Figures 5I–L**). Significant inverse correlations were found for NAI titers after H1N1pdm09 and second TIV, and after H1N1pdm09 and the two first TIVs for $PRNT_{50}$ titers. In contrast, a significant correlation was only found for endpoint titers after the first TIV (**Figures 5A–D**). Although the sample size was low, HCWs did not have a higher fold-increase when they had not been vaccinated during the previous year compared to those who had been vaccinated in the previous year (**Figure 5**). Overall, our results indicate that vaccination boosts and maintains NA-specific antibody titers but the magnitude of fold-increase at day 21 is reduced by repeated vaccination with the same vaccine strain over five years. The level of pre-existing antibody titers influenced the magnitude of fold-increase, particularly for functional antibody titers.

DISCUSSION

NA is required to be present in current influenza vaccines, however, there are no regulatory requirements for the amount

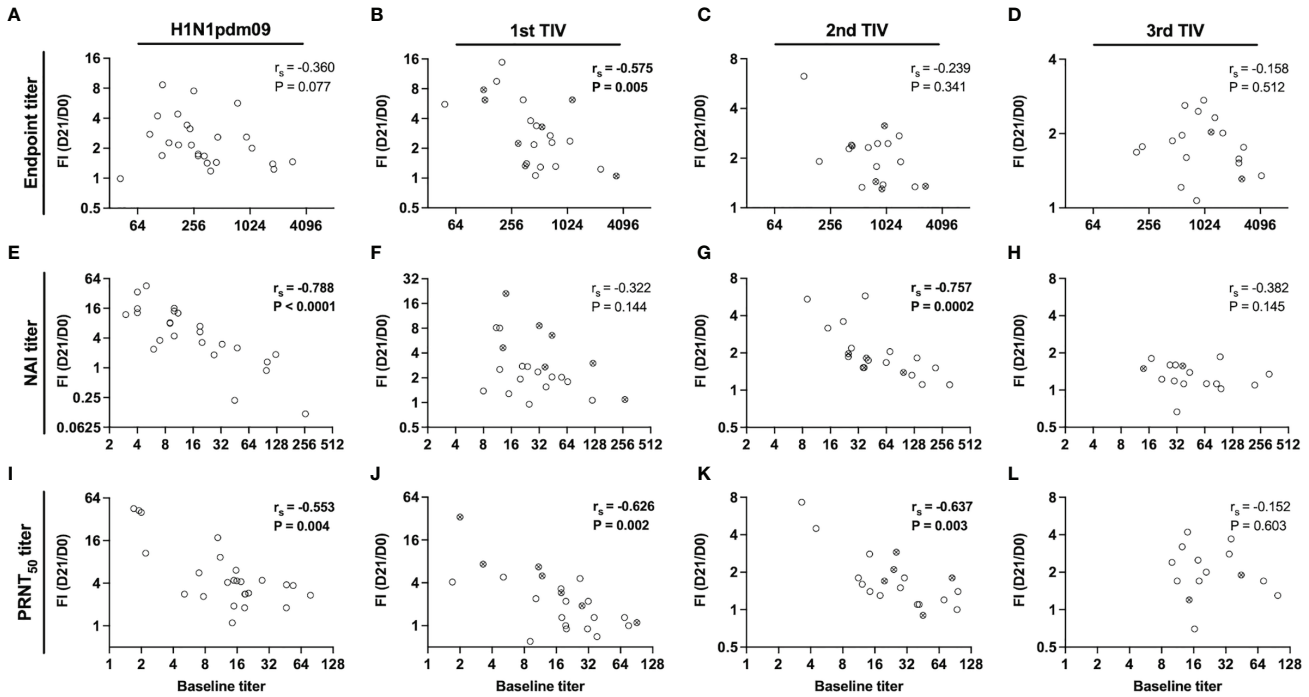

FIGURE 5 | Relationship between pre-existing titers and fold-increase 21 days post-vaccination. Correlation between baseline titers and fold-increase (FI) of titers on day 21 post-vaccination (day 21/day 0) for endpoint **(A–D)**, NAI **(E–H)** and $PRNT_{50}$ titers **(I–L)** in the repeated group. Health care workers (HCWs) were vaccinated with H1N1pdm09 and two or three trivalent influenza vaccines (TIVs) during influenza seasons 2009/2010 – 2013/2014. The antibody responses have been grouped by the vaccine number that were administered. All vaccinated HCWs in the repeated group is included in this figure regardless of their vaccination intervals. Open circles represent HCWs that were vaccinated the previous season and crossed circles represent HCWs that had chosen to not be vaccinated the previous season. The correlation coefficient (r_s) was calculated by non-parametric Spearman correlation.

or the quality of the antigen. Historically, NA content has not been regulated for vaccines due to a lack of standardized assays for measuring the NA concentration and also NA immunogenicity. Recent studies have emphasized the importance of NA-specific antibodies in protection against influenza disease and found that it may be an independent correlate of protection (6, 7). Here, we studied NA-specific antibody responses in HCWs after AS03-adjuvanted monovalent H1N1pdm09 vaccination in 2009 and annual vaccination with TIVs in the four subsequent influenza seasons. Our main finding is repeated influenza vaccination contributes to durable functional H1N1pdm09 NA-specific antibodies, although there is a reduced magnitude of fold-induction with increasing number of TIVs.

Early studies have shown that individuals with high pre-existing HAI titers have reduced boosting after re-vaccination (19, 20). Others have since reported that repeated vaccination and high pre-existing titers may reduce boosting of B cell responses and antibody titers after vaccination (12, 13, 21, 22). These studies have mostly focused on HA-specific antibody responses, however, lower antibody responses to NA after a second vaccination have been reported in individuals vaccinated in two consecutive years (23). Here we show that repeated vaccination has a similar effect on the NA-specific antibody response also after a third and fourth vaccination. We found that, although antibody titers were boosted after repeated vaccination, the magnitude of fold-induction declined, which was most prominent for functional NAI and $PRNT_{50}$ titers. Additionally, the NAI and $PRNT_{50}$ titer fold-increase on day 21 was inversely correlated with pre-existing titers. Others have hypothesized that boosting after repeated vaccination could be limited by pre-existing immunity and several mechanisms has been suggested based on mathematical modeling, which includes epitope masking model (24). This model proposes that pre-existing antibodies will bind and mask epitopes, blocking B cells that bind to the same or nearby epitopes, which results in limited B cell stimulation and expansion. Epitope masking may be a possible explanation for why the functional NA antibodies (measured by fold-increase for NAI and $PRNT_{50}$ titers) peak after H1N1pdm09 vaccination but declines after subsequent TIVs, whereas this effect is less prominent for total NA-specific IgG binding antibodies measured by ELISA. Functional antibodies that are capable of conferring NAI activity bind directly or close to the enzyme active site, however, antigenic sites for human mAbs that do not have functional NAI activity have been described (25). Masking of NAI epitopes would still allow for stimulation of B cells reactive to other parts of the NA, which are readily measured by ELISA. Our observational study

showed that repeated vaccination with the same strain induced durable NA-specific antibodies although it may reduce the magnitude of fold-increase, particularly functional antibodies capable of NAI. The persistence of durable antibody titers suggests that long-lived plasma cells are generated after adjuvanted H1N1pdm09 and subsequent non-adjuvanted TIVs. Further studies are warranted to understand the immunological mechanisms influencing this. This study was unique because the H1N1 vaccine component was the same for five consecutive influenza seasons. Antibody responses after vaccination with TIV during seasons 2006 – 2013 was found to be highest whenever one or more of the vaccine strains varied from year to year (21). More diversification of the H1N1 vaccine strain or addition of adjuvant could possibly have reduced the negative impact of repeated vaccination on antibody responses to NA and should be taken into consideration when choosing the vaccine strains for seasonal vaccines in the future.

A second objective of our study was to investigate the induction of NA-specific antibodies after AS03-adjuvanted monovalent H1N1pdm09 vaccination in healthy adults. This vaccine only contained 3.75 μg HA per dose due to dose-sparing during the 2009 pandemic, whereas TIVs are required to contain 15 μg HA. Quantification of the H1N1pdm09 vaccine composition by mass spectrometry revealed that one dose contained 21% HA and 6.9% NA, demonstrating that the amount of NA was even lower than that of HA per dose. Based on this estimation, the amount of NA would have been 1.23 μg per dose (26). Despite this, we found robust induction of NA-specific antibodies and a 53% seroconversion rate for NAI titers defined seroconversion as >4-fold increase. Other studies have found seroconversion rates ranging from 23 – 64%, however, the definition of seroconversion in these studies varied from 2 – 4-fold increase on day 21 from baseline (7, 10, 11). The seroconversion rate in our study is among the highest reported after influenza vaccination. This shows that robust and durable NA-specific antibody responses can be induced, even with low amounts of antigen when given with an appropriate adjuvant. Our results further support that standardization of the amount and stability of the NA antigen should be implemented for optimization of current influenza vaccines.

NA may undergo antigenic drift and shift independently of HA and NA immunity could provide protection in the event of mismatching of vaccine and circulating strains, and possibly against newly emerging strains. Broadly reactive NA antibodies have been described, demonstrating the breadth of immunity that could potentially be achieved through vaccination (8, 27). Standardizing the amount and supplementing current vaccines with NA have been proposed as a strategy for improving NA immunogenicity (28). A high dosage influenza vaccine containing eight times more NA activity than standard TIVs was found to induce higher levels of NAI antibodies compared to the standard TIV dosage in humans (29). Furthermore, computationally designed NA antigens tested in mice have shown that NA antigens can be designed for optimal cross reactivity (30). These strategies could possibly overcome the influence of pre-existing immunity and aid in the design of diverse antigens for optimal NA immunogenicity.

The current study has several limitations. HCWs may have been infected with influenza virus during the five-year study. This was more easily identified in the single group by increases of HI titers during a season, three HCWs were excluded from further analysis after seroconversion had occurred. However, this was more complicated for HCWs in the repeated group because it is not possible to distinguish increase in HI titer induced by vaccination *versus* infection. Furthermore, HCWs in the repeated group had different intervals of TIV vaccination and the sample size for the various regimens was low. However, we did not find that HCWs that had not been vaccinated for one or two years had higher antibody titer fold-increase compared to those who received TIVs in consecutive years. Only serological responses were measured in this study and therefore it is not known if and how the B cells are affected by repeated vaccination. Others have found inverse correlations between HA-specific pre-existing titers and the number of vaccine-induced antibody secreting cells (12, 21). Investigating this relationship for NA-specific humoral responses is important in future work as it could provide a better understanding of the interplay between pre-existing immunity and boosting, and its role in repeated influenza vaccination.

In conclusion, we found that AS03-adjvuanted pandemic vaccination boosted the NA-specific antibodies that persisted above pre-vaccination levels for 5 years. Repeated vaccination boosted NA-specific antibody titers, although with reduced the magnitude of fold-increase, particularly for functional antibodies. It is important to emphasize that vaccination is the best method of preventing influenza infection and annual vaccination remains beneficial. Our results support continued development and standardization of the NA antigen to supplement current influenza vaccines and reduce the burden of morbidity and mortality.

DATA AVAILABILITY STATEMENT

The raw data supporting the conclusions of this article will be made available by the authors, without undue reservation.

ETHICS STATEMENT

The studies involving human participants were reviewed and approved by Regionale komiteer for medisinsk og helsefaglig forskningsetikk Vest. The patients/participants provided their written informed consent to participate in this study.

AUTHOR CONTRIBUTIONS

LH, FZ, and HA performed the experiments. LH and M-CT performed statistical analyses. LH and RJC wrote the manuscript.

RJC and M-CT conceptualized and designed the study. All authors contributed to the article and approved the submitted version.

FUNDING

LH was supported by Norwegian Research Council grant 271160. This study received intramural funding from the Influenza Centre at the University of Bergen and Haukeland University Hospital. The Influenza Centre is funded by the University of Bergen, Ministry of Health and Care Services, Helse Vest (F-11628), the Trond Mohn Foundation (TMS2020TMT05), the European Union (EU IMI115672 FLUCOP, H2020 874866 INCENTIVE, H2020 101037867 VACCELERATE, EU IMI101007799 Inno4Vac) and Nanomedicines Flunanoair (ERA-NETet EuroNanoMed2, JTC2016), and the Research Council of Norway GLOBVAC program (284930).

ACKNOWLEDGMENTS

We thank all HCWs, clinical staff especially Marianne Sævik and staff at the Influenza Centre for participation in the study. We thank NIBSC for providing the RG virus used in the ELLA assay. We thank Prof. Florian Krammer for providing the baculoviruses used in purifying N1NA proteins.

SUPPLEMENTARY MATERIAL

The Supplementary Material for this article can be found online at: https://www.frontiersin.org/articles/10.3389/fimmu.2021.748264/full#supplementary-material

Supplementary Figure 1 | NA inhibitor oseltamivir was used to verify that the plaque reduction neutralization assay was capable of measuring reduction of plaque forming units per well (PFU/well) as a result of NA inhibition in a dose-dependent manner.

REFERENCES

1. Iuliano AD, Roguski KM, Chang HH, Muscatello DJ, Palekar R, Tempia S, et al. Estimates of Global Seasonal Influenza-Associated Respiratory Mortality: A Modelling Study. *Lancet* (2018) 391(10127):1285–300. doi: 10.1016/S0140-6736(17)33293-2
2. World Health Organization. *Influenza (Seasonal)* (2018). Available at: https://www.who.int/en/news-room/fact-sheets/detail/influenza-(seasonal).
3. Palese P, Tobita K, Ueda M, Compans RW. Characterization of Temperature Sensitive Influenza Virus Mutants Defective in Neuraminidase. *Virology* (1974) 61(2):397–410. doi: 10.1016/0042-6822(74)90276-1
4. Kilbourne ED, Couch RB, Kasel JA, Keitel WA, Cate TR, Quarles JH, et al. Purified Influenza A Virus N2 Neuraminidase Vaccine is Immunogenic and non-Toxic in Humans. *Vaccine* (1995) 13(18):1799–803. doi: 10.1016/0264-410X(95)00127-M
5. Murphy BR, Kasel JA, Chanock RM. Association of Serum Anti-Neuraminidase Antibody With Resistance to Influenza in Man. *N Engl J Med* (1972) 286(25):1329–32. doi: 10.1056/NEJM197206222862502
6. Memoli MJ, Shaw PA, Han A, Czajkowski L, Reed S, Athota R, et al. Evaluation of Antihemagglutinin and Antineuraminidase Antibodies as Correlates of Protection in an Influenza A/H1N1 Virus Healthy Human Challenge Model. *mBio* (2016) 7(2):e00417–16. doi: 10.1128/mBio.00417-16
7. Monto AS, Petrie JG, Cross RT, Johnson E, Liu M, Zhong W, et al. Antibody to Influenza Virus Neuraminidase: An Independent Correlate of Protection. *J Infect Dis* (2015) 212(8):1191–9. doi: 10.1093/infdis/jiv195
8. Chen YQ, Wohlbold TJ, Zheng NY, Huang M, Huang Y, Neu KE, et al. Influenza Infection in Humans Induces Broadly Cross-Reactive and Protective Neuraminidase-Reactive Antibodies. *Cell* (2018) 173(2):417–29.e10. doi: 10.1016/j.cell.2018.03.030
9. Wohlbold TJ, Nachbagauer R, Xu H, Tan GS, Hirsh A, Brokstad KA, et al. Vaccination With Adjuvanted Recombinant Neuraminidase Induces Broad Heterologous, But Not Heterosubtypic, Cross-Protection Against Influenza Virus Infection in Mice. *mBio* (2015) 6(2):e02556. doi: 10.1128/mBio.02556-14
10. Couch RB, Atmar RL, Keitel WA, Quarles JM, Wells J, Arden N, et al. Randomized Comparative Study of the Serum Antihemagglutinin and Antineuraminidase Antibody Responses to Six Licensed Trivalent Influenza Vaccines. *Vaccine* (2012) 31(1):190–5. doi: 10.1016/j.vaccine.2012.10.065
11. Laguio-Vila MR, Thompson MG, Reynolds S, Spencer SM, Gaglani M, Naleway A, et al. Comparison of Serum Hemagglutinin and Neuraminidase Inhibition Antibodies After 2010-2011 Trivalent Inactivated Influenza Vaccination in Healthcare Personnel. *Open Forum Infect Dis* (2015) 2(1): ofu115. doi: 10.1093/ofid/ofu115
12. Sanyal M, Holmes TH, Maecker HT, Albrecht RA, Dekker CL, He XS, et al. Diminished B-Cell Response After Repeat Influenza Vaccination. *J Infect Dis* (2019) 219(10):1586–95. doi: 10.1093/infdis/jiy685
13. Ellebedy AH, Nachbagauer R, Jackson KJL, Dai YN, Han J, Alsoussi WB, et al. Adjuvanted H5N1 Influenza Vaccine Enhances Both Cross-Reactive Memory B Cell and Strain-Specific Naive B Cell Responses in Humans. *Proc Natl Acad Sci USA* (2020) 117(30):17957–64. doi: 10.1073/pnas.1906613117
14. Madhun AS, Akselsen PE, Sjursen H, Pedersen G, Svindland S, Nostbakken JK, et al. An Adjuvanted Pandemic Influenza H1N1 Vaccine Provides Early and Long Term Protection in Health Care Workers. *Vaccine* (2010) 29 (2):266–73. doi: 10.1016/j.vaccine.2010.10.038
15. Margine I, Palese P, Krammer F. Expression of Functional Recombinant Hemagglutinin and Neuraminidase Proteins From the Novel H7N9 Influenza Virus Using the Baculovirus Expression System. *J Vis Exp* (2013) 81):e51112. doi: 10.3791/51112
16. Couzens L, Gao J, Westgeest K, Sandbulte M, Lugovtsev V, Fouchier R, et al. An Optimized Enzyme-Linked Lectin Assay to Measure Influenza A Virus Neuraminidase Inhibition Antibody Titers in Human Sera. *J Virol Methods* (2014) 210:7–14. doi: 10.1016/j.jviromet.2014.09.003
17. Matrosovich M, Matrosovich T, Carr J, Roberts NA, Klenk HD. Overexpression of the Alpha-2,6-Sialyltransferase in MDCK Cells Increases Influenza Virus Sensitivity to Neuraminidase Inhibitors. *J Virol* (2003) 77 (15):8418–25. doi: 10.1128/JVI.77.15.8418-8425.2003
18. Matrosovich M, Matrosovich T, Garten W, Klenk HD. New Low-Viscosity Overlay Medium for Viral Plaque Assays. *Virol J* (2006) 3:63. doi: 10.1186/1743-422X-3-63
19. Hobson D, Baker FA, Curry RL. Effect of Influenza Vaccines in Stimulating Antibody in Volunteers With Prior Immunity. *Lancet* (1973) 2(7821):155–6. doi: 10.1016/S0140-6736(73)93106-1
20. Pyhala R, Kumpulainen V, Alanko S, Forsten T. HI Antibody Kinetics in Adult Volunteers Immunized Repeatedly With Inactivated Trivalent Influenza Vaccine in 1990-1992. *Vaccine* (1994) 12(10):947–52. doi: 10.1016/0264-410X(94)90039-6
21. Andrews SF, Kaur K, Pauli NT, Huang M, Huang Y, Wilson PC. High Preexisting Serological Antibody Levels Correlate With Diversification of the Influenza Vaccine Response. *J Virol* (2015) 89(6):3308–17. doi: 10.1128/JVI.02871-14
22. Ellebedy AH, Krammer F, Li GM, Miller MS, Chiu C, Wrammert J, et al. Induction of Broadly Cross-Reactive Antibody Responses to the Influenza HA Stem Region Following H5N1 Vaccination in Humans. *Proc Natl Acad Sci USA* (2014) 111(36):13133–8. doi: 10.1073/pnas.1414070111
23. Petrie JG, Ohmit SE, Johnson E, Truscon R, Monto AS. Persistence of Antibodies to Influenza Hemagglutinin and Neuraminidase Following One or Two Years of Influenza Vaccination. *J Infect Dis* (2015) 212(12):1914–22. doi: 10.1093/infdis/jiv313
24. Linderman SL, Ellebedy AH, Davis C, Eberhardt CS, Antia R, Ahmed R, et al. Influenza Immunization in the Context of Preexisting Immunity. *Cold Spring Harb Perspect Med* (2020). doi: 10.1101/cshperspect.a040964
25. Yasuhara A, Yamayoshi S, Kiso M, Sakai-Tagawa Y, Koga M, Adachi E, et al. Antigenic Drift Originating From Changes to the Lateral Surface of the Neuraminidase Head of Influenza A Virus. *Nat Microbiol* (2019) 4(6):1024–34. doi: 10.1038/s41564-019-0401-1
26. Jacob L, Leib R, Ollila HM, Bonvalet M, Adams CM, Mignot E. Comparison of Pandemrix and Arepanrix, Two Ph1n1 AS03-Adjuvanted Vaccines

Differentially Associated With Narcolepsy Development. *Brain Behav Immun* (2015) 47:44–57. doi: 10.1016/j.bbi.2014.11.004

27. Stadlbauer D, Zhu X, McMahon M, Turner JS, Wohlbold TJ, Schmitz AJ, et al. Broadly Protective Human Antibodies That Target the Active Site of Influenza Virus Neuraminidase. *Science* (2019) 366(6464):499–504. doi: 10.1126/science.aay0678
28. Giurgea LT, Morens DM, Taubenberger JK, Memoli MJ. Influenza Neuraminidase: A Neglected Protein and Its Potential for a Better Influenza Vaccine. *Vaccines (Basel)* (2020) 8(3):409. doi: 10.3390/vaccines8030409
29. Cate TR, Rayford Y, Nino D, Winokur P, Brady R, Belshe R, et al. A High Dosage Influenza Vaccine Induced Significantly More Neuraminidase Antibody Than Standard Vaccine Among Elderly Subjects. *Vaccine* (2010) 28(9):2076–9. doi: 10.1016/j.vaccine.2009.12.041
30. Skarlupka AL, Bebin-Blackwell AG, Sumner SF, Ross TM. Universal Influenza Virus Neuraminidase Vaccine Elicits Protective Immune Responses Against Human Seasonal and Pre-Pandemic Strains. *J Virol* (2021) 95(7):e0075921. doi: 10.1128/JVI.00759-21

Conflict of Interest: The authors declare that the research was conducted in the absence of any commercial or financial relationships that could be construed as a potential conflict of interest.

frontiers in Immunology

SYSTEMATIC REVIEW
published: 28 October 2021
doi: 10.3389/fimmu.2021.740048

Safety of Influenza A H1N1pdm09 Vaccines: An Overview of Systematic Reviews

Lene Kristine Juvet, Anna Hayman Robertson, Ida Laake, Siri Mjaaland and Lill Trogstad*

Division of Infection Control and Environmental Health, Norwegian Institute of Public Health, Oslo, Norway

Background: In 2009, a new influenza A H1N1 virus emerged causing a global pandemic. A range of monovalent influenza A H1N1pdm09 vaccines with or without adjuvants were developed. After the mass vaccination campaigns safety concerns related to H1N1pdm09 vaccines were reported. More than a decade later, reported AEFIs are still under scrutiny. We performed a systematic review aiming to synthesize the evidence on the safety of the H1N1pdm09 vaccines on reported outcomes from existing systematic reviews.

Methods: Four electronic databases, PubMed, EMBASE, Epistimonikos and the Cochrane Database of Systematic Reviews were searched for articles on H1N1pdm09 vaccination published from 2009 to January 2021. Systematic reviews assessing short- or long-term adverse events after H1N1pdm09 vaccination were considered for inclusion. Data was extracted from all selected reviews. Outcomes were grouped and results from each included review were presented narratively and in tables.

Results: 16 systematic reviews met the inclusion criteria. Reported outcomes were short-term events (3 reviews), fetal/pregnancy outcomes (8 reviews), Guillain-Barré syndrome (GBS) (4 reviews), narcolepsy (2 reviews) demyelinating diseases (1 review based on one study only) and inflammatory bowel disease (IBD) (1 review). Short-term serious adverse events were rare, 3 cases amongst 16725 subjects in 18 randomized controlled trials (0.018%). No deaths were reported. The risks of local events were generally higher for adjuvanted vaccines as compared to unadjuvanted vaccines. Maternal H1N1pdm09 vaccination in any trimester was not associated with an increase in preterm birth, small for gestational age, congenital malformations or fetal death. For GBS, results were conflicting. The main systematic review on narcolepsy found a 5-14-fold increased risk in children, and a 2-7- fold increased risk in adults after vaccination with Pandemrix. The attributable risk of narcolepsy one year after vaccination was 1 case per 18 400 vaccine doses in children/adolescents, and 1 case per 181 000 vaccine doses in adults.

Conclusion: Adjuvanted vaccines had more local but not serious adverse events compared to unadjuvanted vaccines. Vaccination with Pandemrix was strongly associated with narcolepsy, particularly in children. No increased risks of pregnancy outcomes were seen after pandemic vaccination. The findings on GBS were inconclusive.

Keywords: H1N1pdm09 vaccination, pandemic vaccines, influenza vaccines, safety, adverse events

OPEN ACCESS

Edited by:
Michael Schotsaert, Icahn School of Medicine at Mount Sinai, United States

Reviewed by:
Osaretin Emmanuel Asowata, Population Council, United States
David Pejoski, Université de Genève, Switzerland

****Correspondence:***
Lene Kristine Juvet
LeneKristine.Juvet@fhi.no

Specialty section:
This article was submitted to Vaccines and Molecular Therapeutics, a section of the journal Frontiers in Immunology

Received: *12 July 2021*
Accepted: *12 October 2021*
Published: *28 October 2021*

Citation:
Juvet LK, Robertson AH, Laake I, Mjaaland S and Trogstad L (2021) Safety of Influenza A H1N1pdm09 Vaccines: An Overview of Systematic Reviews. Front. Immunol. 12:740048. doi: 10.3389/fimmu.2021.740048

INTRODUCTION

In 2009, a novel H1N1 influenza A virus (H1N1pdm09) emerged causing a global pandemic. According to Centers for Disease Control and Prevention (CDC) an estimated 151,700 - 575,400 people worldwide died from H1N1pdm09 virus infection during the first year the virus circulated (1). Globally, 80 percent of H1N1pdm09 virus-related deaths were estimated to have occurred in people younger than 65 years of age. This differs greatly from typical seasonal influenza epidemics, during which about 70 to 90 percent of deaths are estimated to occur in people 65 years and older (2). Pregnant women were early considered to be at increased risk of severe disease and adverse fetal outcomes (3).

To combat the pandemic virus, a range of monovalent H1N1pdm09 vaccines were developed, mainly drawing on existing egg-based technology from seasonal influenza vaccines. The vaccines were produced with the adjuvants AS03, MF59, aluminium, or without adjuvants. By June 2010, more than 350 million people had received H1N1pdm09 vaccines worldwide (4). In Europe, more than 37 million people were vaccinated with three centrally authorized Influenza A H1N1 vaccines marketed in the European Economic Area: Celvapan (no adjuvants), Focetria (MF59 adjuvanted) and Pandemrix (AS03 adjuvanted). More than 30 million persons received Pandemrix in Europe (4, 5). The overall effectiveness of the pandemic vaccines has been estimated to 80% (95% CI 59-90%) against laboratory confirmed influenza, with adjuvanted vaccines being significantly more effective in children than adults (6). Pandemic vaccination may also have contributed to less severe outcomes related to H1N1pdm09 infection in the following flu season (2010/11) when the same virus strain continued to circulate (7).

The safety of vaccines is a prime concern, also in pandemic situations. Safety monitoring systems require coordinated actions and collaboration between regulatory and immunization program authorities on a national level and concerted international efforts to maintain proper management and public trust. In response to the pandemic influenza A H1N1pdm09 strain, mass vaccination campaigns administrating vaccines to large populations over a short period of time were launched. In such situations, surveillance and evaluation of adverse events following immunization (AEFIs) may be particularly challenging due to large numbers of vaccine adverse events reports. An AEFI is defined as any untoward medical occurrence which follows immunization and which does not necessarily have a causal relationship with the vaccine (8). The fact that a vaccine was administered within a reasonable time period of the occurrence of an event does not automatically suggest that the vaccine caused or contributed to the event. Nevertheless, a temporal association is necessary to imply causation. In many countries, the vaccination campaigns coincided with the pandemic peak. This may have complicated the evaluation of suspected AEFIs, which in some cases may be difficult to separate from symptoms or consequences of the pandemic influenza infection itself, for instance Guillain-Barré Syndrome (GBS) or Chronic fatigue syndrome/Myalgic encephalopathy (CFS/ME) (9, 10). The evidence of a link between a vaccine as a potential cause and a specific event is derived from well-designed population based epidemiological studies (8). Since clinical trials are not powered to detect *rare* adverse events, large, prospective studies including appropriate comparison groups are crucial. Knowledge on the expected background rates of possible adverse events is important for the assessment of possible vaccine adverse reactions. Other health conditions may occur in close proximity to vaccination in a substantial number of people when large populations are vaccinated. Thus, careful evaluation of vaccine safety signals is critical to detect the true vaccine reactions and to establish whether coincidental events were caused by vaccination or not.

A number of reports on suspected AEFIs have been published, among which the unexpected increased incidence of narcolepsy in children and young adults following vaccination with Pandemrix received massive attention among the general public and medical communities, in particular in Europe. A number of observational studies have confirmed the association between Pandemrix vaccination and narcolepsy (11–14), whereas studies on associations between H1N1pdm09 vaccination and other outcomes have shown no or conflicting results (9, 10, 15). More than a decade later, reported AEFIs after H1N1pdm09 vaccination are still under scrutiny and assessment for causality in Norway, and a synthesis of the available evidence warranted. The objective of this systematic review was to synthesize the current evidence on the safety of the H1N1pdm09 vaccines from existing systematic reviews, based on both randomized controlled trials and observational studies.

METHODS

Search Strategy and Selection of Systematic Reviews

The search strategy followed the Preferred Reporting Items for Systematic Review and Meta-analysis (PRISMA) guidelines (16, 17). Four electronic databases, namely, PubMed, EMBASE, Epistimonikos and the Cochrane Database of Systematic Reviews, were searched. Keywords employed were ("H1N1 pdm09" OR "influenza pandemic 2009") AND ("vaccin*" OR "pandemic vaccine*") (**Supplementary Table 1**). The search was designed to identify primary studies and systematic reviews, and covered literature published between 2009 and November 2019. All retrieved studies were imported into the Rayyan QCRI (18) and duplicated articles were removed.

Criteria for inclusion were short- or long-term adverse events after H1N1pdm09 vaccination compared to a control group (**Table 1**). Two independent researchers initially screened all articles based on title and abstract, categorizing them as "included", "excluded" or "maybe". Any disagreements or "maybes" were resolved by consensus with a third reviewer. For this study, only systematic reviews were included. Systematic reviews limited to vaccine efficacy were excluded. Only publications in English were included. An updated search for systematic reviews in Pubmed (systematic review filter) was performed on 22nd January 2021.The reference lists were checked for further systematic reviews not previously identified. Subsequently, full text assessment of the included systematic reviews was performed by two reviewers to determine study eligibility based on the inclusion and exclusion criteria. Disagreements were resolved by discussion including a third reviewer.

TABLE 1 | Review inclusion criteria (PICO).

Population	All children, women and men.
Intervention	Pandemic vaccine during season 2009-2010.
Comparisons	No vaccination, placebo or other vaccines
Outcome	**Safety – outcomes all** • Acute events • Local adverse events • Longterm events • Systemic adverse events **Safety – additional outcomes pregnant women** • Spontaneous abortion, foetal death, stillbirth, preterm birth (less than 37 weeks), pre-eclampsia and eclampsia • Neonatal outcomes: congenital malformations (minor and major), neonatal death.
Study designs	Systematic reviews, health technology assessments

Assessment of Methodological Quality of Included Reviews

Two reviewers independently assessed the quality of each review using the revised "A Measurement Tool to Assess systematic Reviews, version 2" (AMSTAR 2) (19). Disagreements were resolved by discussion and, if necessary, arbitration among the whole review team. The level of confidence in the findings of the reviews was assessed according to the number of critical and minor flaws in the methodology. Only two systematic reviews included a list of excluded studies (Q7) (20, 21). If the systematic review included a flow chart explaining the reason for exclusion, it was scored as partial yes (PY). The source of funding (Q10) for the incorporated observational studies was not reported in the systematic reviews and was categorized as not applicable (NA). For most reviews, too few studies were included to enable assessment of publication bias. If the authors justified why the assessment could not be performed, the item was scored 'yes' (Q15).

Data Extraction and Management

One reviewer extracted data from all selected reviews into a spreadsheet (Microsoft Excel) including number and settings of the included trials, total number and characteristics of participants, intervention(s) assessed, outcomes measured and major limitations. A second reviewer cross-checked the extracted data for accuracy. Extracted variables from each systematic review are presented in detail in the characteristics of included systematic reviews (**Table 2**). Only data on H1N1pdm09 vaccines were extracted.

RESULTS

After exclusion of duplicates, the initial literature search identified 6815 articles for abstract review (**Figure 1**). After excluding articles based on abstract review, 453 remained. In the current study only systematic reviews were included (**Table 1**), and 22 systematic reviews were selected for full-text review according to the inclusion criteria. One additional article was found through hand searching of other literature. Of the 23 systematic reviews, 7 were excluded (**Supplementary Table 2**), and 16 reviews were included in the overview.

Table 2 summarizes the quality assessments of the included reviews. Most of the reviews were of moderate or high quality, but for two reviews there was low confidence in the findings of the review (**Table 2**). Common critical domain deficiencies included failure to preregister the review protocol (Q2), and failure to list excluded studies (Q7). Failure to consider risk of bias when interpreting results (Q13) were also quite frequent.

Table 3 shows an overview of the outcomes covered by the included systematic reviews. The main outcomes were short-term adverse events, narcolepsy, Guillain-Barré syndrome (GBS) and pregnancy- or fetal outcomes. One systematic review also

TABLE 2 | AMSTAR2 rating of 16 included systematic reviews.

Systematic review	AMSTAR2 rating																Confidence in findings of review
	Q1	Q2	Q3	Q4	Q5	Q6	Q7	Q8	Q9	Q10	Q11	Q12	Q13	Q14	Q15	Q16	
Demicheli 2018 (20)	Y	Y	Y	Y	Y	Y	Y	Y	Y	Y	Y	N	N	Y	Y	Y	High
Fell 2015 (22)	Y	Y	Y	Y	Y	Y	PY	Y	Y	NA	NA	NA	Y	Y	Y	Y	High
Foo 2020 (23)	Y	Y	Y	Y	Y	Y	PY	Y	Y	NA	NA	NA	Y	Y	NA	Y	High
Giles 2019 (24)	Y	N	Y	PY	Y	Y	PY	Y	Y	NA	N	N	N	Y	Y	Y	Moderate
Hauser 2019 (25)	Y	Y	Y	Y	Y	Y	PY	Y	Y	Y	Y	N	N	Y	Y	Y	High
Manzoli 2011 (26)	Y	N	Y	Y	Y	Y	PY	Y	Y	Y	N	Y	Y	N	Y	Y	Moderate
Martin Arias 2015 (27)	Y	N	Y	Y	Y	Y	PY	PY	N	NA	Y	N	N	Y	Y	N	Moderate
McMillan 2015 (21)	Y	Y	Y	Y	Y	Y	Y	Y	Y	Y	Y	Y	Y	Y	N	Y	High
Nunes 2016 (28)	Y	N	Y	Y	Y	Y	PY	Y	N	NA	Y	N	N	Y	Y	Y	Moderate
Pineton 2015 (29)	Y	N	Y	Y	Y	N	PY	Y	N	NA	NA	NA	N	Y	NA	Y	Moderate
Polyzos 2015 (30)	Y	N	Y	Y	Y	Y	PY	Y	Y	NA	Y	N	N	Y	Y	Y	Moderate
Sanz Fadrique 2019 (31)	Y	N	Y	PY	N	N	PY	PY	N	NA	NA	NA	N	N	NA	Y	Low
Sarkanan 2018 (32)	Y	N	Y	Y	Y	Y	PY	Y	N	NA	Y	N	Y	Y	Y	Y	Moderate
Stassijns 2016 (33)	Y	N	Y	Y	N	N	N	Y	N	N	Y	N	N	Y	N	Y	Low
Wachira 2019 (34)	Y	PY	Y	PY	Y	Y	PY	Y	Y	NA	NA	NA	Y	N	NA	N	Moderate
Zhang 2018 (35)	Y	N	Y	Y	Y	Y	PY	Y	Y	NA	N	N	N	N	NA	Y	Moderate

1. components of PICO, 2. established protocol prior to review, 3. selection of study design, 4.comprehensive literature search, 5. study selection in duplicate, 6.data extraction in duplicate, 7. list of excluded studies, 8.describe the included studies, 9. assessing the risk of bias, 10. sources of funding, 11.meta-analysis if appropriate, 12. meta-analysis sensitivity RoB, 13. interpreting RoB when discussing the results, 14. discussing heterogeneity, 15. investigation publication bias, 16. potential sources of conflict of interest.
N, no; NA, not applicable no meta-analysis conducted; PY, partial yes; Y, yes.

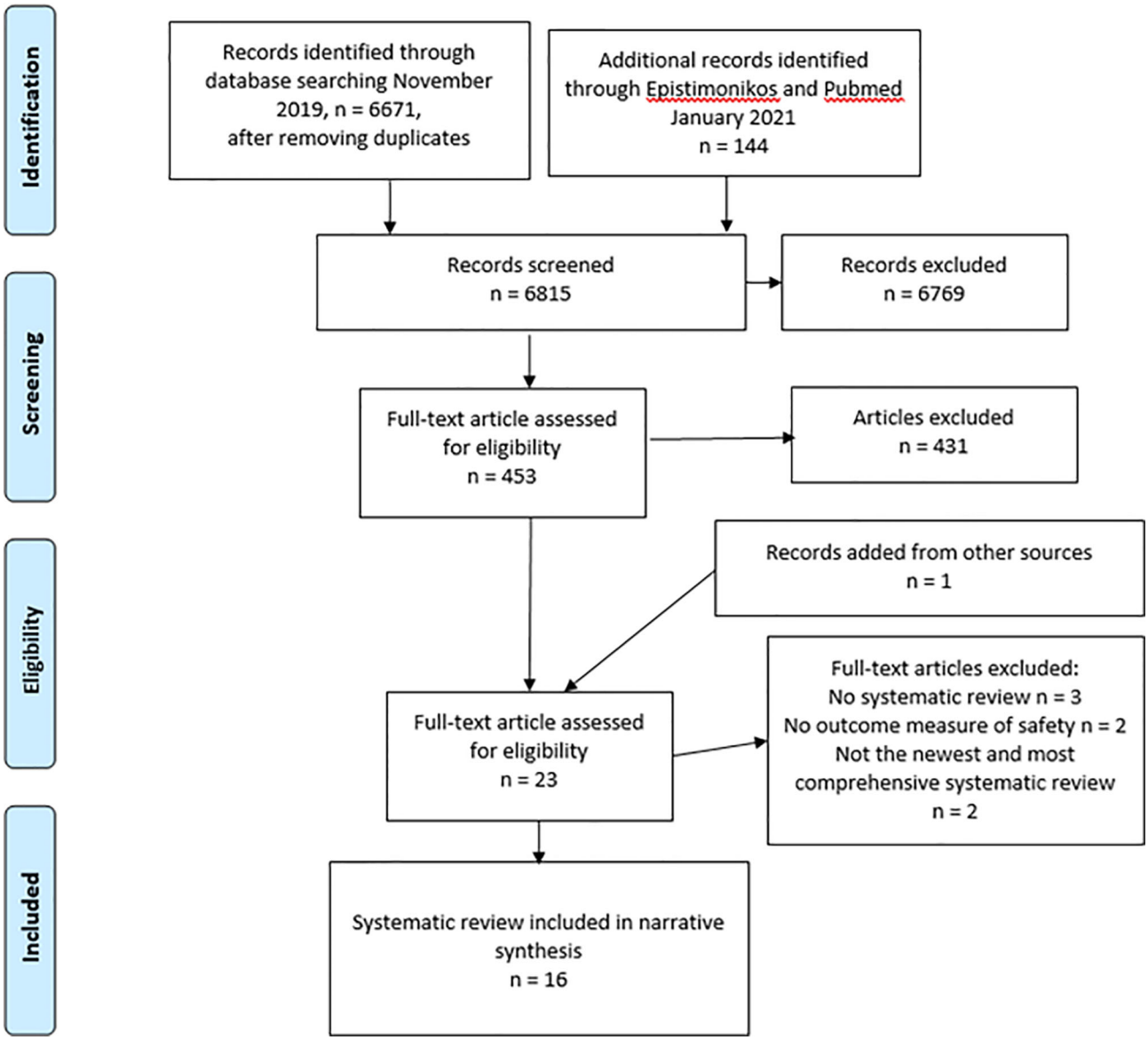

FIGURE 1 | Study selection, PRISMA flow chart.

included a single study on inflammatory bowel disease (IBD) (29), and one systematic review included a single study on demyelinating disease (20). Most studies reporting short-term adverse events were randomized controlled trials (RCTs), whereas reviews on rare or long-term outcomes were based on observational studies.

Short-Term Adverse Events

Three systematic reviews on short-term adverse events were included (25, 26, 33). These reviews included only RCTs. Manzoli addressed all types of adverse events and all types of vaccines (26). Hauser (25) assessed the effects of adjuvants on mild adverse events, whereas Stassijsn (33) was limited to the effect of adjuvants on mild to serious adverse events in pediatric populations only. In general, direct meta-analysis comparing rates of adverse events for different vaccines, dosing regimens and adjuvants was challenging due to varying definitions of adverse events and types of events reported, and events frequently being reported as percentages only. According to Manzoli (26), the proportion of serious adverse events was low (0.018%, 3 cases amongst 16725 subjects, 18 RCTs), and no deaths were reported. They found a minor dose effect on local and systemic events for non-adjuvanted vaccines (based on 6 studies where one dose was used, and 6-7 studies where two doses were used), whereas this was not found for adjuvanted vaccines (one study), but data was scarce.

TABLE 3 | Overview of included systematic reviews on H1N1pdm09 vaccines according to outcome.

OUTCOME	Reference	Total number of studies included[a]	Type of study	Meta-analyses by vaccine type (adjuvants yes/no)	Date of search
Short term adverse events (mild/mod/serious)					
All types	Manzoli, (26)	18	RCT	Yes	Apr. 2011
Effect of adjuvants, pediatric (all types)	Stassijns, [b] (33)	8	RCT	Yes	Apr. 2015
Effect of adjuvants, pediatric/adults (mild only)	Hauser, (25)	22[c]	RCT	Yes	Sep. 2018
Narcolepsy	Sarkanen, (32)	11	Observational studies	Yes	Nov. 2016
	Demicheli, (20)	4		No	Dec. 2016
Guillain-Barré syndrome (GBS)	Sanz Fadrique, [d] (31)	2	Observational studies	No	Jul. 2017
	Martin Aries, (27)	16		Yes	Apr. 2014
	Demicheli, (20)	2		No	Dec. 2016
	Wachira, (34)	15		No	Jun. 2017
Inflammatory bowel disease (IBD)	Pineton, (29)	1	Observational study	NA	Jun. 2014
Demyelinating diseases	Demicheli, (20)	1	Observational study	NA	Dec. 2016
Pregnancy- and fetal outcomes and offspring					
Adverse events in pregnancy (local, systemic, preeclampsia); congenital malformation; spontaneous abortion; still birth; preterm birth; small for gestational age (SGA); low birth weight	McMillan, (21)	17	Observational studies	No	Mar. 2014
Preterm birth; late fetal death; any fetal death	Fell, (22)	12	Observational studies	No	May 2013
Preterm birth; SGA; low birth weight	Nunes, (28)	13	Observational studies	No	Jun. 2015
Congenital malformation	Polyzos, (30)	12	Observational studies	No	Dec. 2014
Spontaneous abortion; fetal death; stillbirth; preterm birth; congenital malformations; neonatal death	Demicheli, (20)	14	Observational studies	No	Dec. 2016
Congenital malformation; spontaneous abortion; still birth; preterm birth; SGA	Zhang, (35)	19	Observational studies	No	Jan. 2017
Congenital malformation; stillbirth/fetal death; SGA; low birth weight	Giles, (24)	9	Observational studies	Yes	May 2017
Early childhood health outcomes	Foo, (23)	6	Observational studies	No	Jul. 2019

[a]*studies from which data extraction on H1N1pdm09 vaccination was possible (i.e. not pooled with seasonal influenza vaccination). In systematic reviews covering more than one outcome, the number of studies may be lower for single outcomes.* [b]*studies also included in Hauser et al. (25).* [c]*unclear if all studies reported adverse events.* [d]*update of Martin Aries et al. (27).*

Aluminium containing vaccines were associated with an increased risk of local events compared to unadjuvanted vaccines (26) (**Supplementary Table 3**). In adults, the risk of local adverse events after vaccination with oil-in water adjuvant containing vaccines (AS03 or MF59) was higher compared to vaccination with unadjuvanted vaccines (25, 26). The increased risk was significantly higher for AS03 adjuvanted vaccines compared to MF59 adjuvanted vaccines, RR = 2.90 (95% CI 2.37-3.54) for AS03 and RR = 1.70 (95% CI 1.25-2.31) for MF59, subgroup difference p< 0.004 (25). No difference in risk associated with adjuvants was observed for systemic events (fever). The data was more limited in children. In Stassijns (33), 29 trials encompassing more than 25 000 children were included, but only four trials included information on AS03, and four trials included information on MF59. No overall increase in serious adverse events was seen in the AS03 trials nor in MF59 trials for children, and no overall increase in solicited or unsolicited AEFIs was found (33). Local pain was reported with rates between 31.7-84.6% for AS03 adjuvanted vaccines, and 1.0-59% for MF59 adjuvanted vaccines (33). Hauser reported a possible increase in local adverse events with MF59 adjuvanted vaccines in children but had no information on AS03 adjuvanted pandemic vaccine. The Hauser review (25) was assessed to high quality, the Manzoli review (26) to moderate and the Stassijns review (33) to low quality (**Table 2**).

Narcolepsy

Two systematic reviews on narcolepsy was included. The systematic review by Sarkanen included 29 studies (32). Only 11 studies, all on Pandemrix, were included in the meta-analysis. The analyses were performed separately for children/adolescents summarized from nine studies: Finland, France, Ireland, the Netherlands, Norway, Sweden and the UK. For adults, the meta-analysisadults included 5 studies: Finland, France, Ireland, Sweden and the UK. The analysis was specified for three different proxy dates for onset of disease (index dates). The studies included 376 narcolepsy cases and 5.1 million subjects/person years in vaccinated children/adolescents; 95 narcolepsy cases and 11.3 million subjects/person years in unvaccinated children/adolescents; 133 narcolepsy cases and 9.0 million subjects/person years in vaccinated adults; and 59 narcolepsy cases and 12.1 million subjects/person years in unvaccinated adults. Increased risk of narcolepsy type 1 after vaccination with Pandemrix was found in children/adolescents for all index dates. In the meta-analysis the overall RRs were 14.3 (95% CI 8.9-23.0), 9.7 (95% CI 4.9- 19.2), and 5.0 (95% CI 3.4-7.5) for onset of symptoms, first healthcare contact, and diagnosis, respectively (**Table 4**). Based on studies included in the meta-analysis, the attributable risk one year after vaccination was 1 case per 18 400 vaccine doses (95% CI 1 per 16 700 to 1 per 20 400) in children/adolescents (based on 5 studies) and 1 case per 181 000 vaccine

TABLE 4 | Systematic review of vaccination with Pandemrix and risk of narcolepsy.

	Children and adolescents			Adults		
	Number of studies	Effect size (95% CI)	I^2	Number of studies	Effect size (95% CI)	I^2
Index date[a]						
Onset date	6	14.32 (8.92, 22.99)	0.0%	3	7.01 (3.40, 14.46)	0.0%
Healthcare contact	3	9.68 (4.88, 19.23)	44.1%	3	8.08 (3.86, 16.89)	0.0%
Diagnosis	5	5.02 (3.36, 7.51)	0.0%	4	2.95 (1.88, 4.62)	0.0%

[a]*Exact date of symptom onset is difficult to remember and prone to recall bias. The studies used different index dates as proxy of disease onset. Some studies are included in analyses of more than one index date.*

doses (95% CI 1 per 141 000 to 1 per 254 000) in adults (based on 3 studies). Increased risk of narcolepsy type 1 was also observed in adults, although the association was not as strong as in children/adolescents, overall RRs were 7.0 (95% CI 3.4-14.5), 8.1 (95% CI 3.9-16.9), and 3.0 (95% CI 1.9-4.62) for onset of symptoms, first healthcare contact, and diagnosis, respectively. The heterogeneity between studies was generally very low.

Narcolepsy incidence was not increased in countries where other H1N1pdm09 vaccines than Pandemrix were used: South Korea, US and Canada (Ontario). In Quebec, Canada, where AS03-adjuvanted Arepanrix vaccine was used, RR 16 weeks after vaccination was 1.48 -4.32 based on different study designs. The vaccine attributable risk was only 1 per 1,000,000, which is significantly lower than in European studies. In a qualitative synthesis of 12 studies, the authors did not find evidence of increased risk of narcolepsy after vaccination with non-Pandemrix H1N1pdm09 vaccines, including Arepanrix (AS03-adjuvanted) and MF59 adjuvanted vaccines. The authors also reported some evidence of rising incidence of narcolepsy in relation to H1N1pdm09 infection, referring to studies from the Beijing and Shanghai area with a 3-fold increase in narcolepsy incidence 3-6 months after the pandemic peak in a largely unvaccinated population. The Sarkanen review (32) was assessed to moderate quality (**Table 2**).

The Cochrane systematic review by Demicheli (20) only provided a brief description of 4 studies (2 of which had overlapping datasets) on narcolepsy following pandemic vaccination, together with other neurological and autoimmune diseases, confirming the increased risk in children. These studies were from Finland, France and Ireland and were also covered by Sarkanan (32). The Cochrane review was assessed to high quality (**Table 2**).

Guillain-Barré Syndrome (GBS)

GBS is an acute autoimmune disorder which attacks the nervous system. A meta-analysis from 2015 (27), an updated review from 2019 (31), a meta-analysis from 2018 (20) and a narrative systematic review from 2019 (34) were included. 16 studies were incorporated in the meta-analysis by Martin, Arias (27) and an overall RR = 1.84 (95% CI 1.36-2.50) of GBS after pandemic vaccination was estimated. However, heterogeneity was high (I^2 = 64%) and only 7 of the 16 studies found a significantly increased risk. A funnel plot did not identify publication bias. Risk estimates were higher in meta-analysis based on self-controlled analyses compared to other study designs. The risk estimates of GBS after vaccination varied according to geographic region, although not significantly, estimates being higher in Australia and Taiwan (RR = 3.54, 95% CI 1.05-11.97), and lower in Europe (RR = 1.62, 95%CI 0.83-3.13). Estimates for adjuvanted vaccines and unadjuvanted vaccines compared to unvaccinated were similar RR = 1.97 (95%CI 1.22–3.17) and RR = 1.75 (95%CI 1.20–2.56). The estimates were based on 7 and 9 studies respectively. The updated review (31) only identified two new studies, one from South Korea which found a significant association (RR = 1.46, 95% CI 1.26-1.68), and a registry study from Norway which found no association after adjustment for influenza infection (HR = 1.1, 95% CI 0.51-2.43) (**Supplementary Table 4**). No updated meta-analysis was performed.

A newer systematic review by Wachira (34) identified 15 articles of which only two found a statistically significant association between H1N1pdm09 vaccines and GBS. Crude estimates from 10 primary studies were presented in a Forrest plot without a pooled estimate. There was a significant association (RR = 2.8 95% CI 1.3-6.0) in one of the studies, but according to the authors, this association disappeared when adjusted for influenza like illness, infections of the respiratory tract and other seasonal influenza vaccines (RR = 1.0. CI 95% 0.3-2.7). Wachira (34) only covered five of the studies included in the analysis of Martin Arias, thus 11 studies were not covered despite similar inclusion criteria with regards to study design (**Supplementary Table 4**).

The Cochrane review by Demicheli (20) from 2018 included two case control studies on H1N1pdm09 vaccination and GBS in general populations in a meta-analysis (**Supplementary Table 4**). In the crude analyses, the odds of GBS after vaccination was two-fold increased. However, the odds ratio was reduced after adjustment for pandemic influenza infection, other diseases and medication, indicating no increased risk (OR 0.92 (0.35-2.4). The studies of Martin Arias and Wachira were both assessed to moderate quality according to the AMSTAR-2 tool, while the Cochrane review by Demicheli (20) was assessed to high quality (**Table 2**).

Inflammatory Bowel Disease (IBD)

One systematic review that assessed risk of IBD after vaccination was included (29). Only one study on H1N1pdm09 vaccine (Pandemrix) was included in the review. Overall, people vaccinated with H1N1pdm09 vaccine did not have significantly higher risk of IBD compared to the unvaccinated, HR = 1.13 (95% CI 0.97-1.32). The Pineton review (29) was assessed to moderate quality (**Table 2**).

Demyelinating Diseases

One review (20) (high quality, **Table 2**) assessed the association between H1N1pdm09 vaccination and risk of demyelinating diseases. The review included only one study, and the presented OR was unadjusted, OR = 2.06 (95% CI 0.51-8.22). The study was conducted in individuals vaccinated with the MF59-adjuvanted H1N1pdm09 vaccine Focetria.

Fetal Outcomes

Seven systematic reviews on fetal outcomes, all based on observational studies were included (**Table 4**) (20–22, 24, 28, 30, 35). Three of the systematic reviews were assessed to high quality (20–22), while the others were assessed to moderate quality (24, 28, 30, 35) (**Table 2**). The reviews provided evidence on the outcomes congenital malformations, spontaneous abortion, stillbirth/fetal death, preterm birth, small for gestational age birth (SGA), and low birth weight (LBW). Not all systematic reviews included all outcomes. A list of included primary studies for each outcome is provided in **Supplementary Table 5**. All the systematic reviews compared vaccinated/exposed individuals to unvaccinated/unexposed individuals. Some of the systematic reviews included studies with both H1N1pdm09 monovalent vaccine and seasonal vaccines, but only the results from studies with H1N1pdm09 vaccines (both adjuvanted and non-adjuvanted) were included here.

Estimates from five systematic reviews on congenital malformations were all close to one (**Table 5**) (20, 21, 24, 30, 35). Only one review found a significant association (OR = 1.14 (95% CI 1.01-1.29) (35), while three other reviews found no significant association with vaccination (OR = 1.02 (95% CI 0.91-1.17) (30), (OR = 1.11 (95% CI 0.99- 1.29) (20) and OR = 1.03 (95% CI 0.99, 1.07) (24). The last review also suggested no association (no pooled estimate) (21). Only two primary studies were included in all five systematic reviews (**Supplementary Table 5**).

Two reviews explored the relationship between maternal H1N1pdm09 vaccination and spontaneous abortion (21, 35) (**Table 5**). Neither review found any association between maternal H1N1pdm09 vaccination (any trimester) and spontaneous abortion. Only Zhang et al. presented a pooled estimate [OR 1.04 (95% CI 0.72-1.52)] for spontaneous abortion prior to gestational week 22 (35).

Five systematic reviews on stillbirth/fetal death/abortion were included (20–22, 24, 35) (**Table 5**). Two concluded there was no evidence of increased risk of preterm birth after H1N1pdm09 vaccination, but the studies were too heterogeneous to be pooled (21, 22). Three other systematic reviews performed meta-analyses (20, 24, 35). All found effect estimates below one, consistent with no increased risk of fetal death following maternal H1N1pdm09 vaccination.

The six systematic reviews on preterm birth found no evidence that maternal H1N1pdm09 vaccination was associated with an increase in preterm birth in any trimester (20–22, 24, 28, 35) (**Table 5**). In five of the reviews, estimates for vaccination in any trimester were below one. In three of these, confidence intervals included one (21, 24, 35). One review did not perform a meta-analysis (22). One review included an estimate for very preterm birth (21) (**Table 5**).

There was consistent evidence of no increased risk of SGA after maternal H1N1pdm09 vaccination in any trimester, reported in four systematic reviews (21, 24, 28, 35) (**Table 5**). Three reviews with meta-analyses found no association (24, 28, 35). The last review suggested a very small protective effect for the vaccine on SGA birth when pooling two studies (21).

Three reviews evaluated the relationship between H1N1pdm09 vaccination and LBW (21, 24, 28) (**Table 5**). There was no association in meta-analyses that included studies of vaccination in any trimester (21), in the second and third trimester combined (24), or in the first trimester (24). One review observed a lower rate of LBW after maternal H1N1pdm09 vaccination, although the confidence interval was wide (28).

One review (24) did a separate analysis for adjuvanted H1N1pdm09 vaccines. The estimates for SGA, LBW, preterm birth and congenital abnormalities were all around 1 with confidence intervals that included 1. These estimates were similar to the estimates combining both adjuvanted and unadjuvanted vaccines.

Only the Cochrane review addressed neonatal death (20). The review was based on two studies and suggested that pandemic vaccine during pregnancy was not associated with an increased risk of neonatal death OR = 1.09 (95% CI 0.4-2.95).

In a narrative systematic review based on five cohort studies, no significant association was found between pandemic vaccination and preeclampsia (21).

Long Term Effects in Children Following Maternal H1N1pdm09 Vaccination

A narrative systematic review by Foo et al. (23) was the only review concerning long-term effects of H1N1pdm09 vaccination during pregnancy on early childhood health outcomes. The review identified six primary studies which assessed the effect on influenza infections, primary infections only, childhood mortality up to the age of 5, and two registry studies assessing the effect on infections, hospitalisations, and general diseases and syndromes. No association between maternal vaccination and adverse health outcomes in early childhood were identified. The review was assessed to high quality (**Table 2**).

DISCUSSION

Overall, 16 systematic reviews on adverse events following vaccination with monovalent H1N1pdm09 vaccines were included. According to the AMSTAR 2 assessment tool, five of the systematic reviews were considered high quality (20–23, 25), two were considered low quality (31, 33). The rest were considered moderate quality.

Overall, the risk of short term serious adverse events was low following H1N1pdm09 vaccination. In clinical trials, adjuvanted vaccines had more local, but not more serious adverse events compared to unadjuvanted vaccines. Vaccination with Pandemrix

TABLE 5 | Adjusted estimates for fetal outcomes after maternal H1N1pdm09 vaccination.

Outcome/ Systematic review	Vaccine adminstrated	Congenital malformations			Spontaneous abortion			Stillbirth/Fetal death/Abortion			Preterm delivery (< 37 weeks)			Small for gestational age birth (SGA)			Low birth weight (LBW)		
		Studies	Effect size (95% CI)	I^2	Studies	Effect size (95% CI)	I^2	Studies	Effect size (95% CI)	I^2	Studies	Effect size (95% CI)	I^2	Studies	Effect size (95% CI)	I^2	Studies	Effect size (95% CI)	I^2
Fell (22)	*Any trimester*							3	Range 0.56-0.79[a] Range 0.89-1.23[ab] Range 0.44-0.77[ac]		10	No association[a]							
McMillan (21)	*Any trimester*	7	No association[a]		5	No association[a]		9	No pooled estimate		6	OR = 0.93 (0.83-1.04)	59%	2	OR = 0.91 (0.87-0.96)	0%	6	OR = 0.94 (0.82-1.08)	39%
											3	HR = 1.00 (0.93-1.07)[d]	0%						
	Any trimester										2	OR = 0.79 (0.61-1.01)[e]	19%						
Polyzos (30)	*Any trimester*	10	OR = 1.02 (0.91-1.14)																
	First trimester	6	OR = 1.02 (0.89-1.17)																
Nunes (28)	*Any trimester*										9	OR = 0.90 (0.82-0.99)	72%	6	OR = 0.98 (0.91-1.07)	54%	7	OR = 0.88 (0.79-0.98)	62%
Zhang (35)	*Any trimester*	6	OR = 1.14 (1.01-1.29)	0%	3	OR = 1.04 (0.72-1.52)	0%	10	OR = 0.80 (0.69-0.92)	8%	12	RR = 0.92 (0.84-1.01)	68%	7	OR = 0.98 (0.91-1.06)	45%			
	First trimester	2	OR = 1.07 (0.59-1.94)	0%															
Demicheli (20)	*Any trimester*	6	OR = 1.11 (0.99-1.23)	0%				5	OR = 0.75 (0.62-0.90)[f]	0%	7	OR = 0.84 (0.76-0.93)	71%						
								3	HR = 0.81 (0.63-1.04)[df]	0%	2	HR = 1.11[d] (0.46-2.68)	59%						
	Second/third trimester										2	OR = 1.08 (0.92-1.28)	0%						
	First trimester										2	OR = 0.96 (0.87-1.90)	0%						
Giles (24)	*Any trimester*	7	OR = 1.03 (0.99-1.07)	0%				3	OR = 0.84 (0.65-1.08)	0%									
	Second/third trimester	1	HR = 0.96 (0.29-3.12)								3	OR = 0.96 (0.87-1.06)	0%	3	OR = 0.96 (0.89-1.04)	0%	2	OR = 0.97 (0.71-1.32)	83%
	First trimester	1	HR = 1.32 (0.78-2.21)								2	OR = 1.08 (0.92-1.28)	0%				2	OR = 1.00 (0.80-1.24)	0%

[a]no pooled estimate, and no I^2 [b]late fetal death [c]early fetal death [d]separate analysis on time metric and calculated HR [e]<32 weeks [f]abortion included spontaneous, internal, foetal death and stillbirth.

was strongly associated with narcolepsy, particularly in children. For GBS, the findings from the systematic reviews were inconsistent. Two other outcomes identified in the systematic reviews were IBD (29) and demyelinating diseases (20). For these outcomes, the estimates were based on only one primary study, thus no conclusions could be drawn.

Almost half of the systematic reviews covered fetal outcomes after maternal vaccination (20–22, 24, 28, 30, 35), and in general indicated no increased risk of adverse pregnancy outcomes. Furthermore, studies did not reveal any adverse effect of maternal H1N1pdm09 vaccination on childhood health outcome during the first 5 years of life (23).

Adverse Events by Vaccine and Adjuvants

All included reviews based on RCTs performed meta-analyses according to vaccine type/adjuvants. Among reviews based on observational studies, only three performed meta-analyses according to vaccine type/adjuvants (24, 27, 32). However, several of the reviews included tables of included primary studies with information on vaccine type (24, 30, 35). For rare events like GBS or adverse pregnancy outcomes (fetal death, SGA, LBW, premature birth or spontaneous abortion), no differences were reported according to adjuvanted or non-adjuvanted pandemic vaccines, or type of adjuvant (MF59, AS03) in any of the included reviews. Increased risk of narcolepsy was only seen following vaccination with the AS03-adjuvanted vaccine Pandemrix, however not for the AS03-adjuvanted vaccine Arepanrix, as discussed below.

Narcolepsy

Although the absolute numbers of children and young adults developing narcolepsy type 1 were limited to around 400 reported cases across the included studies. In Europe, H1N1pdm09 vaccination with Pandemrix was consistently associated with an increased risk of narcolepsy (32). During the first year after vaccination, the relative risk of narcolepsy was increased 5 to 14-fold in children and adolescents and 2 to 7-fold in adults. The vaccine attributable risk in children and adolescents was around 1 per 18,400 vaccine doses and 1 per 181, 000 in adults. The risk was limited to vaccination with the Pandemrix vaccine only and was only found for narcolepsy type 1. Follow-up time in the included studies was up to approximately two years, and onset of symptoms occurred most often during the first three to six months following vaccination. The Cochrane systematic review by Demicheli (20) only provided information from studies also covered by Sarkanan (32). Narcolepsy incidence was not increased in countries where other H1N1pdm09 vaccines than Pandemrix were used: South Korea, US and Canada (Ontario). In Quebec, Canada, where AS03-adjuvanted Arepanrix vaccine was used, the vaccine attributable risk was only 1 per 1,000,000, which is significantly lower and not comparable to the large excess risks demonstrated in European studies. According to the authors, it cannot completely be ruled out that this finding may be due to a confounding effect of H1N1pdm09 influenza infection (36).

Increased incidence of narcolepsy in absence of pandemic vaccination was reported from Beijing and Shanghai following the pandemic peak (37, 38). The incidence decreased back to baseline two years after the H1N1 pandemic, suggesting that infection with the 2009 H1N1 strain was associated with narcolepsy onset. In many countries, the vaccination campaigns coincided with the pandemic peak, thus dual exposure to pandemic influenza infection and vaccine was likely. Also, in Germany the incidence of narcolepsy increased threefold starting in spring 2009, although the overall pandemic vaccine coverage was only 4-8%. Thus, a role also for natural H1N1pdm09 infection in the development of narcolepsy is possible. Moreover, a combined effect of simultaneous exposure to H1N1pdm09 infection and vaccination on the risk of narcolepsy cannot be ruled out, since mass vaccination campaigns coincided with the pandemic peak in some countries (13). Confounding by natural H1N1pdm09 infection was briefly discussed by the authors of the systematic review. Increased risk of narcolepsy was only seen following vaccination with the AS03-adjuvanted vaccine Pandemrix. However, no clear increased risk was reported after vaccination with the AS03 adjuvanted vaccine, Arepanrix, which was made by the same vaccine producer, but at another production facility (32, 39). This observation lends support to the recent hypothesis of molecular mimicry of a specific configuration of the vaccine antigen (40) as a potential causal factor in the development of narcolepsy, rather than the AS03 adjuvant (41).

Guillain-Barré Syndrome (GBS)

One of the systematic reviews found a significant association between H1N1pdm09 vaccination and GBS (27) based on a pooled estimate of 16 studies, whereas another systematic review (34) found few primary studies supporting this finding. There was little overlap between the primary studies included, despite similar inclusion and exclusion criteria in terms of study design (cohort, case control, self-controlled case series and self- controlled risk interval design). However, the objective of Wachira's review was broader, and aimed at discovering any aetiological agents of GBS, and the searches were carried out in different databases (34). In contrast, Demicheli (20) only included two case control studies on GBS. The inclusion criteria were narrow and did not include self-controlled case series, which are commonly used for very rare outcomes, such as GBS. Demicheli (20) assessed the two studies as unclear risk of bias, whereas Wachira (34) gave the same studies a high rating, both according to the Newcastle Ottowa quality assessment Scale. The cohort studies included in Wachira (34) also gained high ratings, though the case series received somewhat lower ratings. These discrepancies illustrate how authors may emphasize certain factors over others when performing systematic reviews.

Wachira (34) explored all known infectious aetiological agents of GBS, reconfirming *Campylobacter jejuni* as one of the main triggers of GBS, in addition to other infections including influenza like illness (6/7 studies). Importantly, one study showed a strong association with H1N1pdm09 infection (HR = 4.22 95%CI 1.01-17.59) in contrast to pandemic vaccination in the same population, where no association was found (9). The review by Demicheli (20) found a two-fold increased risk of GBS in crude analyses. However, similar to

the findings of Wachira (34), the odds ratio was reduced after adjustment for pandemic influenza infection, indicating no increased risk. As the pandemic peak and vaccination campaign coincided in many countries, exposure to both influenza infection and vaccine was likely (13). Also, the epidemiology of gastrointestinal infections like *Campylobacter jejuni* may depend on population and setting, explaining the geographical differences in estimates (27). However, obtaining good data on infection is generally challenging for most study populations/settings and a difficult confounder to control for. Thus, lack of control for coincident infections might to some extent explain the lack of consistency in studies on influenza vaccines and risk of GBS, although other factors cannot be ruled out. Given that the systematic reviews on GBS had different approaches and inconsistent results, novel analysis would be beneficial for this outcome.

Pregnancy Outcomes

In general, no associations with H1N1pdm09 vaccination were found for any of the fetal outcomes assessed. Three of the seven reviews were considered high quality (20–22). Only one review performed sub-analysis according to adjuvated vaccine *versus* no vaccine (24) and did not find any difference in the risk of adverse pregnancy outcome. Early in the pandemic, pregnant women were identified as at high risk of serious complications (3). The WHO therefore recommended that pregnant women regardless of pregnancy length received the vaccine, and policies were widely adopted after 2009 pandemic (42). Consequently, there was an immediate need for knowledge on the safety of pandemic vaccines, especially on fetal outcomes, and these initial studies also formed part of evidence base for the safety of seasonal influenza vaccination. Nearly all the primary studies were conducted in high-income countries, and less is known on safety of maternal H1N1pdm09 vaccination in low- and middle-income countries. Small inconsistencies between the reviews were observed and may be attributable to the difference in inclusion of primary studies (**Supplementary Table 5**). The primary studies included in the reviews may also differ in terms of study design, baseline immunity to influenza, coincidence between vaccine and pandemic influenza season, or not considering immortal time bias. The systematic review on long-term effects of maternal H1N1pdm09 vaccination found no association between maternal vaccination and adverse health outcomes in early childhood (23). The authors of the systematic review concluded that this field is under-investigated.

Strengths and Limitations

Overviews of systematic reviews relating to the adverse effects of an intervention may allow commonalities to be drawn across a broader range of evidence than in a more focused systematic review, with the potential to highlight equivalence or patterns not previously identified (43). The suitability of reanalysis of existing data within an overview is debated. It has been argued that, where novel analyses are the aim, conducting a review of primary studies may be more appropriate than an overview of reviews (43). Using existing results of literature searches may nevertheless save time (44).

Even though systematic reviews increasingly try to consider all outcomes (both beneficial and harmful), data on adverse events may be more fragmented and incomplete, and given more cursory treatment than efficacy/effectiveness data. The decision to perform meta-analysis on included studies can differ between systematic reviews (45), due to different approaches often described as 'lumping' or 'splitting' of information. Lumping refers to finding commonalities across different approaches, whereas splitting creates a more narrowly refined focus within a broader research field (43). Such decisions require both sufficient knowledge of the subject area, both for exposures and outcomes, which often represent different specialities, as well as competence in the methodology of systematic reviews and meta-analysis. This was apparent both for GBS and for the pregnancy outcomes, whereby the systematic reviews seemed to provide different justifications for or against meta-analysis (for e.g. degree of heterogeneity).

A limitation of our systematic review is that we may not have identified all the systematic reviews covering safety outcomes in our search result. This may especially be true for reviews including studies that are primarily designed to address vaccine efficacy/effectiveness, with additional short- term safety data.

Future Challenges

Mass vaccination against the H1N1pdm09 pandemic illustrated that rare, unexpected adverse events can occur, which are almost impossible to predict. Clinical trials are not powered to assess rare or long-term events due to the urgent need for prevention. In practice, rare and/or long-term events will therefore not be detected until mass vaccination is carried out through post-marketing surveillance and well-designed observational studies with comparison groups are conducted. Furthermore, as was the case during the 2009 pandemic, H1N1pdm09 virus circulation and vaccination coincided, and hence it is difficult to disentangle the effects of infection from vaccination, or indeed the effect of dual exposure (9, 13, 38, 44). In hindsight, the H1N1 2009 pandemic was less severe than anticipated, and subsequently led to an adaptation of the WHO pandemic phases to ensure disease severity was incorporated in the pandemic criteria – in addition to incidence of disease (46). In contrast, the current SARS-CoV-2 pandemic has been associated with a significantly higher disease burden and the risk willingness for vaccination may be higher. This will likely affect vaccine uptake.

Relevance in Current and Future Pandemics/Epidemics

In the event of new pandemics, caused by influenza or other agents, novel vaccines will be developed. In a pandemic situation with new vaccines it will be impossible to foresee new serious adverse events. Careful evaluation of the short- and long-term effects of both the infection itself, as well as the vaccine used for prevention, should be performed. This is highly actualized in the COVID-19 pandemic where long-term consequences of COVID-19 infection is becoming evident (47) and mass vaccination campaigns with vaccines based on new technologies have been rolled out (48, 49) where case reports

on serious hematological adverse events have been published for difference vaccines (50–52).

In terms of surveillance and epidemiological studies on safety of pandemic vaccination there are lessons to be learnt from the 2009 H1N1 pandemic. Causality assessment of AEFIs should firstly be performed at the population level, to establish if there is a causal association between the use of a vaccine and a particular AEFI in the population. In the evaluation of individual AEFI case reports, population-based evidence should be reviewed, and a logical deduction performed to determine whether an AEFI in a specific individual is causally related to the use of the vaccine (8). Furthermore, ensuring sufficient data-collection on all relevant outcomes and exposures including both pandemic infection and vaccination, with appropriate control groups is crucial.

CONCLUSION

Twelve years after the 2009 H1N1 pandemic, adverse events following administration of the H1N1pdm09 vaccines have been rigorously studied. Adjuvanted vaccines had more local, but not serious, adverse events compared to unadjuvanted vaccines. Vaccination with Pandemrix was consistently associated with narcolepsy, particularly in children. Although Pandemrix was an adjuvanted vaccine, molecular mimicry of a specific configuration of the vaccine antigen has been suggested as a potential causal factor in the development of narcolepsy, rather than the AS03 adjuvant. Pregnant women were at increased risk of severe influenza illness and adverse pregnancy outcomes, however there is no evidence of adverse effects in mothers nor children following H1N1pdm09 vaccination in pregnancy. The findings on GBS were inconclusive. In conclusion, the risk benefit of the H1N1pdm09 vaccines appear favorable.

DATA AVAILABILITY STATEMENT

The original contributions presented in the study are included in the article/**Supplementary Material**. Further inquiries can be directed to the corresponding author.

AUTHOR CONTRIBUTIONS

All the authors contributed with selection and assessment of the included systematic reviews, in addition to writing and completed the manuscript. All authors contributed to the article and approved the submitted version.

FUNDING

The Norwegian Institute of Public Health funded this study.

ACKNOWLEDGMENTS

The authors wish to thank Kjersti M. Rydland and Atle Fretheim, the Norwegian Institute of Public Health, and Christian Syvertsen, the Norwegian Medicines Agency for valuable input to the study protocol, and Ragnhild A. Tornes and Trude A. Muggerud for conducting the literature search.

SUPPLEMENTARY MATERIAL

The Supplementary Material for this article can be found online at: https://www.frontiersin.org/articles/10.3389/fimmu.2021.740048/full#supplementary-material

REFERENCES

1. 2009 H1N1 Pandemic (H1N1pdm09 virus). *Centers for Disease Control and Prevention (CDC)* . Available at: https://www.cdc.gov/flu/pandemic-resources/2009-h1n1-pandemic.html (Accessed June 30, 2021).
2. Iuliano AD, Roguski KM, Chang HH, Muscatello DJ, Palekar R, Tempia S, et al. Estimates of Global Seasonal Influenza-Associated Respiratory Mortality: A Modelling Study. *Lancet* (2018) 391:1285–300. doi: 10.1016/S0140-6736(17)33293-2
3. The ANZIC Influenza Investigators and Australasian Maternity Outcomes Surveillance System. Critical Illness Due to 2009 A/H1N1 Influenza in Pregnant and Postpartum Women: Population Based Cohort Study. *BMJ* (2010) 340:c1279. doi: 10.1136/bmj.c1279
4. WHO. New Data on Narcolepsy Following the 2009 Pandemic Influenza Vaccine, in: *The Global Advisory Comittee of Vaccine Safety* (2017). Available at: https://www.who.int/groups/global-advisory-committee-on-vaccine-safety/topics/influenza-vaccines/h1n1-vaccines (Accessed June 30, 2021).
5. Kurz X, Domergue F, Slattery J, Segec A, Szmigiel A, Hidalgo-Simon A. Safety Monitoring of Influenza A/H1N1 Pandemic Vaccines in EudraVigilance. *Vaccine* (2011) 29:4378–87. doi: 10.1016/j.vaccine.2011.04.005
6. Lansbury LE, Smith S, Beyer W, Karamehic E, Pasic-Juhas E, Sikira H, et al. Effectiveness of 2009 Pandemic Influenza A(H1N1) Vaccines: A Systematic Review and Meta-Analysis. *Vaccine* (2017) 35:1996–2006. doi: 10.1016/j.vaccine.2017.02.059
7. Gil Cuesta J, Aavitsland P, Englund H, Gudlaugsson Ó, Hauge SH, Lyytikäinen O, et al. Pandemic Vaccination Strategies and Influenza Severe Outcomes During the Influenza A(H1N1)pdm09 Pandemic and the Post-Pandemic Influenza Season: The Nordic Experience. *Euro Surveill* (2016) 21 (16):pii=30208. doi: 10.2807/1560-7917.ES.2016.21.16.30208
8. World Health Organization. *Causality Assessment of an Adverse Event Following Immunization (AEFI): User Manual for the Revised WHO Classification 2nd Ed., 2019 Update*. Geneva: World Health Organization (2019). Licence: CC BY-NC-SA 3.0 IGO. https://apps.who.int/iris/handle/10665/340802.
9. Ghaderi S, Gunnes N, Bakken IJ, Magnus P, Trogstad L, Håberg SE. Risk of Guillain-Barré Syndrome After Exposure to Pandemic Influenza A (H1N1)pdm09 Vaccination or Infection: A Norwegian Population-Based Cohort Study. *Eur J Epidemiol* (2016) 31:67–72. doi: 10.1007/s10654-015-0047-0
10. Magnus P, Gunnes N, Tveito K, Bakken IJ, Ghaderi S, Stoltenberg C, et al. Chronic Fatigue Syndrome/Myalgic Encephalomyelitis (CFS/ME) is Associated With Pandemic Influenza Infection, But Not With an Adjuvanted Pandemic Influenza Vaccine. *Vaccine* (2015) 33:6173–7. doi: 10.1016/j.vaccine.2015.10.018
11. Nohynek H, Jokinen J, Partinen M, Vaarala O, Kirjavainen T, Sundman J, et al. AS03 Adjuvanted AH1N1 Vaccine Associated With an Abrupt Increase in the Incidence of Childhood Narcolepsy in Finland. *PloS One* (2012) 7: e33536. doi: 10.1371/journal.pone.0033536

12. Szakacs A, Darin N, Hallbook T. Increased Childhood Incidence of Narcolepsy in Western Sweden After H1N1 Influenza Vaccination. *Neurology* (2013) 80:1315–21. doi: 10.1212/WNL.0b013e31828ab26f
13. Trogstad L, Bakken IJ, Gunnes N, Ghaderi S, Stoltenberg C, Magnus P, et al. Narcolepsy and Hypersomnia in Norwegian Children and Young Adults Following the Influenza A(H1N1) 2009 Pandemic. *Vaccine* (2017) 35:1879–85. doi: 10.1016/j.vaccine.2017.02.053
14. Miller E, Andrews N, Stellitano L, Stowe J, Winstone AM, Shneerson J, et al. Risk of Narcolepsy in Children and Young People Receiving AS03 Adjuvanted Pandemic A/H1N1 2009 Influenza Vaccine: Retrospective Analysis. *BMJ* (2013) 346:f794. doi: 10.1136/bmj.f794
15. Dieleman J, Romio S, Johansen K, Weibel D, Bonhoeffer J, Sturkenboom M. Guillain-Barre Syndrome and Adjuvanted Pandemic Influenza A (H1N1) 2009 Vaccine: Multinational Case-Control Study in Europe. *BMJ* (2011) 343: d3908. doi: 10.1136/bmj.d3908
16. Moher D, Shamseer L, Clarke M, Ghersi D, Liberati A, Petticrew M, et al. Preferred Reporting Items for Systematic Review and Meta-Analysis Protocols (PRISMA-P) 2015 Statement. *Syst Rev* (2015) 4:1. doi: 10.1186/2046-4053-4-1
17. Shamseer L, Moher D, Clarke M, Ghersi D, Liberati A, Petticrew M, et al. Preferred Reporting Items for Systematic Review and Meta-Analysis Protocols (PRISMA-P) 2015: Elaboration and Explanation. *BMJ* (2015) 350:g7647. doi: 10.1136/bmj.g7647
18. *Rayyan* . Available at: https://www.rayyan.ai/ (Accessed June 30, 2021).
19. Shea BJ, Reeves BC, Wells G, Thuku M, Hamel C, Moran J, et al. AMSTAR 2: A Critical Appraisal Tool for Systematic Reviews That Include Randomised or non-Randomised Studies of Healthcare Interventions, or Both. *BMJ* (2017) 358:j4008. doi: 10.1136/bmj.j4008
20. Demicheli V, Jefferson T, Di Pietrantonj C, Ferroni E, Thorning S, Thomas RE, et al. Vaccines for Preventing Influenza in the Elderly. *Cochrane Database Syst Rev* (2018) 2:Cd004876. doi: 10.1002/14651858.CD004876.pub4
21. McMillan M, Kralik D, Porritt K, Marshall H. Influenza Vaccination During Pregnancy: A Systematic Review of Effectiveness and Safety. *JBI Database Syst Rev Implement Rep* (2014) 12:281–381. doi: 10.11124/jbisrir-2014-1269
22. Fell DB, Platt RW, Lanes A, Wilson K, Kaufman JS, Basso O, et al. Fetal Death and Preterm Birth Associated With Maternal Influenza Vaccination: Systematic Review. *Bjog* (2015) 122:17–26. doi: 10.1111/1471-0528.12977
23. Foo DYP, Sarna M, Pereira G, Moore HC, Fell DB, Regan AK. Early Childhood Health Outcomes Following *In Utero* Exposure to Influenza Vaccines: A Systematic Review. *Pediatrics* (2020) 146. doi: 10.1542/peds.2020-0375
24. Giles ML, Krishnaswamy S, Macartney K, Cheng A. The Safety of Inactivated Influenza Vaccines in Pregnancy for Birth Outcomes: A Systematic Review. *Hum Vaccin Immunother* (2019) 15(3):687–99. doi: 10.1080/21645515.2018.1540807
25. Hauser MI, Muscatello DJ, Soh ACY, Dwyer DE, Turner RM. An Indirect Comparison Meta-Analysis of AS03 and MF59 Adjuvants in Pandemic Influenza A(H1N1)pdm09 Vaccines. *Vaccine* (2019) 37:4246–55. doi: 10.1016/j.vaccine.2019.06.039
26. Manzoli L, De Vito C, Salanti G, D'Addario M, Villari P, Ioannidis JP. Meta-Analysis of the Immunogenicity and Tolerability of Pandemic Influenza A 2009 (H1N1) Vaccines. *PloS One* (2011) 6:e24384. doi: 10.1371/journal.pone.0024384
27. Martin Arias LH, Sanz R, Sainz M, Treceno C, Carvajal A. Guillain-Barre Syndrome and Influenza Vaccines: A Meta-Analysis. *Vaccine* (2015) 33:3773–8. doi: 10.1016/j.vaccine.2015.05.013
28. Nunes MC, Aqil AR, Omer SB, Madhi SA. The Effects of Influenza Vaccination During Pregnancy on Birth Outcomes: A Systematic Review and Meta-Analysis. *Am J Perinatol* (2016) 33:1104–14. doi: 10.1055/s-0036-1586101
29. Pineton de Chambrun G, Dauchet L, Gower-Rousseau C, Cortot A, Colombel JF, Peyrin-Biroulet L. Vaccination and Risk for Developing Inflammatory Bowel Disease: A Meta-Analysis of Case-Control and Cohort Studies. *Clin Gastroenterol Hepatol* (2015) 13:1405–15. doi: 10.1016/j.cgh.2015.04.179
30. Polyzos KA, Konstantelias AA, Pitsa CE, Falagas ME. Maternal Influenza Vaccination and Risk for Congenital Malformations a Systematic Review and Meta-Analysis. *Obstet Gynecol* (2015) 126:1075–84. doi: 10.1097/AOG.0000000000001068
31. Sanz Fadrique R, Martin Arias L, Molina-Guarneros JA, Jimeno Bulnes N, Garcia Ortega P. Guillain-Barre Syndrome and Influenza Vaccines: Current Evidence. *Rev Esp Quimioter* (2019) 32:288–95.
32. Sarkanen TO, Alakuijala APE, Dauvilliers YA, Partinen MM. Incidence of Narcolepsy After H1N1 Influenza and Vaccinations: Systematic Review and Meta-Analysis. *Sleep Med Rev* (2018) 38:177–86. doi: 10.1016/j.smrv.2017.06.006
33. Stassijns J, Bollaerts K, Baay M, Verstraeten T. A Systematic Review and Meta-Analysis on the Safety of Newly Adjuvanted Vaccines Among Children. *Vaccine* (2016) 34:714–22. doi: 10.1016/j.vaccine.2015.12.024
34. Wachira VK, Peixoto HM, Oliveira MRF, de Oliveira MRF. Systematic Review of Factors Associated With the Development of Guillain-Barré Syndrome 2007-2017: What has Changed? *Trop Med Int Health* (2019) 24:132–42. doi: 10.1111/tmi.13181
35. Zhang C, Wang X, Liu D, Zhang L, Sun X. A Systematic Review and Meta-Analysis of Fetal Outcomes Following the Administration of Influenza A/H1N1 Vaccination During Pregnancy. *Int J Gynaecol Obstet* (2018) 141:141–50. doi: 10.1002/ijgo.12394
36. Montplaisir J, Petit D, Quinn MJ, Ouakki M, Deceuninck G, Desautels A, et al. Risk of Narcolepsy Associated With Inactivated Adjuvanted (AS03) A/H1N1 (2009) Pandemic Influenza Vaccine in Quebec. *PloS One* (2014) 9:e108489. doi: 10.1371/journal.pone.0108489
37. Han F, Lin L, Li J, Dong XS, Mignot E. Decreased Incidence of Childhood Narcolepsy 2 Years After the 2009 H1N1 Winter Flu Pandemic. *Ann Neurol* (2013) 73:560. doi: 10.1002/ana.23799
38. Han F, Lin L, Warby SC, Faraco J, Li J, Dong SX, et al. Narcolepsy Onset is Seasonal and Increased Following the 2009 H1N1 Pandemic in China. *Ann Neurol* (2011) 70:410–7. doi: 10.1002/ana.22587
39. Jacob L, Leib R, Ollila HM, Bonvalet M, Adams CM, Mignot E. Comparison of Pandemrix and Arepanrix, Two Ph1n1 AS03-Adjuvanted Vaccines Differentially Associated With Narcolepsy Development. *Brain Behav Immun* (2015) 47:44–57. doi: 10.1016/j.bbi.2014.11.004
40. Luo G, Ambati A, Lin L, Bonvalet M, Partinen M, Ji X, et al. Autoimmunity to Hypocretin and Molecular Mimicry to Flu in Type 1 Narcolepsy. *Proc Natl Acad Sci USA* (2018) 115:E12323–e12332. doi: 10.1073/pnas.1818150116
41. Vaarala O, Vuorela A, Partinen M, Baumann M, Freitag TL, Meri S, et al. Antigenic Differences Between AS03 Adjuvanted Influenza A (H1N1) Pandemic Vaccines: Implications for Pandemrix-Associated Narcolepsy Risk. *PloS One* (2014) 9:e114361. doi: 10.1371/journal.pone.0114361
42. Pandemic Influenza A (H1N1) 2009 Virus Vaccine - Conclusions and Recommendations From the October 2009 Meeting of the Immunization Strategic Advisory Group of Experts. *Wkly Epidemiol Rec* (2009) 84:505–8 https://www.who.int/wer/2009/wer8449.pdf.
43. Hunt H, Pollock A, Campbell P, Estcourt L, Brunton G. An Introduction to Overviews of Reviews: Planning a Relevant Research Question and Objective for an Overview. *Syst Rev* (2018) 7:39. doi: 10.1186/s13643-018-0695-8
44. Harder T, Remschmidt C, Haller S, Eckmanns T, Wichmann O. Use of Existing Systematic Reviews for Evidence Assessments in Infectious Disease Prevention: A Comparative Case Study. *Syst Rev* (2016) 5:171. doi: 10.1186/s13643-016-0347-9
45. Zorzela L, Loke YK, Ioannidis JP, Golder S, Santaguida P, Altman DG, et al. PRISMA Harms Checklist: Improving Harms Reporting in Systematic Reviews. *BMJ* (2016) 352:i157. doi: 10.1136/bmj.i157
46. Implementation of the International Health Regulations. Report of the Review Committee on the Functioning of the International Health Regulations (2005) in Relation to Pandemic (H1N1) 2009, in: *WHO 2011; SIXTY-FOURTH WORLD HEALTH ASSEMBLY* (2005). Available at: https://apps.who.int/gb/ebwha/pdf_files/WHA64/A64_10-en.pdf (Accessed June 30, 2021).
47. Blomberg B, Mohn KG, Brokstad KA, Zhou F, Linchausen DW, Hansen BA, et al. Long COVID in a Prospective Cohort of Home-Isolated Patients. *Nat Med* (2021) 27(9):1607–13. doi: 10.1038/s41591-021-01433-3
48. Cavaleri M, Enzmann H, Straus S, Cooke E. The European Medicines Agency's EU Conditional Marketing Authorisations for COVID-19 Vaccines. *Lancet* (2021) 397:355–7. doi: 10.1016/S0140-6736(21)00085-4
49. Pormohammad A, Zarei M, Ghorbani S, Mohammadi M, Razizadeh MH, Turner DL, et al. Efficacy and Safety of COVID-19 Vaccines: A Systematic Review and Meta-Analysis of Randomized Clinical Trials. *Vaccines (Basel)* (2021) 9:467. doi: 10.2139/ssrn.3812422

50. Greinacher A, Thiele T, Warkentin TE, Weisser K, Kyrle PA, Eichinger S. Thrombotic Thrombocytopenia After ChAdOx1 Ncov-19 Vaccination. *N Engl J Med* (2021) 384(22):2092–101. doi: 10.1056/NEJMoa2104840
51. Karron RA, Key NS, Sharfstein JM. Assessing a Rare and Serious Adverse Event Following Administration of the Ad26.COV2.S Vaccine. *JAMA* (2021) 325(24):2445–47. doi: 10.1001/jama.2021.7637
52. Schultz NH, Sørvoll IH, Michelsen AE, Munthe LA, Lund-Johansen F, Ahlen MT, et al. Thrombosis and Thrombocytopenia After ChAdOx1 Ncov-19 Vaccination. *N Engl J Med* (2021) 384(22):2124–30. doi: 10.1056/NEJMoa2104882

Conflict of Interest: The authors declare that the research was conducted in the absence of any commercial or financial relationships that could be construed as a potential conflict of interest.

Publisher's Note: All claims expressed in this article are solely those of the authors and do not necessarily represent those of their affiliated organizations, or those of the publisher, the editors and the reviewers. Any product that may be evaluated in this article, or claim that may be made by its manufacturer, is not guaranteed or endorsed by the publisher.

frontiers in Immunology

REVIEW
published: 16 November 2021
doi: 10.3389/fimmu.2021.786617

Influenza Neuraminidase Characteristics and Potential as a Vaccine Target

Sarah Creytens[1,2†], *Mirte N. Pascha*[3†], *Marlies Ballegeer*[1,2†], *Xavier Saelens*[1,2*] *and Cornelis A. M. de Haan*[3*]

[1] Vlaams Instituut voor Biotechnologie (VIB)-UGent Center for Medical Biotechnology, VIB, Ghent, Belgium, [2] Department of Biochemistry and Microbiology, Ghent University, Ghent, Belgium, [3] Section Virology, Division Infectious Diseases & Immunology, Department of Biomolecular Health Sciences, Utrecht University, Utrecht, Netherlands

Neuraminidase of influenza A and B viruses plays a critical role in the virus life cycle and is an important target of the host immune system. Here, we highlight the current understanding of influenza neuraminidase structure, function, antigenicity, immunogenicity, and immune protective potential. Neuraminidase inhibiting antibodies have been recognized as correlates of protection against disease caused by natural or experimental influenza A virus infection in humans. In the past years, we have witnessed an increasing interest in the use of influenza neuraminidase to improve the protective potential of currently used influenza vaccines. A number of well-characterized influenza neuraminidase-specific monoclonal antibodies have been described recently, most of which can protect in experimental challenge models by inhibiting the neuraminidase activity or by Fc receptor-dependent mechanisms. The relative instability of the neuraminidase poses a challenge for protein-based antigen design. We critically review the different solutions that have been proposed to solve this problem, ranging from the inclusion of stabilizing heterologous tetramerizing zippers to the introduction of inter-protomer stabilizing mutations. Computationally engineered neuraminidase antigens have been generated that offer broad, within subtype protection in animal challenge models. We also provide an overview of modern vaccine technology platforms that are compatible with the induction of robust neuraminidase-specific immune responses. In the near future, we will likely see the implementation of influenza vaccines that confront the influenza virus with a double punch: targeting both the hemagglutinin and the neuraminidase.

Keywords: influenza, neuraminidase, antigenic drift, monoclonal antibodies, correlate of protection, vaccines

OPEN ACCESS

Edited by:
Corey Patrick Mallett, GlaxoSmithKline (USA), United States

Reviewed by:
Irina V. Kiseleva, Institute of Experimental Medicine (RAS), Russia
Marion Russier, Max Planck Institute of Biochemistry, Germany

***Correspondence:**
Cornelis A. M. de Haan
C.A.M.deHaan@uu.nl
Xavier Saelens
xavier.saelens@vib-ugent.be

†These authors share first authorship

Specialty section:
This article was submitted to Vaccines and Molecular Therapeutics, a section of the journal Frontiers in Immunology

Received: *30 September 2021*
Accepted: *29 October 2021*
Published: *16 November 2021*

Citation:
Creytens S, Pascha MN, Ballegeer M, Saelens X and de Haan CAM (2021) Influenza Neuraminidase Characteristics and Potential as a Vaccine Target. Front. Immunol. 12:786617. doi: 10.3389/fimmu.2021.786617

1 INTRODUCTION

Influenza A and B viruses (IAV and IBV) cause acute respiratory illness and are widespread in the human population, with seasonal appearance in moderate climate zones and year-round manifestation in the tropics (1, 2). The use of licensed influenza vaccines is considered one of the best measures to prevent human influenza. These vaccines are vital in the efforts to alleviate the burden of influenza illness and deaths and are especially recommended for individuals who have an

increased risk of developing complications due to age or underlying disease (3, 4). The effectiveness of currently licensed influenza vaccines however leaves considerable room for improvement. Depending on the IAV subtype and the antigenic match between the influenza strains that are represented in the vaccine and the strains that circulate in the population, the vaccines prevent 10 to 60% of laboratory-confirmed medically attended influenza (5). The composition of seasonal influenza vaccines is reconsidered every year for each hemisphere in an attempt to keep pace with the antigenic drift of the viral hemagglutinin (HA), the major envelope protein on the influenza virions and the principal protective antigen in currently used influenza vaccines. These annual updates come with a risk of suboptimal predictions leading to a mismatch between the vaccine- and circulating influenza virus strains. There is a pressing need for more effective influenza vaccines that can elicit stronger and potentially broader protection against influenza. In the past decade, there has been a renewed interest in the exploration of influenza neuraminidase (NA) as a protective antigen component in influenza vaccines. Here, we review some of the seminal findings on NA structure and function, its immune-protective potential, as well as the current efforts to implement NA in next-generation influenza vaccines that aim for eliciting an immune response with increased magnitude and breadth.

2 NEURAMINIDASE: STRUCTURE AND FUNCTION

2.1 NA Structure

NA is one of the three membrane proteins expressed on IAV and IBV particles, next to HA and matrix protein 2 (M2). Label-free protein quantification of purified influenza A and B virions revealed that the NA : HA ratio ranges from 0.1 to 0.2 (6). NA is a homotetrameric type II membrane protein with a mushroom-like shape. Each protomer comprises approximately 470 amino acid residues and consists of a cytoplasmic tail, a transmembrane domain (TMD), a stalk and a head domain (**Figure 1**).

The cytoplasmic tail of NA consists of 7 highly conserved amino acid residues. Alanine-scanning mutagenesis of the cytoplasmic tail of NA of A/WSN/33 virus indicated a role in virus budding. Notably bud release rather than bud formation was affected in the tested NA cytoplasmic tail mutants (7). The cytoplasmic tail is also important for the association of NA with lipid rafts. Lipid rafts on the apical site of polarized cells are sites where newly formed influenza virions initiate assembly and budding (8). Together with the cytoplasmic tail, the TMD plays a role in the transport of newly expressed NA to the apical plasma membrane (9). The sequence of the TMD is moderately conserved across IAV subtypes and predicted to form an alpha helix. The TMD ensures the membrane anchoring of NA and serves as a translocation signal. In addition, this domain is reported to be an important stabilizing factor for the tetrameric NA formation (10, 11). Substitution of hydrophilic residues in the TMD by alanine reduced or even abolished the interaction between the four TMDs of the NA tetramer (10).

The stalk domain connects the TMD with the catalytic head domain. There is no crystal structure available of the stalk domain. The NA stalk varies in length within and across NA subtypes, carries multiple predicted N-glycosylation sites and, with few exceptions, contains at least one cysteine residue that can form an intermolecular disulphide bond with a neighbouring NA molecule (12). Glycosylation of the stalk region may contribute to NA stability, whereas inter-stalk disulphide bond

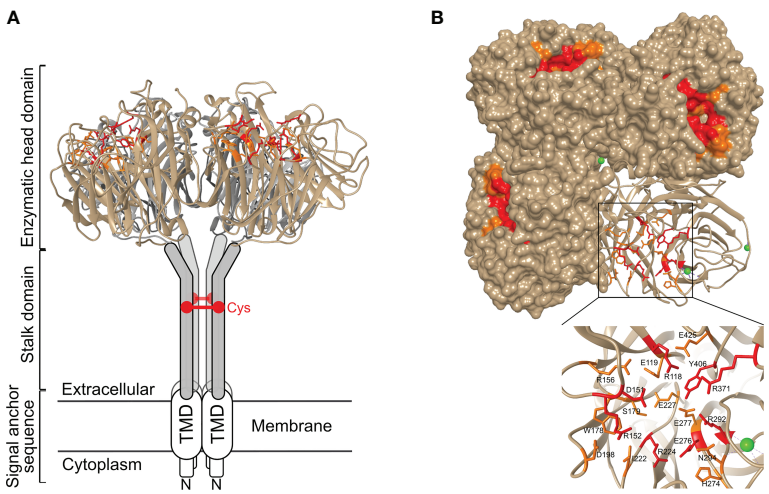

FIGURE 1 | Structure of neuraminidase and its catalytic site. **(A)** Side view and **(B)** top view of N1 NA (PDB 6Q23). NA is a homotetrameric type II membrane protein consisting of a head domain, stalk domain, and a transmembrane domain (TMD) and cytoplasmic tail that together form the signal anchor sequence. In general, NA stalk domains contain a cysteine residue (Cys) involved in intermolecular disulphide bond formation. The inset in panel **(B)** shows the catalytic site with the residues that interact with the sialic acid-containing substrate depicted in red, and the residues that stabilize the catalytic site labelled in orange. Ca^{2+} ions are shown as green spheres.

formation is important for the tetramer formation. Whereas the length of the NA stalk of human influenza viruses seems to be relatively constant, the NA stalk of avian NA subtypes, in particular N1, N2, N3, N5, N6, and N7, tolerate deletions (13). The stalk length affects NA enzymatic activity, presumably by modulating the accessibility to the sialic acid-containing substrates (14).

Crystal structures of the catalytic head domain of at least one representative NA from N1 to N9 and from influenza B NA have been resolved (15–22). The NA head domain is characterized by a six-bladed propeller that is folded around the catalytic site and which is typical for all known sialidases (23). Each blade is made up of four antiparallel β-sheets that are stabilized by disulphide bonds and connected by loops of variable length (12). Each monomer harbours a catalytic site, oriented towards the lateral side of the NA head, that is highly conserved over the different IAV subtypes (**Figure 1**). Remarkably, unlike the tetramer, influenza NA monomers and dimers show very little if any enzymatic activity (24). It is not known why tetramer formation is essential for NA to be active. Possibly, this is linked to calcium binding by tetrameric NA, which contributes to NA activity and stability. NA can bind up to nine $Ca2^{+}$ ions in the case of the 2009 H1N1 pandemic (H1N1pdm09) virus derived NA (16, 25–28).

Despite the significant primary sequence variation between IAV subtype NAs, the catalytic site residues in N1–N9 NAs are highly conserved. Among these, residues R118, D151, R152, R224, E276, R292, R371, and Y406 (N2 numbering) directly contact the substrate, while residues E119, R156, W178, S179, D198, I222, E227, H274, E277, N294, and E425 play a key role in stabilizing the catalytic site residues (19) (**Figure 1**). Phylogenetic analysis indicates that IAV NAs fall into two distinct groups. In group 1 NAs, a cavity adjacent to the catalytic site is observed which is absent in group 2 NAs (29). This cavity is created by the so-called 150-loop that consists of residue 147-152 and is flexible in group 1 NAs such that it can adopt an open and a closed conformation. Group 2 NAs on the other hand lack this second cavity as the formation of a salt bridge between D147 and H150 stabilizes the 150-loop, which is absent in group 1 NAs due to the presence of a G147 there (29, 30). The catalytic site and its adjacent 150-cavity are further explored as targets for NA inhibitors (31). Additionally, most avian influenza NAs, but not NAs of human viruses, have a functional second sialic acid binding site (2SBS) or hemadsorption site next to the catalytic site (32). The 2SBS consists of three loops with residues that facilitate binding to sialic acid in its so-called chair conformation. The catalytic site, in contrast, binds sialic acid in its twisted boat conformation (16). Studies comparing human and avian NA catalytic properties show that the presence of a functional 2SBS in avian NA increases NA activity against multivalent substrates (33, 34).

2.2 NA Function

HA and NA exert different functions in the influenza virus life cycle. HA is vital in the entry process, by mediating binding to sialic acids on host cell glycoproteins or -lipids, which results in virion uptake into endocytic vesicles, and the subsequent fusion of the host cell and virus membrane through a pH-induced conformational change (35). NA, on the other hand, catalyses the removal of the terminal sialic acids and thus functions as a receptor-destroying enzyme. NA activity is involved in multiple steps of the virus life cycle (**Figure 2**). During viral entry NA cleaves decoy receptors present in the mucus that lines the epithelial cells of the respiratory tract, allowing the infection of underlying epithelial cells (36–38). In line herewith, inhibition of NA activity was shown to result in severely decreased infection of differentiated primary human airway epithelium cells (39). NA activity was also reported to stimulate HA-mediated membrane fusion (40). The best-known function of NA in the influenza virus replication cycle is its critical role in the release of newly formed virions from the infected cell and in prevention of HA-mediated virion aggregation by removing sialic acid from the viral and host cell membrane (41).

Given these partly opposing functions, a functional balance between HA and NA is critical for viral replication. If HA binding is much stronger than NA activity, for example, virions may be trapped by decoy receptors present in mucus and eventually be removed by mucociliary clearance before reaching the underlying epithelial cells. On the contrary, if NA activity dominates, the virion will quickly move through the mucus, but will more likely fail to stably bind to an epithelial cell and enter it. HA and NA can be found on the virion surface in a patch-wise distribution, which contributes together with the HA-NA balance to virus motility and entry. In filamentous influenza virions, NA is mainly localized at one pole of the filamentous virus, and the few NA molecules present along the side of the virus tend to cluster in patches as well (42). Such polarized viruses seem to move by Brownian ratchet-like diffusion in a mucus-rich extracellular environment, in which filamentous particles exhibit directed mobility away from their NA-rich pole and toward the HA crowded part of the virus (42). HA binding to sialic acid is reversible due to the low affinity. This reversible binding likely allows NA patches to catalyse the removal of the sialic acid when the HA is no longer bound thereby initiating movement of the virion through mucus and over the cell surface. This NA-driven virion motility presumably allows the virus to find and to dock to specific spots on the cell surface that trigger entry into the host cell (38, 43, 44). Although detailed mechanistic insights into the importance of the HA-NA balance are still lacking, it is clear that besides HA also NA contributes to IAV pathogenicity. For example, truncation of the NA stalk, which has been associated with adaptation of IAV from aquatic birds to poultry, resulted in increased virulence in poultry and mice (13, 45–49).

3 ANTIBODIES DIRECTED AGAINST NA AS A CORRELATE OF PROTECTION

Protection against disease caused by influenza virus infection has traditionally been correlated with the presence of hemagglutination-inhibiting (HAI) antibodies in the blood. Such antibodies can neutralize influenza viruses *in vitro*, by

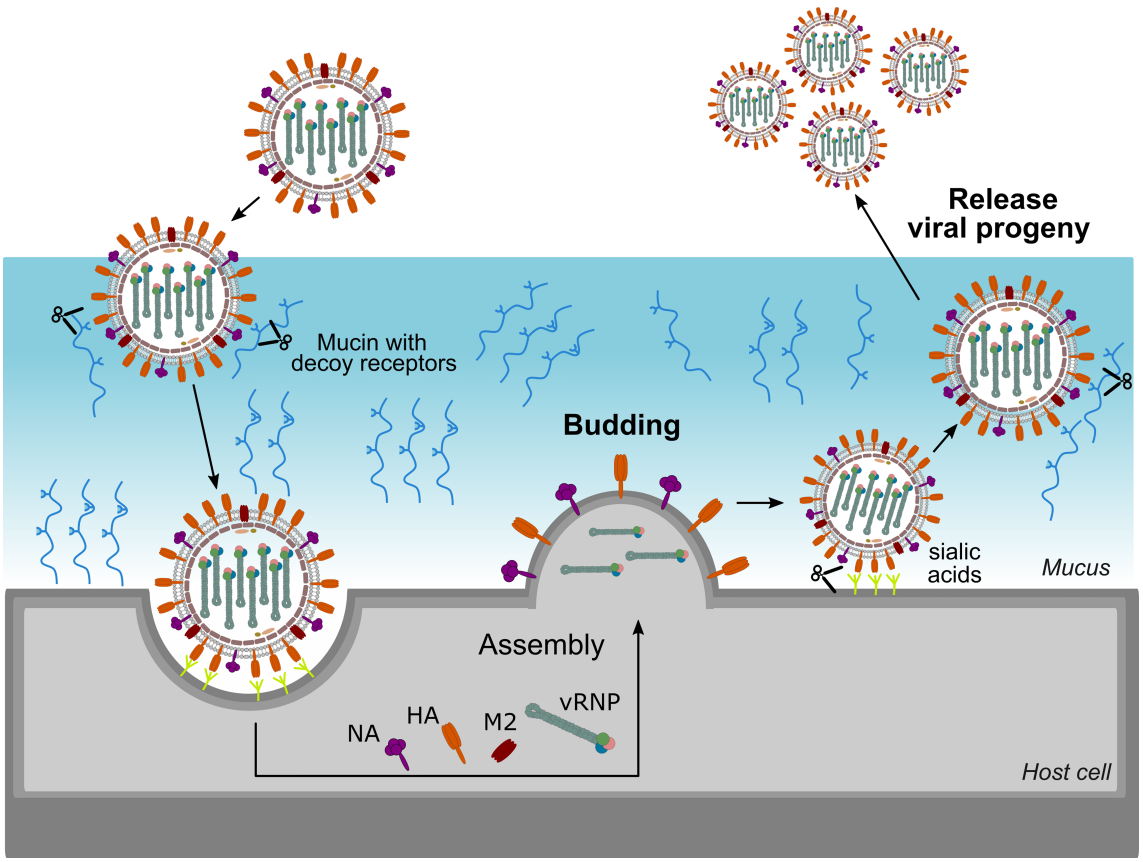

FIGURE 2 | Important role for NA in the virus life cycle. NA contributes to virus motility, allowing the virus to move through the mucus layer and to reach functional receptors at the cell surface. NA also plays an essential role at the end of the virus life cycle by removing sialic acids from the cell surface thereby allowing efficient release of virions and preventing virion aggregation.

preventing the binding of the virus to its sialic acid-containing receptor on the target cell. Therefore, in order to induce such antibodies, current influenza vaccines are standardized for their HA content. Natural infection, however, elicits an immune response against both HA and NA (50). In mice it has been shown that NA inhibiting (NAI) antibodies are associated with a reduction in pulmonary virus titer. More recently, by using a guinea pig model, monoclonal NAI antibodies were demonstrated to reduce airborne transmission of human IAVs, both when the antibodies were administered post infection to the infected animals or to the exposed recipients (51). This observation is in line with the contribution of NA to the release and spread of newly formed viruses after infection (50, 52, 53). Further, a combination of HA and NA provides even enhanced protection against influenza compared to HA alone (54–57). Studies comparing protection in mice induced by conventional inactivated influenza vaccines with or without supplementation with recombinant NA showed that for protection against homosubtypic influenza virus infection anti-HA antibodies sufficed. However, when challenged with an influenza virus with a mismatched HA supplementation of the vaccine with NA was required to reach a clear reduction in pulmonary virus titer (58, 59). In a ferret study it was found that whereas vaccination with HA reduced viral titers, vaccination with NA particularly decreased the clinical effects of infection, with optimal protection being achieved by a combination of the two antigens (54).

Evidence of NA-based protection in human has also been observed during the 1968 Hong-Kong pandemic. This pandemic was caused by a H3N2 virus with the same N2 as the previously H2N2 circulating virus. Individuals with pre-existing antibodies against the NA of H2N2 were less likely to be infected with the newly emerged virus (60–63). In humans, NA-inhibiting antibodies in serum correlate with a reduced virus load in nasal wash (62). Couch et al. first showed that serum N2-specific antibodies, elicited by vaccination with H1N2 (H1 HA from A/equine/Prague, N2 NA from A/Aichi/2/68 (H3N2)) in humans who initially lacked anti-HA antibodies, correlate with a reduction of viral shedding after challenge of the subjects with A/Aichi/2/68 (H3N2) virus (62). Three decades later, during the 2009 H1N1 pandemic season, it was demonstrated that HAI and NAI antibodies in serum independently correlated with immunity against infection and infection-associated illness. Moreover, in H1N1pdm09-infected individuals, NAI antibodies

in serum independently predicted reduced illness (64). This correlation of NAI antibodies with protection is also supported by more recent studies in humans. The presence of NAI antibodies in serum was associated with a reduction of PCR-confirmed influenza infection for both H3N2 and H1N1pdm09 virus (65, 66). Memoli et al. divided the participants in their controlled human challenge study with H1N1pdm09 virus in a group based on HAI or NAI titer and showed that subjects with a high (> 1:40) NAI titer at baseline not only presented with reduced symptoms and virus shedding duration, but also with a reduction in the number of symptoms and the symptom severity. In contrast, HAI titers correlated only with a reduction in the number of symptoms and virus shedding duration but not with symptom severity (66). These results highlight that anti-NA immunity can enhance protection against influenza virus infection.

4 EVOLUTION AND ANTIGENIC DRIFT OF NA

HA and NA are prime targets of the host's immune response to influenza virus infection (67). Combined with the relatively high mutation rate of the replicating influenza virus RNA genome, human influenza viruses with antigenically altered HA and NA emerge that have a selective advantage over previously circulating strains because they are less likely to be recognized by antibodies that prevail in the population. This phenomenon of antigenic changes is called antigenic drift, and is at the basis for the frequent updating of human influenza vaccines. The selection of seasonal vaccine strains is based on three types of data: epidemiological information, HA and NA gene sequence phylogeny and serological analysis using an HA inhibition assay. Today, the main focus of genetic and antigenic surveillance is thus on HA since licensed influenza vaccine formulations are standardized for the amount of HA (68). The antigenic drift of HA has been extensively studied (69). In a seminal paper, Smith et al., discerned a pattern of eleven antigenic HA clusters in human H3N2 viruses that circulated between 1968 and 2003 (70). Later, two clusters were added to the antigenic map when HAI data was added up to 2011 showing that the human H3N2 virus continued to evolve antigenically (71). Interestingly, the antigenic change between the HA clusters is the result of a limited set of amino acid changes confined to positions near the receptor binding site of HA (72, 73). In contrast to HA, antigenic drift of NA is not routinely examined. In the next paragraphs, we discuss the genetic evolution of NA and the limited studies on NA antigenic drift.

4.1 Genetic Evolution

Several studies addressed the genetic evolution of HA and NA using IAV and IBV strains, which revealed that their evolution differs and is often asynchronous (74–78). Although the general topology of the NA and HA phylogenetic trees is similar with the typical 'ladder-like' gradual evolution and rapid replacement of old strains by newer ones, NA evolved slower and more gradually at the nucleotide level than HA. Looking at 40 years of evolution of human H3N2 viruses, Westgeest et al. showed that NA had fewer nucleotide substitutions over this time span compared with the HA head HA1, the most variable part of the HA gene (78). Nevertheless, it was concluded by Bhatt et al. (74) that with almost all adaptive evolution in NA being concentrated in residues on the surface of NA, the adaptation rate is higher for surface NA residues than for HA1. The observation that adaptive evolution in NA occurs almost exclusively in solvent-accessible surface residues indicates an important role for antibody-mediated immune responses in NA evolution. In **Figure 3**, the IAV N1, IAV N2 and IBV NA structural conservation for the viruses that were used in seasonal influenza vaccines from 1970 to 2021 are depicted. Overall, a relatively high conservation of the head domain residues is observed for each NA (sub)type. As expected, the catalytic site is for all NA subtypes highly conserved. However, the surface residues do show variation, especially for IAV N2, which is in agreement with a higher rate of adaptation for NA in H3N2 than H1N1 viruses (74).

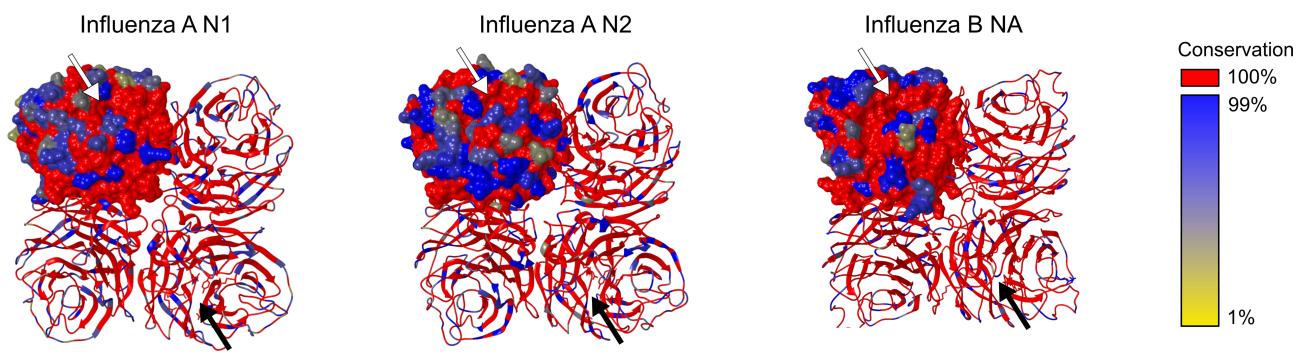

FIGURE 3 | NA structural conservation. Structural alignments of all seasonal influenza vaccine included influenza strains in the period 1970-2021.The sequence conservation of Influenza A N1, Influenza A N2 and Influenza B NA amino acid residues was visualized using MUSCLE and shown on a crystal structure of the respective NA subtype using the render by conservation function in CHIMERA. Residues conserved in all sequences of a specific subtype NA are shown in red. Further distinction of conservation is indicated from dark blue (99% conservation) till yellow (1% conservation). Structure representations based on N1: PDB 4B7Q, N2: PDB 4GZX, and IBV NA: PDB 4CPL. Arrows point towards the catalytic site.

4.2 Antigenic Drift

The analysis of NA antigenic drift usually relies on the determination of NAI titers of polyclonal ferret antisera raised against a particular influenza virus strain (e.g. a vaccine strain) in an enzyme-linked lectin assay (ELLA) (79, 80). The antigenic relatedness of the NAs from two viruses can be assessed by comparing NAI titers, calculating percent relatedness (81) or by performing antigenic cartography (76) to generate an antigenic map (80). On such a map, based on the quantification of the raw data of NAI assays, the antigenic distances between influenza viruses or sera are visualized. Importantly, the reactivity of antisera of ferrets that have experienced a single experimental virus infection is quite different from human sera which have an antibody repertoire that has typically been shaped by multiple prior infections and vaccinations (80, 82). The antigenic changes identified this way based on sera from ferret that were infected once with a particular influenza virus strain may therefore not always accurately reflect the response of an (adult) human individual (83) although such discrepancies have so far only been demonstrated for HA-specific responses (84–86).

Only a few studies have investigated the antigenic drift of NA using large NAI data sets and by constructing antigenic maps. In 2011, Sandbulte et al. reported on the characterization of the antigenic drift of NA in human H1N1 and H3N2 viruses that were recommended for influenza vaccine implementation over a period of 15 years in the USA (76). Similarly, Gao et al. examined the antigenic drift of NA sequences of H1N1pdm09 viruses (80). Overall, the antigenic differences between NAs of human H1N1 viruses occurred in one direction, meaning that antisera raised against older strains reacted weakly with more recent NAs whereas reactivity between antisera against more recent strains and older NAs was high (76, 80, 87). Both raw NAI data and the antigenic map obtained by Sandbulte et al. show that the NA of pre-2009 seasonal human H1N1 was in antigenic stasis for over a decade despite its genetic evolution during that time. For human H3N2 viruses the antigenic drift of NA was also not proportional to the number of amino acid changes induced. Collectively, these data show that there is discordance between the antigenic and genetic evolution of NA. Indeed, For N2 it was found that a single point mutation (E329K) was responsible for the abrupt NA antigenic drift between 2006 and 2007 (76). Similarly, for H1N1pdm09 few substitutions appeared to be largely responsible for the observed antigenic changes (80). The presumed important role in antigenic drift of K432E (80) was later confirmed using recombinant NA proteins that only differed at this position (87). Epistatic interactions as well as by biophysical constraints may also play a role in NA antigenic drift as was shown for the evolution of an antigenic site in H3N2 NA (88, 89). Furthermore, changes in HA receptor binding, e.g. as a result of antigenic drift, may in turn select for substitutions in NA that affect enzymatic activity to restore a functional balance in HA and NA, while additionally affecting NA antigenicity (90).

Bidirectional IAV transmission between humans and swine represents a serious public health challenge. In the last decade, an increasing number of zoonotic infections with IAV from swine has been reported. For example, after two distinct human-to-swine H3N2 spill overs in 1998 and 2002, N2-98 and N2-02 lineage viruses have circulated in swine in the USA and antigenically evolved over the next 20 years. After IAV infection, pigs typically produce broadly cross-reactive NAI antibodies to the N2 protein, but no NAI cross-reactivity between the N2-98 and N2-02 lineages was observed (91). The antigenic distance between swine and human N2 antigens increased over time to the extent that there is by now very little antigenic similarity with the human seasonal H3N2 NA that these viruses were derived from, nor with the NA of currently circulating human H3N2 viruses. This suggest that there will be little to no cross-reactive NA mediated immunity in both the swine and human population which may impact the occurrence of future spill overs (91).

5 NEURAMINIDASE-SPECIFIC MONOCLONAL ANTIBODIES: MECHANISMS OF ACTION AND EPITOPES

Using large panels of monoclonal antibodies (mAbs) or recombinant NA proteins, several studies have set out to identify antigenic sites on NA (12, 52, 92–96). NA activity and inhibition thereof can be evaluated with two types of assays. The so-called 4-methylumbelli-feryl N-acetyl-α-D-neuraminic acid (MUNANA, a fluorogenic NA substrate) or NA-STAR (a chemiluminescent NA substrate) assays allow to quantify the hydrolysis of a small soluble substrate by NA. The small molecule NA inhibitor oseltamivir, which binds precisely inside the catalytic site, inhibits NA activity in these types of assays (97). Only a mAb that binds inside or in very close proximity to the catalytic site will be able to prevent cleavage of the small substrate whereas mAbs that bind distal to the catalytic site are less likely to have an effect in such assays.

ELLA assays use larger substrates compared to MUNANA and NA-STAR assays, such as the glycoprotein fetuin that contains sialylated N- and O-linked glycans. A mAb binding to the NA head domain, even outside of the catalytic site, may still sterically block access of fetuin to the catalytic site and prevent cleavage of the substrate, while cleavage of small soluble substrates may not be affected. Comparing the inhibition profile of NAI mAbs based on the outcome of both types of assays will thus give an indication on their possible binding site. **Table 1** provides an overview of different NA-specific mAbs and their impact on NA activity as determined with a small molecule substrate or in the ELLA. Overall, two different antigenic regions have been described that characterize NAI antibodies: (i) the catalytic site and its rim and (ii) outside of the catalytic site, including the interface between two adjacent monomers. Additionally, several NA-specific mAbs have been described that lack detectable NAI activity in either assay, yet can protect *in vivo* against influenza A virus challenge. These mAbs rely on Fc effector functions and will be discussed separately (**Figure 4**).

TABLE 1 | Overview of NAI mAbs and their epitopes.

Epitope	Mechanism of action	Neuraminidase inhibition?		mAb (reference) * structural data available Bold: mentioned in text
		Small substrate assay	Large substrate assay	
The catalytic site and its rim	(partially) block access to catalytic site	Yes	Yes	NA-73* (98, 99) NA-108 (98, 99) HCA-2 (100, 101) IG05 (102) 2E01 (102) **HF5** (103, 104) 3G1 (52) 229-1 F06 (50) 229-1G03 (50) 229-11)05 (50)
	CDR3 loop insertion in catalytic site	Yes	Yes	**IG01*** (105) IG04* (105) IE01* (105) **Z2B3*** (106, 107) **NA-45*** (98, 99)
	bind loop surrounding the cavity of the catalytic site	Yes	Yes	Mem5* (108) NC10* (109) NC41* (110) IG8* (111) 229-1D05 (50, 112) 229-1C02 (50, 112)
Outside of the catalytic site	bind linear epitope on tip	No	Yes	NA-63* (98, 99) NA-80* (98, 99)
	unknown	No	Yes	IF2 (52) N1-C4 (113)
	bind interface between adjacent monomers causing steric hindrance	No	Yes	**CD6*** (103) **N8-4** (114) 4F11 (52) NA-22* (98, 99)

Neuraminidase inhibition activity is determined via small substrate (MUNANA or NA-STAR) and large substrate (ELLA) assays. mAbs in bold are mentioned in the text, while other mAbs are referenced for completeness.

5.1 NAI mAbs That Target the Catalytic Site and Its Rim

Early antibody characterization and vaccination studies have shown that immunity to NA can be very broad within, but usually not across, subtypes (105). Nevertheless, mAbs that directly bind into the highly conserved catalytic site of NA (115) and inhibit enzymatic activity in small molecule assays are expected to exert a degree of heterosubtypic NAI. Recently, Stadlbauer et al. reported on a human mAb, 1G01, which binds to and inhibits the activity of several group 1 and group 2 NAs as well as NAs from both influenza B virus antigenic lineages *in vitro*. MAb 1G01 was shown to inhibit NA activity in a NA-Star assay and to occupy the catalytic site *via* a long CDR H3 loop by co-crystal structure analysis (**Figure 4**) (105). A similar mechanism of action was described for mAb NA-45 where the CDR H3 loop adopts a protruding conformation with a tip that inserts into the NA catalytic site (98). This type of substrate mimicry is unique among all structurally characterized NA antibodies so far but has also been reported for anti-HA antibodies that target the receptor-binding site (116, 117). Interestingly, the number of residues in the antibody footprint might be important for the cross-reactivity of mAbs. For example, the binding footprint of 1G01 (105) and Z2B3 (106, 107) significantly overlaps. However, the 1G01 footprint includes more catalytic and framework residues which explains the broader cross-reactivity of 1G01 compared to Z2B3 (107). It is important to note that the footprint of mAbs that bind into the highly conserved catalytic site of NA often overlaps with the rim of the catalytic site. The rim is less conserved and can tolerate amino acid substitution without NA losing enzymatic activity.

Next to conventional mAbs, other antibody moieties that target the NA catalytic site have been described. The first NA-specific single domain antibodies or VHHs were described by Harmsen et al. with several candidate cross-NA binders and some VHHs that could affect NA activity (118). The isolation and characterization of a set of alpaca-derived H5N1 NA-specific VHHs (N1-VHH) with NA-inhibitory activity was also described. Two monovalent candidates N1-3-VHHm and N1-5-VHHm could inhibit NA activity with N1-3-VHHm also inhibiting oseltamivir resistant H5N1 virus NA. Bivalency of these constructs enhanced their NA inhibitory capacities and resulted in VHH constructs that could protect mice against H5N1 challenge (119).

5.2 mAbs that Bind to Epitopes Outside the Catalytic Site

A large proportion of the reported NAI mAbs only display NAI activity in the ELLA, but not in assays with small molecule

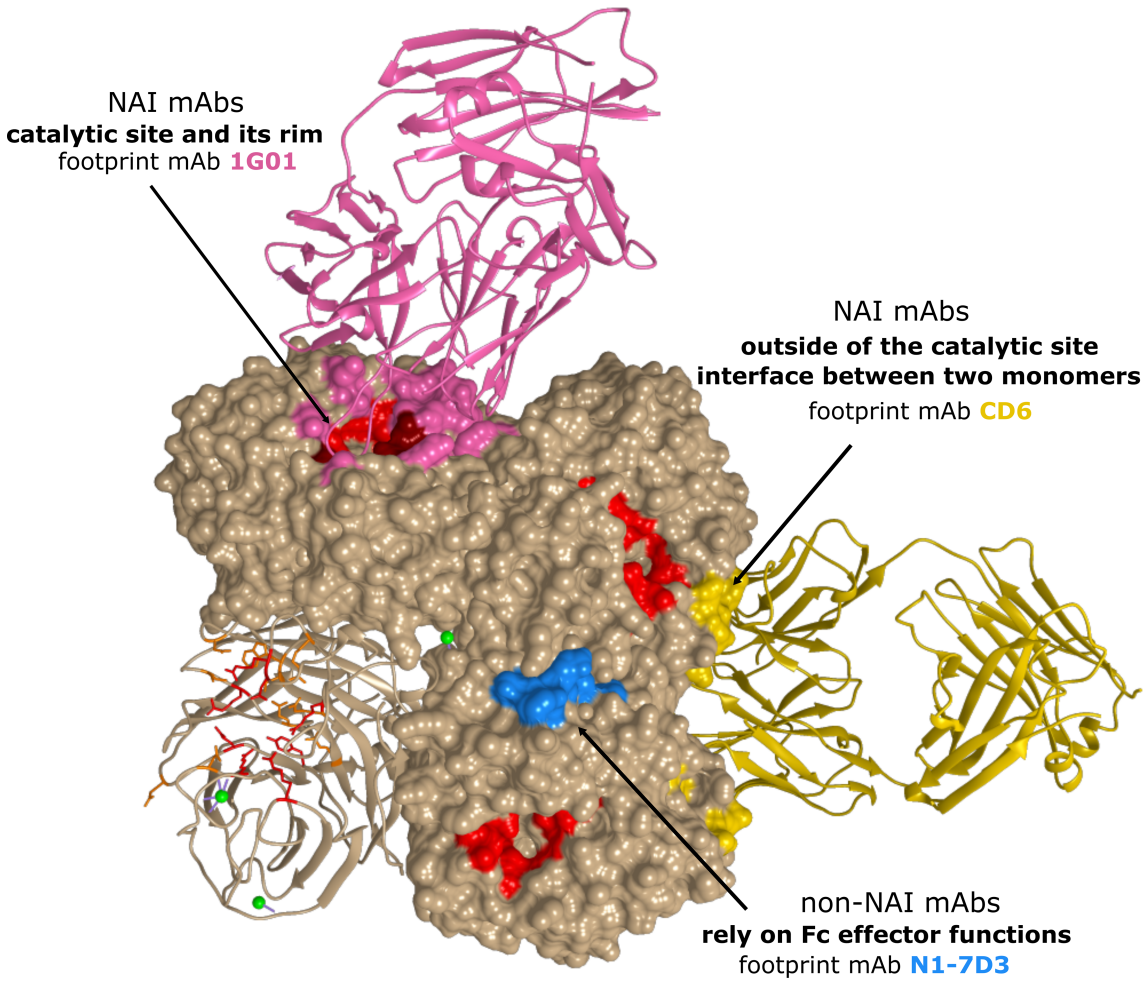

FIGURE 4 | Antigenic regions of N1 NA-specific mAbs. The A/California/04/2009 (H1N1) tetramer is depicted with one protomer in ribbon representation. The catalytic residues are depicted in red. For each region, a representative antibody footprint is shown: 1G01 (105) in pink (PDB 6Q23) with antibody contact residues in NA that overlap with the catalytic site in dark red; CD6 (103) in gold (PDB 4QNP) and N1-7D3 (113) in light blue.

substrates, indicating they do not contact the catalytic site directly (99). Binding of these mAbs likely results in steric hindrance and restricts access of large glycoconjugate substrates to the catalytic site (52). The NAI activity in ELLA assays has been associated with the capacity to block virus egress from infected cells (98, 99). An example of such a mAb is CD6, which effectively inhibited H1N1pdm09 viruses both *in vivo* and *in vitro* (103). Interestingly, CD6 more efficiently inhibited NA as an intact IgG compared to Fab and Fab_2 molecules of CD6, demonstrating that CD6 inhibits NA activity through steric hindrance and not structural distortion. Crystallization studies revealed a quaternary epitope that spans the lateral faces of two neighbouring N1 monomers (**Figure 4**). Such a quaternary epitope present in intact NA dimers had been proposed earlier by Saito et al. for the N8-4 mAb but until then had never been structurally defined (114). For HA, quaternary epitope-specific mAbs that span two HA monomers that are efficient in neutralizing virus *in vitro* have also been described (120, 121). Some studies showed a correlation between the relative distance of epitopes to the NA catalytic site and the *in vitro* properties of mAbs. For example, mAb HF5 which has contact residues that surround the catalytic site pocket, showed more efficient NAI activity compared to other mAbs with an epitope that is located more laterally on the NA head (92, 107). Additionally, murine anti-N9 mAbs that inhibit NA enzymatic activity with a small molecule substrate *in vitro*, provided superior *in vivo* protection compared with mAbs that inhibited NA activity only in the ELLA assay (93).

5.3 mAbs That Depend on Fc Effector Functions for Protection

It is becoming increasingly clear that Fc-mediated effector functions have an important role in providing *in vivo* protection against influenza virus challenge (122). The fragment crystallisable (Fc) region of an antibody can interact with Fc receptors and thereby mediate indirect effector functions

such as antibody-dependent cellular cytotoxicity (ADCC), antibody-dependent cellular phagocytosis (ADCP) and complement-dependent cytotoxicity (CDC) (123). Using Fc receptor knockout mice and DA265 mutant mAbs that are unable to bind Fc receptors, it was demonstrated that broadly reactive HA-stalk antibodies depend on Fc-Fcγ receptor interactions *in vivo* (122, 124, 125). The contribution of Fcγ receptor engagement for *in vivo* protection by some NA-specific mAbs was demonstrated by Job et al. (126). The mouse monoclonal antibody N1-7D3 binds to a conserved linear epitope near the carboxy-terminus of N1 NA and shows no NAI activity (**Figure 4**) (113). However, a recombinant mouse-human chimeric version comprised of the variable domains of mouse N1-7D3 and the constant regions of human IgG1 could engage activating Fcγ receptors and protected FcγR-humanized mice against challenge with H1N1pdm09 virus (126). In addition, mAbs with no detectable NAI activity reported by Yasuhara et al., could protect mice against a lethal influenza virus infection. Interestingly, a N297Q mutant version of these mAbs that lacks Fcγ receptor-binding activity failed to protect, thereby supporting the crucial role for Fcγ effector functions in protection by non-NAI mAbs (127). In line with this, grafting of the non-NAI N1-7-VHH on a mouse IgG2a Fc could protect mice against an otherwise lethal H5N1 challenge (119).

Several studies have demonstrated that the Fc-mediated effector functions might also be crucial for *in vivo* protection by some anti-NA mAbs that possess weak NAI activity (99, 127). Thus, while for potent N9 NAI mAbs Fc effector functions were not needed, the ability to interact with Fc receptors was required for weakly NAI mAbs to protect against challenge (99). Likewise, a broadly cross-reactive mAb with low NAI activity required FcγR interactions to mediate protection, while a strain-specific mAbs with high NAI did not (124). Likely, the sum of the NAI activity and the FcγR-mediated effector functions determines the potency of an anti-NA antibody *in vivo*. An anti-NA mAb with high NAI activity can reduce virus spread *in vivo* mainly through its NAI activity, whereas an anti-NA mAb without NAI activity can suppress virus replication mainly through FcγR-mediated effector cell activation (127).

6 NA-BASED INFLUENZA VACCINES

6.1 NA Immunogenicity in Seasonal Influenza Vaccines

Despite the recognized importance of NA-reactive antibodies in protection against influenza, the current commercially available influenza vaccines do not consistently elicit these antibodies (50, 128). NA immunogenicity of these vaccines varies widely between manufacturers (65, 128–130) and is poor compared to natural infection. Whereas following natural infection the number of NA-reactive B cells were equal to or exceeded HA-reactive B cells, current vaccines rarely induced NA-reactive B cells (50). Furthermore, broadly cross-reactive NAI antibodies elicited by natural infection were unable to bind multiple commercially available inactivated vaccines, indicating that the vaccines lack the NA epitopes targeted by these antibodies (50).

The poor NA immunogenicity of the licensed influenza vaccines can be attributed to a few factors. As mentioned, current vaccines are optimized and standardized specifically for inducing high HAI antibody titers. As a result, the immunogenicity of the NA is not guaranteed. Quantity and quality of the NA antigen varies between manufacturers and vaccine batches (131, 132). Virus inactivation procedures may also affect NA immunogenicity. While treatment with EDTA or formalin did not compromise the immunogenicity of recombinant NA proteins (133), native NA in a viral particle may respond differently to these conditions. The stability and immunogenicity of NA also varies between strains (132). Nevertheless, in case vaccination does elicit NA antibodies, these can be long lived in healthy human subjects (134, 135). Better consideration of the NA component of current vaccines could therefore mean an important step forward in effectivity of the current vaccines. This could be achieved by also considering NA in selection of the vaccine strains, optimizing the manufacturing process to keep NA antigenically intact, and also standardizing the amounts of immunogenic NA in vaccine preparations.

6.2 Next-Generation NA-Based Vaccines

Next-generation seasonal and universal influenza vaccines call for an improved NA-directed immune response. Various options for rational design of the NA antigen and mode of presentation to the immune system are in development aiming to boost the breadth and magnitude of the NA-specific response (**Figure 5**). The following section summarizes promising ideas and the rationale behind them.

6.2.1 Enhancing NA Immunogenicity Within Existing Influenza Virus Vaccines

In addition to optimizing the manufacturing conditions of the current seasonal vaccines, extra steps can be taken to improve the immunogenicity of NA while using the same influenza virion-based vaccine technology as a basis. For example, by re-structuring parts of the viral genome, a higher amount of NA can be incorporated into the viral particles (136, 137). Swapping the packaging signals of HA and NA that contain the viral RNA promoters resulted in virions with more NA, although at the expense of HA. Immunization with this virus resulted in increased levels of NAI and Fc-dependent antibodies directed against NA and induced protection against lethal challenge with an NA-matched IAV strain. HA-directed IgG titers were however significantly lower for the recombinant virus compared to the wild-type (136). Since glycosylation of the NA head domain was also found to affect NA incorporation in the virion (138), altering glycosylation sites could be explored as an alternative strategy to incorporate higher levels of NA in an IAV vaccine strain. Such modifications may, however, also affect NA antigenicity and immunogenicity. Extending the NA stalk so that NA surpassed HA in length was also shown to enhance NA immunogenicity of an inactivated virion-based vaccine in mice. Specifically, increased levels of antibodies with ADCC activity were induced. The authors hypothesized that their extended NA stalk domain

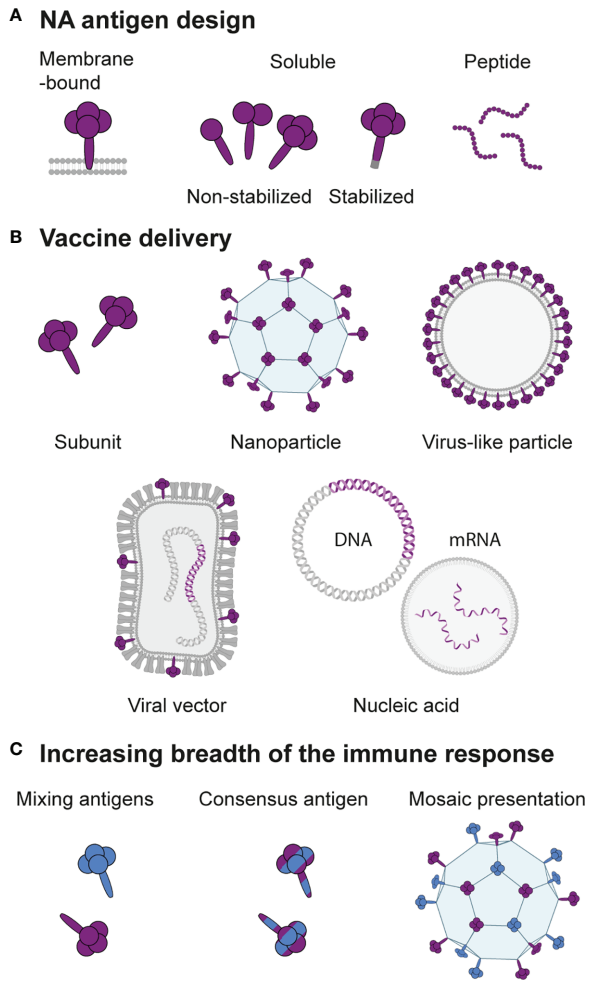

FIGURE 5 | Design of next-generation NA-based vaccines. **(A)** The NA antigen can be presented in the native membrane-bound form, as a soluble protein that lacks the transmembrane domain with or without modifications to retain or stabilize the tetrameric structure, or as peptides containing an epitope of interest. **(B)** Depending on the antigen design, various methods for vaccine delivery are possible. Soluble NA can be administered as a subunit vaccine or coupled to a nanoparticle carrier. Membrane-bound NA can be presented on a virus-like particle or on the cell surface when encoded as RNA or DNA delivered directly or by a viral vector. **(C)** Strategies to increase the breadth of the immune response include mixing of NAs from different strains, computational design of consensus NAs, or hetero-multivalent mosaic presentation of NAs from different strains on a single particle.

method exposes NA epitopes to the immune system that were otherwise hidden (139).

6.2.2 Recombinant Protein Design

An alternative solution to increase the immune response to NA is to add extra NA to vaccine formulations. Johansson et al. supplemented inactivated vaccines with soluble NA purified from viral particles. This approach induced higher titers of NAI antibodies without compromising on HAI antibodies (58, 59). Recombinant soluble NA proteins (**Figure 5A**) are also attractive vaccine antigens to supplement inactivated virus vaccines or as a component of a multi-antigen subunit vaccine. Important in the design of such antigens is that a correctly folded tetrameric structure is essential for optimal immunogenicity (133, 140). Often enzymatic activity is measured as a proxy for a correct conformation of the NA antigen. While this is a reliable proxy for the presence of intact antigenic structure, NA activity in itself is not required to induce protective NA-specific antibodies in mice (133, 141, 142). Early on, recombinant NA was produced by replacing the membrane anchor sequence with a signal sequence derived from a type I membrane protein. This method typically results in a mix of tetrameric, dimeric, and some monomeric protein (24). To produce pure and stable tetrameric NA, ectodomains are better fused to heterologous tetramerization domains. Multiple tetramerization domains have successfully been used to produce immune-protective recombinant NA: VASP, GCN4, and Tetrabrachion (54, 143, 144). Tetrabrachion-stabilized NA proteins appear most stable and enzymatically active, presumably due to the parallel orientation of these domains (145, 146). In addition, a crystal structure of a tetrabrachion-stabilized N9 showed that the head domain maintained its native structure as found on virions (147). Whether immunization with these constructs also results in better quality antibody responses is yet to be determined. Interestingly, a recent study showed that the combined choice of tetramerization domain and inclusion of the stalk domain into recombinant NA profoundly impacts activity and immunogenicity. Thorough evaluation of individual recombinant NAs may therefore be required to determine the optimal antigen design strategy (142).

Mutations in the NA stalk (148) or the interface between protomers (149) can also enhance the stability and immunogenicity of recombinant NA. Cysteine mutations in the stalk led to more efficient dimer formation of recombinant N1, resulting in enhanced enzymatic activity and immune protection. The cysteine-stabilized dimers were however still outperformed by a VASP-stabilized tetrameric NA (148). It was only recently recognized that recombinant NA proteins can adopt an open conformation in addition to the closed conformation that is found on the surface of influenza virions. Structure-guided stabilization of the closed conformation was performed that improved thermal stability. More importantly, it also enhanced the affinity to protective antibodies elicited by viral infection, indicating that these antigens may elicit antibody responses to vulnerable quaternary epitopes more efficiently (149).

To broaden the protection elicited by a recombinant protein antigen, computational methods can be used to design constructs based on a consensus sequence of varying strains (**Figure 5C**). After similar techniques have shown promise for the induction of more broadly reactive HA responses (150), recent studies engineered NA constructs that combined sequences of various human, swine, and avian H1N1 and H5N1 strains (151, 152). The resulting antigens were immunogenic and induced antibodies against a broader range of viruses than wild-type NA antigens, including NAI antibodies against strains not included in the antigen design (151).

Immunization or passive transfer of the sera of immunized mice offered protection against homologous and heterologous viral challenge (151, 152). While the broadened immune response may come at the cost of a lower magnitude compared to immunizations with a matched NA antigen (152), consensus NA antigens are promising candidates for inclusion in multi-antigen universal vaccine formulations.

6.2.3 Multivalent Presentation

The immunogenicity of soluble protein antigens can be substantially improved with multivalent presentation. Multivalent nanoparticles better mimic viruses in terms of size, shape, antigen valency, and repetitive organization, resulting in enhanced uptake by antigen presenting cells and stronger activation of B cell receptors (153). Such nanoparticle designs may constitute virus-like particles (VLPs) containing membrane-anchored NAs or protein nanoparticles to which soluble NAs are coupled (**Figure 5B**).

NA can self-assemble into VLPs, either when expressed alone or in combination with other IAV structural proteins (154–157). VLPs that display N1 alone or in combination with H5 and M2e induced high titers of NAI antibodies (154, 157–159). Vaccination with N1 VLPs derived from H1N1pdm09 provided cross-protection against lethal challenge with heterologous (H5N1) and even heterosubtypic (H3N2) IAV (159). However, in a more recent study N1 VLPs were not able to cross-protect against a historical H3N2 strain (160). N2 VLPs derived from a more recent H3N2 virus did protect against challenge with the distant H3N2. In addition, bivalent vaccination combining the N1 and N2 VLPs induced strong anti-N1 and -N2 antibody responses that exceeded the antibody levels induced by either one of the VLPs individually (160). Protective efficacy of NA-based VLP vaccination has also been demonstrated in ferrets. In these animals, VLPs containing H5N1-derived NA and matrix protein M1 induced high serum NAI antibody titers and protection against lethal homologous challenge. Incorporation of additional H5 or H3 into the VLPs further reduced clinical symptoms of the ferrets after H5N1 challenge. VLPs composed of H3/N2/M1 were however unable to cross-protect against the heterosubtypic H5N1 challenge (154). Efforts to further boost both humoral and cellular immunity of VLP vaccines currently focuses on attachment of adjuvants directly onto the VLPs (161–163).

In a different strategy based on multivalent presentation, nanoparticles consisting of little more than IAV structural proteins were generated (164). A dense core was constructed out of M2e protein and decorated with M2e-NA fusion proteins by chemical cross-linking. These double-layered nanoparticles greatly improved immunogenicity and (cross-)protection over soluble M2e-NA fusion proteins. M2e-NA nanoparticles were generated using NA from H5N1 and H3N2. Mice immunized with the M2e-N1 nanoparticles were fully protected against mortality following challenge with the homologous strain, as well as H1N1 and H3N2. Immunization with the M2e-N2 nanoparticles fully protected against mortality following challenge with the homologous strain and an H9N2 virus and conferred 60% protection against H1N1 (164).

Self-assembling protein nanoparticles are highly ordered, monodisperse carrier platforms that are increasingly used in experimental vaccines. The geometry of these nanoparticles is versatile and can be readily adapted for optimization to a specific antigen (165). While these carriers have not yet been used to generate NA-based nanoparticle vaccines, examples of their application for other viral glycoproteins illustrate their promise. HA nanoparticles, for example, elicited more than 10-fold higher antibody titers compared to the commercial inactivated vaccine, including antibodies directed against conserved vulnerable epitopes (166). The respiratory syncytial virus fusion protein similarly induced 10-fold higher neutralizing antibody titers when presented on a two-component protein scaffold (167). Self-assembling protein scaffolds are also well suited for presenting viral glycoproteins from multiple strains together on mosaic nanoparticles (**Figure 5C**). It was hypothesized that presentation of these diverse antigens alongside each other gives an avidity benefit for cross-reactive B cell receptors, resulting in a broader antibody response. This strategy was applied using the HA receptor binding domains (RBDs) of two H1N1 strains. Mosaic nanoparticles displaying two distinct H1 RBDs were found to induce broader antibody responses than a mixture of homotypic nanoparticles displaying the same set of RBDs (168). These results indicate that mosaic nanoparticles may enhance activation of B cells specific for the otherwise subdominant cross-reactive epitopes, which could be an interesting strategy to evaluate for NA.

6.2.4 Epitope-Based Vaccines

Epitope-based vaccine design aims to precisely direct the immune response towards conserved vulnerable B or T cell epitopes by presenting peptide epitopes (**Figure 5A**) on an immunogenic carrier or in a multi-epitope construct. In doing so, these techniques have potential for eliciting broadly protective immunity. The potential of an universally conserved linear B cell epitope near the NA catalytic site consisting of residues 222 through 228 or 230 (NA_{222}) as an vaccine antigen was recently studied (169, 170). Kim et al. incorporated the epitope into the HA head domain of a H1N1 virus, creating a chimeric virus that was inactivated prior to immunizations. The NA_{222} chimeric virus, but not the inactivated wild-type virus, induced a strong Th1-type antibody response directed to this epitope. The chimeric virus protected against heterosubtypic challenge with H3N2 and H9N2 viruses and at 6 days post-challenge the mice expressed high levels of mucosal IgG and IgA specific for the epitope (169). Zeigler et al. developed a self-assembling protein nanoparticle containing the NA_{222} epitope in addition to two universal CD4 T cell epitopes that mediate high-affinity, long-lived antibody responses. The NA_{222} nanoparticle induced high IgG titers and conferred approximately 50% survival in otherwise lethal H1N1 and IBV challenge, whereas nanoparticles with HA or M2e epitopes were 70-75% protective with similar IgG titers. It was suggested that the NA_{222} epitope was less protective due to limited antibody accessibility (170). Alternative novel B and T cell epitopes may be identified using *in silico* predictions and be combined into a multi-epitope construct. Further *in vivo*

studies are needed, however, to evaluate the protective potential of such vaccine candidates (171).

6.2.5 Viral Vector-Based Vaccines

Antigens delivered in the form of genetic information will be expressed in the natural environment of the cell, which helps to ensure the correct antigen generation and processing that is vital for a potent immune response. Vectored vaccines deliver the genetic material encoding the antigen of interest by incorporation into unrelated live attenuated or replication incompetent viruses (**Figure 5B**). A large number of viral vectors are available that each differ in their ability to stimulate different arms of the immune system, but also in more practical characteristics including genomic stability, accepted insertion size, and safety profile (172).

Experimental NA-based vector vaccines have been described among others for pox virus (173, 174) or parainfluenza virus (175) vectors. Modified Vaccinia Ankara (MVA), a safe and commonly used live poxviral vector, that expressed NA (MVA-NA) of H1N1pdm09 was analyzed for its protective efficacy. The MVA-NA vaccine induced high NAI titers and a potent cellular response characterized by particularly strong activation of CD8 T cells. Immunization conferred partial protection against replication of a homologous virus (173). A raccoonpox vector expressing the NA of avian H5N1 conferred full protection to mice against an otherwise lethal challenge when administered *via* the intranasal (IN) route. Interestingly, depletion of CD4 and CD8 T cells strongly reduced protection, suggesting an important role for cellular immunity in the protection provided by this vector (174). In contrast, parainfluenza 5 (PIV5) expressing the NA of H1N1pdm09 or avian H5N1 induced weak T cell responses and was dependent on antibodies for protection. PIV5 expressing the H1N1pdm09 NA conferred partial cross-protection against H5N1 and H3N2 challenge, whereas PIV5 expressing the H5N1 NA protected against H1N1, but not H3N2 (175). Other NA-expressing viral vectors that have been applied with varied success in a veterinary setting are Newcastle disease virus, infectious laryngotracheitis virus and alphavirus replicons (176–179).

6.2.6 Nucleic Acid-Based Vaccines

Nucleic acid-based vaccines directly deliver the genetic information encoding the antigen without the need for a viral vector (**Figure 5B**). In doing so, these methods exploit the benefits of *in vivo* antigen expression while eliminating the risks for reduced efficacy due to anti-vector immunity and safety concerns associated with viral vector-based vaccines. Production of this type of vaccines is rapid and scalable, which could be a critical advantage over other vaccine platforms in the event of a new emerging strain. Recent advances in stability and delivery of RNA and DNA vaccine formulations have led to improved immunogenicity, resulting in a renewed interest in using these technologies for emerging infectious diseases (172, 180, 181). mRNA vaccine technology was particularly accelerated by the current SARS-CoV-2 pandemic with the development of two highly effective vaccines based on this technology (182, 183).

Several studies reported the protective potential of NA antigens delivered by vaccination with plasmid DNA. An early study comparing the ability of various IAV antigens delivered by plasmid DNA to induce a protective immune response showed that only immunization with HA or NA, but not other internal IAV antigens, protected mice against homologous H1N1 challenge (184). In a follow-up study DNA vaccination with N2 induced full protection against challenge with homologous and drifted H3N2 strains, but was not effective in protecting against H1N1 challenge (185). Plasmid DNA encoding N1 from H1N1 conferred full protection against homologous challenge and 40-50% protection against H5N1 (186). Efficacy of a H5 DNA vaccine against challenge with a distant H5N1 strain was boosted from 75% to 100% with the addition of a N1-encoding plasmid (187).

NA-based mRNA vaccines have demonstrated high potency in some studies, but lower in another (188–190). Lipid encapsulated mRNA vaccines encoding various antigens of H1N1pdm09, separate or in a combination vaccine, elicited a strong humoral and cellular response in mice. The NA component of the vaccine was found to be the only one eliciting high NAI titers and protecting against a highly lethal dose of a matched challenge virus. A vaccine dose as low as 0.05 μg was sufficient to elicit a protective immune response. The NA mRNA vaccine however provided only limited or no protection against heterosubtypic challenge while the other more conserved vaccine components were fully protective (190) Similarly, in a recent study vaccination with mRNA encoding NA of H1N1pdm09 induced high NAI titers and protected against mortality from challenge with pre-pandemic H1N1 and H5N1. Serum antibodies from vaccinated mice however did not cross-react with H3N2 or influenza B virus (189) In an earlier study the immunogenicity of a N1-mRNA vaccine was considerably lower. High dose vaccination induced only 40% protection against a matched challenge in mice. Supplementing a H1-mRNA vaccine with the N1-mRNA however resulted in significantly reduced morbidity over the H1-only vaccine (188). The potential of mRNA vaccines might be boosted further by the use of self-replicating RNAs, which may induce high expression levels after low dose vaccination (191, 192).

7 OUTLOOK

Various studies mentioned in this review describe NA-based vaccine candidates with impressive protective efficacy against homologous and heterologous challenge strains, although most candidates have yet to be tested in models other than mice. In view of the potential of NA to induce protective immunity, efforts to improve vaccine efficacy against influenza should not only focus on HA, but also on NA. Improving the NA component of current vaccines with respect to antigenic match and immunogenicity, would likely improve the efficacy of these vaccines in the short term. NA additionally should be considered in the development of next-generation vaccines, besides the largely HA-focused approaches.

While studying the protective efficacy of isolated NA-based vaccine candidates is informative, NA particularly has potential as a component in a multi-antigen vaccine. Vaccines targeting both HA and NA provide better and broader protection, as evidenced by reduced disease and transmission when compared to HA- or NA-only vaccines. Given that the antigenic drift of HA and NA is discordant (76) a seasonal vaccine combining both antigens would be less likely to be mismatched with circulating strains for both antigens, compared to a HA-focussed vaccine.

Most vaccine candidates described here induce a protective immune response against homologous and in some cases intra-subtypic heterologous NA, but not heterosubtypic NA. The application of strategies aimed at increasing the breadth of the immune response is vital to improve protection against drifted or new emerging strains. The induction of broadly protective heterologous immune responses may be enhanced by computational design of consensus antigens. Protective responses against different NA subtypes may be achieved by simple mixing of NA antigens, though the breadth may in such vaccines still be limited to the strains used for immunization like in the current seasonal vaccines. Additional measures may be required to ensure that the elicited immune response surpasses the immunization strains. To direct the immune responses more towards conserved epitopes the option of combining NAs from multiple strains onto heteromultivalent mosaic nanoparticles could be explored.

The recent market application of mRNA vaccines targeting SARS-CoV-2 is likely to pave the road for the clinical use of this vaccine platform for novel influenza vaccines. Prior to the emergence of SARS-CoV-2 it was already recognized that mRNA vaccines would be suitable specifically in an outbreak setting mostly due to the capacity for rapid development, in addition to the low dose requirement and high potency (180). mRNA vaccines encoding HA of potential pandemic strains have already demonstrated safety and immunogenicity in ferrets, non-human primates and humans (193) and clinical trials for seasonal HA-based mRNA vaccines are underway (Clinical Trials Identifiers NCT04956575 and NCT04969276). Addition of NA-encoding mRNA to such formulations is likely to improve the magnitude and breadth of protection and should be advocated.

AUTHOR CONTRIBUTIONS

SC, MP, MB, XS, and CH wrote the manuscript. SC, MP, and MB created the figures. MB made **Table 1**. All authors contributed to the article and approved the submitted version.

FUNDING

This work was supported in part by the ENDFLU project that has received funding from the European Union's Horizon 2020 research and innovation programme under grant agreement No 874650. The present work was also a part of the research program of the Netherlands Centre for One Health (www.ncoh.nl) and was financially supported through the One Health Investment Fund from the Faculty of Veterinary Medicine of the Utrecht University.

REFERENCES

1. Paget J, Marquet R, Meijer A, van der Velden K. Influenza Activity in Europe During Eight Seasons (1999-2007): An Evaluation of the Indicators Used to Measure Activity and an Assessment of the Timing, Length and Course of Peak Activity (Spread) Across Europe. *BMC Infect Dis* (2007) 7 (1):1–7. doi: 10.1186/1471-2334-7-141
2. Ng S, Gordon A. Influenza Burden and Transmission in the Tropics. *Curr Epidemiol Rep* (2015) 2(2):89–100. doi: 10.1007/s40471-015-0038-4
3. Demicheli V, Jefferson T, Di Pietrantonj C, Ferroni E, Thorning S, Thomas RE, et al. Vaccines for Preventing Influenza in the Elderly. *Cochrane Database Syst Rev* (2018) 2(2):CD004876. doi: 10.1002/14651858.CD004876.pub4
4. Rodrigues BS, David C, Costa J, Ferreira JJ, Pinto FJ, Caldeira D. Influenza Vaccination in Patients With Heart Failure: A Systematic Review and Meta-Analysis of Observational Studies. *Heart* (2020) 106(5):350–7. doi: 10.1136/heartjnl-2019-315193
5. Belongia EA, Kieke BA, Donahue JG, Greenlee RT, Balish A, Foust A, et al. Effectiveness of Inactivated Influenza Vaccines Varied Substantially With Antigenic Match From the 2004-2005 Season to the 2006-2007 Season. *J Infect Dis* (2009) 199(2):159–67. doi: 10.1086/595861
6. Hutchinson EC, Charles PD, Hester SS, Thomas B, Trudgian D, Martinez-Alonso M, et al. Conserved and Host-Specific Features of Influenza Virion Architecture. *Nat Commun* (2014) 5:4816. doi: 10.1038/ncomms5816
7. Barman S, Adhikary L, Chakrabarti AK, Bernas C, Kawaoka Y, Nayak DP. Role of Transmembrane Domain and Cytoplasmic Tail Amino Acid Sequences of Influenza A Virus Neuraminidase in Raft Association and Virus Budding. *J Virol* (2004) 78(10):5258–69. doi: 10.1128/jvi.78.10.5258-5269.2004
8. Rossman JS, Lamb RA. Influenza Virus Assembly and Budding. *Virology* (2011) 411(2):229–36. doi: 10.1016/j.virol.2010.12.003
9. Kundu A, Avalos RT, Sanderson CM, Nayak DP. Transmembrane Domain of Influenza Virus Neuraminidase, A Type II Protein, Possesses an Apical Sorting Signal in Polarized MDCK Cells. *J Virol* (1996) 70(9):6508–15. doi: 10.1128/jvi.70.9.6508-6515.1996
10. Nordholm J, Da Silva DV, Damjanovic J, Dou D, Daniels R. Polar Residues and Their Positional Context Dictate the Transmembrane Domain Interactions of Influenza a Neuraminidases. *J Biol Chem* (2013) 288 (15):10652–60. doi: 10.1074/jbc.M112.440230
11. Da Silva DV, Nordholm J, Madjo U, Pfeiffer A, Daniels R. Assembly of Subtype 1 Influenza Neuraminidase Is Driven by Both the Transmembrane and Head Domains. *J Biol Chem* (2013) 288(1):644–53. doi: 10.1074/jbc.M112.424150
12. Air GM. Influenza Neuraminidase. *Influenza Other Respi Viruses* (2012) 6 (4):245–5. doi: 10.1111/j.1750-2659.2011.00304.x
13. Li J, Dohna H, Cardona CJ, Miller J, Carpenter TE. Emergence and Genetic Variation of Neuraminidase Stalk Deletions in Avian Influenza Viruses. *PloS One* (2011) 6(2):e14722. doi: 10.1371/journal.pone.0014722
14. Baigent SJ, McCauley JW. Glycosylation of Haemagglutinin and Stalk-Length of Neuraminidase Combine to Regulate the Growth of Avian Influenza Viruses in Tissue Culture. *Virus Res* (2001) 79(1–2):177–85. doi: 10.1016/S0168-1702(01)00272-6
15. Wang M, Qi J, Liu Y, Vavricka C, Wu Y, Li Q, et al. Influenza A Virus N5 Neuraminidase Has an Extended 150-Cavity. *J Virol* (2011) 85(16):8431–5. doi: 10.1128/JVI.00638-11
16. Sun X, Li Q, Wu Y, Wang M, Liu Y, Qi J, et al. Structure of Influenza Virus N7: The Last Piece of the Neuraminidase "Jigsaw" Puzzle. *J Virol* (2014) 88 (16):9197–207. doi: 10.1128/jvi.00805-14

17. Li Q, Qi J, Wu Y, Kiyota H, Tanaka K, Suhara Ys, et al. Functional and Structural Analysis of Influenza Virus Neuraminidase N3 Offers Further Insight Into the Mechanisms of Oseltamivir Resistance. *J Virol* (2013) 87 (18):10016–24. doi: 10.1128/JVI.01129-13
18. Xu X, Zhu X, Dwek RA, Stevens J, Wilson IA. Structural Characterization of the 1918 Influenza Virus H1N1 Neuraminidase. *J Virol* (2008) 82 (21):10493–501. doi: 10.1128/JVI.00959-08
19. Russell RJ, Haire LF, Stevens DJ, Collins PJ, Lin YP, Blackburn GM, et al. The Structure of H5N1 Avian Influenza Neuraminidase Suggests New Opportunities for Drug Design. *Nature* (2006) 443(7107):45–9. doi: 10.1038/nature05114
20. Varghese J, Colman P. Three-Dimensional Structure of the Neuraminidase of Influenza Virus A/Tokyo/3/67 at 2.2 A Resolution. *J Mol Biol* (1991) 221 (2):473–86. doi: 10.1016/0022-2836(91)80068-6
21. Tulip WR, Varghese JN, Baker AT, van Donkelaar A, Laver WG, Webster RG, et al. Refined Atomic Structures of N9 Subtype Influenza Virus Neuraminidase and Escape Mutants. *J Mol Biol* (1991) 221(2):487–97. doi: 10.1016/0022-2836(91)80069-7
22. Burmeister WP, Ruigrok RWH, Cusack S. The 2.2 Å Resolution Crystal Structure of Influenza B Neuraminidase and Its Complex With Sialic Acid. *EMBO J* (1992) 11(1):49–5. doi: 10.1002/j.1460-2075.1992.tb05026.x
23. Roggentin P, Rothe B, Kaper JB, Galen J, Lawrisuk L, Vimr ER, et al. Conserved Sequences in Bacterial and Viral Sialidases. *Glycoconj J* (1989) 6 (3):349–53. doi: 10.1007/BF01047853
24. Deroo T, Jou WM, Fiers W. Recombinant Neuraminidase Vaccine Protects Against Lethal Influenza. *Vaccine* (1996) 14(6):561–9. doi: 10.1016/0264-410X(95)00157-V
25. Chong AKJ, Pegg MS, von Itzstein M. Influenza Virus Sialidase: Effect of Calcium on Steady-State Kinetic Parameters. *Biochim Biophys Acta (BBA)/Protein Struct Mol* (1991) 1077(1):65–71. doi: 10.1016/0167-4838(91)90526-6
26. Wang H, Dou D, Östbye H, Revol R, Daniels R. Structural Restrictions for Influenza Neuraminidase Activity Promote Adaptation and Diversification. *Nat Microbiol* (2019) 4(12):2565–77. doi: 10.1038/s41564-019-0537-z
27. Burmeister WP, Cusack S, Ruigrok RWH. Calcium Is Needed for the Thermostability of Influenza B Virus Neuraminidase. *J Gen Virol* (1994) 75(2):381–8. doi: 10.1099/0022-1317-75-2-381
28. Dimmock NJ. Dependence of the Activity of an Influenza Virus Neuraminidase Upon Ca2+. *J Gen Virol* (1971) 13(3):481–3. doi: 10.1099/0022-1317-13-3-481
29. Li L, Li Y, Zhang L, Hou T. Theoretical Studies on the Susceptibility of Oseltamivir Against Variants of 2009 A/H1N1 Influenza Neuraminidase. *J Chem Inf Model* (2012) 52(10):2715–29. doi: 10.1021/ci300375k
30. Amaro RE, Swift RV, Votapka L, Li WW, Walker RC, Bush RM. Mechanism of 150-Cavity Formation in Influenza Neuraminidase. *Nat Commun* (2011) 2(1):388. doi: 10.1038/ncomms1390
31. Wu Y, Qin G, Gao F, Liu Y, Vavricka CJ, Qi J, et al. Induced Opening of Influenza Virus Neuraminidase N2 150-Loop Suggests an Important Role in Inhibitor Binding. *Sci Rep* (2013) 3(1):1–8. doi: 10.1038/srep01551
32. Du W, de Vries E, van Kuppeveld FJM, Matrosovich M, de Haan CAM. Second Sialic Acid-Binding Site of Influenza A Virus Neuraminidase: Binding Receptors for Efficient Release. *FEBS J* (2021) 288(19):5598–612. doi: 10.1111/febs.15668
33. Du W, Guo H, Nijman VS, Doedt J, van der Vries E, van der Lee J, et al. The 2nd Sialic Acid-Binding Site of Influenza a Virus Neuraminidase Is an Important Determinant of the Hemagglutinin-Neuraminidase-Receptor Balance. *PloS Pathog* (2019) 15(6):e1007860. doi: 10.1371/journal.ppat.1007860
34. Uhlendorff J, Matrosovich T, Klenk H, Matrosovich M. Functional Significance of the Hemadsorption Activity of Influenza Virus Neuraminidase and Its Alteration in Pandemic Viruses. *Arch Virol* (2009) 154(6):945–57. doi: 10.1007/S00705-009-0393-X
35. Benton DJ, Gamblin SJ, Rosenthal PB, Skehel JJ. Structural Transitions in Influenza Haemagglutinin at Membrane Fusion PH. *Nature* (2020) 583 (7814):150–3. doi: 10.1038/s41586-020-2333-6
36. Cohen M, Zhang XQ, Senaati HP, Chen HW, Varki NM, Schooley RT, et al. Influenza A Penetrates Host Mucus by Cleaving Sialic Acids With Neuraminidase. *Virol J* (2013) 10(1):1–13. doi: 10.1186/1743-422X-10-321
37. Matrosovich MN, Matrosovich TY, Gray T, Roberts NA, Klenk HD. Human and Avian Influenza Viruses Target Different Cell Types in Cultures of Human Airway Epithelium. *Proc Natl Acad Sci USA* (2004) 101(13):4620–4. doi: 10.1073/pnas.0308001101
38. de Vries E, Du W, Guo H, de Haan CAM. Influenza A Virus Hemagglutinin–Neuraminidase–Receptor Balance: Preserving Virus Motility. *Trends Microbiol* (2020) 28(1):57–67. doi: 10.1016/j.tim.2019.08.010
39. Matrosovich MN, Matrosovich TY, Gray T, Roberts NA, Klenk H-D. Neuraminidase Is Important for the Initiation of Influenza Virus Infection in Human Airway Epithelium. *J Virol* (2004) 78(22):12665. doi: 10.1128/JVI.78.22.12665-12667.2004
40. Su B, Wurtzer S, Rameix-Welti MA, Dwyer D, van der Werf S, Naffakh N, et al. Enhancement of the Influenza a Hemagglutinin (HA)-Mediated Cell-Cell Fusion and Virus Entry by the Viral Neuraminidase (Na). *PloS One* (2009) 4(12):e8495. doi: 10.1371/journal.pone.0008495
41. Palese P, Compans RW. Inhibition of Influenza Virus Replication in Tissue Culture by 2 Deoxy 2,3 Dehydro N Trifluoroacetylneuraminic Acid (FANA): Mechanism of Action. *J Gen Virol* (1976) 33(1):159–63. doi: 10.1099/0022-1317-33-1-159
42. Vahey MD, Fletcher DA. Influenza a Virus Surface Proteins Are Organized to Help Penetrate Host Mucus. *Elife* (2019) 8:e43764. doi: 10.7554/eLife.43764
43. Fei Y, Sun YS, Li Y, Yu H, Lau K, Landry JP, et al. Characterization of Receptor Binding Profiles of Influenza a Viruses Using an Ellipsometry-Based Label-Free Glycan Microarray Assay Platform. *Biomolecules* (2015) 5 (3):1480–98. doi: 10.3390/biom5031480
44. Guo H, Rabouw H, Slomp A, Dai M, van der Vegt F, van Lent JWM, et al. Kinetic Analysis of the Influenza A Virus HA/NA Balance Reveals Contribution of NA to Virus-Receptor Binding and NA-Dependent Rolling on Receptor-Containing Surfaces. *PloS Pathog* (2018) 14(8):e1007233. doi: 10.1371/journal.ppat.1007233
45. Park S, Il Kim J, Lee I, Bae JY, Yoo K, Nam M, et al. Adaptive Mutations of Neuraminidase Stalk Truncation and Deglycosylation Confer Enhanced Pathogenicity of Influenza A Viruses. *Sci Rep* (2017) 7(1):10928. doi: 10.1038/s41598-017-11348-0
46. Hossain MJ, Hickman D, Perez DR. Evidence of Expanded Host Range and Mammalian-Associated Genetic Changes in a Duck H9N2 Influenza Virus Following Adaptation in Quail and Chickens. *PloS One* (2008) 3(9):e3170. doi: 10.1371/journal.pone.0003170
47. Matrosovich M, Zhou N, Kawaoka Y, Webster R. The Surface Glycoproteins of H5 Influenza Viruses Isolated From Humans, Chickens, and Wild Aquatic Birds Have Distinguishable Properties. *J Virol* (1999) 73(2):1146–55. doi: 10.1128/jvi.73.2.1146-1155.1999
48. Munier S, Larcher T, Cormier-Aline F, Soubieux D, Su B, Guigand L, et al. A Genetically Engineered Waterfowl Influenza Virus With a Deletion in the Stalk of the Neuraminidase Has Increased Virulence for Chickens. *J Virol* (2010) 84(2):940–52. doi: 10.1128/jvi.01581-09
49. Zhou H, Yu Z, Hu Y, Tu J, Zou W, Peng Y, et al. The Special Neuraminidase Stalk-Motif Responsible for Increased Virulence and Pathogenesis of H5N1 Influenza A Virus. *PloS One* (2009) 4(7):e6277. doi: 10.1371/journal.pone.0006277
50. Chen YQ, Wohlbold TJ, Zheng NY, Huang M, Huang Y, Neu KE, et al. Influenza Infection in Humans Induces Broadly Cross-Reactive and Protective Neuraminidase-Reactive Antibodies. *Cell* (2018) 173(2):417–29. doi: 10.1016/j.cell.2018.03.030
51. Tan J, O'Dell G, Hernandez M, Sordillo E, Kahn Z, Kriti D, et al. Human Anti-Neuraminidase Antibodies Reduce Airborne Transmission of Clinical Influenza Virus Isolates in the Guinea Pig Model. *J Virol* (2021) JVI0142121. doi: 10.1128/JVI.01421-21
52. Wohlbold TJ, Podolsky KA, Chromikova V, Kirkpatrick E, Falconieri V, Meade P, et al. Broadly Protective Murine Monoclonal Antibodies Against Influenza B Virus Target Highly Conserved Neuraminidase Epitopes. *Nat Microbiol* (2017) 2(10):1415–24. doi: 10.1038/s41564-017-0011-8
53. Xiong FF, Liu XY, Gao FX, Luo J, Duan P, Tan WS, et al. Protective Efficacy of Anti-Neuraminidase Monoclonal Antibodies Against H7N9 Influenza Virus Infection. *Emerg Microbes Infect* (2020) 9(1):78–87. doi: 10.1080/22221751.2019.1708214

54. Bosch BJ, Bodewes R, Vries RP, de; Kreijtz JHCM, Bartelink W, Amerongen Gv, et al. Recombinant Soluble, Multimeric HA and NA Exhibit Distinctive Types of Protection Against Pandemic Swine-Origin 2009 A(H1N1) Influenza Virus Infection in Ferrets. *J Virol* (2010) 84(19):10366. doi: 10.1128/JVI.01035-10
55. Chen Z, Matsuo K, Asanuma H, Takahashi H, Iwasaki T, Suzuki Y, et al. Enhanced Protection Against a Lethal Influenza Virus Challenge by Immunization With Both Hemagglutinin- and Neuraminidase-Expressing DNAs. *Vaccine* (1999) 17(7–8):653–9. doi: 10.1016/S0264-410X(98)00247-3
56. Johansson BE. Immunization With Influenza A Virus Hemagglutinin and Neuraminidase Produced in Recombinant Baculovirus Results in a Balanced and Broadened Immune Response Superior to Conventional Vaccine. *Vaccine* (1999) 17(15–16):2073–80. doi: 10.1016/S0264-410X(98)00413-7
57. Johansson BE, Kilbourne ED. Dissociation of Influenza Virus Hemagglutinin and Neuraminidase Eliminates Their Intravirionic Antigenic Competition. *J Virol* (1993) 67(10):5721–3. doi: 10.1128/jvi.67.10.5721-5723.1993
58. Johansson BE, Matthews JT, Kilbourne ED. Supplementation of Conventional Influenza A Vaccine With Purified Viral Neuraminidase Results in a Balanced and Broadened Immune Response. *Vaccine* (1998) 16(9–10):1009–15. doi: 10.1016/S0264-410X(97)00279-X
59. Johansson BE, Pokorny BA, Tiso VA. Supplementation of Conventional Trivalent Influenza Vaccine With Purified Viral N1 and N2 Neuraminidases Induces a Balanced Immune Response Without Antigenic Competition. *Vaccine* (2002) 20(11–12):1670–4. doi: 10.1016/S0264-410X(01)00490-X
60. Monto AS, Kendal AP. Effect of Neuraminidase Antibody on Hong Kong Influenza. *Lancet* (1973) 301(7804):623–5. doi: 10.1016/S0140-6736(73)92196-X
61. Schulman JL, Khakpour M, Kilbourne ED. Protective Effects of Specific Immunity to Viral Neuraminidase on Influenza Virus Infection of Mice. *J Virol* (1968) 2(8):778–86. doi: 10.1128/jvi.2.8.778-786.1968
62. Couch RB, Kasel JA, Gerin JL, Schulman JL, Kilbourne ED. Induction of Partial Immunity to Influenza by a Neuraminidase Specific Vaccine. *J Infect Dis* (1974) 129(4):411–20. doi: 10.1093/infdis/129.4.411
63. Dowdle WR, Coleman MT, Mostow SR, Kaye HS, Schoenbaum SC. Inactivated Influenza Vaccines. 2. Laboratory Indices of Protection. *Postgrad Med J* (1973) 49(569):159–63. doi: 10.1136/pgmj.49.569.159
64. Couch RB, Atmar RL, Franco LM, Quarles JM, Wells J, Arden N, et al. Antibody Correlates and Predictors of Immunity to Naturally Occurring Influenza in Humans and the Importance of Antibody to the Neuraminidase. *J Infect Dis* (2013) 207(6):974–81. doi: 10.1093/infdis/jis935
65. Monto AS, Petrie JG, Cross RT, Johnson E, Liu M, Zhong W, et al. Antibody to Influenza Virus Neuraminidase: An Independent Correlate of Protection. *J Infect Dis* (2015) 212(8):1191–9. doi: 10.1093/INFDIS/JIV195
66. Memoli MJ, Shaw PA, Han A, Czajkowski L, Reed S, Athota R, et al. Evaluation of Antihemagglutinin and Antineuraminidase Antibodies as Correlates of Protection in an Influenza A/H1N1 Virus Healthy Human Challenge Model. *MBio* (2016) 7(2):e00417-16. doi: 10.1128/mBio.00417-16
67. Kosik I, Yewdell JW. Influenza Hemagglutinin and Neuraminidase: Yin-Yang Proteins Coevolving to Thwart Immunity. *Viruses* (2019) 11(4):346. doi: 10.3390/v11040346
68. Fiore AE, Uyeki TM, Broder K, Finelli L, Euler GL, Singleton JA, et al. Prevention and Control of Influenza With Vaccines: Recommendations of the Advisory Committee on Immunization Practices (ACIP), 2010. *Morb Mortal Wkly Rep* (2010) 6(59):RR–8.
69. Heaton NS, Sachs D, Chen CJ, Hai R, Palese P. Genome-Wide Mutagenesis of Influenza Virus Reveals Unique Plasticity of the Hemagglutinin and NS1 Proteins. *Proc Natl Acad Sci USA* (2013) 110(50):20248–53. doi: 10.1073/pnas.1320524110
70. Smith DJ, Lapedes AS, De Jong JC, Bestebroer TM, Rimmelzwaan GF, Osterhaus ADME, et al. Mapping the Antigenic and Genetic Evolution of Influenza Virus. *Science* (2004) 305(5682):371–6. doi: 10.1126/science.1097211
71. De Jong JC, Donker GA, Meijer A, van der Hoek W, Rimmelzwaan GF, Osterhaus ADME. Het Influenzaseizoen 2010/2011 in Nederland: Het Nieuwe A(H1N1)-Virus Van 2009 Blijft Actief. *Ned Tijdschr Voor Med Microbiol* (2011) 19(4):21–7.
72. Koel BF, Burke DF, Bestebroer TM, van der Vliet S, Zondag GCM, Vervaet G, et al. Substitutions Near the Receptor Binding Site Determine Major Antigenic Change During Influenza Virus Evolution. *Science* (2013) 342(6161):976–9. doi: 10.1126/science.1244730
73. Doud MB, Hensley SE, Bloom JD. Complete Mapping of Viral Escape From Neutralizing Antibodies. *PloS Pathog* (2017) 13(3):e1006271. doi: 10.1371/journal.ppat.1006271
74. Bhatt S, Holmes EC, Pybus OG. The Genomic Rate of Molecular Adaptation of the Human Influenza A Virus. *Mol Biol Evol* (2011) 28(9):2443–51. doi: 10.1093/molbev/msr044
75. Kilbourne ED, Johansson BE, Grajower B. Independent and Disparate Evolution in Nature of Influenza A Virus Hemagglutinin and Neuraminidase Glycoproteins. *Proc Natl Acad Sci USA* (1990) 87(2):786–90. doi: 10.1073/pnas.87.2.786
76. Sandbulte MR, Westgeest KB, Gao J, Xu X, Klimov AI, Russell CA, et al. Discordant Antigenic Drift of Neuraminidase and Hemagglutinin in H1N1 and H3N2 Influenza Viruses. *Proc Natl Acad Sci USA* (2011) 108(51):20748–53. doi: 10.1073/pnas.1113801108
77. Laver WG, Air GM, Webster RG, Markoff LJ. Amino Acid Sequence Changes in Antigenic Variants of Type A Influenza Virus N2 Neuraminidase. *Virology* (1982) 122(2):450–60. doi: 10.1016/0042-6822(82)90244-6
78. Westgeest KB, de Graaf M, Fourment M, Bestebroer TM, van Beek R, Spronken MIJ, et al. Genetic Evolution of the Neuraminidase of Influenza a (H3N2) Viruses From 1968 to 2009 and Its Correspondence to Haemagglutinin Evolution. *J Gen Virol* (2012) 93(Pt 9):1996–2007. doi: 10.1099/vir.0.043059-0
79. Kilbourne ED, Laver WG, Schulman JL, Webster RG. Antiviral Activity of Antiserum Specific for an Influenza Virus Neuraminidase. *J Virol* (1968) 2(4):281–8. doi: 10.1128/jvi.2.4.281-288.1968
80. Gao J, Couzens L, Burke DF, Wan H, Wilson P, Memoli MJ, et al. Antigenic Drift of the Influenza A(H1N1)Pdm09 Virus Neuraminidase Results in Reduced Effectiveness of A/California/7/2009 (H1N1pdm09)-Specific Antibodies. *MBio* (2019) 10(2):e00307–19. doi: 10.1128/MBIO.00307-19
81. Archetti I, Horsfall FL. Persistent Antigenic Variation of Influenza A Viruses After Incomplete Neutralization in Ovo With Heterologous Immune Serum. *J Exp Med* (1950) 92(5):441–62. doi: 10.1084/jem.92.5.441
82. Xie H, Wan XF, Ye Z, Plant EP, Zhao Y, Xu Y, et al. H3N2 Mismatch of 2014-15 Northern Hemisphere Influenza Vaccines and Head-To-Head Comparison Between Human and Ferret Antisera Derived Antigenic Maps. *Sci Rep* (2015) 5:15279. doi: 10.1038/srep15279
83. Linderman SL, Chambers BS, Zost SJ, Parkhousea K, Li Y, Herrmann C, et al. Potential Antigenic Explanation for Atypical H1n1 Infections Among Middle-Aged Adults During the 2013-2014 Influenza Season. *Proc Natl Acad Sci USA* (2014) 5:15279. doi: 10.1073/pnas.1409171111
84. Li GM, Chiu C, Wrammert J, McCausland M, Andrews SF, Zheng NY, et al. Pandemic H1N1 Influenza Vaccine Induces a Recall Response in Humans That Favors Broadly Cross-Reactive Memory B Cells. *Proc Natl Acad Sci USA* (2012) 109(23):9047–52. doi: 10.1073/pnas.1118979109
85. Chen Z, Wang W, Zhou H, Suguitan AL, Shambaugh C, Kim L, et al. Generation of Live Attenuated Novel Influenza Virus A/California/7/09 (H1N1) Vaccines With High Yield in Embryonated Chicken Eggs. *J Virol* (2010) 84(1):44–51. doi: 10.1128/jvi.02106-09
86. Lee MS, Yang CF. Cross-Reactive H1N1 Antibody Responses to a Live Attenuated Influenza Vaccine in Children: Implication for Selection of Vaccine Strains. *J Infect Dis* (2003) 188(9):1362–6. doi: 10.1086/379045
87. Dai M, Du W, Martínez-Romero C, Leenders T, Wennekes T, Rimmelzwaan GF, et al. Analysis of the Evolution of Pandemic Influenza a(H1N1) Virus Neuraminidase Reveals Entanglement of Different Phenotypic Characteristics. *MBio* (2021) 12(3):e00287–21. doi: 10.1128/mBio.00287-21
88. Lässig M, Mustonen V, Walczak AM. Predicting Evolution. *Nat Ecol Evol* (2017) 1(3):77. doi: 10.1038/s41559-017-0077
89. Wang Y, Lei R, Nourmohammed A, Wu NC. Antigenic Evolution of Human Influenza H3N2 Neuraminidase Is Constrained by Charge Balancing. *bioRxiv* (2021) 2021.07.10.451918. doi: 10.1101/2021.07.10.451918
90. Hensley SE, Das SR, Gibbs JS, Bailey AL, Schmidt LM, Bennink JR, et al. Influenza a Virus Hemagglutinin Antibody Escape Promotes Neuraminidase

Antigenic Variation and Drug Resistance. *PloS One* (2011) 6(2):e15190. doi: 10.1371/journal.pone.0015190
91. Kaplan BS, Anderson TK, Chang J, Santos J, Perez D, Lewis N, et al. Evolution and Antigenic Advancement of N2 Neuraminidase of Swine Influenza A Viruses Circulating in the United States Following Two Separate Introductions From Human Seasonal Viruses. *J Virol* (2021) 95 (20):e0063221. doi: 10.1128/JVI.00632-21
92. Wan H, Gao J, Xu K, Chen H, Couzens LK, Rivers KH, et al. Molecular Basis for Broad Neuraminidase Immunity: Conserved Epitopes in Seasonal and Pandemic H1N1 as Well as H5N1 Influenza Viruses. *J Virol* (2013) 87 (16):9290–300. doi: 10.1128/jvi.01203-13
93. Wan H, Qi L, Gao J, Couzens LK, Jiang L, Gao Y, et al. Comparison of the Efficacy of N9 Neuraminidase-Specific Monoclonal Antibodies Against Influenza A(H7N9) Virus Infection. *J Virol* (2018) 92(4):e01588–17. doi: 10.1128/jvi.01588-17
94. Wilson JR, Guo Z, Reber A, Kamal RP, Music N, Gansebom S, et al. An Influenza A Virus (H7N9) Anti-Neuraminidase Monoclonal Antibody With Prophylactic and Therapeutic Activity *In Vivo*. *Antiviral Res* (2016) 135:48–55. doi: 10.1016/j.antiviral.2016.10.001
95. Guo Z, Wilson JR, York IA, Stevens J. Biosensor-Based Epitope Mapping of Antibodies Targeting the Hemagglutinin and Neuraminidase of Influenza A Virus. *J Immunol Methods* (2018) 461:23–9. doi: 10.1016/j.jim.2018.07.007
96. Eichelberger M, Wan H. Influenza Neuraminidase as a Vaccine Antigen. *Curr Top Microbiol Immunol* (2015) 386:275–99. doi: 10.1007/82_2014_398
97. Wang B, Wang K, Meng P, Hu Y, Yang F, Liu K, et al. Design, Synthesis, and Evaluation of Carboxyl-Modified Oseltamivir Derivatives With Improved Lipophilicity as Neuraminidase Inhibitors. *Bioorg Med Chem Lett* (2018) 28 (21):3477–82. doi: 10.1016/j.bmcl.2018.09.014
98. Zhu X, Turner HL, Lang S, McBride R, Bangaru S, Gilchuk IM, et al. Structural Basis of Protection Against H7N9 Influenza Virus by Human Anti-N9 Neuraminidase Antibodies. *Cell Host Microbe* (2019) 26(6):729–38. doi: 10.1016/j.chom.2019.10.002
99. Gilchuk IM, Bangaru S, Gilchuk P, Irving RP, Kose N, Bombardi RG, et al. Influenza H7N9 Virus Neuraminidase-Specific Human Monoclonal Antibodies Inhibit Viral Egress and Protect From Lethal Influenza Infection in Mice. *Cell Host Microbe* (2019) 26(6):715–28. doi: 10.1016/j.chom.2019.10.003
100. Doyle TM, Hashem AM, Li C, Van Domselaar G, Larocque L, Wang J, et al. Universal Anti-Neuraminidase Antibody Inhibiting All Influenza A Subtypes. *Antiviral Res* (2013) 100(2):567–74. doi: 10.1016/j.antiviral.2013.09.018
101. Doyle TM, Li C, Bucher DJ, Hashem AM, Van Domselaar G, Wang K, et al. A Monoclonal Antibody Targeting a Highly Conserved Epitope in Influenza B Neuraminidase Provides Protection Against Drug Resistant Strains. *Biochem Biophys Res Commun* (2013) 441(1):226–9. doi: 10.1016/j.bbrc.2013.10.041
102. Madsen A, Dai YN, McMahon M, Schmitz AJ, Turner JS, Tan J, et al. Human Antibodies Targeting Influenza B Virus Neuraminidase Active Site Are Broadly Protective. *Immunity* (2020) 53(4):852–863.e. doi: 10.1016/j.immuni.2020.08.015
103. Wan H, Yang H, Shore DA, Garten RJ, Couzens L, Gao J, et al. Structural Characterization of a Protective Epitope Spanning A(H1N1)Pdm09 Influenza Virus Neuraminidase Monomers. *Nat Commun* (2015) 6(1):1–10. doi: 10.1038/ncomms7114
104. Jiang L, Fantoni G, Couzens L, Gao J, Plant E, Ye Z. Comparative Efficacy of Monoclonal Antibodies That Bind to Different Epitopes of the 2009 Pandemic H1N1 Influenza Virus Neuraminidase. *J Virol* (2016) 90(1):117–28. doi: 10.1128/JVI.01756-15
105. Stadlbauer D, Zhu X, McMahon M, Turner JS, Wohlbold TJ, Schmitz AJ, et al. Broadly Protective Human Antibodies That Target the Active Site of Influenza Virus Neuraminidase. *Science* (2019) 366(6464):499–504. doi: 10.1126/science.aay0678
106. Rijal P, Wang BB, Tan TK, Schimanski L, Janesch P, Dong T, et al. Broadly Inhibiting Antineuraminidase Monoclonal Antibodies Induced by Trivalent Influenza Vaccine and H7N9 Infection in Humans. *J Virol* (2020) 94(4): e01182–19. doi: 10.1128/jvi.01182-19
107. Jiang H, Peng W, Qi J, Chai Y, Song H, Bi Y, et al. Structure-Based Modification of an Anti-Neuraminidase Human Antibody Restores Protection Efficacy Against the Drifted Influenza Virus. *MBio* (2020) 11 (5):e02315–20. doi: 10.1128/mBio.02315-20
108. Gulati U, Hwang C-C, Venkatramani L, Gulati S, Stray SJ, Lee JT, et al. Antibody Epitopes on the Neuraminidase of a Recent H3N2 Influenza Virus (A/Memphis/31/98). *J Virol* (2002) 76(23):12274–80. doi: 10.1128/jvi.76.23.12274-12280.2002?
109. Malby RL, Tulip WR, Harley VR, McKimm-Breschkin JL, Laver WG, Webster RG, et al. The Structure of a Complex Between the NC10 Antibody and Influenza Virus Neuraminidase and Comparison With the Overlapping Binding Site of the NC41 Antibody. *Structure* (1994) 2(8):733–46. doi: 10.1016/S0969-2126(00)00074-5
110. Tulip WR, Varghese JN, Laver WG, Webster RG, Colman PM. Refined Crystal Structure of the Influenza Virus N9 Neuraminidase-NC41 Fab Complex. *J Mol Biol* (1992) 227(1):122–48. doi: 10.1016/0022-2836(91)80069-7
111. Wan Z, Ye J, Sang J, Shao H, Qian K, Jin W, et al. Identification of Amino Acids in H9N2 Influenza Virus Neuraminidase That Are Critical for the Binding of Two Mouse Monoclonal Antibodies. *Vet Microbiol* (2016) 187:58–63. doi: 10.1016/j.vetmic.2016.03.011
112. Kirkpatrick Roubidoux E, McMahon M, Carreño JM, Capuano C, Jiang K, Simon V, et al. Identification and Characterization of Novel Antibody Epitopes on the N2 Neuraminidase. *mSphere* (2021) 6(1):e00958–20. doi: 10.1128/msphere.00958-20
113. Job ER, Schotsaert M, Ibañez LI, Smet A, Ysenbaert T, Roose K, et al. Antibodies Directed Toward Neuraminidase N1 Control Disease in a Mouse Model of Influenza. *J Virol* (2018) 92(4):e01584–17. doi: 10.1128/jvi.01584-17
114. Saito T, Taylor G, Laver WG, Kawaoka Y, Webster RG. Antigenicity of the N8 Influenza A Virus Neuraminidase: Existence of an Epitope at the Subunit Interface of the Neuraminidase. *J Virol* (1994) 68(3):1790–6. doi: 10.1128/jvi.68.3.1790-1796.1994
115. Colman PM, Hoyne PA, Lawrence MC. Sequence and Structure Alignment of Paramyxovirus Hemagglutinin-Neuraminidase With Influenza Virus Neuraminidase. *J Virol* (1993) 67(6):2972–80. doi: 10.1128/jvi.67.6.2972-2980.1993
116. Schmidt AG, Therkelsen MD, Stewart S, Kepler TB, Liao HX, Moody MA, et al. Viral Receptor-Binding Site Antibodies With Diverse Germline Origins. *Cell* (2015) 161(5):1026–34. doi: 10.1016/j.cell.2015.04.028
117. Lee PS, Ohshima N, Stanfield RL, Yu W, Iba Y, Okuno Y, et al. Receptor Mimicry by Antibody F045-092 Facilitates Universal Binding to the H3 Subtype of Influenza Virus. *Nat Commun* (2014) 5:3614. doi: 10.1038/ncomms4614
118. Harmsen M, Blokker J, Pritz-Verschuren S, Bartelink W, van der Burg H, Koch G. Isolation of Panels of Llama Single-Domain Antibody Fragments Binding All Nine Neuraminidase Subtypes of Influenza A Virus. *Antibodies* (2013) 2(2):168–92. doi: 10.3390/antib2020168
119. Cardoso FM, Ibanez LI, Van den Hoecke S, De Baets S, Smet A, Roose K, et al. Single-Domain Antibodies Targeting Neuraminidase Protect Against an H5N1 Influenza Virus Challenge. *J Virol* (2014) 88(15):8278–96. doi: 10.1128/jvi.03178-13
120. Barbey-Martin C, Gigant B, Bizebard T, Calder LJ, Wharton SA, Skehel JJ, et al. An Antibody That Prevents the Hemagglutinin Low PH Fusogenic Transition. *Virology* (2002) 294(1):70–4. doi: 10.1006/viro.2001.1320
121. Iba Y, Fujii Y, Ohshima N, Sumida T, Kubota-Koketsu R, Ikeda M, et al. Conserved Neutralizing Epitope at Globular Head of Hemagglutinin in H3N2 Influenza Viruses. *J Virol* (2014) 88(13):7130–44. doi: 10.1128/jvi.00420-14
122. Dilillo DJ, Tan GS, Palese P, Ravetch JV. Broadly Neutralizing Hemagglutinin Stalk-Specific Antibodies Require Fcγr Interactions for Protection Against Influenza Virus *In Vivo*. *Nat Med* (2014) 20(2):143–51. doi: 10.1038/nm.3443
123. Jegaskanda S, Vanderven HA, Wheatley AK, Kent SJ. Fc or Not Fc; That Is the Question: Antibody Fc-Receptor Interactions Are Key to Universal Influenza Vaccine Design. *Hum Vaccines Immunother* (2017) 13(6):1–9. doi: 10.1080/21645515.2017.1290018

124. DiLillo DJ, Palese P, Wilson PC, Ravetch JV. Broadly Neutralizing Anti-Influenza Antibodies Require Fc Receptor Engagement for *In Vivo* Protection. *J Clin Invest* (2016) 126(2):605–10. doi: 10.1172/JCI84428
125. Henry Dunand CJ, Leon PE, Huang M, Choi A, Chromikova V, Ho IY, et al. Both Neutralizing and Non-Neutralizing Human H7N9 Influenza Vaccine-Induced Monoclonal Antibodies Confer Protection. *Cell Host Microbe* (2016) 19(6):800–13. doi: 10.1016/j.chom.2016.05.014
126. Job ER, Ysenbaert T, Smet A, Van Hecke A, Meuris L, Kleanthous H, et al. Fcγ Receptors Contribute to the Antiviral Properties of Influenza Virus Neuraminidase-Specific Antibodies. *MBio* (2019) 10(5):e01667–19. doi: 10.1128/mBio.01395-19
127. Yasuhara A, Yamayoshi S, Kiso M, Sakai-Tagawa Y, Koga M, Adachi E, et al. Antigenic Drift Originating From Changes to the Lateral Surface of the Neuraminidase Head of Influenza A Virus. *Nat Microbiol* (2019) 4(6):1024–34. doi: 10.1038/s41564-019-0401-1
128. Ito H, Nishimura H, Kisu T, Hagiwara H, Watanabe O, Kadji FMN, et al. Low Response in Eliciting Neuraminidase Inhibition Activity of Sera Among Recipients of a Split, Monovalent Pandemic Influenza Vaccine During the 2009 Pandemic. *PloS One* (2020) 15(5):e0233001. doi: 10.1371/JOURNAL.PONE.0233001
129. Powers DC, Kilbourne ED, Johansson BE. Neuraminidase-Specific Antibody Responses to Inactivated Influenza Virus Vaccine in Young and Elderly Adults. *Clin Diagn Lab Immunol* (1996) 3(5):511–6. doi: 10.1128/CDLI.3.5.511-516.1996
130. Couch RB, Atmar RL, Keitel WA, Quarles JM, Wells J, Arden N, et al. Randomized Comparative Study of the Serum Antihemagglutinin and Antineuraminidase Antibody Responses to Six Licensed Trivalent Influenza Vaccines. *Vaccine* (2012) 31(1):190–5. doi: 10.1016/J.VACCINE.2012.10.065
131. Getie-Kebtie M, Sultana I, Eichelberger M, Alterman M. Label-Free Mass Spectrometry-Based Quantification of Hemagglutinin and Neuraminidase in Influenza Virus Preparations and Vaccines. *Influenza Other Respi Viruses* (2013) 7(4):521–30. doi: 10.1111/IRV.12001
132. Sultana I, Yang K, Getie-Kebtie M, Couzens L, Markoff L, Alterman M, et al. Stability of Neuraminidase in Inactivated Influenza Vaccines. *Vaccine* (2014) 32(19):2225–30. doi: 10.1016/J.VACCINE.2014.01.078
133. McMahon M, Strohmeier S, Rajendran M, Capuano C, Ellebedy AH, Wilson PC, et al. Correctly Folded - But Not Necessarily Functional - Influenza Virus Neuraminidase Is Required to Induce Protective Antibody Responses in Mice. *Vaccine* (2020) 38(45):7129–37. doi: 10.1016/J.VACCINE.2020.08.067
134. Petrie J, Ohmit S, Johnson E, Truscon R, Monto A. Persistence of Antibodies to Influenza Hemagglutinin and Neuraminidase Following One or Two Years of Influenza Vaccination. *J Infect Dis* (2015) 212(12):1914–22. doi: 10.1093/INFDIS/JIV313
135. Kilbourne E, Couch R, Kasel J, Keitel W, Cate T, Quarles J, et al. Purified Influenza A Virus N2 Neuraminidase Vaccine Is Immunogenic and Non-Toxic in Humans. *Vaccine* (1995) 13(18):1799–803. doi: 10.1016/0264-410X(95)00127-M
136. Zheng A, Sun W, Xiong X, Freyn AW, Peukes J, Strohmeier S, et al. Enhancing Neuraminidase Immunogenicity of Influenza A Viruses by Rewiring RNA Packaging Signals. *J Virol* (2020) 94(16):e00742–20. doi: 10.1128/JVI.00742-20
137. Gao J, Wan H, Li X, Martinez MR, Klenow L, Gao Y, et al. Balancing the Influenza Neuraminidase and Hemagglutinin Responses by Exchanging the Vaccine Virus Backbone. *PloS Pathog* (2021) 17(4):e1009171. doi: 10.1371/JOURNAL.PPAT.1009171
138. Östbye H, Gao J, Martinez MR, Wang H, Gier JW de, Daniels R. N-Linked Glycan Sites on the Influenza A Virus Neuraminidase Head Domain Are Required for Efficient Viral Incorporation and Replication. *J Virol* (2020) 94(19):e00874–20. doi: 10.1128/JVI.00874-20
139. Broecker F, Zheng A, Suntronwong N, Sun W, Bailey MJ, Krammer F, et al. Extending the Stalk Enhances Immunogenicity of the Influenza Virus Neuraminidase. *J Virol* (2019) 93(18):e00840–19. doi: 10.1128/JVI.00840-19
140. Deng X, Wang Q, Liu M, Zheng Q, Wu F, Huang J. Tetrameric Neuraminidase of Influenza A Virus Is Required to Induce Protective Antibody Responses in Mice. *Front Microbiol* (2021) 12:729914. doi: 10.3389/FMICB.2021.729914
141. Sultana I, Gao J, Markoff L, Eichelberger MC. Influenza Neuraminidase-Inhibiting Antibodies Are Induced in the Presence of Zanamivir. *Vaccine* (2011) 29(14):2601–6. doi: 10.1016/J.VACCINE.2011.01.047
142. Gao J, Klenow L, Parsons L, Malik T, Phue J-N, Gao Z, et al. Design of the Recombinant Influenza Neuraminidase Antigen Is Crucial for Protective Efficacy. *J Virol* (2021), JVI0116021. doi: 10.1101/2021.04.29.442077
143. Schotsaert M, Ysenbaert T, Smet A, Schepens B, Vanderschaeghe D, Stegalkina S, et al. Long-Lasting Cross-Protection Against Influenza A by Neuraminidase and M2e-Based Immunization Strategies. *Sci Rep* (2016) 6:24402. doi: 10.1038/SREP24402
144. Liu WC, Lin CY, Tsou YT, Jan JT, Wu SC. Cross-Reactive Neuraminidase-Inhibiting Antibodies Elicited by Immunization With Recombinant Neuraminidase Proteins of H5N1 and Pandemic H1N1 Influenza A Viruses. *J Virol* (2015) 89(14):7224–34. doi: 10.1128/JVI.00585-15
145. Schmidt PM, Attwood RM, Mohr PG, Barrett SA, McKimm-Breschkin JLA. Generic System for the Expression and Purification of Soluble and Stable Influenza Neuraminidase. *PloS One* (2011) 6(2):e16284. doi: 10.1371/JOURNAL.PONE.0016284
146. Dai M, Guo H, Dortmans JCFM, Dekkers J, Nordholm J, Daniels R, et al. Identification of Residues That Affect Oligomerization and/or Enzymatic Activity of Influenza Virus H5N1 Neuraminidase Proteins. *J Virol* (2016) 90(20):9457. doi: 10.1128/JVI.01346-16
147. Streltsov VA, Schmidt PM, McKimm-Breschkin JL. Structure of an Influenza A Virus N9 Neuraminidase With a Tetrabrachion-Domain Stalk. *Acta Crystallogr Sect F Struct Biol Commun* (2019) 75(Pt 2):89–97. doi: 10.1107/S2053230X18017892
148. Strohmeier S, Carreño JM, Brito RN, Krammer F. Introduction of Cysteines in the Stalk Domain of Recombinant Influenza Virus N1 Neuraminidase Enhances Protein Stability and Immunogenicity in Mice. *Vaccines* (2021) 9(4):404. doi: 10.3390/VACCINES9040404
149. Ellis D, Lederhofer J, Acton OJ, Tsybovsky Y, Kephart S, Yap C, et al. Structure-Based Design of Stabilized Recombinant Influenza Neuraminidase Tetramers. *bioRxiv* (2021), 2021.05.17.444468. doi: 10.1101/2021.05.17.444468
150. Bullard BL, Weaver EA. Strategies Targeting Hemagglutinin as a Universal Influenza Vaccine. *Vaccines* (2021) 9(3):257. doi: 10.3390/VACCINES9030257
151. Job ER, Ysenbaert T, Smet A, Christopoulou I, Strugnell T, Oloo EO, et al. Broadened Immunity Against Influenza by Vaccination With Computationally Designed Influenza Virus N1 Neuraminidase Constructs. *NPJ Vaccines* (2018) 3:55. doi: 10.1038/S41541-018-0093-1
152. Skarlupka AL, Bebin-Blackwell A-G, Sumner SF, Ross TM. Universal Influenza Virus Neuraminidase Vaccine Elicits Protective Immune Responses Against Human Seasonal and Pre-Pandemic Strains. *J Virol* (2021) 95(17):e0075921. doi: 10.1128/JVI.00759-21
153. Bachmann MF, Jennings GT. Vaccine Delivery: A Matter of Size, Geometry, Kinetics and Molecular Patterns. *Nat Rev Immunol* (2010) 10(11):787–96. doi: 10.1038/NRI2868
154. Smith GE, Sun X, Bai Y, Liu YV, Massare MJ, Pearce MB, et al. Neuraminidase-Based Recombinant Virus-Like Particles Protect Against Lethal Avian Influenza A(H5N1) Virus Infection in Ferrets. *Virology* (2017) 509:90–7. doi: 10.1016/J.VIROL.2017.06.006
155. Lai JCC, Chan WWL, Kien F, Nicholls JM, Peiris JSM, Garcia J-M. Formation of Virus-Like Particles From Human Cell Lines Exclusively Expressing Influenza Neuraminidase. *J Gen Virol* (2010) 91(9):2322–30. doi: 10.1099/VIR.0.019935-0
156. Tao P, Luo M, Zhu D, Qu S, Yang Z, Gao M, et al. Virus-Like Particle Vaccine Comprised of the HA, NA, and M1 Proteins of an Avian Isolated H5N1 Influenza Virus Induces Protective Immunity Against Homologous and Heterologous Strains in Mice. *Viral Immunol* (2009) 22(4):273–81. doi: 10.1089/VIM.2009.0017
157. Wu C-Y, Yeh Y-C, Chan J-T, Yang Y-C, Yang J-R, Liu M-T, et al. A VLP Vaccine Induces Broad-Spectrum Cross-Protective Antibody Immunity Against H5N1 and H1N1 Subtypes of Influenza A Virus. *PloS One* (2012) 7(8):e42363. doi: 10.1371/JOURNAL.PONE.0042363
158. Easterbrook JD, Schwartzman LM, Gao J, Kash JC, Morens DM, Couzens L, et al. Protection Against a Lethal H5N1 Influenza Challenge by Intranasal Immunization With Virus-Like Particles Containing 2009 Pandemic H1N1

Neuraminidase in Mice. *Virology* (2012) 432(1):39–44. doi: 10.1016/J.VIROL.2012.06.003
159. Kim KH, Lee YT, Park S, Jung YJ, Lee Y, Ko EJ, et al. Neuraminidase Expressing Virus-Like Particle Vaccine Provides Effective Cross Protection Against Influenza Virus. *Virology* (2019) 535:179–88. doi: 10.1016/J.VIROL.2019.07.008
160. Menne Z, Pliasas VC, Compans RW, Glover S, Kyriakis CS, Skountzou I. Bivalent Vaccination With NA1 and NA2 Neuraminidase Virus-Like Particles Is Protective Against Challenge With H1N1 and H3N2 Influenza A Viruses in a Murine Model. *Virology* (2021) 562:197–208. doi: 10.1016/J.VIROL.2021.08.001
161. Liu J, Ren Z, Wang H, Zhao Y, Wilker PR, Yu Z, et al. Influenza Virus-Like Particles Composed of Conserved Influenza Proteins and GPI-Anchored CCL28/GM-CSF Fusion Proteins Enhance Protective Immunity Against Homologous and Heterologous Viruses. *Int Immunopharmacol* (2018) 63:119–28. doi: 10.1016/J.INTIMP.2018.07.011
162. Skountzou I, Quan F-S, Gangadhara S, Ye L, Vzorov A, Selvaraj P, et al. Incorporation of Glycosylphosphatidylinositol-Anchored Granulocyte-MacrophageColony-Stimulating Factor or CD40 Ligand Enhances Immunogenicity of Chimeric Simian Immunodeficiency Virus-Like Particles. *J Virol* (2007) 81(3):1083–94. doi: 10.1128/JVI.01692-06
163. Patel JM, Kim MC, Vartabedian VF, Lee YN, He S, Song JM, et al. Protein Transfer-Mediated Surface Engineering to Adjuvantate Virus-Like Nanoparticles for Enhanced Anti-Viral Immune Responses. *Nanomedicine* (2015) 11(5):1097–107. doi: 10.1016/J.NANO.2015.02.008
164. Wang Y, Deng L, Gonzalez GX, Luthra L, Dong C, Ma Y, et al. Double-Layered M2e-NA Protein Nanoparticle Immunization Induces Broad Cross-Protection Against Different Influenza Viruses in Mice. *Adv Healthc Mater* (2020) 9(2):1901176. doi: 10.1002/ADHM.201901176
165. Ueda G, Antanasijevic A, Fallas JA, Sheffler W, Copps J, Ellis D, et al. Tailored Design of Protein Nanoparticle Scaffolds for Multivalent Presentation of Viral Glycoprotein Antigens. *Elife* (2020) 9:1–30. doi: 10.7554/ELIFE.57659
166. Kanekiyo M, Wei C-J, Yassine HM, McTamney PM, Boyington JC, Whittle JRR, et al. Self-Assembling Influenza Nanoparticle Vaccines Elicit Broadly Neutralizing H1N1 Antibodies. *Nature* (2013) 499(7456):102–6. doi: 10.1038/NATURE12202
167. Marcandalli J, Fiala B, Ols S, Perotti M, Schueren W devd, Snijder J, et al. Induction of Potent Neutralizing Antibody Responses by a Designed Protein Nanoparticle Vaccine for Respiratory Syncytial Virus. *Cell* (2019) 176 (6):1420–31. doi: 10.1016/J.CELL.2019.01.046
168. Kanekiyo M, Joyce MG, Gillespie RA, Gallagher JR, Andrews SF, Yassine HM, et al. Mosaic Nanoparticle Display of Diverse Influenza Virus Hemagglutinins Elicits Broad B Cell Responses. *Nat Immunol* (2019) 20 (3):362–72. doi: 10.1038/S41590-018-0305-X
169. Kim KH, Jung YJ, Lee Y, Park BR, Oh J, Lee YN, et al. Cross Protection by Inactivated Recombinant Influenza Viruses Containing Chimeric Hemagglutinin Conjugates With a Conserved Neuraminidase or M2 Ectodomain Epitope. *Virology* (2020) 550:51–60. doi: 10.1016/J.VIROL.2020.08.003
170. Zeigler DF, Gage E, Clegg CH. Epitope-Targeting Platform for Broadly Protective Influenza Vaccines. *PloS One* (2021) 16(5):e0252170. doi: 10.1371/JOURNAL.PONE.0252170
171. Behbahani M, Moradi M, Mohabatkar H. In Silico Design of a Multi-Epitope Peptide Construct as a Potential Vaccine Candidate for Influenza A Based on Neuraminidase Protein. *Silico Pharmacol* (2021) 9(1):36. doi: 10.1007/S40203-021-00095-W
172. Rauch S, Jasny E, Schmidt KE, Petsch B. New Vaccine Technologies to Combat Outbreak Situations. *Front Immunol* (2018) 9:1963. doi: 10.3389/FIMMU.2018.01963
173. Hessel A, Schwendinger M, Fritz D, Coulibaly S, Holzer GW, Sabarth N, et al. A Pandemic Influenza H1N1 Live Vaccine Based on Modified Vaccinia Ankara Is Highly Immunogenic and Protects Mice in Active and Passive Immunizations. *PloS One* (2010) 5(8):e12217. doi: 10.1371/JOURNAL.PONE.0012217
174. Kingstad-Bakke B, Kamlangdee A, Osorio JE. Mucosal Administration of Raccoonpox Virus Expressing Highly Pathogenic Avian H5N1 Influenza Neuraminidase Is Highly Protective Against H5N1 and Seasonal Influenza Virus Challenge. *Vaccine* (2015) 33(39):5155–62. doi: 10.1016/J.VACCINE.2015.08.005
175. Mooney AJ, Gabbard JD, Li Z, Dlugolenski DA, Johnson SK, Tripp RA, et al. Vaccination With Recombinant Parainfluenza Virus 5 Expressing Neuraminidase Protects Against Homologous and Heterologous Influenza Virus Challenge. *J Virol* (2017) 91(23):e01579–17. doi: 10.1128/JVI.01579-17
176. Sylte M, Hubby B, Suarez D. Influenza Neuraminidase Antibodies Provide Partial Protection for Chickens Against High Pathogenic Avian Influenza Infection. *Vaccine* (2007) 25(19):3763–72. doi: 10.1016/J.VACCINE.2007.02.011
177. Ramp K, Veits J, Deckers D, Rudolf M, Grund C, Mettenleiter TC, et al. Coexpression of Avian Influenza Virus H5 and N1 by Recombinant Newcastle Disease Virus and the Impact on Immune Response in Chickens. *Avian Dis* (2011) 55(3):413–21. doi: 10.1637/9652-011111-REG.1
178. Nayak B, Kumar S, DiNapoli J, Paldurai A, Perez D, Collins P, et al. Contributions of the Avian Influenza Virus HA, NA, and M2 Surface Proteins to the Induction of Neutralizing Antibodies and Protective Immunity. *J Virol* (2010) 84(5):2408–20. doi: 10.1128/JVI.02135-09
179. Pavlova S, Veits J, Keil G, Mettenleiter T, Fuchs W. Protection of Chickens Against H5N1 Highly Pathogenic Avian Influenza Virus Infection by Live Vaccination With Infectious Laryngotracheitis Virus Recombinants Expressing H5 Hemagglutinin and N1 Neuraminidase. *Vaccine* (2009) 27 (5):773–85. doi: 10.1016/J.VACCINE.2008.11.033
180. Pardi N, Hogan MJ, Porter FW, Weissman D. MRNA Vaccines — a New Era in Vaccinology. *Nat Rev Drug Discovery* (2018) 17(4):261–79. doi: 10.1038/NRD.2017.243
181. Xu Z, Patel A, Tursi NJ, Zhu X, Muthumani K, Kulp DW, et al. Harnessing Recent Advances in Synthetic DNA and Electroporation Technologies for Rapid Vaccine Development Against COVID-19 and Other Emerging Infectious Diseases. *Front Med Technol* (2020) 0:571030. doi: 10.3389/FMEDT.2020.571030
182. Baden LR, Sahly HM El, Essink B, Kotloff K, Frey S, Novak R, et al. Efficacy and Safety of the MRNA-1273 SARS-CoV-2 Vaccine. *N Eng J Med* (2021) 384(5):403–16. doi: 10.1056/NEJMOA2035389
183. Polack FP, Thomas SJ, Kitchin N, Absalon J, Gurtman A, Lockhart S, et al. Safety and Efficacy of the BNT162b2 MRNA Covid-19 Vaccine. *N Eng J Med* (2020) 383(27):2603–15. doi: 10.1056/NEJMOA2034577
184. Chen Z, Sahashi Y, Matsuo K, Asanuma H, Takahashi H, Iwasaki T, et al. Comparison of the Ability of Viral Protein-Expressing Plasmid DNAs to Protect Against Influenza. *Vaccine* (1998) 16(16):1544–9. doi: 10.1016/S0264-410X(98)00043-7
185. Chen Z, Kadowaki SE, Hagiwara Y, Yoshikawa T, Matsuo K, Kurata T, et al. Cross-Protection Against a Lethal Influenza Virus Infection by DNA Vaccine to Neuraminidase. *Vaccine* (2000) 18(28):3214–22. doi: 10.1016/S0264-410X(00)00149-3
186. Sandbulte MR, Jimenez GS, Boon ACM, Smith LR, Treanor JJ, Webby RJ. Cross-Reactive Neuraminidase Antibodies Afford Partial Protection Against H5N1 in Mice and Are Present in Unexposed Humans. *PloS Med* (2007) 4 (2):e59. doi: 10.1371/JOURNAL.PMED.0040059
187. Torrieri-Dramard L, Lambrecht B, Ferreira HL, Van Den Berg T, Klatzmann D, Bellier B. Intranasal DNA Vaccination Induces Potent Mucosal and Systemic Immune Responses and Cross-Protective Immunity Against Influenza Viruses. *Mol Ther* (2011) 19(3):602–11. doi: 10.1038/MT.2010.222
188. Petsch B, Schnee M, Vogel AB, Lange E, Hoffmann B, Voss D, et al. Protective Efficacy of *In Vitro* Synthesized, Specific MRNA Vaccines Against Influenza A Virus Infection. *Nat Biotechnol* (2012) 30(12):1210–6. doi: 10.1038/NBT.2436
189. Freyn AW, Pine M, Rosado VC, Benz M, Muramatsu H, Beattie M, et al. Antigen Modifications Improve Nucleoside-Modified MRNA-Based Influenza Virus Vaccines in Mice. *Mol Ther - Methods Clin Dev* (2021) 22:84–95. doi: 10.1016/J.OMTM.2021.06.003
190. Freyn AW, Silva JR da, Rosado VC, Bliss CM, Pine M, Mui BL, et al. A Multi-Targeting, Nucleoside-Modified MRNA Influenza Virus Vaccine Provides Broad Protection in Mice. *Mol Ther* (2020) 28(7):1569–84. doi: 10.1016/J.YMTHE.2020.04.018
191. Bloom K, Berg Fvd, Arbuthnot P. Self-Amplifying RNA Vaccines for Infectious Diseases. *Gene Ther* (2021) 28(3–4):117–29. doi: 10.1038/S41434-020-00204-Y

192. Blakney AK, Ip S, Geall AJ. An Update on Self-Amplifying MRNA Vaccine Development. *Vaccines* (2021) 9(2):97. doi: 10.3390/VACCINES9020097
193. Bahl K, Senn JJ, Yuzhakov O, Bulychev A, Brito LA, Hassett KJ, et al. Preclinical and Clinical Demonstration of Immunogenicity by MRNA Vaccines Against H10N8 and H7N9 Influenza Viruses. *Mol Ther* (2017) 25(6):1316–27. doi: 10.1016/J.YMTHE.2017.03.035

Conflict of Interest: XS declares to receive funding from Sanofi Pasteur for research related to influenza vaccine development.

The remaining authors declare that the research was conducted in the absence of any commercial or financial relationships that could be construed as a potential conflict of interest.

Publisher's Note: All claims expressed in this article are solely those of the authors and do not necessarily represent those of their affiliated organizations, or those of the publisher, the editors and the reviewers. Any product that may be evaluated in this article, or claim that may be made by its manufacturer, is not guaranteed or endorsed by the publisher.

frontiers in Immunology

ORIGINAL RESEARCH
published: 23 November 2021
doi: 10.3389/fimmu.2021.747774

Matrix M Adjuvanted H5N1 Vaccine Elicits Broadly Neutralizing Antibodies and Neuraminidase Inhibiting Antibodies in Humans That Correlate With *In Vivo* Protection

Fan Zhou[1]*, *Lena Hansen*[1], *Gabriel Pedersen*[1,2], *Gunnveig Grødeland*[3] and *Rebecca Cox*[1,4]

[1] Influenza Center, Department of Clinical Science, University of Bergen, Bergen, Norway, [2] Center for Vaccine Research, Statens Serum Institut, Copenhagen, Denmark, [3] Department of Immunology, University of Oslo and Oslo University Hospital, Oslo, Norway, [4] Department of Microbiology, Haukeland University Hospital, Bergen, Norway

OPEN ACCESS

Edited by:
Mingtao Zeng,
Texas Tech University Health Sciences Center El Paso, United States

Reviewed by:
Rupsa Basu,
Helaina Inc., United States
Carolien Emma van de Sandt,
The University of Melbourne, Australia

***Correspondence:**
Fan Zhou
fan.zhou@uib.no

Specialty section:
This article was submitted to Vaccines and Molecular Therapeutics, a section of the journal Frontiers in Immunology

Received: 26 July 2021
Accepted: 05 November 2021
Published: 23 November 2021

Citation:
Zhou F, Hansen L, Pedersen G, Grødeland G and Cox R (2021) Matrix M Adjuvanted H5N1 Vaccine Elicits Broadly Neutralizing Antibodies and Neuraminidase Inhibiting Antibodies in Humans That Correlate With In Vivo Protection. Front. Immunol. 12:747774. doi: 10.3389/fimmu.2021.747774

The highly pathogenic avian influenza H5N1 viruses constantly evolve and give rise to novel variants that have caused widespread zoonotic outbreaks and sporadic human infections. Therefore, vaccines capable of eliciting broadly protective antibody responses are desired and under development. We here investigated the magnitude, kinetics and protective efficacy of the multi-faceted humoral immunity induced by vaccination in healthy adult volunteers with a Matrix M adjuvanted virosomal H5N1 vaccine. Vaccinees were given escalating doses of adjuvanted vaccine (1.5μg, 7.5μg, or 30μg), or a non-adjuvanted vaccine (30μg). An evaluation of sera from vaccinees against pseudotyped viruses covering all (sub)clades isolated from human H5N1 infections demonstrated that the adjuvanted vaccines (7.5μg and 30μg) could elicit rapid and robust increases of broadly cross-neutralizing antibodies against all clades. In addition, the adjuvanted vaccines also induced multifaceted antibody responses including hemagglutinin stalk domain specific, neuraminidase inhibiting, and antibody-dependent cellular cytotoxicity inducing antibodies. The lower adjuvanted dose (1.5μg) showed delayed kinetics, whilst the non-adjuvanted vaccine induced overall lower levels of antibody responses. Importantly, we demonstrate that human sera post vaccination with the adjuvanted (30μg) vaccine provided full protection against a lethal homologous virus challenge in mice. Of note, when combining our data from mice and humans we identified the neutralizing and neuraminidase inhibiting antibody titers as correlates of *in vivo* protection.

Keywords: H5N1 (Avian influenza), correlate of protection, adjuvant, Matrix M, pseudotype neutralization, neuraminidase inhibiting antibodies

INTRODUCTION

Enveloped RNA viruses, such as influenza viruses and coronaviruses, constantly evolve, thus causing zoonotic outbreaks and occasional pandemics in humans. Mutations accumulate over time and enable the virus to escape existing immunity established from previous infection and/or vaccination. This mechanism leads to the emergence of geographic and temporal novel variants, which hamper the effectiveness and efficacy of the vaccines designed based on ancestral viruses. As a result, vaccines targeting enveloped RNA viruses need to be updated at regular intervals. Vaccines capable of inducing broadly cross-protective immune responses are urgently needed.

Since its first isolation in 1996, the highly pathogenic avian influenza (HPAI) H5N1 virus have caused outbreaks in domestic and wild birds worldwide, as well as sporadic animal-human transmissions. To date, 862 human infections have been laboratory confirmed which resulting in 455 deaths (1). Tens of thousands of HPAI H5N1 virus strains have emerged in the last two decades. These variant strains are grouped into 10 clades and dozens of subclades according to the main surface glycoprotein hemagglutinin (HA) gene sequences. All the variants isolated from human infections are from clades 0, 1, 2 and 7 (2–4). To combat the HPAI H5N1 viruses in situations of potential human-to-human transmission, a panel of pre-pandemic H5N1 vaccine candidates from each of the most common (sub)clades have been prepared (3). Different vaccines formats, including subunit, live attenuated, and adenoviral vectores have been tested in clinical trials alone, or in combination with adjuvants such as AS03 and MF59 (5–9). These vaccines elicited protective homologous antibody responses and low to moderate levels of neutralizing antibodies to closely related strains. However, the breadth of cross-neutralizing antibody responses after vaccination has not been fully elucidated.

Compared to the highly variable HA head domain, HA stalk and neuraminidase (NA) are more conserved among circulating strains across different continents and seasons (10–12). Recent studies have revealed functions of non-neutralizing antibodies targeting these more conserved domains. For example, HA stalk specific antibodies can block viral genome release into the cytoplasm; whilst NA specific antibodies reduce progeny virion release from infected cells (13). In addition, non-neutralizing antibodies can trigger cytotoxicity and phagocytosis to clear infected cells (14, 15). However, whether these non-neutralizing antibodies correlate with *in vivo* protection against the highly pathogenic H5N1 virus remains unclear.

We have conducted a clinical trial with a virosomal H5N1 vaccine with Matrix M adjuvant in 60 adults. We have previously demonstrated that the adjuvanted H5N1 vaccines elicited potent vaccine specific neutralizing antibodies, and to a lesser extent cross-reactive hemagglutination inhibition (HI) antibodies and Th1 and Th2 CD4+ T cell responses against closely related strains (16–18). Here, we established an expanded panel of H5N1 pseudotypes covering all (sub)clades isolated from human infections; and characterized the kinetics and breadth of antibody responses after vaccination, including dissection of the multifaceted non-neutralizing antibody responses. We also assessed the *in vivo* protection from vaccine induced antibodies in a passive transfer murine model and investigated immunological candidates for correlates of protection.

MATERIAL AND METHODS

Study Design

Sixty healthy adult volunteers (20-49 years old) were enrolled in an open label phase I dose escalating clinical trial early 2009 at Haukeland University Hospital, Bergen, Norway (www.clinicaltrials.gov, NCT00868218) (16). The study was approved by the Regional Committee for Medical Research Ethics, Northern Norway and the Norwegian Medicines Agency. All participants provided written informed consent before inclusion into the study.

Participants were randomized into 4 groups, and intramuscularly vaccinated twice with the H5N1 virosomal vaccine (Crucell Berna Biotech) containing 30μg HA alone, or 1.5, 7.5 or 30μg HA with 50μg Matrix M adjuvant (Novavax) at 3-week interval (16). None of the participants had previously received an H5N1 vaccine.

Vaccine and Sampling

A monovalent inactivated virosomal H5N1 vaccine, containing vaccine strain NIBRG-14, a virus derived from A/Vietnam/1194/2004 (H5N1) and A/Puerto Rico/8/1934 (H1N1) using reverse genetics, was used in the clinical trial. The influenza surface antigens HA and NA were purified from beta-propiolactone (BPL) inactivated egg grown viruses, mixed with lecithin and incorporated into the phospholipid bilayer by spontaneous formation of the virosomes. The HA content of the vaccine was quantified by single radial diffusion, and the presence of NA was confirmed.

The adjuvant Matrix M used in the trial was the 3rd generation immune stimulating complex, which contains Matrix-A and Matrix-C fractions produced from purified *Quillaja* saponin fractions A and C, at the proportion of 91:9. The vaccine was formulated as 30μg HA alone, or 1.5, 7.5 or 30μg HA with 50μg Matrix M adjuvant, filled into single use syringes, and stored at 4°C until use. All participants (n=60) received 2 doses of the vaccine at a 3-week interval, except one withdrawal from the 7.5μg HA adjuvanted vaccine group.

Blood samples were collected before, and up to 42 days after vaccination. Sera were separated, aliquoted and stored at -80°C until use.

Hemagglutination Inhibition Assay

All sera were treated with receptor-destroying enzyme (RDE, Seiken) at a ratio of 1 in 4 at 37°C for 18h, and heat treated at 56°C for 1h. The treated sera were analysed in duplicate (2-fold serial dilution, starting from 1:10) with 4 hemagglutinating units of viruses and 0.8% horse red blood cells, as previously described (16, 17). A panel of reassortant H5N1 viruses were used, including A/Vietnam/1194/2004 (NIBRG-14, vaccine strain,

clade 1), A/Indonesia/5/2005 (IBCDC-RG2, subclade 2.1.3.2), A/turkey/Turkey/1/2005 (NIBRG-23, subclade 2.2.1), and A/Cambodia/R0405050/2007 (NIBRG-88, subclade 1.1). The hemagglutination inhibition (HI) titer was determined as the reciprocal of the highest sera dilution giving 50% inhibition of hemagglutination. Non-detected samples were assigned a value of 4 for calculation purpose.

Pseudotype-Based Neutralization Assay

H5N1 pseudotypes were generated by co-transfecting lentiviral vectors pHR'CMV-Luc, pCMVRΔ8.2, pCMVR-H5HA, and pCMVR-N1NA into HEK293T cells as previously described (19, 20). A panel of pCMVR-HA constructs encoding H5HA from A/Vietnam/1203/2004 (Vietnam, clade 1), A/Indonesia/5/2005 (Indonesia, subclade 2.1.3.2), A/Turkey/65596/2006 (Turkey, subclade 2.2.1), A/common magpie/Hong Kong/5052/2007 (HK5052, subclade 2.3.2.1), A/Shenzhen/406H/2006 (Shenzhen, subclade 2.3.4), A/Shanxi/2/2006 (Shanxi, clade 7), and pCMVR-N1NA construct encoding NA from A/Thailand/(KAN-1)/2004 were used to prepare H5N1 pseudotypes.

All sera were heat inactivated and analysed in duplicate (4-fold serial dilution, starting from 1:10) with H5N1 pseudotypes corresponding to 20,000 to 200,000 relative luciferase activity (RLA), as previously described (20). The pseudotype-based neutralization (PN) titer (IC_{80}) was determined as the reciprocal of the sera dilution giving 80% reduction of RLA. PN titers were normalized based on HIV-1 gag p24 quantities for different pseudotypes. Non-detected samples were assigned a value of 2 for calculation purpose.

Enzyme-Linked Immunosorbent Assay

H5HA stalk and N1NA specific immunoglobulin G (IgG) were quantified in sera using the enzyme-linked immunosorbent assay (ELISA) developed in-house, as previously described (21). Serially diluted sera were analysed in Maxi Sorp 96-well plates coated with 1 μg/ml recombinant chimeric HA (cH9/5HA) that combines the H5HA stalk domain from NIBRG-14 strain with an HA globular head domain from A/guinea fowl/Hong Kong/WF10/1999 H9 influenza A virus, or 1 μg/ml recombinant N1 neuraminidase. Immunoglobulin concentrations were interpolated from standard human IgG curves. For calculation purposes, non-detected samples were assigned as 0.04 μg/ml against cH9/5HA and 0.005 μg/ml against N1NA.

Virus Neutralization Assay

All sera were heat inactivated and analysed in duplicate (2-fold serial dilution, starting from 1:10) with 100 $TCID_{50}$ reassortant cH9/1N3 virus in MDCK cells, as previously described (22). The cH9/1N3 virus contains the HA stalk domain from A/California/07/2009 H1 strain, an HA globular head domain from A/guinea fowl/Hong Kong/WF10/1999 H9 strain, and N3NA from A/swine/Missouri/4296424/2006 virus. The virus neutralization (VN) titer was measured with 0.7% turkey red blood cells and determined as the highest serum dilution giving complete hemagglutination. Non-detected samples were assigned a value of 5 for calculation purpose.

Enzyme-Linked Lectin Assay

All sera were treated at 56°C for 45min and analysed in duplicate (3-fold serial dilution, starting from 1:5) with a reassortant NIBRG-73 virus, as previously described (22). The NIBRG-73 virus has N1NA from the NIBRG-14 strain and H7HA from A/equine/Prague/1956 virus. The neuraminidase enzymatic activity was measured with fetuin, horseradish peroxidase-conjugated peanut agglutinin and o-phenylenediamine dihydrochloride (Sigma-Aldrich), and read as optical density (OD) value at 490nm. The neuraminidase inhibition (NI) titer (IC_{50}) was calculated as the reciprocal dilution of sera giving 50% reduction in enzymatic activity. Non-detected samples were assigned a value of 2 for calculation purpose.

Antibody-Dependent Cellular Cytotoxicity Reporter Assay

All sera were heat inactivated, serially diluted and analysed using ADCC Reporter Bioassay kit (Promega), as previously described (22). MDCK cells infected with NIBRG-14 virus at multiplicities of infection (MOI) 0.34 were used as target cells, and Jurkat/NFAT-luc cells were used as effect cells. The antibody-dependent cellular cytotoxicity (ADCC) reporter activity was measured with Bio-Glo Luciferase Assay Reagent (Promega) as relative luciferase activity (RLA). ADCC titer (EC_{50}) was calculated as the reciprocal dilution of sera giving 50% of maximum RLA. Non-detected samples were assigned a value of 2 for calculation purpose.

Passive Transfer and Viral Challenge in Mice

Six to eight weeks old female BALB/c mice (Taconic, Denmark) were housed under specific-pathogen free conditions at Rikshospitalet, Oslo University Hospital. All animal experiments were approved by the Norwegian Food Safety Authority.

Pooled human sera or saline (400μl/mouse) were injected intraperitoneally (i.p.) into mice (n=12/group) 1 day prior to viral challenge. Mice were anaesthetized by subcutaneous (s.c.) injection of Hypnorm/Dormicum (0.05ml working solution/10g) and infected intranasally (i.n.) with 5 MLD_{50} of NIBRG-14 virus in 20 μl/mouse (10μl/nostril). Mice were monitored for survival and weight loss for 2 weeks after challenge, with an endpoint of 20% weight reduction, as required by the Norwegian Food Safety Authority. Mice that lost more than 20% body weight were euthanized by cervical dislocation. For mice that did not lose weight during the 2-week monitoring, the maximum body weight loss was assigned as 0.01% for calculation purpose. At days 3 and 5 post challenge, both lobes of lungs were harvested (n=3 mice/group), snap frozen and stored at -80°C until use.

Virus Quantification

Frozen lung tissues were weighted and homogenized in DMEM with 1% antibiotics. NIBRG-14 virus was quantified in $TCID_{50}$ on MDCK cells (23). Hemagglutination assay with 0.7% human red blood cells was used to measure the viral load. The limit of detection was 22.49 $TCID_{50}$/ml of homogenate.

Phylogenetic Tree

Full-length HA protein amino acid sequences from influenza type A viruses were downloaded from NCBI Influenza Virus Database. Phylogenetic analyses were performed at ngPhylogeny.fr using MAFFT (Multiple Alignment using Fast Fourier Transform, default settings), BMGE (Block Mapping and Gathering with Entropy, default settings), and PhyML (Phylogeny software based on the Maximum-likelihood, default settings) (24, 25). See **Supplementary Table 1** for the accession no. of all HA amino acid sequences used.

Statistical Analyses

Biological replicates were used in all experiments, unless otherwise stated. Antibody quantification results including HI, PN, VN, NI, ADCC titers, and IgG concentrations, and lung viral load results were Ln transformed prior to statistical tests. Turkey's multiple comparisons and Fisher's LSD test were performed in two-way analysis of variance (ANOVA). False Discovery Rate controlled multiple comparisons were performed in Nonparametric Kruskal-Wallis test. Nonparametric Spearman correlations and Pearson correlations were tested, linear fitting curves were plotted when Spearman or Pearson P <0.10. In multiple linear regression analyses, all independent variables were centered prior to test. * P<0.05, ** P<0.01, *** P<0.001, all P values are two-tailed. All statistical analyses were performed with GraphPad Prism 7 and SPSS 25.

RESULTS

Study Design

Sixty adults were divided into 4 groups and vaccinated with the H5N1 virosomal vaccine alone or escalating doses of adjuvanted vaccine: Group 30μg - (30μg HA alone, 15 subjects), Group 1.5μg + (1.5μg HA with adjuvant Matrix M, 15 subjects), Group 7.5μg + (7.5μg HA with adjuvant Matrix M, 15 subjects), and Group 30μg + (30μg HA with adjuvant Matrix M, 15 subjects). All subjects received a boosting dose 3 weeks after the first priming dose, except for one withdrawal after the first dose in 7.5μg + group (**Figure 1A**). Twenty-five subjects had earlier received seasonal influenza vaccine(s) or reported influenza virus infection (**Table 1**). Sequential pre- and post-vaccination serum samples up to 42 days were collected from all vaccinees.

Adjuvanted H5N1 Vaccines Rapidly Elicits Strain Specific and Broadly Cross-Clades Neutralizing Antibodies

We assessed HA specific antibodies using the HI assay. None of the vaccinees had detectable antibodies before vaccination. After priming, only the 30μg + group showed potent increases of vaccine specific antibodies. After boosting, all 3 adjuvanted groups had antibodies above the protective level (HI titer ≥32), while the non-adjuvanted 30μg - group remained below the protective level (**Figure 1B**). The 1.5μg + group had significantly lower antibody fold-induction after priming compared to the 30μg + group, while after boosting the difference diminished. On the contrary, the 30μg - group showed significant antibody induction after priming but limited further increase after boosting (**Figure 1C**).

We further analysed antibody responses using pseudotype-based neutralization (PN) assay. In 24 subjects, low levels of pre-existing vaccine specific neutralizing antibodies were detected. Of note, the vaccine elicited potent homologous antibody responses 7 days after priming in all 4 groups, which were further significantly elevated to higher level in the 1.5μg + and 7.5μg + groups after boosting. The 1.5μg + group had lower antibody fold-induction after priming compared to the 30μg + group but reached similar neutralizing antibody titer after boosting; whilst the 30μg - group had rapid antibody increase 7 days after priming but no significant boost after the second dose (**Figures 1E, F**).

To explore the breadth of the vaccine elicited cross-neutralizing antibodies, we developed a panel of H5N1 pseudotypes expressing divergent H5 hemagglutinins covering multiple (sub)clades of H5N1 viruses isolated from humans (**Figure 1D** and **Supplementary Table 1**). Remarkably, cross-neutralizing antibodies were elicited to equivalent titers as compared to vaccine specific antibodies in all 4 groups when tested against the 3 closely related pseudotypes, namely HK5052 (subclade 2.3.2.1), Turkey (subclade 2.2.1) and Shenzhen (subclade 2.3.4). Meanwhile, although significantly boosted by vaccination, lower levels of cross-neutralizing antibodies were detected to the 2 more distant pseudotypes: Indonesia (subclade 2.1.3.2) and Shanxi (clade 7). Nevertheless, broadly neutralizing antibodies were detected in all the subjects in the 30μg + group across all the (sub)clades (**Figure 1G**).

Multifaceted Antibody Responses After H5N1 Vaccines

Total HA stalk specific antibodies were measured in ELISA against the recombinant chimeric protein cH9/5HA, which consists of the HA stalk domain from the vaccine strain and an irrelevant H9HA head. All subjects were found to have pre-existing HA stalk specific antibodies. As early as 7 days after priming, we observed significant antibody increases in all 4 groups. The 30μg + group had significantly higher antibody fold-induction as compared to the 1.5μg + and 30μg - groups (**Figures 2A, B**).

We next assessed neuraminidase (NA) specific antibodies by ELISA (**Figures 2C, D**). In 51 subjects, NA specific antibodies were detected prior to vaccination. The H5N1 vaccines elicited potent antibody increases in all 4 groups at 7 days after priming. Further significant antibody increases were found after boosting in 1.5μg + and 7.5μg + H5N1 groups (**Figure 2C**). Overall, the 7.5μg + and 30μg + groups showed equivalently potent responses, while the 1.5μg + and 30μg - groups had lower fold change of NA specific antibodies (**Figure 2D**).

To quantify the antibodies that inhibit NA enzymatic activity, we performed enzyme-linked lectin assay (ELLA). Before vaccination, detectable NA inhibition (NI) titers were observed in 36 of 60 subjects. Vaccinees in the groups 30μg -, 7.5μg + and 30μg + had significant antibody increases 7 days after priming. While vaccinees in the 1.5μg+ group showed antibody induction

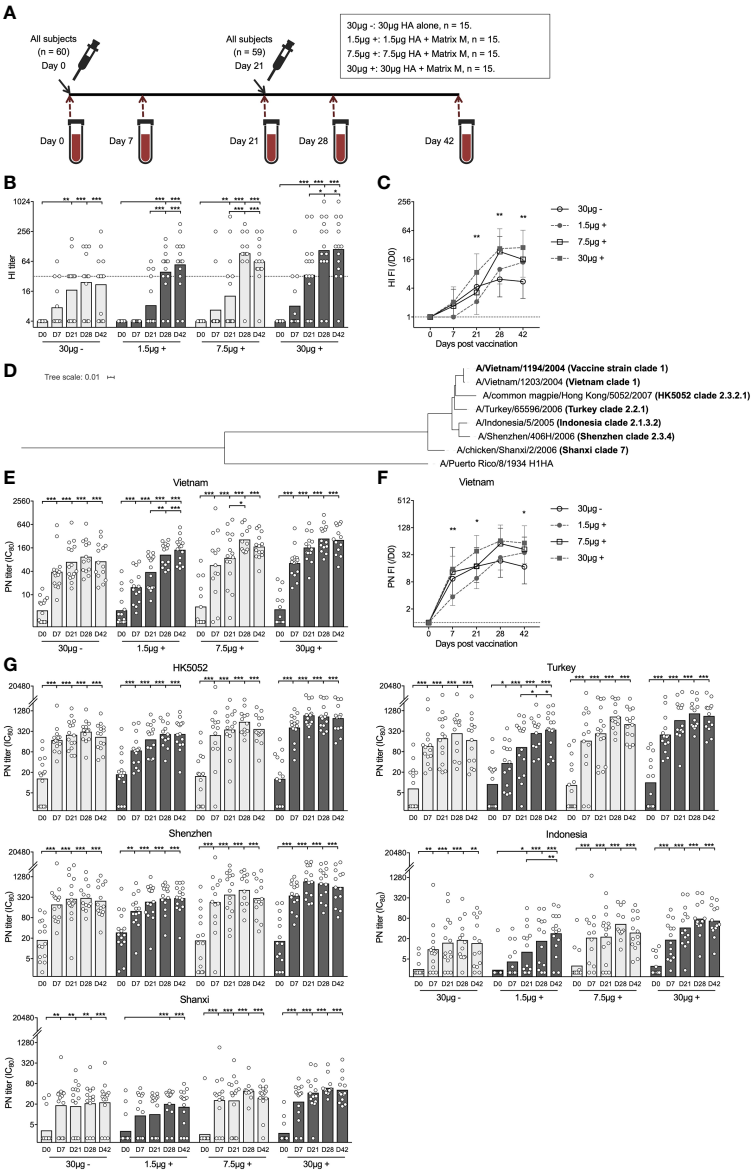

FIGURE 1 | Adjuvanted H5N1 vaccine rapidly elicited strain specific and cross-reactive neutralizing antibody responses. **(A)** An Illustration of the study design. Sixty adults (20 to 49 years old) were enrolled in this study and vaccinated with inactivated virosomal H5N1 vaccine (Crucell| Berna Biotech, Switzerland). The adults were randomized into 4 groups of 15 subjects and received two doses of H5N1 vaccine with 30 μg hemagglutinin (HA) alone (30μg -), or 1.5, 7.5 and 30 μg HA adjuvanted with Matrix M (1.5 μg +, 7.5 μg +, and 30 μg +, respectively), at an interval of 21 days. Serum samples pre- (day 0), 7 days, 21 days, 28 days, and 42 days post-vaccination were collected. One subject withdrew after first dose vaccine in 7.5μg + group. **(B, C)** Hemagglutination inhibiting titer (HI titer, **B**) and fold-induction (FI) after vaccination (HI FI,/D0, **C**) was measured against NIBRG-14 virus (vaccine strain). **(D)** Phylogenetic tree shows the genetic divergence between H5HA from the vaccine strain and heterologous H5HAs tested in pseudotype-based neutralization (PN) assay. H1HA from A/Puerto Rico/8/1934 was used as a reference. Phylogenetic analyses were performed at ngPhylogeny.fr. **(E, F)** Vaccine specific neutralizing antibodies were measured in PN assay against pseudotyped virus derived from A/Vietnam/1203/2004 virus (Vietnam). The PN titer (IC_{80}, **E**) was calculated as the reciprocal dilutions of the sera that gave 80% inhibition. Fold-induction after vaccination (PN FI,/D0, **F**) is shown. **(G)** Cross-neutralizing antibody titers (IC_{80}) were measured against 5 strains of pseudotypes expressing heterologous H5HAs listed in D All antibody responses were measured using serum samples before (D0) and after vaccination (D7, D21, D28, and D42). The geometric mean values are shown as bars, and each symbol represents one subject **(B, E, G)**. The geometric mean of fold-inductions in each group ± geometric standard deviation as error bar is shown **(C, F)**. *P < 0.05, **P < 0.01, ***P < 0.001 (Antibody titers and fold-inductions were Ln transformed in statistical analyses. Turkey's multiple comparisons between pre-prime (D0) and post-prime (D7, D21, D28, D42), and between pre-boost (D21) and post-boost (D28 and D42) in each group were performed in two-way ANOVA in **(B, E, G)** Turkey's multiple comparisons between 30 μg + and 1.5 μg + after prime (D7 and D21), and between 30 μg + and 30 μg - after boost (D28 and D42) were performed in two-way ANOVA in **C, F**). The horizontal dotted lines indicate HI titer of 32 **(B)**, and fold-induction of 1 **(C, F)**. Duplicates were performed in all experiments.

TABLE 1 | The demographics of the subjects enrolled in the study.

Group (Vaccine administered[1])	Total (N/A[2])	30μg - (30μg HA)	1.5μg +(1.5μg HA adjuvanted with 50μg Matrix M)	7.5μg +(7.5μg HA adjuvanted with 50μg Matrix M)	30μg +(30μg HA adjuvanted with 50μg Matrix M)
No. of subjects	60	15	15	15[3]	15
Gender, M/F	22/38	6/9	5/10	7/8	4/11
Median age, years	30	30	26	28	30
(Range)	(20-49)	(20-41)	(21-44)	(22-42)	(25-49)
No. of subjects with previous vaccinations and/or infection[4]	25	6	8	4	7

[1]*The vaccine was supplied as prefilled syringes of pre-formulated virosomal vaccine with Matrix M.*
[2]*Not applicable (N/A).*
[3]*One withdrawal after first dose vaccine in 7.5μg + group.*
[4]*Annual seasonal influenza vaccines during 2005/06-2008/09 seasons were included as previous vaccinations. Influenza infection during 2008/09 season was included as infection. In addition, three subjects received the H7N1 vaccine in a clinical trial in 2006, which was not included in the table.*

21 days after priming, which increased significantly after boosting (**Figure 2E**). The kinetics of NI antibody fold change among 4 vaccine groups was similar to the kinetics of NA specific binding antibodies by ELISA (**Figures 2D, F**).

Lastly, we measured ADCC inducing antibodies. Thirty-seven out of 60 subjects had pre-existing ADCC inducing antibodies. The H5N1 vaccines further elevated the antibody levels, which remained high after boosting in all groups, especially the 30μg+ group (**Figures 2G, H**).

In summary, the virosomal H5N1 vaccines elicited potent and multifaceted antibody responses. The adjuvanted intermediate (7.5μg +) and high (30μg +) dose vaccines potently induced antibody increases 7 days after priming, which were further elevated or maintained after boosting. By comparison, the adjuvanted low (1.5μg +) dose vaccine showed delayed antibody kinetics; whilst the non-adjuvanted (30μg -) vaccine elicited antibodies of an overall lower magnitude.

H5N1 Vaccines Induced Robust Antibody Responses

As the majority of our subjects had some detectable antibodies against the H5N1 vaccine components prior to vaccination, we investigated whether pre-existing immunity hampers the H5N1 vaccine elicited antibody responses. Firstly, the age of the subjects enrolled in this study ranged from 20 to 49 years old (**Table 1**). We saw significant correlations between the age and pre-existing level of neutralizing antibodies, HA stalk and NA specific binding antibodies (**Figure 3A**). In contrast, the antibody levels after H5N1 vaccination had inverse or no correlation with age (**Figure 3B**). Next, subjects who had had seasonal influenza vaccination or infection within 5 years prior to the current study showed significantly higher levels of pre-existing neutralizing, NA specific and ADCC inducing antibodies. H5N1 vaccination boosted antibodies to comparably high levels in all subjects (**Figure 3C**). Collectively, the H5N1 vaccines induced robust and multifaceted antibody responses regardless of age, vaccination/infection history or pre-existing antibody levels.

Human Immune Post H5N1 Vaccination Sera Confer *In Vivo* Protection

To study whether the H5N1 vaccine induced antibodies are protective against infection, we performed passive serum transfer and virus challenge in a murine model. Briefly, we pooled pre-vaccination sera from groups 1.5μg + and 30μg + as D0 sera, and post-vaccination sera were pooled within each group from all vaccinees in the 1.5μg + and 30μg + groups for days 7, 21 and 42. Pooled immune sera or saline were then transferred into mice one day prior to a viral challenge ($5\times MLD_{50}$) with the NIBRG-14 virus. Body weight was monitored for 14 days after challenge (**Figure 4A**). Mice that received saline or D0 sera became ill and rapidly lost weight. All 5 mice receiving saline and 2 out of 6 mice receiving D0 sera died between days 7 and 8 after challenge. By contrast, all mice that received post-vaccination sera survived. Mice that received sera 7 and 21 days post-vaccination from group 1.5μg + showed mild symptoms and lost a maximum of 16% and 9.3% of body weight, respectively, although they quickly recovered. Mice receiving day 42 sera from the group 1.5μg + and sera at all 3 time points from the group 30μg + displayed no symptoms of disease and had < 3% body weight loss at maximum (**Figures 4B–D**).

We measured the lung weight and viral load at 3 and 5 days after challenge. Mice that received days 21 and 42 sera from group 30 μg + showed lower lung weight at 5 days post challenge, and lower viral loads at days 3 and 5, compared to the mice receiving saline (**Figures 4E, F**). In addition, we observed good correlations between the lung viral load and body weight loss, as well as between the lung viral load and the lung weight (**Figures 4G, H**). To summarise, immune sera elicited by H5N1 vaccination, especially the adjuvanted high dose (30μg +), conferred full protection against a lethal *in vivo* challenge.

Neutralizing Antibody and Neuraminidase Inhibiting Antibody Titers Act as Correlates of Protection

Our final aim was to study which of the H5N1 vaccine elicited antibody responses correlated with *in vivo* protection. We included the widely used hemagglutination inhibition (HI) titer, neutralizing antibody titer measured in pseudotype-based assay (PN titer), hemagglutinin stalk specific antibody level (HA stalk IgG) and neuraminidase inhibition (NI) titer as candidates for correlates of protection. As the Fc receptors involved in ADCC are different between humans and mice, the ADCC inducing antibody titer was not included in analyses.

Importantly, we observed inverse correlations between the antibody levels in the pooled human sera that mice received by

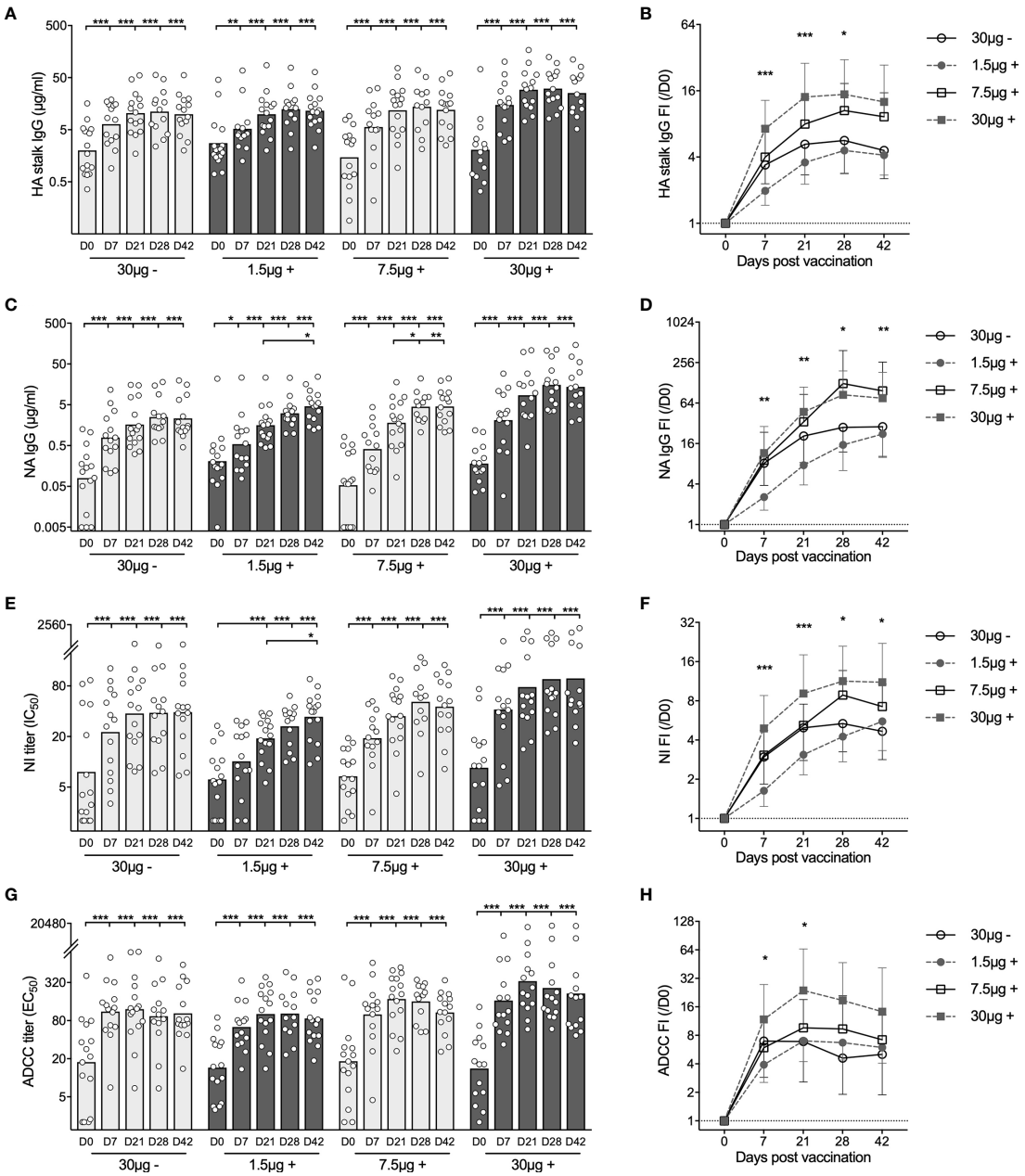

FIGURE 2 | Adjuvanted H5N1 vaccines elicit multifaceted antibody responses. **(A, B)** H5HA stalk specific antibodies were measured against the recombinant chimeric protein cH9/5HA, which consists of HA stalk domain from H5 A/Vietnam/1203/2004 strain and irrelevant H9HA head domain. Concentrations of total H5HA stalk specific antibody measured in ELISA **(A)** and fold-induction (FI) after vaccination (IgG FI,/D0, **B**) are shown. **(C, D)** Total neuraminidase (NA) specific antibodies were measured in ELISA against N1NA from A/Vietnam/1203/2004 virus. Antibody concentrations **(C)** and fold-induction after vaccination (IgG FI,/D0, **D**) are shown. **(E, F)** Pre- and post-vaccination sera were tested for inhibiting NA enzymatic activity in ELLA against reassortant NIBRG-73 virus, which expresses NA from H5N1 vaccine strain and irrelevant H7HA. The neuraminidase enzymatic activity inhibition titer (NI IC50, **E**) was calculated as the reciprocal dilutions of the sera that gave 50% inhibition. Fold-induction after vaccination (NI FI,/D0, **F**) is shown. **(G, H)** Sera were tested for inducing antibody-dependent cellular cytotoxicity (ADCC) in ADCC Reporter Bioassay against the vaccine strain (NIBRG-14). The ADCC titer (EC50, **G**) was calculated as the reciprocal dilutions of the sera that gave 50% of the maximal biological response. Fold-induction after vaccination (ADCC FI,/D0, **H**) is shown. The geometric mean titers are shown as bars, and each symbol represents one subject **(A, C, E, G)**. The geometric means of fold-induction in each group ± geometric standard deviation as error bar are shown **(B, D, F, H)**. *P < 0.05, **P < 0.01, ***P < 0.001 (Antibody titers and fold-inductions were Ln transformed in statistical analyses. Turkey's multiple comparisons between pre-prime (D0) and post-prime (D7, D21, D28, D42), and between pre-boost (D21) and post-boost (D28 and D42) in each group were performed in two-way ANOVA in **A, C, E, G.** Turkey's multiple comparisons between 30 µg + and 1.5 µg + after prime (D7 and D21), and between 30 µg + and 30 µg - after boost (D28 and D42) were performed in two-way ANOVA in **B, D, F, H**). The horizontal dotted lines indicate fold-induction of 1 **(B, D, F, H)**. Duplicates were performed in all experiments.

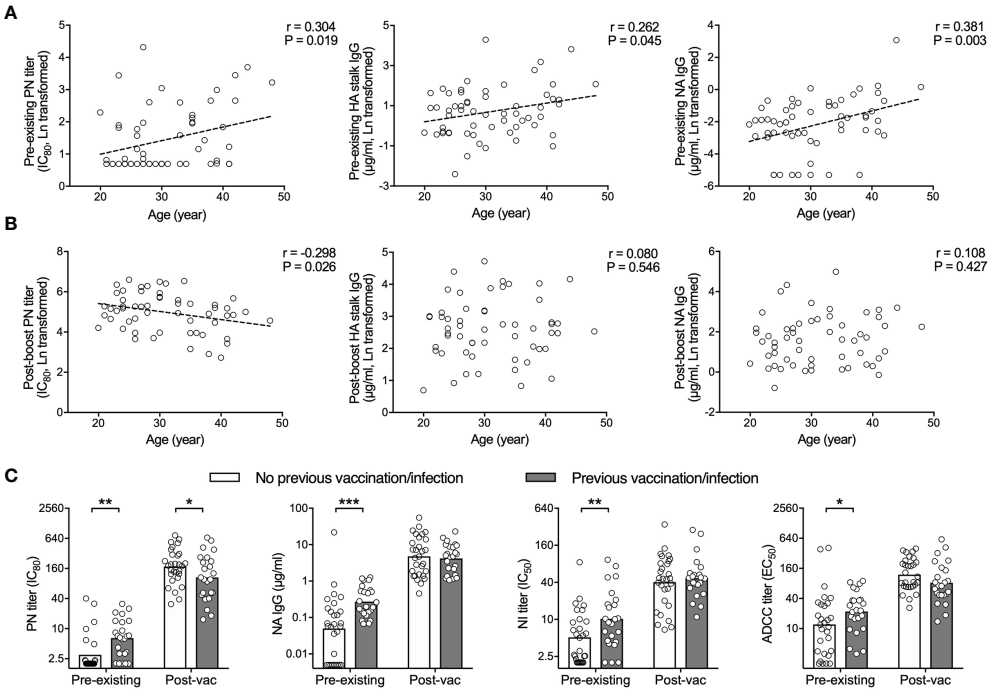

FIGURE 3 | H5N1 vaccines elicit potent antibody responses regardless of pre-existing humoral immunity. **(A, B)** HA specific neutralizing antibodies (PN titer, left), total HA stalk specific antibodies (IgG, center) and total NA specific antibodies (IgG, right) tested in pre-vaccination sera (pre-existing, D0, **A**) correlate with age. Inverse or no significant correlation with age is found in sera after vaccination (post-vac, D42, **B**). **(C)** Subjects with previous vaccination and/or infection had significantly higher pre-existing antibodies, compared to subjects without previous vaccination or infection. After vaccination, the difference was abolished. HA specific neutralizing antibodies (PN titer, far left), total NA specific antibodies (IgG, central left), neuraminidase enzymatic activity inhibiting antibodies (NI titer, central right), and antibody-dependent cell-mediated cytotoxicity (ADCC) inducing antibodies (ADCC titer, far right) were tested in sera before (pre-existing) and 42 days after vaccination (post-vac). The geometric mean titers are shown as bars **(C)**, and each symbol represents one subject **(A–C)**. Linear fitting curve was plotted as dotted line when Pearson correlation P < 0,05. Pearson r and P values are noted for each correlation **(A, B)**. *P < 0.05, **P < 0.01, ***P < 0.001 (Antibody titers and concentrations were Ln transformed in statistical analyses. Fisher's LSD test between subjects with previous vaccination/infection and subjects without was performed in two-way ANOVA in **(C)**.

passive transfer and murine body weight loss, as well as lung viral load after challenge (**Figures 5A, B**). Of note, the NI titer had the closest relationship with both murine body weight loss and lung viral load, followed by PN titer. Whilst the HI titer and HA stalk IgG level showed lower degrees of correlation with *in vivo* protection, determined by the Peason's r values in correlation analyses.

We further dissected the contribution of each antibody parameter to the predictions of *in vivo* protection. The adjusted R square and the standard error of the estimate in the multiple linear regression analyses were used to determine the level of fit in different prediction models. When predicting the maximum body weight loss, PN titer and NI titer alone or combined were among the best-fit models (**Figure 5C** and **Supplementary Table 2**). In the lung viral load predictions, NI titer alone, NI and PN titer combined, and all 4 antibody parameters together were the top 3 models (**Figure 5D** and **Supplementary Table 2**). Notably, NI titer contributed significantly to the top models predicting both body weight loss and lung viral load (**Figures 5C, D** and **Supplementary Table 3**). Together, our correlation and regression analyses on the *in vivo* protection provided by pooled human sera in murine challenge model cohesively demonstrated that PN and NI titers act as correlates of protection. Further study is needed to confirm the roles of PN and NI titers as correlates of protection in human infection scenario.

DISCUSSION

Since 1996, highly pathogenic avian influenza (HPAI) H5N1 have caused outbreaks in domestic and wild birds worldwide, as well as sporadic zoonotic-human transmissions (3, 26). The high mortality rate in confirmed human infections raised alarms about the global pandemic preparedness (1). Dozens of pre-pandemic H5N1 candidates have been developed, and clinical trials have been conducted with vaccines developed in various platforms (3, 5). Here, we investigated in-depth the multifaceted antibody responses after a virosomal H5N1 vaccine alone or with the Matrix M adjuvant. Our data showed that the adjuvanted H5N1 vaccines elicited potent vaccine-specific and broadly cross-neutralizing antibodies, as well as HA stalk and NA specific functional antibodies. The multifaceted antibody responses were found as early as 7 days after the first dose and were further boosted and

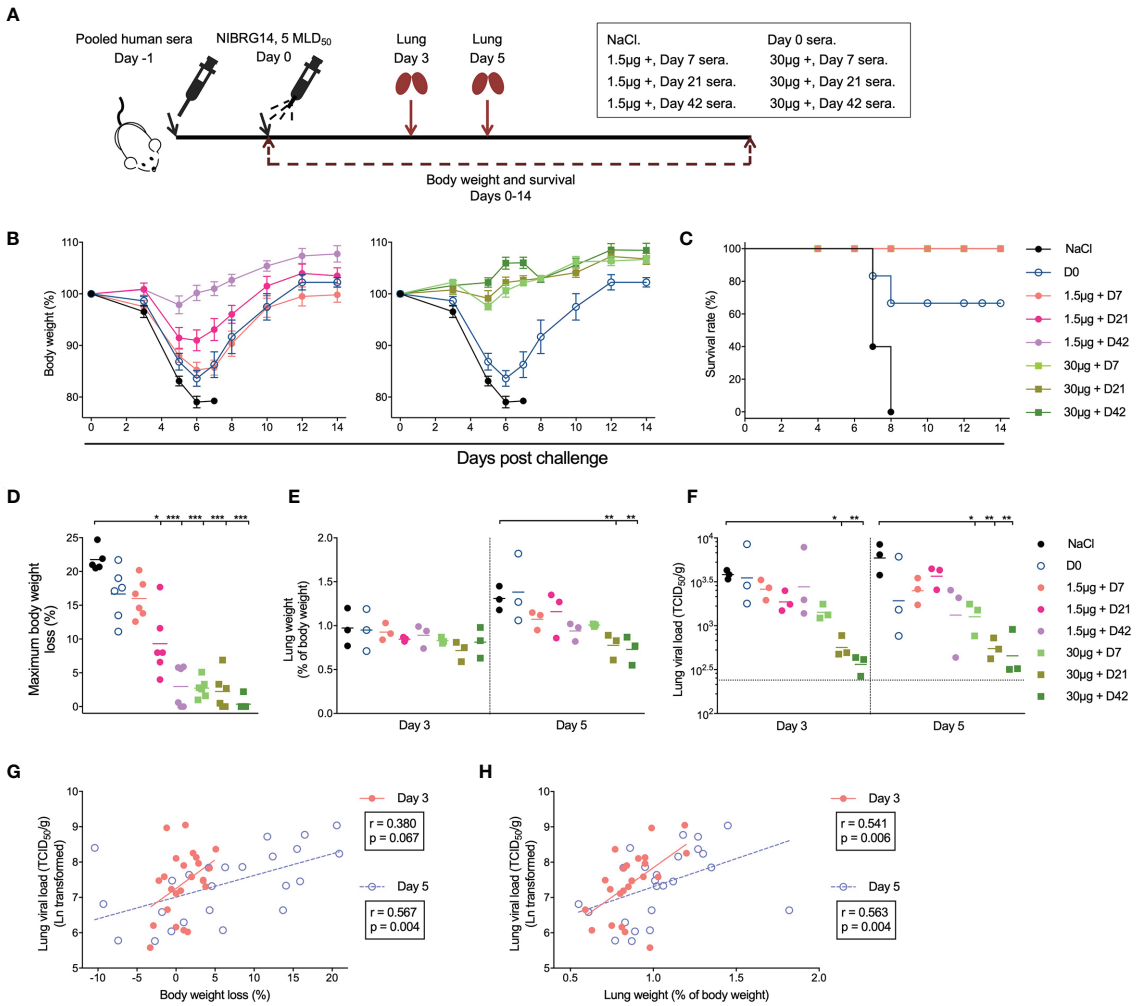

FIGURE 4 | Adjuvanted H5N1 vaccines elicit antibodies provided *in vivo* protection against lethal virus challenge. **(A)** Illustration of the experiment set-up for serum transfer and virus challenge. Pre-vaccination sera from subjects in 1.5μg + and 30μg + groups were pooled together as D0 sera. Sera from days 7, 21 and 42 after vaccination from subjects in 1.5μg + or 30μg + groups were pooled separately. Group-and time-point-wise pooled sera were administered intraperitoneally to female BALB/c mice (n=12 per group). NaCl was given as control. One day later, the mice were infected intranasally with 5× 50% mice lethal dose (MLD50) of NIBRG-14 virus. Body weight and survival were monitored for 14 days after challenge. Lungs from 3 mice per group were collected 3 and 5 days after infection for weight and viral load measurement. **(B, C)** The body weight loss **(B)** and survival rate **(C)** of the mice in different groups are shown. **(D)** Maximum body weight loss was calculated for each individual mouse as the maximum body weight loss through 14 days monitoring, which occurred at 5, 6 or 7 days after challenge. For mice with no body weight loss observed through monitoring, maximum weight loss was assigned as 0,01%. **(E, F)** The lung weight of the 3 mice sacrificed on days 3 and 5 after virus challenge was measured and is shown as the mean of percentage of pre-infection body weight (% of body weight, **E**). The viral load of NIBRG-14 virus was measured in MDCK cells as the reciprocal dilutions of lung homogenates that gave 50% tissue culture infection dose (TCID50) and standardized based on the lung weight (TCID50/g, **F**). The dotted line indicates the lowest detectable viral load in the assay. **(G, H)** The standardized lung viral load (TCID50/g) 3 and 5 days after infection correlate with the body weight loss **(G)** and the lung weight **(H)**. The body weight of mice in each group is shown as mean ± standard deviation as error bar **(B)**. Means **(D, E)** and geometric means **(F)** are shown as horizontal lines, and each symbol represents one mouse **(D–H)**. *P < 0.05, **P < 0.01, ***P < 0.001 (lung viral load was Ln transformed in statistical analyses. False Discovery Rate controlled multiple comparisons between mice receiving NaCl and pooled sera were performed in Nonparametric Kruskal-Wallis test in **D–F**). The standardized lung viral load was Ln transformed in statistical analyses. Linear fitting curve is plotted as solid line (Day 3) or dotted line (Day 5) when nonparametric Spearman P < 0.10. Spearman r and P values are noted for each correlation **(G, H)**. Duplicates were performed in lung weight and viral load measurement.

maintained at high levels after the second dose. These antibodies provided full protection against H5N1 virus challenge in mice. Of note, the levels of neutralizing antibodies and NA inhibiting antibodies could predict *in vivo* protection against infection and disease progression.

Like other enveloped RNA virus, influenza viruses evolve continuously due to its error-prone replication and large host reservoirs. Newly emerged strains may thus escape existing immunity established from previous infection and vaccination. The HPAI H5N1 viruses have evolved into multiple clades and

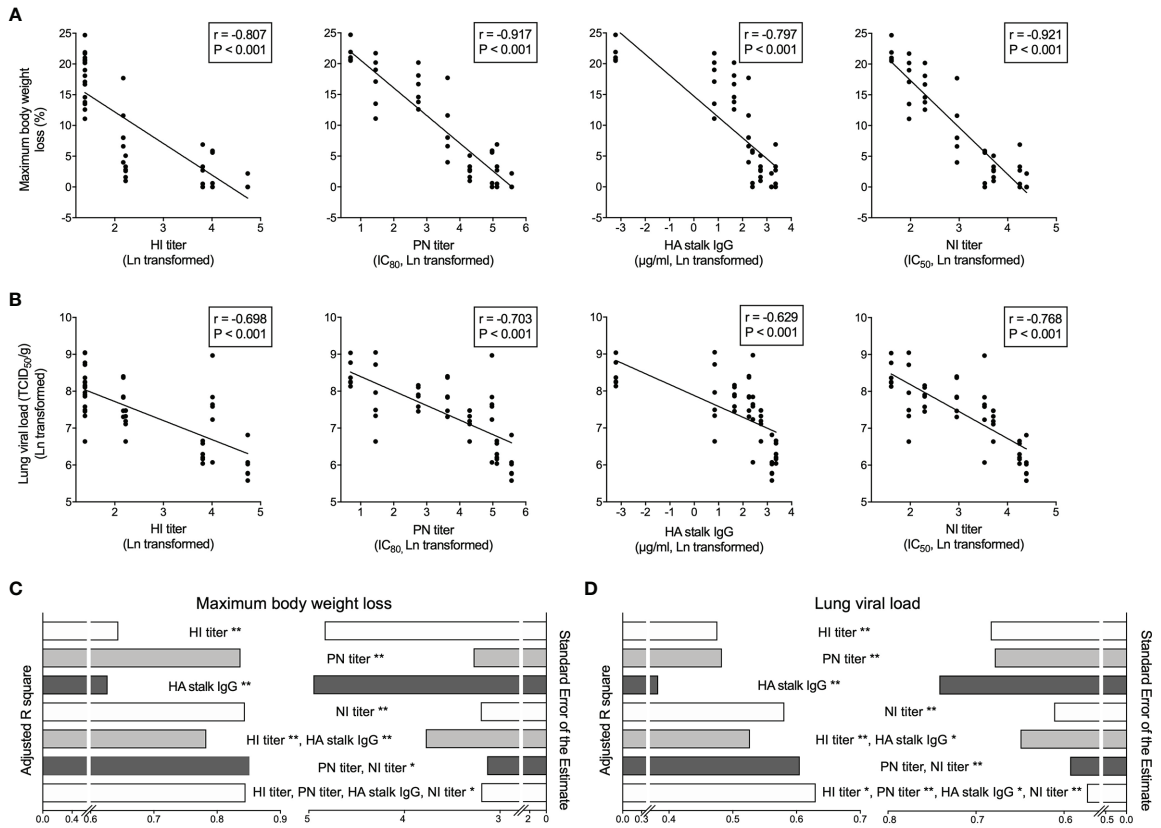

FIGURE 5 | Vaccine elicited HA and NA specific antibodies predict *in vivo* protection after challenge. **(A, B)** Hemagglutination inhibition antibodies (HI titer, far left), HA specific neutralizing antibodies (PN titer, central left), total HA stalk specific antibodies (HA stalk IgG, central right), and neuraminidase enzymatic activity inhibiting antibodies (NI titer, far right) significantly and inversely correlate with the maximum body weight loss **(A)** and lung viral load **(B)** in mice after NIBRG-14 virus challenge. Each symbol represents one mouse **(A, B)**. The linear fitting curve is plotted as line. Pearson r and P values are noted in each correlation. **(C, D)** Antibody parameters including HI titer, PN titer, HA stalk IgG and NI titer results were used to predict mice maximum body weight loss **(C)** and lung viral load **(D)** in uni- and multiple linear regression models. Adjusted R square (left half) and Standard Error of the Estimate (right half) are shown to indicate the goodness of different models explaining dependent variables. In each model, predictors contributing significantly are noted. *P < 0.05, **P < 0.01. For detailed model summary and coefficients, see **Supplementary Tables 2–3**. Antibody parameters from each individual subject in clinical trial were put together in silico the same way as sera were combined to make group-and-time-point-wise pooled human sera for mice passive transfer. Geometric mean of antibody parameter was calculated, Ln transformed and centered before being used as independent variables. Maximum body weight loss and Ln-transformed lung viral load were used as dependent variables in regression analyses in SPSS 25.

subclades. Therefore, vaccines capable of eliciting cross-protective immunity are highly desired. Previous studies on cross-neutralizing antibodies after H5N1 vaccines were mostly limited to clades 1 and 2 (8, 27–30). To our knowledge, we are the first to report vaccine-induced cross-neutralizing antibody responses against all H5 clades found from human infections, including (sub)clades 1, 2.1.3.2, 2.2.1, 2.3.2.1, 2.3.4 and 7. To our surprise, most of the subjects had low to moderate level of antibodies cross-reactive to multiple (sub)clades prior to vaccination. Importantly, the Matrix M adjuvanted virosomal H5N1 vaccine elicited potent neutralizing antibody responses against all 6 (sub)clades, as quickly as 7 days after the first vaccine dose. Similarly, rapid increases in functional non-neutralizing antibodies, such as HA stalk IgG, NA inhibiting and ADCC inducing antibodies, were observed after vaccination (**Figures 1**, **2**). In contrast, our early studies using HI, microneutralization and single radial hemolysis assays showed no measurable pre-existing antibodies; and 2 doses of vaccine were required for induction of low to moderate levels of antibodies that could cross neutralize clades 1 and 2 [**Supplementary Figure 1** and references (16–18)]. The detection of pre-existing antibodies in this study could be attributed to the higher sensitivity of pseudotype-based neutralization compared to the traditional assays used earlier. The protective potential of these pre-existing antibodies has not yet been fully elucidated, but our results from the sera passive transfer and viral challenge in mice indicate that efficient vaccines will still be needed for protection. The different magnitude and kinetics of the antibody response emphasize the necessity of implementing and harmonizing highly sensitive serological assays to fully understand the immune responses. For example, a more balanced distribution of surface glycoproteins and sensitive luminescence readout

make pseudotype-based neutralization assay more sensitive, quantitative and better suited in detecting zoonotic virus specific antibodies (19, 31, 32).

Compared to the variable HA head domain, the HA stalk domain and NA are more conserved. Thus, functional antibodies against HA stalk and NA broaden vaccine responses against heterologous strains. Ellebedy et al. reported robust HA stalk antibody responses measured in ELISA after receiving inactivated H5N1 vaccine (7). Boudreau C. et al. demonstrated that the MF59-adjuvanted H5N1 vaccine elicited antibodies that stimulated robust neutrophil phagocytosis and complement activity (33). In our study, we observed potent increases of HA stalk specific IgGs and ADCC inducing antibodies, which peaked after priming with no further boost after the second vaccine dose. By contrast, cross-neutralizing and NA inhibiting antibodies were significantly elicited after both the priming and boosting dose, especially in the low and intermedium adjuvanted (1.5μg + and 7.5μg +) groups (**Figures 1**, **2**).

Adjuvants enhance vaccine immunogenicity, especially in the absence of pre-existing immune memory. The Matrix M has been tested in vaccines against malaria and is currently used in the NVX-CoV2373 vaccine against COVID-19 (34–38). Here we demonstrated that the Matrix M adjuvanted H5N1 influenza vaccine induced potent increases of broadly cross-neutralizing antibodies, as well as HA stalk and NA specific non-neutralizing antibodies. The adjuvanted 7.5μg + and 30μg + vaccines induced significantly higher titers and better breadth of antibodies as compared to the non-adjuvanted 30μg - group. More importantly, days 21 and 42 post-vaccination sera from 30μg + group provided full protection in mice against both disease progress and viral infection (**Figure 4**).

The controlled human influenza virus infection model and vaccine field studies are useful in assessing the vaccine effectiveness and establishing correlates of protection (39, 40). Unfortunately, it is difficult to conduct such studies with HPAI H5N1 viruses due to the high morbidity and mortality rate associated. We therefore transferred human sera into naïve mice before an *in vivo* challenge to study relevant correlates of protection. Other studies applying human sera transfer and mice challenge have shown that HA stalk specific antibodies predict *in vivo* protection against heterologous virus challenge (41, 42). Here, our results demonstrated that PN and NI titers had closer correlations with *in vivo* protection against a homologous virus challenge, as compared to HI titer or HA stalk specific IgG (**Figure 5**). These results are in agreement with other human challenge (43) and cohort studies (44–46). A caveat here is that our multiple linear regression analyses suffer from inherited collinearity issues due to the similar kinetics of vaccine-elicited antibody responses. Therefore, the coefficients of each predictor may be subject to variance inflation (**Supplementary Table 3**). Nevertheless, the overall level of predictions should hold accurate (**Figures 5C, D** and **Supplementary Table 2**).

In this study, we assessed the kinetics, magnitude and *in vivo* protection efficacy of the multifaceted antibody responses after the adjuvanted virosomal H5N1 vaccines. This vaccine was developed in preparation for a potential H5N1 pandemic. Nevertheless, lessons learnt from H5N1 vaccine development could help preparation for the ongoing and future pandemics: 1) Highly sensitive assays help better understand the breadth of cross-reactive immune responses after infection and vaccination. 2) Adjuvants allow vaccine dose sparing and enhance both the magnitude and breadth of responses against vaccine strain and heterologous variants.

DATA AVAILABILITY STATEMENT

The raw data supporting the conclusions of this article will be made available by the authors, without undue reservation.

ETHICS STATEMENT

The studies involving human participants were reviewed and approved by The Regional Committee for Medical Research Ethics, Northern Norway and the Norwegian Medicines Agency. The patients/participants provided their written informed consent to participate in this study. The animal study was reviewed and approved by Norwegian Food Safety Authority.

AUTHOR CONTRIBUTIONS

FZ and RC conceived the project. FZ, GG, and RC designed the experiments. RC and GP conducted the clinical study and collected samples. FZ, LH, and GG conducted the experiments. FZ analyzed the data. FZ, LH, GP, GG, and RC prepared and edited the manuscript. All authors contributed to the article and approved the submitted version.

FUNDING

This study received intramural funding from the Influenza Center at the University of Bergen and Haukeland University Hospital. The Influenza Center is funded by the University of Bergen, Ministry of Health and Care Services, the Trond Mohn Foundation (TMS2020TMT05), the European Union (EU IMI115672 FLUCOP, H2020 874866 INCENTIVE, H2020 101037867 VACCELERATE, EU IMI 101007799 Inno4Vac) and Nanomedicines Flunanoair (ERA-NETet EuroNanoMed2, JTC2016), and the Research Council of Norway GLOBVAC program (284930).

ACKNOWLEDGMENTS

We thank all volunteers, clinical staff and staff at the Influenza Center for participation in the study. We thank Crucell Berna Biotech, the Netherlands, for providing the vaccine. We thank Prof. Paul Zhou for providing all the plasmids for H5N1 pseudotypes. We thank NIBSC for providing all HPAI H5N1

antigens used in HI assay. We thank Prof. Florian Krammer for providing the baculoviruses used in purifying cH9/5HA and N1NA proteins. We also thank the staff at the department of comparative medicine at Oslo University Hospital for technical help in association with the mouse experiments.

SUPPLEMENTARY MATERIAL

The Supplementary Material for this article can be found online at: https://www.frontiersin.org/articles/10.3389/fimmu.2021.747774/full#supplementary-material

REFERENCES

1. WHO. *Cumulative Number of Confirmed Human Cases for Avian Influenza A (H5N1) Reported to WHO, 2003-2021*. (2021). Available at: https://www.who.int/publications/m/item/cumulative-number-of-confirmed-human-cases-for-avian-influenza-a(h5n1)-reported-to-who-2003-2021-15-april-2021 (Accessed Jun 25, 2021).
2. WHO. Update on Avian Influenza A (H5N1) Virus Infection in Humans. *N Engl J Med* (2008) 358:261–73. doi: 10.1056/NEJMra0707279
3. WHO. Antigenic and Genetic Characteristics of Zoonotic Influenza Viruses and Development of Candidate Vaccine Viruses for Pandemic Preparedness. *Wkly Epidemiol Rec* (2014) 89:105–15.
4. WHO. Avian Influenza A (H5N1) Infection in Humans. *N Engl J Med* (2005) 353:1374–85. doi: 10.1056/NEJMra052211
5. Baz M, Luke CJ, Cheng X, Jin H, Subbarao K. H5N1 Vaccines in Humans. *Virus Res* (2013) 178:78–98. doi: 10.1016/j.virusres.2013.05.006
6. Matsuda K, Huang J, Zhou T, Sheng Z, Kang BH, Ishida E, et al. Prolonged Evolution of the Memory B Cell Response Induced by a Replicating Adenovirus-Influenza H5 Vaccine. *Sci Immunol* (2019) 4:eaau2710. doi: 10.1126/sciimmunol.aau2710
7. Ellebedy AH, Krammer F, Li G-M, Miller MS, Chiu C, Wrammert J, et al. Induction of Broadly Cross-Reactive Antibody Responses to the Influenza HA Stem Region Following H5N1 Vaccination in Humans. *Proc Natl Acad Sci USA* (2014) 111:13133–8. doi: 10.1073/pnas.1414070111
8. Belshe RB, Frey SE, Graham I, Mulligan MJ, Edupuganti S, Jackson LA, et al. Safety and Immunogenicity of Influenza A H5 Subunit Vaccines: Effect of Vaccine Schedule and Antigenic Variant. *J Infect Dis* (2011) 203:666–73. doi: 10.1093/infdis/jiq093
9. Talaat KR, Luke CJ, Khurana S, Manischewitz J, King LR, McMahon BA, et al. A Live Attenuated Influenza A(H5N1) Vaccine Induces Long-Term Immunity in the Absence of a Primary Antibody Response. *J Infect Dis* (2014) 209:1860–69. doi: 10.1093/infdis/jiu123
10. Kirkpatrick E, Qiu X, Wilson PC, Bahl J, Krammer F. The Influenza Virus Hemagglutinin Head Evolves Faster Than the Stalk Domain. *Sci Rep* (2018) 8:10432. doi: 10.1038/s41598-018-28706-1
11. Eichelberger MC, Morens DM, Taubenberger JK. Neuraminidase as an Influenza Vaccine Antigen: A Low Hanging Fruit, Ready for Picking to Improve Vaccine Effectiveness. *Curr Opin Immunol* (2018) 53:38–44. doi: 10.1016/j.coi.2018.03.025
12. Krammer F, Li L, Wilson PC. Emerging From the Shadow of Hemagglutinin: Neuraminidase Is an Important Target for Influenza Vaccination. *Cell Host Microbe* (2019) 26:712–13. doi: 10.1016/j.chom.2019.11.006
13. Palese P, Tobita K, Ueda M, Compans RW. Characterization of Temperature Sensitive Influenza Virus Mutants Defective in Neuraminidase. *Virology* (1974) 61:397–410. doi: 10.1016/0042-6822(74)90276-1
14. DiLillo DJ, Palese P, Wilson PC, Ravetch JV. Broadly Neutralizing Anti-Influenza Antibodies Require Fc Receptor Engagement for. *Vivo Protect J Clin Invest* (2016) 126:605–10. doi: 10.1172/JCI84428
15. DiLillo DJ, Tan GS, Palese P, Ravetch JV. Broadly Neutralizing Hemagglutinin Stalk–Specific Antibodies Require FcγR Interactions for Protection Against Influenza Virus *In Vivo*. *Nat Med* (2014) 20:143–51. doi: 10.1038/nm.3443
16. Cox RJ, Pedersen G, Madhun AS, Svindland S, Saevik M, Breakwell L, et al. Evaluation of a Virosomal H5N1 Vaccine Formulated With Matrix M Adjuvant in a Phase I Clinical Trial. *Vaccine* (2011) 29:8049–59. doi: 10.1016/j.vaccine.2011.08.042
17. Cox RJ, Major D, Pedersen G, Pathirana RD, Hoschler K, Guilfoyle K, et al. Matrix M H5N1 Vaccine Induces Cross-H5 Clade Humoral Immune Responses in a Randomized Clinical Trial and Provides Protection From Highly Pathogenic Influenza Challenge in Ferrets. *PloS One* (2015) 10: e0131652. doi: 10.1371/journal.pone.0131652
18. Pedersen GK, Sjursen H, Nostbakken JK, Jul-Larsen Å, Hoschler K, Cox RJ. Matrix M(TM) Adjuvanted Virosomal H5N1 Vaccine Induces Balanced Th1/Th2 CD4(+) T Cell Responses in Man. *Hum Vaccin Immunother* (2014) 10:2408–16. doi: 10.4161/hv.29583
19. Tsai C, Caillet C, Hu H, Zhou F, Ding H, Zhang G, et al. Measurement of Neutralizing Antibody Responses Against H5N1 Clades in Immunized Mice and Ferrets Using Pseudotypes Expressing Influenza Hemagglutinin and Neuraminidase. *Vaccine* (2009) 27:6777–90. doi: 10.1016/j.vaccine.2009.08.056
20. Zhou F, Wang G, Buchy P, Cai Z, Chen H, Chen Z, et al. A Triclade DNA Vaccine Designed on the Basis of a Comprehensive Serologic Study Elicits Neutralizing Antibody Responses Against All Clades and Subclades of Highly Pathogenic Avian Influenza H5N1 Viruses. *J Virol* (2012) 86:6970–78. doi: 10.1128/JVI.06930-11
21. Tete SM, Krammer F, Lartey S, Bredholt G, Wood J, Skrede S, et al. Dissecting the Hemagglutinin Head and Stalk-Specific IgG Antibody Response in Healthcare Workers Following Pandemic H1N1 Vaccination. *NPJ Vaccines* (2016) 1:16001. doi: 10.1038/npjvaccines.2016.1
22. Islam S, Zhou F, Lartey S, Mohn KGI, Krammer F, Cox RJ, et al. Functional Immune Response to Influenza H1N1 in Children and Adults After Live Attenuated Influenza Virus Vaccination. *Scand J Immunol* (2019) 90:e12801. doi: 10.1111/sji.12801
23. Szretter KJ, Balish AL, Katz JM. Influenza: Propagation, Quantification, and Storage. *Curr Protoc Microbiol* (2006) 3:15G.1.1–15G.1.22. doi: 10.1002/0471729256.mc15g01s3
24. Dereeper A, Guignon V, Blanc G, Audic S, Buffet S, Chevenet F, et al. Phylogeny.fr: Robust Phylogenetic Analysis for the Non-Specialist. *Nucleic Acids Res* (2008) 36:W465–9. doi: 10.1093/nar/gkn180
25. Lemoine F, Correia D, Lefort V, Doppelt-Azeroual O, Mareuil F, Cohen-Boulakia S, et al. NGPhylogeny.fr: New Generation Phylogenetic Services for Non-Specialists. *Nucleic Acids Res* (2019) 47:W260–5. doi: 10.1093/nar/gkz303
26. WHO. Antigenic and Genetic Characteristics of Zoonotic Influenza A Viruses and Development of Candidate Vaccine Viruses for Pandemic Preparedness. *Wkly Epidemiol Rec* (2021) 96:88–104.
27. Leroux-Roels I, Borkowski A, Vanwolleghem T, Dramé M, Clement F, Hons E, et al. Antigen Sparing and Cross-Reactive Immunity With an Adjuvanted Rh5n1 Prototype Pandemic Influenza Vaccine: A Randomised Controlled Trial. *Lancet* (2007) 370:580–89. doi: 10.1016/S0140-6736(07)61297-5
28. Leroux-Roels I, Bernhard R, Gérard P, Dramé M, Hanon E, Leroux-Roels G. Broad Clade 2 Cross-Reactive Immunity Induced by an Adjuvanted Clade 1 Rh5n1 Pandemic Influenza Vaccine. *PloS One* (2008) 3:e1665. doi: 10.1371/journal.pone.0001665
29. Nolan TM, Richmond PC, Skeljo MV, Pearce G, Hartel G, Formica NT, et al. Phase I and II Randomised Trials of the Safety and Immunogenicity of a Prototype Adjuvanted Inactivated Split-Virus Influenza A (H5N1) Vaccine in Healthy Adults. *Vaccine* (2008) 26:4160–67. doi: 10.1016/j.vaccine.2008.05.077
30. Nolan T, Richmond PC, Formica NT, Höschler K, Skeljo MV, Stoney T, et al. Safety and Immunogenicity of a Prototype Adjuvanted Inactivated Split-Virus Influenza A (H5N1) Vaccine in Infants and Children. *Vaccine* (2008) 26:6383–91. doi: 10.1016/j.vaccine.2008.08.046
31. Andersen Tor K, Zhou F, Cox R, Bogen B, Grødeland G. A DNA Vaccine That Targets Hemagglutinin to Antigen-Presenting Cells Protects Mice Against H7 Influenza. *J Virol* (2017) 91:e01340–17. doi: 10.1128/JVI.01340-17
32. Alberini I, Del Tordello E, Fasolo A, Temperton NJ, Galli G, Gentile C, et al. Pseudoparticle Neutralization Is a Reliable Assay to Measure Immunity and Cross-Reactivity to H5N1 Influenza Viruses. *Vaccine* (2009) 27:5998–6003. doi: 10.1016/j.vaccine.2009.07.079
33. Boudreau CM, Yu W-H, Suscovich TJ, Talbot HK, Edwards KM, Alter G. Selective Induction of Antibody Effector Functional Responses Using MF59-Adjuvanted Vaccination. *J Clin Invest* (2020) 130:662–72. doi: 10.1172/JCI129520

34. Lovgren Bengtsson K, Morein B, Osterhaus AD. ISCOM Technology-Based Matrix M Adjuvant: Success in Future Vaccines Relies on Formulation. *Expert Rev Vaccines* (2011) 10:401–03. doi: 10.1586/erv.11.25
35. Venkatraman N, Anagnostou N, Bliss C, Bowyer G, Wright D, Lövgren-Bengtsson K, et al. Safety and Immunogenicity of Heterologous Prime-Boost Immunization With Viral-Vectored Malaria Vaccines Adjuvanted With Matrix-M™. *Vaccine* (2017) 35:6208–17. doi: 10.1016/j.vaccine.2017.09.028
36. Datoo MS, Natama MH, Somé A, Traoré O, Rouamba T, Bellamy D, et al. Efficacy of a Low-Dose Candidate Malaria Vaccine, R21 in Adjuvant Matrix-M, With Seasonal Administration to Children in Burkina Faso: A Randomised Controlled Trial. *Lancet* (2021) 397:1809–18. doi: 10.1016/S0140-6736(21)00943-0
37. Heath PT, Galiza EP, Baxter DN, Boffito M, Browne D, Burns F, et al. Safety and Efficacy of NVX-CoV2373 Covid-19 Vaccine. *N Engl J Med* (2021) 385(13):1172–83. doi: 10.1056/NEJMoa2107659
38. Keech C, Albert G, Cho I, Robertson A, Reed P, Neal S, et al. Phase 1–2 Trial of a SARS-CoV-2 Recombinant Spike Protein Nanoparticle Vaccine. *N Engl J Med* (2020) 383:2320–32. doi: 10.1056/NEJMoa2026920
39. Hobson D, Curry RL, Beare AS, Ward-Gardner A. The Role of Serum Haemagglutination-Inhibiting Antibody in Protection Against Challenge Infection With Influenza A2 and B Viruses. *J Hyg* (1972) 70:767–77. doi: 10.1017/s0022172400022610
40. Black S, Nicolay U, Vesikari T, Knuf M, Del Giudice G, Della Cioppa G, et al. Hemagglutination Inhibition Antibody Titers as a Correlate of Protection for Inactivated Influenza Vaccines in Children. *Pediatr Infect Dis J* (2011) 30:1081–85. doi: 10.1097/INF.0b013e3182367662
41. Nachbagauer R, Wohlbold TJ, Hirsh A, Hai R, Sjursen H, Palese P, et al. Induction of Broadly Reactive Anti-Hemagglutinin Stalk Antibodies by an H5N1 Vaccine in Humans. *J Virol* (2014) 88:13260–68. doi: 10.1128/JVI.02133-14
42. Jacobsen H, Rajendran M, Choi A, Sjursen H, Brokstad KA, Cox RJ, et al. Influenza Virus Hemagglutinin Stalk-Specific Antibodies in Human Serum Are a Surrogate Marker for *In Vivo* Protection in a Serum Transfer Mouse Challenge Model. *mBio* (2017) 8:e01463–17. doi: 10.1128/mBio.01463-17
43. Memoli MJ, Shaw PA, Han A, Czajkowski L, Reed S, Athota R, et al. Evaluation of Antihemagglutinin and Antineuraminidase Antibodies as Correlates of Protection in an Influenza A/H1N1 Virus Healthy Human Challenge Model. *mBio* (2016) 7:e00417–16. doi: 10.1128/mBio.00417-16
44. Couch RB, Atmar RL, Franco LM, Quarles JM, Wells J, Arden N, et al. Antibody Correlates and Predictors of Immunity to Naturally Occurring Influenza in Humans and the Importance of Antibody to the Neuraminidase. *J Infect Dis* (2013) 207:974–81. doi: 10.1093/infdis/jis935
45. Monto AS, Petrie JG, Cross RT, Johnson E, Liu M, Zhong W, et al. Antibody to Influenza Virus Neuraminidase: An Independent Correlate of Protection. *J Infect Dis* (2015) 212:1191–99. doi: 10.1093/infdis/jiv195
46. Krammer F, Weir JP, Engelhardt O, Katz JM, Cox RJ. Meeting Report and Review: Immunological Assays and Correlates of Protection for Next-Generation Influenza Vaccines. *Influenza Other Respir Viruses* (2020) 14:237–43. doi: 10.1111/irv.12706

Conflict of Interest: The authors declare that the research was conducted in the absence of any commercial or financial relationships that could be construed as a potential conflict of interest.

frontiers in Immunology

ORIGINAL RESEARCH
published: 06 December 2021
doi: 10.3389/fimmu.2021.748281

Functional and Binding H1N1pdm09-Specific Antibody Responses in Occasionally and Repeatedly Vaccinated Healthcare Workers: A Five-Year Study (2009-2014)

Håkon Amdam[1], Anders Madsen[1], Fan Zhou[1], Amit Bansal[1], Mai-Chi Trieu[1†] and Rebecca Jane Cox[1,2†]*

[1] Influenza Centre, Department of Clinical Science, University of Bergen, Bergen, Norway, [2] Department of Microbiology, Haukeland University Hospital, Bergen, Norway

OPEN ACCESS

Edited by:
Pedro A. Reche, Complutense University of Madrid, Spain

Reviewed by:
Dapeng Zhou, Tongji University, China
Hang Xie, United States Food and Drug Administration, United States
S. Sohail Ahmed, Kling Biotherapeutics, Netherlands

***Correspondence:**
Rebecca Jane Cox
rebecca.cox@uib.no

[†]These authors have contributed equally to this work

Specialty section:
This article was submitted to Vaccines and Molecular Therapeutics, a section of the journal Frontiers in Immunology

Received: *27 July 2021*
Accepted: *17 November 2021*
Published: *06 December 2021*

Citation:
Amdam H, Madsen A, Zhou F, Bansal A, Trieu M-C and Cox RJ (2021) Functional and Binding H1N1pdm09-Specific Antibody Responses in Occasionally and Repeatedly Vaccinated Healthcare Workers: A Five-Year Study (2009-2014). Front. Immunol. 12:748281. doi: 10.3389/fimmu.2021.748281

Background: In 2009, a novel influenza A/H1N1pdm09 emerged and caused a pandemic. This strain continued to circulate and was therefore included in the seasonal vaccines up to the 2016/2017-season. This provided a unique opportunity to study the long-term antibody responses to H1N1pdm09 in healthcare workers (HCW) with a different vaccination history.

Methods: HCW at Haukeland University Hospital, Bergen, Norway were immunized with the AS03-adjuvanted H1N1pdm09 vaccine in 2009 (N=55) and divided into groups according to their vaccination history; one vaccination (N=10), two vaccinations (N=15), three vaccinations (N=5), four vaccinations (N=15) and five vaccinations (N=10). HCW are recommended for influenza vaccination to protect both themselves and their patients, but it is voluntary in Norway. Blood samples were collected pre- and at 21 days, 3, 6, and 12 months after each vaccination, or annually from 2010 HCW without vaccination. ELISA, haemagglutination inhibition (HI) and microneutralization (MN) assays were used to determine the antibody response.

Results: Pandemic vaccination induced a significant increase in the H1N1-specific antibodies measured by ELISA, HI and MN. Seasonal vaccination boosted the antibody response, both in HCW with only the current vaccination and those with prior and current vaccination during 2010/11-2013/14. We observed a trend of increased antibody responses in HCW with only the current vaccination in 2013/14. A two- and three-year gap before vaccination in 2013/14 provided a more potent antibody response compared to annually vaccinated HCW.

Conclusions: Our long term follow up study elucidates the antibody response in HCW with different vaccination histories. Our findings contribute to our understanding of the impact of repeated vaccination upon antibody responses.

Keywords: influenza, pandemic vaccination, repeated vaccination, HI, MN, ELISA, H1N1pdm09, healthcare workers

INTRODUCTION

Influenza is a respiratory virus that causes annual epidemics and occasional pandemics. Seasonal influenza is estimated to cause 294,000-518,000 deaths globally each year (1), but mortality can increase dramatically when a pandemic occurs. Vaccination remains the cornerstone of influenza prevention by inducing antibodies against the major surface proteins hemagglutinin (HA) and neuraminidase (NA). In Norway, annual vaccination is recommended for high-risk populations and occupational groups, including healthcare workers, (HCW) to protect the individual and patients (2).

The first pandemic of the 21st century was caused by an influenza A H1N1 virus (A/California/07/2009) which was first detected in April 2009 before spreading globally (3). Norway initiated a mass vaccination campaign in October 2009, and 2.2 million people were vaccinated with the AS03-adjuvanted monovalent H1N1pdm09 vaccine. HCW were among the first to receive the vaccine to maintain the integrity of the healthcare system (4). The H1N1pdm09 strain continued to circulate as a seasonal virus after the pandemic and was included in seasonal influenza vaccines from 2010/11 to 2016/17 seasons.

Mutations in the surface glycoproteins cause antigenic drift. Annual vaccine updates are necessary to match the vaccine strains with circulating viruses, making it difficult to assess the durability of antibody response. The immune response to influenza is multifaceted and shaped by several factors, including previous influenza infections or vaccinations, age and health conditions (5). Despite decades of use, the impact of annual repeated influenza vaccination on antibody responses remains unclear, with conflicting results reported with either increases or decreases in antibody responses (6, 7). Furthermore, the vaccine coverage among recommended high-risk groups and HCW in Norway is far from WHO´s goal of 75% (8). As a result, many HCW are not annually vaccinated, and their vaccination status varies.

We conducted a five-year follow up of HCW vaccinated with the AS03-adjuvanted pandemic vaccine in 2009, followed by seasonal trivalent inactivated influenza vaccines (IIV) during the following years (9). The H1N1pdm09 component (A/California/07/2009) of the vaccine remained unchanged during the five-year period, giving us the unique opportunity to investigate the long-term H1N1pdm09 antibody response in groups of HCW categorized based on their annual vaccination history over the five-year period.

MATERIALS AND METHODS

Clinical Trial

Fifty-five participants were selected from a clinical trial of HCW vaccinated in 2009 with the AS03-adjuvanted monovalent pandemic split H1N1 virus vaccine containing the A/California/07/2009 (H1N1pdm09) virus [Pandemrix, GlaxoSmithKline (GSK), Belgium] at Haukeland University Hospital, Bergen, Norway. The participants were followed up for a five-year period and were selected and grouped based on the number of vaccinations during the study period. Ten HCW received solely the pandemic vaccine, fifteen HCW received the pandemic vaccine and one additional IIV, five HCW received the pandemic vaccine and two additional IIV and fifteen HCW received the pandemic vaccine and three IIV. Ten HCW received four consecutive IIV, in addition to the pandemic vaccine. The trivalent seasonal inactivated influenza vaccine [IIV, either sub-unit (Influvac, Abbott Laboratories) or split-virion (Vaxigrip, Sanofi Pasteur)] was used from 2010/10 to 2013/14 containing the A/California/07/2009 (H1N1pdm09) virus as the A/H1N1 component.

All HCW provided written informed consent before inclusion in the study (10). The study was approved by the regional ethics committee (Regional Committee for Medical Research Ethics, Western Norway (REK Vest 2012/1772) and the Norwegian Medicines Agency. The trial is registered in the European Clinical Trials Database (2009-016456-43), and National Institute for Health Database Clinical trials.gov (NCT01003288).

Sampling

Blood samples were collected pre-pandemic vaccination (day 0), at 21 days, and 3, 6, 12, 24, 36, 48 and 60 months after pandemic vaccination. HCW who were annually vaccinated provided additional blood samples at 21 days, 3, and 6 months after each vaccination. Serum samples were stored at -80°C until analysed.

HA Proteins and Influenza Viruses

Whole H1 HA (trimeric A/California/04/09) was generated using the baculovirus expression system for the ELISA (11). Recombinant baculoviruses were passaged three times through Sf9 cells, before infection of High-five cells. Purified proteins were analysed using sodium dodecyl sulphate polyacrylamide gel electrophoresis (SDS-PAGE) and quantified by infrared spectrometer (DirectDetect®, Milipore Corporation). For the HI assay, A/California/07/2009 (H1N1) virus was beta-propiolactone (BPL) inactivated (Influenza Reagents Resources). For the MN assay, a recombinant A/California/07/2009 (H1N1) virus (X-179A) was propagated in-house in 10-day-old embryonated hen´s eggs and frozen at -80°C until used.

ELISA

HA specific serum IgG antibodies were measured by indirect enzyme-linked immunosorbent assay (ELISA), as previously described (12). Ninety-six-well plates (Invitrogen) were incubated with HA protein overnight (1 µg/ml in PBS). The next day, five-fold serial dilutions of serum were added, followed by one hour incubation at 37°C. Horseradish peroxidase (HRP)-conjugated goat anti-human IgG (BD Biosciences, USA, 555788) were added to the plates, and detected with colorimetric substrate [3,3´,5,5´-3,3´,5,5´-tetramethylbenzidine (TMB) (BD Biosciences, USA)]. Absorbances were measured with a microplate reader (Bio-Tek) at the optical density (OD) of 450nm. ELISA endpoint titres were defined as the reciprocal of the highest dilution of serum to give a detectable measurement (OD value over 3 standard deviations above the mean of blank controls).

Hemagglutination Inhibition Assay

Antibodies directed towards the receptor binding site of HA were analysed using the hemagglutination inhibition (HI) assay, as previously described (10). Sera was heat-inactivated and treated with receptor destroying enzyme (Denka Seiken, Japan). Eight HA units of the A/California/07/2009 (H1N1pdm09) virus were added to 2-fold serial dilutions of RDE treated sera in phosphate buffered saline (PBS) for one hour before incubation with 0.7% turkey red blood cells for 30 minutes. The HI titre was defined as the reciprocal of the highest dilution of serum that inhibited 50% hemagglutination. Negative values were assigned a value of 5 for calculation purposes.

Microneutralization Assay

The microneutralization (MN) assay was used for measuring neutralizing antibodies as previously described (13). Sera were heat-inactivated at 56°C for 30 minutes and added in 3-fold serial dilutions to a ninety-six-well cell culture plate (Nunclone Delta surface, USA), with H1N1pdm09 like-virus (X179a, 2000 TCID50/ml). Madin-Darby Canine Kidney (MDCK) cells were added after one hour incubation in room temperature, and the plates were then incubated in 37°C for 18 hours. The next day, cells were fixed with hydrogenperoxide (Sigma-Aldrich, USA, H-1009) in methanol (Sigma-Aldrich, USA, 32213) (0.6% H_2O_2) in 20 minutes. Mouse anti-influenza A nucleoprotein antibodies (AbD Serotec, USA, MCA400) was added, and the plates were incubated for one hour at 37°C. HRP secondary antibody (Dako, Denmark, P0260) was added followed by one-hour incubation. Influenza virus was detected using TMB, before reading at 450 and 620nm to calculate the OD-value. The dilution of serum that provided 50% inhibition of infection was calculated as the MN titre. Negative values were assigned a value of 5 for calculation purposes.

Statistical Analysis

The appropriate statistical tests were used to detect differences within and between the different groups. All analysis were conducted in GraphPad Prism version 8.0 for Mac, (GraphPad Software, USA). Correlations between the assays are presented as Pearson´s *r*, alpha = 0.05. A p-value <0.05 were considered statistically significant in all analysis.

RESULTS

Demographics of the Healthcare Workers

Pandemic and seasonal influenza vaccination were recommended for all HCW but voluntary and provided free of charge by the hospital. Fifty-five HCW received the AS03-adjuvanted H1N1pdm09 pandemic vaccine in 2009. During the subsequent seasons from 2010/11 - 2013/14, IIV containing the same H1N1pdm09 virus (A/California/07/2009) was used. HCW were retrospectively divided into different groups according to their number of seasonal influenza vaccinations and vaccination history during the study period (**Table 1**). Most of the HCW were female (84%) corresponding to the gender distribution of Norwegian healthcare workers. The majority of the HCW (64%) worked clinically and had a history of previous influenza vaccination (75%) The mean age of the study population was 37 years old.

Pandemic Vaccination Induced a Strong Increase in Antibodies

We measured the IgG-specific antibodies binding to full length HA H1N1pdm09 (A/California/07/2009) in ELISA (**Figures 1A, B**). H1N1pdm09 specific binding antibodies were detected in all HCW (55/55) before pandemic vaccination, although at low levels. Pandemic vaccination significantly increased the IgG titres at day 21, 3, 6 and 12 months after vaccination ($p < 0.05$), with a fold change of 10.2. The titres were significantly higher than pre-vaccination titres at 3, 6 and 12 months after vaccination, despite the titres gradually waned from 21 days after vaccination.

We used HI to measure the functionality of the antibodies (**Figures 1C, D**). An HI titre $\geqq 40$ is considered as protective, with a 50% reduction in the risk of contracting influenza (14). Twelve of the 55 of the HCW had an HI titre ≥40 before pandemic vaccination. Vaccination induced a significant increase in HI titres measured at 21 days, 3 months and 6 months after

TABLE 1 | Demographics and vaccination histories of the healthcare workers.

Number of vaccinations (n)	One vaccination (10)	Two vaccinations (15)	Three vaccinations (5)	Four vaccinations (15)	Five vaccinations (10)
Age (mean)	41	40	27	38	37
Sex (female/male)	8/2	13/2	3/2	12/3	10/0
Clinical work (yes/no)	2/8	11/15	4/1	11/4	7/3
Vaccination status 2009 - 2013 (V/N) [a, b]	V-N-N-N-N (10)	V-V-N-N-N (6) V-N-N-N-V (5) V-N-V-N-N (4)	V-V-N-N-V (5)	V-V-V-V-N (6) V-V-V-N-V (4) V-V-N-V-V (5)	V-V-V-V-V (10)
Year of vaccination (n)	2009 (10)	2009 (15) 2010 (10) 2011 (4) 2012 (0) 2013 (5)	2009 (5) 2010 (5) 2011 (0) 2012 (0) 2013 (5)	2009 (15) 2010 (15) 2011 (10) 2012 (11) 2013 (9)	2009 (10) 2010 (10) 2011 (10) 2012 (10) 2013 (10).
Previous influenza vaccination (yes/no)	7/3	11/4	2/3	12/3	9/1

[a] *V, vaccinated; N, Not vaccinated.*

[b] *We had no virological surveillance of the healthcare workers.*

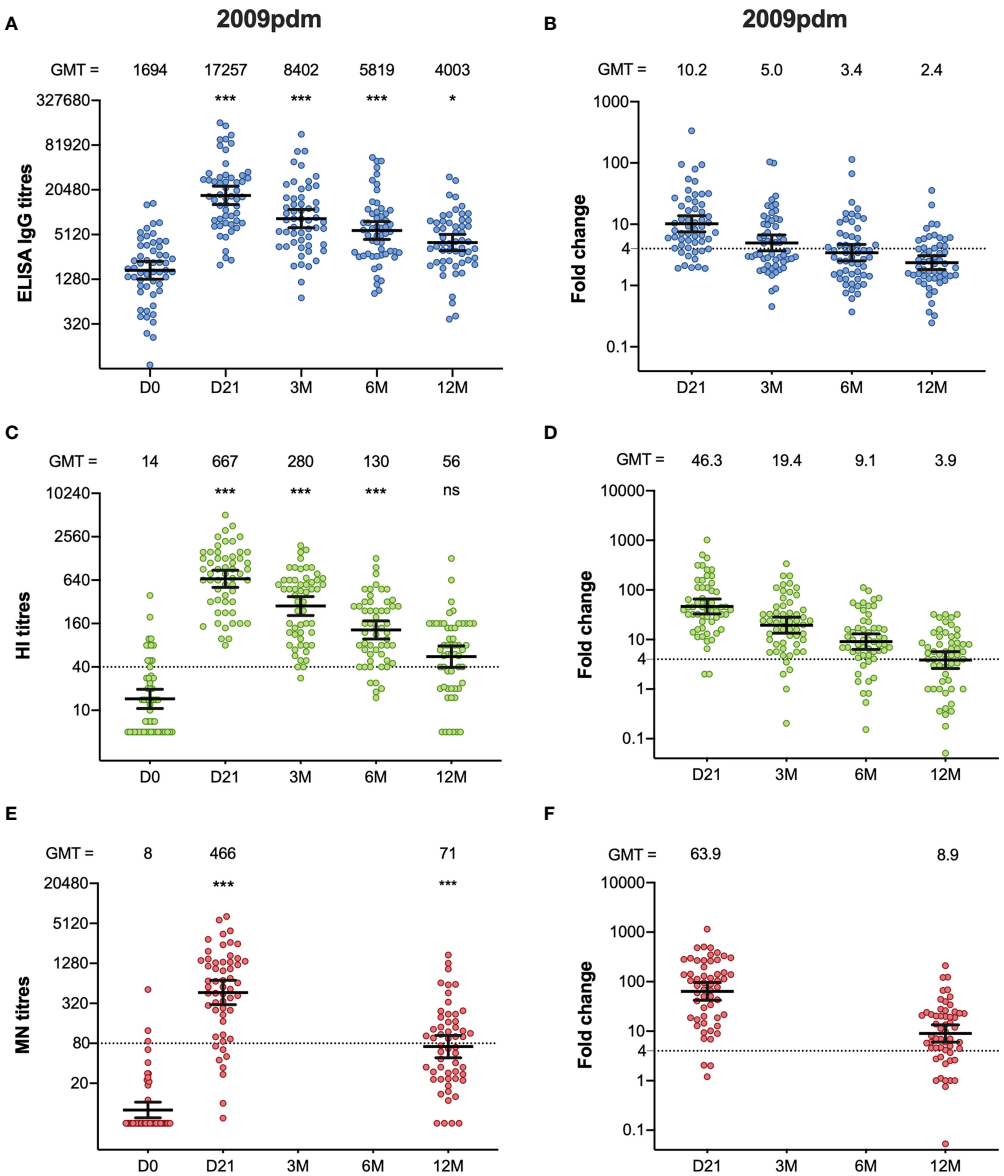

FIGURE 1 | The H1N1pdm09-specific ELISA IgG, HI, and MN antibody response after pandemic vaccination. The ELISA IgG **(A)**, HI **(C)** and MN-titres **(E)** measured in the HCW during 2009/10 (2009pdm). Each symbol represents an individual ELISA, HI and MN titre, and the horizontal line representing the geometric mean titre (GMT) and 95% confidence interval. The GMT for each timepoint in each assay is shown over the graph. The dotted line at 40 and 80 represents the protective titre, in HI and MN respectively. The fold-changes from pre-vaccination ELISA IgG **(B)**, HI **(D)** and MN titres **(F)** measured from pre-vaccination titres (D0) to post- pandemic vaccination (D21, 3M, 6M, 12M) are shown. Each symbol represents an individual ELISA IgG, HI and MN fold-change from pre-vaccination titres to day 21, 3, 6 and 12 months after vaccination. The horizontal line shows the geometric mean with 95% confidence interval. The dotted line at 4 indicates seroconversion, and the GMT is shown above the graph. Statistical differences were tested using the Friedman test, with Dunn´s multiple comparison test. The stars indicate significant differences from pre-vaccination titres, using D0 as a reference. ***P < 0.001, *P < 0.05. Ns, not significant.

vaccination (p <0.001). All HCW had an HI titre ≥40 at 21 days after vaccination, and the fold-change was 46.3. The HI titres waned during the 2009/10-season, but the vaccine fulfilled the criteria of the European Committee for Medicinal Products for Human Use (CHMP), which were pre- and post-vaccination geometric mean ratio >2.5, seroconversion rate >40%, and seroprotection rate >70%, for up to 6 months (10). Two-thirds (37/55) of the HCW had HI titres ≥40 at 12 months.

We further measured the neutralising antibodies using the MN assay, which detects neutralising antibodies that prevent virus infection in cell culture (**Figures 1E, F**). Only three HCW (3/55) had MN titres >80 before pandemic vaccination, which has been suggested to be seroprotective (15). Forty-eight of fifty-five HCW (87%) had titres >80 measured at 21 days after pandemic vaccination, and the titres increased significantly compared to pre-vaccination titres, (p < 0.001) with a fold-change of 63.9.

The titres decreased from 21 days after vaccination from 12 months after vaccination but were significantly higher compared to pre-vaccination titres ($p < 0.001$).

Ten of the HCW received only the pandemic vaccination during the five-year period, but annual serum samples were collected prior to each influenza season. Interestingly, five years after pandemic vaccination, 60% of HCW (6/10) had protective HI titres (≥40) and 50% (5/10) had a MN titre >80 (**Supplementary Figure 1**). None of these HCW who had protective HI or MN titres five years after pandemic vaccination had protective titres pre-pandemic vaccination.

Seasonal Vaccination Boosted the Antibody Response, Regardless of Prior Vaccination

We grouped the HCW according to their vaccination status during the different seasons into three different groups: unvaccinated, prior and current vaccination, or current vaccination only. Since all HCW received the pandemic vaccine, we had no HCW who only received the current vaccine in 2010/11.

Seasonal vaccinations significantly boosted both the quantity (ELISA) and quality (HI and MN) of the antibody response each year, regardless of prior vaccination status (**Figures 2A–L**). The only significant difference among those vaccinated was measured in ELISA in 2012/2013, where HCW who had not taken influenza vaccination in the prior season had significantly higher titres 12 months after vaccination compared to HCW vaccinated in both seasons (**Figure 2C**). We observed no differences in antibody responses during the seasons 2011/12 – 2012/13 between the groups, but HCW vaccinated only in the current 2013/14 season had a trend of a better antibody response compared to those with the prior vaccination. (**Figures 2D, H, L**). HCW without prior

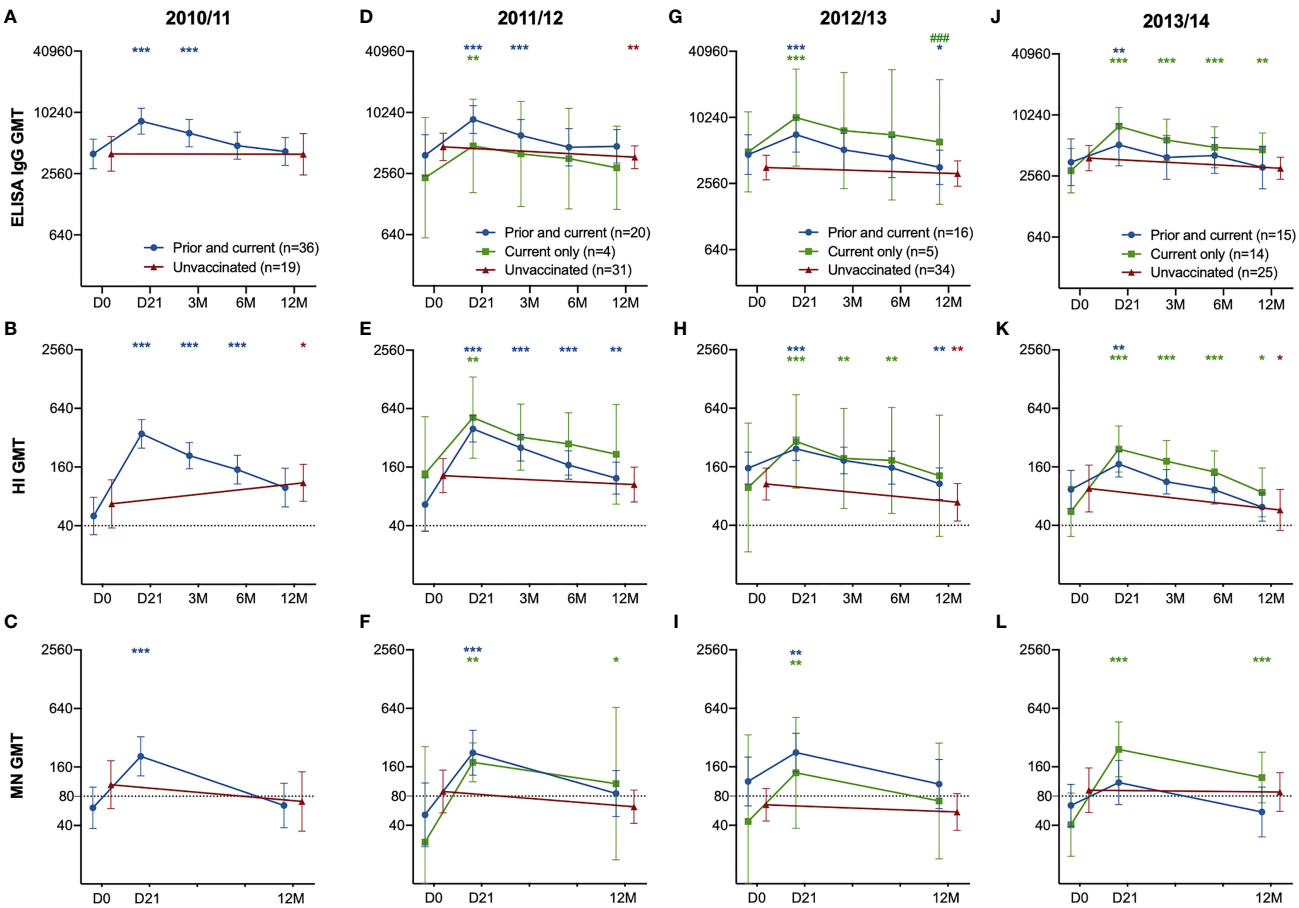

FIGURE 2 | The H1N1pdm09-specific ELISA IgG, HI and MN antibody response in HCW with the prior and current vaccination, current vaccination only and unvaccinated HCW. The ELISA IgG **(A)**, HI **(B)** and MN-titres **(C)** in HCW who received the prior & current vaccination in 2010/11 compared to unvaccinated HCW in 2010/11. The ELISA IgG **(D, G, J)**, HI **(B, E, H, K)** and MN titres **(C, F, I, L)** in HCW who received the prior & current vaccination in 2011/12 – 2013/14 compared to HCW who received only the current vaccination, and unvaccinated HCW. The geometric mean titres with 95% confidence interval are presented. The dotted line at 40 and 80 represents the protective titre, in HI and MN respectively. The data was log-transformed and analysed with the two-way ANOVA with Dunnetts test for multiple comparisons, for detecting differences within a group. Statistical differences between the groups were tested with linear mixed-effect models, with Dunnett´s test for multiple comparisons. The stars indicate significant increases within a group, with pre-vaccination titres (D0) as the reference timepoint. ***P < 0.001, **P < 0.01, *P < 0.05. ### Indicates statistical differences (P<0.05) between groups.

vaccination had significantly higher GMT (Geometric mean titres) 12 months after vaccination in 2013/14 compared to pre-vaccination GMT (**Figures 2J, K, L**). Compared to those who had been vaccinated in 2012/13 and received the current vaccination in 2013/14, the HCW without the prior vaccination had a significantly higher fold-change 21 days after vaccination in the 2013/14 season measured in ELISA and MN ($p < 0.05$) (**Figures 3A, C**).

Each season, HCW who were vaccinated had significant increases in their antibody titres measured at day 21 after vaccination in all assays ($p < 0.05$) (**Figures 2D–L**), except in the MN titres of the HCW with both prior and current vaccination at 21 days post-vaccination 2013/14. (**Figures 2L**). Also, the unvaccinated HCW showed a significant increase in HI titres in 2011/12, probably due to infection (**Figure 2B**).

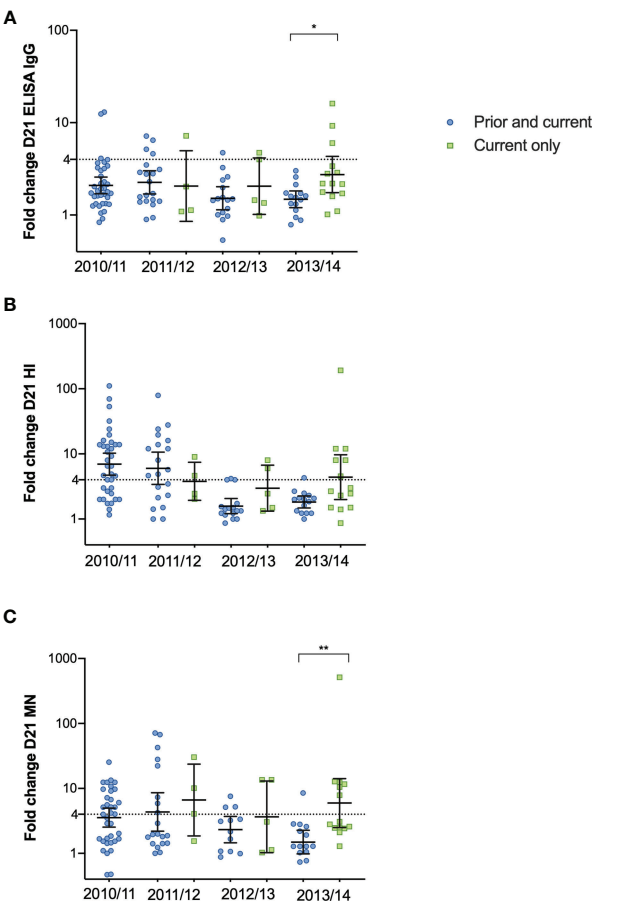

FIGURE 3 | The fold change after vaccination in 2010/11 – 2013/14 in HCW receiving the prior and current vaccination and the current vaccination only. The fold-change from pre-vaccination titres (D0) to post-vaccination titres (D21) measured in ELISA **(A)**, HI **(B)** and MN titres **(C)** in the HCW with the current vaccination only and those with the prior and current vaccination. Each symbol represents an individual ELISA, HI and MN fold change. The horizontal line shows the geometric mean with 95% confidence interval, and the dotted line at 4 indicates seroconversion. Statistical differences between the groups were tested with the Kruskal-Wallis test, with Dunn´s multiple comparisons test. $^{**}P < 0.01$, $^{*}P < 0.05$.

Antibodies decreased over time in subsequent years in the unvaccinated HCW (**Figure 2D–L**).

Time Duration Between Vaccinations Impacted the Fold Change After Vaccination in 2013

We further investigated the antibody responses in HCW with repeated annual vaccination compared to those with one-, two- or three-year gap in vaccination before vaccination in 2013. Antibodies increased after vaccination in all years but with some variations between the subgroups (**Figures 4A–C**). Antibodies declined over time in HCW who choose not to be vaccinated with seasonal vaccine, except in the HI titres in 12M 2009/10 to 12M 2010/11 in the three-year gap group (**Figures 4B**). Interestingly, the group with a two-year gap between vaccinations in 2010/11 and 2013/14 had consistently high antibody titres and had seroprotective HI- and MN antibodies at 12M 2012/13, two years after their last vaccination (**Figures 4B, C**).

When comparing the subgroups against the annually repeated group, the group with a two-year gap had significantly higher titres at day 21, 3, 6 and 12 months after vaccination in 2013/14 measured by ELISA (**Figure 4A**), and HI at 3 months and 6 months (**Figure 4B**). In addition, they had significantly higher MN titres 21 days after vaccination in 2013/14 (**Figure 4C**). The three-year gap group had significantly higher titres compared to the repeated group at 21 days after vaccination in 2013/14.

We assessed the fold changes in the repeated group, and the groups with one-, two, or three-year gap in vaccination before vaccination in 2013 (**Figure 5**). We observed lower antibody fold changes in the repeated group after vaccination in 2012/13 and 2013/14, in all assays (5A, E, I), which were their fourth and fifth vaccinations (5A, B, C). We further analysed the correlation between the different serological assays using all antibody titres (**Supplementary Figure 2**) and all correlations were statistically significant in the Pearson correlation test. The correlation coefficient was highest between the HI and MN titres (0.73) compared to 0.57 between the HI and ELISA titres, and 0.54 between the MN and ELISA titres.

DISCUSSION

HCW have a higher risk of influenza infections due to occupational exposure and are an important target group for influenza vaccination (16). However, the influenza vaccine coverage among HCW in Europe is often low (17). Current IIV offers suboptimal protection but remains the best option to prevent the burden of influenza. Despite IIV being used for decades, there are still unanswered questions regarding the durability of antibody responses and vaccine effectiveness after repeated vaccination. Several studies have shown that repeated vaccination impairs the antibody response (18, 19), while others have found no adverse effect on the antibody response after repeated vaccination (7, 20). The H1N1pdm09 virus from 2009 (A/California/07/2009) was included in seasonal vaccines up to the 2016/2017-season, providing a unique opportunity to study

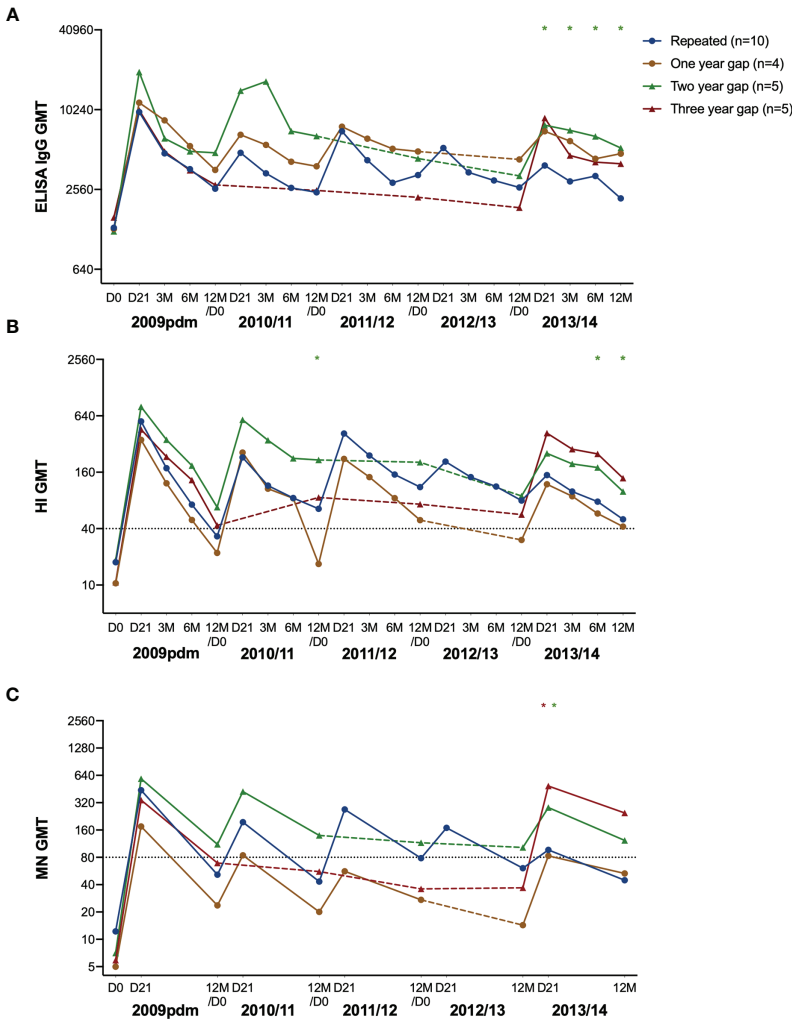

FIGURE 4 | The H1N1pdm09-specific antibody response over five years after pandemic and seasonal vaccinations. The geometric mean titre with 95% confidence interval measured in ELISA **(A)**, HI **(B)**, and MN **(C)** in repeatedly vaccinated HCW, and HCW with a one-, two- and three-year gap in vaccinations before vaccination in 2013/14. The titres at pre-vaccination (D0), and at 21 days (D21), 3, 6, and 12 months after vaccination are shown. The gap-years without vaccination is illustrated with a dotted line. The data was log-transformed and compared between groups with linear mixed-effect models, with Dunnett's test for multiple comparisons. The repeatedly vaccinated HCW was used as the reference group. ***P < 0.001, **P < 0.01, *P < 0.05.

the long-term antibody response to H1N1pdm09 without the complication of strains updates. This five-year study provides insight into antibody responses after pandemic and seasonal vaccinations in HCW with different influenza vaccination histories. Our study elucidates the impact of an AS03-adjuvanted influenza vaccine, and how the vaccination history shapes the antibody response.

The pandemic vaccine induced a potent and durable antibody response. We have previously shown durable HI antibodies in HCW receiving only the pandemic vaccine (9) and we have extended these findings to show that 50-60% of HCW with only pandemic vaccination (n = 10) had protective HI (6/10) and MN (5/10) titres 5 years post-vaccination. Although these unvaccinated HCW had a significant increase in HI titres by the end of the season 2010/11, which could be due to infection, young adults between 20-39 years old had the highest influenza attack rate in Norway in 2010/11 (21, 22). The persistence of antibodies in the HCW with protective titres up to five years after pandemic vaccination was caused by the AS03 adjuvant, which has been shown to induce higher T-and B-cell responses than non-adjuvanted vaccines (23), by activation of more naïve and memory B-cells (24). Others have also found that the AS03-adjuvanted pandemic vaccine was highly immunogenic (23, 25), and superior to non-adjuvanted monovalent H1N1pdm09 vaccines (26). The durability of these antibodies induced after adjuvanted vaccination shows the importance of inclusion of an adjuvant, which could be used in pandemic vaccine development for other possible respiratory virus pandemic threats.

All HCW received the pandemic vaccination, but their seasonal vaccination status varied during the following years.

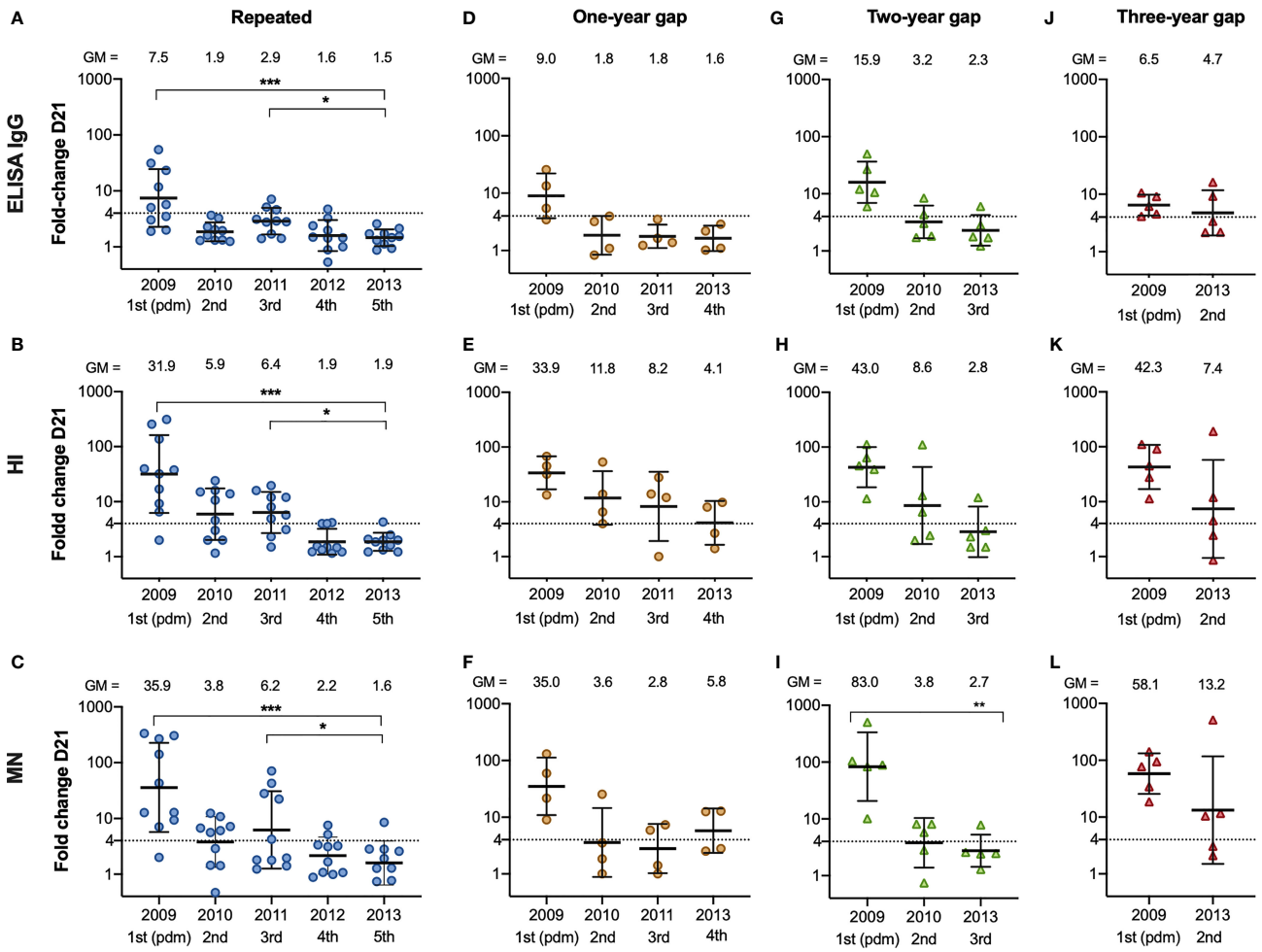

FIGURE 5 | The fold change after vaccination from 2009/10 – 2013/14 in repeatedly vaccinated and HCW with a one-, two- and three-year gap in vaccinations before vaccination in 2013/14. The fold change from pre-vaccination titres (D0) to post-vaccination titres (D21) measured in ELISA **(A)**, HI **(B)** and MN **(C)** in the HCW with repeated vaccinations, one-year gap **(D–F)** two-year gap **(G–I)** and a three-year gap **(J–L)** in vaccinations before getting vaccinated in 2013/14. Each symbol represents an individual ELISA, HI and MN fold change. The horizontal line shows the geometric mean with geometric standard deviation. The geometric mean is shown above the graph, and the number of vaccinations is shown below the graph. The dotted line at 4 indicates seroconversion. The Friedman test was used for detecting differences within the different subgroups, with Dunn´s test for multiple comparisons and the fold change in 2013/14 as the reference timepoint. ***P < 0.001, **P < 0.01, *P < 0.05.

We grouped the HCW to see the differences between the unvaccinated HCW, to those who only received the current vaccination, and those who had received both the previous and current seasonal vaccination. Some studies have reported that prior vaccination can attenuate the antibody response following the current seasonal vaccination (7, 27). We observed no differences between the groups in 2011/12 – 2012/13, but the groups varied in sample size. The groups had similar sample sizes in 2013/14 and we found a trend (although not significant) of a superior antibody response in the group with the current vaccination only compared to those who had previously received seasonal vaccination. Similarly, a recent study found the lowest influenza A/H1N1pdm09 positivity rate in every influenza-season between 2012/13 – 2017/18 in individuals with current vaccination only compared to prior vaccination only or current and prior vaccination (28).

HCW with five subsequent vaccinations had a reduced boosting effect post-vaccination in 2012/2013 and 2013/14, after their fourth and fifth vaccination with the same H1N1pdm09 strain, compared with their third vaccination. This suggests that the fold change after vaccination is reduced after the third vaccination against the same A/California/07/2009 (H1N1pdm09) antigen. Conversely, a gap-year between vaccinations is beneficial in terms of antibody boosting to the same strain with fold changes >4 in HI and MN observed in 2013/14 after their fourth vaccination. We observed that the group with a three-year gap between their two vaccinations (vaccinated in 2009/10 and 2013/14) had the highest fold change after vaccination in 2013/14 compared to the other groups. However, subject numbers were low in the groups of a two-year gap and a three-year gap before vaccination in 2013/14, so the results should be interpreted with caution. Importantly the

HCW were not optimally protected during the years without vaccination and had a higher risk of contracting influenza A/H3N2 or B during this time. Therefore, annual vaccination is favourable despite the probability of a reduced boosting of the antibody titres, as we observed in the repeatedly vaccinated HCW.

A recent study assessed different mathematical models to explain the difference in antibody-boosting in individuals who skipped vaccination for at least three years, compared to repeatedly vaccinated individuals, and found an increased boost in those who skipped vaccinations (29). We observed a reduced boosting in repeatedly vaccinated HCW in 2013/14, which could be a explained by a more rapid clearance of vaccine antigen in individuals with higher baseline titres (30), shortening the germinal center reaction (31). Furthermore, pre-existing antibodies may bind to and mask epitopes in the vaccine antigens, which would limit stimulation and expansion of B-cells (29). Our results agree with previous studies (18, 32) and suggest that the antibody response against the same antigen is diminished following repeated vaccination.

It has been known for decades that the antibody response following seasonal influenza vaccination is shaped by previous influenza encounters (33), either from infection or by vaccination. The "antibody ceiling" effect that we observed in the repeatedly vaccinated HCW has been previously reported in individuals with repeated influenza vaccinations (30, 32, 34), and we found a reduced antibody boosting after vaccination in the repeated group after their fourth and fifth vaccination. The "antibody ceiling" effect has been observed in individuals with high pre-existing titres (34) and may be due to antibody focusing to conserved epitopes on the HA. Although a reduced boosting in antibodies is observed in repeatedly vaccinated individuals, unvaccinated individuals have a higher risk of influenza infection due to the lack of humoral and cellular immunity to circulating strains (28). Further studies that investigates the impact of HA-specific antibodies and T-cells in repeatedly vaccinated individuals upon clinical protection are needed. The use of an adjuvanted vaccine was favourable in terms of priming and maintaining antibodies in our cohort, and perhaps adjuvanted influenza vaccines should be considered when vaccinating individuals that are repeatedly vaccinated, such as HCW and elderly. In future studies, vaccine effectiveness and antibody response of repeatedly vaccinated individuals after receiving an adjuvanted seasonal influenza vaccine should be investigated to see if that could overcome the "antibody ceiling" effect.

Caveats to our study should be considered. The numbers of HCW in the different subgroups were limited, and most were female. Our results cannot be generalized to all influenza seasons due to antigenic drift allowing the virus to escape host immunity and subsequent need for influenza vaccine updates. Since the adjuvanted pandemic vaccine was highly immunogenic, the antibody response may differ in other populations where the first vaccination was a non-adjuvanted vaccine. Although we asked participants if they had experienced influenza like illness, we did not perform virological surveillance during the study period, so we cannot exclude natural influenza infection that may have boosted the antibody responses. However, the main strength of our study is long term follow up with blood samples over a five-year period and the use of three serological assays (ELISA, HI and MN) which complement the limited number of other similar studies (35, 36).

In summary, our findings provide insight into the antibody responses in HCW with different vaccination statuses over a five-year period after pandemic and seasonal influenza vaccinations. We found that the adjuvanted pandemic vaccine elicited a robust antibody response, and HCW with only the current vaccination and with 2- and 3 gap-years before vaccination in 2013/14 had a better antibody response compared to repeatedly vaccinated HCW. However, seasonal vaccinations are the cornerstone of protection, and without vaccination HCW are more likely to be infected with circulating viruses, increasing the potential risk of infecting their patients. Our study supports the policy of annual vaccination to provide optimal protection for each influenza season, and it contributes to our understanding of the antibody response following repeated vaccination.

DATA AVAILABILITY STATEMENT

The raw data will be made available upon reasonable request to the corresponding author.

ETHICS STATEMENT

The studies involving human participants were reviewed and approved by Regional Ethics Committee (REKVest-2012/1772), and the Norwegian Medicines Agency (Clinicaltrials.gov NCT01003288). The participants provided their written consent to participate in this study.

AUTHOR CONTRIBUTIONS

RC and M-CT designed the study. HA, M-CT, FZ, and AM conducted the laboratory analysis. HA, M-CT and AB conducted the statistical analysis. HA and RC analysed the data and wrote the manuscript. All authors have read the final version of the manuscript. All authors contributed to the article and approved the submitted version.

FUNDING

This work was supported by intramural funding by the Influenza Centre at the University of Bergen. The Influenza Centre is funded by the University of Bergen, Ministry of Health and Care Services Norway (F-11628), the Trond Mohn foundation (TMS2020TMT05), the European Union (EU IMI115672 FLUCOP, H2020 877866 INCENTIVE and H2020 101037867 VACCELERATE, EU IMI101007799 Inno4Vac), Nanomedicines Flunanoair (ERA-NETet EuroNanoMed2,

JTC2016) and the Research Council of Norway Globvac program (284930).

ACKNOWLEDGMENTS

We are grateful to HCW who altruistically gave their time and donated blood, the clinical staff, and staff at the Influenza Centre for help with the study. We especially thank Prof. Florian Krammer Mount Sinai, USA for providing the baculoviruses used to purify the H1 protein.

SUPPLEMENTARY MATERIAL

The Supplementary Material for this article can be found online at: https://www.frontiersin.org/articles/10.3389/fimmu.2021.748281/full#supplementary-material

REFERENCES

1. Paget J, Spreeuwenberg P, Charu V, Taylor RJ, Iuliano AD, Bresee J, et al. Global Mortality Associated With Seasonal Influenza Epidemics: New Burden Estimates and Predictors From the GLaMOR Project. *J Glob Health* (2019) 9 (2):20421. doi: 10.7189/jogh.09.020421
2. Poland GA, Tosh P, Jacobson RM. Requiring Influenza Vaccination for Health Care Workers: Seven Truths We Must Accept. *Vaccine* (2005) 23:2251–5. doi: 10.1016/j.vaccine.2005.01.043
3. World Health Organization. *Pandemic (H1N1) 2009 – Update 68*. Available at: http://www.who.int/csr/don/2009_10_02/en/.
4. Helse og omsorgsdepartementet. *Beredskap Mot Pandemisk Influensa Meld. St. 16 (2012–2013)*. Available at: https://www.regjeringen.no/contentassets/a7c7e93dbe8f44d2a8fe892768e429c5/no/pdfs/stm201220130016000dddpdfs.pdf.
5. Castrucci MR. Factors Affecting Immune Responses to the Influenza Vaccine. *Hum Vaccin Immunother* (2018) 14(3):637–46. doi: 10.1080/21645515.2017.1338547
6. Belongia EA, Skowronski DM, McLean HQ, Chambers C, Sundaram ME, De Serres G. Repeated Annual Influenza Vaccination and Vaccine Effectiveness: Review of Evidence. *Expert Rev Vaccines* (2017) 16:7. doi: 10.1080/14760584.2017.1334554
7. Beyer WEP, de Bruijn IA, Palache AM, Westendorp RGJ, Osterhaus ADME. Protection Against Influenza After Annually Repeated Vaccination: A Meta-Analysis of Serologic and Field Studies. *Arch Intern Med* (1999) 159(2):182–8. doi: 10.1001/archinte.159.2.182
8. Folkehelseinstituttet. *Influenza Vaccination Coverage in Norway 2018/2019 Season* (2019). Available at: https://www.fhi.no/sv/influensa/influensavaksine/vaksinasjonsdekningstall-for-influensavaksine/.
9. Trieu MC, Jul-Larsen Å, Sævik M, Madsen A, Nøstebakken JK, Zhou F, et al. Antibody Responses to Influenza A/H1N1pdm09 Virus After Pandemic and Seasonal Influenza Vaccination in Healthcare Workers: A 5-Year Follow-Up Study. *Clin Infect Dis* (2019) 68(3):382–92. doi: 10.1093/cid/ciy487
10. Madhun AS, Akselsen PE, Sjursen H, Pedersen G, Svindland S, Nøstbakken JK, et al. An Adjuvanted Pandemic Influenza H1N1 Vaccine Provides Early and Long Term Protection in Healthcare Workers. *Vaccine* (2010) 29:266–73. doi: 10.1016/j.vaccine.2010.10.038
11. Krammer F, Pica N, Hai R, Margine I, Palese P. Chimeric Hemagglutinin Influenza Virus Vaccine Constructs Elicit Broadly Protective Stalk-Specific Antibodies. *J Virol* (2013) 87(12):6542–50. doi: 10.1128/JVI.00641-13
12. Tete SM, Krammer F, Lartey S, Bredholt G, Wood J, Skrede S, et al. Dissecting the Hemagglutinin Head and Stalk-Specific IgG Antibody Response in Healthcare Workers Following Pandemic H1N1 Vaccination. *NPJ Vaccines* (2016) 1:16001. doi: 10.1038/npjvaccines.2016.1
13. Rowe T, Abernathy RA, Hu-Primmer J, Thompson WW, Lu X, Lim W, et al. Detection of Antibody to Avian Influenza A (H5N1) Virus in Human Serum by Using a Combination of Serologic Assays. *J Clin Microbiol* (1999) 37 (4):937–43. doi: 10.1128/JCM.37.4.937-943.1999
14. Hobson D, Curry RL, Beare AS, Ward-Gardner A. The Role of Serum Haemagglutination-Inhibiting Antibody in Protection Against Challenge Infection With Influenza A2 and B Viruses. *J Hygiene* (1972) 70(4):767–77. doi: 10.1017/s0022172400022610
15. Veguilla V, Hancock K, Schiffer J, Gargiullo P, Lu X, Aranio D, et al. Sensitivity and Specificity of Serologic Assays for Detection of Human Infection With 2009 Pandemic H1N1 Virus in U.S. Populations. *J Clin Microbiol* (2011) 49(6):2210–5. doi: 10.1128/JCM.00229-11
16. Kuster SP, Shah PS, Coleman BL, Lam PP, Tong A, Wormsbecker A, et al. Incidence of Influenza in Healthy Adults and Healthcare Workers: A Systematic Review and Meta-Analysis. *PloS One* (2011) 6(10):e26239. doi: 10.1371/journal.pone.0026239
17. Jorgensen P, Mereckiene J, Cotter S, Johansen K, Tsolova S, Brown C. How Close Are Countries of the WHO European Region to Achieving the Goal of Vaccinating 75% of Key Risk Groups Against Influenza? Results From National Surveys on Seasonal Influenza Vaccination Programmes, 2008/2009 to 2014/2015. *Vaccine* (2018) 36(4):442–52. doi: 10.1016/j.vaccine.2017.12.019
18. Sanyal M, Holmes TH, Maecker HT, Albrecht RA, Dekker CL, He XS, et al. Diminished B-Cell Response After Repeat Influenza Vaccination. *J Infect Dis* (2019) 219:10 1586–1595. doi: 10.1093/infdis/jiy685
19. Leung KYV, Carolan LA, Worth LJ, Harper SA, Peck H, Tilmanis D, et al. Influenza Vaccination Responses: Evaluating Impact of Repeat Vaccination Among Health Care Workers. *Vaccine* (2017) 35;19:2558–68. doi: 10.1016/j.vaccine.2017.03.063
20. Strengell M, Ikonen N, Ziegler T, Kantele A, Anttila VJ, Julkunen I. Antibody Responses Against Influenza A(H1N1)pdm09 Virus After Sequential Vaccination With Pandemic and Seasonal Influenza Vaccines in Finnish Healthcare Professionals. *Influenza Other Respir Viruses* (2013) 7(3):431–8. doi: 10.1111/j.1750-2659.2012.00415.x
21. Künzel W, Glathe H, Engelmann H, Van Hoecke C. Kinetics of Humoral Antibody Response to Trivalent Inactivated Split Influenza Vaccine in Subjects Previously Vaccinated or Vaccinated for the First Time. *Vaccine* (1996) 14(12):1108–10. doi: 10.1016/0264-410x(96)00061-8
22. Hauge SH, Bakken IJ, de Blasio BF, Håberg SE. Burden of Medically Attended Influenza in Norway 2008-2017. *Influenza Other Respi Viruses* (2019) 13:240–7. doi: 10.1111/irv.12627
23. van der Most RG, Clement F, Willekens J, Dewé W, Walravens K, Vaughn DW, et al. Long-Term Persistence of Cell-Mediated and Humoral Responses to A(H1N1)pdm09 Influenza Virus Vaccines and the Role of the AS03 Adjuvant System in Adults During Two Randomized Controlled Trials. *Clin Vaccine Immunol* (2017) 24:e00553–16. doi: 10.1128/CVI.00553-16
24. Galson JD, Trück J, Kelly DF, van der Most R. Investigating the Effect of AS03 Adjuvant on the Plasma Cell Repertoire Following Ph1n1 Influenza Vaccination. *Sci Rep* (2016) 6:37229. doi: 10.1038/srep37229
25. Cohet C, van der Most R, Bauchau V, Bekkat-Berkani R, Doherty TM, Schuind A, et al. Safety of AS03-Adjuvanted Influenza Vaccines: A Review of the Evidence. *Vaccine* (2019) 37(23):3006–21. doi: 10.1016/j.vaccine.2019.04.048
26. Ferguson M, Risi G, Davis M, Sheldon E, Baron M, Li P, et al. Safety and Long-Term Humoral Immune Response in Adults After Vaccination With an H1N1 2009 Pandemic Influenza Vaccine With or Without AS03 Adjuvant. *J Infect Dis* (2012) 205(5):733–44. doi: 10.1093/infdis/jir641
27. Gaglani M, Spencer S, Ball S, Song J, Naleway A, Henkle E, et al. Antibody Response to Influenza A(H1N1)pdm09 Among Healthcare Personnel Receiving Trivalent Inactivated Vaccine: Effect of Prior Monovalent Inactivated Vaccine. *J Infect Dis* (20142014) 209(11):1705–14. doi: 10.1093/infdis/jit825
28. Kim SS, Flannery B, Foppa IM, Chung JR, Nowalk MP, Zimmerman RK, et al. Effects of Prior Season Vaccination on Current Season Vaccine Effectiveness in the United States Flu Vaccine Effectiveness Network, 2012-2013 Through 2017-2018. *Clin Infect Dis* (2021) 73(3):497–505. doi: 10.1093/cid/ciaa706

29. Linderman SL, Ellebedy AH, Davis C, Eberhardt CS, Antia R, Ahmed R, et al. Influenza Immunization in the Context of Preexisting Immunity. *Cold Spring Harb Perspect Med* (2020) 11(11):a040964. doi: 10.1101/cshperspect.a040964
30. Ellebedy AH. Immunizing the Immune: Can We Overcome Influenza's Most Formidable Challenge? *Vaccines (Basel)* (2018) 6(4):68. doi: 10.3390/vaccines6040068
31. Zhang Y, Garcia-Ibanez L, Toellner KM. Regulation of Germinal Center B-Cell Differentiation [Published Correction Appears in Immunol Rev. 2016 Jul;272(1):202]. *Immunol Rev* (2016) 270(1):8–19. doi: 10.1111/imr.12396
32. Sherman AC, Lai L, Bower M, Natrajan MS, Huerta C, Karmali V, et al. The Effects of Imprinting and Repeated Seasonal Influenza Vaccination on Adaptive Immunity After Influenza Vaccination. *Vaccines* (2020) 8(4):663. doi: 10.3390/vaccines8040663
33. Francis T. On the Doctrine of Original Antigenic Sin. *Proc Am Philos Soc* (1960) 104:572–8.
34. Andrews SF, Huang Y, Kaur K, Popova LI, Ho IY, Pauli NT, et al. Immune History Profoundly Affects Broadly Protective B Cell Responses to Influenza. *Sci Transl Med* (2015) 7(316):316ra192. doi: 10.1126/scitranslmed.aad0522
35. Madsen A, Jul-Larsen Å, Trieu MC, Krammer F. Cox. Persistently High Antibody Responses After AS03-Adjuvanted H1N1pdm09 Vaccine: Dissecting the HA Specific Antibody Response. *NPJ Vaccines* (2021) 6:45. doi: 10.1038/s41541-021-00308-5
36. Herrera MT, Gonzalez Y, Juárez E, Hernández-Sánchez F, Carranza C, Sarabia C, et al. Humoral and Cellular Responses to a Non-Adjuvanted Monovalent H1N1 Pandemic Influenza Vaccine in Hospital Employees. *BMC Infect Dis* (2013) 13:544. doi: 10.1186/1471-2334-13-544

Conflict of Interest: The authors declare that the research was conducted in the absence of any commercial or financial relationships that could be construed as a potential conflict of interest.

frontiers in Immunology

ORIGINAL RESEARCH
published: 21 February 2022
doi: 10.3389/fimmu.2022.785975

Supplementation of H7N9 Virus-Like Particle Vaccine With Recombinant Epitope Antigen Confers Full Protection Against Antigenically Divergent H7N9 Virus in Chickens

Dexin Kong[1,2,3,4], *Taoran Chen*[1,2,3,4], *Xiaolong Hu*[1,2,3,4], *Shaorong Lin*[1,2,3,4], *Yinze Gao*[1,2,3,4], *Chunmei Ju*[1], *Ming Liao*[1,2,3,4*] *and Huiying Fan*[1,2,3,4*]

[1] College of Veterinary Medicine, South China Agricultural University, Guangzhou, China, [2] Key Laboratory of Zoonosis Prevention and Control of Guangdong Province, College of Veterinary Medicine, South China Agricultural University, Guangzhou, China, [3] Key Laboratory of Animal Vaccine Development, Ministry of Agriculture, Guangzhou, China, [4] National and Regional Joint Engineering Laboratory for Medicament of Zoonosis Prevention and Control, College of Veterinary Medicine, South China Agricultural University, Guangzhou, China

OPEN ACCESS

Edited by:
Corey Patrick Mallett,
GlaxoSmithKline, United States

Reviewed by:
Edward Rybicki,
University of Cape Town, South Africa
Irina V. Kiseleva,
Institute of Experimental Medicine (RAS), Russia

***Correspondence:**
Huiying Fan
fanhy@scau.edu.cn
Ming Liao
mliao1968@163.com

Specialty section:
This article was submitted to Vaccines and Molecular Therapeutics, a section of the journal Frontiers in Immunology

Received: 29 September 2021
Accepted: 27 January 2022
Published: 21 February 2022

Citation:
Kong D, Chen T, Hu X, Lin S, Gao Y, Ju C, Liao M and Fan H (2022) Supplementation of H7N9 Virus-Like Particle Vaccine With Recombinant Epitope Antigen Confers Full Protection Against Antigenically Divergent H7N9 Virus in Chickens. Front. Immunol. 13:785975. doi: 10.3389/fimmu.2022.785975

The continuous evolution of the H7N9 avian influenza virus suggests a potential outbreak of an H7N9 pandemic. Therefore, to prevent a potential epidemic of the H7N9 influenza virus, it is necessary to develop an effective crossprotective influenza vaccine. In this study, we developed H7N9 virus-like particles (VLPs) containing HA, NA, and M1 proteins derived from H7N9/16876 virus and a helper antigen HMN based on influenza conserved epitopes using a baculovirus expression vector system (BEVS). The results showed that the influenza VLP vaccine induced a strong HI antibody response and provided effective protection comparable with the effects of commercial inactivated H7N9 vaccines against homologous H7N9 virus challenge in chickens. Meanwhile, the H7N9 VLP vaccine induced robust crossreactive HI and neutralizing antibody titers against antigenically divergent H7N9 viruses isolated in wave 5 and conferred on chickens complete clinical protection against heterologous H7N9 virus challenge, significantly inhibiting virus shedding in chickens. Importantly, supplemented vaccination with HMN antigen can enhance Th1 immune responses; virus shedding was completely abolished in the vaccinated chickens. Our study also demonstrated that viral receptor-binding avidity should be taken into consideration in evaluating an H7N9 candidate vaccine. These studies suggested that supplementing influenza VLP vaccine with recombinant epitope antigen will be a promising strategy for the development of broad-spectrum influenza vaccines.

Keywords: H7N9, virus-like particles, influenza conserved epitopes, cross-protection, T-cell immunity

INTRODUCTION

In March 2013, a novel H7N9 subtype of avian influenza virus infection was discovered in human cases in China (1). Since then, the virus has spread rapidly throughout the country, leading to several waves of outbreaks. In particular, after the emergence of the highly pathogenic H7N9 avian influenza virus during the fifth wave, the H7N9 virus caused a sharp rise in human infection, resulting in 1,568

laboratory-confirmed cases and 616 deaths as of July 7, 2021 (http://www.fao.org/ag/againfo/programmes/en/empres/H7N9/situation_update.html). More importantly, some novel biological features of the H7N9 virus, such as immune escape mutations and antigenic drift were discovered in H7N9 variants (2–4). Thus, there is still a possibility of an H7N9 pandemic outbreak. The continuous evolution of the H7N9 virus poses a dual threat to public health and the poultry industry, and thus it is imperative to protect against H7N9 influenza infection.

Vaccination has been considered the most effective way to prevent and control influenza virus infection (5, 6). Available are the conventional influenza vaccine containing live attenuated vaccine, whole-virus inactivated vaccine, recombinant vector vaccine, and recombinant subunit vaccine. The current large-scale production of influenza vaccine depends on the supply of embryonated chicken eggs; it is very fragile for the timely supply of a sufficient influenza vaccine during pandemic outbreaks (7, 8). Therefore, it is necessary to develop a preferable method for the production of influenza vaccines. Virus-like particle (VLP) vaccine is one of the influenza subunit vaccines; the VLPs mimic the structural and immunological properties of a native virus but are innocuous. Thus, the preparation approach of an influenza vaccine based on VLPs is preferable (9, 10). The insect cell-baculovirus expression vector system (IC-BEVS) is widely used for the development of influenza VLP subunit vaccines owing to its unique advantages, including excellent safety, short production times, and straightforward scale-up (11–13). The production of VLPs based on insect cell suspension cultured in a bioreactor system is low cost and high yield (12, 14). Currently, several different influenza VLP constructs contain HA or a combination of HA and neuraminidase (HA-NA) and matrix protein M1. HA is the main target antigen for the development of avian influenza vaccines. Neuraminidase (NA) in influenza VLP contributes to protecting against a high-dose avian influenza virus challenge infection (15).

Current influenza vaccine immunization only induces specific immune responses against strain-matched influenza viruses. This cannot provide effective protection when the circulating viruses generate antigenic drift or a new pandemic virus emerges (4, 16, 17). Therefore, developing an appropriate vaccination strategy is a high priority to improve the crossprotection of influenza vaccines and prevent future pandemic outbreaks. One appropriate approach to improving the crossprotection of the influenza vaccine is by combining it with the toll-like receptor ligand or the influenza conserved epitopes fusion protein adjuvant. Studies have shown that immunization with influenza vaccines based on influenza conserved epitopes induces crossreaction immune responses to confer crossprotection against homologous and heterologous influenza virus challenge (18–23). Nevertheless, influenza vaccines based on influenza conserved epitopes have shown limited protection against homologous and heterologous influenza challenges in reducing signs of clinical symptoms and virus shedding (24–26). These findings indicate that fusion protein of the recombined influenza conserved epitopes can act as an adjuvant to enhance the crossprotection of influenza VLP vaccine against drifted influenza virus. Poly(I:C), a toll-like receptor (TLR)-3 ligand, is a potent adjuvant, intranasal delivery of influenza vaccine with Poly(I:C) elicited robust antigen-specific cell-mediated immune responses (27, 28). Poly(I:C) has been identified to induce strong Th1 immune responses. The induction of protective T-cell responses can enhance the crossprotection of the influenza vaccine.

The main goal of this study was to develop an influenza VLP subunit vaccine and an effective supplement vaccination strategy to provide crossprotection against an influenza virus challenge. A recombinant protein (HMN) consisting of three tandem conserved epitopes: two repeats of $HA_{76\text{-}130}$; four repeats of M2e; and eight repeats of $NP_{55\text{-}69}$ was constructed, and a Poly (I:C) was used as a vaccine supplement in the present study. The result demonstrated that the influenza VLP subunit vaccine induced robust HI and neutralizing antibody titers to crossprotect against challenge with a lethal homologous and heterologous H7N9 virus. The influenza VLP vaccine supplement with HMN or Poly(I:C) enhanced a Th1-biased influenza-specific immune response in chickens, which was significantly inhibited virus shedding.

MATERIALS AND METHODS

Ethics Statement

All experiments involved in the live H7N9 avian influenza viruses (AIVs) were performed in a biosafety level 3 laboratory facility at South China Agricultural University (SCAU) (CNAS BL0011) in accordance with protocols. All animals involved in the experiments were reviewed and approved by the Institution Animal Care and Use Committee at SCAU and treated in accordance with the guidelines (2017A002).

Cells and Viruses

Spodoptera frugiperda 9 (Sf9) and BTI-TN-5B1-4 (High Five™) insect cells were used in this study. Sf9 cells (Invitrogen, Waltham, MA, USA) were maintained in Sf-900 II serum-free medium (Gibco, Carlsbad, CA, USA) and used for the production of recombinant baculovirus. High Five™ cells (Invitrogen, USA) were maintained as a suspension in HF-SFM (World-Medium, Suzhou, China) in shaker flasks at a speed of 100–120 rpm and used for the production of recombinant proteins. Both insect cell lines were cultured at 27°C. Madin-Darby canine kidney (MDCK) cells were maintained at 37°C in 5% CO_2 in Dulbecco's modified Eagle's medium (DMEM) supplemented with 10% (v/v) heat-inactivated fetal bovine serum (Invitrogen, USA).

HPAI H7N9 viruses A/Chicken/Guangdong/16876/2016 (H7N9-16876) (29), A/Chicken/Qingyuan/E664/2017 (H7N9-E664) (3), and A/Chicken/Guangdong/E157/2017 (H7N9-E157) were used in this study. Influenza viruses were propagated in 10-day-old specific-pathogen-free (SPF) embryonated chicken eggs. The viral allantoic fluid was harvested from each embryo and clarified at 4,000×*g* centrifugation for 5 min. The clarified fluid was then ultracentrifuged at 30,000×*g* for 1 h, and the virus solution was further purified using a 20%–30%–45%–60%

discontinuous sucrose gradient. The 50% egg infectious dose (EID_{50}) and the 50% egg lethal dose (ELD_{50}) were calculated using the Reed-Muench method (30). Furthermore, H7N9-16876 and H7N9-E157 AIVs were used as challenge viruses. The inactivated virus using 0.1% formalin was used as hemagglutination inhibition (HI) antigen.

Generation of Recombinant Baculovirus

To generate the VLP, the hemagglutinin (HA), neuraminidase (NA), and matrix protein (M1) genes derived from A/Chicken/Guangdong/16876/2016(H7N9) were biochemically synthesized by BGI (Shenzhen, China). Genes of HA, NA, and M1 were codon optimized for a high level of expression in High Five cells, then a 6xHis epitope tag was simultaneously fused to the C-terminal end of the optimized gene.

A recombinant chimeric protein containing honeybee melittin signal peptide, tandem repeat of $2HA_{76\text{-}130}$, 4M2e, $8NP_{55\text{-}69}$, and a flexible linker sequence (3xG4S) was designed and named HMN (**Table 1**). Each M2e sequence was linked by a linker sequence (PGGSSGGSS). Each $NP_{55\text{-}69}$ sequence was linked by a linker sequence (GGSS), and the 6xHis tag epitope was linked to the 3′ ends of the HMN sequence by a GGSS linker. HMN gene was codon optimized for a high level of expression in the High Five cells and synthesized by BGI.

These four optimized genes were cloned into the pACEBac1 vector plasmid (Invitrogen, Carlsbad, CA, USA), respectively. The recombinant plasmids were transformed into *Escherichia coli* DH10Bac to make recombinant bacmid baculovirus DNA, purified recombinant bacmid DNAs were transfected into sf9 insect cells using Cellfectin™ II reagent (Invitrogen) to obtain the recombinant baculovirus (rBV) in the culture supernatant. Following the manufacturer's instructions, the recombinant baculoviruses were then amplified by infecting sf9 insect cells. All preparations of rBV were plaque purified and titrated using a rapid titration kit (BacPak Baculovirus Rapid Titer Kit; Clontech, Mountain View, CA, USA).

Expression and Purification of H7N9-VLP and HMN

To generate recombinant proteins, High Five cells were maintained as suspension cultures in HF-SFM serum-free medium (World-Medium Biotechnology Co., Ltd., Suzhou, China) in shaker flasks at 27°C. For the production of VLP containing the H7N9 HA, NA, and M1 proteins, High Five cells were coinfected with rBVs expressing HA, NA, and M1, respectively, at a multiplicity of infection (MOI) of 2:1:2. After 3 days postinfection, cell culture supernatants were harvested by centrifugation at 2,000×*g* for 30 min at 4°C to remove debris. The VLPs in the supernatants were purified by ultracentrifugation at 30,000×*g* for 60 min at 4°C. The sedimented particles were resuspended in phosphate-buffered saline (PBS, pH 7.2) at 4°C overnight and further purified through a 20%–30%–45%–60% discontinuous sucrose gradient at 100,000×*g* for 1 h at 4°C (31). The functionality of HA protein incorporated into VLPs was quantified by hemagglutination assay (HA assay) using 1% (v/v) chicken red blood cells.

For the production of HMN proteins, High Five cells were infected with rBV expressing HMN protein in shaker flasks at an MOI of 1. After 3 days postinfection, the infected High Five cells were harvested and disrupted by ultrasonication for 30 min to prepare cell lysates under the condition of maintaining the temperature at 0°C–4°C. The sonicated cell lysates were cleared by low-speed centrifugation (10,000×*g* for 3 min at 4°C) to remove cell debris. The target proteins were purified using Ni-chromatography and used for further studies. The concentration of the purified VLPs and HMN was quantified using the Pierce BCA Protein Assay Kit (Thermo Fisher Scientific, Waltham, MA, USA).

The indirect immunofluorescence assay (IFA) was performed to detect the expression of VLPs and HMN protein in infected sf9 insect cells. Briefly, sf9 insect cells were infected with recombinant baculovirus expressing H7N9 proteins or HMN, respectively. After incubation for 48 h, the cells were fixed with 80% precooled acetone at −20°C for 15 min and incubated with the primary chicken antiserum against H7N9 AIVs or anti-His-tag mouse monoclonal antibody at a dilution of 1:200, and then with the secondary fluorescein isothiocyanate (FITC)-conjugated goat anti-chicken IgG antibody (Invitrogen, Carlsbad, CA, USA) or rabbit anti-mouse IgG antibody (Sigma St. Louis, MO, USA). Fluorescent images were examined under an inverted fluorescence microscope (Nikon, Ti-S, Minato, Japan).

SDS-PAGE and Western Blot

The H7N9 VLPs and HMN proteins were analyzed using SDS-PAGE and Western blot. Briefly, the protein samples were mixed with 5x SDS-PAGE loading buffer (Dingguo, Guangzhou, China) and boiled for 10 min, then separated by 10% Tris-Glycine gels, and stained using Coomassie Brilliant Blue (Dingguo, Guangzhou, China) for SDS-PAGE analysis. The protein bands were also transferred to nitrocellulose membranes (Bio-Rad, Guangzhou, China) for Western blot analysis. The membranes were blocked with 5% (W/V) skim milk in PBST [PBS containing 0.05% (v/v) Tween 20] overnight at 4°C. Membranes were subsequently incubated with an anti-His-tag mouse monoclonal antibody (1:5,000, v/v, BioWorld Technology, Nanjing, China) for 1 h at room temperature. The blots were then washed five times with PBST and incubated with a horseradish-peroxidase-conjugated goat anti-mouse IgG antibody (LI-COR, Lincoln, NE, USA) for 1 h at room temperature. Finally, the proteins were visualized by chemiluminescence (LI-COR Odyssey).

TABLE 1 | Antigen epitopes included in HMN.

Epitope	Sequence
HA2 76-130	QIGNVINWTRDSITEVWSYNAELLVAMENQHTIDLADSEMDKLYERVKRQLRENA
M2e 2-24	SLLTEVETPTRTGWECNCSGSSD
NP 55-69	RLIQNSITIERMVLS
Melittin SP	MKFLVNVALVFMVVYISYIYAD

HA2 76–130, hemagglutinin stem area amino acids 76–130; M2e, the ectodomain of matrix protein M2; NP55–69, nucleoprotein amino acids 55–69; Melittin SP, melittin signal peptide.

Electron Microscopy

Sucrose gradient-purified VLP samples were adsorbed onto a carbon parlodion-coated copper grid for 2 min. Excess VLP suspension was removed by blotting with filter paper, and the grid was immediately stained with 1% phosphotungstic acid for 10 min. Excess stain was removed by filter paper, and the samples were examined using a transmission electron microscope (Talos L120C, FEI, Czech).

Vaccination and Challenge

Three-week-old SPF chickens were purchased from the Experimental Animal Center (Xinxing Dahuanong Eggs Co., Ltd., Guangdong, China). They were maintained according to the South China Agricultural University's guidelines for the care and use of laboratory animals and used to determine the immunogenicity and efficacy of the H7N9 VLPs. The commercial avian influenza trivalent inactivated vaccine [Reassortant Avian Influenza Virus (H5+H7) Trivalent Vaccine, Inactivated (H5N2 Strain rSD57+ Strain rFJ56, H7N9 Strain rLN79)] was provided from South China Biological Medicine Co., Ltd. (Guangzhou, China). For a homologous protection study, a group (N = 10) of chickens were subcutaneously immunized once with 30 μg of (total protein) VLPs in combination with EOLANE 150 (Total Energies, Paris, France). The commercial avian influenza trivalent inactivated vaccine (H7 +H5) was set as comparison control, and one group of chickens was inoculated with PBS as a negative control. Three weeks after immunization, chickens were intranasally challenged with $2 \times 10^{6.0}$ ELD_{50} (0.2 ml) HPAI H7N9-16876.

For a crossprotection study, groups (N = 13 each group) of chickens were subcutaneously immunized once with 30 μg of VLP with ISA 201 VG, ISA 201 VG supplemented with 30 μg of HMN, and ISA 201 VG supplemented with 30 μg of Poly(I:C) (*In vivo*Gen, San Diego, CA, USA); one group (N = 13) of chickens was immunized intramuscularly once with 30 μg of VLP with ISA 71VG (Seppic, Paris, France), and one group of chickens was inoculated PBS as a negative control. Nineteen days after immunization, the peripheral blood and spleen of chickens (N = 3) in each group were obtained for the determination of cytokine levels. Three weeks after immunization, other chickens (N = 10) of each test group were inoculated intranasally with $10^{6.0}$ EID_{50} of H7N9-E157 virus in a 200-μl volume. Chickens were monitored for clinical signs and mortality for 14 days postchallenge (PC). All surviving chickens were killed humanely at the end of monitoring experiments.

To determine virus positivity or shedding from individual chickens, the oropharyngeal and cloacal swab samples were collected at 5 days postchallenge in the homologous protection study. The oropharyngeal and cloacal swab samples were collected at 3, 5, 7, and 9 days postchallenge in the crossprotection study. The swab samples were resuspended in 1 ml of PBS supplemented with 2,000 mg/ml streptomycin and 2,000 IU/ml penicillin. The suspensions were centrifuged at 3,000×*g* for 10 min, and 0.1 ml of the supernatants from the oropharyngeal or cloacal swabs were used to inoculate the allantoic cavities of 10-day-old SPF chicken embryos (3 eggs/sample). After incubation for 48 h at 37°C, the allantoic fluids were tested for hemagglutination activity. A virus isolation positive swab means one or more of the inoculated egg allantoic fluids reciprocal to the hemagglutination titers was higher than 4.

Serology Assays

To determine the immunogenicity of the vaccines, serum antibody levels were titrated by hemagglutination inhibition (HI) assay or neutralization assay. Hemagglutination inhibition (HI) assay was performed using standard methods (32). Briefly, sera were pretreated with a receptor destroying enzyme (RDE, Seiken, Japan) for 20 h at 37°C followed by inactivation of the RDE at 56°C for 30 min. Twofold serial dilutions of 50 μl pretreated sera were incubated with an equal volume of 4 HA units of the inactivated H7N9 virus antigen for 1 h at room temperature. Then, 50 μl of a 1% suspension of chicken red blood cells (RBC) was added to each well and incubated at room temperature for 30 min. The HI titer was expressed as the reciprocal of the highest serum dilution that completely inhibited hemagglutination of 4 HA units of the virus. The neutralization assay was performed as follows. Briefly, MDCK cells were plated into 96-well plates. The twofold serial dilutions of heat-inactivated (56°C, 30 min) serum samples were mixed with equal volumes of 100 mean tissue culture infective doses (TCID50) of H7N9 influenza viruses (E157 or E664). After 1 h of incubation at 37°C, the mixtures of serum and virus were added to the MDCK cells. Cells were then incubated for 1 h at 37°C. After 1 h of incubation, the culture supernatants were replaced by medium supplemented with 0.5 μg/μl TPCK-trypsin (Dingguo, Guangzhou, China), and cells were incubated for an additional 72 h. After 72 h of incubation, cell supernatants were harvested and transferred to V-bottom 96-well plates. The presence of virus was detected using a hemagglutination assay (33). Neutralizing antibody titers were defined as the reciprocal of the highest serum dilution that neutralized the virus in cell supernatants.

Isolation and Stimulation of Chicken PBMCs and Splenocytes

Peripheral blood mononuclear cells (PBMCs) and splenocytes were prepared for cytokine assays. PBMCs were isolated from peripheral blood using Ficoll-Hypaque density sedimentation (Tbdscience, Tianjin, China). Splenocytes were obtained from the spleens of chickens by density gradient centrifugation using Lymphoprep (Tbdscience, Tianjin, China) according to the manufacturer's instructions. After contaminating red blood cells (RBC) present in the isolated cells lysed using RBC lysis buffer (Solarbio, Beijing, China), single cells were collected. PBMCs and splenocyte single-cell suspensions were cultured in complete Roswell Park Memorial Institute (RPMI) 1640 medium containing 10% FBS and 1% penicillin-streptomycin/L-glutamine (Gibco, Carlsbad, CA, USA) at a final concentration of 1×10^6 cells/ml. Cells were stimulated with 20 μg of inactivated H7N9-E157 virus or H7N9 VLPs and incubated for 8 h at 37°C. Cells were then harvested for RNA extraction. Cytokine expression levels of cells were evaluated using qRT-PCR.

Cytokine Assays Using Quantitative Real-Time PCR (qRT-PCR)

Total mRNA was extracted using total RNA extraction kits (Feijie, Shanghai, China); 500 ng of total mRNA was converted into cDNA using HiScript Reverse Transcriptase (Vazyme, Nanjing, China) according to the manufacturer's instructions. mRNA expressions were examined using quantitative real-time PCR (qRT-PCR) with ChamQ Universal SYBR qPCR master mix (Vazyme, Nanjing, China) using a Bio-Rad CFX Applied System PCR instrument (Bio-Rad Laboratories Inc., Hercules, CA, USA). Sequences of primers used for qRT-PCR are shown in **Table 2**. The analyzed specific gene level was normalized with a housekeeping gene β-actin of the respective treatment group, and results were expressed in fold change.

Statistical Analysis

Experimental data are presented as mean ± SD of the mean. GraphPad Prism 7 software was used for data analysis. The results of serum antibody titers and cytokine level were evaluated using one-way ANOVA and Tukey's multiple-comparison test. Significant differences are denoted by an asterisk as follows: $^{*}p < 0.05$, $^{**}p < 0.01$, $^{***}p < 0.001$, or $^{****}p < 0.0001$.

RESULTS

Production and Characterization of H7N9 VLPs and HMN

The H7N9 VLPs were produced in High Five insect cells, which were coinfected with recombinant baculovirus (rBVs) expressing HA, NA, and M1. Based on optimization results, the H7N9 VLPs in the study were produced using High Five cells coinfected with rBVs expressing HA, NA, and M1 at an MOI of 2:1:2. The expression of H7N9 proteins was observed with indirect IFA with chicken antiserum against H7N9 AIVs in sf9 cells 48 h after coinfection with HA, NA, and M1 rBVs (**Figure 1A**), whereas there was no specific fluorescence in the control baculovirus-infected cells (**Figure 1B**). The production of VLPs from cell culture supernatants was confirmed using SDS-PAGE and Western blotting (**Figure 1E**). The molecular mass of HA, NA, and M1 proteins was ~70, ~53, and ~28 kDa, respectively. The VLPs were then purified using the sucrose gradient centrifugation. The purity of the H7N9 VLPs was confirmed using SDS-PAGE and Western blotting (**Figure 2A**). The hemagglutination activity of the purified H7N9 VLPs reached 2^{13}. The size and morphology of H7N9 VLPs were examined by

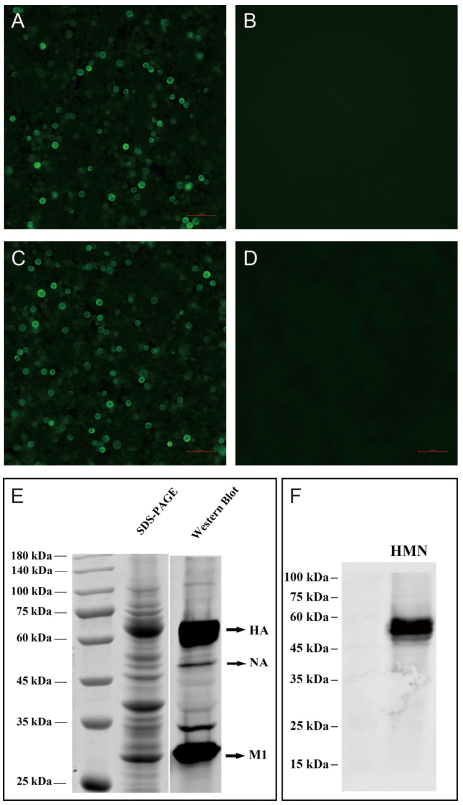

FIGURE 1 | Characterization of H7N9 VLPs and HMN by indirect immunofluorescence assay (IFA), SDS-PAGE, and Western blotting. IFA detection of expression of the baculovirus in sf9 infected cells. Sf9 cells infected with rBV-HA, rBV-NA, and rBV-HA **(A)**, rBV-HMN **(C)**, or only empty baculoviruses **(B)**, **(D)** after 48 h. H7N9 chicken antiserum and anti-His-tag mouse monoclonal antibodies were used in the IFA assay. **(E)** The expression of the HA, NA, and M1 proteins on the VLPs was analyzed using SDS-PAGE gels with Coomassie blue staining and validated by Western blot using the anti-His-tag mouse monoclonal antibody. The molecular mass of H7N9 HA, NA, and M1 were ~70, ~55, and ~28 kDa, respectively. **(F)** The expression of HMN protein was validated by Western blot using the anti-His-tag mouse monoclonal antibody. The molecular mass of HMN was ~52 kDa.

TABLE 2 | Sequences of primers used for quantitative real-time PCR.

Gene	Primer Sequences (5′–3′)	Product Size (bp)	Accession No.
IFN-γ	F: ACCTTCCTGATGGCGTGAAG R: TGAAGAGTTCATTCGCGGCT	102	AJ634956.1
IL-4	F: ATGACATCCAGGGAGAGGTTT R: ATTGGAGTAGTGTTGCCTGCT	235	GU119892.1
IL-17	F: ACAGGAGATCCTCGTCCTCC R: TGACACATGTGCAGCCCAC	95	AY744450.1
β-Actin	F: TGGGTATGGAGTCCTGTGGT R: CTGTCAGCAATGCCAGGGTA	136	NM_205518.1

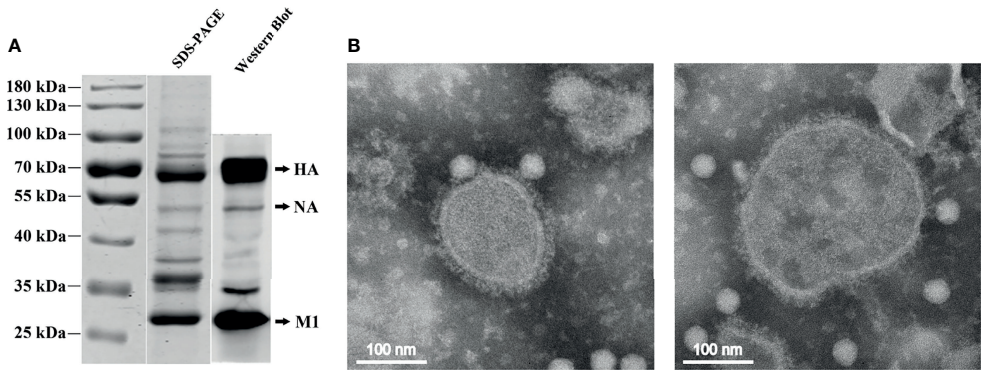

FIGURE 2 | SDS-PAGE, Western blotting, and electron microscopy of the purified H7N9 VLPs. **(A)** The purity of the purified H7N9 VLPs was analyzed using SDS-PAGE and validated by Western blotting with the anti-His-tag mouse monoclonal antibody. **(B)** Negative staining electron microscopy of the H7N9 VLPs. Purified VLPs were stained using 1% phosphotungstic acid.

transmission electron microscopy (**Figure 2B**). The average size of the VLPs was 100 nm; the morphology of the VLPs resembles that of influenza virus particles, and the spikes were observed on spherical surfaces which mimic influenza virus HA and NA proteins on the native virions.

The HMN fusion construct was generated as described in **Figure 3**. HMN gene consists of the $2HA2_{76\text{-}130}$, 4M2e, and $8NP_{55\text{–}69}$ epitope sequences, a linker sequence, melittin signal peptide, and 6xHis tag epitope. The expression of HMN proteins was observed using an IFA in HMN rBV-infected sf9 cells (**Figure 1C**), whereas there was no specific fluorescence in control baculovirus-infected cells (**Figure 1D**). Western blot analysis was used to validate HMN protein (**Figure 1F**). The determined molecular mass of the HMN protein was ~52 kDa.

H7N9 VLP Vaccines Elicit Immune Responses in Chickens

To examine the capacity of H7N9 VLP vaccine to induce immune responses in chickens, groups of 3-week-old SPF chickens were subcutaneously vaccinated one time with 30 μg of H7N9 VLPs formulated with adjuvant EOLANE 150 and H7N9 commercial vaccine as controls. The level of serum antibody against homologous virus H7N9-16876 was measured by HI assay at 3 weeks after a single-dose vaccination. The result showed that all vaccine groups effectively elicited anti-H7N9 AIV HI antibodies; the HI titers of chickens receiving the H7N9 commercial vaccine were higher than those induced by receiving the H7N9 VLP vaccine (**Figure 4A**). The mean HI titers of the H7N9 VLP vaccine reached 6.5 $\log_2$, which showed that the H7N9 VLP vaccine induced a high antibody response in chickens.

H7N9 VLP Vaccines Offer Protection Against a High Lethal Dose Challenge of Homologous H7N9 Virus

Groups of 3-week-old SPF chickens were subcutaneously vaccinated once with EOLANE 150-adjuvanted H7N9 VLP vaccine or H7N9 commercial vaccine, respectively; the control group was treated with PBS. All chickens were intranasally challenged with $2 \times 10^{6.0}$ ELD_{50} (0.2 ml) of A/Chicken/Guangdong/16876/2016 (H7N9) virus 3 weeks after immunization. The survival rates and morbidity of chickens in each group were monitored for 2 weeks after the challenge. All chickens in the H7N9 VLPs and H7N9 commercial vaccine group survived the infection. In contrast, all chickens in the control group died of infection 2 days postchallenge (**Figure 4B**). The clinical signs of the vaccinated chickens were not observed, and the bodyweight still slightly increased in chickens that received the H7N9 VLPs and commercial vaccines during 14 days of the monitoring period (date not shown).

The excreted viruses *via* the oropharynx and cloaca were analyzed to determine the virus replication at 5 days postchallenge (**Table 3**). After the challenge, virus shedding was not detected in chickens from the H7N9 commercial

FIGURE 3 | Schematic representation of HMN structure. HMN: melittin signal peptide; two repeated copies of the hemagglutinin stem area amino acids 76-130 (2HA2); four repeated copies of the ectodomain of matrix protein M2 (4M2e); eight repeated copies of the nucleoprotein amino acids 55-69 (8NP); 6xHis tag epitope. 3xG4S, GGGGSGGGGSGGGGS.

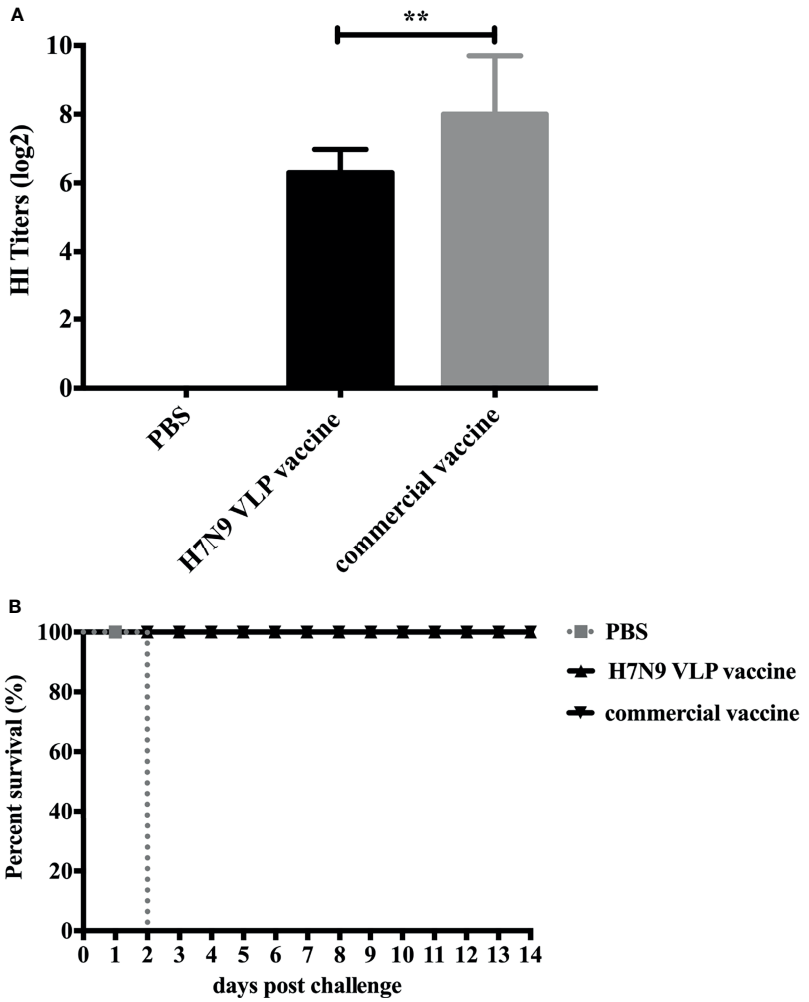

FIGURE 4 | Hemagglutinin inhibition (HI) titers of SPF chickens after immunization and survival rates of SPF chickens after challenge. **(A)** The SPF chickens were immunized with the H7N9 VLP vaccine and the H7N9 commercial vaccine. The serum samples were collected at 3 weeks postvaccination to measure the HI antibody titers. The HI titers of SPF chicken sera were measured with 4 HAU testing antigens of the H7N9 GD16 virus. The HI titers among vaccination groups were compared using one-way ANOVA followed by Tukey's multiple-comparison test. $^{**}p < 0.01$, statistically significant differences. **(B)** At 3 weeks postvaccination, groups of SPF chickens ($n = 10$) were intranasally challenged with a high lethal dose ($2 \times 10^{6.0}$ ELD_{50}) of A/Chicken/Guangdong/GD16/2016 H7N9 AIVs. Survival rates of chickens were measured daily for 2 weeks after challenge.

vaccine group, and one chicken was positive for virus isolation in the H7N9 VLP vaccine group. Overall, although the HI titers induced by the H7N9 VLP vaccine were lower than those by the commercial vaccine, the protective efficacy of the H7N9 VLP vaccine was comparable with the commercial vaccine.

H7N9 VLP Vaccines Induce Crossreactive HI and Neutralizing Antibody Against Antigenically Divergent H7N9 Viruses

To evaluate the crossreactivity of the serum antibodies from the H7N9 VLP-vaccinated chickens against antigenically divergent

TABLE 3 | Virus shedding after a lethal-dose homologous influenza virus challenge of chickens.

Group	Challenge Virus	5 dpc		Total Virus Shedding/total	No. Clinical Symptoms	Survival/Total
		Oropharyngeal Swab	Cloacal Swab			
H7N9 VLP vaccine	16876	1/10	0/10	1/10	0	10/10
Commercial vaccine	16876	0/10	0/10	0/10	0	10/10
PBS	16876	NA	NA	NA	10	0/10

16876 is virus of A/Chicken/Guangdong/16876/2016 (H7N9). The oropharyngeal and cloacal swab samples were collected at 5 days postchallenge. Virus positivity or shedding was determined by inoculating each swab solution into 3 eggs of 10-day-old specific-pathogen-free chicken embryos.
dpc, days postchallenge; NA, not applicable due to death of chickens.

H7N9 AIVs from wave 5, HI and neutralization assay were carried out against H7N9 variant viruses E157 and E664 (3). Groups of 3-week-old SPF chickens were immunized once with 30 μg of H7N9 VLPs formulated with ISA 201 VG, ISA 201 VG plus HMN (30 μg), ISA 201 VG plus Poly(I:C) (30 μg), and ISA 71 VG. Antisera were collected at 14 and 19 days after a single-dose vaccination (**Figure 5A**). For HI assay, using 4 HA units (HAU) of H7N9-E157 as a testing virus, the results showed that ISA 71 VG-adjuvanted H7N9 VLP vaccine immunization could induce a higher level of HI antibody titers, which was significantly higher than that induced by the ISA 201 VG-containing adjuvant H7N9 VLP vaccine. Furthermore, the use of ISA 201 VG adjuvant alone showed slightly higher HI titers than the titer observed with ISA 201 VG plus HMN and ISA 201 VG plus Poly(I:C), but the difference was not statistically significant at 3 weeks after immunization (**Figure 5B**). Using 4 HAU of H7N9-E664 as a testing virus, the results showed the mean HI titers of the ISA 71 VG adjuvant group were 6.5 $\log_2$ 14 days after immunization, which was significantly higher than the titers of other adjuvant groups. The serum HI levels of all vaccine groups 19 days after immunization were substantially increased compared with those on day 14. The ISA 71 VG adjuvant group demonstrated significantly higher HI titers than the ISA 201 VG-containing adjuvant groups. There were no significant differences among ISA 201 VG-associated vaccine groups (**Figure 5C**).

Neutralization assay was carried out against the H7N9 AIV E157 or E664. Serum samples from the VLP+ISA 71 vaccine group demonstrated significantly higher neutralizing antibody titers than those from other vaccine groups (**Figures 5D, E**).

Q226 Mutation on H7N9 Influenza Virus Hemagglutinin May Lead to Biased Antigenicity Evaluation

The study has shown that the Q226 mutation in the HA of H7N9 influenza virus [A/Guangdong/17SF003/2016 (H7/GD16)] from the fifth wave increases the viral receptor-binding avidity to RBC, leading to decreasing HI titers against viruses containing HA Q226 and resulting in a biased antigenic evaluation based on HI assay (34). In this study, the fifth wave of H7N9 influenza virus

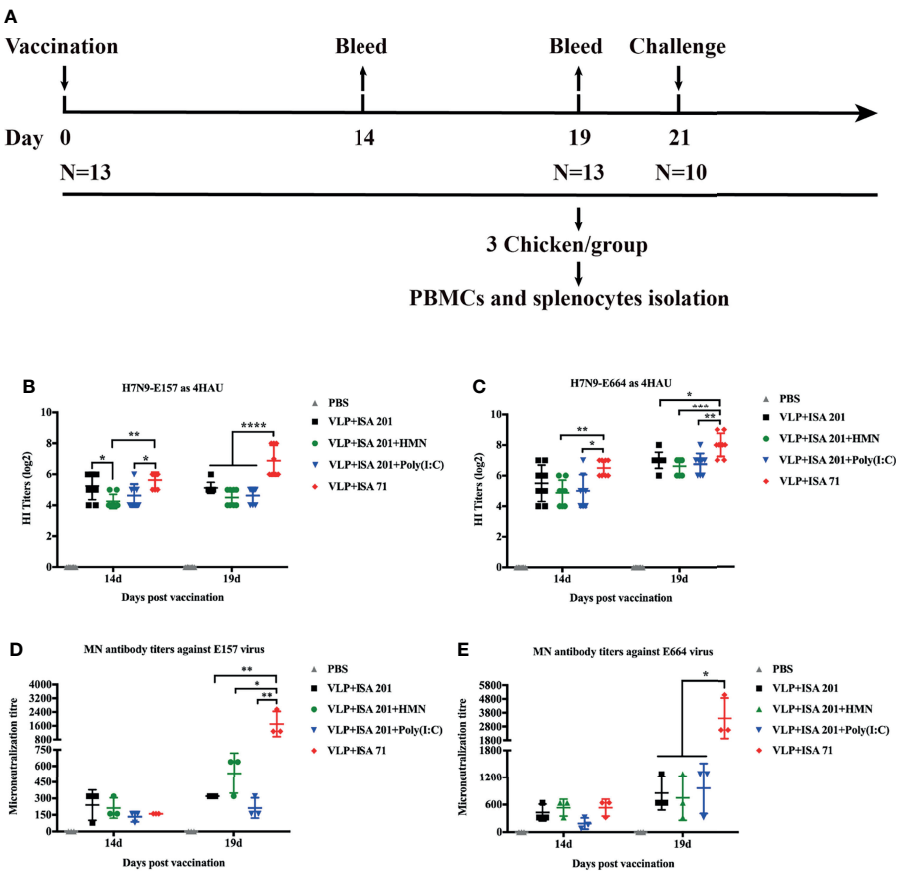

FIGURE 5 | Hemagglutinin inhibition (HI) and neutralizing antibody titers of immune sera from vaccinated specific pathogen-free (SPF) chickens. **(A)** The timeline and vaccination and challenge study in chicken. SPF chickens were immunized with H7N9 VLP vaccine candidates, and the serum samples were collected 14 and 19 days after immunization. The HI titers of SPF chicken sera were measured with 4 HAU of E157 **(B)** and E664 **(C)**. Viral neutralizing antibody titers in serum were determined with E157 **(D)** and E664 **(E)** AIVs. The neutralizing and HI antibody titers among vaccination groups were compared using one-way ANOVA followed by Tukey's multiple-comparison test. Statistically significant differences are indicated by an asterisk as follows: $^{*}p < 0.05$, $^{**}p < 0.01$, $^{***}p < 0.001$, or $^{****}p < 0.0001$.

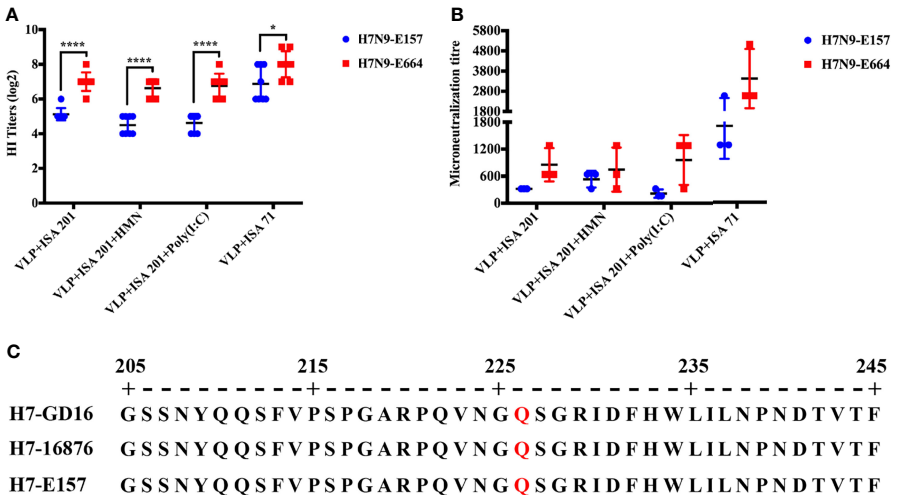

FIGURE 6 | Q226 mutation of H7 HA decreases readouts of HI and neutralizing antibody titers. **(A)** HI titers of H7N9-VLP immune sera from chickens to H7N9-E157 and H7N9-E664 viruses. **(B)** Neutralizing antibody titers of H7N9-VLP immune sera from chickens to H7N9-E157 and H7N9-E664 viruses. **(C)** Sequence alignment of HA gene of the H7N9-GD16, H7N9-E157, and H7N9-E664 viruses. H7N9-GD16, A/Guangdong/17SF003/2016 (H7/GD16). Statistically significant differences are indicated by an asterisk as follows: $^{*}p < 0.05$, $^{****}p < 0.0001$.

E157 and E664 were used to evaluate the crossreactivity of H7N9 VLP vaccine sera. Nineteen days after immunization, the H7N9-E157 virus displayed significantly lower HI titers to H7N9-VLP immune sera from all vaccine groups than the H7N9-E664 virus (**Figure 6A**). Similar results were observed in the neutralizing antibody titers (**Figure 6B**). By aligning the amino acid sequence of the HA gene of H7N9-GD16, H7N9-16876, and H7N9-E157 viruses, the results showed that the receptor-binding site of the HA gene of H7N9-16876 and H7N9-E157 viruses has the same Q226 mutation as that of the H7N9-GD16 virus (**Figure 6C**). These results showed that the Q226 mutation in the receptor-binding site of H7 HA decreased readouts of HI and neutralizing antibody titers by impacting the receptor-binding avidity to red blood cells.

HMN and Poly(I:C) Enhance Th1-Type Immune Responses of H7N9 VLP Vaccine

To evaluate the ability of vaccine candidates to induce immune responses and to further estimate the immune types, PBMCs and splenocytes were isolated from the vaccinated chickens 19 days after immunization and stimulated with inactivated influenza virus or purified H7N9 VLP antigen *in vitro*. The level of the cytokines IFN-γ, IL-4, and IL-17, associated with Th1-type, Th2-type, and Th17-type immune responses, respectively, were determined to evaluate the immune types induced by H7N9 VLP vaccine candidates. After virus stimulation *in vitro*, mRNA expression levels of IFN-γ and IL-4 were significantly higher in the PBMCs of chickens that received ISA 71 VG-adjuvanted vaccine than levels of IFN-γ and IL-4 in the PBMCs of chickens that received ISA 201 VG-containing adjuvanted vaccine. The mRNA levels of IFN-γ were significantly higher in the PBMCs of VLPs in combination with ISA 71 VG-vaccinated chickens than that of the IL-4, indicating that Th2-biased immune responses were induced by ISA 71 VG-adjuvanted vaccine (**Figure 7A**). The splenocytes of chickens that received the ISA 71 VG-adjuvanted vaccine demonstrated significantly higher IL-4 and IL-17 mRNA expression levels than those immunized with the ISA 201 VG-containing adjuvant vaccine (**Figure 7C**). After antigen stimulation *in vitro*, the lowest levels of IFN-γ and IL-4 were observed in the PBMCs of chickens that received ISA 201 VG-adjuvanted vaccine in the presence of Poly(I:C) or HMN, respectively (**Figure 7B**). In contrast, the splenocytes of chickens that received Poly(I:C)-supplemented ISA 201 VG-adjuvanted vaccine could induce the highest expression levels of IFN-γ. mRNA levels of IFN-γ were significantly higher in the splenocytes of chickens vaccinated with HMN- or Poly(I:C)-supplemented ISA 201 VG-adjuvanted vaccine than with ISA 201 VG-adjuvanted vaccine alone. The splenocytes of chickens that received the ISA 201 VG-adjuvanted vaccine showed the highest IL-4 mRNA expression levels, which was significantly higher than the IL-4 levels in the splenocytes of chickens that received other H7N9 vaccine candidates (**Figure 7D**). The results indicated that the ISA 201 VG adjuvant vaccine supplement with Poly(I:C) or HMN induced Th1-biased immune responses. The use of ISA 201 VG or ISA 71 VG adjuvant alone induced Th2-biased immune responses.

H7N9 VLP Vaccine Confers Crossprotection Against Heterologous H7N9 Virus

Prior to challenge, the results showed that the titers of HI and neutralizing antibody titers against H7N9-E157 AIVs were lower

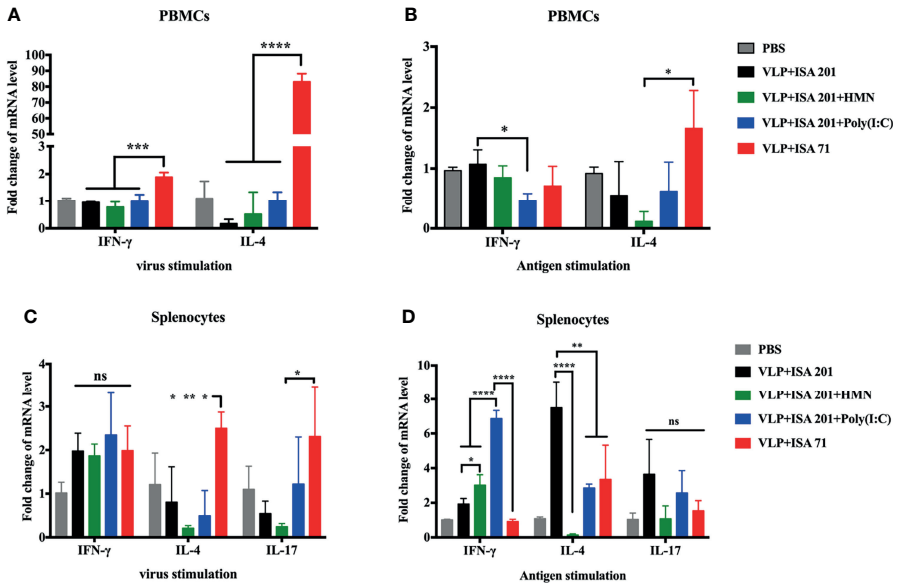

FIGURE 7 | Cytokine expression levels in PBMCs and splenocytes of SPF chickens (N=3). PBMCs and splenocytes were isolated from the vaccinated chickens 19 days after immunization and stimulated with inactivated influenza virus or purified H7N9 VLPs antigen for 8 h in vitro. The expression levels of cytokines in PBMCs **(A, B)** and splenocytes **(C, D)** were measured using qRT-PCR. Data are presented as the mean ± standard error of the mean. Statistical significance of differences is illustrated as follows: *P < 0.05, **P < 0.01, ***P < 0.001, ****P < 0.0001, or ns, not significant.

than those against H7N9-E664 AIVs. Therefore, to effectively evaluate the crossprotective efficacy of the H7N9 VLP vaccine, the H7N9-E157 AIVs were selected as challenge virus. Groups of 3-week-old SPF chickens were vaccinated once with VLP+ISA 201, VLP+ISA 201+HMN, VLP+ISA 201+Poly(I:C), and VLP +ISA 71 vaccines, respectively; the control group was treated with PBS. All chickens were intranasally challenged with $10^{6.0}$ EID_{50} (0.2 ml) of the H7N9-E157 virus 3 weeks after immunization. All chickens in the vaccine groups of VLP+ISA 201, VLP+ISA 201+HMN, VLP+ISA 201+Poly(I:C), and VLP+ISA 71 survived the infection. In contrast, all chickens in the control group died of infection 3 days PC (**Figure 8**). The clinical signs of the vaccinated chickens were not observed, and the bodyweight still slightly increased in chickens that received the H7N9 VLP vaccine candidates during 14 days of the monitoring period (data not shown).

The excreted viruses *via* the oropharynx and cloaca were analyzed to determine the virus replication at 3, 5, 7, and 9 days PC (**Table 4**). After the challenge, virus shedding was not detected in chickens from the VLP+ISA 201+HMN group, and

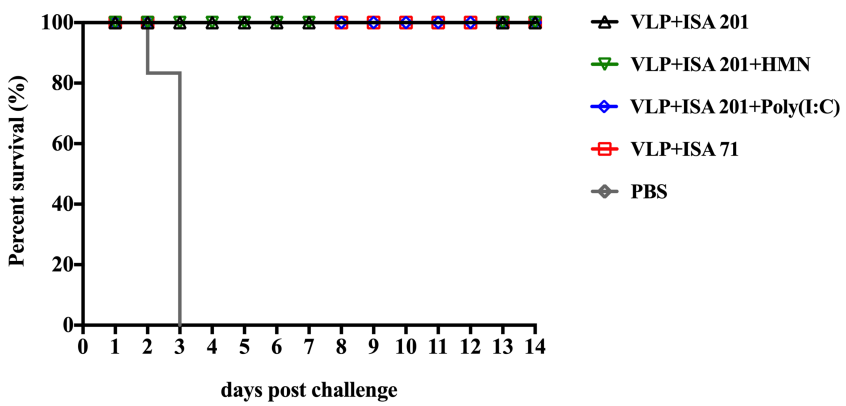

FIGURE 8 | Survival rates of the specific pathogen-free (SPF) chickens after H7N9-E157 virus challenge. At 3 weeks postvaccination, groups of SPF chickens (*n* = 10) were intranasally challenged with a high lethal dose ($10^{6.0}$ EID_{50}) of A/Chicken/Guangdong/E157/2017 H7N9 AIVs. Survival rates of chickens were measured daily for 2 weeks after challenge.

TABLE 4 | Virus shedding after a lethal-dose E157 AIV challenge of chickens.

Group	Oropharyngeal swab (virus shedding number/total number)				Cloacal swab (virus shedding number/total number)				No. clinical symptoms
	3 dpc	5 dpc	7 dpc	9 dpc	3 dpc	5 dpc	7 dpc	9 dpc	
VLP+ISA 201	0/10	0/10	0/10	0/10	0/10	2/10	0/10	0/10	0
VLP+ISA 201+HMN	0/10	0/10	0/10	0/10	0/10	0/10	0/10	0/10	0
VLP+ISA 201+Poly(I:C)	0/10	0/10	0/10	0/10	0/10	1/10	0/10	0/10	0
VLP+ISA 71	0/10	0/10	0/10	0/10	0/10	0/10	0/10	1/10	0
PBS	NA	NA	NA	NA	NA	NA	NA	NA	10

E157 is virus of A/Chicken/Guangdong/E157/2017. The oropharyngeal and cloacal swab samples were collected at 3, 5, 7, and 9 days postchallenge. Virus positivity or shedding was determined by inoculating each swab solution into 3 eggs of 10-day-old specific-pathogen-free chicken embryos.
dpc, days postchallenge; NA, not applicable due to death of chickens.

one chicken in the VLP+ISA 201+ Poly(I:C) group, two chickens in the VLP+ISA 201 group, and one chicken in the VLP+ISA 71 group recovered viruses from cloacal swab samples.

DISCUSSION

The continuous evolution and mutation of the H7N9 avian influenza virus poses a dual threat to human health and the poultry industry (4), and thus it is imperative to develop a safe and effective vaccine against H7N9 virus infections. A variety of the influenza vaccine formations were designed to protect against influenza virus (35–38). Avian influenza VLPs retain the structural and antigenic properties of native viruses but lack the genetic material, which is a better selection as vaccine antigen for the development of influenza vaccine. Influenza VLPs have been generated in various production platforms, including plant cells (39, 40), hepatitis B virus core (HBc) (41, 42), insect cells (11, 43), and mammalian cells (44). Commercially, the method for producing influenza VLPs using a baculovirus expression vector system (BEVS) is safe and low cost. High-throughput production of avian influenza VLPs is possible by optimizing the BEVS process (12, 45). A previous study showed that intramuscular and intranasal immunization with insect cell-derived H7 VLPs induces protective immunity against lethal H7N9 virus challenge (13), which supports the hypothesis that influenza VLPs are a promising candidate H7N9 vaccine antigen.

HA and NA proteins are the major surface glycoproteins of influenza viruses. Reports have shown that the recombinant H7 HA subunit vaccine protects mice from H7N9 influenza virus challenge (16, 17). NA expressing VLPs induced effective crossprotective immunity against influenza virus (46). On the other hand, M1 is a central component of the virus particle. In this study, we developed VLPs containing H7N9 HA, NA, and M1 proteins. The expression of VLP was detected using SDS-PAGE, and VLP antigenicity was validated *via* IFA and Western blotting. The hemagglutination activity of VLPs further confirmed that HA proteins anchored on surface VLPs retained functional stability and cRBC-binding activity. The water-in-oil-in-water emulsion adjuvant Montanide ISA 201 VG was used as an adjuvant in conjunction with VLPs to improve the crossprotection of vaccination. Report has shown that Montanide ISA 201 VG combined with inactivated influenza virus induces both humoral and cell-mediated immune responses to protect against a homologous H1N1 challenge in swine (47). We demonstrated that vaccination with H7 VLPs combined with ISA 201 VG induced strong HI antibody titers after single-dose vaccination and homologous protection against H7N9-16876 virus challenge in chickens. However, the influenza VLP vaccine induced a lower HI antibody titer and presented virus shedding in vaccinated chickens compared with the commercial H7N9 inactivated vaccine. A previous study also showed that H7N9 VLPs combined with ISA 71 R adjuvant induced lower levels of HI and MN antibody titers compared with commercial whole-virus inactivated vaccine (6). The protective efficacy of the H7N9 VLPs vaccine can be further improved by increasing the dose of VLP (13). Previous studies have shown that recombinant baculovirus vaccine expressing H7N9 HA protein confers better protection to the inactivated vaccine in chickens (48), and a plant-derived H6N2 VLP elicited a better protective immunity than a commercial inactivated H6N2 vaccine (49). Therefore, the efficacy of the H7N9 VLP vaccine needs to be further evaluated.

In the present study, we developed a series of vaccination strategies for VLP vaccine aiming to enhance crossprotection and eliminate viral shedding in vaccinated chickens. Previous studies have shown that influenza conserved fusion epitopes vaccine can induce broad crossprotection against different influenza viruses (50, 51). However, the influenza vaccine based on influenza conserved epitopes cannot provide complete protection against influenza virus challenge in the presence of morbidity, mortality, and virus shedding (52–54). Therefore, a single recombinant protein based on influenza conserved epitopes is not sufficient as an influenza vaccine antigen. Reports have shown that supplementing influenza vaccines with tandem repeat M2e VLPs enhances crossprotection against homologous and heterologous influenza virus challenge in an animal model (55, 56). Therefore, the influenza conserved epitopes can be used as an antigen supplement to enhance the crossprotection ability of influenza VLP vaccines. In this study, we constructed and expressed a recombinant protein (HMN) based on influenza conserved peptides to improve the crossprotective immunity of influenza VLP vaccines. HMN protein antigenicity was validated *via* Western blotting. In this study, we demonstrated that supplementation of the VLP+ISA 201 vaccine with HMN

protein cannot increase HI and neutralizing antibody titers to the VLP+ISA 201 vaccine. Nevertheless, following the heterologous H7N9-E157 virus challenge, viral shedding was completely abolished in chickens of the HMN supplement vaccine group, but two chickens in the VLP+ISA 201 group recovered viruses. Meanwhile, the HMN-supplemented VLP+ISA 201 vaccine induces significantly higher IFN-γ mRNA expression levels in splenocytes than the VLP+ISA 201 vaccine, which enhances the Th1-type immune responses of VLP+ISA 201 vaccine. A previous study showed that Th1 immune responses play a critical role in crossprotective immunity and virus removal against influenza virus challenge (57). Although this study is limited to not being able to determine the immune response induced by HMN, we speculate that the HMN protein may induce a broad crossprotective immune response and play an important role in virus clearance. Therefore, HMN protein as an antigen supplement is a promising vaccination strategy for crossprotection against the H7N9 influenza virus.

Influenza-specific cell-mediated immune responses play an important role in eliminating the virus in chickens receiving the influenza VLP vaccine (6). Poly(I:C) was selected as an adjuvant supplement to improve cell-mediated immune responses of the VLP+ISA 201 vaccine. Previous studies have shown that Poly(I:C)-adjuvanted influenza vaccines induce a cell-mediated immune response, conferring protection against homologous and heterologous virus challenge (28, 58). In this study, we demonstrated that the Poly(I:C)-supplemented vaccine stimulates the highest mRNA expression levels of IFN-γ in splenocytes that enhanced a Th1-mediated immune response of the VLP + ISA 201 vaccine and provided a crossprotection against a heterologous H7N9 E157 virus challenge in chickens. However, the supplementation of Poly(I:C) did not significantly increase HI and MN antibody titers and did not completely inhibit virus shedding in vaccinated chickens, which may be related to the injection route of Poly(I:C). Reports have shown that intranasal immunization with Poly(I:C)-adjuvanted influenza vaccines induces robust mucosal, humoral, and cellular immunity to protect against homologous and heterologous influenza virus challenge (28, 58, 59). The potency of VLPs with Poly(I:C) needs to be further investigated in chickens administered intranasally.

Montanide ISA 71 VG was used as an adjuvant for comparison with Montanide ISA 201 VG. Montanide ISA 71 VG is a commercial water-in-oil emulsion adjuvant and has been confirmed to stimulate both humoral and cellular immune responses (60). Recent studies have shown that combining influenza VLPs with ISA 71 VG induces protective immunity against lethal homologous virus challenge (6, 61). These findings indicated that ISA 71 VG is a promising VLP subunit vaccine adjuvant. This study has shown that H7N9 VLPs combined with ISA 71 VG induce higher titers of HI and MN antibody against heterologous H7N9 virus than the ISA 201 VG-adjuvanted vaccine. Meanwhile, ISA 71 VG stimulated significantly higher IFN-γ, IL-4, and IL-17 mRNA expression levels in PBMCs and splenocytes than stimulated by ISA 201 VG. Following the H7N9-E157 virus challenge, the ISA 71 VG vaccine group showed less virus shedding than the ISA 201 VG vaccine group. In comparison, the ISA 201 VG-adjuvanted VLP vaccine induced lower serum HI and MN antibody titers against the heterologous H7N9-E157 and H7N9-E664 viruses and Th2-biased immune responses in chickens. Following the E157 virus challenge, the VLP+ISA 201 vaccine did not eliminate virus shedding in chickens. However, supplementing the VLP +ISA 201 vaccine with HMN protein can achieve the goal of virus clearance in chickens. This study demonstrated that Q226 mutation in the receptor-binding site of H7 HA plays a crucial role in reducing the readouts of HI and neutralizing antibody titers by impacting the receptor-binding avidity to red blood cells. Therefore, viral receptor-binding avidity should be considered in evaluating an H7N9 candidate vaccine.

In the future, H7N9 VLP from this study may be further modified by combining with mucosal or nanoparticle adjuvant. Mucosal immune responses play an important role in defense against influenza virus infection. Several studies showed that the intranasal administration of influenza vaccine combined with the mucosal adjuvant induced crossprotection against divergent influenza subtypes (62, 63). Influenza nanoparticle vaccine is one of the strategies for developing a universal influenza vaccine. Previous studies showed that influenza nanoparticles induce broad protection against heterosubtypic influenza viruses (64, 65).

In summary, our results indicate that H7N9 VLP vaccine candidates induce a crossreactive serum immune response and provide effective crossprotection against homologous and heterologous H7N9 influenza viruse challenge. In addition, we successfully developed a combo vaccine consisting of H7N9 VLP and polyepitope HMN that confers full protection against antigenically divergent H7N9 virus challenge. Our results collectively suggest that the supplementation of the H7N9 VLP vaccine with polyepitope antigen will be a promising strategy for broad protection against an antigenically divergent H7N9 virus.

DATA AVAILABILITY STATEMENT

The raw data supporting the conclusions of this article will be made available by the authors, without undue reservation.

ETHICS STATEMENT

All experiments involved in the live H7N9 avian influenza viruses (AIVs) were performed in a biosafety level 3 laboratory facilities at South China Agricultural University (SCAU) (CNAS BL0011) in accordance with protocols. All animals involved in the experiments were reviewed and approved by the Institutional Animal Care and Use Committee at SCAU and treated in accordance with the guidelines (2017A002).

AUTHOR CONTRIBUTIONS

HF, ML, and DK designed the research. DK, TC, XH, SL, and YG performed the experiments. DK, TC, and CJ analyzed the data.

DK, ML, and HF participated in writing the paper. All authors reviewed the manuscript.

FUNDING

This work was supported by the Innovation Leading Team Program of Guangzhou City (202009020009) and the Key Research and Development Program of Guangdong Province (2019B020218004).

ACKNOWLEDGMENTS

Special thanks to Ming Liao for providing three avian influenza A (H7N9) virus samples.

REFERENCES

1. Liu D, Shi W, Shi Y, Wang D, Xiao H, Li W, et al. Origin and Diversity of Novel Avian Influenza A H7N9 Viruses Causing Human Infection: Phylogenetic, Structural, and Coalescent Analyses. *Lancet* (2013) 381 (9881):1926–32. doi: 10.1016/S0140-6736(13)60938-1
2. Bao L, Bi Y, Wong G, Qi W, Li F, Lv Q, et al. Diverse Biological Characteristics and Varied Virulence of H7N9 From Wave 5. *Emerg Microbes Infect* (2019) 8 (1):94–102. doi: 10.1080/22221751.2018.1560234
3. Wu Y, Hu J, Jin X, Li X, Wang J, Zhang M, et al. Accelerated Evolution of H7N9 Subtype Influenza Virus Under Vaccination Pressure. *Virol Sin* (2021) 36(5):1124-32. doi: 10.1007/s12250-021-00383-x
4. Zhang J, Ye H, Li H, Ma K, Qiu W, Chen Y, et al. Evolution and Antigenic Drift of Influenza A (H7N9) Viruses, China, 2017-2019. *Emerg Infect Dis* (2020) 26(8):1906–11. doi: 10.3201/eid2608.200244
5. Maurice A, Halasa N. Preparing for the 2019-2020 Influenza Season. *Pediatr Transplant* (2020) 24(1):e13645. doi: 10.1111/petr.13645
6. Li J, Li R, Zhang Q, Peng P, Wang X, Gu M, et al. H7N9 Influenza Virus-Like Particle Based on BEVS Protects Chickens From Lethal Challenge With Highly Pathogenic H7N9 Avian Influenza Virus. *Vet Microbiol* (2021) 258:109106. doi: 10.1016/j.vetmic.2021.109106
7. Erlewyn-Lajeunesse M, Brathwaite N, Lucas JSA, Warner JO. Recommendations for the Administration of Influenza Vaccine in Children Allergic to Egg. *BMJ* (2009) 339:b3680. doi: 10.1136/bmj.b3680
8. Parker L, Wharton SA, Martin SR, Cross K, Lin Y, Liu Y, et al. Effects of Egg-Adaptation on Receptor-Binding and Antigenic Properties of Recent Influenza A (H3N2) Vaccine Viruses. *J Gen Virol* (2016) 97(6):1333–44. doi: 10.1099/jgv.0.000457
9. Durous L, Rosa-Calatrava M, Petiot E. Advances in Influenza Virus-Like Particles Bioprocesses. *Expert Rev Vaccines* (2019) 18(12):1285–300. doi: 10.1080/14760584.2019.1704262
10. Frietze KM, Peabody DS, Chackerian B. Engineering Virus-Like Particles as Vaccine Platforms. *Curr Opin Virol* (2016) 18:44–9. doi: 10.1016/j.coviro.2016.03.001
11. Huang D, Chao Y-C, Lv Z, Jan J-T, Yang Y-C, Hsiao P-W, et al. Comparison of Chicken Immune Responses After Inoculation With H5 Avian Influenza Virus-Like Particles Produced by Insect Cells or Pupae. *J Vet Res* (2021) 65 (2):139–45. doi: 10.2478/jvetres-2021-0026
12. Lai C-C, Cheng Y-C, Chen P-W, Lin T-H, Tzeng T-T, Lu C-C, et al. Process Development for Pandemic Influenza VLP Vaccine Production Using a Baculovirus Expression System. *J Biol Eng* (2019) 13(1):78. doi: 10.1186/s13036-019-0206-z
13. Ren Z, Zhao Y, Liu J, Ji X, Meng L, Wang T, et al. Intramuscular and Intranasal Immunization With an H7N9 Influenza Virus-Like Particle Vaccine Protects Mice Against Lethal Influenza Virus Challenge. *Int Immunopharmacol* (2018) 58:109–16. doi: 10.1016/j.intimp.2017.12.020
14. Steele KH, Stone BJ, Franklin KM, Fath-Goodin A, Zhang X, Jiang H, et al. Improving the Baculovirus Expression Vector System With Vankyrin-Enhanced Technology. *Biotechnol Prog* (2017) 33(6):1496–507. doi: 10.1002/btpr.2516
15. Kang H-J, Chu K-B, Yoon K-W, Eom G-D, Mao J, Kim M-J, et al. Neuraminidase in Virus-Like Particles Contributes to the Protection Against High Dose of Avian Influenza Virus Challenge Infection. *Pathogens* (2021) 10(10):1291. doi: 10.3390/pathogens10101291
16. Chen T-H, Liu W-C, Chen IC, Liu C-C, Huang M-H, Jan J-T, et al. Recombinant Hemagglutinin Produced From Chinese Hamster Ovary (CHO) Stable Cell Clones and a PELC/CpG Combination Adjuvant for H7N9 Subunit Vaccine Development. *Vaccine* (2019) 37(47):6933–41. doi: 10.1016/j.vaccine.2019.02.040
17. Liu B, Shi P, Wang T, Zhao Y, Lu S, Li X, et al. Recombinant H7 Hemagglutinin Expressed in Glycoengineered Pichia Pastoris Forms Nanoparticles That Protect Mice From Challenge With H7N9 Influenza Virus. *Vaccine* (2020) 38(50):7938–48. doi: 10.1016/j.vaccine.2020.10.061
18. Bernasconi V, Bernocchi B, Ye L, Lê MQ, Omokanye A, Carpentier R, et al. Porous Nanoparticles With Self-Adjuvanting M2e-Fusion Protein and Recombinant Hemagglutinin Provide Strong and Broadly Protective Immunity Against Influenza Virus Infections. *Front Immunol* (2018) 9:2060. doi: 10.3389/fimmu.2018.02060
19. Bhide Y, Dong W, Gribonika I, Voshart D, Meijerhof T, de Vries-Idema J, et al. Cross-Protective Potential and Protection-Relevant Immune Mechanisms of Whole Inactivated Influenza Virus Vaccines Are Determined by Adjuvants and Route of Immunization. *Front Immunol* (2019) 10:646. doi: 10.3389/fimmu.2019.00646
20. Choi A, Bouzya B, Cortés Franco K-D, Stadlbauer D, Rajabhathor A, Rouxel RN, et al. Chimeric Hemagglutinin-Based Influenza Virus Vaccines Induce Protective Stalk-Specific Humoral Immunity and Cellular Responses in Mice. *Immunohorizons* (2019) 3(4):133–48. doi: 10.4049/immunohorizons.1900022
21. Kim Y-J, Lee Y-T, Kim M-C, Lee Y-N, Kim K-H, Ko E-J, et al. Cross-Protective Efficacy of Influenza Virus M2e Containing Virus-Like Particles Is Superior to Hemagglutinin Vaccines and Variable Depending on the Genetic Backgrounds of Mice. *Front Immunol* (2017) 8:1730:1730. doi: 10.3389/fimmu.2017.01730
22. Liu W-C, Nachbagauer R, Stadlbauer D, Solórzano A, Berlanda-Scorza F, García-Sastre A, et al. Sequential Immunization With Live-Attenuated Chimeric Hemagglutinin-Based Vaccines Confers Heterosubtypic Immunity Against Influenza A Viruses in a Preclinical Ferret Model. *Front Immunol* (2019) 10:756. doi: 10.3389/fimmu.2019.00756
23. McMahon M, Asthagiri Arunkumar G, Liu W-C, Stadlbauer D, Albrecht RA, Pavot V, et al. Vaccination With Viral Vectors Expressing Chimeric Hemagglutinin, NP and M1 Antigens Protects Ferrets Against Influenza Virus Challenge. *Front Immunol* (2019) 10:2005:2005. doi: 10.3389/fimmu.2019.02005
24. Liu J, Ren Z, Wang H, Zhao Y, Wilker PR, Yu Z, et al. Influenza Virus-Like Particles Composed of Conserved Influenza Proteins and GPI-Anchored CCL28/GM-CSF Fusion Proteins Enhance Protective Immunity Against Homologous and Heterologous Viruses. *Int Immunopharmacol* (2018) 63:119–28. doi: 10.1016/j.intimp.2018.07.011
25. Song L, Xiong D, Song H, Wu L, Zhang M, Kang X, et al. Mucosal and Systemic Immune Responses to Influenza H7N9 Antigen HA1–2 Co-Delivered Intranasally With Flagellin or Polyethyleneimine in Mice and Chickens. *Front Immunol* (2017) 8:326. doi: 10.3389/fimmu.2017.00326
26. Zhang Z, Zhang J, Zhang J, Li Q, Miao P, Liu J, et al. Coimmunization With Recombinant Epitope-Expressing Baculovirus Enhances Protective Effects of Inactivated H5N1 Vaccine Against Heterologous Virus. *Vet Microbiol* (2017) 203:143–8. doi: 10.1016/j.vetmic.2017.03.004
27. Patil V, Renu S, Feliciano-Ruiz N, Han Y, Ramesh A, Schrock J, et al. Intranasal Delivery of Inactivated Influenza Virus and Poly(I:C) Adsorbed Corn-Based Nanoparticle Vaccine Elicited Robust Antigen-Specific Cell-Mediated Immune Responses in Maternal Antibody Positive Nursery Pigs. *Front Immunol* (2020) 11:596964. doi: 10.3389/fimmu.2020.596964
28. Renu S, Feliciano-Ruiz N, Ghimire S, Han Y, Schrock J, Dhakal S, et al. Poly(I:C) Augments Inactivated Influenza Virus-Chitosan Nanovaccine Induced

Cell Mediated Immune Response in Pigs Vaccinated Intranasally. *Vet Microbiol* (2020) 242:108611. doi: 10.1016/j.vetmic.2020.108611
29. Dong J, Chen P, Wang Y, Lv Y, Xiao J, Li Q, et al. Evaluation of the Immune Response of a H7N9 Candidate Vaccine Virus Derived From the Fifth Wave A/Guangdong/17sf003/2016. *Antiviral Res* (2020) 177:104776. doi: 10.1016/j.antiviral.2020.104776
30. Reed LJ, Muench H. A Simple Method of Estimating fifty Per Cent Endpoints. *Am J Epidemiol* (1938) 27(3):493–7. doi: 10.1093/oxfordjournals.aje.a118408
31. Quan FS, Huang C, Compans RW, Kang SM. Virus-Like Particle Vaccine Induces Protective Immunity Against Homologous and Heterologous Strains of Influenza Virus. *J Virol* (2007) 81(7):3514–24. doi: 10.1128/JVI.02052-06
32. Pushko P, Tumpey TM, Bu F, Knell J, Robinson R, Smith G. Influenza Virus-Like Particles Comprised of the HA, NA, and M1 Proteins of H9N2 Influenza Virus Induce Protective Immune Responses in BALB/c Mice. *Vaccine* (2005) 23(50):5751–9. doi: 10.1016/j.vaccine.2005.07.098
33. Budimir N, Huckriede A, Meijerhof T, Boon L, Gostick E, Price DA, et al. Induction of Heterosubtypic Cross-Protection Against Influenza by a Whole Inactivated Virus Vaccine: The Role of Viral Membrane Fusion Activity. *PloS One* (2012) 7(1):e30898. doi: 10.1371/journal.pone.0030898
34. Wang Y, Lv Y, Niu X, Dong J, Feng P, Li Q, et al. L226Q Mutation on Influenza H7N9 Virus Hemagglutinin Increases Receptor-Binding Avidity and Leads to Biased Antigenicity Evaluation. *J Virol* (2020) 94(20):e00667–20. doi: 10.1128/JVI.00667-20
35. Asthagiri Arunkumar G, McMahon M, Pavot V, Aramouni M, Ioannou A, Lambe T, et al. Vaccination With Viral Vectors Expressing NP, M1 and Chimeric Hemagglutinin Induces Broad Protection Against Influenza Virus Challenge in Mice. *Vaccine* (2019) 37(37):5567–77. doi: 10.1016/j.vaccine.2019.07.095
36. Lu Y, Landreth S, Liu G, Brownlie R, Gaba A, Littel-van den Hurk S, et al. Innate Immunemodulator Containing Adjuvant Formulated HA Based Vaccine Protects Mice From Lethal Infection of Highly Pathogenic Avian Influenza H5N1 Virus. *Vaccine* (2020) 38(10):2387–95. doi: 10.1016/j.vaccine.2020.01.051
37. Wang W, Li R, Deng Y, Lu N, Chen H, Meng X, et al. Protective Efficacy of the Conserved NP, PB1, and M1 Proteins as Immunogens in DNA- and Vaccinia Virus-Based Universal Influenza A Virus Vaccines in Mice. *Clin Vaccine Immunol* (2015) 22(6):618–30. doi: 10.1128/CVI.00091-15
38. Xu X, Qian J, Qin L, Li J, Xue C, Ding J, et al. Chimeric Newcastle Disease Virus-Like Particles Containing DC-Binding Peptide-Fused Haemagglutinin Protect Chickens From Virulent Newcastle Disease Virus and H9N2 Avian Influenza Virus Challenge. *Virol Sin* (2020) 35(4):455–67. doi: 10.1007/s12250-020-00199-1
39. Pillet S, Racine T, Nfon C, Di Lenardo TZ, Babiuk S, Ward BJ, et al. Plant-Derived H7 VLP Vaccine Elicits Protective Immune Response Against H7N9 Influenza Virus in Mice and Ferrets. *Vaccine* (2015) 33(46):6282–9. doi: 10.1016/j.vaccine.2015.09.065
40. Ward BJ, Makarkov A, Séguin A, Pillet S, Trépanier S, Dhaliwall J, et al. Efficacy, Immunogenicity, and Safety of a Plant-Derived, Quadrivalent, Virus-Like Particle Influenza Vaccine in Adults (18-64 Years) and Older Adults (≥65 Years): Two Multicentre, Randomised Phase 3 Trials. *Lancet* (2020) 396 (10261):1491–503. doi: 10.1016/S0140-6736(20)32014-6
41. Gao X, Wang W, Li Y, Zhang S, Duan Y, Xing L, et al. Enhanced Influenza VLP Vaccines Comprising Matrix-2 Ectodomain and Nucleoprotein Epitopes Protects Mice From Lethal Challenge. *Antiviral Res* (2013) 98(1):4–11. doi: 10.1016/j.antiviral.2013.01.010
42. Ramirez A, Morris S, Maucourant S, D'Ascanio I, Crescente V, Lu IN, et al. A Virus-Like Particle Vaccine Candidate for Influenza A Virus Based on Multiple Conserved Antigens Presented on Hepatitis B Tandem Core Particles. *Vaccine* (2018) 36(6):873–80. doi: 10.1016/j.vaccine.2017.12.053
43. Sequeira DP, Correia R, Carrondo MJT, Roldão A, Teixeira AP, Alves PM. Combining Stable Insect Cell Lines With Baculovirus-Mediated Expression for Multi-HA Influenza VLP Production. *Vaccine* (2018) 36(22):3112–23. doi: 10.1016/j.vaccine.2017.02.043
44. Buffin S, Peubez I, Barrière F, Nicolaï M-C, Tapia T, Dhir V, et al. Influenza A and B Virus-Like Particles Produced in Mammalian Cells Are Highly Immunogenic and Induce Functional Antibodies. *Vaccine* (2019) 37 (46):6857–67. doi: 10.1016/j.vaccine.2019.09.057
45. Sari-Ak D, Bahrami S, Laska MJ, Drncova P, Fitzgerald DJ, Schaffitzel C, et al. High-Throughput Production of Influenza Virus-Like Particle (VLP) Array by Using VLP-Factory™, a MultiBac Baculoviral Genome Customized for Enveloped VLP Expression. *High Throughput Protein Production Purif: Methods Protoc* (2019) 2025:213–26. doi: 10.1007/978-1-4939-9624-7_10
46. Kim K-H, Lee Y-T, Park S, Jung Y-J, Lee Y, Ko E-J, et al. Neuraminidase Expressing Virus-Like Particle Vaccine Provides Effective Cross Protection Against Influenza Virus. *Virology* (2019) 535:179–88. doi: 10.1016/j.virol.2019.07.008
47. Bouguyon E, Goncalves E, Shevtsov A, Maisonnasse P, Remyga S, Goryushev O, et al. A New Adjuvant Combined With Inactivated Influenza Enhances Specific CD8 T Cell Response in Mice and Decreases Symptoms in Swine Upon Challenge. *Viral Immunol* (2015) 28(9):524–31. doi: 10.1089/vim.2014.0149
48. Hu J, Liang Y, Hu Z, Wang X, Gu M, Li R, et al. Recombinant Baculovirus Vaccine Expressing Hemagglutinin of H7N9 Avian Influenza Virus Confers Full Protection Against Lethal Highly Pathogenic H7N9 Virus Infection in Chickens. *Arch Virol* (2019) 164(3):807–17. doi: 10.1007/s00705-018-04142-4
49. Smith T, O'Kennedy MM, Wandrag DBR, Adeyemi M, Abolnik C. Efficacy of a Plant-Produced Virus-Like Particle Vaccine in Chickens Challenged With Influenza A H6N2 Virus. *Plant Biotechnol J* (2020) 18(2):502–12. doi: 10.1111/pbi.13219
50. Wang Q, Zhang Y, Zou P, Wang M, Fu W, She J, et al. Self-Assembly M2e-Based Peptide Nanovaccine Confers Broad Protection Against Influenza Viruses. *Front Microbiol* (2020) 11:1961. doi: 10.3389/fmicb.2020.01961
51. Wang Y, Deng L, Gonzalez GX, Luthra L, Dong C, Ma Y, et al. Double-Layered M2e-NA Protein Nanoparticle Immunization Induces Broad Cross-Protection Against Different Influenza Viruses in Mice. *Adv Healthc Mater* (2020) 9(2):e1901176–e. doi: 10.1002/adhm.201901176
52. Ravin NV, Blokhina EA, Kuprianov VV, Stepanova LA, Shaldjan AA, Kovaleva AA, et al. Development of a Candidate Influenza Vaccine Based on Virus-Like Particles Displaying Influenza M2e Peptide Into the Immunodominant Loop Region of Hepatitis B Core Antigen: Insertion of Multiple Copies of M2e Increases Immunogenicity and Protective Efficiency. *Vaccine* (2015) 33(29):3392–7. doi: 10.1016/j.vaccine.2015.04.066
53. Shokouhi H, Farahmand B, Ghaemi A, Mazaheri V, Fotouhi F. Vaccination With Three Tandem Repeats of M2 Extracellular Domain Fused to Leismania Major HSP70 Protects Mice Against Influenza A Virus Challenge. *Virus Res* (2018) 251:40–6. doi: 10.1016/j.virusres.2018.05.003
54. Stepanova LA, Mardanova ES, Shuklina MA, Blokhina EA, Kotlyarov RY, Potapchuk MV, et al. Flagellin-Fused Protein Targeting M2e and HA2 Induces Potent Humoral and T-Cell Responses and Protects Mice Against Various Influenza Viruses a Subtypes. *J Biomed Sci* (2018) 25(1):33. doi: 10.1186/s12929-018-0433-5
55. Music N, Reber AJ, Kim M-C, York IA, Kang S-M. Supplementation of H1N1pdm09 Split Vaccine With Heterologous Tandem Repeat M2e5x Virus-Like Particles Confers Improved Cross-Protection in Ferrets. *Vaccine* (2016) 34(4):466–73. doi: 10.1016/j.vaccine.2015.12.023
56. Song B-M, Kang H-M, Lee E-K, Jung SC, Kim M-C, Lee Y-N, et al. Supplemented Vaccination With Tandem Repeat M2e Virus-Like Particles Enhances Protection Against Homologous and Heterologous HPAI H5 Viruses in Chickens. *Vaccine* (2016) 34(5):678–86. doi: 10.1016/j.vaccine.2015.11.074
57. Miller SM, Cybulski V, Whitacre M, Bess LS, Livesay MT, Walsh L, et al. Novel Lipidated Imidazoquinoline TLR7/8 Adjuvants Elicit Influenza-Specific Th1 Immune Responses and Protect Against Heterologous H3N2 Influenza Challenge in Mice. *Front Immunol* (2020) 11:406. doi: 10.3389/fimmu.2020.00406
58. Moriyama M, Chino S, Ichinohe T. Consecutive Inoculations of Influenza Virus Vaccine and Poly(I:C) Protects Mice Against Homologous and Heterologous Virus Challenge. *Vaccine* (2017) 35(7):1001–7. doi: 10.1016/j.vaccine.2017.01.025
59. Wong PT, Goff PH, Sun RJ, Ruge MJ, Ermler ME, Sebring A, et al. Combined Intranasal Nanoemulsion and RIG-I Activating RNA Adjuvants Enhance Mucosal, Humoral, and Cellular Immunity to Influenza Virus. *Mol Pharm* (2021) 18(2):679–98. doi: 10.1021/acs.molpharmaceut.0c00315
60. Jang SI, Lillehoj HS, Lee SH, Lee KW, Lillehoj EP, Bertrand F, et al. Montanide™ ISA 71 VG Adjuvant Enhances Antibody and Cell-Mediated Immune Responses to Profilin Subunit Antigen Vaccination and Promotes Protection Against Eimeria Acervulina and Eimeria Tenella. *Exp Parasitol* (2011) 127(1):178–83. doi: 10.1016/j.exppara.2010.07.021

61. Zhu W-Z, Wen Y-C, Lin S-Y, Chen T-C, Chen H-W. Anti-Influenza Protective Efficacy of a H6 Virus-Like Particle in Chickens. *Vaccines* (2020) 8(3):465. doi: 10.3390/vaccines8030465
62. Chowdhury MYE, Kim T-H, Uddin MB, Kim J-H, Hewawaduge CY, Ferdowshi Z, et al. Mucosal Vaccination of Conserved Sm2, HA2 and Cholera Toxin Subunit A1 (CTA1) Fusion Protein With Poly Gamma-Glutamate/Chitosan Nanoparticles (PC NPs) Induces Protection Against Divergent Influenza Subtypes. *Vet Microbiol* (2017) 201:240–51. doi: 10.1016/j.vetmic.2017.01.020
63. Wang SH, Smith D, Cao Z, Chen J, Acosta H, Chichester JA, et al. Recombinant H5 Hemagglutinin Adjuvanted With Nanoemulsion Protects Ferrets Against Pathogenic Avian Influenza Virus Challenge. *Vaccine* (2019) 37(12):1591–600. doi: 10.1016/j.vaccine.2019.02.002
64. Deng L, Chang TZ, Wang Y, Li S, Wang S, Matsuyama S, et al. Heterosubtypic Influenza Protection Elicited by Double-Layered Polypeptide Nanoparticles in Mice. *Proc Natl Acad Sci U S A* (2018) 115(33):E7758–67. doi: 10.1073/pnas.1805713115
65. Deng L, Mohan T, Chang TZ, Gonzalez GX, Wang Y, Kwon Y-M, et al. Double-Layered Protein Nanoparticles Induce Broad Protection Against Divergent Influenza A Viruses. *Nat Commun* (2018) 9(1):359. doi: 10.1038/s41467-017-02725-4

Conflict of Interest: The authors declare that the research was conducted in the absence of any commercial or financial relationships that could be construed as a potential conflict of interest.

Publisher's Note: All claims expressed in this article are solely those of the authors and do not necessarily represent those of their affiliated organizations, or those of the publisher, the editors and the reviewers. Any product that may be evaluated in this article, or claim that may be made by its manufacturer, is not guaranteed or endorsed by the publisher.

Advantages of publishing in Frontiers

OPEN ACCESS
Articles are free to read for greatest visibility and readership

FAST PUBLICATION
Around 90 days from submission to decision

HIGH QUALITY PEER-REVIEW
Rigorous, collaborative, and constructive peer-review

TRANSPARENT PEER-REVIEW
Editors and reviewers acknowledged by name on published articles

Frontiers
Avenue du Tribunal-Fédéral 34
1005 Lausanne | Switzerland

Visit us: www.frontiersin.org
Contact us: frontiersin.org/about/contact

REPRODUCIBILITY OF RESEARCH
Support open data and methods to enhance research reproducibility

DIGITAL PUBLISHING
Articles designed for optimal readership across devices

FOLLOW US
@frontiersin

IMPACT METRICS
Advanced article metrics track visibility across digital media

EXTENSIVE PROMOTION
Marketing and promotion of impactful research

LOOP RESEARCH NETWORK
Our network increases your article's readership